



T.C.

ÇANAKKALE ONSEKİZ MART ÜNİVERSİTESİ  
LİSANSÜSTÜ EĞİTİM ENSTİTÜSÜ

***CANAKKALE ONSEKİZ MART UNIVERSITY  
JOURNAL OF ADVANCED  
RESEARCH IN NATURAL AND  
APPLIED SCIENCES***



ISSN 2757-5195

**Journal of Advanced Research in Natural  
and Applied Sciences**

**e-ISSN: 2757-5195**

**Volume 8 / Issue 4**

**Sayı 8 / Cilt 4**

**2022-Aralık/December**

**Yayıncı/Publisher:** Çanakkale Onsekiz Mart Üniversitesi

**Rektör /Rector:** Prof. Dr. Sedat MURAT

**Dergi Editör Kurulu /Editorial Board**

Doç. Dr. Filiz UĞUR NİGİZ (Editor-in-Chief)

Dr. Öğretim Üyesi Ayça AYDOĞDU

Doç. Dr. Tuğba GÜNGÖR

Doç. Dr. Deniz ŞANLIYÜKSEL YÜCEL

Doç. Dr. Necati KAYA

Doç. Dr. Mehmet Ali YÜCEL

Doç. Dr. Özgür Turay KAYMAKÇI

Dr. Öğretim Üyesi Gülçin ÖZCAN ATEŞ

Dr. Öğretim Üyesi Şebnem ÖNDER

Dr. Öğretim Üyesi Doğukan TAŞER

**Dil Editörü**

Doç. Dr. Sercan Hamza BAĞLAMA

**Önsöz:**

Journal of Advanced Research in Natural and Applied Sciences Dergisi Fen, Mühendislik, Doğa ve Temel bilimler alanlarında daha önce yayımlanmamış orijinal araştırma makalesi, derleme yazılar, teknik not türünde araştırmaları yayınlayan ulusal ve uluslararası indekslerde taranan, hakemli ve bilimsel bir dergidir. Journal of Advanced Research in Natural and Applied Sciences Dergisi Mart, Haziran, Eylül, Aralık olmak üzere yılda dört sayı yayımlanacaktır. Tr-Dizin’de taranan Journal of Advanced Research in Natural and Applied Sciences Dergisi’nin 8.cilt 4.sayısında 21 adet araştırma makalesi yayına kabul edilmiştir.

	TÜBİTAK TR DİZİN tarafından taranmaktadır. Indexed by TR-DİZİN Database.
	TÜBİTAK-ULAKBİM DergiPark Akademik tarafından yayımlanmaktadır. Published by TÜBİTAK-ULAKBİM Turkish Journal Park Academic Database.
	CROSSREF® veri tabanı tarafından taranmakta ve makaleler DOI numarası ile yayımlanmaktadır. Indexed by CROSSREF® Database and articles are published with DOI number.
	Google Scholar'da ve SOBIAD'da taranmaktadır. Indexed by Google Scholar and SOBIAD Database.

### İletişim Adresi / Publisher Address

Çanakkale Onsekiz Mart Üniversitesi Lisansüstü Eğitim Enstitüsü  
Terzioğlu Yerleşkesi Çanakkale (Sağlık Hizmetleri Meslek Yüksekokulu Binası)

**Tel:** 0286 218 05 23

**Belgegeçer / Fax:** 0286 218 05 24

**E-posta / E-mail:** [jarnas.journal@gmail.com](mailto:jarnas.journal@gmail.com)

### Dergi Web Sayfası / Journal Home Page:

<http://jarna.dergi.comu.edu.tr/>

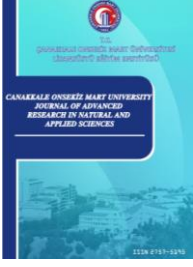
<https://dergipark.org.tr/tr/pub/jarnas>





**CONTENTS / İÇİNDEKİLER**  
**(2022, 8:4)**

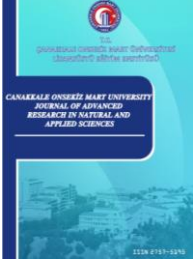
No	Articles & Authors / Makaleler & Yazarlar	Pages / Sayfa No
1	Improving The Physical Stability Of Virgin Olive Oil Mayonnaise Melis COSKUN, Sinem ARGUN, Emrah KIRTIL* Research/Araştırma	543 - 554
2	STEAM Dijital Oyun Platformunda Bulunan Eğitici İçerikli Dijital Oyunların Elektrik-Elektronik Mühendisliği Öğretim Müfredatına Entegrasyonu İçin Öneriler Şehmus FİDAN*, Ömer Ali KARAMAN, Abdullah YILDIRMAZ Research/Araştırma	555 - 568
3	Enhancing the Process of AES: A Lightweight Cryptography Algorithm AES for Ad-hoc Environments Mustafa ALHANDHAL, Alharith A. ABDULLAH, Oğuz ATA*, Çağatay AYDİN Research/Araştırma	569 - 582
4	The Effect of Nitrogen and Phosphorus Limitations at Different Salt Ratios on Growth and Biochemical Composition of Tetraselmis suecica (Chlorodendrophyceae) Cananur SİSALAN PİHAVA, Leyla USLU* Research/Araştırma	583 - 599
5	Comparative analysis and manufacturing of airfoil structures suitable for use at low speeds Satılmış ÜRGÜN, Mert GÖKDEMİR*, Sinan FİDAN Research/Araştırma	600 - 613
6	Deniz Ulaştırma İşletme Mühendisliği Bölümlerindeki Hiyerarşik Yapının Öğrenciler Üzerindeki Psikolojik Etkilerinin SPSS ile Kapsamlı Analizi Devran YAZIR*, Sefa YAY Research/Araştırma	614 - 623
7	An Integrated Risk Management Framework for Global Supply Chains Mualla Gonca AVCI* Research/Araştırma	624 - 640
8	Culturable Bacterial Communities Related to Different Larval Stages of Sanys irrosea (Guenee, 1852) (Lepidoptera: Noctuoidea) Ali SEVİM*, Elif SEVİM Research/Araştırma	641 - 650



Çanakkale Onsekiz Mart University Journal of Advanced Research in Natural and Applied Sciences

Aralık (December) 2022 / Cilt (Volume) 8 / Sayı (Issue) 4 / e-ISSN 2757-5195

9	Üretim Sektöründe Sürdürülebilirlik için Sosyal Yaşam Döngüsü Değerlendirmesi: Çimento Üretimi Örneği Büşra CİCİ, Beyhan PEKEY, Simge ÇANKAYA* Research/Araştırma	651 - 661
10	Makine Öğrenmesi Yöntemleri ile Türkiye’de Covid-19’a İlişkin Günlük Vaka, Ağır Hasta, Vefat ve İyileşen Sayısı Tahmini Figen ÖZEN* Research/Araştırma	662 - 676
11	Group-Based Authentication Methods in The OneM2M Ecosystem İbrahim Uğur ABA*, Erhan TAŞKIN Research/Araştırma	677 - 694
12	Validation of Colchicine Assay Method for Therapeutic Drug Monitoring in Human Plasma Fadime CANBOLAT* Research/Araştırma	695 - 702
13	Evaluation of Consumers' Aspects on Organic Farming Products by Regions Başak AYDIN*, Murat DOĞU, Ayten AŞKIN KILINÇ, Sunay DEMİR, Bülent TARIM, Duygu AKTÜRK, Filiz PEZİKOĞLU, Volkan BURUCU, Mustafa ASLAN Research/Araştırma	703 - 721
14	Metalik-Benek Dokulu Sanatsal Seramik Sırların Geliştirilmesi: Yüzey Aşınma Özelliklerinin İncelenmesi Nihan ERCİOĞLU AKDOĞAN*, Elif UBAY Research/Araştırma	722 - 735
15	Sentiment Analysis from Face Expressions Based on Image Processing Using Deep Learning Methods Orhan Emre AKSOY, Selda GÜNEY* Research/Araştırma	736 - 752
16	A Methodology for Clustering Items with Seasonal and Non-seasonal Demand Patterns for Inventory Management Burak KANDEMİR* Research/Araştırma	753 - 761



Çanakkale Onsekiz Mart University Journal of Advanced Research in Natural and Applied Sciences

Aralık (December) 2022 / Cilt (Volume) 8 / Sayı (Issue) 4 / e-ISSN 2757-5195

17	Fretting behavior of piston ring-cylinder liner components of a diesel engine running on TiO <sub>2</sub> nanolubricant Ali Can YILMAZ* Research/Araştırma	762 - 776
18	Kocavşar Deresi (Balıkesir) Fitoplankton Ekolojisi Kemal ÇELİK* Research/Araştırma	777 - 784
19	Effect of Growth Medium on Dopa and Dopamine Production Using <i>Citrobacter freundii</i> (NRRL B-2643) Meltem ÇAKMAK, Veyis SELEN, Dursun ÖZER, Fikret KARATAŞ*, Sinan SAYDAM Research/Araştırma	785 - 795
20	The Changes in Biochemical Compositions of Five Different Macroalgae and Seagrass ( <i>Halophila stipulacea</i> (Forsskal) Ascherson 1867) Collected from Iskenderun Bay Mehmet NAZ*, Selin SAYIN, Zafer ÇETİN, Eyüp İlker SAYGILI, Ergün TAŞKIN, Oktay SÖYLER Research/Araştırma	796 - 804
21	Yer Radarı (GPR) Uygulaması ile Kısmi Yıkılmış Bir Köprünün Sağlık Durumunun Belirlenmesi Gökhan KILIÇ* Research/Araştırma	805 - 819



# Improving the Physical Stability of Virgin Olive Oil Mayonnaise

Melis Coskun<sup>1</sup>, Sinem Argun<sup>1</sup>, Emrah Kirtil<sup>1,\*</sup>

<sup>1</sup>Food Engineering Department, Engineering Faculty, Yeditepe University, Istanbul, Türkiye

## Article History

Received: 03.04.2022

Accepted: 01.06.2022

Published: 15.12.2022

## Research Article

**Abstract** – Mayonnaise is a popular solid like sauce obtained typically from the ingredients; vegetable oil, vinegar, egg yolk, and salt. For mayonnaise production, vegetable oils with low costs are preferred. Extra virgin olive oil (EVOO), despite its high cost, is unique in that it has some very exceptional nutritional and sensorial properties and positive health promoting effects. However, EVOO mayonnaises pose some challenges in preparation and particularly in maintaining their stability for elevated periods. This study explored some options that could extend the shelf life of mayonnaise prepared from EVOO. For this purpose, two different stabilizer sodium alginate and gellan gum at two different concentrations (0.1% and 0.2%) were added to mayonnaise formulations, additionally ultrasound was applied at two different powers (40% and 70%) for 2 min. Rheological characterization revealed that all mayonnaise samples displayed a pseudoplastic behaviour which is desirable in condiments like mayonnaise. Particle size measurements revealed that oil particle diameters ranged between 2.1-25.5 µm. Real time and accelerated emulsion stability measurement were in line with each other. According to these, sodium alginate resulted in mayonnaise with the highest physical stability. Real time emulsion stability measurements revealed that all samples except control maintained their physical stability up to 20 days after preparation.


**Keywords** – Emulsion stabilization, EVOO, mayonnaise, olive oil, sodium alginate


## 1. Introduction


Mayonnaise is a popular solid like sauce obtained typically from the ingredients; vegetable oil, vinegar, egg yolk, and salt. The sensorial properties of this condiment is very much affected by the mouth feel of the product as well as taste. Thus, properties like appearance, structure, creaminess, and rheological properties are exceptionally important for mayonnaise. For condiments like mayonnaise, customer satisfaction is shaped by these parameters that make up the texture of the final product along with the product's physical stability (Giacintucci et al., 2016).

From a colloidal standpoint, mayonnaise is an emulsion, and like all emulsions, it is thermodynamically unstable. It is a low-pH oil-in-water emulsion characterized by high oil content, varying between 65 to 85% based on the formulation. The high oil content makes it particularly hard to maintain stability with the major component, oil being the dispersed phase and the minor component, water being the continuous phase. The final texture and stability of the emulsion are modified by the distribution of the oil phase, the overall size of oil droplets, and the interaction between different components in the formulation. The micro-sized oil particles are stabilized by a layer of egg phospholipids present in egg yolk. These small surface-active molecules position themselves spontaneously at the interface and prevent the droplets from coalescence (Kiosseoglou & Sherman, 1983; Langton et al., 1999).

As the type of oil, mayonnaise formulations typically contain worldwide spread vegetable oils with low cost. Most used oils for this purpose are rapeseed, corn, soybean, sunflower, and canola oil. Olive oil, with its higher

<sup>1</sup>  melis.coskun@std.yeditepe.edu.tr

<sup>2</sup>  sinem.argun@yeditepe.edu.tr

<sup>3</sup>  emrah.kirtil@yeditepe.edu.tr\*

\* Corresponding Author

cost is not particularly preferred for mayonnaise preparation. However, extra virgin olive oil (EVOO) is unique in that it has some very exceptional nutritional and sensorial properties and positive health-promoting effects. EVOO makes up a very crucial part of dietary lipids acquired from olive tree crops especially in Mediterranean region countries such as Greece, Italy, Turkey, and Spain (Bendini et al., 2007; Boskou et al., 2006; Zampounis, 2006).

However, despite being a very nutritious oil, the use of EVOO oils as an ingredient in complex crafted foods is quite rare. This has a few different reasons. One of them is the high cost of this oil with respect to other vegetable oils, and the other reason is its unique sensorial properties. The consumers from Mediterranean regions where olive oil consumption is high are more familiar with the taste of olive oil, and mayonnaise and other sauces from olive oil could be a preference for many individuals in these regions not only because of its health benefit but also for its sensorial attributes (Bendini et al., 2007; Zampounis, 2006).

Nevertheless, replacing another vegetable oil with olive oil in complicated formulated systems like a low stability food emulsion such as mayonnaise could introduce many problems. The high dispersion degree could pose a problem in maintaining the physical stability of the product throughout its whole shelf life. The intrinsic features of an emulsion, like the main ingredients, define the colloidal attributes like the kinetic and thermodynamic stability. The existence of some components that can either negatively or positively affect emulsion stability by changing the composition of the bulk phase and especially the interface (Freer et al., 2004; Kontogiorgos, 2019).

Olive oil, particularly extra virgin olive oil, contains bioactive molecules that also have a surface affinity. These bioactive molecules are of diverse nature, but a major portion of these is made up of phenolic compounds that show powerful antioxidant activity (Bendini et al., 2007; Giacintucci et al., 2016). Recently, researchers have focused on exploring the emulsification properties of emulsions prepared with EVOO and investigating the role of surface-active compounds in it like phospholipids, free fatty acids, and phenolics. The results of these studies indicated that olive oil is unique in that the abundance of these surface-active endogenous amphiphilic molecules greatly differentiates the dynamics of emulsions prepared by it. This was related to the difference in the composition of the olive oil-water interfaces compared to other vegetable oils (C. D. Di Mattia et al., 2009; Carla D. Di Mattia et al., 2011).

To the best of our knowledge, there currently are very few studies to investigate the effect of polyphenols on the structure of real food emulsions such as mayonnaise, presumably owing to the sophistication of their formulation that could restrict the interpretation of the role of these surface-active bioactive compounds that are very low in concentration. The objective of this work was to explore the physical and structural attributes of mayonnaise prepared by extra virgin olive oils (EVOO) and go one step further than previous research on the subject; this study also aims to come up with ways to improve the physical stability of virgin olive oil mayonnaise. Mayonnaise samples were produced by using a single recipe, only differentiating in the type and amount of hydrocolloids (incorporated as a stabilizer). For this purpose, guar gum and sodium alginate was used. In addition to a standardized homogenization procedure, some samples were further homogenized via ultrasonication. Produced mayonnaise samples were then characterized by physical stability, droplet size distribution, and rheological properties.

## **2. Materials and Methods**

### **2.1. Materials**

Eggs (Jumbo, Large, Keskinöglü, Turkey), apple cider vinegar (Gurme Elma Sirkesi, Kemal Kükrer, Turkey), salt (İyotlu tuz, Billur Tuz, Turkey), extra virgin olive oil (Ege Soğuk Lezzetler Naturel Sızma Zeytinyağı, Komili, Turkey) was purchased from a local grocery store in İstanbul, Turkey. Gellan Gum (CP Kelco UK Ltd, UK), Sodium Alginate (FMC Biopolymer Ltd., UK) was purchased from Sigma Aldrich.

### **2.2. Methods**

#### **2.2.1. Sample Preparation**

Mayonnaises were prepared following a recipe studied in Giacintucci et al. (2016). Mayonnaise ingredients were used in the relative amounts of; oil (500 g), eggs (120 g), vinegar (30 g), salt (1 g). To this mixture,

depending on formulation, either 0.1 and 0.2% of gellan gum or sodium alginate were added. Mayonnaises were prepared with a two-step procedure. Initially, egg yolk, vinegar, salt, and gum were mixed with a kitchen-type mixer. Then to this mixture, oil is added slowly by vigorous mixing with a lab-style high-speed homogenizer (Ultraturrax, WiseTis HG-15D, Wertheim, Germany) at 5000 rpm for 10 min. For ultrasound applied samples, the mayonnaise was later subjected to an ultrasound treatment (UW 2200, Bandelin, Sonopuls, Berlin) at either 40% or 70% max power for 2 minutes. Samples treated with ultrasound at 70% of the instrument's maximum power did not provide stable emulsions and thus were excluded from some of the measurements.

### 2.2.2. Experimental Design

The experimental design is given in Table 1.

Table 1  
Experimental Design

Formulation	Control	G0.1	G0.2	S0.1	S0.2	US70	US40
Olive oil	+	+	+	+	+	+	+
Vinegar	+	+	+	+	+	+	+
Eggs	+	+	+	+	+	+	+
Salt	+	+	+	+	+	+	+
Ultrasound Treatment	-	-	-	-	-	+	+
Gum		0.1 % w/v Gellan Gum	0.2 % w/v Gellan Gum	0.1 % w/v Sodium Alginate	0.2 % w/v Sodium Alginate		

### 2.2.3. Real-time emulsion Stability

Real-time emulsion studies were conducted by monitoring of the physical stability of emulsions by taking pictures of the samples. Mayonnaises, after preparation, were placed into cylindrical sealed tubes, and these samples were put to rest at either 25°C or 40 °C. Photos were taken every 2-3 days over the course of 40 days.

### 2.2.4. Accelerated Emulsion Stability

Accelerated Emulsion Stability measurements were performed to mimic real-time emulsion stability results. Since we had limited time to observe the emulsions, it might not be possible to see the destabilization of some of the metastable mayonnaise formulations. For this, following preparation, mayonnaises were centrifuged (Sartorius, Sigma 1-14, Germany) at 6000 rpm for 20 min at 25 °C. In case of a visible phase separation, the upper layer was identified as the oil portion, and the lower layer was identified as the serum layer. Percent creaming index (%CI) values were calculated by measuring the height of each layer and taking the ratio as shown in the following equation;

$$\%CI = \frac{H_C}{H_T} \times 100 \quad (2.1)$$

where  $H_C$  is the height of the cream layer and  $H_T$  is the total height.

### 2.2.5. Rheological Characterization

To characterize the flow behaviour and viscoelastic properties of mayonnaises, shear rate ramp and amplitude and frequency sweep tests were conducted. For the measurements, a cone-and-plate (40 mm diameter and 4° cone angle, 0.1425 mm gap) dynamic rheometer (Malvern, Kinexus Pro Rheometer, UK) was

employed. Shear rate ramp measurements give shear stress values for changing shear rate values. For this purpose shear rate was changed between  $0.1 \text{ s}^{-1}$  to  $100 \text{ s}^{-1}$ , and shear stress values were recorded for 20 sampling points for a total measurement time of 2 min. The results were found to be suitable to be defined with a power-law model;

$$\tau = K\gamma^n \quad (2.2)$$

where  $\tau$  (Pa) is shear stress,  $K$  ( $\text{Pa} \cdot \text{s}^n$ ) is the consistency index,  $\gamma$  ( $\text{s}^{-1}$ ) is shear rate,  $n$  is flow behavior index.

### 2.2.6. Particle Size Measurement

Light diffraction method was utilized for the measurement of the sizes of oil droplets. For this, a particle size analyzer (Mastersizer 3000, Malvern, UK) was employed. The reported droplet sizes are volume-moment mean diameter, calculated from the following equation;

$$d_{43} = \frac{\sum n_i d_i^4}{\sum n_i d_i^3} \quad (2.3)$$

where  $n_i$  is the number of particles in emulsion with diameter  $d_i$ . For olive oil droplets, a refractive index of 1.46 and absorption of 0.01, and for water, a refractive index of 1.33 was used (Kirtil & Oztop, 2016). To prevent potential multi-scattering effects, emulsions were diluted approximately  $10^{-4}$  to  $10^{-7}$  of their initial concentration. Particle size measurements were conducted within 24 h of sample preparation.

### 2.2.7. Statistical Analysis

All measurements were carried out in at least three replicates. Statistical analysis software Minitab (Version 16, State College, PA, USA) was used for the analysis of variance (ANOVA) and Tukey's multiple comparison tests. Differences were considered significant for  $p \leq 0.05$ .

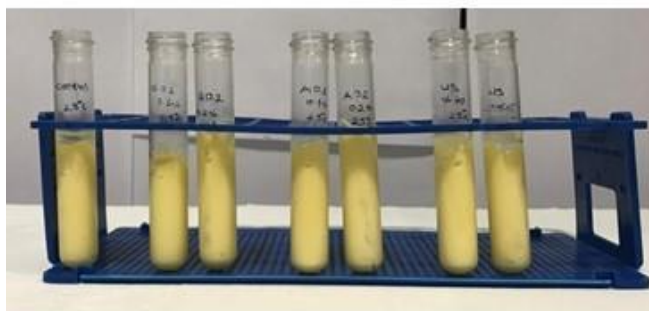
## 3. Results and Discussion

### 3.1. Real-time Emulsion Stability

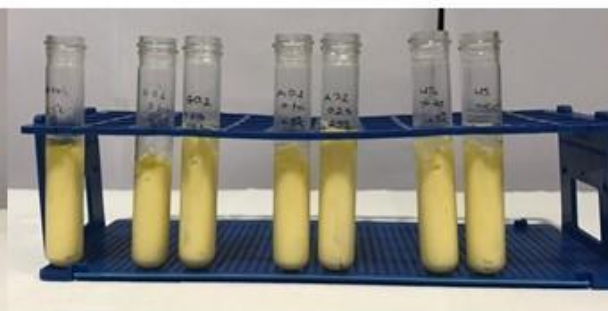
Results of real-time emulsion stability can be seen in Figure 1 and Figure 2. As evident from the figures, emulsions kept at  $40 \text{ }^\circ\text{C}$  were much quicker to destabilize than emulsions kept at  $25 \text{ }^\circ\text{C}$ . It was possible to see the first signs of creaming 5 days after preparation for  $40 \text{ }^\circ\text{C}$  samples, whereas  $25 \text{ }^\circ\text{C}$  samples were relatively stable up until the 25 day mark. Temperature increases the rate of molecular movement by increasing the kinetic energy of the molecules. Viscosity is also known to be negatively correlated with temperature.



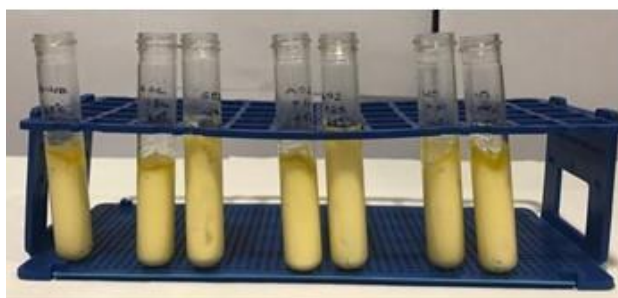
**Day 1**



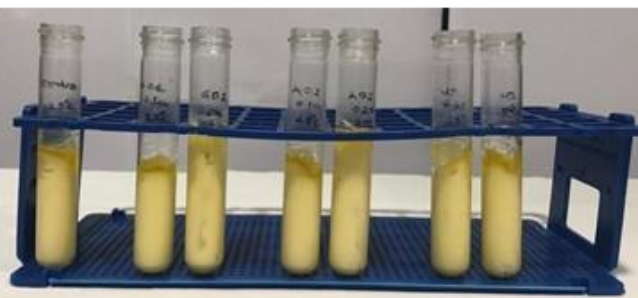
**Day 5**



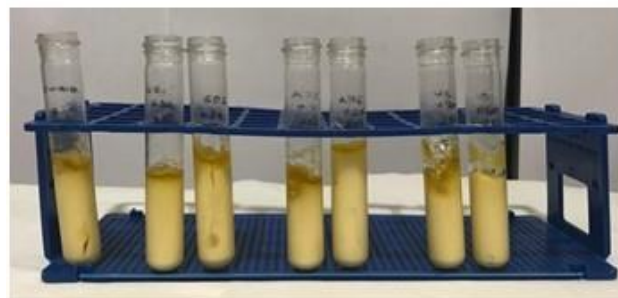
**Day 10**



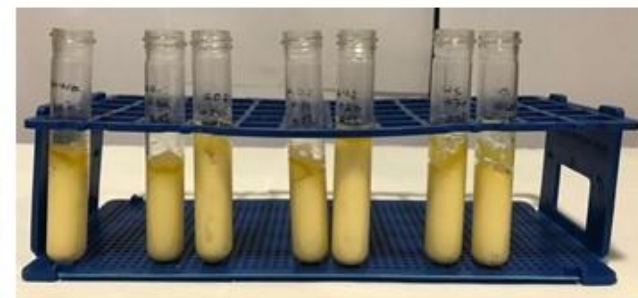
**Day 15**



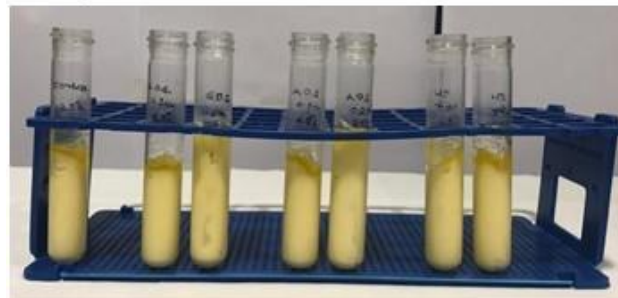
**Day 20**



**Day 25**



**Day 30**



**Day 35**

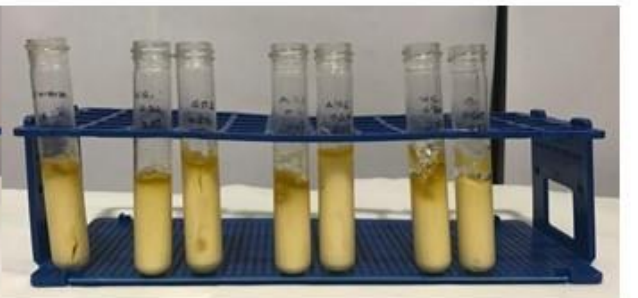


Figure 1. Real time emulsion stability measurement results at 25 °C

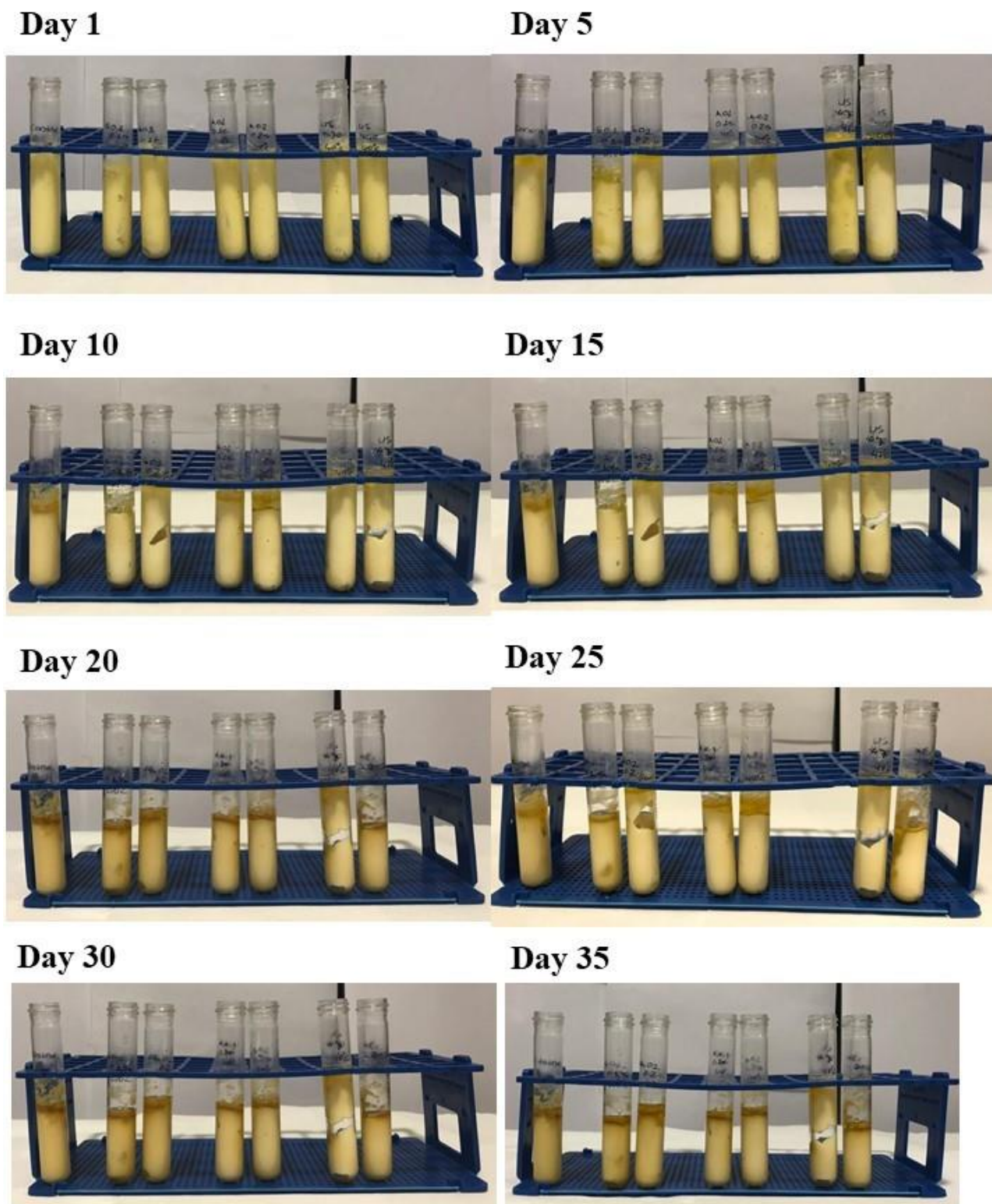


Figure 2. Real-time emulsion stability measurement results at 40 °C

The increased molecular mobility coupled with the decreasing viscosity accelerates the rate of movement of the oil droplets. Mayonnaises are a kinetically stable system; hence they are stabilized by retardation of particle movement and collisions. However, oil particles are always under the effect of gravitational and buoyancy forces, and despite being slow they always try to move against gravity and form a cream layer at the top (Berg, 2010; Kirtil et al., 2022; Kontogiorgos, 2019). This movement is expectedly much faster at 40 °C. At 25 °C, mayonnaises were mostly stable for the first 20 days. After 20 days, all samples showed signs of phase separation. The control sample phase-separated before the others and had a final cream layer thicker than the

other samples. This is in line with our expectation that extra virgin olive oil mayonnaises destabilize quickly and have a shorter shelf life than other plant oil-based mayonnaises. All other samples destabilized at similar rates and showed similar sizes of cream layers. At 40 °C, the control sample was again the first to destabilize at around 5 days after preparation. This is followed by the other samples, all of which showed signs of phase separation at varying degrees at the end of 35 days.

### 3.2. Accelerated Emulsion Stability

Creaming index (%CI) results indicate the extent of destabilization that the mayonnaise sample went through by the vigorous centrifugal force. If there was a phase separation, it was easy to recognize it. Some of the olive oil separates itself from the rest of the emulsion and forms a clear layer on top. %CI data can be seen in Table 2. The photos of samples taken after accelerated emulsion experiments are given in Figure 3.

Table 2

Creaming index (%CI) results gathered from accelerated emulsion stability experiments

Samples	CI %
Control	7.61±0.68 <sup>d</sup>
G0.1	5.88±0.71 <sup>d</sup>
G0.2	17.9±1.83 <sup>c</sup>
S0.1	0
S0.2	0
US40	38.6±1.11 <sup>b</sup>
US70	54.3±0.98 <sup>a</sup>

Means within the same column, followed by the different letters are significantly different ( $p < 0.05$ ).

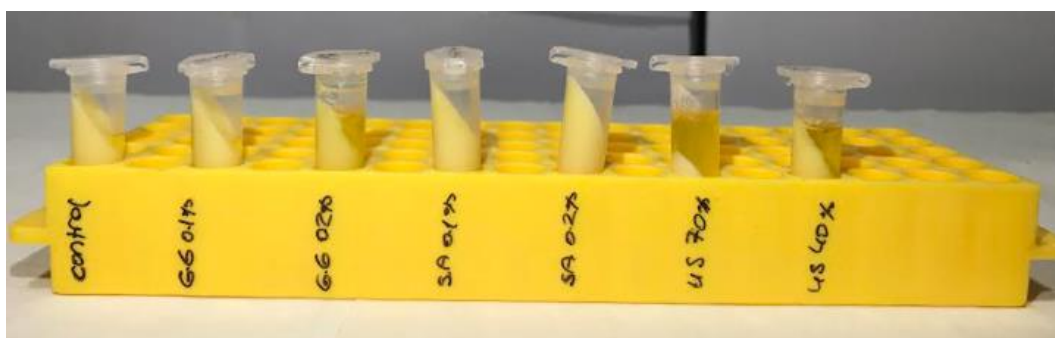


Figure 3. Results of accelerated emulsion measurements

As evident from both the photos and the %CI data, samples prepared with sodium alginate showed no phase separation. These were the only samples that didn't show any phase separation. Mayonnaises prepared with sodium alginate were found to be the most stable samples. Sodium alginate is a hydrocolloid with a high molecular weight and is commercially used as a stabilizer in many food products (Rosell et al., 2001; Vélez-Eraza et al., 2020; Yang et al., 2012). Alginate increased the viscosity of the continuous phase thereby retarded particle collisions and upward movement of particles under the effect of buoyancy force (Berg, 2010; Kontogiorgos, 2019). The accelerated emulsion studies show that alginate at both concentrations (0.1 and 0.2%) was a successful emulsion stabilizer for extra virgin olive oil mayonnaise. However, other methods were not as effective. Gellan gum was not successful in preventing phase separation. At %0.1 concentration gellan gum sample's %CI was not significantly different ( $p > 0.05$ ) than control samples. Interestingly when the amount of gellan gum increased to 0.2%, this introduced a further instability to emulsions. This could be related to the complex interactions between gellan gum and other mayonnaise ingredients and requires further analysis. Ultrasound samples showed the highest %CI values. As US power increased, %CI values also increased (up to 54.3%).

Ultrasound application was not suitable for this type of emulsion. We had observed this even right after US treatment, as there were visible signs of instability on the samples. It is a known phenomenon that if, during emulsification, samples are subjected to a homogenization method for too long after sample formation, this



could break the emulsion (Berg, 2010; Dickinson, 2009). Ultrasound homogenizes emulsions by sending sound waves that can help disperse oil particles by separating large particles into smaller ones. However, if it is over-applied to an already homogenized emulsion, it can act inversely and can cause the droplets to flocculate and even merge (Dickinson, 1998, 2008). Ultrasound most likely caused the particles to merge and increase in size, which greatly accelerated the rates of creaming, and this is observed as higher %CI values. The 70% US sample was visibly unstable. Thus, it was removed from some of the analyses.

### 3.3. Rheological Characterization

4 shows the change of shear viscosities (Pa.s) with shear stress ( $s^{-1}$ ) for all samples, including US70. As seen from the figure, shear viscosities decrease with increasing shear rate. This behavior is characteristic of pseudoplastic materials. The hydrocolloids that cause this behavior in such fluids, during flow, align themselves with the direction of flow and ease the movement of other molecules over one another. With increasing shear, this alignment is even more and more complete; thus, molecular mobility increases, which decreases viscosity (Dickinson, 2011; Vogt et al., 2015).

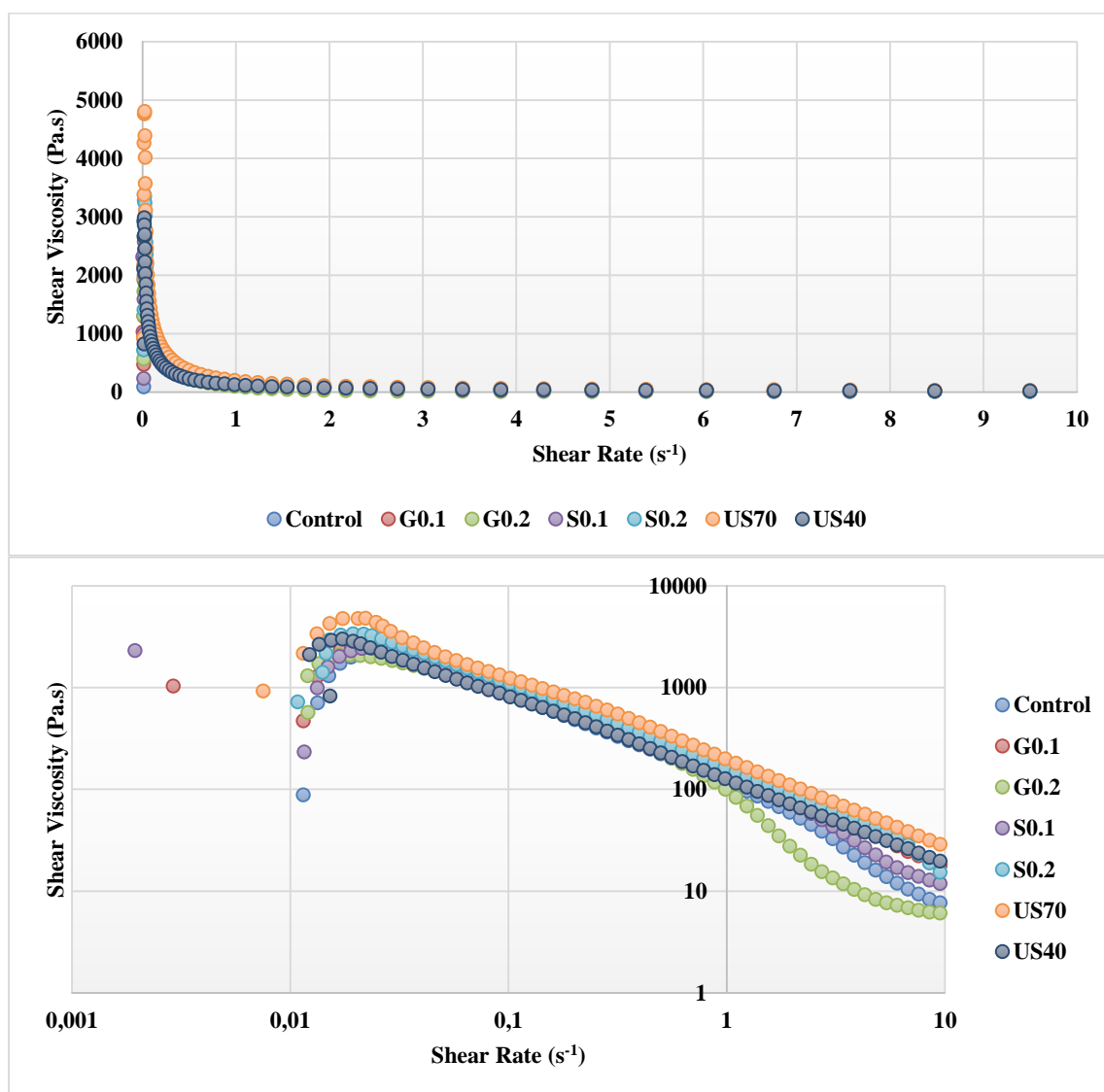


Figure 4. Change of shear viscosity with shear stress for mayonnaise samples

Shear-thinning behavior is especially essential and desirable in sauces because these condiments have to stay solid like at rest but should act more fluid-like under stress, such as during pumping or consumption (Marcotte et al., 2001). With the addition of sodium alginate and gellan gum, the shear-thinning behavior is not restricted, which is a positive result. The strong negative correlation between shear rate and viscosities was linear on a

logarithmic scale. Hence, a power model fit was found to be suitable for fitting the data. This assumption was confirmed with correlation coefficients of  $R^2 > 0.90$  for power-law fitting of shear rate ramp experiment results.

Table 0

Power-law fitting results of shear rate and shear stress data

	<b>K</b>	<b>n</b>	<b>R<sup>2</sup></b>
<b>Control</b>	91.7±2.7 <sup>e</sup>	0.813±0.07 <sup>b</sup>	0,90
<b>G0.1</b>	138.6±3.3 <sup>c</sup>	0.709±0.08 <sup>d</sup>	0,90
<b>G0.2</b>	66.7±2.1 <sup>f</sup>	0.957±0.05 <sup>a</sup>	0,93
<b>S0.1</b>	118.6±4.1 <sup>de</sup>	0.752±0.03 <sup>c</sup>	0,90
<b>S0.2</b>	154.1±4.7 <sup>b</sup>	0.768±0.07 <sup>c</sup>	0,95
<b>US40</b>	124.5±5.3 <sup>cd</sup>	0.768±0.09 <sup>c</sup>	0,98
<b>US70</b>	193.5±4.8 <sup>a</sup>	0.754±0.03 <sup>c</sup>	0,95

Means within the same column, followed by the different letters, are significantly different ( $p < 0.05$ ).

Table shows the coefficients of the power-law equation for each of the mayonnaise samples. US70 displayed the highest consistency index values. All mayonnaises displayed a shear-thinning behaviour as identified with  $n$  values lower than 1. Consistency index values are correlated with the system's resistance against the flow (Chakraborty et al., 2018; Krstonošić et al., 2020; Nikzade et al., 2012). A higher consistency index ( $K$ ) indicates a more viscous structure. Considering this, US70 mayonnaise was thicker in terms of texture than others. This could be related to an abundance of oil particles of large particle sizes. It is known that in emulsions, as the particle size of the dispersed phase increases, the solution becomes more viscous (Berg, 2010; Wilde et al., 2004). The addition of sodium alginate seemed to result in higher  $K$  values than control, and  $K$  also increased with an increase in the concentration of the gum, whereas shear thinning behavior was not affected by gum concentration. One interesting finding worth noting here is that G0.2 had lower  $K$  and higher  $n$  values than G0.1. Increasing gellan gum concentration seemed to decrease mayonnaise consistency. This is in line with the accelerated emulsion stability results that showed higher %CI values in G0.2 compared to G0.1.

### 3.4. Particle Size Measurements

Table 4

Volume-moment mean diameter results of mayonnaise samples

<b>Samples</b>	<b>d<sub>43</sub> (µm)</b>
<b>Control</b>	8.21±1.1 <sup>b</sup>
<b>S0.1</b>	6.39±1.2 <sup>b</sup>
<b>S0.2</b>	25.42±2.1 <sup>a</sup>
<b>G0.1</b>	2.11±0.4 <sup>c</sup>
<b>G0.2</b>	2.59±0.2 <sup>c</sup>
<b>US40</b>	3.76±0.3 <sup>c</sup>

Means within the same column, followed by the different letters are significantly different ( $p < 0.05$ ).

The size of oil particles ranged between 2.1-25.5 µm. Other studies have also reported oil particle diameters of similar sizes (Gavahian et al., 2018; Hong et al., 2018; Laca et al., 2010; Langton et al., 1999). The sample was subjected to a minimum of 1000-fold dilution procedure before measurements, and US70 sample phase-separated during this pretreatment. Hence it was not measured. Another sample that also phase-separated was S0.2. Still, we measured the particle size of this sample as, unlike US70, it was a very stable sample before dilution. However, the much larger particle sizes of this sample compared to others shows that this result could be unreliable and will be disregarded during interpretation. There was no statistical difference between the particle size results of control mayonnaise and S0.1 mayonnaise ( $p < 0.05$ ). This shows that alginate addition did not significantly favor emulsion formation. However, the particle sizes of G0.1, G0.2, and US40 ranged between 2.11-3.76 and were lower than the other samples. The presence of gellan gum might have provided a more efficient energy distribution in the continuous phase that resulted in better dispersion of oil particles in

the aqueous phase. US40, on the other hand, despite being easily destabilized with accelerated stabilization measurements, actually displayed smaller droplet sizes than the control. This shows that US40 was mildly successful in decreasing the overall mean droplet diameter. The destabilization introduced by US could be associated with a more heterogeneous particle distribution after US application. Other studies have reported similar results where over-application of US might increase particle size heterogeneity (Dickinson et al., 1994; Kaltsa et al., 2013; Kentish & Feng, 2014; Li et al., 2019). Thus, despite an overall decrease in mean droplet sizes, the presence of large particles could have accelerated Ostwald ripening (which is one of the primary mechanisms of destabilization for mayonnaise), resulting in an overall unstable emulsion.

#### 4. Conclusion

Mayonnaise is a popular solid-like sauce typically obtained from the ingredients; vegetable oil, vinegar, egg yolk, and salt. As the type of oil, mayonnaise formulations typically contain worldwide spread vegetable oils with low cost. Olive oil, with its higher cost, is not particularly preferred for mayonnaise preparation. However, extra virgin olive oil (EVOO) is unique in that it has some very exceptional nutritional and sensorial properties and positive health-promoting effects. EVOO is rich in surface-active compounds such as phenolics and free fatty acids. These surface-active molecules can prevent the adsorption of lecithin on oil droplets and result in emulsion destabilization. That is why it is particularly challenging to prepare mayonnaise from EVOO that has a long shelf life. This study explored some options that could extend the shelf life of mayonnaise prepared from EVOO.

Rheological characterization revealed that all mayonnaise samples displayed a pseudoplastic behaviour which is desirable in condiments like mayonnaise. None of the additives substantially changed the flow behaviour or increased the sauce thickness to levels that would be unacceptable for the consumer. Particle size measurements revealed that oil particle diameters ranged between 2,1-25.5  $\mu\text{m}$ . The addition of gellan gum favored the dispersion of oil by decreasing particle sizes down to around 2  $\mu\text{m}$  from 8.5  $\mu\text{m}$  of control. Real-time and accelerated emulsion stability measurements were in line with each other. According to these, sodium alginate resulted in mayonnaise with the highest physical stability. These emulsions did not show any phase separation upon centrifugation at 6000 rpm for 20 min. Real-time emulsion stability measurements revealed that all samples except control maintained their physical stability up to 20 days after preparation.

In conclusion, with this study, it was possible to observe the physical stability of mayonnaise formulations prepared with different stabilizers and the incorporation of ultrasound as an additional homogenization method for mayonnaise formation. Especially with sodium alginate addition, improvements in the physical stability of EVOO mayonnaise could be achieved.

#### Author Contributions

Melis Coskun: Methodology, Investigation, Writing - Original Draft

Sinem Argun: Methodology, Investigation

Emrah Kirtil: Conceptualization, Data curation, Formal analysis, Writing - Original Draft, Writing - Review & Editing, Supervision, Validation

#### Conflicts of Interest

The authors declare no conflict of interest.

#### References

- Bendini, A., Cerretani, L., Carrasco-Pancorbo, A., Gómez-Caravaca, A. M., Segura-Carretero, A., Fernández-Gutiérrez, A., & Lercker, G. (2007). Phenolic molecules in virgin olive oils: A survey of their sensory properties, health effects, antioxidant activity and analytical methods. An overview of the last decade. *Molecules*, 12(8), 1679–1719. doi:<https://doi.org/10.3390/12081679>
- Berg, J. C. (2010). *An Introduction to Interfaces & Colloids: The Bridge to Nanoscience*. World Scientific. <https://books.google.com/books?id=x-XZBJngdM4C>
- Boskou, D., Blekas, G., & Tsimidou, M. (2006). Olive Oil Composition. *Olive Oil: Chemistry and Technology: Second Edition*, 41–72. doi:<https://doi.org/10.1016/B978-1-893997-88-2.50008-0>
- Chakraborty, S. K., Kotwaliwale, N., & Navale, S. A. (2018). Rheological characterization of gluten free millet

- flour dough. *Journal of Food Measurement and Characterization*, 12(2), 1195–1202. doi:<https://doi.org/10.1007/S11694-018-9733-4>
- Di Mattia, C. D., Sacchetti, G., Mastrocola, D., & Pittia, P. (2009). Effect of phenolic antioxidants on the dispersion state and chemical stability of olive oil O/W emulsions. *Food Research International*, 42(8), 1163–1170. doi:<https://doi.org/10.1016/j.foodres.2009.05.017>
- Di Mattia, Carla D., Sacchetti, G., & Pittia, P. (2011). Interfacial Behavior and Antioxidant Efficiency of Olive Phenolic Compounds in O/W Olive oil Emulsions as Affected by Surface Active Agent Type. *Food Biophysics*, 6(2), 295–302. doi:<https://doi.org/10.1007/S11483-010-9195-7>
- Dickinson, E. (1998). Proteins at interfaces and in emulsions. Stability, rheology and interactions. *Journal of the Chemical Society - Faraday Transactions*, 94(12), 1657–1669. doi:<https://doi.org/10.1039/a801167b>
- Dickinson, E. (2008). Interfacial structure and stability of food emulsions as affected by protein-polysaccharide interactions. *Soft Matter*, 4(5), 932–942. doi:<https://doi.org/10.1039/b718319d>
- Dickinson, E. (2009). Hydrocolloids as emulsifiers and emulsion stabilizers. *Food Hydrocolloids*, 23(6), 1473–1482. doi:<https://doi.org/10.1016/j.foodhyd.2008.08.005>
- Dickinson, E. (2011). Mixed biopolymers at interfaces: Competitive adsorption and multilayer structures. *Food Hydrocolloids*, 25(8), 1966–1983. doi:<https://doi.org/10.1016/j.foodhyd.2010.12.001>
- Dickinson, E., Ma, J., & Povey, M. J. W. (1994). Creaming of concentrated oil-in-water emulsions containing xanthan. *Topics in Catalysis*, 8(5), 481–497. doi:[https://doi.org/10.1016/S0268-005X\(09\)80090-8](https://doi.org/10.1016/S0268-005X(09)80090-8)
- Freer, E. M., Yim, K. S., Fuller, G. G., & Radke, C. J. (2004). Interfacial Rheology of Globular and Flexible Proteins at the Hexadecane/Water Interface: Comparison of Shear and Dilatation Deformation. *The Journal of Physical Chemistry B*, 108(12), 3835–3844. doi:<https://doi.org/10.1021/jp037236k>
- Gavahian, M., Chen, Y. M., Mousavi Khaneghah, A., Barba, F. J., & Yang, B. B. (2018). In-pack sonication technique for edible emulsions: Understanding the impact of acacia gum and lecithin emulsifiers and ultrasound homogenization on salad dressing emulsions stability. *Food Hydrocolloids*, 83, 79–87. doi:<https://doi.org/10.1016/j.foodhyd.2018.04.039>
- Giacintucci, V., Di Mattia, C., Sacchetti, G., Neri, L., & Pittia, P. (2016). Role of olive oil phenolics in physical properties and stability of mayonnaise-like emulsions. *Food Chemistry*, 213, 369–377. doi:<https://doi.org/10.1016/J.FOODCHEM.2016.06.095>
- Hong, L. F., Cheng, L. H., Gan, C. Y., Lee, C. Y., & Peh, K. K. (2018). Evaluation of starch propionate as emulsion stabiliser in comparison with octenylsuccinate starch. *LWT - Food Science and Technology*, 91, 526–531. doi:<https://doi.org/10.1016/j.lwt.2018.01.076>
- Kaltsa, O., Michon, C., Yanniotis, S., & Mandala, I. (2013). Ultrasonic energy input influence on the production of sub-micron o/w emulsions containing whey protein and common stabilizers. *Ultrasonics Sonochemistry*, 20(3), 881–891. doi:<https://doi.org/10.1016/j.ultsonch.2012.11.011>
- Kentish, S., & Feng, H. (2014). Applications of Power Ultrasound in Food Processing. *Annual Review of Food Science and Technology*, 5(1), 263–284. <https://doi.org/10.1146/annurev-food-030212-182537>
- Kiosseoglou, V. D., & Sherman, P. (1983). Influence of Egg Yolk Lipoproteins on the Rheology and Stability of O/W Emulsions and Mayonnaise 1. Viscoelasticity of Groundnut Oil-in-Water Emulsions and Mayonnaise. *Journal of Texture Studies*, 14(4), 397–417. doi:<https://doi.org/10.1111/j.1745-4603.1983.tb00358.x>
- Kirtil, E., & Oztop, M. H. M. H. (2016). Characterization of emulsion stabilization properties of quince seed extract as a new source of hydrocolloid. *Food Research International*, 85, 84–94. doi:<https://doi.org/10.1016/j.foodres.2016.04.019>
- Kirtil, E., Svitova, T., Radke, C. J., Oztop, M. H., & Sahin, S. (2022). Investigation of surface properties of quince seed extract as a novel polymeric surfactant. *Food Hydrocolloids*, 123(September 2021), 107185. doi:<https://doi.org/10.1016/j.foodhyd.2021.107185>
- Kontogiorgos, V. (2019). Polysaccharides at fluid interfaces of food systems. *Advances in Colloid and Interface Science*, 270, 28–37. doi:<https://doi.org/10.1016/j.cis.2019.05.008>
- Krstonošić, V. S., Kalić, M. D., Dapčević-Hadnadev, T. R., Lončarević, I. S., & Hadnadev, M. S. (2020). Physico-chemical characterization of protein stabilized oil-in-water emulsions. *Colloids and Surfaces A: Physicochemical and Engineering Aspects*, 602, 125045. doi:<https://doi.org/10.1016/j.colsurfa.2020.125045>
- Laca, A., Sáenz, M. C., Paredes, B., & Díaz, M. (2010). Rheological properties, stability and sensory evaluation of low-cholesterol mayonnaises prepared using egg yolk granules as emulsifying agent. *Journal of Food Engineering*, 97(2), 243–252. doi:<https://doi.org/10.1016/j.jfoodeng.2009.10.017>



- Langton, M., Jordansson, E., Altskär, A., Sørensen, C., & Hermansson, A. M. (1999). Microstructure and image analysis of mayonnaises. *Food Hydrocolloids*, *13*(2), 113–125. doi:[https://doi.org/10.1016/S0268-005X\(98\)00076-9](https://doi.org/10.1016/S0268-005X(98)00076-9)
- Li, Y., Xiang, D., Wang, B., & Gong, X. (2019). Oil-in-water emulsions stabilized by ultrasonic degraded polysaccharide complex. *Molecules*, *24*(6). doi:<https://doi.org/10.3390/molecules24061097>
- Marcotte, M., Hoshahili, A. R. T., & Ramaswamy, H. S. (2001). Rheological properties of selected hydrocolloids as a function of concentration and temperature. *Food Research International*, *34*(8), 695–703. doi:[https://doi.org/10.1016/S0963-9969\(01\)00091-6](https://doi.org/10.1016/S0963-9969(01)00091-6)
- Nikzade, V., Tehrani, M. M., & Saadatmand-Tarzjan, M. (2012). Optimization of low-cholesterol-low-fat mayonnaise formulation: Effect of using soy milk and some stabilizer by a mixture design approach. *Food Hydrocolloids*, *28*(2), 344–352. doi:<https://doi.org/10.1016/j.foodhyd.2011.12.023>
- Rosell, C. M., Rojas, J. A., & Benedito de Barber, C. (2001). Influence of hydrocolloids on dough rheology and bread quality. *Food Hydrocolloids*, *15*(1), 75–81. doi:[https://doi.org/10.1016/S0268-005X\(00\)00054-0](https://doi.org/10.1016/S0268-005X(00)00054-0)
- Vélez-Erazo, E. M., Bosqui, K., Rabelo, R. S., Kurozawa, L. E., & Hubinger, M. D. (2020). High internal phase emulsions (HIPE) using pea protein and different polysaccharides as stabilizers. *Food Hydrocolloids*, *105*, 105775. doi:<https://doi.org/10.1016/j.foodhyd.2020.105775>
- Vogt, S. J., Smith, J. R., Seymour, J. D., Carr, A. J., Golding, M. D., & Codd, S. L. (2015). Assessment of the changes in the structure and component mobility of Mozzarella and Cheddar cheese during heating. *Journal of Food Engineering*, *150*, 35–43. doi:<https://doi.org/10.1016/j.jfoodeng.2014.10.026>
- Wilde, P., Mackie, A., Husband, F., Gunning, P., & Morris, V. (2004). Proteins and emulsifiers at liquid interfaces. *Advances in Colloid and Interface Science*. doi:<https://doi.org/10.1016/j.cis.2003.10.011>
- Yang, J. S., Jiang, B., He, W., & Xia, Y. M. (2012). Hydrophobically modified alginate for emulsion of oil in water. *Carbohydrate Polymers*, *87*(2), 1503–1506. doi:<https://doi.org/10.1016/j.carbpol.2011.09.046>
- Zampounis, V. (2006). Olive Oil in the World Market. *Olive Oil: Chemistry and Technology: Second Edition*, 21–39. doi:<https://doi.org/10.1016/B978-1-893997-88-2.50007-9>



## STEAM Dijital Oyun Platformunda Bulunan Eğitici İçerikli Dijital Oyunların Elektrik-Elektronik Mühendisliği Öğretim Müfredatına Entegrasyonu İçin Öneriler

Şehmus Fidan<sup>1\*</sup>, Ömer Ali Karaman<sup>2</sup>, Abdullah Yıldırım<sup>3</sup>

<sup>1,2</sup>Elektronik ve Otomasyon Bölümü, Teknik Bilimler Meslek Yüksekokulu, Batman Üniversitesi, Batman, Türkiye

<sup>3</sup>Pazarlama ve Reklamcılık Bölümü, Sosyal Bilimler Meslek Yüksekokulu, Batman Üniversitesi, Batman, Türkiye

### Makale Tarihi

Gönderim: 28.01.2022

Kabul: 06.01.2022

Yayın: 15.12.2022

### Araştırma Makalesi

**Öz-** Bu makalede eğitici içeriğe sahip dijital video oyunları ele alınmış olup Elektrik-Elektronik Mühendisliğine entegrasyonu için STEM (Bilim, Teknoloji, Mühendislik, Matematik) felsefesi içinde bazı değerlendirilmeler yapılmıştır. STEM kavramına daha sonradan sanat kavramı da eklenerek genişletilen STEAM (Bilim, Teknoloji, Mühendislik, Sanat, Matematik) felsefesiyle aynı ismi taşıyan STEAM dijital oyun dağıtım platformu 30.000'i geçen sayıda oyun sunmaktadır. Bu platform ayrıca en fazla eğitici içerikli dijital video oyunu sunan platform olarak dikkat çekmektedir. Eğitici içeriğe sahip dijital oyunlar öğrencilerin derse daha fazla katılımını sağlayarak motivasyonun artırılmasına, alan yeterliliğine ve takım çalışmasına olumlu katkı sunmaktadır. Eğitici içerikli oyunların belirlenmesi için STEAM oyun platformu içinde 100'den fazla oyun değerlendirmeye alınmış ve eğitici içeriğe sahip olanlar belirlenmiştir. Örnek olarak seçilen bazı oyunlar için incelemeler sunulduktan sonra en fazla indirilme ve olumlu yorum alma durumlarına göre değerlendirilmiştir. Literatürde seçilen eğitici içerikli oyunlar için bir sınıflandırma yapılmadığı için öneride bulunulmuştur. Yapılan incelemeler sonunda belirtilen oyunların Elektrik-Elektronik Mühendisliği bölümü müfredatına eklenebileceği ancak dikkate alınması gereken eksiklikler bulunduğu belirtilmiş ve öneriler sunulmuştur.

**Anahtar Kelimeler** – Bilim teknolojisi, elektrik-elektronik mühendisliği eğitimi, mühendislik matematik (stem), STEAM platformu

## Recommendations for the Integration of Educational Digital Games on the STEAM Digital Game Platform into the Electrical and Electronics Engineering Teaching Curriculum

<sup>1,2</sup>Department of Electronics and Automation, Vocational School of Technical Sciences, Batman University, Batman, Türkiye

<sup>3</sup>Department of Marketing and Advertising, Vocational School of Social Sciences, Batman University, Batman, Türkiye

### Article History

Received: 28.01.2022

Accepted: 06.01.2022

Published: 15.12.2022

### Research Article

**Abstract-** In this article, digital video games with educational content are discussed and some evaluations have been made within the STEM (Science, Technology, Engineering, Mathematics) philosophy for their integration into Electrical-Electronics engineering. STEAM, digital game distribution platform, which bears the same name with the STEAM (Science, Technology, Engineering, Arts, Mathematics) philosophy, which was expanded by adding the concept of art to the STEM concept, offers more than 30,000 games. This platform also stands out as the platform that offers the most educational digital video games. Digital video games with educational content make a positive contribution to increasing motivation, field proficiency and teamwork by enabling students to participate more in the lesson. In order to determine the educational games, more than 100 games were evaluated in STEAM game distribution platform and those with educational content were determined. After the selected-game reviews were presented, it was evaluated according to the most downloaded and positive comments. Since the absence of classification for the digital video games with educational content, a recommendation are proposed. As a result, it has been stated that the mentioned games can be added to the curriculum of the Department of Electrical and Electronics Engineering, but there are deficiencies that need to be taken into account and suggestions are presented.

**Keywords** – Electrical-electronics, engineering education, math (STEM), science technology engineering, STEAM platform

<sup>1</sup> sehmus.fidan@batman.edu.tr

<sup>2</sup> omerali.karaman@batman.edu.tr

<sup>3</sup> abdullah.yildirim@batman.edu.tr

\* Sorumlu yazar

## 1. Giriş

Küresel anlamda eğitimin daha iyi hale getirilmesi için problem çözme becerileri yüksek, eleştirel düşünebilen, ekip çalışmasına yatkın insan gücünün yetiştirilmesinde modern eğitim yaklaşımlarına ihtiyaç duyulmaktadır (Çınar ve Çiftçi, 2016). Bu noktada ‘STEM (Bilim, Teknoloji, Mühendislik, Matematik) Yaklaşımı’ yenilikçi bir eğitim yöntemi olarak 2000’li yıllardan beri üzerinde çokça çalışılan konulardan birisi olarak dikkat çekmektedir. Art, yani sanatın da eklenmesiyle birlikte STEAM olarak genişletilen bu yeni eğitim felsefesini benimseyen eğitimciler, STEAM’in öğrencilerin yaratıcılığını ve düşünme becerilerini geliştirdiğini belirtmişlerdir (Perignat ve Katz-Buonincontro, 2019).

Oyunlar ile ilgili geleneksel, dijital ve sanal oyunlar olmak üzere çeşitli sınıflandırma yöntemleri bulunmaktadır. Geleneksel oyunlar kovalamaca, saklambaç gibi fiziksel çabaya dayanırken dijital oyunlar bilgisayar, oyun konsolları ve mobil cihazlarda oynanabilen oyunlar olarak tanımlanmaktadır (Sağlam ve Topsümer, 2019). Son yıllarda teknolojik imkânların gelişmesiyle birlikte sanal gerçeklik oyunları da yaygınlık kazanmaya başlamıştır (Bayram ve Çalışkan, 2019). Özellikle evren ötesi kavramı (metaverse) hayatımıza girdikçe sanal gerçeklik oyunları ve bu oyunlara yönelik olarak verilen eğitimlerin hayatımızda çok daha fazla yer kaplayacağı düşünülmektedir (Collins, 2008). Oyunları eğitsel, dijital eğitsel ve ciddi oyunlar olarak amaçlarına göre de sınıflandırmak mümkündür. Eğitsel ve dijital eğitsel oyunlarda, oyunun öncelikli amacı öğretim olmamakla birlikte, ciddi oyunlarda oyun, belirli bir öğretim hedefine yönelik olarak tasarlanır veya kullanılır (Sezgin, 2016).

Oyun sayılarının ve oyunu oynayanların sayısındaki artışa paralel olarak bu alanda hizmet sağlayan dijital video oyun dağıtım sektörü de hızla büyümektedir. Dijital oyun dağıtım platformları içinde Steam, Epic Games, Humble Store, Itch.io, GOG (Green Man Gaming), Uplay, Fanatical vd. gibi çok fazla sayıda olmasa da oyun dağıtım platformları bulunmaktadır. Bu platformlar arasında sektör lideri olan STEAM oyun dağıtım platformu, 2003 yılından beri hızla büyümektedir. Steam üzerinden alınan verilerde günlük eş zamanlı oyuncu sayısı 25 milyon rakamını geçerek bu alanda rekor kırmıştır. Hatta bu platformda aynı gün içinde 7,4 milyon oyuncuya online oyun hizmeti sunulmuştur (Valve, 2001a). Online olarak büyük bir insan topluluğunu bir araya getirip bütün türlerde oyunları, oyun severlere sunan dijital oyun dağıtım platformları yorumlar, yorum istatistikleri, oyun türü vb. birçok özelliği bünyesinde barındırmakta ve kullanıcılara sunmaktadır. STEAM dağıtım platformu üzerinde farklı türde oyunlar kullanıcılara sunulmaktadır.

STEAM dijital oyun dağıtım platformu, en fazla eğitici içeriğe sahip oyun sunan platform olma özelliğine sahiptir. Bu platformda yapılan araştırmalarda STEAM felsefesi çerçevesinde sınıf içinde öğrencilere oynatılabilecek çeşitli oyunlar tespit edilmiştir. Seçilen oyunlar öğrencilerin yaratıcılık becerilerini, konu ile ilgili bilgilerini ve farkındalıklarını arttıracak niteliktedir. Bu oyunlardan bazıları Car Mechanic Simulator, Hacknet, TIS-100, Infinifactory, Shenzen-IO, EXAPUNKS, Opus-Magnum, While True Learn, Factorio, LogicBots, Hardware Engineers, 911 Operator, Hardware Engineering, Silicon Zeroes, Project Hospital, PC Building Simulator, Kerbal Space Program, Poly Bridge, Diesel Brothers, comet 64, Rover Mechanic Simulator, Main Assembly vb. oyunlardır. Bu oyunlar incelendiğinde oldukça eğitici olmanın yanında STEAM felsefesine uygun bir şekilde ele alınabileceği belirlenmiştir. Bu sebeple alt bölümlerde örneği verilen oyunlardan bazılarının içeriğinden bahsedilmiştir.

Srinivasan ve arkadaşları, 13 lisans öğrencisine dijital elektronik temellerini öğretmek için kullanılan bir dijital 3B bulmaca oyununu oynatarak sonuçları açıkladılar. Katılımcılar video oyununun dijital elektronik kavramlarını öğrenmede geleneksel yöntemlerden daha etkili bir yol olduğuna ve ayrıca video oyunlarının genel olarak elektrik mühendisliği konularını öğretmek için iyi araçlar olduğuna inandıklarını bildirdiler (Srinivasan ve diğ., 2011). Oyunlar, iyi bir mühendis olmaya katkıda bulunabilecek kişisel özellikleri geliştirir. Oyun ve simülasyon ortamları, gerçek bağlamları kopyalayabildikleri için mükemmel öğrenme araçlarıdır. Oyun tabanlı öğrenme özellikle mühendisler için gerekli olan yeterlilikleri ve becerileri geliştirdiğini göstermektedir (Carvalho, 2012). Topallı ve Çağıtay, Bilgisayar Mühendisliği, Yazılım Mühendisliği ve Bilişim Sistemleri Mühendisliği öğrencileri üzerinde oyun temelli bir araştırma projesi gerçekleştirmişlerdir. Bu üç bölümde ortak ders olan bilgisayar programlamaya giriş dersi pilot ders olarak seçilmiş olup öğrencilerin bir kısmı klasik dersi alırken diğer kısmı oyun tabanlı zenginleştirilmiş bilgisayar programlamaya giriş dersini aldılar. Yapılan çalışmada oyun temelli projenin öğrencilerin dersi daha iyi anlamalarına vesile olduğu ortaya konmuştur (Topallı ve Çağıtay, 2018). Velaora ve Kakarountas, Elektrik-Elektronik ve Bilgisayar mühendisliği bölümlerinde verilen sayısal tasarım dersi için oyun temelli uzaktan eğitimin mümkün olduğu

bir çalışma önermişlerdir. Bu yeni öğrenme yaklaşımı öğrencilerin dikkatini çekmeyi başarmış olup daha odaklı çalışmalarını sağlamıştır. Öğrenciler tarafından iyi tasarlanmış bir model olarak kabul edilen bu yeni eğitim materyali öğrencilerin özgüvenini artırmıştır. Önerilen yöntemle öğrencilerin devrelerle sürekli tasarım yapması sağlanarak dersi daha iyi anlamaları sağlandı (Velaora ve Kakarountas, 2021).

Ülkemiz mühendislik fakültelerinde, özellikle son dönemlerde açılan bölümlerde, öğretim kalitesindeki seviye farklılıkları, laboratuvar yetersizlikleri, malzeme eksikliği, ekipmanların güncel olmayışı vb. önemli sorunlar bulunmaktadır (EMO, 2020). Bununla birlikte pek çok öğrenci, ilgi çekici olarak algılamadıkları derslere güçlü bir şekilde katılım göstermemektedir. Öğrencilerin ilgisini çekmeye yardımcı olacak bir yöntem olarak dijital oyunların müfredat içine yerleştirilmesi genel olarak daha motive edici olabilir. Eğitsel oyunlar, öğrencilere öğrenmeyi teşvik etmek için anında geri bildirim sağlarken; bunun yanında motive ve teşvik edici bir ortam sağlayabilir (Bodnar vd., 2016). Bu bağlamda, eğitici içerikli dijital oyunların, Elektrik-Elektronik Mühendisliğinde bazı laboratuvar derslerine entegre edilmesinin, öğrenmenin artırılması ile birlikte daha nitelikli zaman geçirilmesini sağlayacağı düşünülmektedir (Marston ve Kowert, 2020).

Mühendislik fakültelerinde karşılaşılan problemler Elektrik-Elektronik Mühendisliği gibi yoğun laboratuvar uygulamaları yapan bölümlerde daha büyük sorunlara neden olmaktadır. Özellikle algoritmalar, programlama, dijital elektronik, programlanabilir lojik kontrolörler ve mikrodenetleyiciler derslerinde uygulama geliştirmeye başlamadan önce yoğun soyut düşünme, problemin iyi tanımlanması ve problem çözümünün sistematik olarak yapılması gerekmektedir. Bu süreçte laboratuvar eksikliği yanında öğretim elemanın gerçek hayat uygulamalarını aktarmasındaki deneyimsizliği, derslerin yoğun içeriğe sahip olması derslerin anlaşılmasında problemi daha büyütme ve nitelikli bir eğitimin oluşmasına engel olmaktadır.

Örnek verilecek olursa; laboratuvar eksiklikleri olan üniversite bölümlerinde dijital elektronik ve mikrodenetleyiciler dersleri çoğunlukla sadece kâğıt üzerinde çözüm yaparak geçiştirilmektedir. Bazen de öğretim elemanı yeterliyse bilgisayar kullanılarak benzetim uygulamaları yapılmaktadır. Bilgisayarda benzetim programlarının kullanılması durumunda aslında bir benzetim programı gibi niteliklere sahip ancak dijital oyunlarda bulunan ekstra özellikler ile birlikte bir öykü çerçevesinde sunulan Silicon Zeroes, Shenhzen-IO gibi dijital oyunlar bu benzetim programlarının yerini kolaylıkla alabilir. Böylelikle STEM felsefesi dâhilinde ele alınan eğitici içerikli dijital oyunlar ders içeriğine haftalık bir saatlik uygulama olarak eklenebilir ve eğitim süreci daha kalıcı, kaliteli hale getirilebilir. Elbette ki dijital oyunlar gerçek laboratuvar uygulamasının yerini alamayacaktır ancak soyut becerilerin geliştirilmesi ve ders içeriğinde sunulan bütün elemanların fonksiyonlarına ait özellikler çok kolay bir şekilde öğrenilebilir. Bu çalışmanın amacı, oyun dağıtım platformlarında sunulan bazı dijital video oyunların öğretim amaçlı kullanılabilmesi üzerinde durularak oyunların STEM felsefesine uygunluğunun değerlendirilmesi ve bu doğrultuda literatüre katkıda bulunmaktır.

## 2. Materyal ve Yöntem

### 2.1. Dijital Oyun Tabanlı Öğrenme Yaklaşımı

Son yıllarda STEAM ile ilgili araştırma yapan akademisyenler dijital teknolojilerin eğitim alanına daha fazla entegre edilmesi için çalışmalar yapmaktadır. Bunun yanında bugünün öğrencileri yaşamlarının her alanında bilgisayar, video oyunları, akıllı telefonlar ve diğer tüm dijital araçlarla kuşatılmış bir ortamla karşı karşıya kalmaktadır. Bu öğrencilerin klasik ve durağan eğitim yaklaşımları karşısında dikkat ve odaklanma problemleri yaşadıkları ifade edilmektedir. Bu olumsuzlukları ortadan kaldırmanın bir yolu öğrencilerin motivasyonlarını artıracak, eğitimi daha eğlenceli ve dikkat çekici hale getirecek öğrenme deneyimleri sağlamaktır (Prensky, 2001). Bu bağlamda oyun düşüncesini temel alan yaklaşımlar önemli görülmektedir.

İyi bir bilgisayar ya da video oyunu, insanların kendilerini yeni bir dünyada yeniden güncellemelerinin yanında eğlence ve öğrenme imkânlarına ulaşmaları bakımından önemli görülmektedir. Bu bağlamda oyun tabanlı öğrenme yaklaşımının güçlü bir öğrenme yaklaşımı olduğuna dikkat çekilebilir. Bu oyunların öğrenciyi öğrenmenin merkezi haline getirmesi bakımından STEAM felsefesine uygunluğu değerlendirilerek sistemin içerisine entegre edilmesi, öğrenmeyi daha eğlenceli ve katılımlı bir süreç haline getirebilir (Gee, 2003). Bu da öğrenme sürecinin daha kolay, ilginç ve etkili olmasına imkân sağlamaktadır.

Genel olarak oyunlar, anında geri bildirim vermesi, katılımcıların ilerlemelerini gözlemleyebilmesi ve onları oyun boyunca ilerlemeleri için ödüllerle motive etmede başarılıdır. Bu ödüller, gerçek fiziksel ödüller gibi somut olanlardan, zafer duygusu gibi soyut olana kadar değişebilir. Bu nedenle, oyunlarda ortak olan birçok yön, örneğin öğrenmeye yönelik deneme-yanılma yaklaşımı ve hızlı geri bildirim, doğrudan birçok öğrencinin

tercihlerine hitap eder ve bu özellikler onların öğrenme sürecine daha fazla ilgi duymalarını ve meşgul olmalarını sağlar. Bu şekilde ilgi duyma ve derse katılım, bugün birçok öğrencinin içeriğine ilgi duymayabileceği derslere katılımı artırarak mühendislik eğitimine katkı sağlayabileceği öngörülmektedir (Joiner vd., 2011; Morelock ve Matusovich, 2018).

Dijital oyun platformlarında oyunlar sınıflandırılırken genellikle bulmaca, platform, simülasyon, rol yapma vb. kavramlar kullanılmaktadır. Oyun incelemeleri içinde oyunların bu sınıflandırmalardan hangisi ya da hangilerine dâhil olduğu belirtilmiştir. Bunun yanında çalışmanın amacına da uygun olması açısından eğitim amaçlı bir sınıflandırma yapılmasının da önemli olduğu düşünülmektedir. Elektrik-Elektronik Mühendisliği bölümünde mikroişlemciler/mikrodenetleyiciler, sayısal/dijital elektronik, programlama vb. dersler, öğrenciler tarafından kavranması nispeten daha zor olmaktadır. Hatta öğrenciler tarafından bu soyut kavramlı dersler bazen hiç anlaşılammakta ve bu dersleri geçmek için genel olarak ezber yöntemi tercih edilmektedir. Uzun süren ders saatleri takip etmesi zor olmakla birlikte hızlı tüketim kültürüne alışmış Z kuşağı için takip etmesi daha zor olmaktadır. Ancak Z kuşağı nesli için dijital oyunlar hem eğlenceli hem de motive edicidir. Bu sebeple dijital oyun oynayarak ders anlatmak önemli bir fırsat olarak görülmelidir. Oyun platformlarında hâlihazırda sunulan bazı oyunlar eğlendirmenin ötesinde bu alanda çalışan ya da çalışacak olan kişilere soyut olan bazı kavramları algılamaları noktasında yardımcı olduğu çalışmalarla ortaya konulmuştur (Kuk vd., 2012). Dijital oyunların Elektrik-Elektronik Mühendisliği eğitiminde yardımcı yaklaşım olarak kullanılmasıyla ders müfredatlarındaki eşitsizlik, altyapı ve laboratuvar eksikliği gibi olumsuz etkenlerin minimum seviyelere indirilmesi noktasında alana katkıda bulunulacağı öngörülmektedir. Özellikle yeni açılan üniversitelerde laboratuvar noktasında ciddi altyapı eksikliği göze çarpmaktadır. Eski üniversitelerde dahi bazı laboratuvarlar tam değildir ya da laboratuvarlar güncel malzemelerle donatılmamıştır. Şayet laboratuvarlar eksiksiz ve güncel malzemelerden oluşsa bile dersin saati hem teorik hem de uygulama yapmaya yetmemektedir. Çoğu deney yapılamamaktadır. Bu anlamda ders saati dışında derslerle ilgili eğitsel dijital oyunlar, konunun anlaşılması ve bazı deneyler sonucunda ulaşılabilecek neticeyi kazandırabilir. Elektrik Elektronik ve Bilgisayar Mühendisliği bölümü öğrencileri için Mikroişlemciler ve CPU (Central Process Unit) tasarımı gibi konular soyut kalmakta bazen laboratuvar imkanları da yukarıda yazılan nedenlerden dolayı tam değerlendirilememektedir. Tam bu noktadan hareketle özellikle cep telefonu ile çok zaman geçiren ve oyun oynamaya meraklı Z kuşağı öğrencileri için dijital oyunlar derslerin anlaşılmasında yardımcı olabilir. Örneğin aşağıda detaylı açıklanan Silicon Zeroes oyununu kullanarak toplayıcılar, mandallar ve çoklayıcılar gibi çeşitli basit bileşenlerden karmaşık elektronikler oluşturulabiliyor. Söz konusu oyunda işin mantığını öğretmeye yönelik basit devrelerden başlayıp karmaşık devre oluşturmaya kadar çeşitli seviyeler bulunmaktadır. Bu durum bu çalışmada önerilen diğer oyunlar için de geçerlidir. Aşağıda Elektrik-Elektronik Mühendisliği alanında bu amaçla kullanılacak oyunlara yönelik bazı uygulamalar örnek olarak sunulacaktır.

## 2.2. Elektrik-Elektronik Mühendisliği Öğretim Müfredatında Kullanılacak Bazı Oyunların İncelenmesi

Yeni açılan üniversitelerde Elektrik-Elektronik Mühendisliği bölümlerinin laboratuvar imkânları nispeten kısıtlıdır. Teknik bilimlere odaklanan meslek yüksekokulları ise laboratuvar noktasında çok daha eksiktir. Bu eksiklikleri gidermek için derslerde çoğu zaman giriş seviyesinde benzetim uygulamaları yapılmaktadır. Ancak bazı durumlarda ders sadece teorik olarak verilmekte ve çok kısıtlı problemler çözümlenmenin ötesine geçilememektedir. Laboratuvar olanakları eksik olunca ağırlıklı olarak teorik işlenen derslerde öğrenciler motive olmakta zorlanmaktadır. Eğlendirici içeriğe sahip eğitici dijital oyunlar bu problemleri aşmak için kullanılabilir. Bu çalışma belirtilen problemleri aşmak için önerilebilecek oyunlara odaklanmaktadır.

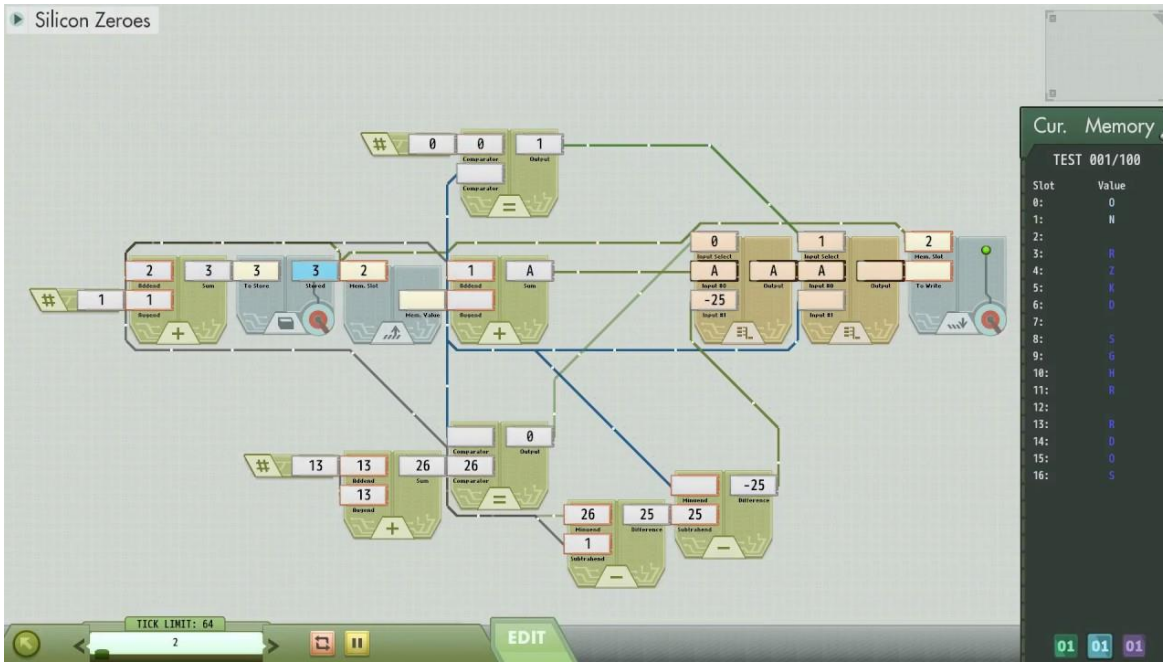
Bu öneri bütün mühendislik bölümlerinin müfredatları için yapılabileceği gibi Bilgisayar mühendisliği için de çok uygundur. Elektrik-Elektronik Mühendisliği müfredatındaki bazı dersler Bilgisayar mühendisliği müfredatında da okutulmaktadır. Bu makalede hem elektrik elektronik mühendisliği hem de bilgisayar mühendisliği bölümü öğrencileri için Silicon Zeroes, Shenhzen-IO ve benzeri oyunlar önerilmiş olup aşağıda detaylı incelenmiştir. Bu oyunlar vasıtasıyla hem CPU tasarım mantığı hem de Assembly yazılım dili öğrenilmiş olacaktır.

STEAM platformunda, STEAM felsefesi çerçevesinde değerlendirilebilecek ve Elektrik-Elektronik Mühendisliği eğitiminde yardımcı materyal olarak kullanılacak oyunlar bulunmaktadır. Ancak öncelikle bu oyunların belirlenmesi ve niteliğinin incelenmesi gerekmektedir. Oyunlar belirlenirken temel olarak Elektrik-Elektronik Mühendisliğinde bulunan bazı derslerin içeriğine yakınlığı göz önüne alınmıştır. Örneğin

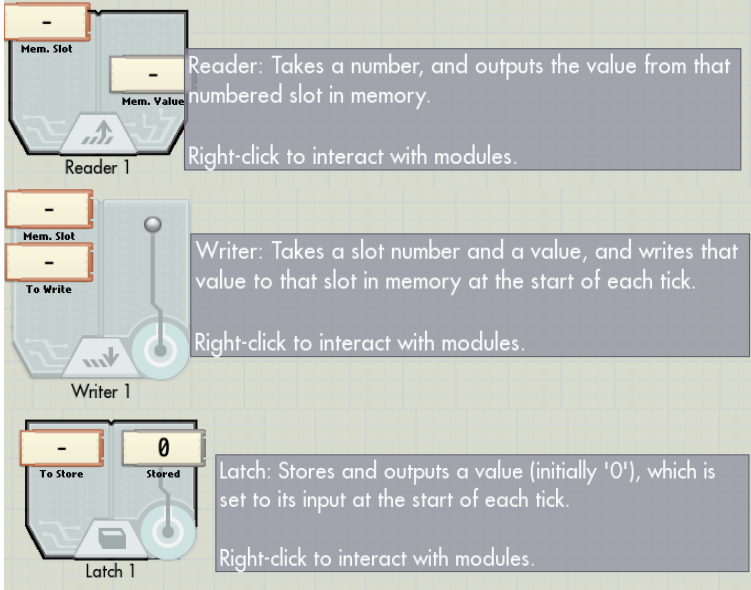
dijital elektronik dersinde ve (and), veya (or) gibi lojik kapılar en temel konulardır. Bu sebeple araştırılan oyunlar içinde lojik kapıların kullanıldığı Silicon Zeroes oyunu belirlenmiştir. Oyun belirlendikten sonra oyun ile ilişkili gerçek yorumlar incelenmiş ve derslere ek materyal olarak sunmak için gerçekten faydalı olup olmayacağı araştırılmıştır. Temel alınan bu yönetime uygun olarak belirlenen oyunların bir kısmı alt bölümlerde sunulmuştur.

### 2.2.1. Silicon Zeroes

Silicon Zeroes oyunu, sayısal elektronik dersi içeriğinde bulunan temel bileşenler, kapılar, toplayıcı vb. elemanları içeren karmaşık elektronik devreleri tasarlamayı amaçlayan bir oyundur. Oyun içeriği şu şekildedir. Kullanıcılar oyuna 60'lı yıllarda Silikon Vadi 'sinde bir start-up firması olarak başlamaktadır. Sonrasında müşterilerden gelen çeşitli projeler yapılarak oyunda ilerlenmektedir. Oyunun belli seviyelerinden sonra CPU tasarımı gibi çok daha karmaşık görevler yapılmaktadır. Eğitimde Elektrik-Elektronik veya bilgisayar ile alakalı bölümlerde bu oyun laboratuvar eksikliği olması durumunda ek bir ders materyali gösterilebilir veya tamamlanması gereken bir ödev olarak öğrencilere sunulabilir. Fikir vermesi açısından Silicon Zeroes oyun görünümü (Şekil 1)'de sunulmuştur. Bu şekil biraz incelenecek olursa sayısal elektronik dersinde temeli oluşturan lojik kapılar, kaydırma işlemleri, aritmetik işlem blokları, hafıza okuma/yazma bloğu vb. bulunmaktadır.



Şekil 1. Silicon Zeroes oyun görünümü



Reader: Belirlenen bir hafıza alanından okuma yapmayı sağlar.

Writer: Belirlenen bir hafıza alanına yazma yapmayı sağlar.

Latch Bloğu : Hafıza elemanı olarak kullanılan bir modüldür.

Şekil 2. Silicon Zeroes oyununa ilişkin bazı modüllerin tanıtımı

(Şekil 2)'de Silicon Zeroes oyununa ilişkin bazı modüller daha detaylı olarak sunulmuştur. Daha başka birçok modül içeren bu oyun incelendiğinde aslında bir senaryoya oturtulmuş sayısal elektronik uygulamalarının puzzle şeklinde sunulduğu görülmektedir.

Silicon Zeroes oyunu, Pleasing Fungus Games tarafından 29 Eylül 2016 yılında yayınlanmıştır. STEAM üzerinden alınan fiyatlar incelendiğinde 3 dolar civarı bir etikete sahip olan bu oyun 12+ yaş sınırlaması ile sunulmuştur. Oyun ile ilgili olarak yaklaşık olarak 185 adet yorum tespit edilmiş ve %95'inin olumlu olduğu görülmüştür. Olumsuz yorumlar ise çoğunlukla optimizasyon veya zorlukla ilgilidir. Eğitici içeriğe sahip olan bu oyun lise, ön lisans hatta lisans döneminde bile öğrencilere oynatılabilir. STEAM üzerinde yapılan yorumlara bakıldığında oyunun oldukça sevildiği ve eğitici bulunduğu değerlendirilmeleri dikkat çekmektedir. Ayrıca ilgili alanda profesyonel olmayan oyuncuların bile dijital tasarıma dönük birçok şey öğrendikleri ile ilgili geri dönüşler olmuştur. SpaceChem ve TIS-100 oyunlarının geliştiricisi Zach Barth, Silicon Zeroes oyunu için "CPU tasarımı hakkında hayal edebileceğim en iyi oyun" şeklinde yorum yapmıştır. (Steam, 2017a).

### 2.2.2. PC Building Simulator

E-posta üzerinden gelen siparişler doğrultusunda, ekran kartı yanan, güç kaynağı arızalanan, ana kartı sorunlu bilgisayarları tamir etme gibi görevleri yerine getirme üzerine geliştirilmiş bir oyundur. Oyunda gösterilen her bir ekipmanın lisanslı olması oyuncunun hem motivasyonunu hem de bilgisayar donanım piyasasında bulunan ekipmanlarla ilgili bilgisini oldukça arttırmaktadır. PC Building Simulator oyunu, Elektrik-Elektronik ve bilgisayar temelli bölümler için uygun olmasının ötesinde ilgisi olan birçok kişiye bilgi kazandırabilecek bir yapıya sahip olması tam olarak STEM oyun felsefesine uygunluğunu göstermektedir. (Şekil 3)'de STEAM üzerinden alınan PC Building Simülör oyununun çalışma ortamı görünümü verilmiştir.

29 Ocak 2019 yılında piyasaya sunulan PC Building Simülör oyunu, STEAM mağazası üzerinden alınan verilerde 24912 adet kullanıcı yorumunun %94'ü olumlu geri dönüş bildirmiştir. Satış rakamları bilinmese de yorumların genellikle olumlu olması ve oyun beğenme oranının yüksek olması, sunulan içeriğin sunum biçiminin sevildiği anlamına gelmektedir. Yorumlara bakıldığında ise oyunun eğitici olduğu birçok parçayı ve kavramı oyun üzerinden öğrenmenin mümkün olduğu anlaşılmaktadır (Steam, 2019a).





Şekil 3. PC Building Simülör oyununda çalışma ortamı görünümü

(Şekil 4)'te tasarlanmış bir PC'nin (Personal Computer) daha detaylı bir görünümü verilmiştir. Detaylara dikkat edilirse bir çalışma alanı, 3 boyutlu tasarlanmış PC kasası, fan vb. gibi özellikleri aslında bir PC tamir atölyesinin benzeri ortam mevcuttur. Oyun vasıtasıyla bilgisayar parçalarını montajlama, tamirat ve müşterilerden gelen sipariş üzerine istenilen teknik özellikte bir kasa tasarlama öğrenilmektedir. Oyunun ileri seviyelerinde işler biraz daha zorlaşmaktadır. Tasarlanan bilgisayar kasasının performansı oyun vasıtasıyla test edilebilmekte ve deneme yanılmayla birçok tecrübe kazanılmaktadır. Yaptıkça kişilerin tasarım performansı geliyor ve 3 boyutlu görünümüyle gerçek ortamı aratmayan bir ortam sunuyor. Özellikle laboratuvar eksikliğinin olduğu durumlar için çok iyi bir ortam sağladığı anlaşılmaktadır.

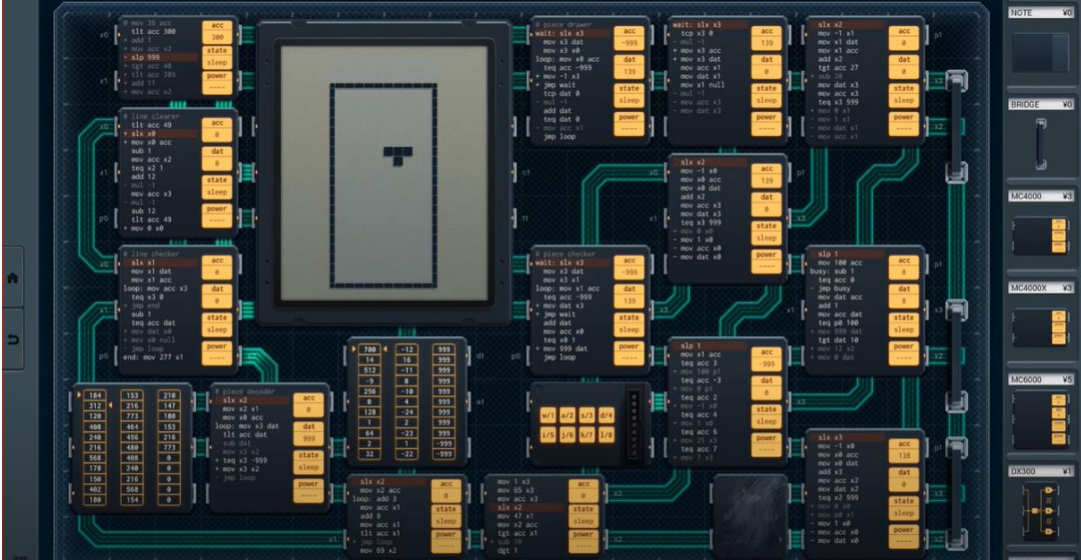


Şekil 4. PC Building Simülör oyununda tasarlanmış bir PC'nin görünümü

### 2.2.3. Shenhzen-IO

Shenhzen-IO oyununda mikrodenetleyiciler, bellek, mantık kapıları ve LCD (liquid-crystal display) ekranlar gibi farklı üreticilerin çeşitli bileşenlerini kullanarak devreler oluşturulabilmektedir. Oyunda her

komutun koşullu olarak yürütülebileceği kompakt ve güçlü bir Assembly dilinde kod yazılabilir. Assembly yazılım dili, Elektrik-Elektronik Mühendisliği ve bilgisayar mühendisliği öğrencileri tarafından zorlayıcı olarak belirtilen bir programlama dilidir. Shenhzen-IO oyunu sayesinde geleneksel öğretim yöntemleri yerine yenilikçi ve eğlendirici bir öğrenme yöntemi sunulmaktadır. Oyun ile ilgili yorumlarda biraz bilgi altyapısı gerektiği, her oyuncuya hitap etmediği, tasarım ve belge okumanın oldukça önemli olduğu belirtilmiştir (West, 2016). (Şekil 5)'de STEAM üzerinden alınan Shenhzen-IO oyununun genel görünümü verilmiştir. 17 Kasım 2016 yılında Zachtronix şirketi tarafından yayınlanan Shenhzen-IO oyunu hakkında STEAM dijital oyun platformu üzerinde 3109 adet inceleme belirlenmiştir ve oyun hakkında oldukça eğitici olduğu, derslerde tam olarak öğrenilemeyen bilgilerin öğrenilebileceği hakkında yorumlar yapılmıştır (West, 2016).

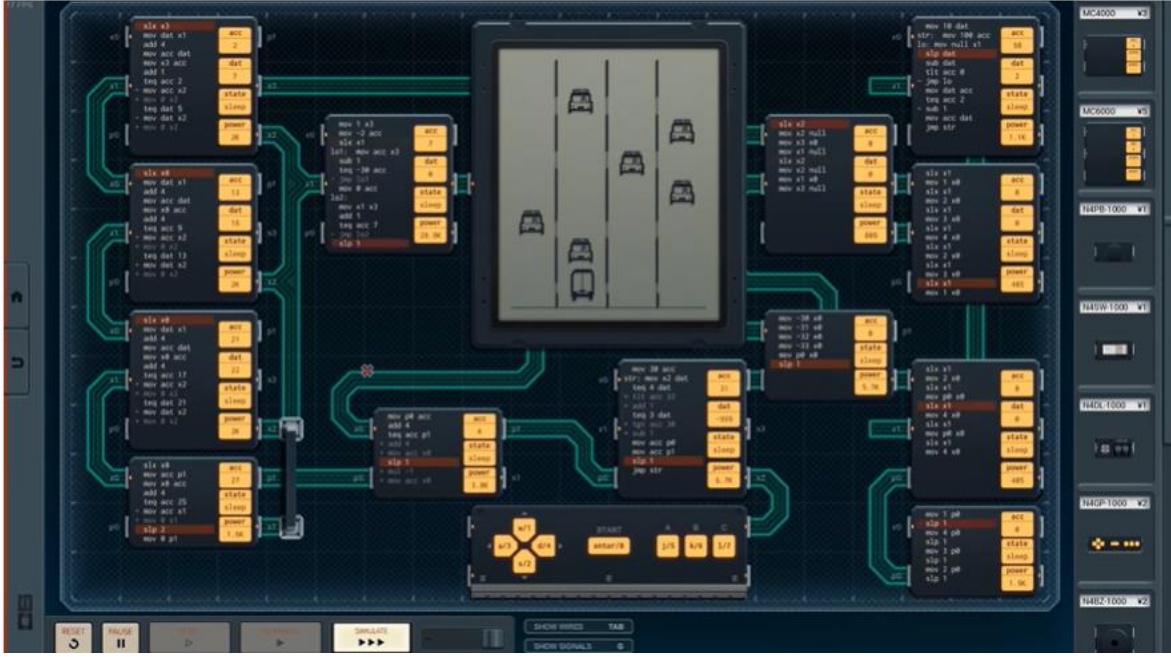


Şekil 5. Shenhzen-IO oyununun genel görünümü

(Şekil 5) klasik olarak bilinen Tetris oyununun Shenhzen-IO içinde tasarımı verilmiştir. Şekle bakıldığında farklı tetris şemalarının oyun vasıtasıyla tasarlanıp bu şemaların sağa, sola ve aşağı hareket etmesi ve bu sayede Assembly yazılım dilinin kavranması amaçlanmıştır. Görüldüğü üzere önerilen oyunların sadece eğlence amaçlı veya basit olmadığı ileri tasarımın mümkün olduğu anlaşılmaktadır. Hatta mikrodenetleyici/mikroişlemci konularını temel alan derslerin laboratuvarlarının tam olduğu durumlarda bile bu derece ileri bir tasarım yapmak oldukça zordur. Bu noktada böyle bir oyunun öğrenciye çok önemli bilgiler katacağı açıktır.

Şekil 6'da Shenhzen-IO oyunu ile Assembly yazılım dili ve mikrodenetleyiciler, bellek, mantık kapıları ve LCD ekranlar kullanılarak trafik oyunu tasarlanmıştır. Bu oyunda 4 şeritli bir yol var. Oyunda minibüs'ün karşıdan gelen arabalara çarpmamak için sürekli şerit değiştirmesi amaçlanmıştır. Öğrenciler, Shenhzen-IO oyunu ile bu şekilde çeşitli oyunlar tasarlayarak hem Assembly yazılım diline hâkim olma hem de mikrodenetleyici ve mantık kapılarını sanal ortamda uygulamalı olarak öğrenebilme imkanına sahip olacaklardır.

Shenhzen-IO oyunu, Elektrik-Elektronik Mühendisliği ve bilgisayar mühendisliği öğrencilerini mesleki olarak geliştirmek için önemli bir oyundur.



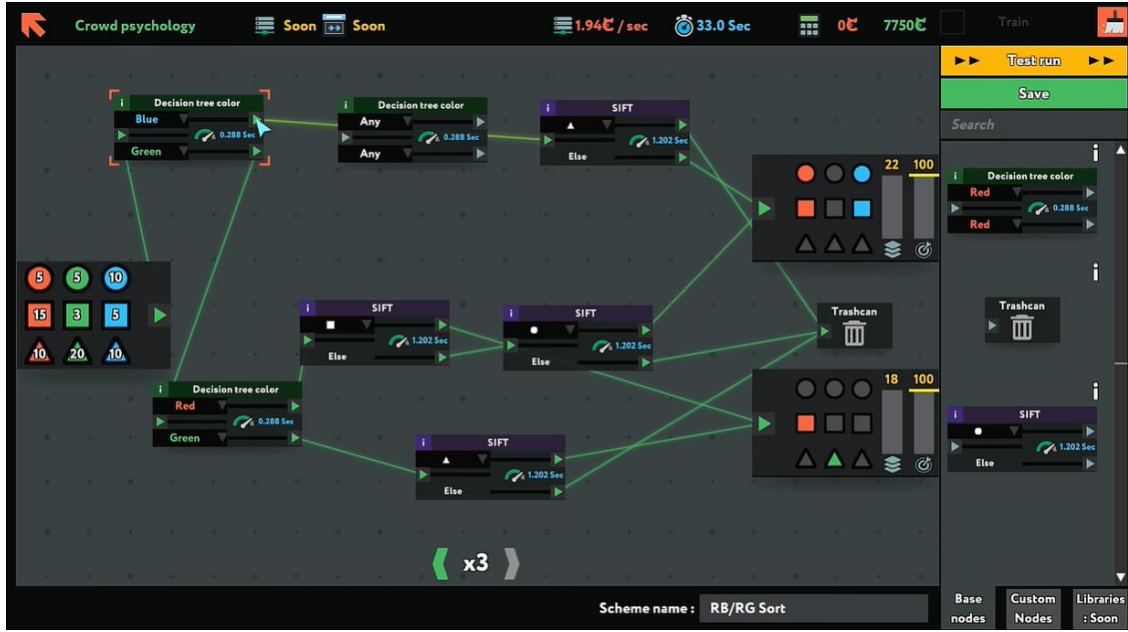
Şekil 6. Shenzhen-IO ile geliştirilmiş Trafik Oyunu

#### 2.2.4. While True Learn

While True Learn oyunu ile ilgili STEAM platformundaki oyun açıklamasında “Sinir ağları üreten bir makine öğrenimi uzmanısın ama kedin bu konuda senden daha iyi. Kedinin daha neler yapabileceğini öğrenmek amacıyla bulmacaları çözerek kedinin dilini anlamak için bir çeviri sistemi kur. Büyük bir servet kazan, kedi kıyafetleri al ve makine öğreniminin gerçekte nasıl çalıştığını öğren!” denilmiştir (Steam, 2019b). Oyun, makine öğrenimi ve ilgili teknolojilerin nasıl çalıştığını öğrenmek isteyenler için neredeyse benzersiz durumdadır. Oyun, uzman sistemlerden, tekrarlanan sinir ağlarına kadar gerçek hayattaki makine öğrenimi teknolojilerini temel almaktadır. Oldukça olumlu yorumlar alan bu oyun, makine öğrenme konularını tam olarak işlemese de genel konseptin anlaşılmasında oldukça orijinal bir içerik sunmaktadır. (Şekil 7)’de While True Learn oyununun görünümü verilmiştir.

Luden.io şirketi tarafından 17 Ocak 2019 yılında yayınlanan bu oyun yaklaşık 6 dolar fiyat etiketine sahiptir. 13+ yaş sınırlaması sahip olan oyun bazı zihinsel becerilerin gelişmesinin ardından rahatlıkla oynanabilir durumdadır. Oyun hakkında 4460 adet yoruma incelenmiş ve %92 oranında olumlu geri dönüşü sahip olduğu görülmüştür (Steam, 2019b). (Şekil 7)’de Karar Ağacı (Decision Tree) metodu ile nesne sınıflandırmaya bir örnek olması açısından önemlidir. Bu oyun Silicon Zeroes, Shenzhen-IO gibi laboratuvar ekşiğini giderme potansiyeli olan oyunlardan farklı olarak daha soyut kavramları öğretmektedir. Giriş seviyesinde makine öğrenme kavramlarını öğretme potansiyeli olan bu oyun ileri seviyede bir bulmaca oyunudur. Tasarımın bir puzzle şeklinde olması öğrencilerin kendini zihinsel olarak geliştirmesi için önemli fırsatlar sunmaktadır. Ayrıca oyun içinde makine öğrenmesi konularının gelişim tarihi, çalışma mantığını anlatan eğitici içerikler de bulunmaktadır.





Şekil 7. While True Learn oyunu ile nesne sınıflandırma

### 2.2.5. Comet 64

Comet 64, piyasada muadili olan 'Software Puzzle' oyunlarına kıyasla görsellik ve anlaşılabilirlik açısından en dikkat çekici olan ve 2021 yılı itibari ile yayına alınan programlama amaçlı bulmaca oyunu olarak tanımlanmaktadır. (Şekil 8)'te Comet 64 oyununa ait bir görsel sunulmuştur. Görselden görüleceği üzere yazılımın bir kısmı verilmekte ve boşluk kısmı oyunu oynayan kişi tarafından tamamlanması beklenmektedir.



Şekil 8. Comet 64 oyunundan bir kesit

İlk olarak 1984 yılında yayınlanan ve daha sonra geliştiriciler tarafından revize edilen ve mevcut 51 yorumu bulunan oyunun olumlu geri dönüş oranı ise %90'dır. Özellikle temel programlama becerisi gereken bölümlerde okuyan öğrenciler için comet 64 oyununu önermek mümkündür. Sadece dersi geçmenin ötesinde oyun içi senaryodaki gizemleri çözerek ve seviyeleri teker teker geçerek lider tablosuna girmek, motivasyon için önemlidir (Steam, 2021a).

### 3. Bulgular ve Tartışma

Çalışma kapsamında STEAM platformu üzerinde yapılan araştırmalarda tamamı incelenmemiş olsa bile, incelenen oyunlar arasından eğitici içeriğe sahip olabilecek nitelikte olan ve Elektrik-Elektronik mesleği ile ilişkilendirilebilecek oyunların bir kısmı (Tablo 1)'de verilmiştir. (Tablo 1)'de oyunların adı, yorum sayısı, olumlu geri dönüş yüzdesi ve oyun sınıflandırmasını gösteren bilgiler verilmiştir. Oyun dağıtım platformlarında oyunlar sınıflandırılırken genellikle bulmaca, platform, benzetim, rol yapma vb. kavramlar kullanılmaktadır. Bunun yanında çalışmanın amacına da uygun olması açısından eğitim amaçlı bir sınıflandırma yapılmasının da önemli olduğu belirlenmiştir. Buna göre oyunlar, elektronik tasarım tabanlı, fabrika kurulum ve optimizasyon tabanlı, yazılım geliştirme tabanlı, tabanlı, yönetim tabanlı olmak üzere 4 gruba ayrılmıştır. Yazılım geliştirme tabanlı olarak sınıflandırılan oyunlar temel olarak oyun içinde kod yazma, komut satırı kullanımı gibi kodlamaya dayalı becerileri geliştirmektedir. Fabrika kurulum ve optimizasyon tabanlı oyunlar seri üretim, fabrika kurulumu, otomasyon tasarımı gibi içeriklere sahip olan oyunları tanımlamaktadır. Yönetim tabanlı oyunlar kaynak yönetimi, strateji geliştirme, maliyeti minimize etme, üretim optimizasyonu gibi içeriklere sahip oyunları tanımlamaktadır. Son olarak Elektronik tasarım tabanlı oyunlar devre tasarımı yapılabilen ve oluşturulan devrelerin çalışma sırasını test edebileceğiniz nitelikte oyunlardır. Böyle bir sınıflandırma sayesinde seçilen oyunların hangi bölümlere ve derslere uygun olduğunu kolayca ayırt etmek mümkün olacaktır. Örneğin; elektronik tasarım tabanlı bir oyun, devre tasarımı ile ilgili olan dijital elektronik dersi ile ilgilidir.

Tablo 1

Oyun adı, yorum sayısı, olumlu yorum yüzdesi, oyun sınıflandırması ve öğrenim türü bilgileri

Oyun Adı	Yorum	Olumlu	Yorum	Oyun Sınıflandırması
Hacknet	10863	%93		Yazılım geliştirme tabanlı
TIS-100	2564	%97		Yazılım geliştirme tabanlı
Infinifactory	1459	%95		Fabrika Kurulum ve Optimizasyon tabanlı
Shenzen-IO	2324	%96		Elektronik tasarım tabanlı
EXAPUNKS	838	%96		Yazılım geliştirme tabanlı
While True Learn	4460	%92		Yazılım geliştirme tabanlı
Factorio	88822	%98		Fabrika Kurulum ve Optimizasyon tabanlı
Hardware Engineers	267	%86		Yönetim tabanlı
Hardware Engineering	166	%55		Elektronik tasarım tabanlı
Silicon Zeroes	185	%95		Elektronik tasarım tabanlı
PC Building Simulator	24912	%94		Elektronik tasarım tabanlı
Comet 64	51	%90		Yazılım geliştirme tabanlı

(Tablo 1)'de görüldüğü gibi bu kısımda STEAM Platformu üzerinden oynanan eğitici içerikli dijital öğrenme oyunlarının hâlihazırda yorum sayıları ve bu yorumların olumlu geri dönüş oranları verilmiştir. Bu oyunların hangi sınıflandırmaya dâhil olacağı, hem oyun açıklamalarından hem de oyunu oynayanların yorumları tek tek incelenerek karar verilmiştir. Ancak bu noktada dikkat edilmesi gereken bir diğer husus, örneğin bir oyunun yazılım geliştirme tabanlı olması diğer alanlarda kullanılamayacağı anlamına gelmemektedir. Bu bağlamda çalışma kapsamında değerlendirilen Elektrik-Elektronik alanında eğitim gören araştırmacı ve öğrenciler platform içerisinde yüzlerce oyunun eğitim amaçlı olarak kullanılabileceği öngörülmektedir. Tablo 1'de Hardware Engineers oyunu ve Hardware Engineering oyunları isim olarak birbirine oldukça benzemekle birlikte Hardware Engineers oyunu bir IT (Information Technologies) şirketini yönettiğiniz yönetim tabanlı bir oyun, Hardware Engineering ise elektronik devre tasarımı yapabildiğiniz bir benzetim içerikli oyundur.

### 4. Sonuç ve Öneriler

Dijitalleşmenin giderek yaygınlaştığı göz önünde bulundurulduğunda dijital oyunların eğitim amaçlı kullanılmasının eğitime destek amaçlı değerlendirilmesi açısından önemli olduğu düşünülmektedir. Bu çalışmada eğitici içeriğe sahip oyunların bir kısmı örnek olarak ele alınarak değerlendirilmiş ve öğretim

müfredatına entegrasyonu hakkında önerilerde bulunulmuştur. Oyunların dağıtım görevini üstlenen çeşitli platformlar bulunmakla birlikte STEAM bu alanda sektör lideri olması açısından önemlidir. STEAM platformunun tasarımı incelendiğinde bireysel kullanım için tasarlandığı ancak eğitim kurumlarına dönük özel bir tasarımının bulunmadığı görülmektedir.

STEAM oyun platform üzerinde eğitici içeriğe sahip olarak belirlenen oyunların yorumları incelendiğinde yorum yapanlardan bazılarının “derslerden çok daha eğitici ve eğlenceli” yorumu dikkate alındığında oyunların öğrenmeyi daha nitelikli hale getirebileceği iddia edilmektedir. Bu sebeple eğitim içinde bu tür oyunların kullanılıp kullanılmayacağı değerlendirilmeli ancak öneriler kısmında belirtilen hususlar üzerinde çalışılmalıdır. EEM müfredatının yoğun matematik, teorik ve laboratuvar eğitimine dayandığı hususunun -pedagojik yaklaşımın yanında- değerlendirilmesi önem arz etmektedir.

Örnek olarak sunulan Silicon Zeroes, PC Building Simulator, Shenhzen-IO ve While True Learn gibi oyunları bir süre oynayan araştırma ekibi Elektrik-Elektronik Mühendisliği öğrencilerine ders içinde bu oyunları oynatarak eğitim verilebileceğine kanaat getirmişlerdir. Belirtilen oyunlar dışında diğer bölümlerde oynatılmaya müsait oyunlar bulunmaktadır ancak bununla ilgili çalışmalar yapılması önerilmektedir.

Belirtilen öneriler sonraki çalışmalara yön vermek ve dijital oyunların eğitime entegrasyonunu sağlamak açısından önemlidir. Bu noktada çalışmada ortaya çıkan sonuçlar ışığında getirilen öneriler aşağıdaki gibi sıralanabilir:

- Çok fazla dikkat dağıtıcı içeriğe sahip oyun platformları eğitim kurumları için özelleştirilmelidir.
- Dijital oyunları incelemeye odaklanmış akademik çalışmaların sayısı azdır. Bu sebeple oyunlar ve eğitime entegrasyonu hakkında mevcut problemleri çözecek akademik çalışmalar yapılmalıdır.
- Eğitici oyunların eğitime entegrasyonu çalışmalarını yürütecek dijital oyun inceleme komisyonu kurulmalıdır.
- Eğitsel içeriğe sahip dijital oyunlar belirlenmeli, içeriği incelenmeli ve STEAM felsefesi içinde uygulanabilirliği araştırılmalıdır.
- Dijital oyunların dil seçeneklerinin artırılması farklı dillerin konuşulduğu ülkelerde eğitimde fırsat eşitliği sağlanması bakımından önemlidir.
- Dijital oyunların derslerde oynatılabilmesi için eğitim yöneticilerine ve öğretmenlere farkındalık eğitimleri verilmelidir.
- Belirlenen oyunlar sürekli güncellenmekte ve yeni versiyonları çıkmaktadır. Yapılacak çalışmalarla oyun üreticilerinin geliştirdikleri oyunların, derslerde oynanabilir hale getirilmesi için nasıl güncelleme yapacaklarına dönük olarak önerilerde bulunulmalıdır.
- Oyunlar sadece oyun olmanın ötesinde görsellikleri ve müzikleri ile de bir sanat çalışması olarak düşünülmelidir. Belirlenen oyunların sanatsal açıdan değerlendirilerek STEAM yaklaşımında öğrenmenin daha iyi olacağı bir dönüşüme girmesi sağlanabilir.
- Başarı değerlendirme kriterlerinin nasıl olacağına dönük çalışmalar yapılmalıdır.
- Oyunların şiddet içeriği ve gayri ahlaki öğeleri incelenmelidir.
- Oyunlara ilişkin yaş sınırlaması kavram olarak şiddet öğeleri hakkında bilgi vermektedir. Ancak oyunun zihinsel olarak hangi yaştan itibaren oynanması gerektiği ile ilgili çalışma yapılmalıdır.
- Oyunların okullarda oynatılması durumunda lisanslama ile ilgili problemler ortaya çıkmaktadır. Bu problemler ilgili mevzuatlar çerçevesinde tekrar değerlendirilerek alandaki yasal engellerin ortadan kaldırılması gerektiği düşünülmektedir.

### Yazar Katkıları

Şehmus Fidan: Çalışma kapsamındaki eğitici içeriğe sahip dijital oyunları analiz ederek gerekli verileri toplamıştır.

Ömer Ali Karaman: Çalışma kapsamındaki eğitici içeriğe sahip dijital oyunları analiz ederek gerekli verileri toplamıştır.

Abdullah Yıldırım: Çalışmanın teorik kısmı ile ilgili gerekli verileri toplayıp makaleyi yazmıştır.

### Çıkar Çatışması

Çıkar çatışması bildirmemişlerdir.

**Kaynaklar**

- Bayram, Ş. B., & Çalışkan, N. (2019). *Oyun tabanlı sanal gerçeklik uygulamasının psikomotor beceri öğretiminde kullanımı: Bir deneyim paylaşımı*. *Journal of Human Sciences*, 16(1), 155-163. Erişim adresi: <https://www.j-humansciences.com/ojs/index.php/IJHS/article/view/5508>.
- Bodnar, C. A., Anastasio, D., Enszer, J. A., & Burkey, D. D. (2016). Engineers at play: Games as teaching tools for undergraduate engineering students. *Journal of Engineering Education*, 105(1), 147-200. <https://doi.org/10.1002/jee.20106>
- Carvalho, C. V. (2012, April). Is game-based learning suitable for engineering education?., *2012 IEEE Global Engineering Education Conference (EDUCON)* (pp. 1-8). IEEE. <https://doi.org/10.1109/EDUCON.2012.6201140>
- Collins, C. (2008). Looking to the future: Higher education in the Metaverse. *Educause Review*, 43(5), 51-63. Erişim adresi: <https://er.educause.edu/articles/2008/9/looking-to-the-future-higher-education-in-the-metaverse>
- Çınar, S., Çiftçi, M. (2016). Disiplinler Arası Stem Yaklaşımına Yönelik Yapılan Çalışmaların İçerik Analizi. *10th International Computer and Instructional Technologies Symposium* (pp:1031-1038). Rize, Turkey. Erişim adresi: <https://avesis.erdogan.edu.tr/yayin/07afe3bb-0b4b-48be-a69a-b191bc8c69f8/disiplinler-arasi-stem-yaklasimina-yonelik-yapilan-calismalarin-icerik-analizi>
- Elektrik Mühendisleri Odası (2020). *Emo Bursa Şubesi 2020 Eğitim Raporu*, Bursa, Erişim adresi: [https://www.emo.org.tr/ekler/815cef00803e307\\_ek.pdf?tipi=1&turu=X&sube=15](https://www.emo.org.tr/ekler/815cef00803e307_ek.pdf?tipi=1&turu=X&sube=15)
- Gee, J. P. (2003). What video games have to teach us about learning and literacy. *Computers in Entertainment (CIE)*, 1(1), 20-20. <https://doi.org/10.1145/950566.950595>.
- Joiner, R., Iacovides, J., Owen, M., Gavin, C., Clibbery, S., Darling, J., Drew, B. (2011). Digitalgames, gender and learning in engineering: do females benefit as much as males? *Journal of Science Education and Technology*. 20(2), 178–185. <https://dx.doi.org/10.1007/s10956-010-9244-568>.
- Kuk, K., Jovanovic, D., Jokanovic, D., Spalevic, P., Caric, M., & Panic, S. (2012). Using a game-based learning model as a new teaching strategy for computer engineering. *Turkish Journal of Electrical Engineering & Computer Sciences*, 20(2), 1312-1331. <https://doi.org/10.3906/elk-1101-962>
- Marston, H. R., & Kowert, R. (2020). What role can videogames play in the COVID-19 pandemic?. *Emerald Open Research*, 2, 34. <https://doi.org/10.35241/emeraldopenres.13727.2>
- Morelock, J. R., & Matusovich, H. M. (2018), All Games Are Not Created Equally: How Different Games Contribute to Learning Differently in Engineering, *Annual Conference & Exposition*, Salt Lake City, Utah. <https://dx.doi.org/10.18260/1-2--29766>
- Perignat, E., Katz-Buonincontro, J. (2019). STEAM in practice and research: An integrative literature review. *Thinking Skills and Creativity*, 31 (2019), pp. 31-43, <https://doi.org/10.1016/j.tsc.2018.10.002>
- Prensky, M. (2001), Digital Natives, Digital Immigrants Part 1, *On the Horizon*, Vol. 9 No. 5, pp. 1-6. <https://doi.org/10.1108/10748120110424816>
- Sağlam, M., Topsümer, F. (2019). Üniversite Öğrencilerinin Dijital Oyun Oynama Nedenlerine İlişkin Nitel Bir Çalışma. *Akdeniz Üniversitesi İletişim Fakültesi Dergisi*, (32), 485-504. Erişim adresi: <https://dergipark.org.tr/tr/pub/akil/issue/51740/617102>
- Sezgin, S. (2016). İnsan ve Oyun: Oyunların Dünü, Bugünü, Yarını. *VIII. Uluslararası Eğitim Araştırmaları Kongresi Bildiriler Kitabı* (343-354). Çanakkale Onsekiz Mart Üniversitesi. Mayıs 5-8, 2016. Çanakkale/Türkiye Erişim adresi: <https://atif.sobiad.com/index.jsp?modul=AW4RFtZbyZgeuuwfeBikmakaleAW4RFtZbyZgeuuwfeBik>
- Srinivasan, V., Butler-Purpy, K., & Pedersen, S. (2011). Developing Educational Games for Engineering Education: A Case Study. In P. Felicia (Ed.), *Handbook of Research on Improving Learning and Motivation through Educational Games: Multidisciplinary Approaches* (pp. 913-938). IGI Global. <https://doi.org/10.4018/978-1-60960-495-0.ch042>
- Steam (2017a), *Silicon Zeroes*, Erişim adresi: [https://store.steampowered.com/app/Silicon\\_Zeroes/](https://store.steampowered.com/app/Silicon_Zeroes/)
- Steam (2019a), *PC Building Simulator*, Erişim adresi: [https://store.steampowered.com/PC\\_Building/](https://store.steampowered.com/PC_Building/)
- Steam (2019b), *while True: learn*, Erişim adresi: [https://store.steampowered.com/while\\_True\\_learn/](https://store.steampowered.com/while_True_learn/)
- Steam (2021a), *Comet\_64*, Erişim adresi: [https://store.steampowered.com/app/1397290/Comet\\_64/](https://store.steampowered.com/app/1397290/Comet_64/)
- Topallı, D., Çağıltay, N.E. (2018). Improving programming skills in engineering education through problem-based game projects with Scratch, *Computers & Education*, Volume 120, Pages 64-74, ISSN 0360-1315, <https://doi.org/10.1016/j.compedu.2018.01.011>.
- Valve(2021a), *SteamAbout*. Erişim adresi: <https://store.steampowered.com/about/>



- Velaora, C., Kakarountas, A. (2021) Game-Based Learning for Engineering Education, *2021 6th South-East Europe Design Automation, Computer Engineering, Computer Networks and Social Media Conference (SEEDA)*, pp. 1-6, [https://doi.org/10.1109/SEEDA\\_CECNSM53056.2021.9566215](https://doi.org/10.1109/SEEDA_CECNSM53056.2021.9566215)
- West B. (2016), *Shenzen I-O*, Eriřim adresi: <https://gamecloud.net.au/review/shenzhen-io>



## Enhancing the Process of AES: A Lightweight Cryptography Algorithm AES for Ad-hoc Environments

Mustafa Al-handhal<sup>1</sup>, Alharith A. Abdullah<sup>2</sup>, Oğuz Ata<sup>3,\*</sup>, Çağatay Aydın<sup>4</sup>

<sup>1</sup>Department of Information Technology, Faculty of Computer Engineering, Altınbaş university, Istanbul, Türkiye

<sup>2</sup>Department of Information Network, Faculty of Information Technology, University of Babylon, Hillah, Iraq

<sup>3</sup>Department of Software Engineering, Faculty of Computer Engineering, Altınbaş university, Istanbul, Türkiye

<sup>4</sup>Department of Electrical-Electronics Engineering, Faculty of Engineering, Ege University, Izmir, Türkiye

### Article History

Received: 07.02.2022

Accepted: 10.06.2022

Published: 15.12.2022

### Research Article

**Abstract** – Ad hoc networks have become more widespread and important because they support mobility and can be used in different situations and some difficult areas such as rescue missions, military, and vehicular communications. Security is stated among the most significant challenges facing Ad Hoc networks due to its characteristic features such as the topology dynamicity, lack of infrastructure centralization, and open architecture. Ad hoc networks work on battery power, and this kind of networks tend to consume more power and time to process data and memory resources through data encryption, eventually requiring a higher amount of power and more time. Therefore, an AES lightweight algorithm is proposed, which is one of the complicated encryption algorithms. This algorithm will be modified to improve the security as well as reduce the amount of time and energy consumed in comparison with the original algorithm. The enhanced version is based on the outputs of sub byte and shift row, in addition to an exclusive X-OR operator between them, whereby the output of the X-OR operator is added to the round key layer. The results confirm that this enhanced algorithm is efficient, accurate, and robust against multiple types of attacks related to ad hoc networks.

**Keywords** – Ad-hoc network, advanced encryption standard (aes), lightweight cryptography (LWC)

## 1. Introduction

Throughout the last few decades, an exponential development is observed regarding the wireless areas. Great advances have been achieved in network infrastructures, which in turn increase the provision of wireless applications, and the appearance of omnipresent wireless devices like portable or handled computers, PDAs, and mobile phones. These devices are remarkably increasing in terms of their capabilities and tend to play a significant role in human life at the present time (Basangi et al., 2004).

Ad hoc networks consist of a set of wireless nodes which communicate in a direct way through common wireless channels (Rani et al., 2013). Ad-Hoc networks do not need any extra infrastructure like base stations or wired access points. The created network can be independent from the infrastructure network. On the other hand, these nodes are able to build their own networks. Additionally, communication among nodes only takes place whenever they are located within their transmission range. Security is an important problem in ad hoc networks, as it produces integrity, confidentiality, and availability (Elmahdi et al., 2018). Providing security

<sup>1</sup> [mostafayousif36@gmail.com](mailto:mostafayousif36@gmail.com)

<sup>2</sup> [alharith@itnet.uobabylon.edu.iq](mailto:alharith@itnet.uobabylon.edu.iq)

<sup>3</sup> [oguzata@gmail.com](mailto:oguzata@gmail.com)

<sup>4</sup> [cagatay.aydin@ege.edu.tr](mailto:cagatay.aydin@ege.edu.tr)

\*Corresponding Author

affects the power management in ad hoc networks, as the consumption of power occurs within the nodes whenever the packet is transmitted or received.

One of the efficient mechanisms which could be used for solving the security challenges in Ad Hoc networks is cryptography (Costa et al., 2017). It seems to have a major role in protecting data from opponents through converting it into a form of data that is unintelligible for unauthorized access. Lightweight cryptography is a novel sub-field designed to deal with more developed technologies (Alyas and Abdullah, 2021). Applying traditional cryptography within constrained devices is not sufficiently practical because of the mathematical complexity of cryptographic primitives (Vanda et al. 2021). Traditional cryptography requires a large memory space and relatively more power for processing. Thus, the motive behind using Lightweight algorithms is the speed of execution, the comparatively less energy and time consumed, and the need for less memory use (Abdullah and Obeid, 2021). Lightweight algorithms consist of two parts: Symmetric figures and Asymmetric figures. The symmetric ciphers consist of Block and Stream Ciphers.

Lightweight cryptography has many effective algorithms, one of which is the Advanced Encryption Standard (AES), a commonly used method in wireless environments. AES has a high security with low complexity (Agwa et al., 2017), and it has become more attractive to researchers for modification and enhancement. Several researchers have proposed different techniques to enhance the security in many networks, as outlined in the related literature reviews below.

Usman et al. (2017) present a lightweight encryption algorithm for securing IoT. A 64-bit block cipher model is proposed, requiring a 64-bit key for data encryption. It represents a hybrid between festal and uniform substituting-permutating networks. Kunchok et al. (2018) proposed three ways of security to encryption data. It combines the advantages of different encryption algorithms, so that the process of transmitting data through the network is encrypted. Aziz and Singh. (2018) proposed a compressive sensing for providing lightweight cryptographic security for IoT. They made use of compressive sensing to encrypt data, which in turn contributed to the protection of power consumption. Abdullah et al. (2018) introduced a super-encryption cryptography using international data and word auto key encryption algorithms. It combines several cryptographic algorithms for providing higher data security. Mohanty et al. (2020) introduced a lightweight algorithm with distributed throughput management in blockchain, which is applicable to IoT networks to enhance security and reduce the consumption of resources like time and power. Keshav Kumar et al. (2020) proposed AES lightweight algorithm to encrypt voice signal on peer-to-peer communication. And it is applied on Field Programmable Gate Array (FPGA) simulation. Fadhil et al. (2021) proposed Lightweight AES encryption algorithm to provide security when the data received from physical environment in IOT system. It is worked on Raspberry. Hussein M. et al. (2022) proposed AES lightweight algorithm in IoT systems to provide security and delay in time. It is implementation on Asp net.

In this paper, the AES lightweight algorithm will be used in Ad-hoc networks to provide security for data that is sent across such kinds of networks, as well as to reduce the time and power consumption required for encrypting data and transmitting packets among nodes.

The research paper could be outlined as follows. Section II describes the AES algorithm adopted in this work. Section III states the experiment and discussion result. A comparison with other previous works is drawn in Section IV, and Section V states the conclusions drawn.

## **2. Materials and Methods**

This section discusses the modified AES lightweight algorithm that is used in this paper to reduce the power and time consumption in ad hoc networks. In the standard AES algorithm, there are four steps to encrypt and decrypt data, namely: Sub Byte, Shift Row, Mix Column and Add Round Key. In the modified form of AES lightweight algorithm, the output of both the Sub byte and Shift row are taken to create an exclusive OR (XOR) to be used instead of the MixColumns.

### 2.1. Encryption Process

The process of encrypting in the AES algorithm (Daemen et al, 1999) consists of a set of steps or transformations that are carried out onto the data. There are also additional steps which are iterative and fixed, also known as rounds. The number of rounds in cryptocurrencies is determined by the key length. If the available one consists of 128 bits, then the number of rounds is 10. The key lengths 192 and 256 are accompanied with 12 and 14 rounds respectively (NIST, 2001). The encryption process is shown in Figure 1.

### 2.2. Decryption Process

The decryption process takes place through reversing the encryption process. However, the sequence of conversions is different from the encryption process. In decryption processes, the InvSubBytes and the InvShiftRows are interchangeable with no effect on the decryption processes. 128 bit used in our work. The decrypting and encryption (William S. 2000) procedure is illustrated in Figure 1.

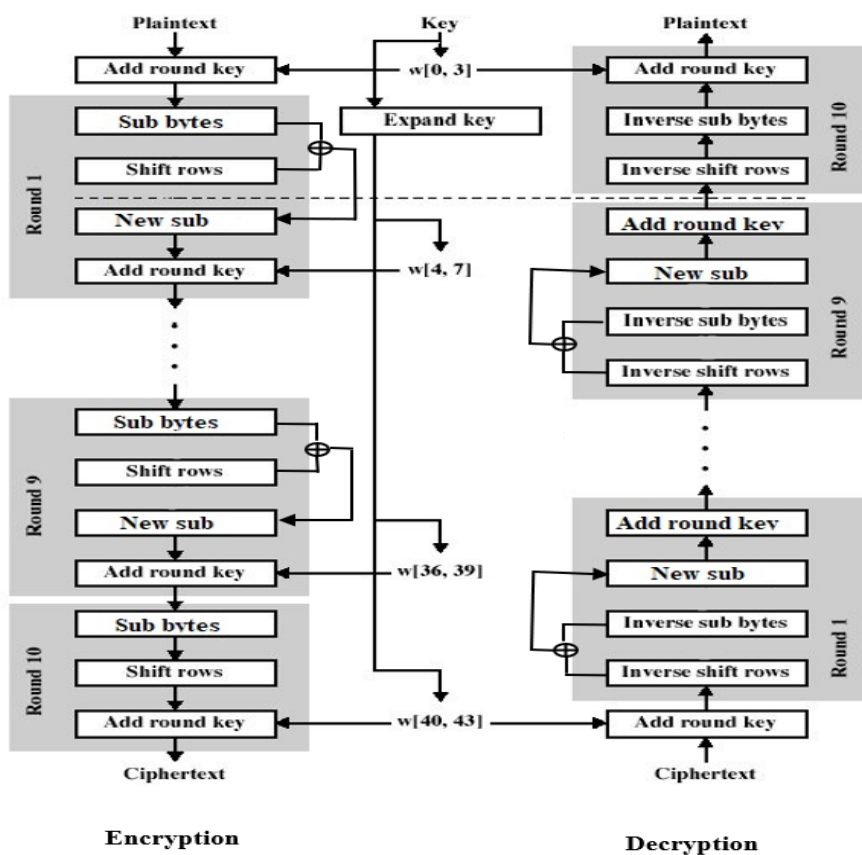


Figure 1. Encrypting and decrypting processes in the modified AES lightweight

Algorithm (1) below outlines the steps of the proposed AES lightweight

**Input:** Plain Text.  
**Output:** Cipher Text.

**Step 1:** Divide the plain text to groups, each group contains (4\*4) byte. Then, perform the XOR operation with the key (This operation is called Initial key).

**Step 2:** Take the initial key and perform the XOR operation with S-Box (This step is called Sub Byte).

**Step 3:** The results of the Sub Byte are shifted. Every byte in the row shifts to the left with a certain indent. The first row undergoes no change. The second row makes a shift to the left, and the third row makes two shifts to the left (This step is called Shift Row).

**Step 4:** This step is called New Sub:

```

if (keyBits == 128) {
    for (;) {
        temp = rk[3];
        rk[4] = rk[0] ^
            (Te4[(temp >> 16) & 0xff] & 0xff000000) ^
            (Te4[(temp >> 8) & 0xff] & 0x00ff0000) ^
            (Te4[(temp >> 0) & 0xff] & 0x0000ff00) ^
            (Te4[(temp >> 24) & 0xff] & 0x000000ff) ^
    }
}
    
```

**Step 5:** Add-Round Key

Figure 2. The steps of the proposed AES lightweight

In Figure 2 above the steps of proposed algorithm in step 4, the key is 128-bit. The term temp refers to the cipher text. Thus, Round 1 takes the Te4, representing the data in the algorithm which is determined by the bytes. Each byte has a different data, for example the data of 16 differs from the data in 8. Thus, this step (Te4[(temp >> 16) & 0xff] represents the Sub Byte and will make XOR operation with Shift Row (0xff000000). This operation reduces the New Sub to be used instead of the Mix Column. These steps will be represented in every round.

### 2.3. Sub Byte and Inverse Sub Byte Transformations

Each byte within the array will be replaced with an 8-byte Sub Byte taken from the S-Box. The benefit of using the Sub Byte is the non-linearity that is provided in the cipher. The S-Box is obtained through the inverse over the Galois Field (2^8) (Shastry et al. 2011). As for the Inverse Sub Byte, all bytes in the matrix are replaced by the Inverse Sub Byte that corresponds with it.

For example, if S<sub>1,1</sub>={1a}, then the substitution value determined by the intersected the column with index '1' and the row with index 'a'. So, the result of S<sub>1,1</sub> will be {A2}. as shown in Figure 3.

	Y															
	0	1	2	3	4	5	6	7	8	9	a	b	c	d	e	f
0	63	7c	77	7b	f2	68	6f	c5	30	01	67	2b	fe	d7	ab	76
1	ca	82	c9	7d	fa	59	47	f0	ad	d4	a2	af	9c	a4	72	c0
2	b7	fd	93	26	36	3f	f7	cc	34	a5	e5	f1	71	d8	31	15
3	04	c7	23	c3	18	96	05	9a	07	12	80	e2	eb	27	b2	75
4	09	83	2c	1a	1b	6e	5a	a0	52	38	d6	b3	29	e3	2f	84
5	53	d1	00	ed	20	fc	b1	58	6a	cb	be	39	4a	4c	58	cf
6	do	ef	aa	fb	43	4d	33	85	45	f9	02	7f	50	3c	9f	a8
7	51	a3	40	8f	92	9d	38	f5	bc	86	da	21	10	ff	f3	d2
8	cd	0c	13	ec	5f	97	44	17	c4	a7	7e	3d	64	5d	19	73
9	60	81	4f	dc	22	2a	90	88	46	ee	b8	14	de	5e	0b	db
a	e0	32	3a	0a	49	06	24	5c	c2	d3	ac	62	91	95	e4	79
b	e7	c8	37	6d	8d	d5	4e	a9	6c	56	f4	ea	65	7a	ae	08
c	ba	78	25	2e	1c	a6	b4	c6	e8	dd	74	1f	4b	bd	8b	8a
d	70	3e	b5	66	48	03	f6	0e	61	35	57	b9	86	c1	1d	9e
e	e1	f8	98	11	69	d9	8e	94	9b	1e	87	e9	ce	55	28	df
f	8c	a1	89	0d	bf	e6	42	68	41	99	2d	0f	80	54	bb	16

Figure 3. Sub Byte Operation

### 2.4. Shift Row and Inverse Shift Row Transformations

In the shift row, each byte in the row undergoes a certain indent to the left. In AES, the first row remains with no changes whereas the second one makes a single shift to the left and the thirft one makes two left shifts. Meanwhile, the inverse shift row is the opposite of the forward shift row. The first row remains with no changes whereas the second shifts once to the right, and the third shifts two bytes to the right as well. The shifts are determined by the adopted matrix in (Scheier, 2015).

For example, if we have this data 85, 01, A2, ed, a4, 21, 30, b2, d2, e6, 97, 44, 53, fc, 3f and 59. So, each 4 bytes will be in row as shown in Figure 4.

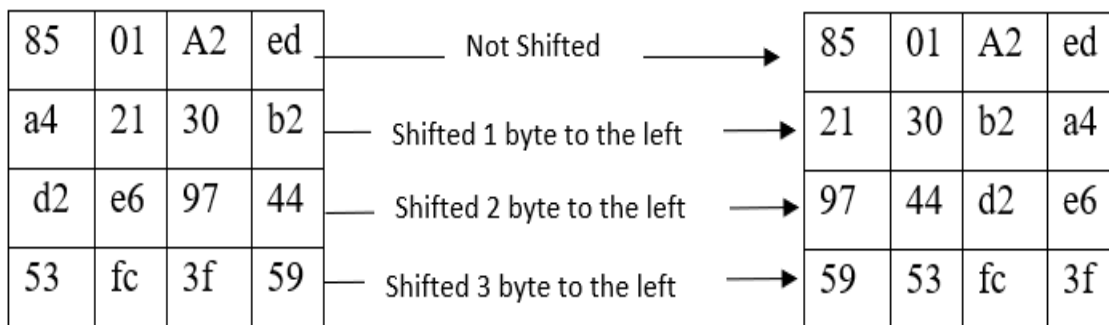


Figure 4. Shift Row Operation

### 2.5. New Sub

The new sub is the result of merging the Sub byte with the Shift row by using the XOR operation. The output is to be used instead of the Mix column. This operation aims to reduce time and energy consumption. Figure 5 shows the result of this step

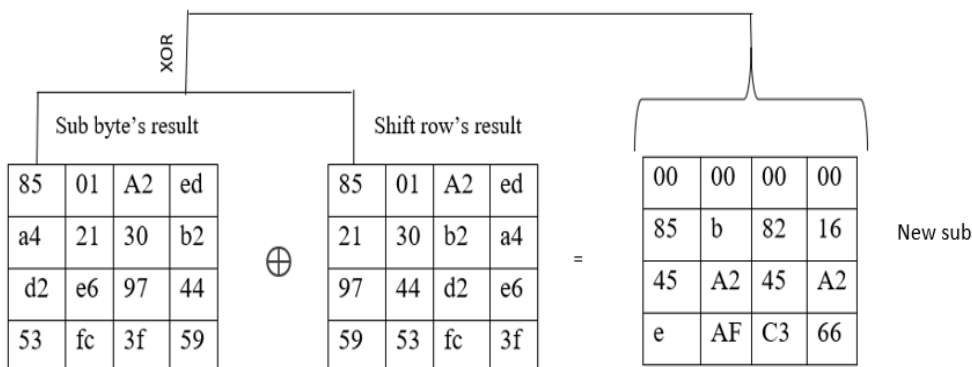


Figure 5. The New Sub

### 2.6. Add Round Key

Next, the round key is added to the state through the X-OR operation. The round keys are composed of several words taken from the key table. The round key undergoes the X0OR operation for every byte in the state matrix, generating a new round key for each round through altering the cipher key.

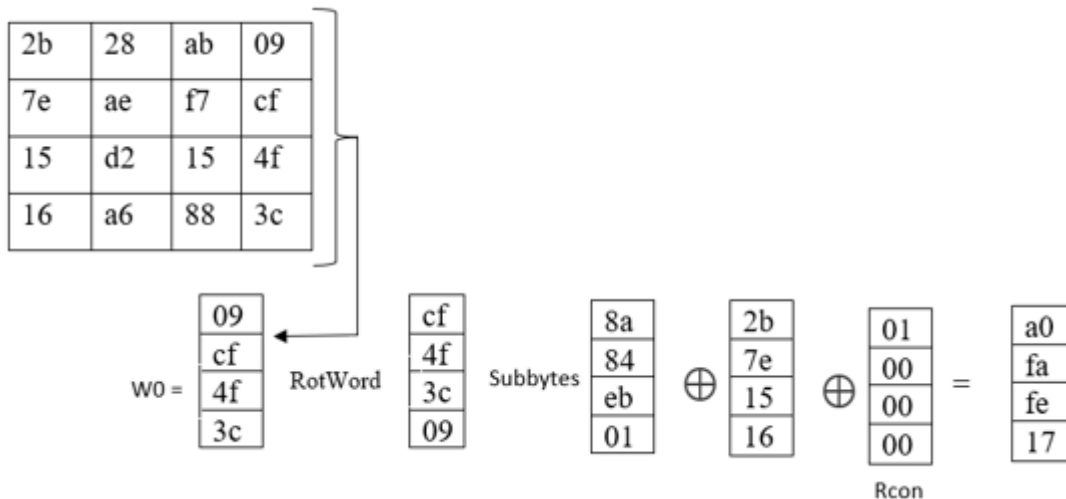


Figure 6. Add Round Key Operation

### 2.7. Key Schedule

The key schedule takes the original key ( the length of 128 bit , 192 bit, and 256 bit) then the subkeys will derive in AES. The subkeys number is equal to the number of rounds plus one. So, the key length of 128 bit is  $n_r = 10$  and there are 11 subkeys because the plus one

### 3. Results and Discussion

After designing the Ad-Hoc network, it is used within this simulation after which the connection between the clients and server is observed. Figure 7 shows this Ad-Hoc network. To prove the enhancement of the AES lightweight algorithm, the implementation of the Ad-Hoc network in the cooja simulator is shown and discussed. Cooja is used for the reduction of power and time consumption.

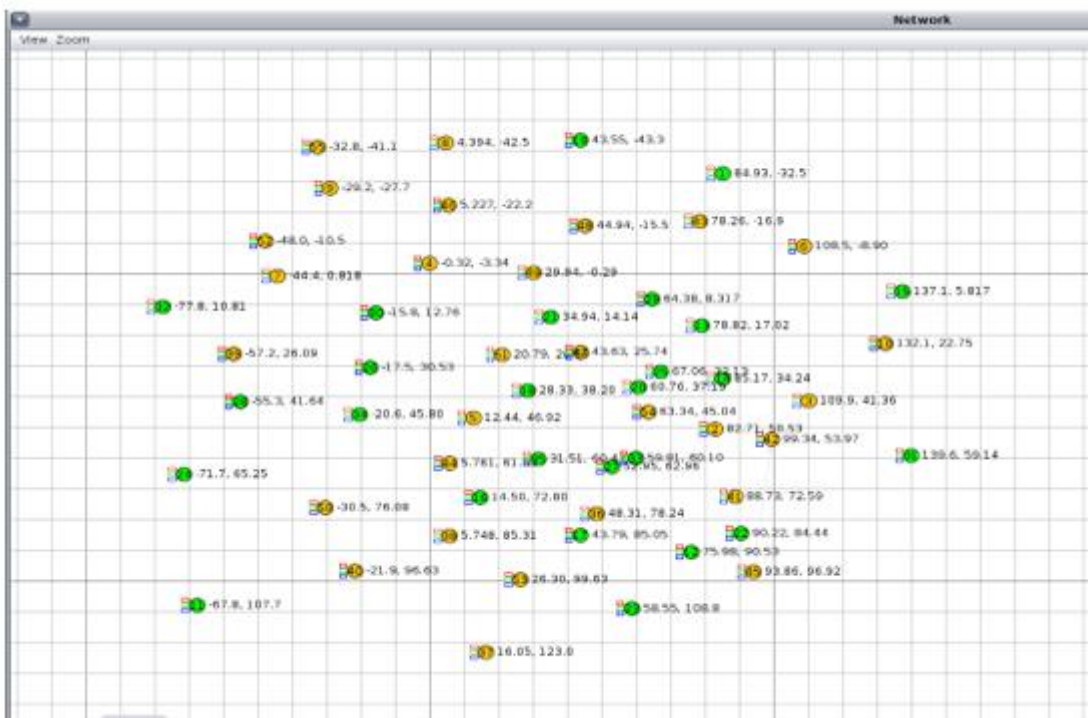


Figure 7. Ad-hoc network implementation.



In Figure 8 below presents the output of the network. It shows the time that is consumed when the message sent between motes as sender and receiver.

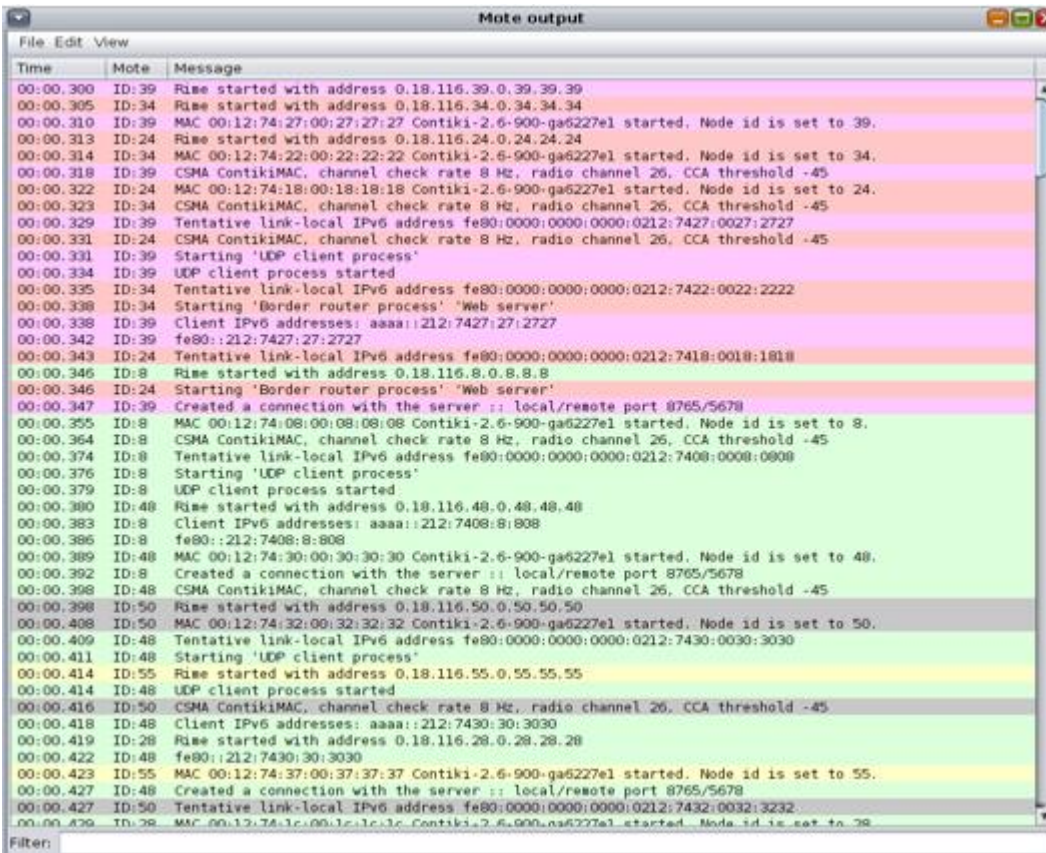


Figure 8. The output of ad hoc network implementation.

In power trace, a loss in power is observed when using the Standard AES algorithm to send data between sender (Radio TX) and receiver (Radio RX), as shown in Table 1. Therefore, the lost power in Radio TX and RX for 55 mote (node) for a lot of nodes. The total loss in power for Radio TX is 0.32% and for Radio RX is 0.03%.

Table 1  
The power trace for Standard AES algorithm

Mote	Radio on (%)	Radio TX (%)	Radio RX (%)
Sky1	0.00%	0.00%	0.00%
Sky 2	1.34%	0.48%	0.02%
Sky 3	1.28%	0.49%	0.00%
Sky 4	0.80%	0.00%	0.07%
Sky 5	1.39%	0.48%	0.06%
Sky 6	1.4 1%	0.48%	0.03%
Sky 7	0.73%	0.00%	0.03%
Sky 8	0.73%	0.00%	0.02%
Sky 9	1.37%	0.48%	0.03%
Sky 10	1.37%	0.49%	0.02%
Sky 11	0.81%	0.00%	0.04%
Sky 12	0.78%	0.00%	0.04%
Sky 13	1.37%	0.49%	0.02%
Sky 14	1.32%	0.48%	0.01%
Sky 15	0.85%	0.00%	0.09%
Sky 16	1.46%	0.48%	0.05%
Sky 17	1.35%	0.49%	0.02%
Sky 18	1.48%	0.48%	0.07%
Sky 19	0.68%	0.00%	0.02%
Sky 20	1.36%	0.48%	0.03%
Sky 21	1.33%	0.49%	0.02%
Sky 22	1.34%	0.49%	0.03%
Sky 23	0.74%	0.00%	0.03%
Sky 24	1.38%	0.49%	0.03%
Sky 25	1.39%	0.48%	0.05%
Sky 26	1.39%	0.48%	0.03%
Sky 27	0.79%	0.00%	0.05%
Sky 28	1.49%	0.49%	0.09%
Sky 29	1.29%	0.49%	0.00%
Sky 30	0.77%	0.00%	0.03%
Sky 31	0.82%	0.00%	0.06%
Sky 32	1.4 1%	0.48%	0.03%
Sky 34	1.47%	0.48%	0.04%
Sky 35	0.71%	0.00%	0.03%
Sky 36	1.31%	0.48%	0.00%
Sky 37	1.32%	0.49%	0.02%
Sky 38	1.33%	0.48%	0.03%
Sky 39	0.73%	0.00%	0.05%
Sky 40	1.38%	0.49%	0.01%
Sky 41	1.38%	0.49%	0.02%
Sky 42	1.30%	0.49%	0.00%
Sky 43	0.75%	0.00%	0.03%
Sky 45	1.36%	0.48%	0.03%
Sky 46	1.47%	0.48%	0.06%
Sky 47	1.38%	0.48%	0.01%
Sky 48	0.85%	0.00%	0.07%
Sky 49	1.40%	0.49%	0.03%
Sky 50	0.81%	0.00%	0.08%
Sky 51	1.35%	0.48%	0.03%
Sky 52	1.34%	0.48%	0.03%
Sky 53	0.81%	0.00%	0.06%
Sky 54	1.47%	0.48%	0.03%
Sky 55	1.35%	0.49%	0.02%
Average	1.16%	0.32%	0.03%

In proposed AES lightweight algorithm, the power loss for sender and receiver is better than the standard algorithm. Table 2 presents the power trace for the proposed algorithm.

Table 2  
The power trace for the proposed AES algorithm

Mote	Radio on (%)	Radio TX (%)	Radio RX (%)
Sky1	0.00%	0.00%	0.00%
Sky 2	1.48%	0.48%	0.06%
Sky 3	1.39%	0.48%	0.00%
Sky 4	0.76%	0.00%	0.07%
Sky 5	1.43%	0.48%	0.06%
Sky 6	1.38%	0.48%	0.03%
Sky 7	0.75%	0.00%	0.03%
Sky 8	0.74%	0.00%	0.02%
Sky 9	1.34%	0.48%	0.03%
Sky 10	1.36%	0.48%	0.03%
Sky 11	0.00%	0.00%	0.00%
Sky 12	0.00%	0.00%	0.00%
Sky 13	0.00%	0.00%	0.00%
Sky 14	0.00%	0.00%	0.00%
Sky 15	0.00%	0.00%	0.00%
Sky 16	0.00%	0.00%	0.00%
Sky 17	0.00%	0.00%	0.00%
Sky 18	0.00%	0.00%	0.00%
Sky 19	0.00%	0.00%	0.00%
Sky 20	0.00%	0.00%	0.00%
Sky 21	0.00%	0.00%	0.00%
Sky 22	0.00%	0.00%	0.00%
Sky 23	0.00%	0.00%	0.00%
Sky 24	0.00%	0.00%	0.00%
Sky 25	0.00%	0.00%	0.00%
Sky 26	0.00%	0.00%	0.00%
Sky 27	0.00%	0.00%	0.00%
Sky 28	0.00%	0.00%	0.00%
Sky 29	0.00%	0.00%	0.00%
Sky 30	0.00%	0.00%	0.00%
Sky 31	0.00%	0.00%	0.00%
Sky 32	0.00%	0.00%	0.00%
Sky 34	0.00%	0.00%	0.00%
Sky 35	0.00%	0.00%	0.00%
Sky 36	1.37%	0.48%	0.03%
Sky 37	1.33%	0.48%	0.02%
Sky 38	0.80%	0.00%	0.05%
Sky 39	1.35%	0.48%	0.02%
Sky 40	1.35%	0.48%	0.04%
Sky 41	1.46%	0.48%	0.07%
Sky 42	0.82%	0.00%	0.02%
Sky 43	1.35%	0.48%	0.04%
Sky 45	1.34%	0.48%	0.01%
Sky 46	0.75%	0.00%	0.05%
Sky 47	1.36%	0.48%	0.03%
Sky 48	1.38%	0.48%	0.01%
Sky 49	0.72%	0.00%	0.03%
Sky 50	0.73%	0.00%	0.00%
Sky 51	1.35%	0.48%	0.02%
Sky 52	1.36%	0.48%	0.01%
Sky 53	0.76%	0.00%	0.03%
Sky 54	1.43%	0.48%	0.05%
Sky 55	1.34%	0.48%	0.02%
Average	0.69%	0.19%	0.02%

As shown in tables above, the power loss for the sender (Radio Tx) is better than the Standard in many motes (nodes), as the power lost in Radio TX and Radio RX is relatively low. The total loss in power is 0.19% for Radio TX and 0.02% for Radio RX. This is an improvement by merging Sub Byte and Shift Row, which results in the formation of a new sub instead of Mix Column. This leads to less consumption of time and power in the proposed algorithm. Additionally, these values are presented as charts below to show the difference between algorithms:

Figure 9 below shows the motes, Radio TX and Radio RX in proposed algorithm. The motes from 11 to 35 show no power lost for Radio TX and Radio RX, being 0. Meanwhile, other motes have values that represent the loss of power.

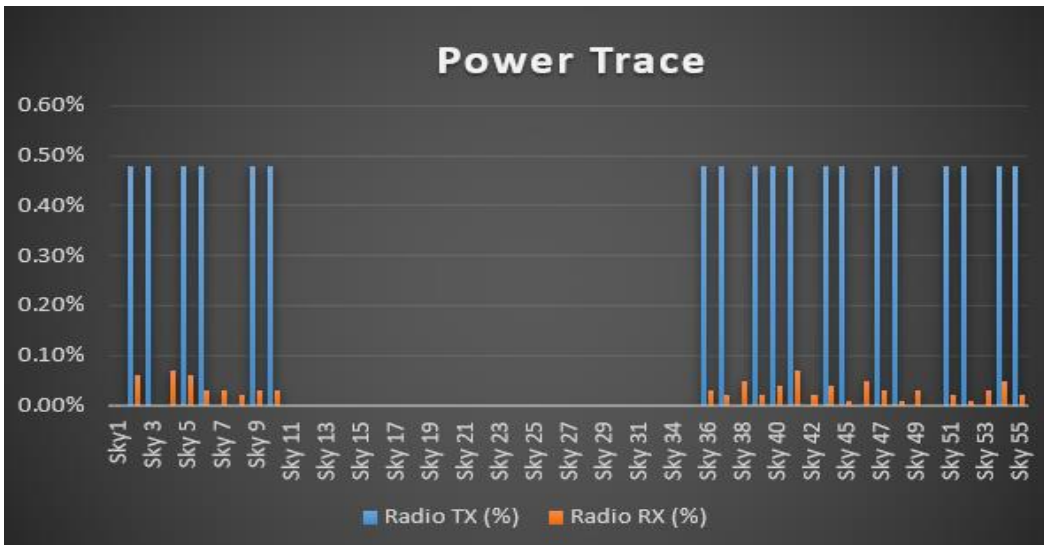


Figure 9. The power trace for the proposed algorithm

In addition, Figure 10 shows the motes, Radio TX and Radio RX in the standard algorithm. A large amount of power is lost in a lot of motes in Radio TX and Radio RX as compared to the proposed algorithm

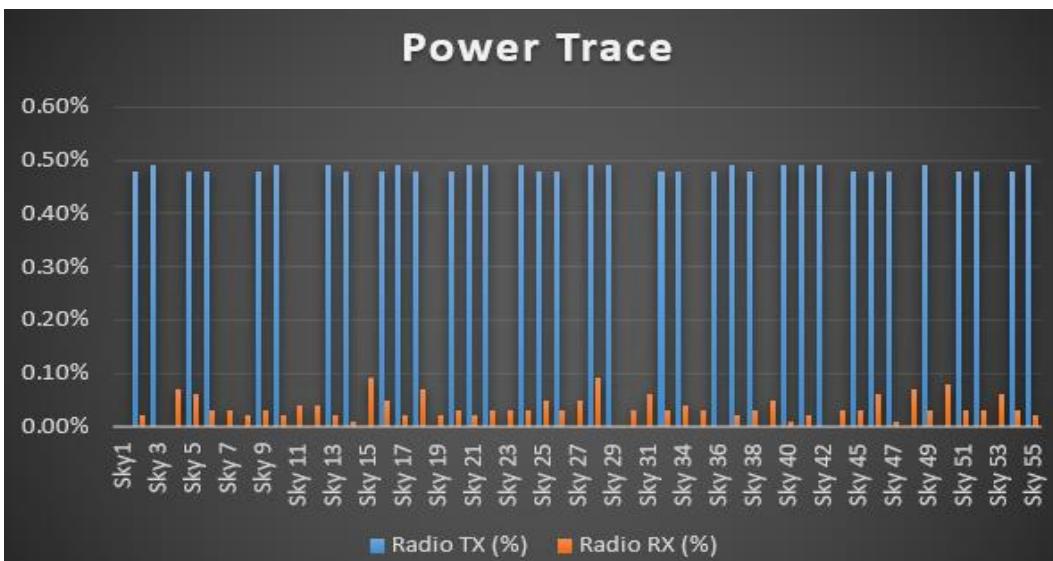


Figure 10. The power trace for the Standard algorithm

The result of the work analysis is presented using the Wireshark, Figure 11 represents the captured packet using the proposed AES lightweight algorithm for clients and servers, Ip Address for the source and destination, clarification of the throughput, and packet loss of Ad-Hoc network.

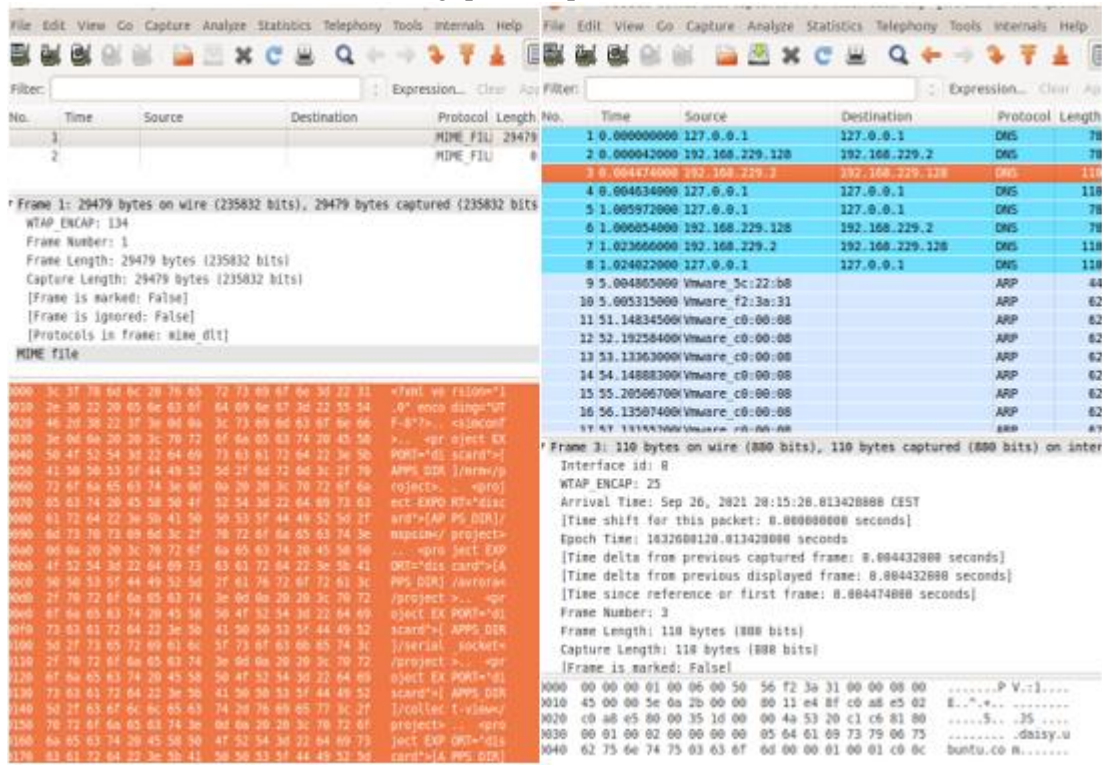


Figure 11. Wireshark Analysis Results

According to the simulation and Wireshark analysis, it is concluded that the time used in the proposed AES lightweight algorithm is less than that of the standard AES algorithm by **8 seconds and some milliseconds**, as shown in Figure 12.

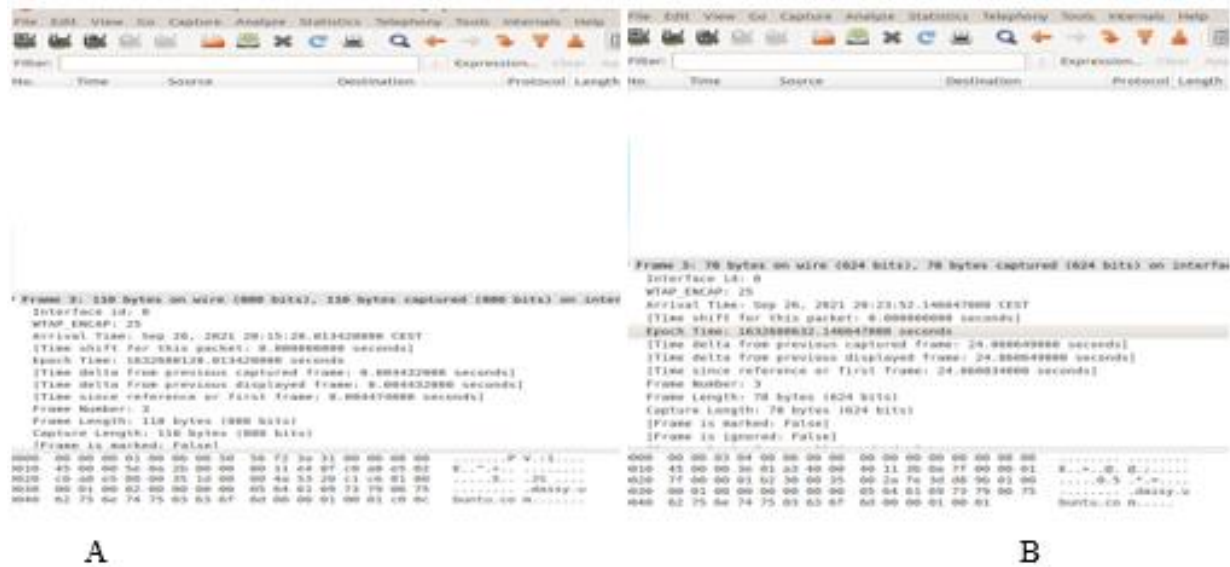


Figure 12. A. Arrival time for the proposed algorithm, B. Arrival time for the Standard algorithm.

#### 4. Comparison of Previous Works

The present work is considered an extension of previous works, with the main objective of solving security problems in Ad-hoc networks. This section draws a comparison between this work and earlier related researches, as summarized in Table 3.

Table 3  
Comparison of previous works

Ref No.	Algorithm used	Technology used	Environment work	Implementation tool	Enhance security	Enhance time and power consuming
Usman et al. (2017)	Secure IoT (SIT).	mix of feistel and uniform substituting-permutating networks.	IOT	MATLAB	✓	✗
Kunchok and Kirunbanand (2018)	Lightweight hybrid encryption system with ECDH and AES.	ECDH key exchange mechanism to generate keys and establish connections, digital signatures for authenticating, followed by the AES algorithm to encrypt and decrypt user data files.	IOT	IOT	✓	✗
Aziz and Singh (2019)	efficient lightweight security scheme (LSS).	CS method used to solve security issue and energy.	IOT	Intel Berkeley research lab	✓	✗
Mohanty et al. (2018)	lightweight integrated Blockchain (ELIB)	ELIB with public blockchain for enhancing security and privacy.	IOT	Block chain	✓	✗
Keshav Kumar et al. (2020)	AES lightweight algorithm	AES lightweight algorithm to encrypt voice signal on peer-to-peer communication.	IOT	FPGA	✓	✗
Fadhil et al. (2021)	Lightweight AES encryption algorithm	Lightweight AES encryption algorithm to provide in IOT system. It is worked on Raspberry	IOT	Raspberry	✓	✗
Hussein M. et al. (2022)	AES lightweight algorithm	Lightweight AES encryption algorithm to provide security in IOT system. However, enhance the delay in time	IOT	Asp.net	✓	✓
The proposed work	AES lightweight algorithm	Using the outputs of Sub byte and Shift row to make an exclusive or (XOR) to be used instead of the MixColumns	Ad-Hoc	Cooja	✓	✓



## 5. Comparison of Standard AES and Enhanced AES Lightweight Algorithm

Table 4

Comparison between standard AES and enhanced AES lightweight algorithm

Item	Standard AES	Enhanced AES lightweight
Security	High	High
Time	Using a lot of time	Using a little time
Key Exchange Algorithm	Classical Algorithms	Lightweight algorithms
Packet loss	More	Less
Power saving	Less	More

## 5. Conclusion

Lightweight cryptography is a technique used for securing information in a developed manner that uses low assets and gives high throughput while consuming less power. This paper proposed an AES lightweight algorithm for reducing the amount of time and power that is consumed in ad hoc network. An XOR operation is conducted between the Sub byte and the Shift row, resulting in a new sub. This sub is used as a replacement of the Mix Column, thereby eventually resulting in the reduction of overall time and power consumption. The results for the proposed AES lightweight algorithm are found to be better than the standard AES algorithm in power and time consumption when transmitting the packets between nodes.

## Author Contributions

Mustafa AL-handhal: Collected data and wrote the article.

Alharith A. Abdullah: Planned the analysis and wrote the article.

Oğuz Ata: Made the statistical analysis.

Çağatay Aydın: Worked on simulations.

## Conflicts of Interest

The authors declare no conflict of interest.

## References

- Abdullah, A. A., & Obeid, N. R. (2021). Efficient Implementation for PRINCE Algorithm in FPGA Based on the BB84 Protocol. In *Journal of Physics: Conference Series*, 1818(1), 122-216. Retrieved from: <http://psychologyandeducation.net/pae/index.php/pae/article/view/3215/2869>
- Abdullah, D.; Rahim, R.; Siahaan, A.P.U.; Ulva, A.F.; Fitri, Z.; Malahayati, M.; Harun, H. (2018). Super-Encryption Cryptography with IDEA and WAKE Algorithm. *Journal of Physics: Conference Series*. doi: <https://doi.org/10.1088/1742-6596/1019/1/012039>
- Alyas, H. H., & Abdullah, A. A. (2021). Enhancement the ChaCha20 Encryption Algorithm Based on Chaotic Maps. In *Next Generation of Internet of Things Springer, Singapore*, 91-107. doi: [https://doi.org/10.1007/978-981-16-0666-3\\_10](https://doi.org/10.1007/978-981-16-0666-3_10)
- Aziz, A., & Singh, K. (2018). Lightweight security scheme for Internet of Things. *Wireless personcommunication Issue, Springer online available* doi:<https://doi.org/10.1007/s11277-018-6035-4>.
- Basagni, S., Conti, M., Giordano, S., & Stojmenovic, I. (Eds.). (2004). *Mobile ad hoc networking. John Wiley & Sons* Retrieved from: <https://doc.lagout.org/network/Mobile%20Ad%20Hoc%20Networking.pdf>
- Costa, D. G., Figuerêdo, S., & Oliveira, G. (2017). *Cryptography in wireless multimedia sensor networks: A*



- survey and research directions. *Cryptography*, 1(1), 4. doi:<https://doi.org/10.3390/cryptography1010004>
- Elmahdi, E., Yoo, S. M., & Sharshembiev, K. (2018). Securing data forwarding against blackhole attacks in mobile ad hoc networks. In *IEEE 8th annual computing and communication workshop and conference (CCWC)*, 463-467. doi: <https://doi.org/10.1109/CCWC.2018.8301683>
- Fadhil, Meryam Saad, Alaa Kadhim Farhan, and Mohammad Natiq Fadhil. (2021)"A lightweight AES Algorithm Implementation for Secure IoT Environment." *Iraqi Journal of Science* 62.8: 2759-2770. doi:10.24996/ij.s.2021.62.8.29
- Hussein M. Mohammad, Alharith A. Abdullah. (2022). Enhancement process of AES: a lightweight cryptography algorithm-AES for constrained devices, *Journal of TELKOMNIKA Telecommunication Computing Electronics and Control*, 551-560. doi: 10.12928/TELKOMNIKA.v20i3.23297
- I.Vanda, L. Buttyán . (2003).Lightweight authentication protocols for low-cost RFID tags, in *Second Workshop on Security in Ubiquitous Computing-Ubicomp*. Retrieved from: <http://www.mscs.mu.edu/~iq/papers/rfid/Lightweight%20Authentication%20protocols%20for%20low%20cost%20RFIDs.pdf>
- J. Daemen, V. Rijmen, and K. U. Leuven.(1999), AES Proposal: Rijndael. (NIST), *National Institute of Standards* Retrieved from: <http://citeseerx.ist.psu.edu/viewdoc/summary?>
- Kumar, K., Ramkumar, K.R., Kaur, A., (2020) A Lightweight AES Algorithm Implementation for Encrypting Voice Messages using Field Programmable Gate Arrays, *Journal of King Saud University - Computer and Information Sciences*. doi: <https://doi.org/10.1016/j.jksuci.2020.08.005>
- Mohanty, S.N.; Ramya, K.C.; Rani, S.S.; Gupta, D.; Shankar, K.; Lakshmanprabu, S.K.; Khanna, A. (2020).An efficient Lightweight integrated Blockchain (ELIB) model for IoT security and privacy. *Future Generation. Computer System*, doi: <https://doi.org/10.1016/j.future.2019.09.050>
- Muhammad Usman, Irfan Ahmed, M. Imran Aslam, Shujaat Khan and Usman Ali Shah.(2017). SIT: A Lightweight Encryption Algorithm for Secure Internet of Things, *International Journal of Advanced Computer Science and Applications*, 8( 1). Retrieved from: <https://arxiv.org/pdf/1704.08688.pdf>
- N. I. of Standards-(NIST), Advanced Encryption Standard (AES). (2001). *Federal Information Processing Standards Publication197*. Retrieved from: <https://nvlpubs.nist.gov/nistpubs/fips/nist.fips.197.pdf>.
- P.V.S. Shastry, A. Agnihotri, D. Kachhwaha, J. Singh and M.S. Sutaone.(2011). A Combinational Logic Implementation of S-Box of AES, *IEEE 54th Int. Midwest Symp on Circuits and Systems (MWSCAS)*, 1-4. doi: <https://doi.org/10.1109/MWSCAS.2011.6026559> .
- S. Agwa, E. Yahya, and Y. Ismail. (2017). Power efficient AES core for IoT constrained devices implemented in 130nm CMOS, *Proc. - IEEE International Symposium on Circuits & System.*, 2–5. doi: <https://doi.org/10.1109/ISCAS.2017.8050361>
- Schneier, B. (2015). *Secrets and lies: digital security in a networked world*. John Wiley & Sons. Retrieved from:<https://www.wiley.com/enus/Secrets+and+Lies%3A+Digital+Security+in+a+Networked+World%2C+15th+Anniversary+Edition-p-9781119092438>
- Tenzin Kunchok, Prof. Kirubanand V. B. (2018). A lightweight hybrid encryption technique to secure IoT data transmission, *International Journal of Engineering & Technology*, 7 (2), 236-240. doi: <https://doi.org/10.14419/ijet.v7i2.6.10776>
- V.Rani, Dr. Renu Dhir. (2013). A Study of Ad Hoc Network: A Review, *International Journal of Advanced Research in Computer and Communication Engineering*, 3, Issue 3. Retrieved from: <http://www.ijarcse.com>.
- William Stallings.(2000). *Cryptography and Network Security: Advanced Encryption Standard*.Retrieved from: <http://www.cs.man.ac.uk/~banach/COMP61411.Info/CourseSlides/Wk2.3.AES.pdf>



# The Effect of Nitrogen and Phosphorus Limitations at Different Salt Ratios on Growth and Biochemical Composition of *Tetraselmis suecica* (Chlorodendrophyceae)

Cananur Sisalan Pihava<sup>1</sup>, Leyla Uslu<sup>2,\*</sup>

<sup>1,2</sup>Fisheries Faculty, Çukurova University, Balcalı Campüs, Adana, Türkiye

## Article History

Received: 26.04.2022

Accepted: 16.06.2022

Published: 15.12.2022

## Research Article

**Abstract** – Algae are plant organisms that produce organic molecules in the aquatic environment and absorb carbon. Since algae are photosynthetic organisms, they give oxygen to the environment. Algae, one of the most important living resources of the seas, are used in many fields such as food, agriculture, cosmetics, medicine, pharmacy, industry and also as a biofuel source thanks to the metabolites they store in the cell. In the study carried out to determine the effects of nitrogen and phosphorus limitations at different salinity rates on the chlorophyll *a*, dry weight, optical density, protein, lipid and fatty acid contents of the microalgae *Tetraselmis suecica* from the class Chlorodendrophyceae cultured in the laboratory conditions, at %15, 30 and 45 salinity rates 50% N and 50% P reductions were applied. The lowest growth was detected in the culture containing 50% N(-). The highest lipid ratio was determined as 39.8±1% in the 50% N(-) group, while the closest ratio was 34.6% in the 50% P(-) group. The highest polyunsaturated fatty acids were determined in the group containing 50% P(-) at all salinity values. The protein value was determined as 22.3% in the 50% P(-) group and 15.7% in the 50% N(-) group at %30 salinity.

**Keywords** – Fatty acids, growth, lipid, protein, N limitation, P limitation, salinity, *tetraselmis suecica*.

## 1. Introduction

Various factors affect the development of algae; In addition to factors such as light, temperature, pH, salinity is one of the most important environmental factors affecting phytoplankton development, metabolism and distribution (Alsull et al., 2012). Marine phytoplanktonic organisms have a very good tolerance to salinity changes. According to the salinity in the natural environment, many algae species also grow well at lower or higher salinities. Although many algae grow in the %12-44 salinity range, they prefer the optimum %20-24 salinity. However, there are algae species that can survive even at %140 salinity, where most of them cannot survive (Ben-Amotz, & Avron, 1983; Borowitzka, & Borowitzka, 1988). E.g; While *Isochrysis galbana* shows maximum growth at %15, *Tetraselmis suecica* prefers %25-35 salinity (Vonshak, & Tomaselli, 2000). Microalgae, like land plants, require light, carbon dioxide, water and inorganic salts for growth. Although their production seems to be costlier when compared to agricultural crops, it is more advantageous in that they can be divided within hours and produced throughout the year (Siaut et al, 2007; Grobbelaar, 2004). Reducing the cost of algae production is possible with the use of sunlight, seawater and carbon dioxide from greenhouse gases. The main elements used in algae production are nitrogen (N), phosphorus (P), sodium (Na), iron (Fe). Since most of these elements are in seawater, it can reduce the cost of the culture medium in the production of marine microalgae (Mirón et al., 2003). After carbon, the most important nutrient for living mass production is N. In general, N constitutes between 1% and 10% of their dry weight (Gökpınar and Cirik, 1991). N is one

<sup>1</sup> cananursisalan@gmail.com

<sup>2</sup> hizarcil@cu.edu.tr

\*Corresponding Author

of the most important factors affecting growth and biochemical composition in algae cultures. The lack of N in the culture medium causes a decrease in the amount of dry matter and chl *a*, and an increase in carotene and lipids (Sukenik et al., 1989). Chemical and physical factors in the culture medium can also affect the content of fatty acids. Increased lipid content has been observed in many microalgae species grown with N restriction. In the late 1940s, N starvation was found to be effective on fat storage and a lipid level of 70-85% in dry weight was reported. *Dunaliella* sp. and some algae species, such as *T. suecica*, contain low lipids and generally produce carbohydrates rather than lipids. Besides N, some other nutritional deficiencies can also cause an increase in lipid content (Piorreck and Pohl, 1984). P is an important nutrient for algae and a component of molecules such as phospholipids and nucleic acids. In plants, P plays an important role in many critical metabolic processes, especially photosynthesis and respiration (Plaxton and Tran, 2011). The presence of P in the aquatic environment is especially important for algae and other aquatic organisms. The use of P in seawater not only affects cell volume, nutritional status, photosynthetic activity, and other biochemical and physiological properties of algal cells, but also affects the composition and quantity of the marine phytoplankton community (Benitez-Nelson, 2000; Paytan and McLaughlin, 2007). Two of the most important problems in our world today are undoubtedly environmental pollution and increasing energy needs. Environmentally-friendly production, sustainable environment and sustainable green economy have started to form the agenda of countries. The use of microalgae in environmental applications is increasing and microalgae technology is developing rapidly. The use of microalgae in preventing water pollution and in bioenergy is seen as an important ecological investment for the future. For this purpose, many studies need to investigate the environmental uses of rapidly developing microalgae technology and its potential in meeting energy needs (Sisman-Aydin, 2019). In this study, the effects of 3 different salinity (‰15, 30 and 45) and nutrient deficiencies (50% N(-) and 50% P(-)) on growth, protein, lipid and fatty acid changes in *T. suecica* were investigated.

## 2. Materials and Methods

### 2.1. Inoculum source and cultivation conditions

*T. suecica* (UTEX LB 2286) used in the study was obtained from UTEX Culture Laboratory. The study was carried out in Çukurova University Fisheries Faculty Algal Biotechnology laboratory. *T. suecica* belonging to the class Chlorodendrophyceae was used in the study. *T. suecica* is a green, four flagellated and motile marine microalgae. It is usually 10 µm long by 14 µm wide. *Tetraselmis* is a promising microalgae species for biofuel use due to its rapid growth rate and high lipid content (Alonso et al., 2012).

In the experiment, the F/2 culture medium (Guillard, 1973) was used as the medium. The experiment was carried out in a laboratory environment. Cultures were replicated first in flasks and then in balloons and sufficient amount of inoculum was prepared. In the experiment, N and P deficiency were tested at 3 different salinity ratios. Salinity ratios were adjusted to be ‰15, 30 and 45 and a control group for each salt concentration was formed. In other groups, experiments were established by making 50% N and 50% P deficiency. The inoculation rate to be used in the trial was adjusted to be 20% and the trial was set up in 5L volumes. From the beginning of the experiment to the last day of the experiment, samples were taken from the trial dishes in order to determine the optical density (OD), biomass and chl *a* value.

### 2.2. Biomass (Dry weight), Chlorophyll *a* (Chl *a*) and Optical Density (OD)

Dry weight amount was determined according to Vonshak, 1997. To determine the amount of Chl *a* throughout the experiment, 5 ml samples were taken from the balloons of each treatment group. The samples taken were filtered through GFC filter. 10 ml of 95% ethanol was added to the samples. Samples were left in the refrigerator (+4°C) for 24 hours in the dark after shaking. At the end of the extraction period, the upper clear part was taken and the absorption values were measured at 649 and 665 nm in the visible spectrophotometer. The results were calculated using the following formulas (Eq. 2.1.) (Kulkarni, & Nikolov, 2018).

$$\text{Chl } a \left(\frac{\text{mg}}{\text{g}}\right) = 13.36 * \text{Abs}_{665\text{nm}} - 5.19 * \text{Abs}_{649\text{nm}} \quad (2.1)$$

In order to measure OD, after the cultures were mixed homogeneously daily, 3 ml of sample was taken with the help of a pipette. The samples taken from the tubes were placed in quartz cuvettes and the visible spectrophotometer was read at a wavelength of 680 nm (Wong, & Franz, 2013).

### 2.3. Lipid, fatty acids and protein analysis

Lipid analysis was performed according to the method applied by Bligh and Dyer (1959). 0.2g homogenized sample was mixed with a Warring blender after adding 120 ml of methanol/chloroform (1/2). Then, these samples were added to 20 ml of 0.4% CaCl<sub>2</sub> solution and filtered through filter paper (Scliecher & Schuell, 5951/2 185 mm) and kept in an oven at 105 °C for 2 hours and then filtered into flasks that were tared. These balloons were closed in such a way that their mouths were not airtight and kept in a dark environment for 1 night, and the next day, the top layer consisting of methanol-water was removed with the help of a separating funnel. Chloroform from the chloroform-lipid part remaining in the balloons was evaporated using a rotary evaporator in a water bath at 60 °C. Then, the balloons were kept in the oven at 90 °C for 1 hour, allowing all the chloroform in them to evaporate, and cooled to room temperature in a desiccator and weighed on a precision balance with 0.1 mg sensitivity. The following formula was used to calculate the lipid ratio (Eq. 2.2).

$$\text{Lipid}\% = \frac{(\text{Ballon tare}(g) + \text{Lipid}(g)) - (\text{Ballon tare}(g)) * 100}{\text{amount of sample}(g)} \quad (2.2)$$

From the extracted lipid, fatty acid methyl esters were made according to the method of Ichihara et al. (1996). 4mL of 2M KOH and 2mL of n-heptane were added to 25 mg of extracted lipid sample. Then, it was vortexed for 2 minutes at room temperature and centrifuged at 4000 rpm for 10 minutes, and the heptane layer was analyzed by gas chromatography (GC).

#### 2.3.1. Gas chromatographic conditions

Fatty acid content was analyzed using a GC Clarus 500 instrument (Perkin–Elmer, USA), a flame ionization detector (FID) and an SGE (60mx0.32mm ID BPX70x0.25 μm, USA) column. Injector and detector temperatures were adjusted as 260°C and 230°C, respectively. In the meantime, the oven temperature was kept at 140°C for 8 minutes, then it was increased by 4°C every minute until 220°C, from 220°C to 230°C by 4°C every minute and kept at 230°C for 15 minutes, the analysis was completed after a total of 45.5 minutes. By controlling the sample size at 1 μl and the carrier gas at 16ps, the split current ratio of 40.0mL/min (1:40) was used. Fatty acids were determined depending on the arrival times of the FAME mixture consisting of standard 37 components (Supelco 37 F.A.M.E. Mix C4-C24 Component, Catalogue No. 18919).

Total crude protein was made in the Kjeldahl apparatus according to the Kjeldahl method (AOAC, 1998). The amount of protein was calculated according to the formula in the following equation (Eq. 2.3)

$$\%N = \frac{14.01 * (A - B) * M}{g * 10} * 100$$

$$\%Protein = \%N * 6.25 \quad (2.3)$$

A: The amount of HCl consumed for the sample

B: The amount of HCl consumed for the blind

M: Acid molarity

g: Sample quantity

### 3. Result and Discussion

In this study, which was carried out to determine the effect of nutrient deficiency on the growth and biochemical structure of *T. suecica* in the Çukurova University Fisheries and Algal Biotechnology Laboratory, at ‰15, 30 and 45 salinities; 50% N and 50% P deficiencies were tried and the trial was completed on different days. In the experiment, chl *a*, dry weight analysis, OD, protein, lipid and fatty acid analyzes were performed.

#### 3.1. Optical Density (OD)

Optical densities were determined in order to monitor the growth of *T. suecica*, which was cultured in environments where salt concentrations of ‰15, 30 and 45 were applied and N and P were reduced by 50%. When the growth curve of *T. suecica* cultures at ‰45 salt concentration is examined, it is seen that the logarithmic phase starts with 50% N(-), 50% P(-) with inoculation, and a lag phase lasting approximately one day in the control group (Figure 1). While the OD values were lower in the 50% P-reduced culture than in the control group, the lowest OD values were determined in the 50% N-reduced culture. The highest OD values in cultures treated with 50% P(-) and 50% N(-) were determined as  $0.376 \pm 0.01$  and  $0.269 \pm 0.02$ , respectively.

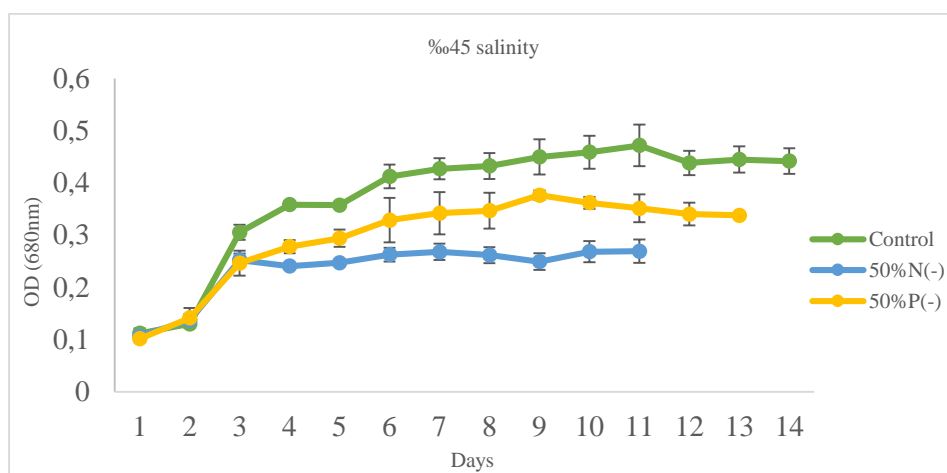


Figure 1. OD values of *T. suecica* groups at ‰45 salinity.

When the growth curve of *T. suecica* cultures at ‰30 salt concentration is examined, it is seen that the logarithmic phase begins with the inoculation in 50% N(-), 50% P(-) and control groups (Figure 2). As seen in the growth curve, OD values in 50% N(-), 50% P(-) and control groups show a similar increase until the 4<sup>th</sup> day, and after the 4<sup>th</sup> day, the OD values in 50% N(-), 50% P(-) cultures decrease is observed. After the 6<sup>th</sup> day of growth, the growth was lower in the culture containing 50% N(-). The highest OD values in cultures treated with 50% P(-) and 50% N(-) were determined as  $0.377 \pm 0.02$  and  $0.291 \pm 0.007$ , respectively.

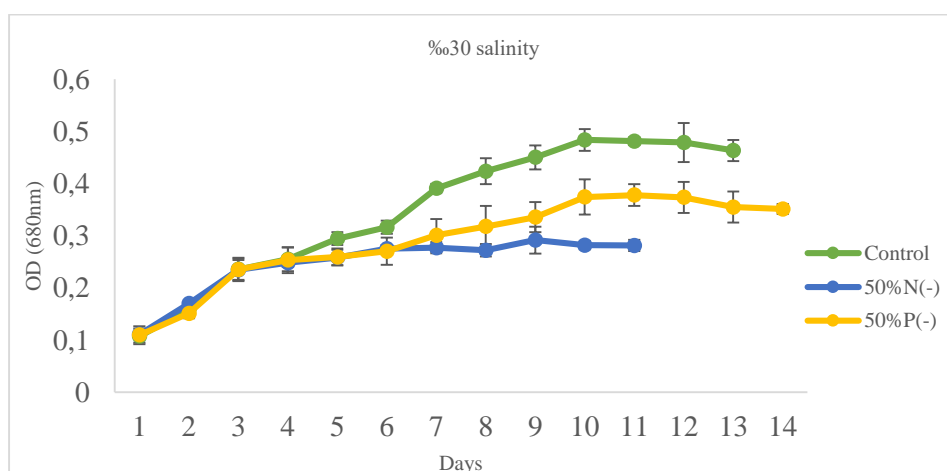


Figure 2. OD values of *T. suecica* groups at ‰30 salinity.

When the growth curve of *T. suecica* cultures at %15 salt concentration is examined, 50% N(-), 50% P(-) and in the control group, the logarithmic phase started with inoculation and as seen in the growth curve, 50% N(-), 50% P(-) and the control group showed a similar increase in OD values until the 3<sup>rd</sup> day. From the 3<sup>rd</sup> day of growth, a decrease in OD values was observed in 50% P(-) cultures compared to the control group, and the lowest OD values were recorded in 50% N(-) cultures (Figure 3). While the highest determined OD value was  $0.402\pm 0.01$  in the control group, the highest OD values were determined as  $0.350\pm 0.01$  and  $0.311\pm 0.03$  in cultures treated with 50% P(-) and 50% N(-), respectively.

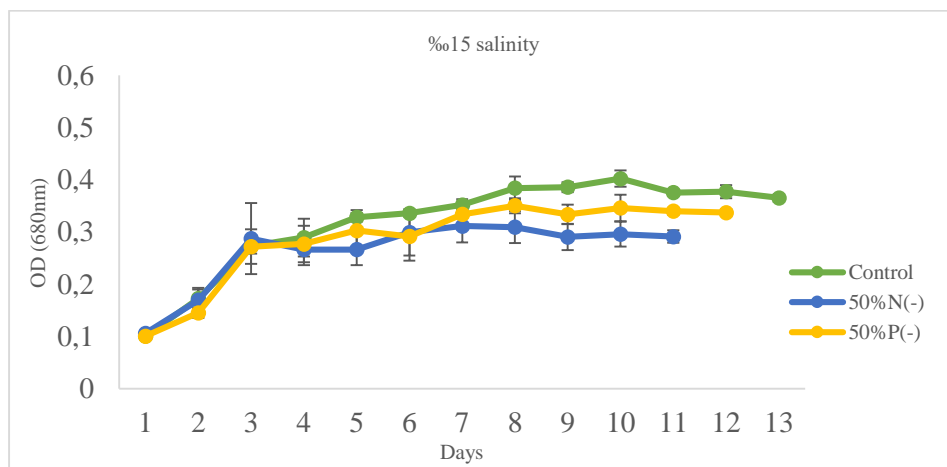


Figure 3. OD values of *T. suecica* groups at 15‰ salinity.

At %15, 30 and 45 salt concentrations, OD values were higher in cultures treated with 50% P(-) compared to 50% N(-) cultures. It is observed that the salinity ratios applied in cultures treated with N and P deficiency have no effect.

### 3.2. Dry Weight

The amounts of dry weight in the groups applied 50% N(-) and 50% P(-) at %45, 30 and 15 salt concentrations are as summarized in the table below (Table 1). As seen in the table, the lowest dry weight values at all three salinity concentrations were determined in the culture applied with 50% N(-). The amount of dry weight in the culture treated with 50% P(-) was higher than the group treated with 50% N(-) and lower than the control group.

Table 1

Dry weight (dw) of groups ( $\text{gL}^{-1}$ )

Salinity (‰)		Control	50% N(-)	50% P(-)
45	dw <sub>first</sub>	$0.045\pm 0.004$	$0.042\pm 0.01$	$0.403\pm 0.002$
	dw <sub>last</sub>	$0.218\pm 0.001^a$	$0.128\pm 0.01^c$	$0.164\pm 0.001^b$
	dw <sub>max.</sub>	$0.223\pm 0.01^a$	$0.128\pm 0.01^c$	$0.184\pm 0.004^b$
30	dw <sub>first</sub>	$0.043\pm 0.007$	$0.045\pm 0.008$	$0.044\pm 0.002$
	dw <sub>last</sub>	$0.229\pm 0.005^a$	$0.134\pm 0.02^c$	$0.173\pm 0.02^b$
	dw <sub>max.</sub>	$0.240\pm 0.006^a$	$0.139\pm 0.01^c$	$0.185\pm 0.03^b$
15	dw <sub>first</sub>	$0.040\pm 0.001$	$0.042\pm 0.001$	$0.039\pm 0.003$
	dw <sub>last</sub>	$0.178\pm 0.003^a$	$0.139\pm 0.006^c$	$0.163\pm 0.003^b$
	dw <sub>max</sub>	$0.197\pm 0.008^a$	$0.150\pm 0.01^c$	$0.170\pm 0.007^b$

There is a statistical difference between the means of lines symbolized by the letters a, b, c ( $p < 0.05$ ).



### 3.3. Chlorophyll *a*

Consistent with the OD measurements and dry weight amounts in the treatment groups, it was determined that chl *a* values were higher in the 50% P(-) applied group at %15, 30 and 45 salt concentrations than in the 50% N(-) applied group and lower than the control group. %The chl *a* value of the group administered 50% P(-) at 30 salt concentration was 0.198 mgL<sup>-1</sup>, the chl *a* value of the group with 50% N deficiency was higher than 0.121 mgL<sup>-1</sup>, and the chl *a* value of the control group was lower than 0.261 mgL<sup>-1</sup> has been. %30 salinity was the salt concentration with the highest chl *a* values in all three groups (Table 2).

Table 2

Chl *a* amounts of all groups (mgL<sup>-1</sup>)

Salinity(‰)		Control	50% N(-)	50% P(-)
45	Chl <sub>first</sub>	0.064±0.001	0.067±0.01	0.062±0.002
	Chl <sub>last</sub>	0.148±0.002 <sup>a</sup>	0.089±0.01 <sup>c</sup>	0.111±0.001 <sup>b</sup>
30	Chl <sub>first</sub>	0.063±0.007	0.067±0.008	0.064±0.002
	Chl <sub>last</sub>	0.261±0.005 <sup>a</sup>	0.121±0.02 <sup>c</sup>	0.198±0.0 <sup>b</sup>
15	Chl <sub>first</sub>	0.068±0.001	0.061±0.001	0.065±0.003
	Chl <sub>last</sub>	0.138±0.003 <sup>a</sup>	0.09±0.006 <sup>c</sup>	0.114±0.003 <sup>b</sup>

There is a statistical difference between the means of lines symbolized by the letters a, b, c (p<0.05).

### 3.4. Protein Values

A significant effect of 50% N(-) and 50% P(-) treatments on protein content were found at %15, 30 and 45 salt concentrations applied in the experiment (p<0.05). The highest protein value was determined in %30 salinity groups, while the lowest values were determined in %45 salinity groups. While the high protein rate at %30 salinity was determined as 22.3% in the 50% P(-) applied group, the protein rate was determined as 20.1% at %30 salinity in the 50% N(-) applied group. The highest protein content was recorded at 26.8%, %30 salinity in the control group (Table 3).

Table 3

Protein amounts of the groups (%)

Salinity(‰)	Control	50%N(-)	50%P(-)
45	20.6±2 <sup>c</sup>	10.3±1 <sup>c</sup>	16.4±2 <sup>c</sup>
30	26.8±1 <sup>a</sup>	15.7±1 <sup>a</sup>	22.3±1 <sup>a</sup>
15	25.3±1 <sup>b</sup>	12.8±2 <sup>b</sup>	20.1±2 <sup>b</sup>

There is a statistical difference between the means of lines symbolized by the letters a, b, c (p<0.05).

### 3.5. Lipid Amount

Salinity, N(-) and P(-) treatments applied in the experiment were found to have a significant effect on lipid content (p<0.05). The highest lipid value was found to be 39.8% in the group treated with %30 salinity and 50% N(-) (Table 4).

Table 4

Lipid amounts of the groups (%)

Salinity(‰)	Control	50%N(-)	50%P(-)
45	21.6±2 <sup>c</sup>	33.2±2 <sup>b</sup>	30.4±2 <sup>b</sup>
30	23.7±3 <sup>a</sup>	39.8±1 <sup>a</sup>	34.6±1 <sup>a</sup>
15	22.9±1 <sup>b</sup>	31.1±2 <sup>c</sup>	29.3±1 <sup>b</sup>

There is a statistical difference between the means of lines symbolized by the letters a, b, c (p<0.05).

### 3.6. Fatty acids

The fatty acid changes of the groups treated with nutrient deficiencies at different salinities are given in Tables 5, 6 and 7. Among the saturated fatty acids (SFA) C16:0 (palmitic acid) in the groups cultured at %45 salinity, the highest N(-) group was determined. Monounsaturated fatty acids ( $\Sigma$ MUFA) were higher in the 50% P(-) group compared to the control group, while it was lower in the 50% N(-) group and this group was statistically different from the other groups (p<0.05). C16:1 (palmitoleic acid) from MUFA was found in the group with the highest P (-), while C18:1 $\omega$ 9 (Oleic acid) showed similar values and lower in both groups compared to the control group. Polyunsaturated fatty acids ( $\Sigma$ PUFA) were found in the group with the highest P(-) and the lowest N(-), and differences were determined between the groups (p<0.05). C18:3 $\omega$ 3 ( $\alpha$ - Linoleic acid) was the most dominant fatty acids within the PUFA group. While C18:2 $\omega$ 6c (linoleic acid) from PUFA was found to be similar in both groups, C18:3 $\omega$ 3 ( $\alpha$ - Linoleic acid) was determined as 11.155% in the group with the highest P(-). In the phosphorus deficient group, EPA was determined as the highest group with 4.425%. Accordingly, total unsaturated fatty ( $\Sigma$ UFA) acids with 45.41% were highest in the group with 50% P(-) and the lowest in the group with 50% N(-) (Table 5).

Table 5  
Fatty acid profile of *T. suecica* (at %45 salinity)

Fatty Acids	Name	Control(%45)	%50N(-)	%50 P(-)
C6:0	Caproic acid	1.125±0.075	0.23±0.03	0.34
C8:0	Caprylic acid	1.26±0.01	1.37	1.25
C10:0	Capric acid	1.86±0.05	2.86±0.02	2.055±0.05
C11:0	Undecylic acid	0	0.03	0
C12:0	Lauric acid	2.035±0.045	3.34	2.31±0.01
C14:0	Myristic acid	1.77±0.06	2.945±0.015	1.995±0.005
C16:0	Palmitic acid	29.24±0.68	24.12±0.04	22.2±0.05
C17:0	Margaric acid	0.51±0.01	0.72	0.65
C18:0	Stearic acid	4.41±0.1	4.925±0.005	7.61±0.01
C20:0	Arachidic acid	2.055±0.045	1.655±0.005	3.565±0.075
C22:0	Behenic acid	0.35±0.01	0.525±0.005	0.06
C24:0	Lignoceric acid	0.03	0.04	0.05
<b>ΣSFA</b>		<b>44.64±1.085<sup>a</sup></b>	<b>42.76±0.12<sup>b</sup></b>	<b>42.08±0.2<sup>b</sup></b>
C14:1	Myristoleic acid	1.15±0.03	1.1	1.07
C15:1	Ginkgolic acid	0.115±0.005	0	0.185±0.005
C16:1	Palmitoleic acid	2.13±0.05	2.385±0.025	2.805±0.015
C17:1		1.725±0.045	1.35±1.3	1.835±0.015
C18:1ω9	Oleic acid	14.79±0.27	12.42±0.01	12.685±0.055
C18:1ω7	Vaccenic acid	3.805±0.045	5.79±0.011	4.9±0.08
C20:1ω9	Gondoic acid	0.21±0.01	0.23	0.255±0.025
C22:1ω9	Erucic acid	0.055±0.005	0.06	0.595±0.005
C24:1ω9	Nervonic acid	0.15±0.06	0.305±0.005	0.13±0.01
<b>ΣMUFA</b>		<b>24.13±0.52<sup>a</sup></b>	<b>23.64±1.351<sup>b</sup></b>	<b>24.46±0.21<sup>a</sup></b>
C18:2ω6c	Linoleic acid	5.02±0.12	4.44±0.02	4.39±0.01
C18:3ω6	γ- Linoleic acid	0.71±0.02	1.22±0.01	0.245±0.012
C18:3ω3	α- Linoleic acid	7.85±0.11	8.34±0.05	11.155±0.03
C20:2	Eicosadienoic acid	0.04	0.06	0.045±0.005
C20:4ω6	Arachidonic acid	0.14	0.225±0.005	0.135±0.005
C20:3ω6	Dihomo-γ-linolenic acid	0.03	0.05	0.485±0.005
C20:5ω3	Eicosapentaenoic acid (EPA)	3±0.07	4.05±0.03	4.425±0.005
C22:6ω3	Docosahexaenoic acid (DHA)	0.07	0.11	0.07
<b>ΣPUFA</b>		<b>16.68±0.32<sup>b</sup></b>	<b>15.13±0.11<sup>c</sup></b>	<b>20.95±0.072<sup>a</sup></b>
<b>ΣUFA</b>		<b>40.81</b>	<b>38.77</b>	<b>45.41</b>
<b>Defined</b>		<b>85.45±0.65</b>	<b>81.53±0.52</b>	<b>87.49±0.16</b>

There is a statistical difference between the means of the columns symbolized by the letters a, b, c (p<0.05).

Among the groups cultured at %30 salinity, SFA was the opposite of that at %45 salinity and was determined in the group with the highest N reduction. In the other two groups, the results were similar (p>0.05). ΣMUFA, on the other hand, was found to be the highest in the P(-) group and the lowest in the N(-) group, and all three groups differed statistically (p<0.05). Oleic acid is the predominant fatty acid in MUFA and it was determined the highest in the N(-) group with 15.72%, while it was found in the control group with 11.595%. In the PUFA group, the dominant fatty acid was α-Linoleic acid, as at %45 salinity. At this salinity, α- Linoleic acid was determined as 10.93% in the group with the highest P(-). EPA was determined in the group with the lowest control and the highest P(-). While ΣPUFA was 21.35% in the group with the highest P(-), total UFA acids were determined with the highest 48% in the control group (Table 6).

Table 6

Fatty acid profile of *T. suecica* (at 30‰ salinity)

Fatty Acids	Name	Control(‰30)	50% N(-)	50% P(-)
C6:0	Caproic acid	0	1.69±0.04	1.88
C8:0	Caprylic acid	1.45±0.01	1.52	1.47±0.02
C10:0	Capric acid	3.33±0.01	2.42±0.01	2.37±0.015
C12:0	Lauric acid	3.9±0.01	2.675±0.005	2.57±0.025
C14:0	Myristic acid	3.41±0.02	2.3±0.01	2.24±0.01
C16:0	Palmitic acid	21.885±0.035	24.425±0.025	22.24±0.285
C17:0	Margaric acid	0.21	0.465±0.005	0.88±0.015
C18:0	Stearic acid	6.6±0.02	5.64±0.01	8.33±0.09
C20:0	Arachidic acid	2.765±0.005	2.15	3.27±0.06
C22:0	Behenic acid	0.08±0.001	0.65±0.005	0.05
C24:0	Lignoceric acid	0.06	0.065±0.005	0.06
<b>ΣSFA</b>		<b>43.85±0.121<sup>b</sup></b>	<b>44±0.115<sup>b</sup></b>	<b>45.46±0.52<sup>a</sup></b>
C14:1	Myristoleic acid	1.235±0.005	0.85	0.69±0.005
C15:1	Ginkgolic acid	0.175±0.005	0	0.18±0.005
C16:1	Palmitoleic acid	4.915±0.015	1.565±0.005	1.76±0.02
C17:1		3.13±0.01	2.045±0.015	2.04±0.02
C18:1ω9	Oleic acid	11.595±0.005	15.72±0.03	13.69±0.0165
C18:1ω7	Vaccenic acid	6.015±0.105	4.92±0.06	4.3±0.11
C20:1ω9	Gondoic acid	0.245±0.005	0.15	0.17
C22:1ω9	Erucic acid	0.295±0.005	0.69±0.02	0.6±0.01
C24:1ω9	Nervonic acid	0.225±0.005	0.365±0.005	0
<b>ΣMUFA</b>		<b>27.83±0.16<sup>a</sup></b>	<b>26.30±0.135<sup>b</sup></b>	<b>23.43±0.7<sup>c</sup></b>
C18:2ω6c	Linoleic acid	3.76±0.02	4.56±0.04	4.45±0.06
C18:3ω6	γ- Linoleic acid	0.235±0.015	0.125±0.005	0.13
C18:3ω3	α- Linoleic acid	8.7±0.02	9.59	10.93±0.125
C20:2	Eicosadienoic acid	0	0.05	0.06
C20:4ω6	Arachidonic acid	0.83±0.01	0.805±0.005	0.14
C20:3ω6	Dihomo-γ-linolenic acid	0.29	0.065	0.72±0.01
C20:5ω3	acid Eicosapentaenoic acid (EPA)	3.11±0.01	4.39	4.87±0.08
C22:6ω3	Docosahexaenoic acid (DHA)	0.1±0.04	0.06	0.05
<b>ΣPUFA</b>		<b>20.23±0.115<sup>b</sup></b>	<b>19.64±0.05<sup>c</sup></b>	<b>21.35±0.275<sup>a</sup></b>
<b>ΣUFA</b>		<b>48.06</b>	<b>45.95</b>	<b>44.78</b>
<b>Defined</b>		<b>91.91±0.132</b>	<b>89.95±0.1</b>	<b>90.34±0.49</b>

There is a statistical difference between the means of the columns symbolized by the letters a, b, c ( $p < 0.05$ ).

ΣSFA at ‰15 salinity was determined as 46.615% in the N(-) group and all groups differed from each other ( $p < 0.05$ ). The most dominant fatty acid in the SFA group was palmitic acid, and the highest N(-) was determined in the group applied. MUFA group fatty acids were the most in the N(-) group (24.29%), and oleic acid was the most dominant fatty acid in all groups. Oleic acid was found to be 10.335% in the group with the lowest P(-). The most dominant fatty acid in ΣPUFA was α- Linoleic acid as in the other groups, and it was determined as 7.235% in the group with the lowest P(-). Linoleic acid (7.47%) and EPA (5.425) were also determined in the group with the highest P(-). ΣPUFA was determined with the highest rate of 21.335% in the P(-) group, and there was a difference between the groups ( $p < 0.05$ ). Total UFA were found to be 41.44% in the control group and 41.49% in the P group, while it was 44.125% in the N group (Table 7).

Table 7  
Fatty acid profile of *T. suecica* (at ‰15 salinity)

Fatty Acids	Name	Control(‰15)	50% N(-)	50% P(-)
C6:0	Caproic acid	0.26±0.04	2.34±0.042	2.02±0.32
C8:0	Caprylic acid	1.51±0.02	2.375±0.005	1.865±0.035
C10:0	Capric acid	3.58±0.04	3.56±0.03	3.43±0.04
C12:0	Lauric acid	4.205±0.045	3.94±0.05	3.89±0.01
C14:0	Myristic acid	3.71±0.05	3.4±0.07	3.415±0.025
C16:0	Palmitic acid	18.315±0.215	23.335±0.095	20.04±0.04
C17:0	Margaric acid	0.39±0.01	0.185±0.005	0.74
C18:0	Stearic acid	7.645±0.085	4.705±0.065	5.69±0.01
C20:0	Arachidic acid	3.88±0.07	2.02±0.01	3.95±0.01
C22:0	Behenic acid	0.06±0.03	0.7	0.06
C24:0	Lignoceric acid	0.03	0.045±0.005	0.04
<b>∑SFA</b>		<b>43.71±0.605<sup>c</sup></b>	<b>46.61±0.377<sup>a</sup></b>	<b>45.31±0.49<sup>b</sup></b>
C14:1	Myristoleic acid	0.73±0.01	0.795±0.025	0.745±0.005
C15:1	Ginkgolic acid	0	0	0
C16:1	Palmitoleic acid	2.44±0.02	1.955±0.005	2.29
C17:1		3.295±0.025	3.065±0.045	2.985±0.005
C18:1ω9	Oleic acid	11.34±0.11	11.9±0.12	10.335±0.035
C18:1ω7	Vaccenic acid	3.44±0.06	3.315±0.135	3.505±0.065
C20:1ω9	Gondoic acid	0.325±0.045	2.21±0.01	0.15±0.01
C22:1ω9	Erucic acid	0.305±0.225	0.6±0.01	0.06
C24:1ω9	Nervonic acid	0.515±0.115	0.45±0.07	0.385±0.005
<b>∑MUFA</b>		<b>22.39±0.6<sup>b</sup></b>	<b>24.29±0.42<sup>a</sup></b>	<b>20.45±0.125<sup>c</sup></b>
C18:2ω6c	Linoleic acid	4.055±0.065	4.53±0.05	7.47
C18:3ω6	γ- Linoleic acid	0.84±0.069	1.46±0.02	0.175±0.025
C18:3ω3	α- Linoleic acid	9.095±0.225	8.665±0.075	7.235±0.015
C20:2	Eicosadienoic acid	0.05	0.05	0.09
C20:4ω6	Arachidonic acid	0.088±0.05	0.145±0.005	0.215±0.005
C20:3ω6	Dihomo-γ-linolenic acid	0.335±0.005	0.445±0.005	0.52
C20:5ω3	Eicosapentaenoic acid (EPA)	4.56±0.05	4.49±0.03	5.425±0.005
C22:6ω3	Docosahexaenoic acid (DHA)	0.03	0.05	0.205±0.005
<b>∑PUFA</b>		<b>19.05±0.464<sup>c</sup></b>	<b>19.83±0.185<sup>b</sup></b>	<b>21.33±0.05<sup>a</sup></b>
<b>∑UFA</b>		<b>41.44</b>	<b>44.12</b>	<b>41.79</b>
<b>Defined</b>		<b>85.15±0.55</b>	<b>90.74±0.32</b>	<b>87.10±0.22</b>

There is a statistical difference between the means of the columns symbolized by the letters a, b, c (p<0.05).

As a result, among all three salinity groups, total UFA were determined highest in ‰30 salinity N(-) and lowest in ‰45 salinity N(-) group. While MUFA fatty acids were found at ‰30 salt concentration in the group made with 50% N(-) the highest, PUFA fatty acids were found in the groups made with P(-) at ‰30 and ‰15 salinity the highest. The lowest PUFA values were determined at ‰45 salinity N(-), and the highest values were determined in all salinity groups in the groups with P(-) (Table 8).

Table 8  
Fatty acid values of all groups (%)

	Control			50% N(-)			50% P(-)		
	%45	%30	%15	%45	%30	%15	%45	%30	%15
<b>SFA</b>	44.645 <sup>c</sup>	43.85 <sup>d</sup>	43.71 <sup>de</sup>	42.76 <sup>e</sup>	44 <sup>d</sup>	46.61 <sup>a</sup>	42.08 <sup>f</sup>	45.46 <sup>b</sup>	45.31 <sup>b</sup>
<b>MUFA</b>	24.13 <sup>c</sup>	27.83 <sup>a</sup>	22.39 <sup>e</sup>	23.64 <sup>d</sup>	26.30 <sup>b</sup>	24.29 <sup>c</sup>	24.46 <sup>c</sup>	23.43 <sup>d</sup>	20.45 <sup>f</sup>
<b>PUFA</b>	16.68 <sup>d</sup>	20.23 <sup>b</sup>	19.05 <sup>c</sup>	15.13 <sup>e</sup>	19.64 <sup>c</sup>	19.83 <sup>bc</sup>	20.95 <sup>ab</sup>	21.35 <sup>a</sup>	21.33 <sup>a</sup>
<b>UFA</b>	40.81 <sup>e</sup>	48.06 <sup>a</sup>	41.44 <sup>d</sup>	38.77 <sup>f</sup>	45.95 <sup>b</sup>	44.12 <sup>c</sup>	45.41 <sup>b</sup>	44.78 <sup>c</sup>	41.79 <sup>d</sup>

There is a statistical difference between the means of the columns symbolized by the letters a, b, c, d, e, f (p<0.05).

#### 4. Discussion

N and P deficiency and different salt concentration treatments, which are stress conditions that stimulate the increase of lipid content of *T. suecica* from the green microalgae group, have been studied in vitro. In this study, the effects of 3 different salinity (%15, 30 and 45) and nutrient deficiencies (50% N(-) and 50% P(-)) on growth, protein, lipid and fatty acid changes in *T. suecica* were investigated. Environmental factors are effective in the growth and biochemical structure of algae, as well as the type and density of nutrient elements in the culture medium (Brown et al, 1989). It is known that the change in N sources (such as ammonium, nitrate, and nitrite) and their concentrations are effective in the growth and biochemical structure of algae (Gökpinar, 1991; Fidalgo et al, 1995). In general, F/2 medium is used for the growth of marine microalgae in the laboratory environment. NaNO<sub>3</sub> is used as N source and NaH<sub>2</sub>PO<sub>4</sub>.H<sub>2</sub>O is used as P source in the nutrient medium. This study is based on NO<sub>3</sub>-N 882 µmol/l and PO<sub>4</sub> 36.3 µmol/l (Guillard, 1973). N limitation by 50% (441 µmol/l) reduction in N source and P limitation by 50% (18.15 µmol/l) reduction in P source. N and P addition rates were among the parameters affecting growth in *T. suecica*. It was observed that there were decreases in OD and biomass amounts in *T. suecica* cultured at all three salinity values where 50% N and P restriction were applied. In a study, it was stated that low N concentration reduced growth in *N. oculata*, but did not affect it in *C. vulgaris* (Converti et al, 2009). It has been reported that when cultured in different N sources and N-free media, the growth of *Ellipsoidion* sp. slows down in N-free media (Xu et al, 2001). Khozin-Goldberg, & Cohen (2006) reported that when the freshwater species *Monodus subterraneus* was cultured in an environment with P restriction, the amount of dry weight decreased with P restriction. Salinity is the most important environmental factor affecting the development, biochemical structure and distribution of algae. It is known that with the decrease in photosynthesis rate of algae cells due to the increase in salinity, protein synthesis from their biochemical content also decreases. At the same time, it has been reported that with the increase in salinity, the growth slows down and there is a significant decrease in production (Zhang et al, 2010). Marine algae have a very high tolerance to salinity changes. It has been stated that many species show good growth at salinities lower than the optimum salinity values. While most of the marine algae prefer %12-44, optimum %20-24 salinity, some algae species can continue their photosynthetic activities for a while even if the growth rate decreases very much at %140 salinity (Ben-Amotz, & Avron, 1983; Borowitzka, & Borowitzka, 1988). While *T. suecica* prefers %25-35 salinity, *I. galbana* %15, *S. platensis* shows good growth at %1 salinity (Vonshak, & Tomaselli, 2000). In this study, the best growth was obtained in the group containing %30 salinity. The closest to this was determined at %45 salinity. The lowest growth was found at %15. *T. suecica* showed good growth in a wide salinity range of 15-45 ppt. It is in agreement with the results reported in previous studies. According to Alsull, & Maznah Omar (2012); At different salinity concentrations (%20, %25, %30, %33, %35 and %38), *Tetraselmis* sp. and *Nannochloropsis* sp. achieved the best growth at %33 salinity concentration. Durmaz, & Pirinç (2017) reported in their study that the highest cell number of *T. chunii* species was obtained in cultures with a salinity concentration of %40, the highest amount of dry weight in culture media adjusted at %30 and %40 salinity. They stated that *T. suecica* developed in the range of 15-60 ppt (Venckus et al, 2021), 20-60ppt (Pugkaew et al, 2019), 25-35 ppt (Fabregas et al, 1986). In the studies, *T. suecica* was cultured in four different salinity values (15, 30, 60 and 90 ppt). They reported that the highest growth was achieved at 15 ppt salinity, while growth slowed down at other salinity values. They also stated that the highest protein content (56.9%) was found in this group, while the highest lipid ratio was 27.7% at 30ppt salinity. They reported that the protein and lipid content decreased as the salt content increased (Venckus et al, 2021). Pugkaew et al. (2019) also found that when *T. suecica* is cultured under 6 different salinities (10,



20, 30, 40, 50 and 60 ppt), the species can be cultured between 20 and 60 ppt values, but 10ppt is essential for the development of the species. They reported that there is no suitable salinity and that the growth is lower than other salinity rates. At the same time, they reported that the highest growth was at 30 ppt, and the growth at 20, 40, 50 and 60 ppt values was similar to each other. They reported that while the protein content was found at the highest 10 ppt, this ratio decreased as the salinity increased, and the highest lipid content was at 60 ppt. Gu et al. (2012) reported that *N. oculata* had the highest lipid content at 25 and 35 salinity, and the lowest at 15 salinity. At the same time, they determined that the protein content decreased with salinity. In our study, the highest protein was found in the control group with 30 salinity, while the closest value was obtained in the control group at 15 salinity. In this study, highest lipid content was found as 39.8% in the group with the 30 salinity and 50% N(-). Salinity is the most important factor affecting microalgal production yield, especially in uncontrolled environments of growing systems. Uncovering the optimal salinity range and high-value biochemical production pathways for algal biomass helps increase production potential and reduce cost (Pugkaew et al, 2018). In our study, it was observed that salinity variations caused a decrease or increase in the amount of biomass by affecting the biochemical structure of *T. suecica*. Elements such as N, P, S, Ca, Mg, Si are essential elements in algae, and these elements are significantly needed in the environment. N(-) and P(-) caused decreases in OD and dry weight values. The highest OD and dry weight amounts obtained in the culture were determined in the control groups at all three salinity values, while the lowest values were determined in the N(-) groups. In their study, Bondioli et al. (2012) determined that while the dry weight efficiency was  $7.8 \text{ g m}^{-2}\text{day}^{-1}$  at the end of the first week in cultures with N restriction in *T. suecica*, this value was  $2.2 \text{ g m}^{-2}\text{day}^{-1}$  in the second week of the experiment.

The application of N and P deficiency, which is effective in the growth of algae, among the elements used in the nutrient medium, increases the lipid ratio in many algae species and causes a decrease in the protein ratio. In the late 1940s, N starvation in algae was found to be effective on lipid storage, and a lipid level of 70-85% in dry weight was reported. *Dunaliella* sp. or *T. suecica* species, on the other hand, contain low lipid and generally produce carbohydrates rather than lipids (Piorreck et al., 1984). Uslu et al. (2011) cultured *S. platensis* in media containing different amounts of N and obtained the highest lipid content in media containing 100%N(-). They also determined the highest protein ratio in the control group. Mutlu et al. (2011) found the highest lipid in *C. vulgaris* as 35.6% in the 100% N(-) group in their study. In their study, Gouveia et al. (2009) found the maximum total lipid ratio of 56% in *N. oleabundans* species cultured with N limitation. In their study, Roopnarain et al. (2014) determined that the highest lipid contents were obtained in cultures containing 25%P and lower levels of P in *I. galbana*, which they cultured with different levels of P restriction. *Nephrochlamys yushanlensis* control was cultured with N, N-P and P deficiency and lipid contents were determined. Total lipid contents were found to be 31% control, 58.6% N(-), 34% P(-), and 49% N-P(-), respectively (Maltsev et al, 2021). In this study, both N and P deficiencies caused an increase in lipid ratios and a decrease in protein ratios in all salinity groups. It shows that applied N deficiency increases the amount of lipid more than P deficiency. Nutritional and environmental factors can affect the ratio of fatty acids relative to each other as well as the total lipid content. Many studies have reported that fatty acids or total lipid productivity can be increased when salinity is higher (Takagi and Karseno 2006; Xia et al, 2013; Ho et al, 2014) or lower (Kim et al. 2016a). The main role of fatty acids in algae is related to cell membrane functions and metabolic processes (Guschina and Harwood, 2006). The degree of unsaturation of fatty acids is also an important parameter in the adaptation of algae to environmental conditions. Changes in the lipid fatty acid profile in response to the high salinity of the environment are necessary to retain membrane fluid and prevent its degradation. However, data on the effect of sodium chloride on the fatty acid composition of algal lipids are scarce and conflicting. *Isochrysis* cells grown under high concentrations of NaCl in medium contain increasing proportions of the PUFA C18 and C22 (Ben-Amotz et al. 1985), whereas Renaud, & Parry (1994) found C18:5 in high-salinity *Isochrysis* sp. and reported a reduction in C22:6. It has been reported that *Dunaliella*, *Nannochloropsis* and *N. frustulum* contain less UFA at high NaCl concentrations (Renaud and Parry 1994; Xu and Beardall 1997; Hu and Gao 2006). In our study, total SFA were highest in the 15 salinity N and P deficiency groups (46% and 45%) and in the 30 P deficiency group (45%); Total UFA were highest in the 30 salinity control group (48%), and the lowest in the 45 salinity N(-) group (38.77%). In their

study, Kim et al. (2016) determined that the UFA values of *Tetraselmis* sp. (35-22ppt) at 2 different salinities were higher at 35 ppt (58%) and SFA values at 22ppt. In our study, the most dominant fatty acids in all groups were palmitic acid (C16:0), oleic acid (C18:1 $\omega$ 9),  $\alpha$ -Linoleic acid (C18:3 $\omega$ 3) and EPA (C20:5 $\omega$ 3). The predominant presence of these fatty acids in *Tetraselmis* members has also been reported previously (Griffiths et al, 2012; Adarme-Vega et al, 2014; Kim et al, 2016). Our results indicate that salinity levels have an effect on fatty acids. EPA, which is an important fatty acid in terms of human health, constituted 3-5.425% of fatty acids. Similar but slightly higher EPA levels of 6% to 7% have been reported in *Tetraselmis* sp. (Adarme-Vega et al, 2014). The main fatty acids Palmitic acid (C16:0) and oleic acid (C18:1) found in vegetable lipids are widely used in biodiesel production and are important determinants of biodiesel quality (Kaur et al.2012; Knothe 2008) and in high amounts in *T. suecica*. found. It seems possible that the lipid obtained from *Tetraselmis* can be used as a biodiesel raw material. However, linoleic acid (C18:3) and PUFAs, which greatly reduce the oxidation stability of biodiesel, may require the addition or blending of antioxidants to improve biodiesel quality (Griffiths et al, 2012). Huang et al. (2013) determined in their study that *T. subcordiformis* contains a high amount of 18:3 $\omega$ 3 (17.68-22.22%) at different N concentrations. In our study, 18:3 $\omega$ 3 ( $\alpha$ -Linoleic acid) fatty acid (7.235-11.155%) was the most dominant among PUFAs. Reducing the amount of N and P in the microalgae medium causes a decrease in the cell density and protein amount, and due to the inability to produce the energy molecules (ATP and NADPH) that provide chlorophyll synthesis, the amount of chl *a* decreases. (Shifrin, & Chisholm, 1981; Sukenik et al, 1989; Roopnarain et al, 2014). In this study, decreases in the amount of chl *a* and protein in the groups treated with N and P deficiency; Increases in lipid content were observed.

One of the factors affecting the growth and biochemical structure of algae is the period of illumination. As the illumination period gets longer, the growth rate of the algae increases and the cell numbers increase. Studies have reported that there is not much difference in terms of algal development between the 18-hour illumination period and the 12-hour illumination period (Oh et al, 2009). In this study, 16:8 light-dark period and 80  $\mu\text{molm}^{-2}\text{s}^{-1}$  light intensity were applied to the cultures. In a study, *P. cruentum* species were grown in growth media (12:12 light-dark period and CO<sub>2</sub> carbon source, 6:18 light-dark period and CO<sub>2</sub> carbon source, 18:6 light-dark and CO<sub>2</sub> carbon source, 24 hours dark and glucose. carbon source, 24 hours dark and glycerol carbon source) were cultured and the highest lipid content was found with 19.3% in the 12:12 light-dark period group (Oh et al, 2009). In another study, *I. galbana* was cultured with 24 hours of continuous light and 8 hours of continuous light, and the highest PUFA was obtained in cultures with 8 hours of illumination (Bandarra et al, 2003). It is concluded that these studies and the light-dark period applied in our study positively affect the lipid increase. The biochemical content of the biomass obtained in different phases of the growth period in microalgae cultures also differs. The amount of lipid is related to the age of the algae culture, and the amount of lipid obtained increases as the culture ages. The total amount of lipid obtained in the stationary phase of the culture is higher than that obtained from other phases (Ying et al, 2002). In this study, the culture was harvested after entering the stationary phase and the lipid amounts were examined in this phase. In a study in which nitrate, nitrite and urea were used as N sources in the medium, *I. galbana* was cultured and no difference was found between them in terms of growth. However, the highest lipid ratio was found with urea (42.05%) and nitrite (41.61%) at the end of the stationary phase in the culture harvested at the beginning of the stationary phase of the study. Fatty acids PUFA (62.27%), EPA (27.66%) and DHA (14.13%) were found in the group cultured with the highest urea and at the beginning of the stationary phase. In the group cultured with urea, the protein was found to be the highest (44.96%) in the phase where the logarithmic stage increased (Fidalgo et al, 1998).

## 5. Conclusion

In the study, different salinity and nutrient deficiencies caused changes in cell densities, chl *a*, dry weight, protein, lipid and fatty acids of microalgae. It was determined that the most suitable salinity value in terms of growth dynamics of *T. suecica* was ‰30. Protein and lipid values were determined at high values at ‰30 salinity, followed by ‰15 salt concentration. In the nutrient deficiency studies, it was determined that the

control groups still had the highest growth dynamics, and the closest group was the 50% P(-) group. The growth was lowest in the N(-) treated groups. When the protein values were examined, the lowest was found in this group. On the contrary, lipid values were found at the highest level in this group, while the lowest was determined in the control group. When lipid enhancement studies are desired, it can be said that the most suitable salinity for this species is 30‰ and it is appropriate to use a medium whose N is reduced by half. UFA were highest in the control group with 30‰ salinity and lowest in the group with high salinity and N(-). PUFA group fatty acids, which we have to take from outside in terms of the health of living things, were at the highest levels in all salinity groups made with P(-). EPA, which is included in PUFA, was also higher in P(-) made groups. Accordingly, it can be said that the reduction of phosphorus in the medium at different levels may cause an increase in PUFA.

### Acknowledgement

This study is a master's thesis. The authors thank the Scientific Research Projects Unit at Çukurova University for their financial support. Project No: FYL-2019-11802.

### Author Contributions

Cananur Pihava: Collected data and performed the analysis.

Leyla Uslu: Planned, analysed data, conducted experiments and wrote all parts of manuscript.

### Conflicts of Interest

There is no conflict of interest.

### References

- Adarme-Vega, T. C., Thomas-Hall, S. R., Lim, D. K., & Schenk, P. M. (2014). Effects of long chain fatty acid synthesis and associated gene expression in microalga *Tetraselmis* sp. *Marine drugs*, 12(6), 3381-3398. doi: <https://doi.org/10.3390/md12063381>
- Alonso, M., Lago, F. C., Vieites, J. M., & Espiñeira, M. (2012). Molecular characterization of microalgae used in aquaculture with biotechnology potential. *Aquaculture International*, 20(5), 847-857. doi: <https://doi.org/10.1007/s10499-012-9506-8>
- Alsull, M., & Omar, W. M. W. (2012). Responses of *Tetraselmis* sp. and *Nannochloropsis* sp. isolated from Penang National Park coastal waters, Malaysia, to the combined influences of salinity, light and nitrogen limitation. In *International Conference on Chemical, Ecology and Environmental Sciences (ICEES 2012)*.
- Bandarra, N. M., Pereira, P. A., Batista, I., & Vilela, M. H. (2003). Fatty acids, sterols and  $\alpha$ -tocopherol in *Isochrysis galbana*. *Journal of Food Lipids*, 10(1), 25-34. doi: <https://doi.org/10.1111/j.1745-4522.2003.tb00003.x>
- Ben-Amotz, A., Tornabene, T. G., & Thomas, W. H. (1985). Chemical profile of selected species of microalgae with emphasis on lipids 1. *Journal of Phycology*, 21(1), 72-81. doi: <https://doi.org/10.1111/j.0022-3646.1985.00072.x>
- Ben-Amotz, A., & Avron, M. (1983). On the factors which determine massive  $\beta$ -carotene accumulation in the halotolerant alga *Dunaliella bardawil*. *Plant Physiology*, 72(3), 593-597. doi: <https://doi.org/10.1104/pp.72.3.593>
- Benitez-Nelson, C. R. (2000). The biogeochemical cycling of phosphorus in marine systems. *Earth-Science Reviews*, 51(1-4), 109-135. doi: [https://doi.org/10.1016/S0012-8252\(00\)00018-0](https://doi.org/10.1016/S0012-8252(00)00018-0)
- Borowitzka, M. A., & Borowitzka, L. J. (1988). *Micro-algal biotechnology*. Cambridge University Press.
- Brown, M. R., Jeffrey, S. W., & Garland, C. D. (1989). *Nutritional aspects of microalgae used in mariculture: a literature review*. Hobart, Tas., CSIRO Marine Laboratories. doi: <https://doi.org/10.25919/5bbb9b2e71b6e>
- Converti, A., Casazza, A. A., Ortiz, E. Y., Perego, P., & Del Borghi, M. (2009). Effect of temperature and nitrogen concentration on the growth and lipid content of *Nannochloropsis oculata* and *Chlorella vulgaris* for biodiesel production. *Chemical Engineering and Processing: Process*

- Intensification*, 48(6), 1146-1151. doi: <https://doi.org/10.1016/j.cep.2009.03.006>
- Durmaz, Y., & Piring, P. (2017). Bazı deniz mikroalglerinin (*Nannochloropsis oculata*, *Tetraselmis chuii* ve *Dunaliella salina*) kültüründe tuzluluk konsantrasyonunun büyüme ve pigment yapısına etkisinin araştırılması Investigation of the effect of salinity concentration on growth and pigment composition on the some marine microalgae (*Nannochloropsis oculata*). *Ege Journal of Fisheries and Aquatic Sciences*, 34(1), 75-80. doi:10.12714/egejfas.2017.34.1.11
- Fabregas, J., Herrero, C., Cabezas, B., & Abalde, J. (1986). Biomass production and biochemical composition in mass cultures of the marine microalga *Isochrysis galbana* Parke at varying nutrient concentrations. *Aquaculture*, 53(2), 101-113. doi:[https://doi.org/10.1016/0044-8486\(86\)90280-2](https://doi.org/10.1016/0044-8486(86)90280-2)
- Fidalgo, J. P., Cid, A., Torres, E., Sukenik, A., & Herrero, C. (1998). Effects of nitrogen source and growth phase on proximate biochemical composition, lipid classes and fatty acid profile of the marine microalga *Isochrysis galbana*. *Aquaculture*, 166(1-2), 105-116. doi: [https://doi.org/10.1016/S0044-8486\(98\)00278-6](https://doi.org/10.1016/S0044-8486(98)00278-6)
- Fidalgo, J., Cid, A., Abalde, J., & Herrero, C. (1995). Culture of the marine diatom *Phaeodactylum tricornutum* with different nitrogen sources: growth, nutrient conversion and biochemical composition. *Cahiers de biologie marine*, 36(3), 165-173.
- Gökpınar, Ş., & Cirik, S. (1991). *Phaeodactylum tricornutum*'un geniş ölçekli yağın kültürleri üzerine tuzluluk faktörünün etkisi. *Ege Ü. Su Ürünleri F. Eğitiminin*, 10, 12-14.
- Gouveia, L., Marques, A. E., Da Silva, T. L., & Reis, A. (2009). *Neochloris oleabundans* UTEX# 1185: a suitable renewable lipid source for biofuel production. *Journal of Industrial Microbiology and Biotechnology*, 36(6), 821-826. doi: <https://doi.org/10.1007/s10295-009-0559-2>
- Griffiths, M. J., van Hille, R. P., & Harrison, S. T. (2012). Lipid productivity, settling potential and fatty acid profile of 11 microalgal species grown under nitrogen replete and limited conditions. *Journal of Applied Phycology*, 24(5), 989-1001. doi: <https://doi.org/10.1007/s10811-011-9723-y>
- Grobbelaar, J. U. (2004). *Handbook of microalgal culture: biotechnology and applied phycology*. Israel: Wiley-Blackwell.
- Gu, N., Lin, Q., Li, G., Tan, Y., Huang, L., & Lin, J. (2012). Effect of salinity on growth, biochemical composition, and lipid productivity of *Nannochloropsis oculata* CS 179. *Engineering in life sciences*, 12(6), 631-637. doi: <https://doi.org/10.1002/elsc.201100204>
- Guillard, R.R.L. (1973). Division Rates. In: Stein, R.J. (Ed.) *Handbook of phycological methods: culture methods and growth measurements* (No. 589.3 S84). Cambridge Univ. Press, N. Y., 283-311.
- Guschina, I. A., & Harwood, J. L. (2006). Lipids and lipid metabolism in eukaryotic algae. *Progress in lipid research*, 45(2), 160-186. doi: <https://doi.org/10.1016/j.plipres.2006.01.001>
- Ichihara, K. I., Shibahara, A., Yamamoto, K., & Nakayama, T. (1996). An improved method for rapid analysis of the fatty acids of glycerolipids. *Lipids*, 31(5), 535-539. doi:<http://dx.doi.org/10.1007/BF02522648>
- Kaur, S., Sarkar, M., Srivastava, R. B., Gogoi, H. K., & Kalita, M. C. (2012). Fatty acid profiling and molecular characterization of some freshwater microalgae from India with potential for biodiesel production. *New Biotechnology*, 29(3), 332-344. doi: <https://doi.org/10.1016/j.nbt.2011.10.009>
- Khozin-Goldberg, I., & Cohen, Z. (2006). The effect of phosphate starvation on the lipid and fatty acid composition of the fresh water eustigmatophyte *Monodus subterraneus*. *Phytochemistry*, 67(7), 696-701. doi: <https://doi.org/10.1016/j.phytochem.2006.01.010>
- Kim, G., Lee, C. H., & Lee, K. (2016). Enhancement of lipid production in marine microalga *Tetraselmis* sp. through salinity variation. *Korean Journal of Chemical Engineering*, 33(1), 230-237. doi: <https://doi.org/10.1007/s11814-015-0089-8>
- Knothe, G. (2008). "Designer" biodiesel: optimizing fatty ester composition to improve fuel properties. *Energy & Fuels*, 22(2), 1358-1364. doi: <https://doi.org/10.1021/ef700639e>
- Maltsev, Y., Maltseva, I., Maltseva, S., Kociolek, J. P., & Kulikovskiy, M. (2021). A new species of freshwater algae *Nephrochlamys yushanlensis* sp. nov. (Selenastraceae, Sphaeropleales) and its lipid accumulation during nitrogen and phosphorus starvation. *Journal of Phycology*, 57(2), 606-618. doi: <https://doi.org/10.1111/jpy.13116>
- Mutlu, Y. B., Isik, O., Uslu, L., Koç, K., & Durmaz, Y. (2011). The effects of nitrogen and phosphorus deficiencies and nitrite addition on the lipid content of *Chlorella vulgaris* (Chlorophyceae). *African*

- Journal of Biotechnology*, 10(3), 453-456. doi:10.5897/AJB10.1390.
- Oh, S. H., Han, J. G., Kim, Y., Ha, J. H., Kim, S. S., Jeong, M. H., ... & Lee, H. Y. (2009). Lipid production in *Porphyridium cruentum* grown under different culture conditions. *Journal of bioscience and bioengineering*, 108(5), 429-434. doi: <https://doi.org/10.1016/j.jbiosc.2009.05.020>
- Piorreck, M., & Pohl, P. (1984). Formation of biomass, total protein, chlorophylls, lipids and fatty acids in green and blue-green algae during one growth phase. *Phytochemistry*, 23(2), 217-223. doi: [https://doi.org/10.1016/S0031-9422\(00\)80305-2](https://doi.org/10.1016/S0031-9422(00)80305-2)
- Plaxton, W. C., & Tran, H. T. (2011). Metabolic adaptations of phosphate-starved plants. *Plant physiology*, 156(3), 1006-1015. doi:<https://doi.org/10.1104/pp.111.175281>
- Paytan, A., & McLaughlin, K. (2007). The oceanic phosphorus cycle. *Chemical reviews*, 107(2), 563-576. doi: <https://doi.org/10.1021/cr0503613>
- Pugkaew, W., Meetam, M., Yokthongwattana, K., Leeratsuwan, N., & Pokethitiyook, P. (2019). Effects of salinity changes on growth, photosynthetic activity, biochemical composition, and lipid productivity of marine microalga *Tetraselmis suecica*. *Journal of Applied Phycology*, 31(2), 969-979. doi: <https://doi.org/10.1007/s10811-018-1619-7>
- Renaud, S. M., & Parry, D. L. (1994). Microalgae for use in tropical aquaculture II: Effect of salinity on growth, gross chemical composition and fatty acid composition of three species of marine microalgae. *Journal of Applied Phycology*, 6(3), 347-356. doi: <https://doi.org/10.1007/BF02181949>
- Roopnarain, A., Gray, V. M., & Sym, S. D. (2014). Phosphorus limitation and starvation effects on cell growth and lipid accumulation in *Isochrysis galbana* U4 for biodiesel production. *Bioresource technology*, 156, 408-411. doi: <https://doi.org/10.1016/j.biortech.2014.01.092>
- Mirón, A. S., Garcia, M. C. C., Gómez, A. C., Camacho, F. G., Grima, E. M., & Chisti, Y. (2003). Shear stress tolerance and biochemical characterization of *Phaeodactylum tricorutum* in quasi steady-state continuous culture in outdoor photobioreactors. *Biochemical Engineering Journal*, 16(3), 287-297. doi: [https://doi.org/10.1016/S1369-703X\(03\)00072-X](https://doi.org/10.1016/S1369-703X(03)00072-X)
- Shifrin, N. S., & Chisholm, S. W. (1981). Phytoplankton lipids: Interspecific differences and effects of nitrate, silicate and light-dark cycles 1. *Journal of phycology*, 17(4), 374-384. doi: <https://doi.org/10.1111/j.1529-8817.1981.tb00865.x>
- Siaut, M., Heijde, M., Mangogna, M., Montsant, A., Coesel, S., Allen, A., ... & Bowler, C. (2007). Molecular toolbox for studying diatom biology in *Phaeodactylum tricorutum*. *Gene*, 406(1-2), 23-35. doi: <https://doi.org/10.1016/j.gene.2007.05.022>
- Sukenik, A., Carmeli, Y., & Berner, T. (1989). Regulation of fatty acid composition by irradiance level in the eustigmatophyte *Nannochloropsis* sp. 1. *Journal of Phycology*, 25(4), 686-692. doi: <https://doi.org/10.1111/j.0022-3646.1989.00686.x>
- Sisman-Aydin, G. (2019). Mikroalg teknolojisi ve çevresel kullanımı. *Harran Üniversitesi Mühendislik Dergisi*, 4(1), 81-92.
- Takagi, M., & Yoshida, T. (2006). Effect of salt concentration on intracellular accumulation of lipids and triacylglyceride in marine microalgae *Dunaliella* cells. *Journal of bioscience and bioengineering*, 101(3), 223-226. doi: <https://doi.org/10.1263/jbb.101.223>
- Uslu, L., İçik, O., Koç, K., & Göksan, T. (2011). The effects of nitrogen deficiencies on the lipid and protein contents of *Spirulina platensis*. *African Journal of Biotechnology*, 10(3), 386-389.
- Venckus, P., Cicchi, B., & Chini Zittelli, G. (2021). Effects of medium salinity on growth and biochemical composition of the green microalga *Tetraselmis suecica*. *Journal of Applied Phycology*, 33(6), 3555-3563. doi: <https://doi.org/10.1007/s10811-021-02560-7>
- Vonshak, A. (Ed.). (1997). *Spirulina platensis arthrospira: physiology, cell-biology and biotechnology*. CRC press.
- Vonshak, A., & Tomaselli, L. (2000). Arthrospira (Spirulina): systematics and ecophysiology. In *The ecology of cyanobacteria* (pp. 505-522). Springer, Dordrecht. doi:[https://doi.org/10.1007/0-306-46855-7\\_18](https://doi.org/10.1007/0-306-46855-7_18)
- Ying, L., Kang-sen, M., & Shi-chun, S. (2002). Effects of harvest stage on the total lipid and fatty acid composition of four *Cylindrotheca* strains. *Chinese Journal of Oceanology and Limnology*, 20(2), 157-161. doi: <https://doi.org/10.1007/BF0284965>
- Xu, N., Zhang, X., Fan, X., Han, L., & Zeng, C. (2001). Effects of nitrogen source and concentration on growth

rate and fatty acid composition of *Ellipsoidion* sp.(Eustigmatophyta). *Journal of Applied Phycology*, 13(6), 463-469. doi:<https://doi.org/10.1023/A:1012537219198>

Xu, X. Q., & Beardall, J. (1997). Effect of salinity on fatty acid composition of a green microalga from an antarctic hypersaline lake. *Phytochemistry*, 45(4), 655-658. doi: [https://doi.org/10.1016/S0031-9422\(96\)00868-0](https://doi.org/10.1016/S0031-9422(96)00868-0)

Zhang, T., Gong, H., Wen, X., & Lu, C. (2010). Salt stress induces a decrease in excitation energy transfer from phycobilisomes to photosystem II but an increase to photosystem I in the cyanobacterium *Spirulina platensis*. *Journal of Plant Physiology*, 167(12), 951-958. doi: <https://doi.org/10.1016/j.jplph.2009.12.020>





# Comparative Analysis and Manufacturing of Airfoil Structures Suitable for Use at Low Speeds

Satılmış Ürgün<sup>1</sup>, Mert Gökdemir<sup>2\*</sup>, Sinan Fidan<sup>3</sup>

<sup>1,3</sup>Faculty of Aeronautics and Astronautics, Kocaeli University, Kocaeli, Türkiye

<sup>2</sup>Institute of Natural and Applied Science, Kocaeli University, Kocaeli, Türkiye

## Article History

Received: 07.02.2022

Accepted: 22.06.2022

Published: 15.12.2022


## Research Article


**Abstract** – An aerodynamic technique to calculating lift and drag coefficients is one of the required instruments in the wing design process. During the last decades, several tools and software have been developed according to aerodynamics and numerical methods. Nowadays, aeronautical architecture requires many calculations. Today's technologists use a variety of simulation techniques to avoid a expensive model testing. This paper explains how wing profiles can be modelled using ANSYS Fluent and tested by low-speed tests considering experimental literature results. With the selected wing profile, the geometry is shaped in two dimensions and designed in three dimensions. Computational fluid dynamics (CFD) was adopted as the method for studying wing profiles. Wing profiles created at 0 to 20-degree attack angles are calculated in the simulation area equal to the actual wind tunnel scale, and equations are solved using the RNG k-Epsilon turbulence model. The process of developing the grids was realized with Ansys Mesher software. The solution stage and the result show operations were carried out with the CFD Post software. The study of the low velocity and high transport wing profiles, the drag coefficient, the lift coefficient, and the effect on the lift-drag ratio were studied using a numerical procedure. After determining the high efficiency of wing profiles, production of a selected profile began with a static examination.


**Keywords** – Airfoil, ANSYS, CFD, lift, NACA

## 1. Introduction

A wing represents a surface used to travel in an air medium perpendicular to the direction of motion to produce aerodynamic forces. A wing is a device used for producing lift with distinct contour structures. The aerodynamic efficiency of some gliders will exceed 60 or higher when expressed by the ratio of lift to drag coefficient. To achieve lift (Chitte, Jadhav, & Bansode, 2013), this means that less thrust is necessary. To obtain the limits, we require, there are two methods (lift, drag, moment coefficient, etc.). These are simulation and experiment. The item or object is inserted in the air stream for the study, and a few holes are opened on it and pressure calculation is performed. The pressure can be determined ahead of the time at each stage, and the drag rise, etc. It is used in coefficient estimation. Be it as it might, this procedure takes time, and the error margin is high. Then again, more developed PC (Personal Computer) simulations allow one to achieve the ideal characteristics in a much more limited period. The most widespread programming of PC programs is CFD (computational fluid dynamics). Inside the measurement field, the point is to illustrate. During simulation, with the assistance of the software, stream conditions are discussed in the ideal process. Simulation gives us the most rational yield characteristics. In this review, CFD programming, which provides faster performance, was preferred because the wind tunnel experiments were expensive and lengthy.

<sup>1</sup>  [urgun@kocaeli.edu.tr](mailto:urgun@kocaeli.edu.tr)

<sup>2</sup>  [mertgokdemir26@gmail.com](mailto:mertgokdemir26@gmail.com)

<sup>3</sup>  [sfidan@kocaeli.edu.tr](mailto:sfidan@kocaeli.edu.tr)

\*Corresponding Author

Carbon fibre reinforced polymers (CFRP) have commonly been used for about forty years in various applications. For e.g., their boss features, low weight, and high efficiency make them an enticing opportunity for certain products in different fields, including aircraft, automobile, and sea applications. In the aviation industry, the early use of composites was essentially for auxiliary non-basic applications, such as coatings and flight control surfaces (Kumara, Raghavendra, Venkata, & Ramachandra, 2012). Given the strict logistical nature of the aviation sector, various subtleties of accreditation and continuity should have appeared to precede the expanded use of these products over the airframe, recognizing that these guidelines are continuously evolving to ensure the general population's well-being (Schmid, Kruse, Korwien, & Geistbeck, 2015). The use of composites in both industrial and military airframes currently approach 40% and is used for critical load manner elements. The change was possible because of the company's dedication to this creation and the steady growth as the manufacturing approaches in the test, material, and cycle strategies. The modelling network gained the certainty of dealing with composites from such tests with numerous wins, numerous misfortunes, and exercises learned (Davies, Choqueuse, & Devaux, 2012). Despite the specialized angle, the conservative hand primarily influenced grasping composites. Compared to metal, the use of lighter-weight fabrics meant that airlines and operators could get a decent deal during operation on fuel prices. It was found that with every pound saved of weight; a saving of \$46 can be made, accepting \$3.44 per gallon of jet fuel (Aviation Outlook, 2021).

With respect to composites, the basic cost factors are the crude material, tooling, function, amount of manufacturing, the scale of output, and machinery. In such areas, any changes will theoretically bring down the prices. With the developments in these fields over the next few decades, the cost of constructing plastic products is agreed to be extreme for metallic materials, which would make them a substantially greater candidate for potential items (Shama, Simha, Rao, & Kumar, 2020). By combining two separate materials that have properties that are obtained by consolidating multiple elements, composite materials are produced. Composite materials are often referred to as composition materials, which are the materials created using at least two constituent materials with various physical and synthetic properties, which coat a substance with different characteristics from its constituents when consolidated. In addition, the constituent components for composites are referred to as 'Reinforcement material and matrix material' that are correctly mixed to achieve the optimal properties, such as dimensional protection, electrical opposition, etc. To obtain adequate consistency in the composite material, the re-enforcement material, and the matrix material must be joined in suitable places. In general, the efficiency of the composite materials depends on the ratio of the reinforcement material and the matrix material. There is a big overview of composite materials, including polymer matrix, ceramic matrix, and metal matrix composites, which are commonly used in the industry. Current research and engineering involve a completely different category of cutting-edge materials, particularly in the areas related to shipping, aviation, and military architecture (Choubey et al., 2018, Lee et al., 2017, Delogu et al., 2017, Karthigeyan et al., 2017, Yadav et al., 2017). For aircraft frames, exceptional corrosion, and fatigue-damage tolerance, composites have demonstrated weight savings. Applications for commercial aircraft have gone from limited flight control surfaces to an ever-increasing number of critical structures (Schwartz, 1992).

Onour (2011) conducted the hypothetical study of AG24, AG35, AG455ct, CAL1215j, CAL2263m, and CAL40411 profiles. Using MATLAB tools at low Reynold's coefficients, test estimations were obtained. As per the results, in the low Reynolds number, the maximum value for the angle of attack and drag coefficient was achieved, and in the high Reynolds number, the minimum value was reached. A high Reynolds number and a minimum value for a low Reynolds number were obtained for the highest lift coefficient/angle of attack. The comparative results show the AG35 airfoil is the most acceptable profile for the design.

Parashar (2015) planned the study of NACA2415, NACA23012, and NACA23105 airfoils, using the GAMBIT and Fluent commercial CFD systems. For flow, using the regular  $k-\epsilon$  disruption model, momentum continuity equations are studied. With CATIA's guidance, 2D wing geometries were obtained at a chord ratio of 0.5 C. At differing attack angles at -15 and +15 degrees, the two streamlined limits were calculated. In determining aerodynamic efficiency, these two limits are of prime importance. Contrary to NACA2415, NACA23015 and NACA23012, at the extreme angle of attack, NACA23012 airfoil produced the least drag at = 0. If the limit is NACA23012 (at the lift coefficient), the lowest drag has been reached.

In this study, Syamsuar, et al., (2016) proficient low-speed airfoil determination and optimization was conducted using multi-directional analysis for unmanned aerial vehicles. The enhancement period involves low-speed airfoil details and design optimization measures as shown by the design needs provided. In unmanned

aerial vehicles, the stability criteria are of high importance due to low clutter and poor stability. Using computational fluid dynamics (CFD), tests were conducted. In XFOIL and ANSYS, studies were conducted using the model of Navier Stokes. In selecting the required airfoil for the design criteria, the weighting technique was used to find the greatest weight value. When the calculations of lift, drag, moment coefficient, and angle of attack were compared with 29 wing profiles as a database, the TL54 wing profile got the highest score.

In the Jony (2014), The drag lift force and overall pressure distributions affecting the NACA6409 and NACA4412 profile profiles were also considered, and flow analysis was analysed. Different variables were obtained by adjusting the angle of attack. In the analysis, the ANSYS Workbench 14.5 programming finite element approach and computational fluid dynamics (CFD) were used to render connections. On the top surface of the NACA4412 airfoil; there is less negative pressure than on the top surface of the NACA6409 airfoil. Separately, the lift/drag ratios for NACA4412 are 3.365 and 5.382 for 0 and 5 degrees. Then again, for the NACA6409 profile, the lift/drag proportions are 0.39 and 0.66 at the attack angle between 0 and 5 degrees, individually. The optimal profile should regularly have a high proportion of lift/drag. The NACA4412 profile is more suitable for aerodynamic applications by comparing the results.

Based on the examples above, the wing profiles, which are widely used today, were analysed at varying angles of attack, and the targeted optimum profile was tried to be obtained. Fuel consumption is of high importance for operator companies and developers in today's aircraft. The way to increase fuel consumption on an aircraft or airfoil is to have the best efficiency that can be requested from its profile. Considering these interests, our aim in our study is to compare 4 different wing profiles in terms of their specific characteristics (carrying, drag coefficient, aerodynamic efficiency) and to produce the most efficient profile in order to set an example for later studies. Creation from composite material was chosen as a new technique in the production of the wing profile, which was examined using simulation software. It has been determined that the application potential of composite material wings and load-bearing parts in wing structures of the proposed size is high. Because of their complex geometry, load-bearing parts inside the wing are challenging to produce from composite material. Precision molding and surface smoothing procedures were used to ensure that the tolerances and dimensions of the composite load-bearing parts were met throughout the manufacturing phase. During assembly, a holistic structure was built by using unique processes to each piece manufactured as a composite part in order to construct a full wing structure.

## **2. Design and Analysis**

The main feature in determining the consistency of acceptance is finite element mesh since the nodes generated characterized the performance parameters for the analysis (Kanesan, Mansor, & Abdul-Latif, 2014). The primary motive behind any configuration of the airfoil is to create an airfoil that offers a more notable lift calculation without drag expansion. Even, without stalling, the airfoil should have the option of operating at high angles of attack (Fertis, 1994). The philosophies of airfoil and wing design have taken huge strides forward with the accessibility of fast computing resources that consider precise aerodynamic efficiency targets. These aims are mainly to improve an efficiency measurement, such as the proportion of lift over drag, or its item with flight Mach number in higher-speed systems. The need for extended lift at higher flight levels, with drag held low has prompted the creation of information bases for streamlined design (Sobieczky, 1999). Currently, wing prototypes are not made by hand, but with the aid of PCs. Two classes of methods are usually based on these new computerized modelling techniques. They either use quasi-experimental equations or use lower-fidelity mathematical devices to help determine the appropriate limits, such as streamlined properties, flight efficiency, applied loads (Jaroslaw, & Raphael, 1996, Cm Erep, 1986). There are several steps toward developing a wing and carrying it to the testing level. The importance of the demand opportunity and the needs of analysis and the area of use (Anderson, 1999, Anderson, 2001) form it. It is important that before the design can begin, the task needs to be characterized. The corresponding stage is to create a concrete design following the design proposal. For another aircraft, the conceptual architecture constructs the main general scale and structure. It requires the load evaluations and the determination of simplified qualities that would be most relevant to the prerequisites of the mission expressed in the proposal for a design. The iterative circle in the flow map demonstrates this. The design transitions to the following level, which is the preliminary design (Meganathan, 2014), at the point where the mission prerequisites are met. It is important to distinguish and address conflicts of need and to place the required measure of focus on specifications that arise as the concept matures. The visible proof and regulation of significant performance attributes (Henne, 1990), are the key

challenge in airfoil configuration. During the wing design process, 18 boundaries must be resolved. They are as per the following:

1. Wing reference (or planform) area ( $S_w$ ,  $S_{ref}$  or  $S$ ).
2. Number of wings.
3. Vertical position relative to the fuselage (high, mid-, or low wing).
4. Horizontal position relative to the fuselage.
5. Cross-section (or airfoil).
6. Aspect ratio (AR).
7. Taper ratio ( $\lambda$ ).
8. Tip chord ( $C_t$ ).
9. Root chord ( $C_r$ ).
10. Mean aerodynamic chord (MAC or  $C$ ).
11. Span ( $b$ ).
12. Twist angle (or washout) ( $\alpha_t$ ).
13. Sweep angle ( $\Lambda$ ).
14. Dihedral angle ( $\Gamma$ ).
15. Incidence ( $i_w$ ) (or setting angle,  $\alpha_{set}$ ).
16. High-lifting devices such as flap.
17. Aileron.
18. Other wing accessories.

Of the above considerable rundown, until this point (during the preliminary design step), only the first (i.e., planform region) has been determined. An iterative period is the wing configuration, and the determinations/computations are normally repeated a few times (Sadraey, 2013). In a wing structure, where the airflow first meets, the leading edge is known, and the trailing edge is known when the airflow leaves. The wing cross-section beamline (veter) is called the line joining these two points. The arc that goes around the middle of the upper and lower surfaces and joins the leading edge and the chord is known as the trailing edge. If analysing, there are two variables that we consider thickness and chord. The highest curvature of the NACA23012 airfoil is 2% of the beam length and 12% of the beam length is the maximum thickness. In low-speed airplane wings, the wing area of NACA23012 is commonly used. The proportion of thickness in the NACA4412 profile is 12% and the proportion of curvature is 4%. Airfoil NACA4412 has a large range of aircraft applications, from wind turbines to air cushion aircraft. The TL54 is usually favoured because, like Rc Motors, it creates lower profile drag at low speeds. The proportion of thickness in the TL54 profile is 9.99% and the proportion of curvature is 2.41% like hovering boats, miniature quad copters etc. The AG35 profile used in low speed unmanned aerial vehicles has an 8.7% thickness and a 2.3% curvature proportion. It was only developed when the aerodynamic efficiency 4412 wing profile achieved the highest score. The design process must be undergone before a component can be made. Two major steps are performed in this step, to be specific to the drawing and examination of the component. A specification is rendered during the section's drawing time in conjunction with the role where it will be used. In this design, things are mulled over, for example, function and aesthetics. Nonetheless, it is not clear if the operational conditions of the design carried out would accomplish the purpose here. Significant engineering measurements and observations should be made to address this question.

Aerodynamic coefficients depend on attack angle, geometry (geometry of the profile, geometry of the wing, configuration of the airplane), number of Reynolds, and number of Mach. The airfoil lift and drag coefficients are experimentally acquired or applications that can be used during profile selection causes estimated values to be used. A PC with a 3.5 GHz 4-core AMD Ryzen 5 1500X CPU, 16 GB RAM, and a 64-bit Windows 10 operating system was used for the simulation. To evaluate the fluid streaming over the profiles, the program ANSYS Fluent (version-16) was used. To maximize outcomes, an organized mesh is used. The angle of attack is defined as the angle on the plane or wing between the air and relative wind over the wing and a reference line (veter). This angle determines the aerodynamic powers of drag that exist.

Table 1  
Specification of input parameters

Parameters	Magnitude
Solver Type	Pressure-based
Time	Steady
Velocity of flow	22.22 m/s
Operating temperature	300 K
Operating pressure	1 atm
Viscous model	K-epsilon (2 eqn)
Density of fluid	1.225 kg/m <sup>3</sup>
AoA of airfoil	Steady
Kinematic viscosity	1.79E-05
Reynolds number	Vary with air velocity
Number of iterations	1000
Angle of attack	0 to 20
Solution method	Second order upwind
Length	1 m

The k-ε realizable turbulence model was used to assess the aerodynamic efficiency of the two-dimensional flow on the wing profiles in computational fluid dynamics. The input values are specified in Table 1 above.

### 2.1. Realizable k-e turbulence Model

The most well-known model used in Computational Fluid Dynamics (CFD) to simulate average flow properties under turbulent flow conditions is the K-epsilon turbulence model. To view turbulence flow, it has two additional transport equations. These two models of equations, for instance, convection and diffusion, help to understand the impacts of turbulent energy.

- The first variable is turbulent kinetic energy, k
- The second variable is the turbulent distribution, ε

The variable determines the turbulence scale, while the primary variable k determines the energy in turbulence (Jones, & Launder, 1972, Launder, & Sharma, 1974). The K-epsilon model can be derived as follows:

$$\frac{\partial}{\partial t}(\rho k) + \frac{\partial}{\partial x_j}(\rho k u_j) = \frac{\partial}{\partial x_j} \left[ \left( \mu + \frac{\mu_t}{\sigma_k} \right) \frac{\partial k}{\partial x_j} \right] + P_k + P_b - \rho \epsilon - Y_M + S_k, \frac{\partial}{\partial t}(\rho \epsilon) + \frac{\partial}{\partial x_j}(\rho \epsilon u_j) = \frac{\partial}{\partial x_j} \left[ \left( \mu + \frac{\mu_t}{\sigma_\epsilon} \right) \frac{\partial \epsilon}{\partial x_j} \right] + \rho C_1 S \epsilon - \rho C_2 \frac{\epsilon^2}{k + \sqrt{\nu \epsilon}} + C_{1\epsilon} \frac{\epsilon}{k} C_{3\epsilon} P_b + S_\epsilon \quad (2.1)$$

Turbulent viscosity is modeled as follows,

$$\mu_t = \frac{\rho C_\mu k^2}{\epsilon} \quad (2.2)$$

K generation can be written as,

$$P_k = \overline{\rho u_i u_j} \frac{\partial u_j}{\partial x_i} \quad (2.3)$$

S is the modulus of the average strain rate tensor defined as:

$$S \equiv \sqrt{2 S_{ij} S_{ij}} \quad (2.4)$$

The model constants used for these equations are:

$$C_{1\epsilon} = 1.44, C_{2\epsilon} = 1.92, C_{3\epsilon} = -0.33, C_{\mu} = 0.09, \sigma_k = 1.0, \sigma_{\epsilon} = 1.3 \quad (2.5)$$

## 2.2. Lift to-drag ratio

The lift-to-drag ratio, or L/D ratio, in aerodynamics is the division of the lift produced by a wing or vehicle by the aerodynamic drag it creates by flying. One of the key targets of wing/airplane architecture is a higher or greater L/D proportion. Low drag offers fuel savings and improved climbing performance, as the required lift is acclimatized to the weight. Lift/drag is the speed vector that shows in the 2D map. The image produces a U shape in almost all situations since the drag has two main components. Wind tunnel flight simulation, measurements, or testing (Wu, Sun, Luo, Sun, Chen, & Sun, 2018), can calculate lift-to-drag ratios. The obtained aerodynamic efficiency values are shown in Table 2.

Table 2

Aerodynamic efficiency comparison

AoA	4412	AG35	23012	TL54
0	16.94	19.3	7.28	8.33
5	12.54	13.85	15.52	13.78
10	8.78	8.87	10.27	9.1
15	6.5	6.19	7.25	5.91
20	5.09	3.45	5.47	2.82

## 2.3. Drag and Lift Coefficient

The drag coefficient in fluid dynamics is a dimensionless quantity in a fluid medium, such as air or water that is used to measure an item's drag or opposition. A low drag coefficient allows an object to have less aerodynamic drag. The drag coefficient is continuously bound to a particular region of the surface (Stollery, 2017). In the drag coefficient condition, the drag coefficient utilizes the wing region as the reference region. The drag coefficient is an unfathomable value that is used to determine the fluid opposition of moving objects. The lift force (coefficient) is a mechanical aerodynamic force generated by the fluid flowing through a rigid body, and this force opposes and maintains the weight of the moving mass in the air. A vector acts against the flying item's centre of pressure. The lift is obtained from the fluid velocity differential around the flying object. If the object is flowing through or fluid, streaming through an object does not make a difference. Usually, the lift coefficient is determined without dimensions (Sharma, 2016).

$$c_D = \left( \frac{2F_D}{\rho u^2 A} \right), c_L = \left( \frac{2F_L}{\rho u^2 A} \right) \quad (2.6)$$

Table 3

Lift coefficients

AoA	4412	AG35	23012	TL54
0	0.192	0.1467	0.043	0.08
5	0.439	0.3866	0.2795	0.3142
10	0.685	0.6342	0.527	0.5411
15	0.936	0.8713	0.775	0.722
20	1.171	0.7433	1	0.7615



Table 4  
Drag coefficients

AoA	4412	AG35	23012	TL54
0	0.011	0.0076	0.0059	0.0096
5	0.035	0.0279	0.018	0.0228
10	0.078	0.0715	0.0513	0.0594
15	0.144	0.1407	0.1068	0.122
20	0.23	0.2151	0.1827	0.27

The above Table 3 and 4 shows the lift and drag coefficients. The data obtained are calculated depending on the lift coefficient ( $c_L$ ), drag coefficient ( $c_D$ ), free flow velocity ( $u$ ), free flow density ( $\rho$ ) and profile veter length. For the NACA23012 and NACA4412 profile, the lift coefficient reached the threshold of 1 value.

### 3. Manufacturing

After the review and saved in phase format our NACA4412 airfoil was modelled in the SolidWorks software. Then, by running an output in ANSYS Mechanical, the material properties of the profile (ribs and stringers) to be used are allocated. The manufacturing process eventually began. In our research, we chose EPIKOTETM Resin MGS ® L285 (Epoksi hexion, 2021), which are used with extremely strong mechanical and thermal properties in aviation and model aircraft. For the mold, polystyrene material (white foam) was used. The use of polystyrene is effective, so it will be useful for airfoil model growth. Only the NACA4412 airfoil with a 2750 mm chord and a 2300 mm span width was planned. There are nine ribs and five stringers of skin in the wing system. As seen in Figure 2, the wing structure is shaped.

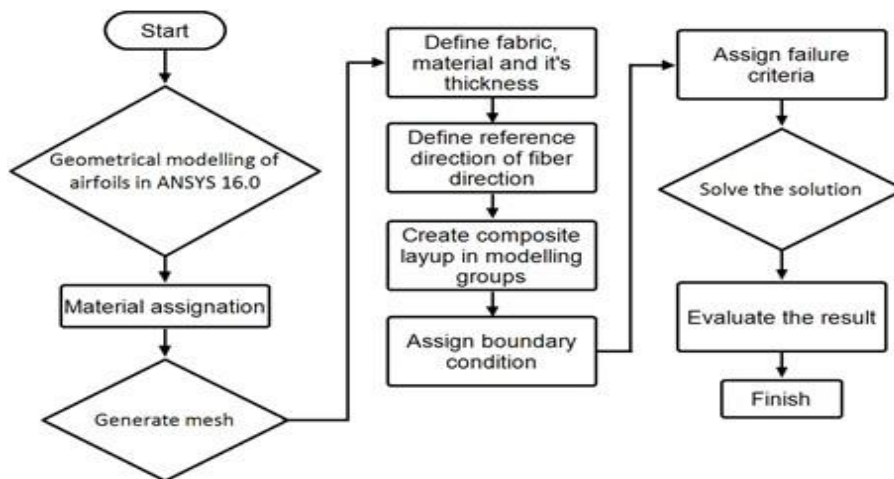


Figure 1. Design parameters

In Figure 2 above, the steps to be taken to build a wing profile are given. First, the wing profile was modelled with Ansys package program. After the material assignment, the meshing process is performed to determine the thickness and fabric of the material. After modelling, fault assignment is made and the results are evaluated, and the design is completed. The method proceeds in the event of a potential mistake by returning to the previous stage. Airfoil structure and construction phase are given in figure 3 and 4.



Figure 2. Wing structure

Two carrier aluminum spars were used in the production of the blade shown in Figure 3. Ribs are primarily produced with XPS polyurethane and covered in 3 layers with epoxy and glass fiber fabric. Ribs are connected at different points with stringers produced with glass fiber fabric and epoxy. Finally, as can be seen in Figure 4, the wing skeleton formed is covered with glass fiber fabric and epoxy, thus creating a very light and strong wing.



Figure 3. Construction of NACA4412 profile

#### 4. Results and Discussion

Using a denser mesh of the wing area, 727946 Elements and 167323 Nodes were made for a performance that is more accurate. As the leading and trailing edges are the focuses that first take the air and leave the air, in these regions the solved equations should be more sensible. These regions are, however, filled with a mesh of 0.002 units. To define the boundary region of the flow, an extra zone has been inserted along with the wing profile. The air's inlet and exit points are overcome. The chord was picked to be 1 meter and the flow area behind the wing was 10 meters of laminar flow. The goal of this analysis is to use the ANSYS Fluent software

to generate a virtual model of the external flow across the wing profiles AG35, NACA4412, NACA23012, and TL54 and to validate it by measuring it at a low speed (22.22 m/s) in the light of the experimental data acquired from the literature. Changing the airfoil's attack angle indicates important speed changes. There is a greater value for the velocity on the top surface of the wing than on the lower surface. As a result, the friction on the upper surface is minimal relative to the wing's lower surface. The entity would shift from the higher-pressure zone to the lower pressure region, as per Bernoulli's theorem. Therefore, on the wing, lift exists. The turbulence grows, as in the writing, as the angle of attack increases at the end of the study. The velocity or AOA must be altered to keep up the laminar flow. The wing angle and velocity of the incoming fluid (air) were held steady throughout the simulation. As a working setting, 15°C 1 ATM pressure and 22.22 m/s speed were used. The methodology of the Coupled Scheme approach was used, which is time-dependent and can arrive at a fast solution. Since our geometries are large, long and there are various regions with pressure variations over them, the Realizable model was picked.

In the rest of the study, the pressure, and velocity-dependent behaviours of all airfoils at 0 and 20 degrees were envisioned. The high-pressure zone at the leading edge and the low-pressure zone on the lower surface of the airfoil system can be seen from the contours. The photos in the figures demonstrate simulation effects of static pressure and velocity changes with the K-epsilon turbulence model at an angle of attack of 0° to 20°. The profile of NACA4412 reached 28.8 m/s on the upper surface of the wing at the maximum velocity. At the same time, as the velocity-pressure is equal to the opposite, the NACA4412 profile with ~ (-250) Pa. was the least pressure on the wing. This makes us the most notable lift at 0° on the NACA4412 profile. While the profiles tend to display smooth flow, the maximum speed of the NACA4412 profile was 48.4 m/s and the maximum speed of the NACA23012 profile was 48.2 m/s. At the leading edges, the NACA4412 and NACA23012 profiles are somewhat stalled, and the entire profile has dropped into stall by decreasing the speed at the trailing edges to 0 m/s. The analysis provides improved results in all profiles below 16 degrees of attack angle for 22.22 m/s velocity. The results show that the predicted drag coefficient in the K-epsilon turbulence model is in good accordance with the experimental evidence. The findings obtained from the simulations demonstrate that lift and drag coefficients for the wings are not greatly influenced by the free flow velocity. Compared to low speeds, the airfoil experiences an increase in lift coefficient and a decrease in drag coefficient at high altitudes. The disparity between airfoil lift and drag coefficients can be explained by the existence of low-velocity separation at a lower attack angle as opposed to high velocity. In different scenarios during the cycle, the simulation provided incredibly interesting results for pressure distribution. Compared to the root, the lower static pressure distribution near the wing tip affirms the three-dimensional movement across the wing. As the angle of attack increased, it was observed, and values increased. The stall happened after 15 degrees because the speed diminished to 0 m/s. With the flow rate, the pressure on the lower and upper surfaces of the profile grew. This result revealed that when in the air, a wing profile or airplane needed to exceed a certain speed to take off and fall below a specific speed. The literature has stated that the pressure differential increases with the effect of the lift on the wing, the difference of pressure below or more with the speed and angle of attack on the wing. The analysis of four airfoils indicates that in applications where the theory is attempted, the NACA4412 airfoil configuration should be preferred as it achieves greater lift force with the least drag force.

#### **4.1. Structural Static Analysis of NACA4412 Airfoil in Ansys**

An airfoil was previously developed and stored in the Solid Works program. In Ansys Workbench, stage format is entered. In the engineering details in the Ansys library, the content properties are entered. In Figure 5 below, the material properties are added. The body (fixed support) has one end of the wing fixed to it. The wing's other end is open. In this manner, deformation and stress values added to the wing can be obtained by correcting one foot. Analysis of stress is essential to structural architecture. Wing construction geometry, with the most optimal range of structural parameters such as material and width, should be light and robust to critical loads.

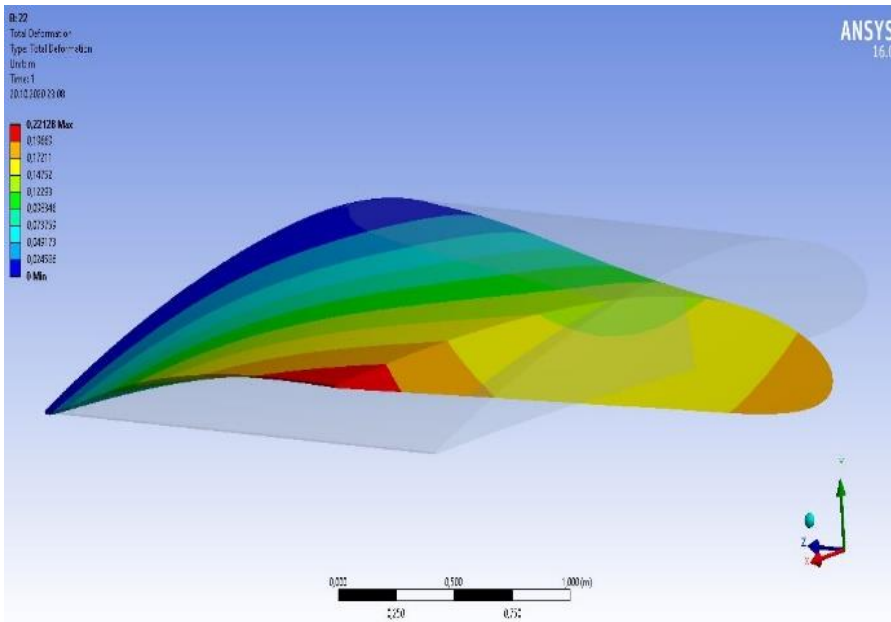


Figure 4. Total deformation on NACA4412

The cumulative displacement of the wing at the pressure and speeds applied to the NACA4412 airfoil is 0.221 m, as can be seen in the visuals above. These values give us knowledge about the changes in the angle of the base and the wings' deformation.

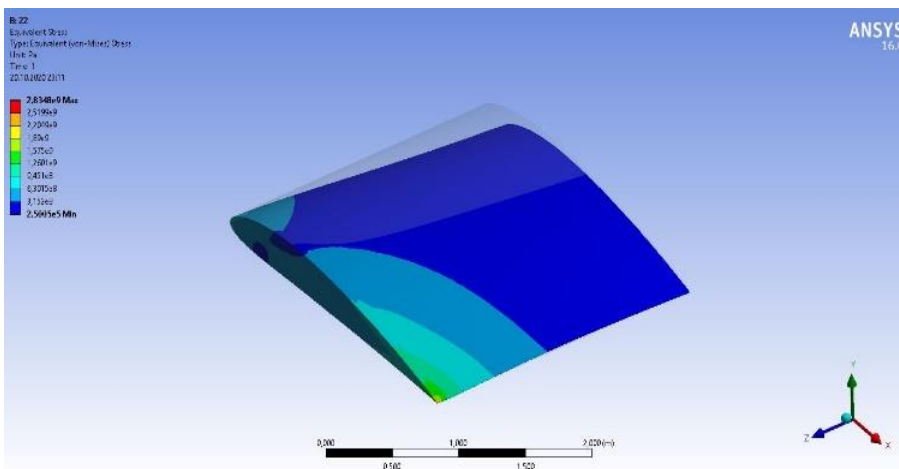


Figure 5. Von-mises stress

In Figure 6 above, Von-mises stress is observed. The stress distribution on the airfoil decreases from the wing root to the wing tip. The stress on the wing is observed from the root of the wing. It is colored lighter at the root of the wing and with a darker color chart as it moves away from the root of the wing.

**4.2. Modal Analysis of NACA4412**

To perform modal analysis to determine the wing model's normal frequency and mode shape. The wing subjected to unpredictable aerodynamic loads will easily fail due to resonance if the normal frequency of the wing coincides with the frequency of the load. For detailed dynamic analysis of wing models in the future, modal analysis is a prerequisite. A classic problem of self-value is modal analysis. The kinematic equation is the basic harmonic vibration of the free vibration of the structure, which means that the displacement meets the function of the sinus.

$$x = x \sin(\omega t) \tag{4.1}$$

$$([K] - \omega^2[M])\{x\} = \{0\} \tag{4.2}$$

Equation (8) is a classic eigenvalue problem, the equation eigenvalue is, the extraction of a root is auto oscillation circular frequency, and the natural vibration frequency is. Vector related to is mode of vibration related to natural vibration frequency (Yongchang, Zhang, Li, Wang, & Tang, 2017).

Table 5  
Mode Frequencies

Mode	Frequency [Hz]
1,2	0
3	2.8184e-005
4	6.6268e-005
5	1.4164e-004
6	2.8383e-004

The consequence of the modal analysis is that, under these frequencies, the frequencies of 6 distinct modes and the deformation values are obtained. In the typical free frequency, the profile does not vibrate, but due to self-weight, certain timeline vibrations occur. Each natural frequency has a distinctive mode shape comparable to different amplitudes. Different modes can be seen in the Figure 7 below (deformed and unreformed).

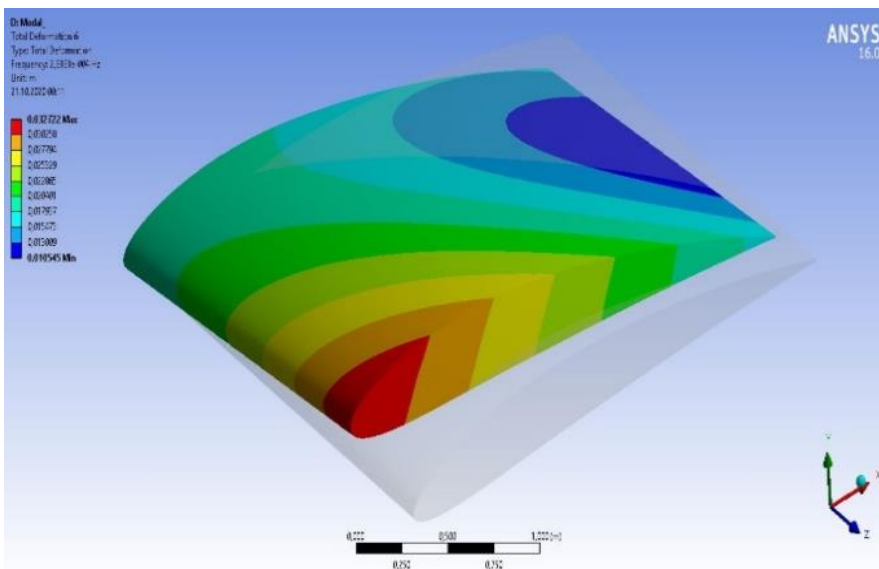


Figure 6. Modal analysis

The most appealing thing is to select an adequate airfoil profile in an airplane configuration. In this way, under the boundary conditions indicated for that airplane, the ideal measure of lift can be made. The most important values to be considered for the best possible aerodynamic configuration of the wing are lift-drag ratio, lift and drag coefficient. CFD simulation was used in this analysis to analyse the flow area and aerodynamic properties of airfoils AG35, NACA4412, NACA23012, and TL54, and numerical simulation was conducted at different attack angles (0°, 5°, 10°, 15°, and 20°). Using a realizable k-epsilon turbulence model and finite volume diagrams, flow properties were roughly analysed. It has been shown that the drag coefficient also increases as AoA increases. This rise is due to the increasing separation zone on the airfoil's upper surface and the increased pressure drag becoming greater than that under the airfoil. The lift generated by the wing profile increases as the angle of attack increases. The lift force decreased after the stall angle (15°). The discrepancy in the flow characteristics of the wing profiles can be deduced as follows, according to this study:

Max:

- 0°-5° AoA, AG35,
- 5°-15°-20° AoA, in the NACA23012 profile

Max:

- 0°-5°-15°-20° AoA, in the NACA4412 profile

Max:

- 0°-5°-10°-15° AoA, NACA4412
- 15°-20° AoA, in the TL54 profile

Even though the NACA4412 profile has the second-best performance among the profiles in terms of aerodynamic efficiency at reference values, the maximum drag and lift coefficient at all attack angles (0°, 5°, 10°, 15°, 20°) has been identified. Accordingly, considering these values under different circumstances, the NACA4412 airfoil should be selected for the specified conditions from among these four airfoils. In the 'static structure' portion of the Ansys workbench, pick the content first. A network of solutions, called meshes, was generated on the wings after choosing the materials. In addition, the values of deformation and Von-Mises stress were obtained. The contrary was not found, given the characteristics of the products we picked depending on the findings of the study. The consequence of the equation is that the final load does not surpass the safe value. The maximum value of the corresponding stress is 2.8348e9 Pa., with a gross wing displacement of 0.221 m at the pressure and speeds applied to the NACA4412 airfoil. These values give us knowledge about the changes in the angle of the base and the wings' deformation.

## 5. Conclusion

A plane wing construction is developed and constructed in this examination using Solid Works, a 3D modelling tool. The Rib and Spars provided structure for the wing. Typically, aluminium composites are components that are used for aircraft wings. Anyway, we used polystyrene for ribs, the spars, the skeleton, and the fibreglass composite for exterior coating in our own review. In the Ansys programme, a structural static analysis was carried out, which prevented the cost of experience. The deflection and strain on the wing were acquired through static analysis. The module was analysed to determine the normal wing frequency, which was subjected to continuous vibration during the flight. There is a possibility that the composite structure will resonate and fail to accomplish its mission. Today, the use of air vehicles for recreational, military and commercial purposes is becoming more frequent. Manufacturers require the design of the blades to satisfy the desired criteria. This includes developing blade geometries in response to needs, modifications, etc. Our study aims to lead the way for future studies by comparing wing profiles, which have different uses in aviation, with each other. Consequently, among the AG35, NACA 4412, NACA 23012, and TL54 airfoils that are commonly used in various aviation applications, the NACA 4412 airfoil with the best efficiency should be preferred. Since the study's conclusions were not validated in actual tests, outcomes will vary among designs. Afterwards, inside a larger flow volume and a more continuous arrangement organization, flow analysis may be presented within the work of this approach. Attacks, hyper-extends, and heated responses should be noted for further investigation. Landing gear, engine, and other analyses should be verified later in the construction stage.

## Author Contributions

Satılmış Ürgün: Conceived and designed the analysis.

Sinan Fidan: Collected data and performed the analysis.

Mert Gökdemir: Performed statistical analysis and wrote the paper.

## Conflicts of Interest

The authors declare no conflict of interest.

## References

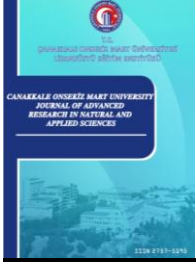
- Anderson, J. D. (1999). Aircraft Performance and Design, Boston, WCB/McGraw-Hill. Retrieved from: [https://www.academia.edu/40606141/AIRCRAFT\\_PERFORMANCE\\_AND\\_DESIGN](https://www.academia.edu/40606141/AIRCRAFT_PERFORMANCE_AND_DESIGN)
- Anderson, J. D. (2001). Introduction to Flight, McGraw-Hill, New York. Retrieved from:



- <http://ae.sharif.edu/~iae/Download/Introduction%20to%20flight.pdf>
- Aviation Outlook. (2021). Retrieved from: <https://www.compositesworld.com/articles/aviation-outlook-fuel-pricing-ignites-demand-for-composites-in-commercial-transport>.
- Chitte, P., Jadhav, P. K., & Bansode, S. S. (2013). Statistic and Dynamic Analysis of Typical Wing Structure of Aircraft Using Nastran. *International Journal of Application or Innovation in Engineering & Management*, ISSN: 2319-4847.
- Choubey, G., Suneetha, L., Pandey, K. M. (2018). Composite Materials Used in Scramjet- A Review. *Materials Today: Proceedings*, 5, pp. 1321-1326. doi: <https://doi.org/10.1016/j.matpr.2017.11.217>
- Davies, P., Choqueuse, D., & Devaux, H. (2012). Failure of Polymer Matrix Composites in Marine and Off-shore Applications. *Failure Mechanisms in Polymer Matrix Composites*. 1st ed., Woodhead Publishing, Cambridge, pp. 300-336. ISBN-13: 978-1845697501.
- Delogu, M., Zanchi, L., Dattilo, C.A., Pierini, M. (2017). Innovative Composites and Hybrid Materials for Electric Vehicles Lightweight Design in a Sustainability Perspective. *Materials Today Communications*, 13, pp. 192-209. doi: <https://doi.org/10.1016/j.mtcomm.2017.09.012>
- Epoksi hexion. (2021). Retrieved from: <https://www.dostkimya.com/tr/urunler/epoksi-sistemler/laminasyon-epoksi-hexion-mgs-l285-sistemi>
- Fertis, D. G. (1994). New Airfoil-Design Concept with Improved Aerodynamic Characteristics. *Journal of Aerospace Engineering*, 7(3), pp. 328-339. doi: [https://doi.org/10.1061/\(ASCE\)0893-1321\(1994\)7:3\(328\)](https://doi.org/10.1061/(ASCE)0893-1321(1994)7:3(328))
- Henne, P. A. (1990). *Applied Computational Aerodynamics*, Washington DC, American Institute of Aeronautics and Astronautics. ISBN: 093040369X 9780930403690
- Jaroslawn, S., Raphael, T. (1996). Multidisciplinary Aerospace Design Optimization: Survey of Recent Developments, *Structural Optimization*, 14, pp. 1-23. doi:10.1007/BF01197554
- Jones, W. P., Launder, B. E. (1972). The Prediction of Laminarization with a Two-Equation Model of Turbulence. *International Journal of Heat and Mass Transfer*, vol. 15, pp. 301-314. doi: [https://doi.org/10.1016/0017-9310\(72\)90076-2](https://doi.org/10.1016/0017-9310(72)90076-2)
- Jony, H. N., Hossain, S., Raiyan, F. M., Akanda, U. N. M. (2014). A Comparative Flow Analysis of Naca6409 and Naca4412 Aerofoil. *International Journal of Research in Engineering and Technology*, 03(10), pp. 342–350.
- Kanesan, G., Mansor, S., Abdul-Latif, A. (2014). Validation of UAV Wing Structural Model for Finite Element Analysis. *J Teknol*, 71, pp. 1-5. doi:10.11113/jt.v71.3710
- Karthigeyan, P., Raja, M. S., Hariharan, R., Karthikeyan, R., Prakash, S. (2017). Performance Evaluation of Composite Material for Aircraft Industries. *Materials Today: Proceedings*, 4, pp.3263-3269. doi: <https://doi.org/10.1016/j.matpr.2017.02.212>
- Kumara, S. M., Raghavendra, K., Venkataswamy, A. M., Ramachandra, H. V. (2012). Fractographic Analysis of Tensile Failures of Aerospace Grade Composites. *Material Research*, 15(6), 990-997. doi: <https://doi.org/10.1590/S1516-14392012005000141>
- Launder, B. E., Sharma, B. I. (1974). Application of the Energy Dissipation Model of Turbulence to the Calculation of Flow Near a Spinning Disc. *Letters in Heat and Mass Transfer*, vol. 1, no. 2, pp. 131-138. doi: [https://doi.org/10.1016/0094-4548\(74\)90150-7](https://doi.org/10.1016/0094-4548(74)90150-7)
- Lee, J. Y., Yan, J. A., Chua, C. K. (2017), Fundamentals, and applications of 3D printing for novel materials. *Applied Materials Today*, 7, pp. 120-133. doi: <https://doi.org/10.1016/j.apmt.2017.02.004>
- Meganathan, V. (2014). Aircraft Design Project-I: Heavy Business Jet. Retrieved from: [https://www.researchgate.net/publication/263850415\\_AIRCRAFT\\_DESIGN\\_PROJECT\\_I\\_Heavy\\_Business\\_Jet](https://www.researchgate.net/publication/263850415_AIRCRAFT_DESIGN_PROJECT_I_Heavy_Business_Jet)
- Onour, H. K., Jahangiri, M., Sedaghat, A. (2011). Theoretical Aerodynamic Analysis of Six Airfoils for Use on Small Wind Turbines, *Proceedings of the 1st International Conference on Emerging Trends in Energy Conservation – ETEC*, Tehran, Iran, 20-21 November.
- Parashar, H. (2015). Calculation of Aerodynamic Characteristics of NACA 2415, 23012, 23015 Airfoils Using Computational Fluid Dynamics (CFD). *International Journal of Science, Engineering and Technology Research*, 4(3), pp. 610–614. Retrieved from: <http://ijsetr.org/wpcontent/uploads/2015/03/IJSETR-VOL-4- ISSUE-3-610-614.pdf>
- Sadraey, M. (2013). *Aircraft Design: A Systems Engineering Approach*, 1st ed., Wiley, New Hampshire. ISBN: 978-1-119-95340-1.
- Schmid Fuertes, T.A., Kruse, T., Korwien, T., & Geistbeck, M. (2015). Bonding of CFRP Primary Aerospace



- Structures - Discussion of the Certification Boundary Conditions and Related Technology Fields Addressing the Needs for Development. *Composite Interfaces*, 22(8), pp. 795-808. doi: <https://doi.org/10.1080/09276440.2015.1077048>
- Schwartz, M. (1992). *Composite Materials Handbook*, 2nd ed., McGraw-Hill, New York. ISBN: 0070558191 9780070558199
- Shama, R. N., Simha, T. G. A., Rao K, P., Kumar, R. G. V. V. (2020), Carbon Composites Are Becoming Competitive and Cost Effective, Infosys Limited, Retrieved from: <https://www.infosys.com/engineering-services/white-papers/Documents/carbon-composites-cost-effective.pdf>
- Sharma, S. (2016). An Aerodynamic Comparative Analysis of Airfoils for Low-Speed Aircrafts, *International Journal of Engineering Research*, V5 (11), pp. 525–529. doi:10.17577/IJERTV5IS110361
- Sobieczky, H. (1999). Parametric Airfoils and Wings, In: Fujii K., Dulikravich G.S., Recent Development of Aerodynamic Design Methodologies, Notes on Numerical Fluid Mechanics (NNFM), vol 65, Vieweg+Teubner Verlag, doi:10.1007/978-3-322-89952-1\_4
- Stollery, J. L. (2017). Aerodynamics, Aeronautics and Flight Mechanics, *In Proceedings of the Institution of Mechanical Engineers, Part G: Journal of Aerospace Engineering*, Vol. 211, doi: <https://doi.org/10.1177/095441009721100102>
- Syamsuar, S., Djatmiko, E. B., Erwandi, E., Mujahid, A. S., Subchan, S. (2016). The Hydroplaning Simulation of Flying Boat Remote Control Model, *Jurnal Teknologi*, 78(6), pp. 191–197, doi: <https://doi.org/10.11113/jt.v78.4267>
- Wu, W., Sun, Q., Luo, S., Sun, M., Chen, Z., & Sun, H. (2018). Accurate calculation of aerodynamic coefficients of parafoil airdrop system based on computational fluid dynamic. *International Journal of Advanced Robotic Systems*, 15(2). doi: <https://doi.org/10.1177/1729881418766190>
- Yadav, S., Gangwar, S., Singh, S. (2017). Micro/Nano Reinforced Filled Metal Alloy Composites: A Review Over Current Development in Aerospace and Automobile Applications. *Materials Today: Proceedings*, 4, pp. 5571-5582. doi: <https://doi.org/10.1016/j.matpr.2017.06.014>
- Yongchang, Y., Zhang, S., Li, H., Wang, X., Tang, Y. (2017). Modal and Harmonic Response Analysis of Key Components of Ditch Device Based on ANSYS, *Procedia Engineering*, 174, pp. 956–64, doi: <https://doi.org/10.1016/j.proeng.2017.01.247>
- См, Егер. (1986). Основы автоматизированного проектирования самолетов.Машиностроение, pp. 232, Москва. Retrieved from: <https://www.dissercat.com/content/avtomatizatsiya-dokumentirovaniya-protsesta-formirovaniya-otseka-magistralnogo-samoleta>



## Deniz Ulaştırma İşletme Mühendisliği Bölümlerindeki Hiyerarşik Yapının Öğrenciler Üzerindeki Psikolojik Etkilerinin Kapsamlı Analizi

Devran Yazır<sup>1\*</sup>, Sefa Yay<sup>2</sup>

<sup>1</sup>Deniz Ulaştırma İşletme Mühendisliği Bölümü, Sürmene Deniz Bilimleri Fakültesi, Karadeniz Teknik Üniversitesi, Trabzon, Türkiye

<sup>2</sup>İstatistik ve Bilgisayar Bilimleri Anabilim Dalı, Fen Bilimleri Enstitüsü, Karadeniz Teknik Üniversitesi, Trabzon, Türkiye

### Makale Tarihi

Gönderim: 20.09.2021

Kabul: 23.06.2022

Yayın: 15.12.2022

### Araştırma Makalesi

**Öz** – Hiyerarşik yapının olduğu kurum ve kuruluşlarda ast-üst ilişkisinin olduğu bilinmektedir. Hiyerarşinin olduğu kurum ve kuruluşlarda hayatının belirli bir kısmını geçiren bireyler hem bireysel hem de gruplar halinde psikolojik olarak olumlu veya olumsuz etkiler yaşamaktadırlar. Bu çalışmada, hiyerarşik yapının Deniz Ulaştırma İşletme Mühendisliği Bölümlerinde (DUİM) öğrenim gören öğrencilerin psikolojilerine yönelik olumlu veya olumsuz etkileri SPSS 23 paket programıyla kapsamlı olarak analiz edilmiştir. Uzman görüşleri alınarak DUİM öğrencilerine uygulanmak için anket hazırlanmıştır. Uygulanan ankete verilen 218 cevaptan 195'i geçerli sayılmıştır. Geçerli anketler üzerinden betimsel istatistikler yapılmış ve öğrencilerin sınıf düzeyleri ve cinsiyetleri tespit edilmiştir. Analizler gerçekleştirilirken hipotezlere ve kullanılacak veriye göre kararlar verilmiştir. Analiz için Bağımsız t-Testi, Tek Yönlü Varyans Analizi (ANOVA), Çok Faktörlü Varyans Analizi (MANOVA), Pearson'ın Ki-Kare testi, korelasyon analizleri yapılmıştır. Pearson'ın Ki-Kare testi ve Çok Yönlü Varyans Analizi için sonuçların derecelerini tespiti içinde ayrıca testler uygulanmıştır. Ankete verilen cevaplar analiz edildiğinde Öğrenciler Arasındaki Hiyerarşik Yapının (ÖAHY), öğrenciler tarafından desteklenmekte olduğunun ve öğrencilere katkı sağladığının tespiti yapılmıştır. Ayrıca öğretim üyelerinin ÖAHY'ye olan desteklerinin öğrenciler arasında negatif unsurların oluşmasında etki ettikleri ortaya çıkmıştır. DUİM öğrencileri arasında ÖAHY'yi oluşturan değerlerin korunmasına destek verilmesi önerilmektedir. ÖAHY'nin sağlıklı işleyebilmesi için öğretim üyelerinin etkilerinin gözden geçirilmesi önerilmekte ve nedenleri bir başka araştırma konusu olarak görülmektedir.

**Anahtar Kelimeler** – Ast-üst ilişkisi, denizcilikte örf ve âdet, öğrenci psikolojisi, SPSS, üniversitede hiyerarşik yapılaşma

## Comprehensive Analysis of The Psychological Effects of Hierarchical Structure in Maritime Transportation and Management Engineering Departments on Students

<sup>1\*</sup> Department of Maritime Transportation and Management Engineering, Sürmene Faculty of Marine Sciences, Karadeniz Technical University, Trabzon, Turkey

<sup>2</sup>Department of Statistics and Computer Sciences, Graduate School of Science and Engineering, Karadeniz Technical University, Trabzon, Turkey

### Article History

Received: 20.09.2021

Accepted: 23.06.2022

Published: 15.12.2022

### Research Article

**Abstract** – It is known that there is a subordinate-superior relationship in institutions and organizations with a hierarchical structure. Individuals who spend a part of their lives in institutions and organizations where there are a hierarchy experience positive or negative psychological effects both individual and in groups. In this study, the effects of the hierarchical structure on the psychology of the students studying in the Maritime Transportation and Management Engineering Departments (MTME) have been analysed with the SPSS 23 package program. A questionnaire was prepared to be applied to MTME students by taking expert opinions. Of the 218 answers given to the questionnaire, 195 were considered valid. Descriptive statistics were made through valid questionnaires and the class levels and genders of the students were determined. The analyses to be made were determined according to the hypotheses and the available data. Independent t-Test, One-Way and Multivariate Analysis of Variance, Pearson's Chi-Square test, and correlation analysis were used for analysis. For Pearson's Chi-Square test and Multivariate Analysis of Variance, additional tests were applied to determine the degrees of the results. According to the results, it was determined that the Hierarchical Structure Among Students (HSAS) was supported by the students and contributed to the students. In addition, it has been revealed that the support of the faculty members to HSAS influences the formation of negative elements among the students. It is recommended to support the preservation of the values that make up the HSAS among MTME students and review the effects of faculty members for the HSAS to function properly and its causes are seen as another research topic.

**Keywords** – Antiquities in maritime, hierarchical structure in the university, student psychology, SPSS, subordinate-superior relationship

<sup>1</sup> [dyazir@ktu.edu.tr](mailto:dyazir@ktu.edu.tr)

<sup>2</sup> [362503@ogr.ktu.edu.tr](mailto:362503@ogr.ktu.edu.tr)

\*Sorumlu Yazar

## 1. Giriş

Deniz Ulaştırma İşletme Mühendisliği Bölümü (DUİM) lisans eğitimi Türkiye’de 10 farklı üniversite tarafından verilmektedir (Gönülalçak, 2016; URL-1). Bölüm öğrencilerine verilen eğitim müfredatı, Gemiadamlarının Eğitim Belgelendirmesi ve Vardiya Tutma Standartları Sözleşmesi’ne (STCW) göre uygulanmaktadır. Bölümde öğrenim gören öğrencilerin uyması gereken bazı kurallar vardır. Bu kurallardan bazıları üniforma giymek, denizcilik örf adetlerine uymak ve Yüksek Öğretim Kurumu (YÖK) müfredatına uygun şekilde ders almaktır (Yıldırım vd., 2019; URL-2). Örf, Türkçede “yasalarla belirlenmeyen, halkın kendiliğinden uyduğu gelenek” anlamına gelmektedir. Adet, Türkçede “görenek, alışkanlık, topluluk içinde eskiden beri uyulan kural” anlamına gelmektedir. Örf ve âdet kavramları yazılı olmayan sözlü kuralları tanımlamaktadır (URL-3).

Denizcilik eğitiminde ve gemi yaşantısında örf ve adetlerin yanı sıra gemiadamlarının çalışma ortamında bulunan organizasyon yapısında diğer işyerlerine nazaran farklı olarak hiyerarşik zincire dayalı bir iletişim sistemi yer almaktadır (Demir ve Çolak Gürkan, 2020). Uygulanan hiyerarşik yapının sektör için gerekli olduğu düşünülmektedir. Hiyerarşi, emir-komuta zincirinden oluşmuş üstün asta emir vermesi ile kurum içi düzenin sağlanmasında etkili yapıya denilmektedir. Kurum veya topluluklarda astın, üst tarafından denetlenmesini sağlayan ve kurum içindeki bütünlüğü sağlıklı iletişim kurarak korumanın temeli hiyerarşik yapılanma olmaktadır (Türk, 2019). Hiyerarşik örgüt kültürü, organik bir yapıda yukarıdan daralarak aşağıya doğru genişleyen, her kademedeki personelin, görevlerinin belli olduğu, çalışanların örgütsel bir çevre içerisinde davranışlarını gözlemleyen yönetim silsilesi olarak tanımlanmaktadır (Var, 2016; Hasırcı ve Örcü, 2021). Hiyerarşik yapı, gemi adamlarının derece olarak üstünde bulunan personelden aldığı görevleri yerine getirmesi gerekliliğini meydana getirmektedir (Demir ve Çolak Gürkan, 2020). Marume ve Chikasha (2016)’ya göre hiyerarşi “Bir kurum veya kuruluş içerisinde basamak şeklinde ve birbirlerine bağlı olarak en üst birimden en alt birime doğru aralarında emir komuta zinciri olacak şekilde düzenlenmesidir.” Hiyerarşide her ast bir üste bağlıdır. Astlık ve üstlük ilişkisinde, amir, emrinde bulunan astın memuriyet durumuna ilişkin işlem yapma, asta emir ve yönerge verme, astın işlemlerini hem hukukilik hem de yerindelik açısından denetleme yetkisine sahiptir. Ayrıca hiyerarşi olağan bir yetkidir ve Anayasada yer almamaktadır (Gözler ve Kaplan, 2017).

Hiyerarşik yapıya sahip kurum ve topluluklarda bir veya birden fazla kişiyi psikolojik olarak olumlu veya olumsuz etkileyen unsurlar ast-üst ilişkisinin içerisinde barınmaktadır. Bu unsurlar iletişim, motivasyon, güven, psikolojik taciz gibi bireyleri duygusal ve psikolojik olarak etkilemektedir (Gülver vd., 2014). Ayrıca, gemi organizasyonundaki hiyerarşik yapıda zayıf iletişimin denizcilerin iş yeri yalnızlık düzeyini etkilediği söylenebilir (Demir ve Çolak Gürkan, 2020). Yüksel (2005) ast-üst ilişkisinin olduğu yerlerde iletişim ve iş tatmini üzerindeki etkilerini araştırmış ve analiz ettiği çalışmada; ast ve üstler arasındaki iletişimin iş tatmininin olumlu çıkması sonucunda çalışanların işe bağlılıkları, personel bağlarının kuvvetlendiği ve çalışanların motive olduğunu tespit etmiştir. Bu bağlamda hiyerarşik yapıya sahip kurum ve topluluklarda olumlu psikolojik etkileri belirlemek için ast ve üst konumundaki kişilerin bağlarının, iş tatmini ve motive olma gibi duyguların tespiti ile hiyerarşinin öğrenciler üzerindeki olumlu psikolojik etkilerini tespit etmekte yardımcı başlık olarak kullanılması gerekeceği ileri sürülmüştür (Timuroğlu ve Balkaya, 2016).

Kurum veya toplulukların içerisindeki hiyerarşik yapı bireyler arasında güven, motivasyon, iş tatminliği, inanç gibi pozitif duygusal etkiler görülmektedir. Pozitif duygusal etkiler bireylerin psikolojik olarak güçlenmesini sağlar, örgüt içerisindeki bağlılığı kuvvetlendirir ve çalışanların yaratıcılığına katkıda bulunur (Kanbur, 2018; Zhao, Kessel ve Kratzer, 2014). Özler ve Yıldırım (2015), örgütsel güven ve psikolojik sermaye arasında bağ olup olmadığı ile ilgili yaptığı araştırmada işveren ile çalışan ve çalışma arkadaşları arasındaki güvenin olumlu psikolojik etkileri tespit etmişlerdir. Yapılan tespitlerde örgütsel güven arttıkça kurum içerisindeki bağların ve kuruma bağlılığın geliştiği aynı zamanda insan psikolojisini destek olma, motive olma, özgüven gibi olumlu duygusal psikolojik etki sağladığı görülmüştür. Öğretim üyelerinin dahil edildiği dönüşümcü liderliğin işe katılıma etkisinin araştırıldığı çalışmada, psikolojik güvenlik dönüşümcü liderlik ve işe bağlılık arasındaki ilişkiye aracı olduğu belirlenmiştir. Aynı zamanda öğretim üyelerinin geleneksel olmaları psikolojik güvenliğin işe bağlılık üzerindeki etkisini güçlendirmekte olduğu anlaşılmıştır (Xu, Zeng, Wang vd., 2022).

Bireyler arasındaki bağlılığı güven ve iletişimin sağlaması ile bireylerde birlik, beraberlik, özgüven, önemsenme gibi duyguların ortaya çıkması olumlu psikoloji olarak görünmektedir (Baloğlu ve Karadağ, 2008). Kurumlardaki çalışma ortamlarında ast-üst ilişkisi veya aynı mertebeye sahip personeller arasındaki

ilişki her zaman bireyin psikolojisini olumlu etkilememektedir. Psikolojik tacize (mobbing) maruz kalan kişilerde tükenmişlik, stres gibi olumsuz durumlara yol açmaktadır. (Albar ve Ofluoğlu, 2017). Denizcilik Fakültelerinin DUİM Bölümlerinde, ast-üst ilişkisi yani hiyerarşik yapı uygulanmaktadır. Özdemir (2018)'in araştırmasında hiyerarşik yapı öğrencilerin sosyal hayatlarını ve psikolojilerini olumsuz yönde etkilediği şeklinde belirtilmiştir. Çalışma ortamında bireyin psikolojisini olumsuz etkileyen en önemli etmen psikolojik taciz olmaktadır. Yapılan çalışmada psikolojik tacizin mağdur üzerinde ekonomik, sosyal, ruhsal ve fiziksel sağlığa olumsuz sonuçlara sebep olduğu belirtmiştir (Erdirençelebi ve Yazgan, 2017). Mobbingin Türkçe karşılığı olarak; psikolojik taciz, psikolojik terör, duygusal taciz, yıldırma, psikolojik şiddet, manevi taciz kavramları yaygın olarak kullanımına rastlanan terimlerdir (Göktürk ve Bulut, 2012). İnsan yapısı gereği sosyal bir varlık olduğundan sevmeye, sevilme, değer görme, önemsenme gibi duygusal ve psikolojik ihtiyaçlara gereksinim duyar. Bu ihtiyaçlara karşılık alamadığında kızgınlık, yalnızlık, içine kapanıklık ve kendini yetersiz görme gibi psikolojisini olumsuz etkileyen hislerle tanışmaktadır (Demirel ve Yücel, 2017).

Bu çalışma, Deniz Ulaştırma İşletme Mühendisliği Bölümü'nde öğrenim görmekte olan öğrencilerin hiyerarşik yapıdan kaynaklı olarak olumlu ve olumsuz psikolojik etkilerine, oluşturulan hipotezler çerçevesinde cevap aramaktadır. Bu araştırma 7 üniversitenin Denizcilik Fakültelerinin DUİM bölümü öğrencilerine uzman kişilerin görüşleri alınarak hazırlanan anket uygulanarak yapılmıştır. Analizler SPSS 23 paket programı ile kapsamlı şekilde yapılmıştır. Araştırma sonucunda eğitim kurumlarındaki hiyerarşik uygulamanın öğrenciler üzerindeki olumlu veya olumsuz etkilerinin tespiti ve çözüm önerilerinin sunulması amaçlanmıştır.

## 2. Materyal ve Yöntem

Bu çalışmanın amacı, 7 üniversitenin Denizcilik Fakültelerinin DUİM bölümü öğrencilerinin Öğrenciler Arasında Hiyerarşik Yapılanma (ÖAHY) hakkındaki düşünce ve fikirlerinin değerlendirilmesine yönelik, aynı zamanda öğrencilerin düşünce ve fikirlerini etkileyen faktörlerin tespitine yönelik istatistiksel analizler uzman kişilerin yardımıyla yapılmıştır. Çalışmada, SPSS 23 paket programı kullanılmıştır. Toplanan veriler için tanımlayıcı istatistikler ve frekans analizinden sonra verilerin türü ve dağılım tipine uygun olan testler uygulanmıştır. Önceden belirlenen hipotezlere göre gerekli karşılaştırma ve ilişki testleri ile analizler yapılmış ve sonuçları yorumlanmıştır.

### 2.1. Veri Toplama

Araştırmanın konusu itibarıyla Denizcilik Fakültelerinin DUİM bölümü öğrencilerinin değerlendirilmesine yönelik yapılacak istatistiksel analiz için uzman kişilerin görüşleri alınarak anket formu tasarlanmıştır. Anket formları, İstanbul Teknik Üniversitesi, Piri Reis Üniversitesi, Dokuz Eylül Üniversitesi, Ordu Üniversitesi, Recep Tayyip Erdoğan Üniversitesi, İskenderun Teknik Üniversitesi ve Karadeniz Teknik Üniversitesi Denizcilik Fakültesi DUİM öğrencilerine online olarak gönderilmiştir. Toplamda 218 yanıt alınmıştır. Bunlardan 23 tane öğrencinin okullarında ÖAHY olmadığını belirtmelerinden dolayı cevapları anketten çıkartılmış ve 195 örnek ile analizler gerçekleştirilmiştir.

### 2.2. Veri Analizi

Toplanan verilerle betimsel istatistikler gerçekleştirilmiş, grafik ve tablolarla değerlendirilmiştir. Uygun analizlerin belirlenebilmesi için verinin istatistiksel varsayımları sağlaması gerekmektedir. Bu varsayımlar veri sayısının 30'dan büyük olması ve normal dağılım göstermesidir. Toplanan veri sayısı 30'dan büyüktür. Normal dağılım gösterip göstermedikleri ise Skewness (Çarpıklık) ve Kurtosis (Yığılma) testleri ile karşılaştırılmıştır. Toplanan verilerin normal dağılım göstermeleri ve kategorik değişkenlerin skor hesabı yapılarak nicel veri tipine dönüştürülmesi nedeniyle Bağımsız Değişkenlerde t-Testi ve Regresyon testleri uygulanmıştır.

Bu işlemi uygulayabilmek için öncelikle SPSS 23 paket programında gerekli veri kolonları seçildikten sonra skor hesabı yapılmıştır. Hipotezlere uygun olarak karşılaştırmaları daha net görebilmek için çapraz çizelgeler oluşturulmuştur. Normallik analizlerinde çarpıklık ve basıklık değerlerine göre normal dağılım gösterip göstermediklerine karar verilmiştir. Hipotezlere uygun olarak karşılaştırılmış kolonlar seçilerek uygun testler uygulanmıştır. Kategorik değişkenlerin faktör olduğu ve bağımsız değişkenlerin sürekli olduğu durumlarda ise Çok Faktörlü Varyans Analizi (MANOVA) yapılmıştır. Test sonuçlarının anlamlı olup olmadığını kararına anlamlılık düzeyine yani p değerine bakılarak karar verilmiştir. p değeri, anlamlı bir farklılığın var olmasının ve kanıt seviyesinin belirlenmesi amacı ile kullanılmıştır. p değerini 0.05 ( $p < 0.05$ ) olarak baz alıp analizlere

karar verilmiştir (Bhattacharya ve Habtzghi, 2002; Kul, 2014). p değerinin yorumlanması Tablo 1'e göre yapılmıştır (Rosner, 2010).

Tablo 1  
p değer aralıklarının yorumlanması

p değeri	Yorumu
$p < 0.001$	Çok yüksek düzeyde istatistiksel anlamlılık
$0.001 \leq p < 0.01$	Yüksek düzeyde istatistiksel anlamlılık
$0.01 \leq p < 0.05$	İstatistiksel anlamlılık
$0.05 \leq p < 0.10$	Anlamlılık eğilimi (sınırdan anlamlılık)
$p > 0.10$	Fark tesadüfen ileri gitmiştir (istatistiksel olarak anlamlı farklılık saptanmamıştır)

Tablo 2  
İlişkinin gücünü tanımlama

Cramer'in V Katsayısı	Yorumu
$> 0.5$	Yüksek ilişki
$0.3$ 'ten $0.5$ 'e	Orta dereceli ilişki
$0.1$ 'den $0.3$ 'e	Düşük ilişki
$0$ 'dan $0.1$ 'e	Eğer varsa çok az ilişki

p değerinin yorumlanmasından ve istatistiksel olarak anlamlı bir sonuca erişildikten sonra ilişkinin derecesini yani kuvvetini ölçmek için çeşitli testler yapılmıştır. Simetrik Ölçümler, Korelasyon analizi gibi. Kullanılan veri tipinin kategorik olduğu durumlarda Simetrik Ölçümler çizelgesinde Cramer'in V katsayısına göre karar alınmıştır (Cramer, 1946). Elde edilen değerlerin yorumlanması Tablo 2'ye göre yapılmıştır (URL-4).

### 3. Bulgular

Faktör analizi ile veri setinin iki faktör olduğu tespit edilmiştir. Faktör analizine uygun olup olmadığı KMO ve Bartlett test sonuçlarına göre belirlenmiştir. KMO sonucu 0.937 ve Bartlett test sonucu ise 0.05'ten düşük çıkarak anlamlı bir sonuç elde edilmiştir. Böylece faktör analizi yapmaya uygun bir seti olduğu tespit edilmiştir. Bu faktörlerden birisi ÖAHY nedeniyle olumsuz olguların olduğu diğeri ise ÖAHY'nın olumlu katkılarının olduğunun ölçümünü yapacak ifadeler olarak faktörleştikleri görülmüştür. Belirlenen iki faktörün kümülatif değeri %73.417 olarak elde edilmiştir.

Ankette ÖAHY'nin olumlu ve olumsuz düşüncelere sahip ifadeler Cochran'ın Alpha katsayısına göre güvenilirlik analizi yapılmıştır. ÖAHY'nin olumlu etkilerini araştıran ifadeler %95 güvenilirlik, olumsuz etkilerini içeren ifadeler %90 güvenilirlik ile çok yüksek güvenilirlik seviyelerinde ölçülmüştür.

Güvenilirlik analizinin artması için çıkartılabilecek ifadeler bakıldığında ÖAHY'nin olumlu etkilerini araştıran ifadelerde bir artış olmadığı tespit edilmiştir. ÖAHY'nin olumsuz etkilerini araştıran ifadelerde ise ÖAHY'nin öğrenciler arasında yaptırma yol açıp açmadığını ölçen ifade çıkartıldığında güvenilirliğin %90'dan %91'e çıktığı tespit edilmiştir. Ancak güvenilirlik seviyesinin çok yüksek olması ve çok büyük bir artış sağlamadığı için tespit edilen ifade analizden çıkartılmamıştır.

Bu çalışmadaki amacın çözümüne yönelik analiz ve inceleme yapılması için; elde edilen veriler, uzman görüşleri ve literatür taraması nihayetinde literatüre katkı sunabileceği düşünülen 4 hipotez belirlenmiştir.

**H<sub>1</sub>:** ÖAHY'ya destek veren veya vermeyen öğrenciler arasında sınıf düzeyleri arasında fark vardır.

**H<sub>2</sub>:** Öğrencilerin sınıf düzeylerine göre ÖAHY'yı pozitif veya negatif algılamaları arasında fark vardır.

**H<sub>3</sub>:** ÖAHY'nin pozitif değerlendirilmesinde öğretim üyeleri ve öğrencilerin desteklemelerinin etkisi vardır.

**H<sub>4</sub>:** ÖAHY'nin negatif değerlendirilmesinde öğretim üyeleri ve öğrencilerin desteklemelerinin etkisi vardır.

### 3.1. Öğrencilerin Sınıf Düzeylerine Göre ÖAHY Farklılığı

Katılımcıların çoğunluğunu erkeklerin oluşturduğu ankette Şekil 1'e bakarak 174 erkek ve 21 kadın öğrenci ile anket gerçekleştirilmiştir. Tablo 3'te sınıflara göre cinsiyetlerin dağılımı gösterilmiştir. Erkek öğrencilerden birinci sınıftakiler 68 kişi ile çoğunluğu oluşturmaktadırlar. 4. sınıftan 54 kişi ile erkek öğrencilerde ikinci en çok katılımın olduğu sınıf olmuştur. Erkek öğrenci katılımcıların 2. sınıftan 40, 3. sınıftan 8 erkek öğrenci ankete katılmıştır. Mezun olan erkek öğrencilerden 4 kişi katılmıştır. Kadın öğrencilerden mezun olup ankete katılan kimse olmamıştır.

Tablo 3

Cinsiyet ve Sınıf bilgilerini oluşturan çapraz tablo

		Cinsiyet		Toplam
		Erkek	Kadın	
Sınıf	1. Sınıf	68	8	76
	2. Sınıf	40	6	46
	3. Sınıf	8	1	9
	4. Sınıf	54	6	60
	Mezun	4	0	4
Toplam		174	21	195

Kadın öğrencilerden 1. sınıftan 8, 2. sınıftan 6, 3. sınıftan 1, 4. sınıftan 6 kişi ankete katılım göstermiştir. Hazırlanan ankette öğrencilerin görüşleri 1-10 arasında değerlendirmeleri istenmiştir.

Şekil 2 incelendiğinde az destekleyenler ÖAHY'ye 1'den 5'e kadar değerlendirmede bulunan öğrencileri ifade ederken çok destekleyenler ÖAHY'ye 6'dan 10'a kadar destek veren öğrencileri ifade etmektedir. Genel itibariyle sınıf seviyelerinde destekleyenlerin sayısı, az destekleyenlere göre daha fazla olduğu görülmüştür. Frekansı çok düşük olan 3. sınıftakilerde ise durum terse dönmektedir. Frekansı düşük olmasının bir etki oluşturup oluşturmadığı test edilmiştir. Tablo 4'teki sonuçlarda ÖAHY'yi destekleyip desteklememe noktasında sınıf düzeyleri arasında bir fark olup olmadığı araştırılmıştır. Pearson'ın Ki-Kare testi sonucu 0.05 değerine çok yakın çıkmasına rağmen büyük çıkmıştır. İstatistiksel olarak anlamlı bir fark oluşturmadığı belirlenmiştir. Tablo 4'teki Cramer'in V katsayısı sonucu Tablo 2'ye göre değerlendirildiğinde aralarındaki ilişkinin düşük olduğu çıkarımı yapılmaktadır. Şekil 2'de 195 katılımcıdan %74'ünün destek verdiği bilgisine göre sınıf düzeylerinde fark etmeksizin ÖAHY'nin desteklediği sonucuna varılmıştır.

Tablo 4

Sınıf düzeylerine göre ÖAHY'sını destekleyip desteklemeyenlerdeki ayrımın ölçüsü

Pearson'ın Ki-kare Testi	0.052
Cramer'in V katsayısı	0.198

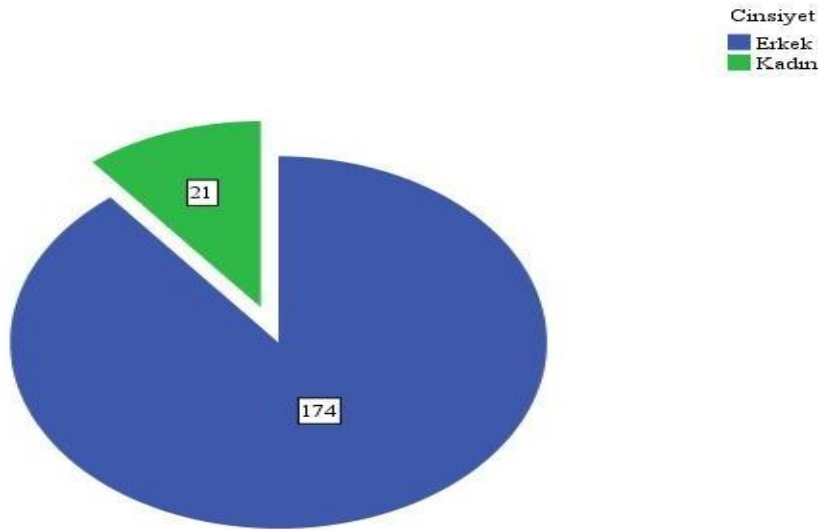
### 3.2. Öğrencilerin Sınıf Düzeylerine Göre ÖAHY'yı Pozitif ve Negatif Algılamaları Arasındaki Farklılıklar

Faktör analizi sonucunda psikolojik baskı, çatışma ortamı, ego, mutsuzluk, stres olguları negatif değerlendirmeler olarak skorlaştırılmış, saygı, liderlik, motivasyon, özgüven gibi olgular pozitif değerlendirmeler olarak skorlaştırılmıştır. Bu iki değişkenin sınıf düzeylerine göre bir fark oluşturup oluşturmadığı analiz edilmiştir. Bir bağımsız değişkenin iki bağımlı değişken üzerindeki etkisini incelemek için MANOVA analizi yapılmıştır. Öncesinde değişkenlerin varsayımları sağlayıp sağlamadığı kontrol edilmiştir. Box'ın kovaryans matrislerinin eşitliği testinin önemlilik (significant) değeri 0.682 olarak elde edilmiştir. Bu sonuca göre verinin MANOVA için uygun olduğu belirlenmiştir. Tablo 5'e bakıldığında yığılma ve çarpıklık +/-2 arasında değer almış olması test edilen iki değişkenin normal dağıldığını göstermiştir. Varsayımlardan bir diğeri varyansların eşitliğidir. Bunun için Levene'nin varyans eşitliği sonuçlarına bakılmış ve sonuçlar her iki bağımlı değişken içinde 0.05'ten büyük çıkmıştır. Tablo 5'te ifade edildiği gibi olumlu ifadeler 0.476, olumsuz ifadelerin test sonucu 0.935 olarak hesaplanmıştır.

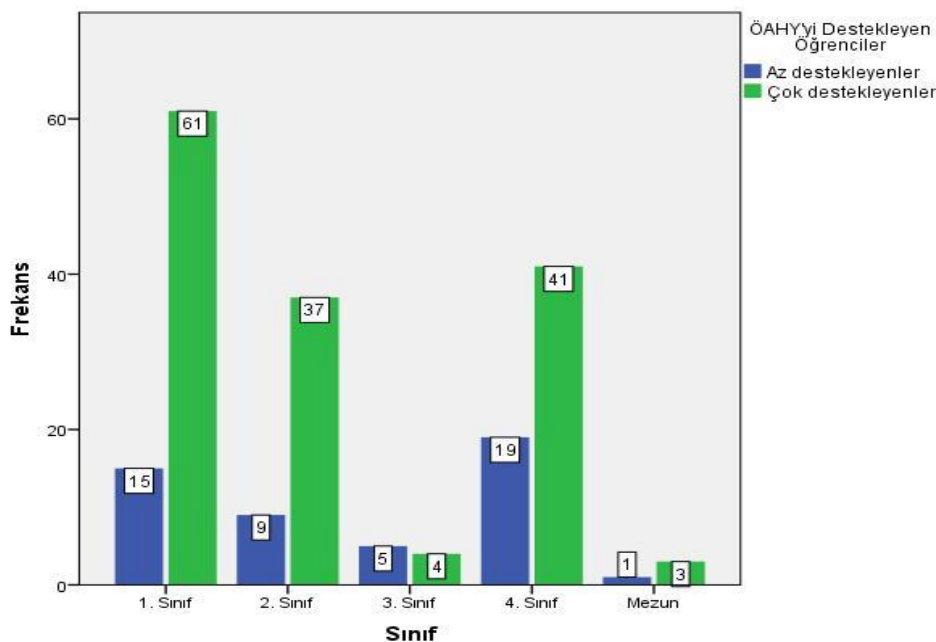
Tablo 5  
Hipotezlerdeki değişkenlerin yığılma ve çarpıklık değerleri

	Yığılma	Çarpıklık	Levene'nin varyans eşitliği testi
ÖAHY pozitif değerlendirme	-0.117	0.763	0.476
ÖAHY negatif değerlendirme	-0.783	0.092	0.935

Varsayımların sağlanması ile MANOVA analizine geçilmiştir. Tablo 6'da MANOVA analizi sonuçları verilmiştir. Sonuçların 0.05 değerinden daha düşük olmasına rağmen gruplar arası etkilerinin yapıldığı Tablo 7'de sınıf düzeylerine göre pozitif ve negatif değerlendirmeler arasında farklılık olmadığı görülmüştür. Post Hoc testleri olarak Tukey, LSD, Bonferroni ve Gabriel yapılmıştır. Yapılan Post Hoc testleri ile de pozitif ve negatif değerlendirmelerin sınıf düzeylerinde önemlilik (significant) değerleri 0.05'ten daha büyük çıkmıştır. Böylece gruplar arası farklılık göstermedikleri belirlenmiştir.  $H_0$  hipotezinin reddedilemeyeceği anlaşılmıştır. Tablo 6'da ifade edilen Kısmi Eta kareleri, korelasyon analizindeki r değeri olarak kabul edilir. Sınıf düzeylerinin bağımlı değişkenlerdeki değişimin ne kadarını açıkladığını göstermektedir. 0.04 gibi düşük bir değer tespit edilmiştir.



Şekil 1. Ankete katılım gösteren DUİM öğrencilerinin cinsiyetlerine göre pasta grafiği



Şekil 2. ÖAHY'ya destek veren ve desteklemeyen grupların sınıflarına göre çubuk grafiği



Tablo 6

Pozitif ve negatif olguların sınıf düzeylerine göre farklılaşmasının MANOVA tablosu

Sınıf Değişkeni	Önemlilik		Kısmi Eta Kareleri
	Pillai's Trace	Wilks' Lambda	
	.040	.041	
	.041	.041	

Tablo 7

Gruplar arası etki testi (Test of Between-Subjects Effects)

Sınıf	Bağımlı Değişkenler	Önemlilik
		ÖAHY pozitif değerlendirme
	ÖAHY negatif değerlendirme	.096

### 3.3. ÖAHY'nın Pozitif Değerlendirilmesinde Öğretim Üyeleri ve Öğrencilerin Desteklemelerinin Etkisi

Öğretim üyeleri ve öğrencilerin ÖAHY'yı destekleme durumlarının ÖAHY'nin pozitif olgulara etkisi araştırılmıştır. İki sürekli değişken içermesinden çoklu regresyon analizi yapılmıştır. Çoklu regresyon analizinde bağımsız değişkenlerin birbirleri ile çok fazla korelasyon içerisinde olmamaları gerekmektedir. Tablo 8'de korelasyon değerlerinin çok düşük olduğu görülmektedir. VIF değerlerinin 2.5 veya 4 değerinin altında olması da çoklu doğrusallık sorununun olmadığını göstermektedir (Hair, Black, Babin ve Anderson, 2010; Allison, 1999).

Düzeltilmiş R<sup>2</sup> istatistiksel olarak modeldeki bağımsız değişkenlerin bağımlı değişkeni yüzde olarak ne kadar açıkladığını ifade etmektedir. Tablo 9'da, oluşturulan modelin bağımsız değişkenleri bağımlı değişkeni R<sup>2</sup> değerine göre %25 oranında açıkladığı tespit edilmiştir. Tek Yönlü Varyans Analizi (ANOVA) anlamlılık değerinin 0.05 değerinden düşük olması modeldeki bağımsız değişkenlerden en az bir tanesinin modeli açıkladığını ifade etmektedir. Öğretim üyelerinin ve öğrencilerin anlamlılık değerlerinin 0.05'ten düşük olmaları her iki değişkeninde pozitif olguları etkilediği, açıkladığı sonucuna varılmıştır. Katsayılarına bakıldığında öğretim üyelerinin negatif yönde bir etkiye sahip oldukları, öğrencilerin ise pozitif yönde etki oluşturdukları tespit edilmiştir.

Tablo 8

Hipotez 3 için korelasyon tablosu

	ÖAHY pozitif olguların skorları	Öğretim üyeleri destekleri	Öğrencilerin destekleri	VIF
ÖAHY pozitif olguların skorları	1000	.090	.496	
Öğretim üyeleri destekleri	.090	1.000	.433	1.231
Öğrencilerin destekleri	.496	.433	1.000	1.231

Tablo 9

Modelin R<sup>2</sup> ve ANOVA değerleri

	Düzeltilmiş R <sup>2</sup>	ANOVA anlamlılık değeri	Öğretim üyeleri anlamlılık değeri	Öğrencilerin anlamlılık değeri
Katsayılar	0.258	0.00	0.027	0.00
			-0.188	0.677

### 3.4. ÖAHY'nın Negatif Değerlendirilmesinde Öğretim Üyeleri ve Öğrencilerin Desteklemelerinin Etkisi

Hipotez 3'teki bağımsız değişkenlerle kurulan modelin pozitif olguları açıklamakta kullanılacağı tespit edilmişti. Aynı şekilde negatif olgular için kurulacak bir modeldeki etkileri ne ölçüde olacağı hipotez 4 ile araştırılmıştır. ÖAHY'nın pozitif olguların dışında negatif olguları oluşturan etkenlerin analizi için öğretim üyelerinin desteklemeleri ile öğrencilerin desteklemelerinin etkisi olup olmadığı araştırılmıştır. Tablo 10'da korelasyon değerlerinin çok düşük olduğu görülmüştür. VIF değerlerinin 2.5 veya 4 değerinin altında olması

da çoklu doğrusallık sorununun olmadığını göstermiştir. Böylece bağımsız değişkenlerin bağımlı değişkeni açıklayabildiği görülmüştür.

Tablo 11'deki ANOVA anlamlılık değerinin 0.05'ten düşük olması değişkenlerden en az birinin negatif olguları etkilediği anlamına gelmektedir. İki bağımsız değişkenin anlamlılık değerlerinin 0.05'ten düşük olması ise her iki değişkeninde bağımsız değişkeni etkilediğini göstermektedir. Bu iki bağımsız değişken ile oluşturulan modelin istatistiksel olarak anlamlı olduğu sonucuna varılmıştır. Katsayılarının ise hipotez 3'e göre farklı şekillendiği görülmektedir. Öğretim üyelerinin negatif değerlendirmelere olan etkilerinin pozitif yönde olduğu görülmektedir. Yani öğretim üyelerinin ÖAHY'yi desteklemeleri öğrenciler üzerinde negatif etkisi olduğu belirlenmiştir. Hipotez 3 ile beraber uyumlu olduğu anlaşılmıştır.

Tablo 10

Hipotez 4 için korelasyon tablosu

	ÖAHY pozitif olguların skorları	Öğretim üyeleri destekleri	Öğrencilerin destekleri	VIF
ÖAHY negatif olguların skorları	1.000	0.118	-0.274	
Öğretim üyeleri destekleri	0.118	1.000	0.433	1.231
Öğrencilerin destekleri	-0.274	0.433	1.000	1.231

Tablo 11

Modelin R<sup>2</sup> ve ANOVA değerleri

	Düzeltilmiş R <sup>2</sup>	ANOVA anlamlılık değeri	Öğretim üyeleri anlamlılık değeri	Öğrencilerin anlamlılık değeri
	0.144	0.00	0.00	0.00
Katsayılar			0.300	-0.405

#### 4. Sonuçlar

Bu çalışmada, ÖAHY uygulanan üniversitelerin DUİM bölümlerinde hiyerarşik yapının öğrenciler arasındaki karşılığı, sınıf düzeyindeki farklılıkları, öğrenciler ve öğretim üyelerinin olumlu ve olumsuz etkileri SPSS 23 paket programı kullanılarak araştırılmıştır. Toplanan veriler için tanımlayıcı istatistikler ve frekans analizinden sonra verilerin türü ve dağılım tipine uygun olan testler yapılmıştır. Bu çalışmadaki anket 21 kadın ve 174 erkek öğrenciye uygulanmıştır. Ankete katılanların 76'sı 1. sınıf, 46'sı 2. sınıf, 9'u 3. sınıf, 60'ı 4. sınıf, 4'ü mezun öğrencidir. ÖAHY'nin stres, ego, psikolojik baskı, öğrenciler arası yaptırım, çatışma ortamı, mutsuzluk, öğrencilerin psikolojilerine etkileri ve ÖAHY'nin liderlik, saygı, ast üst ilişkisi, motivasyon, özgüven, derslere katkısı, öğrencilik hayatına katkısı, öğrenciler arası iletişime katkısı ve gemiye hazırlamadaki etkileri 1-10 arası değerlendirilmiştir. Öğrencilerin sınıf düzeylerine göre ÖAHY'yi pozitif ve negatif algılamaları arasındaki farklılıklar incelenmiştir. Box'ın kovaryans matrislerinin eşitliği testinin önemlilik (Significant) değeri 0.682 olarak elde edilmiştir. Levene'nin varyans eşitliği sonuçlarına bakılmış ve sonuçlar her iki bağımlı değişken içinde 0.05'ten büyük çıkmıştır. Sonuçlara göre verinin MANOVA testi için uygun olduğu belirlenmiştir. Yapılan analizler neticesinde ÖAHY'nin öğrenciler arasında değer gördüğü ve öğrencilere katkı sağladığı sonucuna varılmıştır. ÖAHY'nin pozitif ve negatif değerlendirilmesinde öğretim üyeleri ve öğrencilerin desteklemelerinin etkisi incelenmiş ve katsayılarına bakıldığında öğretim üyelerinin negatif yönde bir etkiye sahip oldukları, öğrencilerin ise pozitif yönde etki oluşturdukları tespit edilmiştir. 195 katılımcıdan %74'ünün destek verdiği ve sınıf düzeylerinde fark etmeksizin ÖAHY'nin desteklediği sonucuna varılmıştır.

Özdemir (2018)'in denizcilik eğitiminde üniforma giyme zorunluluğu, ilgili yönetmelikler, hiyerarşik sistemin neden olduğu sorunları belirlediği çalışmasının aksine yapılan bu çalışma ile öğrencilerin ÖAHY'yi sınıflar arasında fark göstermeksizin destekledikleri ve olumlu olguların oluşumunda kaynak olarak gördükleri belirlenmiştir. Öğretim üyelerinin ÖAHY'ye olan desteklerinin öğrenciler arasında negatif unsurların

oluşmasında etki ettikleri ortaya çıkmıştır. DUİM öğrencileri arasında ÖAHY'yi oluşturan değerlerin korunmasına destek verilmesi önerilmektedir. ÖAHY'nin sağlıklı işleyebilmesi için öğretim üyelerinin etkilerinin “işlemsel liderlik” yerine “dönüşümcül liderlik” ile gözden geçirilmesi önerilmekte ve bir başka araştırma konusu olarak görülmektedir (Uluköy, 2014; Xu vd., 2022). Literatürde öğrenciler ve öğretim üyelerinin görüşleri alınarak hiyerarşik düzen ve hiyerarşik yapı üzerine yapılan çalışma sayısı oldukça kısıtlıdır. Yapılan bu çalışma gelecekte bu konuda yapılacak çalışmalarını destekleyecek ve kaynak olarak gösterilebilecektir.

### Yazar Katkıları

Devran Yazır: Çalışmayı organize etme, veri toplama ve taslağın son haline getirilmesini sağlama.

Sefa Yay: Çalışmadaki analizlerin tasarlanmasına katkı sağlama, istatistiksel analizleri yapma ve makaleyi yazma.

### Çıkar Çatışması

Yazarlar çıkar çatışması bildirmemişlerdir.

### Kaynaklar

- Albar, B. Ö., ve Ofluoğlu, G. (2017). *Çalışma hayatında mobbing ve tükenmişlik ilişkisi. Hak İş Uluslararası Emek ve Toplum Dergisi*, 6(16), 538-550. Erişim adresi: <https://dergipark.org.tr/tr/download/article-file/393168>
- Allison, P. D. (1999). *Multiple regression: a primer*. Pine Forge Press. Erişim adresi: <https://books.google.com.tr/books?hl=tr&lr=&id=20tgP-Wr4QMC&oi=fnd&pg=PR13&dq>
- Baloğlu, N., ve Karadağ, E. (2008). Öğretmen yetkinliğinin tarihsel gelişimi ve ohio öğretmen yetkinlik ölçeği: Türk kültürüne uyarlama, dil geçerliği ve faktör yapısının incelenmesi. *Kuram ve Uygulamada Eğitim Yönetimi*. 56(56), 571-606. Erişim adresi: <https://dergipark.org.tr/tr/download/article-file/108274>
- Bhattacharya, B., ve Habtzghi, D. (2002). Median of the p value under the alternative hypothesis. *The American Statistician*, 56(3), 202-206. doi:<https://doi.org/10.1198/000313002146>
- Cramer, H. (1946). *Mathematical methods of statistics*. Princeton: Princeton University Press. s. 260-290. Erişim adresi: [https://books.google.com.tr/books?hl=tr&lr=&id=jV2YDwAAQBAJ&oi=fnd&pg=PA62&dq=Mathematical+methods+of+statistics.+Princeton:+Princeton+University+Press.+s.+260-290.+Eri%C5%9Fim+adresini:&ots=OYvYDdSqJg&sig=IWKGxAWKqdGt1iSRQZhU0HYJQY&redir\\_esc=y#v=onepage&q&f=false](https://books.google.com.tr/books?hl=tr&lr=&id=jV2YDwAAQBAJ&oi=fnd&pg=PA62&dq=Mathematical+methods+of+statistics.+Princeton:+Princeton+University+Press.+s.+260-290.+Eri%C5%9Fim+adresini:&ots=OYvYDdSqJg&sig=IWKGxAWKqdGt1iSRQZhU0HYJQY&redir_esc=y#v=onepage&q&f=false)
- Demirel, Y., ve Yücel, M. (2017). Sosyal destek ve psikolojik güçlendirmenin duygusal tükenmişlik üzerine etkisi. *Kastamonu Üniversitesi İktisadi ve İdari Bilimler Fakültesi Dergisi*, 310-321. Erişim adresi: <https://dergipark.org.tr/tr/download/article-file/361253>
- Demir, M., ve Çolak Gürkan, N. (2020). Gemi adamlarının iş yerinde yalnızlık düzeylerinin ve işten ayrılma niyetlerinin çeşitli demografik değişkenlere göre incelenmesi. *Mersin Üniversitesi Denizcilik ve Lojistik Araştırmaları Dergisi*, 2(2), 1-22. Erişim adresi: <https://dergipark.org.tr/en/pub/denlojad/issue/59303/779562>
- Erdirençelebi, M., ve Yazgan, E. (2017). Mobbing, örgütsel sinizm, örgütsel bağlılık ve bunların algılanan çalışan performansı üzerine etkileri. *Süleyman Demirel Üniversitesi İktisadi ve İdari Bilimler Fakültesi Dergisi*, 22(2), 267-284. Erişim adresi: <https://dergipark.org.tr/tr/download/article-file/1004361>
- Göktürk, G. Y., ve Bulut, S. (2012). Mobbing: işyerinde psikolojik taciz. *Abant İzzet Baysal Üniversitesi Sosyal Bilimler Enstitüsü Dergisi*, 1(24), 53-70. Erişim adresi: <https://dergipark.org.tr/tr/download/article-file/154618>
- Gönülalçak, M. M. (2016). Türkiye’de denizcilik eğitimi. *Deniz Ticareti Dergisi*, 2106. Erişim adresi: <https://www.denizticaretodasi.org.tr/yayinlarimiz/dergi/detay/2016/4?type=6>
- Gözler, K., ve Kaplan, G. (2017). İdare hukukuna giriş. 23. Baskı, Ekin Kitapevi, Bursa, 46-48.
- Gülver, M., Harmancı, F. M., Gözübenli, M., ve Alaç, A. E. (2014). Örgütsel iletişim ve ast üst ilişkileri. Güvenlik sektöründe insan ilişkileri, *Nobel Yayınevi*, 25-44. Erişim adresi: [https://www.academia.edu/44543030/ÖRGÜTSEL\\_İLETİŞİM\\_VE\\_AST\\_ÜST\\_İLİŞKİLERİ\\_2014\\_Gülver\\_M](https://www.academia.edu/44543030/ÖRGÜTSEL_İLETİŞİM_VE_AST_ÜST_İLİŞKİLERİ_2014_Gülver_M)
- Hair, J. F., Black, W. C., Babin, B. J., ve Anderson, R.E. (2010). *Multivariate data analysis: a global perspective*. 7th Edition, Pearson Education, Upper Saddle River. 152-231. Erişim adresi:

- <https://www.drnishikantjha.com/papersCollection/Multivariate%20Data%20Analysis.pdf>
- Hasırcı, I., ve Örucü, E. (2021). Örgüt kültürünün inovatif davranış eğilimleri ile ilişkisinde öz yeterlilik algısının aracılık rolü ve bir uygulama. *Afyon Kocatepe Üniversitesi Sosyal Bilimler Dergisi*, 23(2), 642-661. doi:<https://doi.org/10.32709/akusosbil.820141>
- Kanbur E. (2018), Havacılık sektöründe psikolojik güçlendirme, iş performansı ve işten ayrılma niyeti arasındaki ilişkilerin incelenmesi. *Uluslararası Yönetim İktisat İşletme Dergisi*, 14(1), 147-162. doi:<https://doi.org/10.17130/ijmeh.2018137578>
- Kul, S. (2014). İstatistik sonuçlarının yorumu: p değeri ve güven aralığı nedir. *Plevra Bülteni*, 8(1), 11-13. Erişim adresi: [https://www.toraks.org.tr/site/sf/books/pre\\_migration/c19fa28083ae026a97e3878c26e1b03eaacfd74d114c8d66f832d8d806c56307.pdf](https://www.toraks.org.tr/site/sf/books/pre_migration/c19fa28083ae026a97e3878c26e1b03eaacfd74d114c8d66f832d8d806c56307.pdf)
- Marume, S. B. M., ve Chikasha, A. S. (2016). The concept hierarchy in organisational theory and practice. *International Journal of Engineering Science Invention*, 5(7), 55-58. Erişim adresi: [http://www.ijesi.org/papers/Vol\(5\)7/H0507055058.pdf](http://www.ijesi.org/papers/Vol(5)7/H0507055058.pdf)
- Özdemir, Ü. (2018). Researching of uniform and hierarchical system in maritime education with multi criteria decision making approach. *Journal of Turkish Studies Educational Sciences*, 13(19), 1409-1426. doi:<http://dx.doi.org/10.7827/TurkishStudies.13861>
- Özler, N. D., ve Yıldırım, H. (2015). Örgütsel güven ile psikolojik sermaye arasındaki ilişkiyi belirlemeye yönelik bir araştırma. *Nevşehir Hacı Bektaş Veli Üniversitesi SBE Dergisi*, 5(1), 163-188. Erişim adresi: <https://dergipark.org.tr/tr/download/article-file/184927>
- Rosner, B. (2010). Fundamentals of biostatistics. 7. Baskı, Cengage Learning. Erişim adresi: [https://books.google.com.tr/books?hl=tr&lr=&id=yn4yBgAAQBAJ&oi=fnd&pg=PP1&dq=Rosner,+B.++\(2010\).+Fundamentals+of+biostatistics.+7th.+Bask%C4%B1,+Cengage+Learning.&ots=IfksTp5Fzn&sig=st3LDab-wkg5uHE02e\\_4oxzYlu0&redir\\_esc=y#v=onepage&q&f=false](https://books.google.com.tr/books?hl=tr&lr=&id=yn4yBgAAQBAJ&oi=fnd&pg=PP1&dq=Rosner,+B.++(2010).+Fundamentals+of+biostatistics.+7th.+Bask%C4%B1,+Cengage+Learning.&ots=IfksTp5Fzn&sig=st3LDab-wkg5uHE02e_4oxzYlu0&redir_esc=y#v=onepage&q&f=false)
- Timuroğlu, M. K., ve Balkaya, E. (2016). Örgütsel iletişim ve motivasyon ilişkisi: bir uygulama. *International Journal of Social Inquiry*, 9(2), 89-113. Erişim adresi: <http://hdl.handle.net/11452/7286>
- Türk, M. S. (2019). Örgüt içi iletişim ve kriz yönetimi. Erişim adresi: [https://www.academia.edu/30636810/ÖRGÜT\\_İÇİ\\_İLETİŞİM\\_VE\\_KRİZ\\_YÖNETİMİ](https://www.academia.edu/30636810/ÖRGÜT_İÇİ_İLETİŞİM_VE_KRİZ_YÖNETİMİ)
- Uluköy, M., Kılıç, R., ve Bozkaya, E. (2014). Hiyerarşik yapısı yüksek olan kurumlarda liderlik yaklaşımlarının çalışanların motivasyonu üzerine etkisi. *Süleyman Demirel Üniversitesi İktisadi ve İdari Bilimler Fakültesi Dergisi*, 19(1), 191-206. Erişim adresi: <https://dergipark.org.tr/tr/download/article-file/194264>
- URL-1: YÖK (2019). Yükseköğretim Kurumu Program Atlası. Erişim adresi: <https://yokatlas.yok.gov.tr/lisans-bolum.php?b=10046> . Erişim Tarihi: 10.07.2021
- URL-2: KTÜ (2018). Karadeniz Teknik Üniversitesi Öğrenci Kıyafet Yönergesi. Erişim adresi: [https://www.ktu.edu.tr/dosyalar/19\\_01\\_00\\_7ac53.pdf](https://www.ktu.edu.tr/dosyalar/19_01_00_7ac53.pdf). Erişim Tarihi: 07.07.2021
- URL-3: TDK (2019). Türk Dil Kurumu. Güncel Türkçe Sözlüğü. Erişim adresi: <https://sozluk.gov.tr> . Erişim Tarihi: 26.07.2021
- URL-4: AcaStat Software (2015). Applied Statistics Handbook. Erişim adresi: <https://www.acastat.com/statbook/chisqassoc.htm> . Erişim Tarihi: 23.02.2021.
- Var, M. (2016). *Mobbing davranışları ile örgüt kültürü arasındaki ilişki: bir kamu kurumu örneği* (Yüksek lisans tezi). Erişim adresi: <https://tez.yok.gov.tr/UlusalTezMerkezi>.
- Yıldırım, U., Tuncel, A. L., ve Başar, E. (2019). *Study on maritime education in turkey and other countries in regard to STCW and innovative approachings*. IMLA 26, Batum, Gürcistan, 58-65.
- Yüksel, İ. (2005). *İletişimin iş tatmini üzerindeki etkileri: bir işletmede yapılan görgül çalışma*. Doğu Üniversitesi Dergisi. 6(2), 291-306. Erişim adresi: <https://dergipark.org.tr/tr/download/article-file/215187>
- Zhao, H., Kessel, M., ve Kratzer, J. (2014). Supervisor–Subordinate Relationship, Differentiation, and Employee Creativity: A Self-Categorization Perspective. *The Journal of Creative Behavior*. 48(3), 165-184. doi: <https://doi.org/10.1002/jocb.46>.
- Xu, G., Zeng, J., Wang, H., Qian, C., ve Gu, X. (2022). How Transformational Leadership Motivates Employee Involvement: The Roles of Psychological Safety and Traditionality. *SAGE Journals*. 12(1), 1-10. doi: <https://doi.org/10.1177/21582440211069967>



# An Integrated Risk Management Framework for Global Supply Chains

Mualla Gonca Avci<sup>1,\*</sup>

<sup>1</sup> Department of Industrial Engineering, Engineering Faculty, Dokuz Eylul University, Izmir, Türkiye

## Article History

Received: 18.04.2022

Accepted: 26.06.2022

Published: 15.12.2022

## Research Article


**Abstract** – In this study, a risk management framework is developed to support risk management decisions in global supply chains. The proposed framework covers all phases of risk management, namely, risk identification, risk mitigation and control. In the risk identification phase of the framework, the supply chain is decomposed into either material-level or product-level sub-networks according to the decision maker's preference. Afterwards, the most critical sub-network is modelled to evaluate different risk mitigation strategies. In particular, a combination of redundancy and flexibility strategies is considered for risk mitigation. These strategies are evaluated by simulation models in terms of their effectiveness and efficiency. While inventory holding cost is used as efficiency measure, effectiveness of the strategies is measured by premium freight ratio. The proposed framework provides a comprehensive and reliable decision support since it covers all phases of risk management and relies on quantitative data, and statistical analysis in risk modelling. Moreover, it is flexible as it can be easily adapted to any change in supply chain environment and strategy. In order to show the applicability of the framework, a practical demonstration is presented for a European automotive company. The results indicate that the proposed framework improves the supply chain performance in terms of efficiency and effectiveness.

**Keywords** – Premium freight, simulation, supply chain risk management, TOPSIS,

## 1. Introduction

As a result of the advances in communication and transportation technologies, today's supply chains have geographically expanded. This fact drives inter-firm competition into global scale. Consequently, supply chains adopt lean principles, and partners in supply chain become more connected to gain cost advantage. However, these strategies make supply chains vulnerable in terms of supply chain risks. Today, an adverse event affected a supply chain partner can influence the entire chain. Therefore, supply chain risk management (SCRM) has gained importance in both industry and academia. Nowadays, firms must evaluate interdependencies in their supply chain, identify their risks and measure likelihoods, effects and severities of the identified risks. Firms should develop risk management plans to avoid, mitigate or control the identified risks (Tummala and Schoenherr 2011).

In global supply chains, SCRM is challenging due to the complex supply chain structures and interrelationships. In fact, global supply chains can be investigated by decomposing them into sub-systems under several scales by using different viewpoints such as a geographical zone, a hazard level, a supplier group or a particular type of product. Then, risk management activities can proceed conveniently for the pre-specified critical sub-systems. In addition, risk management in global supply chains should be flexible so that it can be adapted easily to rapid changes in supply chain environment and competition strategy. Furthermore, SCRM should mainly rely on quantitative data to perform more realistic and reliable risk analysis.

<sup>1</sup>  gonca.yunusoglu@deu.edu.tr

\*Corresponding Author

This study proposes an integrated SCRM framework for operational supply chain risk management in global scale. The proposed framework covers all phases of risk management, namely, risk identification, risk mitigation, risk monitoring and control phases. Particularly, the framework involves a risk identification phase in which the supply chain is decomposed into material-level or product-level sub-networks according to the decision maker's preference. Afterwards, risk mitigation strategies are simulated for the specified critical sub-network, and the best factor levels for risk mitigation strategies are determined by an experimental design approach. In particular, redundancy and flexibility strategies are considered for risk mitigation. In this study, holding safety stock and excess production which is more than forecasted demand size are considered as redundancy strategies. Additionally, supplier's quantity flexibility is the flexibility strategy. These strategies are considered in combined manner and evaluated in terms of both efficiency and effectiveness. Herein, the annual holding cost of the supply chain is employed as a measure of efficiency. In addition, the ratio of premium freights to regular orders is used to measure the effectiveness of the strategies. Specifically, in case of a shortage or delay risk, requesting a premium freight is an effective contingency strategy. However, premium freight is a type of last-minute shipment transported by airlines. It incurs very high costs to the responsible agent in a short time frame due to its setup cost and transportation mode. Additionally, it is an indicator of vulnerability of the supply chain. Hence, premium freight is used as an additional performance measure in this study to measure the effectiveness of the strategies.

The proposed framework consisting of all phases of SCRM provides a comprehensive decision support for SCRM unlike the majority of the studies in this field. The proposed framework is a reliable and realistic tool as it uses quantitative data and employs statistical risk models relying on real historical data. Additionally, it is flexible in determining the focus of risk management and can be easily adapted to any changes in supply chain management strategy or environment. Furthermore, to our knowledge, premium freight is used as an effectiveness measure for the first time for risk mitigation strategies in SCRM field.

The rest of the paper is organized as in the following. In Section 2, related studies in literature are overviewed. In Section 3, the proposed framework is presented. Section 4 presents an application of the proposed framework to an automotive supply chain. In Section 5, results of the application are discussed, and managerial implications are provided. Section 6 concludes the study.

## **2. The Related Literature**

As SCRM is still an emerging research field, definition of risk concepts and risk mitigating strategies are still unclear. Therefore, several review studies such as (Singhal, Agarwal, and Mittal 2011), (Tang and Nurmaya Musa 2011), (Colicchia and Strozzi 2012), (Sodhi, Son, and Tang 2012), (Rangel, de Oliveira, and Leite 2014), (Heckmann, Comes, and Nickel 2015), (Ho et al. 2015) and Pournader et al. (2020) have been published with the aim of classifying the studies on SCRM. Additionally, the reader can find broad descriptions of risk concepts and risk management strategies in (Chopra and Sodhi 2004), (Christopher and Peck 2004), and (Sheffi 2005). In this section, recent quantitative studies related to SCRM field are presented.

The majority of the recent studies in the related field deal with the risk assessment phase of SCRM. In recent studies, multi-criteria decision making techniques, mathematical programming approaches, system analysis and simulation are utilized to assess supply chain risks. Among these approaches, multi-criteria decision making techniques are the most widely used tools in risk assessment. Wang et al. (2012) utilize a fuzzy analytical hierarchy process (AHP) model for risk assessment of implementing green initiatives in a fashion supply chain. Chaudhuri, Mohanty, and Singh (2013) utilize Failure Mode and Effects Analysis (FMEA) to prioritize the failure modes of vulnerable suppliers in new product development process. Chen and Wu (2013) propose an FMEA to categorize existing suppliers and select new suppliers by considering risk. Samvedi, Jain, and Chan (2013) utilize fuzzy AHP and fuzzy TOPSIS methods to obtain a supply chain risk index. Aqlan and Lam (2015a) propose a risk assessment framework which employs Bow-Tie analysis and fuzzy inference system for supply chains. In another study, Aqlan and Lam (2015b) quantify supply chain risks by Bow-Tie analysis, and select mitigation strategy by an optimization model. Govindan and Jepsen (2015) model supply chain uncertainties as intuitionistic fuzzy numbers and assess them via ELECTRE-C. Oliveira et al. (2022) identify and assess the supply chain risks of a home-care service provider via FMEA.

There exist a few mathematical programming applications in risk assessment context. Cardoso et al. (2015) develop a mathematical model for supply chain design and planning to assess resilience of alternative supply chain structures under different disruption types. Klibi and Martel (2012) propose a risk modelling approach considering random, hazardous and deeply uncertain events causing supply chain disruptions. They utilize a Monte-Carlo approach to assess the disruption impact based on the descriptive models.

Recently, system analysis and simulation approaches have become popular in risk assessment. Ghadge et al. (2013) develop a risk management framework by using systems approach to capture the dynamic characteristics of supply chain risks. Bueno-Solano and Cedillo-Campos (2014) investigate the impact of disruptions originated from terrorist acts via a system dynamics model. Wagner, Mizgier, and Arnez (2014) propose Monte-Carlo approach to evaluate possible losses due to disruptions in the US offshore oil industry. Guertler and Spinler (2015) demonstrate the criticality of the operational risks by using a system dynamics model that assesses the intra-organizational dynamics of risks.

In view of the related body of knowledge, it can be stated that the number of studies building comprehensive SCRM frameworks considering all phases of SCRM is limited. Among them, Giannakis and Louis (2011) propose a multi-agent based decision support system for supply chain disruption management. Schmitt and Singh (2012) analyse inventory placement and back-up strategies against supply chain risks by a simulation model. Carvalho et al. (2012) use a supply chain simulation model to evaluate the effects of mitigation strategies on performance of each supply chain entity under a set of scenarios. Rajesh and Ravi (2015) employ a grey-DEMATEL approach to investigate cause-effect relationships between supply chain risk mitigation strategies. Simchi-Levi et al. (2015) develop a SCRM framework for Ford Motor Company to identify new risks, evaluate proactive risk mitigation plans, and derive optimal contingency plans. Oliveira et al. (2019) propose hybrid and flexible simulation-based optimization models for SCRM. However, they do not present a real world application of their model. Kara et al. (2020) present an integrated SCRM framework which employs data mining algorithms. Talukder et al. (2021) propose a multi-indicator supply chain management framework that provides leanness, agility, sustainability, and resilience in the dairy business.

In this study, supply chain risks related to the physical flow in global supply chain networks are considered. In related literature, there exist a few study considering such large supply chain networks ((Chaudhuri, Mohanty, and Singh 2013), (Klibi and Martel 2012), (Wagner, Mizgier, and Arnez 2014), (Simchi-Levi et al. 2015)). As global supply chains consist of several facilities spread on several countries, risk management in these supply chains is challenging. A possible solution to overcome this challenge may be decomposition of the supply chain network into sub-networks by a risk assessment procedure as Chaudhuri, Mohanty, and Singh (2013) and Klibi and Martel (2012) do. Hence, in this study, the supply chain network is decomposed into critical sub-networks to according to their risk level. Unlike the previous studies, the proposed framework has a more comprehensive risk identification phase in which the supply chain can be decomposed into the single-product level or single-material level sub-networks. Therefore, the risks can be assessed at material or product-level by considering the preference of supply chain managers. Consequently, the proposed framework enables the flexibility essential for the real-world SCRM practices.

As stated previously, the proposed framework consists of a risk mitigation phase in addition to risk identification phase. In risk mitigation phase, redundancy and flexibility strategies are investigated to the aim of effective and efficient SCRM. In particular, holding safety stock and excess production which is more than forecasted demand size are considered as redundancy strategies. Additionally, supplier's quantity flexibility is considered as the flexibility strategy. These strategies have been utilized in previous studies. However, they have not been evaluated from effectiveness and efficiency perspectives simultaneously. Effectiveness is the ability to achieve a predefined goal in case of adverse conditions. Efficiency is to ensure minimal spending of resources to reach the goal (Heckmann, Comes, and Nickel 2015). In this study, premium freight ratio and annual holding cost are utilized as effectiveness and efficiency measures, respectively. To the best of our knowledge, there exists no study in related literature considering premium freight as a SCRM performance measure.



### 3. The Proposed Supply Chain Risk Management Framework

In this study, an integrated SCRM framework is developed to support SCRM decisions by considering holding costs and premium freights. The proposed framework considers not only premium freights but also supply chain costs to ensure both effectiveness and efficiency objectives in SCRM. Moreover, the proposed framework covers all commonly acknowledged phases of SCRM namely, risk identification, risk mitigation and risk monitoring and control. Furthermore, the proposed framework has the flexibility in executing material or product-level risk analyses according to preference of the decision maker. The process flow diagram summarizing the phases of the proposed framework is illustrated in Figure 1. In subsequent sections, general process of the framework is explained through risk management phases.

#### 3.1. Risk Identification

Firstly, the risks affecting supply and delivery processes of the supply chain are identified. Basically, supply chain risks can be classified into inbound and outbound risks by considering physical flow direction. The inbound risks are related to the supply-side adverse events such as supplier delivery delay, delivery quantity loss and supplier disruptions. The outbound risks are arisen from customer-side adverse events such as customer demand variability, product delivery delay and shifting customer demand. As stated previously, the proposed framework has the flexibility in focusing on the inbound or outbound risks. In this context, inbound and/or outbound risks are quantified according to the preference of the manager. In particular, the supply chain risks are quantified through statistical models developed by using past order, premium freight and customer sales data. The risk models are obtained by fitting the historical data to probability distributions.

Once the supply chain risks related to each agent are quantified, the most critical sub-network in terms of risk is identified. The critical sub-network may be related to a material or a product type. To identify the critical sub-network, the most critical material or product is determined. In this context, the criteria for critical sub-network identification should be specified. In criteria determination, the adverse effects of risks related to the focal material or product and criticality of them should be considered. Hence, the critical sub-network identification stage involves multi-criteria decision making. Therefore, utilization of a multi-criteria decision making technique in this stage is appropriate. TOPSIS (Hwang & Yoon, 1981) is a suitable technique for this stage as it ranks the alternatives according to their criticality.

Assume that a multi-criteria decision making problem has  $m$  alternatives,  $A_1, A_2, \dots, A_m$  and  $n$  criteria,  $C_1, C_2, \dots, C_n$ . The ratings associated with the alternatives with respect to each criterion is included in a decision matrix,  $D = (x_{ij})_{m \times n}$ . Then, the ratings are normalized to form the normalized decision matrix.

In particular, in identification of material or product-level sub-networks, more than one decision matrices may come into consideration. As the suppliers and customers may be connected with more than one plant in the supply chain, more than one assessment for a criterion may come out. In this case, group decision making approaches can be used to merge the decision matrices into single decision matrix.

The criteria weights are determined by using entropy weighting method (Deng, Yeh, & Willis, 2000). Entropy weighting method considers intrinsic information in each criterion, and does not require decision maker's judgment. In this sense, entropy weighting method is utilized to determine criteria weights to reduce human effort in decision making.

The entropy value indicating the amount of information contained in each criterion is calculated as follows.

$$e_j = -\frac{1}{\ln(n)} \sum_{i=1}^m x_{ij} \ln(x_{ij}) \quad (3.1)$$

The degree of divergence ( $d_j$ ) of the average intrinsic information related to each criterion is calculated as follows.

$$d_j = 1 - e_j \quad (3.2)$$

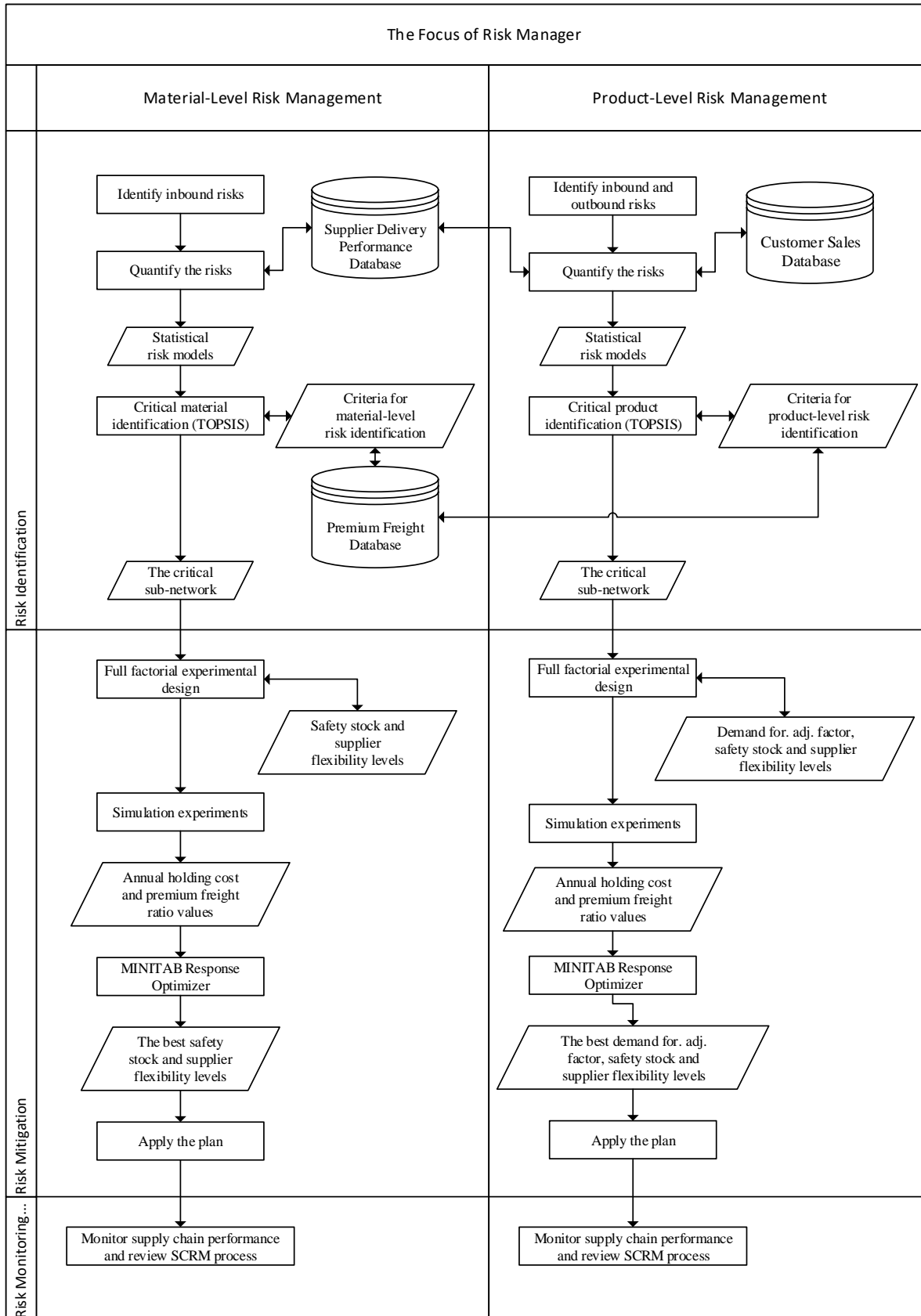


Figure 1. Process flow diagram of the proposed framework

As the degree of divergence represents divergence of the ratings in terms of criterion  $j$ , higher degree of divergence leads to higher criterion weight. In this sense, criteria weights are calculated as follows.

$$w_j = \frac{d_j}{\sum_{j=1}^n d_j} \quad (3.3)$$

Aggregation procedure of TOPSIS is based on weighted Euclidian distances to negative and positive ideal solution.

$$d_i^+ = \sqrt{\sum_{j=1}^n w_j (x_{ij} - p_j)^2} \quad (3.4)$$

$$d_i^- = \sqrt{\sum_{j=1}^n w_j (x_{ij} - n_j)^2} \quad (3.5)$$

where  $d_i^+$  is the distance of the alternative  $i$  to positive ideal solution,  $d_i^-$  is the distance of alternative  $i$  to negative ideal solution,  $p_j$  is the positive ideal value for criterion  $j$ , and  $n_j$  is the negative ideal value for criterion  $j$ .

The overall criticality index for alternative  $i$  is calculated as follows.

$$CC_i = \frac{d_i^-}{d_i^- + d_i^+} \quad (3.6)$$

In the proposed framework, the overall criticality index obtained by TOPSIS present the criticality of material or product in terms of risk. The material (or product) with the highest level of overall criticality is identified as the most critical material (or product). The network related to the most critical material or product is specified as the critical sub-network. Afterwards, the critical sub-network is modelled to develop and evaluate risk mitigation strategies. Concept of the critical sub-network identification is illustrated with an example in Figure 2. An example supply chain system is demonstrated in Figure 2. In case of material-level analysis, the most critical material is identified as the material consumed by P1, P2, P3, and supplied by S2. Hence, the sub-network consisting of S2, P1, P2, and P3 is identified as the critical sub-network. Alternatively, in case of product-level analysis, the most critical product is identified as the product demanded by C3. Therefore, the critical sub-network consists of the customer demanding the product (C3), the plant producing the product (P3) and the suppliers supplying the materials required for production of the product (S2 and S4).

### 3.2 Risk Mitigation

In this stage, a discrete event system simulation model of the critical sub-network is developed. By utilizing the simulation model, a number of risk mitigation strategies are evaluated in terms of their effectiveness and efficiency. In evaluation of the risk mitigation strategies, interrelationships between the strategies must be taken into account. For example, there is a strong relationship between redundancy and flexibility strategies. These strategies are effective in mitigating supply chain risks. However, combinations of these strategies often yield more effective and efficient risk mitigation due to their systemic effects. Herein, we cannot conclude that one strategy is superior to another strategy in terms of both effectiveness and efficiency. Therefore, in this study, these strategies are quantitatively described and evaluated by simulation experiments. The best combination of these strategies is determined in terms of effectiveness and efficiency. To evaluate the effectiveness and efficiency together, a multi-objective evaluation is required. Hence, both cost and premium freight performance are considered to measure efficiency and effectiveness together. To observe the effects of risk mitigation parameter levels a full factorial experiment is designed. Minitab Response Optimizer Tool is used to obtain the best parameter levels that give minimum annual holding cost and premium freight ratio.

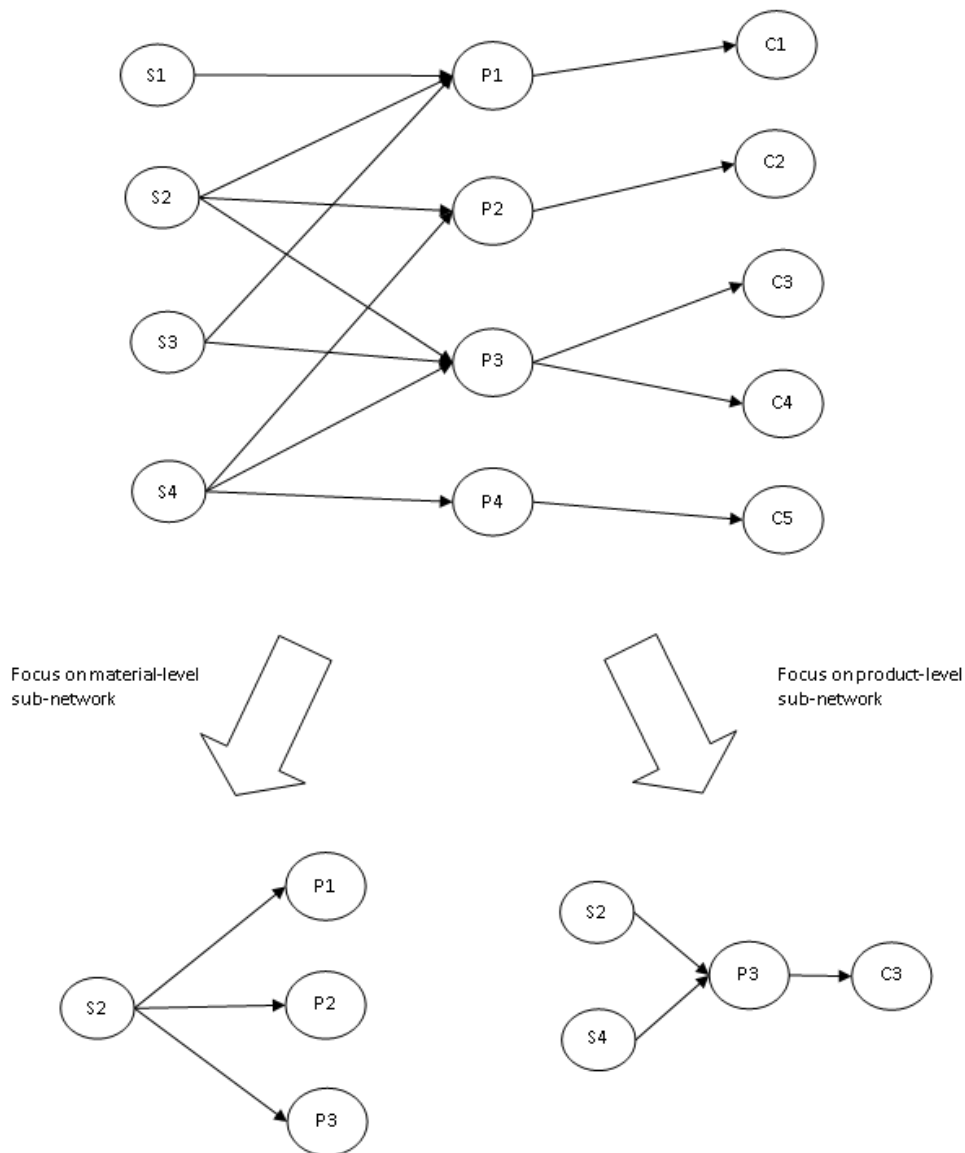


Figure 2. An example to critical sub-network identification

### 3.3 Risk Monitoring and Control

After the risk mitigation strategies are determined, outcomes of these strategies are continually monitored and reviewed. To ensure the continuous improvement in supply chain competitiveness, the management take actions in cases of any change in supply chain environment and risk levels. In particular, costs and premium freights related to the critical sub-network are continuously monitored. The supply chain manager can revise the mitigation plan according to the changes in critical sub-network performance. In a stationary supply chain environment, the manager will mainly focus on supply chain efficiency. In this case, the effects of low safety stock levels or low supplier flexibility on supply chain performance should be analysed. In turbulent environments, the manager will focus on keeping premium freights under control. Moreover, risk identification and mitigation phases can be reiterated in case of a major change in supply chain environment. Furthermore, the criteria for critical sub-network identification can be reconsidered.

#### 4. Application of the Proposed Framework

The proposed framework is applied to a supply chain of a European automotive company. The supply chain consists of 752 suppliers, 12 plants and 55 customers. The plants assemble the materials into a semi-finished product specialized to the customer. The customers are just-in-time automobile manufacturers. Therefore, backlogging is not allowed in the supply chain. In case of a shortage risk, a premium freight is requested.

The supply chain under concern operates six days in a week and 48 weeks in a year. Customers share their demand forecast with the plants in weekly basis. The plants adjust the customer demand forecast information by a demand forecast adjustment factor. In particular, customer demand forecast information is adjusted by multiplying it with demand forecast adjustment factor. The plants use the adjusted demand forecast information in developing their production plan and determining the order sizes to be placed to their suppliers.

The plants use a periodic order-up-to policy for the materials' inventory. At the beginning of each week, the weekly requirements for each material are calculated. Then, if it is needed, an order is placed. The order quantities are determined by considering safety stock level, transportation lead time and average daily consumption of material, as well as, quantity flexibility limits of the suppliers. The orders are processed by suppliers immediately and are delivered after a transportation lead time. Shipments and deliveries are made only in working days. Production and storage processes of the suppliers are not considered in this study.

Inventory position of each plant is reviewed on daily basis. If inventory position of a material is below of the safety stock level and it is not the regular ordering day, an inbound premium freight must be requested from the supplier of the material. At the end of each week, customer demand is realized and filled from the inventory. The customer demand cannot be backordered. If it is not possible to deliver on time, final products are delivered to the customer by an outbound premium freight. The premium freights are delivered at the next day of the shipment.

The required data for the analysis are obtained from the plan for every part spreadsheets which are used by the plants for production planning. The demand forecast adjustment factor for each plant is 1.07. The plants holds 3.5 days of safety stock for each material. Supplier flexibility is presented as a percentage in the quantity flexibility contracts. In these contracts,  $Fl\%$  flexibility means that the order quantity of a plant can be  $Fl\%$  below or above of the contracted quantity. Currently, quantity flexibility of the suppliers is 50%. The quantity flexibility can be increased by making a new contract. However, the contracted unit price will be higher in case of a higher quantity flexibility. By consulting a supply chain manager, we model the relationship between supplier flexibility and unit price as in the following.

$$unit\ price^{new} = \left[ \frac{100 + 20(Fl^{new} - Fl^{curr})}{100} \right] unit\ price^{curr} \quad (4.1)$$

where  $unit\ price^{curr}$  is the current unit price under current quantity flexibility ( $Fl^{curr}$ ), and  $unit\ price^{new}$  is the new unit price which is specified for  $Fl^{new}$  quantity flexibility.

In subsequent sections, identification and modeling of the critical sub-networks through material-level and product level risk management considerations are presented.

##### 4.1 Material-Level Risk Management

This section focuses on the supply chain risks related to materials. Hence, the materials are investigated in terms of their criticality by the proposed risk identification procedure. As the inbound supply chain inventory consists of 7300 materials consumed by 12 plants, it is unreasonable to assess the risks related to all materials. Therefore, the materials that have a considerable share on annual inbound premium freight costs are identified by using Pareto principle. As a result, 37 out of 7300 materials presenting 80% of annual inbound premium cost are selected for risk identification.

### 4.1.1 Risk Identification

The inbound risks of the focal supply chain are identified as supplier delivery delay and delivery quantity loss. The inbound risks are modelled by their occurrence and severity values. The fractions of late and under-shipped deliveries are obtained by historical data and used as the occurrence values of delivery delay and delivery quantity loss, respectively. To quantify the severity values of inbound risks, delivery lateness and quantity loss data are obtained from historical order records. The historical data are fitted to a number of probability distributions such as normal, lognormal, exponential, Weibull and gamma distributions to obtain the risk models.

The outbound risk is identified as variability in the material consumption. However, since a material type can be used in production of hundreds of different product types, it is impractical to model material consumption variability based on customer demand variability. Therefore, material consumption variability is assumed to follow a uniform distribution varying between 50% and 150% of average daily consumption in parallel with the supply chain manager’s opinion.

Afterwards, the focal supply chain is decomposed into a critical sub-network by considering inbound supply chain risk performance. The criteria for critical sub-network identification are determined by the supply chain manager as number of inbound premium freights in previous year, monetary value of inbound premium freights in previous year and average weekly consumption of materials. However, these criteria are assessed by the plants with different ratings. Therefore, multiple decision matrices are formed. As stated previously, these decision matrices should be merged into unique decision matrix by using a group decision making approach. In this study, the decision matrices are merged by averaging the ratings of the plants. In the TOPSIS, the decision matrices are normalized into [0,1]. Hence, the positive ideal solution ( $p_j$ ) is one while the negative ideal solution ( $n_j$ ) is zero for all criteria. In the calculation of overall criticality index, the criteria weights are obtained as 0.33, 0.33, and 0.34 for the number of premium freights, the monetary value of premium freights and the average weekly consumption, respectively. The overall criticality indices calculated by using TOPSIS are presented in Table 1. As it can be seen from the table, the most critical material is M1. The critical sub-network related to material M1 is presented in Figure 3.

Table 1  
Overall criticality indices for materials

Material	$CC_i$	Material	$CC_i$	Material	$CC_i$	Material	$CC_i$
M1	0.14	M9	0.03	M8	0.02	M21	0.01
M5	0.11	M24	0.03	M36	0.02	M31	0.01
M16	0.08	M34	0.03	M18	0.02	M12	0.01
M2	0.05	M6	0.03	M32	0.02	M28	0.01
M3	0.05	M29	0.03	M33	0.02	M20	0.01
M14	0.05	M17	0.02	M30	0.02	M26	0.00
M11	0.04	M19	0.02	M10	0.01	M35	0.00
M7	0.04	M22	0.02	M27	0.01		
M13	0.04	M4	0.02	M23	0.01		
M25	0.03	M15	0.02	M37	0.01		

### 4.1.2 Risk Mitigation

In this phase, a simulation model of the critical sub-network is developed. The inbound risks affecting the critical sub-network are modelled by the aforementioned risk quantification approach. The delivery loss probability is calculated as 0.05. To determine the probability distribution of the delivery loss quantity, the historical delivery loss data are fitted to a number of distributions in MINITAB statistical software. The best fitted distribution is a lognormal distribution with parameters 0.52 and 0.23. The delivery delay probability is 0.06. The delivery delay time distribution is specified as a lognormal (1.43, 0.46). By consulting the supply chain manager, material consumption variability distribution is specified as a uniform distribution varying between 50% and 150% of average daily consumption.

The performance measures are annual holding cost of supply chain and inbound premium freight ratio. Annual holding cost of supply chain involves annual holding costs of the plants associated with the critical material. Inbound premium ratio is the ratio of total amount of premium freights to total amount of orders associated with the critical material in the supply chain.

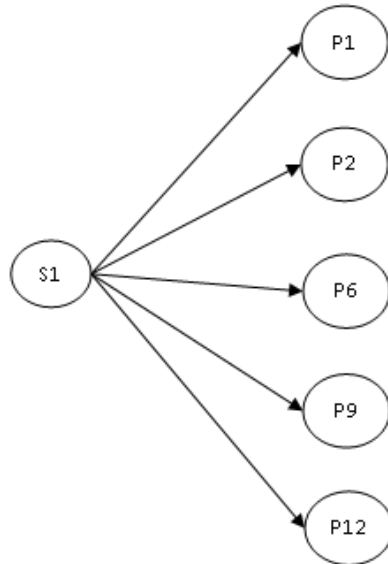


Figure 3. The critical sub-network identified in case of material-level risk management

The critical sub-network model is simulated for 104 weeks. The warm-up period is determined as two weeks by inspecting the variability in orders. Furthermore, required number of replications are determined by analysing the simulation outputs. In particular, a number of confidence intervals are calculated for annual holding cost and inbound premium freight ratio at the end of each replication. Until the confidence intervals become narrow enough, the replications proceed. The required half-length for the confidence intervals are 0.15. As a result, 15 replications are found to be sufficient to predict the performance measures within the predefined error rate.

To analyse the effects of risk mitigation strategies, a full factorial experimental design (Montgomery, 2008) is developed by considering five factor levels for safety stock and supplier flexibility (see Table 2). The response variables of the design are the annual holding cost and the premium freight ratio. The values for the response variables are obtained by the simulation model. According to the results of ANOVA, the effects of safety stock and supplier flexibility are significant on both annual holding cost and premium freight performances. To determine the best factor levels yielding minimum annual holding cost and premium freight ratio, MINITAB Response Optimizer tool is used. The best factor levels are determined as 4.5 days for safety stock and 30% for supplier flexibility. Comparison of the performances corresponding to the best factor levels and current factor levels is presented in Table 3. As one can see from the table, the new factor levels reduce the annual holding cost by 8% and the premium freight ratio by 3%.

Table 2  
Factor levels considered in case of material-level risk management

Factors	Levels				
Safety stock	2.5	3	3.5*	4	4.5
Flexibility	30%	40%	50%*	60%	70%

\*The current levels used in the supply chain



Table 3

Performance comparison in case of material-level risk management

	Safety Stock	Supplier Flexibility	Annual Holding Cost	Inbound Premium Freight Ratio
New factor levels	4.5	30%	€4015	0.19
Current factor levels	3.5	50%	€4349	0.20

## 4.2 Product-Level Risk Management

In this section, the products are investigated in terms of their criticality by the proposed risk assessment procedure. Since there exist 2700 different types of products produced by the plants, it is unreasonable to deal with the risks associated with all products. Hence, the products that have a considerable share on annual outbound premium freight costs are identified by using Pareto principle. As a result, 13 out of 2700 products presenting 80% of annual outbound premium cost are selected for risk identification.

### 4.2.1 Risk Identification

In the product-level risk management case, the inbound risks are identified as supplier delivery delay and delivery loss. The occurrence and severity values are quantified by the probability distributions derived from past order data as the in material-level risk management case. Outbound risks are identified as the customer demand variability and the deviation of actual customer demand from the shared demand information. These risks are modelled as ordinary variabilities that occur every week and only severity values of them are modelled. To model outbound risks, the demand data are obtained from the historical customer demand records.

Then, the focal supply chain is decomposed into a critical sub-network by considering outbound supply chain risk performance. By consulting the supply chain manager, the criteria for critical sub-network identification are determined as the number of outbound premium freights in previous year, monetary value of the outbound premium freights in previous year and average annual sales of the products. As in the material-level risk management case, the decision matrices are normalized into [0,1]. Therefore, the positive ideal solution is one and the negative ideal solution is zero for all criteria. The entropy weights are obtained as 0.34, 0.34, and 0.32 for the number of outbound premium freights, the monetary value of premium freights and the average annual sales, respectively. The overall criticality indices calculated by using TOPSIS method are presented in Table 4. As can be inferred from the table, the most critical product is PR1. The critical sub-network related to PR1 is presented in Figure 4.

### 4.2.2 Risk Mitigation

In this phase, a simulation model of the critical sub-network is developed. The bill of material information related to PR1 is reported in Table 5.

The inbound risks affecting the critical sub-network are modelled by the aforementioned risk quantification approach. The probability distributions that are best fitted to historical data are given in Table 6. The best fitted distributions are normal and Weibull distributions for delivery loss quantity and delivery delay, respectively. The customer demand is modelled by the demand forecast and the deviation of actual customer demand from the demand forecast. The best fitted probability distributions for the demand forecast and the deviation are Lognormal(6.27, 0.51) and Lognormal(0.07, 0.21), respectively.

The performance measures are annual holding cost of supply chain, inbound premium freight ratio, and outbound premium freight ratio. Annual holding cost and inbound premium freight ratio are calculated as in Section 4.1.2. Outbound premium freight ratio is the ratio of total amount of the premium freights related to the products to the total amount of products sold.

Table 4  
Overall criticality indices for the products

Products	$CC_i$
PR1	0.18
PR11	0.14
PR6	0.14
PR2	0.12
PR3	0.10
PR5	0.10
PR4	0.08
PR12	0.07
PR7	0.05
PR13	0.05
PR8	0.04
PR10	0.03
PR9	0.03

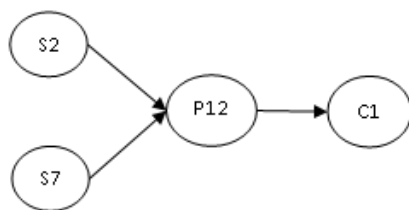


Figure 4. The critical sub-network identified in case of product-level risk management

Table 5  
Bill of material for PR1

Material	Supplier	Quantity
M2	S2	1
M22	S2	3
M71	S7	3
M73	S7	3
M76	S7	1
M79	S7	3

Table 6  
The inbound risk model in case of product-level risk management

Suppliers	Delivery Loss		Delivery Delay	
	Probability	Quantity distribution	Probability	Time distribution
S2	0.05	Normal(0.45,0.17)	0.09	Weibull(1.65,1.61)
S7	0.03	Normal(0.51,0.25)	0.07	Weibull(1.20,2.30)

The warm-up period length and the number of replications are determined in the same manner described in Section 4.1.2. The critical sub-network model is simulated for 104 weeks and 15 replications. The warm-up period is specified as one week. To analyse the effects of risk mitigation strategies, a full factorial experimental design is developed for five factor levels for demand forecast adjustment factor, safety stock and supplier

flexibility. (see Table 7). The response variables are the annual holding cost, inbound and outbound premium freight ratios. The response values are obtained from the simulation model.

Table 7  
Factor levels considered in the experiment

Factors	Levels				
Demand adj.	1	1.03	1.07*	1.11	1.15
Safety stock	2.5	3	3.5*	4	4.5
Flexibility	30%	40%	50%*	60%	70%

\*The current levels used in the supply chain

According to the ANOVA results, all the factors have significant effect on the holding cost and the outbound premium freight ratio. However, only the supplier flexibility affects the inbound premium freight ratio significantly. The best factor levels yielding minimum annual holding cost, inbound and outbound premium freight ratios are determined via MINITAB Response Optimizer Tool. The best factor levels are 1.15, 2.5 and 30% for demand forecast adjustment factor, safety stock and supplier flexibility, respectively. Comparison of the performances corresponding to these factor levels and current factor levels is presented in Table 8. The results reveal that the new factor levels reduce annual holding cost by 10%, inbound premium freight ratio by 26%, and outbound premium freight ratio by 28%.

Table 8  
Performance comparison of in case of product-level risk management

	Demand Adj. Fac.	Safety Stock	Supplier Flexibility	Annual Holding Cost	Inbound Premium Freight Ratio	Outbound Premium Freight Ratio
New factor levels	1.15	2.5	30%	€20254	0.07	0.04
Current factor levels	1.07	3.5	50%	€22425	0.10	0.06

### 5. Discussion and Managerial Implications

According to the results, the proposed framework is capable of ensuring a substantial improvement in terms of holding cost and premium freight performances. In this application, emphasizing on redundancy strategies improves the supply chain risk performance in both holding cost and premium freight aspects. In Figure 5, the main effects of safety stock and supplier flexibility levels on holding cost and premium freight ratio are given for the material-level risk management case. The ANOVA results shows that the effects of supplier flexibility on annual holding cost and premium freight ratio are significant. Moreover, safety stock level has a significant effect on premium freight ratio. In this case, higher supplier flexibility levels yield lower premium freight ratio, but increase holding cost. On the other hand, main effects of safety stock levels on premium freight ratio is nonlinear where the current safety stock level (3.5 days) incurs the worst premium freight performance. Thus, a compromise solution can be obtained among two objectives by decreasing supplier flexibility level and increasing safety stock level. In accordance with this result, the proposed framework improves both holding cost and premium freight ratio by reducing supplier flexibility and increasing safety stock levels (see Table 3).

In Figure 6, main effects of demand forecast adjustment factor, safety stock, and supplier flexibility levels on supply chain performance are illustrated for product-level risk management case. According to the ANOVA results, demand forecast adjustment factor, safety stock and supplier flexibility have significant effect on annual holding cost and outbound premium freight ratio. Moreover, supplier flexibility has a significant effect on inbound premium freight ratio. As one can infer from the figure, demand forecast adjustment factor has lower effect on holding cost and higher effect on outbound premium freight ratio than the other parameters. Therefore, to reduce outbound premium freight ratio, demand forecast adjustment factor can be increased. Moreover, to reduce holding cost supplier flexibility can be reduced by considering its significant relationship with demand forecast adjustment factor in terms of outbound premium freight ratio. Furthermore, we can infer from the figure that safety stock has relatively low effect on outbound premium freight ratio. Accordingly, the proposed framework ensures better supply chain performance in three objectives by increasing demand forecast adjustment factor and decreasing safety stock and supplier flexibility levels (Table 8).

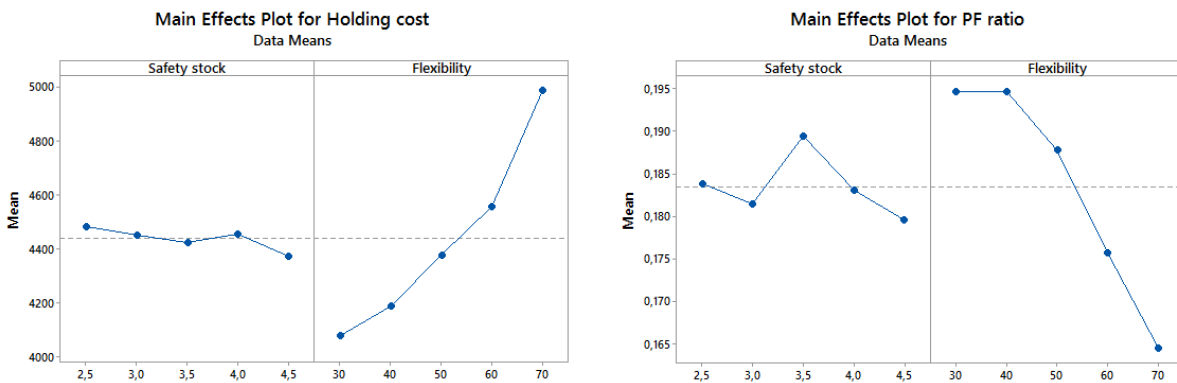


Figure 5. Main effects of parameter levels on supply chain performance in material-level risk management case

In both cases, the framework suggests lower supplier flexibility levels than the current levels. In material-level risk management case, safety stock levels are increased. In the product-level risk management case, demand forecast adjustment factor is increased. Consequently, redundancy strategies are preferred rather than flexibility strategy in this application. Therefore, the managers of the focal supply chain should put more emphasis on redundancy strategies (high demand forecast adjustment factor and safety stock levels).

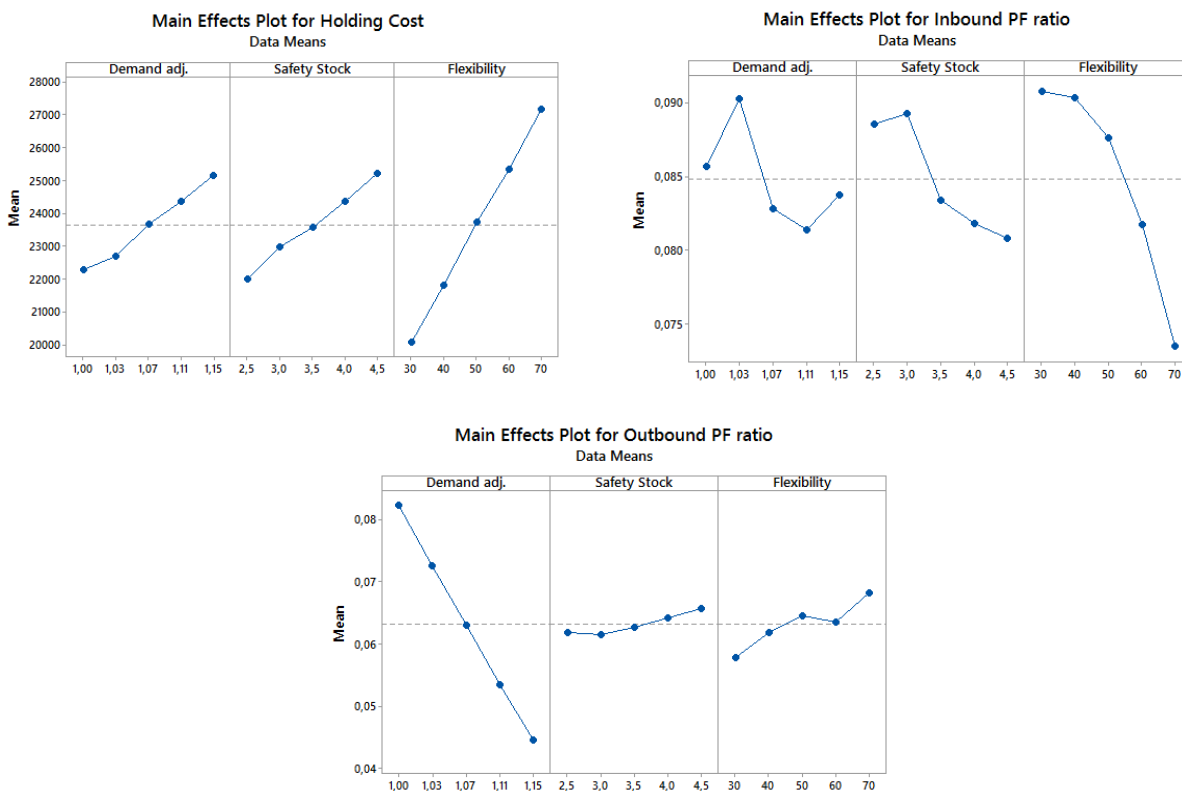


Figure 6. Main effects of parameter levels on supply chain performance in product-level risk management case

Supply chain managers can use the proposed framework in cases of any changes in supply chain environment, competition strategy, and new supplier contracts. Although the objectives have equal importance in this application, the proposed framework provides the flexibility in evaluating risk mitigation plans by considering different weights for the objectives. In a stable supply chain environment, the manager can give more importance to holding costs. In turbulent supply chain environment, the manager will mainly focus on supply chain risks and reduce premium freights. Moreover, in case of a change in competition strategy, the manager

may consider reducing holding costs to gain cost advantage, or focus on supply chain risks to ensure customer satisfaction. Furthermore, the proposed framework will be beneficial in making new supplier contracts, since it considers both cost and resilience objectives.

The proposed framework provides a comprehensive decision support since it involves both material and product-level risk analyses through the preference of the decision maker. Additionally, it considers redundancy and flexibility strategies in combined manner to improve supply chain risk performance efficiently and effectively. Moreover, it measures the supply chain vulnerability by premium freight ratio. Furthermore, due to its flexible and convenient structure, it can be applied to various supply chain structures.

## 6. Conclusion

This study proposes an integrated risk management framework for global supply chains. In the risk identification phase of the proposed framework, global supply chain is decomposed into material-level or product-level critical sub-networks according to preference of the manager. Consequently, the proposed framework is applicable for both material and product-level risk analyses. This provides the flexibility in choosing the focus of SCRM through the manager's performance objectives. Additionally, the proposed framework enables managers in combining redundancy and flexibility strategies to ensure both effectiveness and efficiency objectives in SCRM. In this study, an application of the proposed framework to an automobile supply chain is presented. The results of both material and product level analyses show that the proposed framework improves the supply chain performance.

A limitation of this study is the assumption of the identical safety stock and supplier flexibility levels throughout the supply chain. These parameters may take different values for each material and supplier. However, this increases the complexity of the problem. Consequently, finding the best parameter levels by using an experimental design approach become challenging. Furthermore, analysis of supply chain risk drivers, and considering rare and severe adverse events in the proposed framework are possible future research directions.

## Author Contributions

Mualla Gonca Avci: Conceptualization, Methodology, Software, Validation, Data curation, Writing

## Conflicts of Interest

The authors declare no conflict of interest.

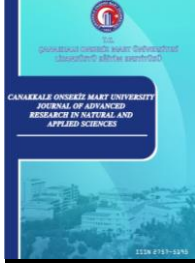
## References

- Aqlan, F., & Lam, S. S. (2015a). A fuzzy-based integrated framework for supply chain risk assessment. *International Journal of Production Economics*, 161, 54-63. doi: <https://doi.org/10.1016/j.ijpe.2014.11.013>
- Aqlan, F., & Lam, S. S. (2015b). Supply chain risk modelling and mitigation. *International Journal of Production Research*, 53(18), 5640-5656. doi: <https://doi.org/10.1080/00207543.2015.1047975>
- Bueno-Solano, A., & Cedillo-Campos, M. G. (2014). Dynamic impact on global supply chains performance of disruptions propagation produced by terrorist acts. *Transportation Research Part E: Logistics and Transportation Review*, 61, 1-12. doi: <https://doi.org/10.1016/j.tre.2013.09.005>
- Cardoso, S. R., Paula Barbosa-Póvoa, A., Relvas, S., & Novais, A. Q. (2015). Resilience metrics in the assessment of complex supply-chains performance operating under demand uncertainty. *Omega*, 56, 53-73. doi: <https://doi.org/10.1016/j.omega.2015.03.008>
- Carvalho, H., Barroso, A. P., Machado, V. H., Azevedo, S., & Cruz-Machado, V. (2012). Supply chain redesign for resilience using simulation. *Computers & Industrial Engineering*, 62(1), 329-341. doi: <https://doi.org/10.1016/j.cie.2011.10.003>
- Chaudhuri, A., Mohanty, B. K., & Singh, K. N. (2013). Supply chain risk assessment during new product development: a group decision making approach using numeric and linguistic data. *International*

- Journal of Production Research*, 51(10), 2790-2804. doi: <https://doi.org/10.1080/00207543.2012.654922>
- Chen, P.-S., & Wu, M.-T. (2013). A modified failure mode and effects analysis method for supplier selection problems in the supply chain risk environment: A case study. *Computers & Industrial Engineering*, 66(4), 634-642. doi: <https://doi.org/10.1016/j.cie.2013.09.018>
- Chopra, S., & Sodhi, M. S. (2004). Managing Risk To Avoid Supply-Chain Breakdown. *MIT Sloan management review*, 46(1), 53-61.
- Christopher, M., & Peck, H. (2004). Building the Resilient Supply Chain. *International Journal of Logistics Management*, 15(2), 1 - 14. doi: <https://doi.org/10.1108/09574090410700275>
- Deng, H., Yeh, C. H., & Willis, R. J. (2000). Inter-company comparison using modified TOPSIS with objective weights. *Computers & Operations Research*, 27(10), 963-973. doi: [https://doi.org/10.1016/S0305-0548\(99\)00069-6](https://doi.org/10.1016/S0305-0548(99)00069-6)
- Colicchia, C., & Strozzi, F. (2012). Supply chain risk management: a new methodology for a systematic literature review. *Supply Chain Management: An International Journal*, 17(4), 403-418. doi: <https://doi.org/10.1108/13598541211246558>
- Ghadge, A., Dani, S., Chester, M., & Kalawsky, R. (2013). A systems approach for modelling supply chain risks. *Supply Chain Management: An International Journal*, 18(5), 523-538. doi: <https://doi.org/10.1108/SCM-11-2012-0366>
- Giannakis, M., & Louis, M. (2011). A multi-agent based framework for supply chain risk management. *Journal of Purchasing and Supply Management*, 17(1), 23-31. doi: <https://doi.org/10.1016/j.pursup.2010.05.001>
- Govindan, K., & Jepsen, M. B. (2015). Supplier risk assessment based on trapezoidal intuitionistic fuzzy numbers and ELECTRE TRI-C: a case illustration involving service suppliers. *Journal of the Operational Research Society*, 67(2), 339-376. doi: <https://doi.org/10.1057/jors.2015.51>
- Guertler, B., & Spinler, S. (2015). When does operational risk cause supply chain enterprises to tip? A simulation of intra-organizational dynamics. *Omega*, 57, 54-69. doi: <https://doi.org/10.1016/j.omega.2015.03.005>
- Heckmann, I., Comes, T., & Nickel, S. (2015). A critical review on supply chain risk – Definition, measure and modeling. *Omega*, 52, 119-132. doi: <https://doi.org/10.1016/j.omega.2014.10.004>
- Ho, W., Zheng, T., Yildiz, H., & Talluri, S. (2015). Supply chain risk management: a literature review. *International Journal of Production Research*, 53(16), 5031-5069. doi: <https://doi.org/10.1080/00207543.2015.1030467>
- Hwang, C. L., & Yoon, K. P. (1981). *Multiple attribute decision making: Methods and applications*: Springer-Verlag, New York.
- Kara, M. E., Firat, S. Ü. O. & Ghadge, A. (2020). A data mining-based framework for supply chain risk management. *Computers & Industrial Engineering*, 139, 105570. doi: <https://doi.org/10.1016/j.cie.2018.12.017>
- Klibi, W., & Martel, A. (2012). Scenario-based Supply Chain Network risk modeling. *European Journal of Operational Research*, 223(3), 644-658. doi: <https://doi.org/10.1016/j.ejor.2012.06.027>
- Montgomery, D. C. (2008). *Design and analysis of experiments*: John Wiley & Sons.
- Oliveira, U. R., de Almeida Muniz, M., Anaia, L. A., & Rocha, H. M. (2022). Medication supply chain risk management for a brazilian home care provider: A business sustainability study. *Cleaner Logistics and Supply Chain*, 3, 100018. doi: <https://doi.org/10.1016/j.clscn.2021.100018>
- Oliveira, J. B., Jin, M., Lima, R. S., Kobza, J. E., & Montevechi, J. A. B. (2019). The role of simulation and optimization methods in supply chain risk management: Performance and review standpoints. *Simulation Modelling Practice and Theory*, 92, 17-44. doi: <https://doi.org/10.1016/j.simpat.2018.11.007>
- Pournader, M., Kach, A., & Talluri, S. (2020). A review of the existing and emerging topics in the supply chain risk management literature. *Decision Sciences*, 51(4), 867-919. doi: <https://doi.org/10.1111/dec.12470>
- Rajesh, R., & Ravi, V. (2015). Modeling enablers of supply chain risk mitigation in electronic supply chains: A Grey-DEMATEL approach. *Computers & Industrial Engineering*, 87, 126-139. doi: <https://doi.org/10.1016/j.cie.2015.04.028>

- Rangel, D. A., de Oliveira, T. K., & Leite, M. S. A. (2014). Supply chain risk classification: discussion and proposal. *International Journal of Production Research*, 1-20. doi: <https://doi.org/10.1080/00207543.2014.910620>
- Samvedi, A., Jain, V., & Chan, F. T. S. (2013). Quantifying risks in a supply chain through integration of fuzzy AHP and fuzzy TOPSIS. *International Journal of Production Research*, 51(8), 2433-2442. doi: <https://doi.org/10.1080/00207543.2012.741330>
- Schmitt, A. J., & Singh, M. (2012). A quantitative analysis of disruption risk in a multi-echelon supply chain. *International Journal of Production Economics*, 139(1), 22-32. doi: <https://doi.org/10.1016/j.ijpe.2012.01.004>
- Sheffi, Y. (2005). A Supply Chain View of the Resilient Enterprise. *MIT Sloan management review, Fall 2005*, 41-48.
- Simchi-Levi, D., Schmidt, W., Wei, Y., Zhang, P. Y., Combs, K., Ge, Y., . . . Zhang, D. (2015). Identifying Risks and Mitigating Disruptions in the Automotive Supply Chain. *Interfaces*, 45(5), 375-390. doi: <https://doi.org/10.1287/inte.2015.0804>
- Singhal, P., Agarwal, G., & Mittal, M. L. (2011). Supply chain risk management: review, classification and future research directions. *International Journal of Business Science and Applied Management*, 6(3), 15-42.
- Sodhi, M. S., Son, B.-G., & Tang, C. S. (2012). Researchers' Perspectives on Supply Chain Risk Management. *Production and Operations Management*, 21(1), 1-13. doi: <https://doi.org/10.1111/j.1937-5956.2011.01251.x>
- Talukder, B., Agnusdei, G. P., Hipel, K. W., & Dubé, L. (2021). Multi-indicator supply chain management framework for food convergent innovation in the dairy business. *Sustainable Futures*, 3, 100045. doi: <https://doi.org/10.1016/j.sftr.2021.100045>
- Tang, O., & Nurmaya Musa, S. (2011). Identifying risk issues and research advancements in supply chain risk management. *International Journal of Production Economics*, 133(1), 25-34. doi: <https://doi.org/10.1016/j.ijpe.2010.06.013>
- Tummala, R., & Schoenherr, T. (2011). Assessing and managing risks using the Supply Chain Risk Management Process (SCRMP). *Supply Chain Management: An International Journal*, 16(6), 474 - 483. doi: <https://doi.org/10.1108/13598541111171165>
- Wagner, S. M., Mizgier, K. J., & Arnez, P. (2014). Disruptions in tightly coupled supply chain networks: the case of the US offshore oil industry. *Production Planning & Control*, 25(6), 494-508. doi: <https://doi.org/10.1080/09537287.2012.705355>
- Wang, X., Chan, H. K., Yee, R. W. Y., & Diaz-Rainey, I. (2012). A two-stage fuzzy-AHP model for risk assessment of implementing green initiatives in the fashion supply chain. *International Journal of Production Economics*, 135(2), 595-606. doi: <https://doi.org/10.1016/j.ijpe.2011.03.021>





# Culturable Bacterial Communities Related to Different Larval Stages of *Sanys irrosea* (Guenee, 1852) (Lepidoptera: Noctuidae)

Ali Sevim<sup>1,\*</sup>, Elif Sevim<sup>2</sup>

<sup>1</sup>Department of Plant Protection, Faculty of Agriculture, Kırşehir Ahi Evran University, Kırşehir, Türkiye

<sup>2</sup>Department of Medical Biology, Faculty of Medicine, Kırşehir Ahi Evran University, Kırşehir, Türkiye

## Article History

Received: 02.04.2022

Accepted: 27.06.2022

Published: 15.12.2022


## Research Article


**Abstract** – Many bacterial species are frequently associated with insects in symbiotic, mutualistic, or parasitic relationships. Symbiotic bacteria living in mostly insect gut have many roles in insect's biology such as nutrition, development, sex determination and evolution. Therefore, studying of symbiotic bacteria in insects is very important to elucidate their roles in their hosts biology. In this study, we purposed to isolate and identify the culturable bacterial species in internal organs (mostly gut parts) of *Sanys irrosea* (Guenee, 1852) (Lepidoptera: Noctuidae) which was selected as model organism. The bacterial flora of different development stages of *S. irrosea* was studied by culture dependent techniques and the isolated bacteria was identified by 16S rRNA sequencing and phylogenetic analysis. A total of 22 bacterial isolates were obtained from different instar larvae of the insect and were identified. Among the identified bacterial species, *Staphylococcus*, *Micrococcus* and *Bacillus* species were dominant. In addition, some potential slug, human and plant pathogenic bacteria (*Moraxella osloensis*, *Kocuria rosea* and *Clavibacter michiganensis*) were isolated. The results were discussed with respect to the bacterial composition of *S. irrosea* regarding effects of bacterial diversity on the larval development of the insect. Results obtained from this study should be beneficial for future studies to understand roles of bacteria in the larval development of Lepidopteran insects.

**Keywords** – Bacteria, insect, symbiosis, 16S rRNA

## 1. Introduction

Bacteria are prokaryotic microorganisms which have different shapes, metabolism and lifestyle and they can survive in different environments from soil to water. They can also live with different organisms such as plants and animals in symbiotic and parasitic relations (Madigan, Martinko & Parker, 2003). They have also some genes and enzymes to sensitize some essential vitamins (such as cobalamin) which are necessary for nearly all animal life (Moore & Warren, 2012). Most of the bacteria in the human and various animal bodies including insects are in the intestinal (gut) system. Many of these bacteria are symbiotically related with their hosts and beneficial (Scudder, 2009; Engel & Moran, 2013). Insects are the biggest animal group on earth, including more than approximately 2 million species. They can be found almost in every ecosystem in the world and can sometimes be seen in very intense populations (Basset et al., 2012; Novotny et al., 2002). These creatures which have a large amount of species and are found in large quantities have been successful in their evolutionary histories partly by dint of beneficial microorganisms living with them (Engel & Moran, 2013). Based on today's information, it can be said that these symbiotic microorganisms are responsible for various functions (making useful nutrient-poor diet, aiding digestion of insect's food compounds, protecting against their enemies and determining mating and reproductive systems) in insects (Douglas, 2015). Especially, some studies showed that bacterial communities within insects can affect the developments stages of insects (Souza

<sup>1</sup>  ali.sevim@ahievran.edu.tr

<sup>2</sup>  esevim@ahievran.edu.tr

\*Corresponding Author

et al., 2019; Peterkova-Koci, Robles-Murguia, Ramalho-Ortigao & Zurek, 2012). Therefore, it is important to study insect-microbial relations to clarify roles of these microorganisms in insect's life.

Therewithal, some microorganisms such as viruses, bacteria, nematodes, fungi, and protozoans can cause infection diseases in various insects (Lacey et al., 2015). These insect pathogenic microorganisms are sometimes harmful in terms of beneficial insects such honeybee and silkworm and sometimes useful for harmful insects (also called pests) in agriculture and forestry. Within these microbial control agents, bacteria (especially *Bacillus thuringiensis*) have special importance since they are the most commercially used and produced in terms of controlling of important pest species (Ben-Dov, 2014). Apart from *B. thuringiensis*, there are many bacterial species (such as *Lysinibacillus sphaericus*, *Brevibacillus laterosporus*, *Serratia* spp. and, *Pseudomonas entomophila*) which are pathogenic to insects (Ruiu, 2015).

The first step is to isolate and characterize bacterial species in insect's gut to elucidate their functions in host's development and biology. In accordance with this purpose, up to now, many studies have been carried out to isolate and identify various bacteria from various insect species (Sevim, Çelebi & Sevim, 2012; Liu et al., 2016; Anand et al., 2010). According to many studies, molecular characterization techniques (especially 16S rRNA sequencing) are the most reliable techniques for identifying bacterial species (Janda & Abbott, 2007). In this study, we purposed to isolate and identify bacterial species from different development stages of *Sanys irrosea*, which was selected as model organism, based on the culture-dependent technique and to characterize them by 16S rRNA gene sequence analysis. This insect was selected as model organism for moths to study the bacterial diversity since it has a wide and intense distribution in the study region. The attained results from here could be beneficial for future and further studies to elucidate the roles of these bacteria in the insect biology, especially Lepidopteran insects.

## 2. Materials and Methods

### 2.1. Collection of *Sanys irrosea* larvae

*Sanys irrosea* larvae were collected from Kırşehir city (steppe fields) in Turkey between May-June 2019. The collected larvae were put into plastic boxes (30 × 25 cm) with leaves of the plant on which they feed and brought to the laboratory. After that, the larvae were separated based on their sizes into different developments stages from first to fifth instar. They were fed with the collected plant leaves in the laboratory for two days and healthy larvae without disease were selected and used for bacterial isolation.

### 2.2. Molecular identification of larvae

Recently, molecular identification techniques such as DNA sequencing are being frequently used for many insects due to difficulties and limitations in morphological taxonomy (Campbell, Lawrence, Hudspath & Gruwell, 2014). Also, one of the most important parts for solution in growing problems with many pest species and the studying of insect-microbe relations require complete and accurate species identification. Therefore, in this study, we used the partial sequence of cytochrome oxidase (subunit I) (*COI*) gene (598 bp long) for identification of the collected larvae samples. Total genomic DNA from larvae were extracted using QIAGEN DNeasy Blood & Tissue kit (Hilden, Germany) based on the manufacturer's recommendations. For isolation, head parts of the larvae were used. The isolated DNAs were stored at -20 °C until use in PCR amplification. After that, approximately 620 bp fragment of *COI* gene was amplified by PCR. The primer pair of LCO1490-5'-GGTCAACAAATCATAAAGATATTGG-3' as forward and HCO2198-5'-TAAACTTCAGGGTGAC-CAAAAATCA-3' as reverse were used in PCR (Folmer, Black, Hoeh, Lutz & Vrijenhoek, 1994). The PCR was performed in 50 µl reaction volume as follow: 1 µl genomic DNA, 5 µl 10 × PCR buffer, 1.5 mM MgCl<sub>2</sub>, 1.25 U *Taq* DNA Polymerase enzyme, 0.25 mM opposing primers and 200 mM of each dNTP. The final volume was completed to 50 µl by sterile ddH<sub>2</sub>O. Thermal cycles were as follow; after first denaturation at 96 °C for 5 min, 95°C for 1 min, 56 °C for 45 s and 72 °C for 1 min as 36 cycles and 72 °C for 10 min for final extension. After PCR, the obtained products were run on 1 % agarose gel containing ethidium bromide for 15 min at 90 V and viewed under UV light. After the correct PCR bands were seen on the gel, one of them was purified, quantified, and sent to Macrogen (the Netherlands) for sequencing. Amplification primers for *COI* gene were also used for sequencing.

### 2.3. Bacterial isolation

The field collected larvae of *S. irrosea* were firstly separated into different development stages (instar) from first to fifth instar and waited for 2-3 days in the laboratory to select healthy larvae for the bacterial isolation. After selection of the healthy larvae, ten larvae for each instar were used for bacterial isolation. Firstly, the larvae were separately immersed in 70% ethanol for 3 min for surface sterilization and then, washed twice with sterile dH<sub>2</sub>O. The surface sterilized larvae were separately (based on different instar) homogenized in 3 ml nutrient broth using a tissue grinder and filtered through two layers of sterile cheese cloth to remove insect debris. After that, five homogenates (for each instar) were diluted with sterile nutrient broth from 10<sup>-1</sup> to 10<sup>-8</sup>. 100 µl from each dilution was taken and spread on nutrient agar (NA) by the spread plate method and incubated at 30 °C for two days in dark. After this, the total colony on each countable petri was counted by eye and the number of bacteria for per larva was calculated as colony forming unit (cfu). Later, each different colony was selected according to their shape, type, color, and morphology. The selected colonies were purified and stored in 20% glycerol at - 20°C for further identification studies.

### 2.4. 16S rRNA gene sequencing

The stock cultures for each bacterial strain were plated on nutrient agar by the streak plate method to obtain a single colony. A single colony for each strain was inoculated into 3 ml of nutrient broth (NB) and incubated in a rotary shaker at 200 rpm overnight. Later, genomic DNA extraction was done using these cultures. Genomic DNAs were extracted using PureLink™ Genomic DNA Mini Kit (Invitrogen). 16S rRNA gene regions belonging to each bacterial strain were amplified by the universal primer pair of 27F (5'- AGAGTTT-GATCMTGGCTCAG-3') as forward and 1492R (5'-TACGGYTACCTTGTTACGACTT-3') as reverse (Macrogen). The PCR was performed in 50 µl reaction volume including 1 µl genomic DNA, 5 µl 10 x PCR buffer, 1.5 mM MgCl<sub>2</sub>, 1.25 U *Taq* DNA Polymerase, 0.25 mM forward and reverse primer for each and 200 mM of each dNTP. The final volume was completed by sterile ddH<sub>2</sub>O to 50 µl. Thermal cycles were as follow; after first denaturation at 96 °C for 5 min, 95°C for 1 min, 55 °C for 1 min and 72 °C for 1,5 min as 36 cycles and 72 °C for 10 min for final extension. After PCR, the obtained products were run on 1 % agarose gel containing ethidium bromide for 15 min at 90 V and viewed under UV light. After the correct PCR bands were seen on the gel, all were sent to Macrogen (the Netherlands) for sequencing. The primer pair 518F (5'-CCAGC AGCCGCGGTAATACG-3') and 800R (5'-TACCAGG GTATCTAATCC-3') were used for sequencing (Macrogen).

### 2.5. Data analysis

The gene sequences were edited and aligned with BioEdit version 7.2.5 (Hall, 1999). The edited sequences were used for Blast search in GenBank to compare each sequence with their closely related insect or bacterial species and percent (%) similarity values were calculated (Altschul, Gish, Miler, Myers & Lipman, 1990; Benson et al., 2012). In addition, these gene sequences were used for phylogenetic analysis using MEGA-X software (Kumar, Stecher, Li, Knyaz & Tamura, 2018). For larvae, the partial sequence of *COI* gene (approximately 598 bp) was used to compare reference species in the study of (Mutanen, Wahlberg & Kaila, 2010). For bacterial strains, the 16S rRNA gene sequences were compared with their most closely related bacterial species based on Blast search in GenBank. For phylogenetic relationships, the neighbor-joining method with p-distance analysis packed in MEGA-X was used. The strength of the internal branches in the final tree was statistically evaluated by bootstrap analysis based on 1.000 pseudoreplicates using MEGA-X.

### 2.6. GenBank accession numbers of the bacterial isolates

GenBank accession numbers for 16S rRNA gene sequences belonging to the bacterial isolates are from MT537942 to MT537963.

## 3. Results and Discussion

The collected larvae were identified by the partial sequence of *COI* gene (approximately 598 bp). Based on the Blast search, *COI* sequence (598 bp) of the collected larvae was found to be similar with *Peactes fuscescens* voucher 11-SRNP-23183 with 90.62 % and *S. irrosea* DHJ04 with 90.10%. Since this similarity was very low

for species identification, we performed a phylogenetic analysis using reference species mentioned in the study of (Mutanen et al., 2010) to perform more correct species identification. Based on the phylogenetic analysis, the larva was identified as *Sanys irrosea* (Guenee, 1852) (Lepidoptera: Noctuidae) (Figure 1).

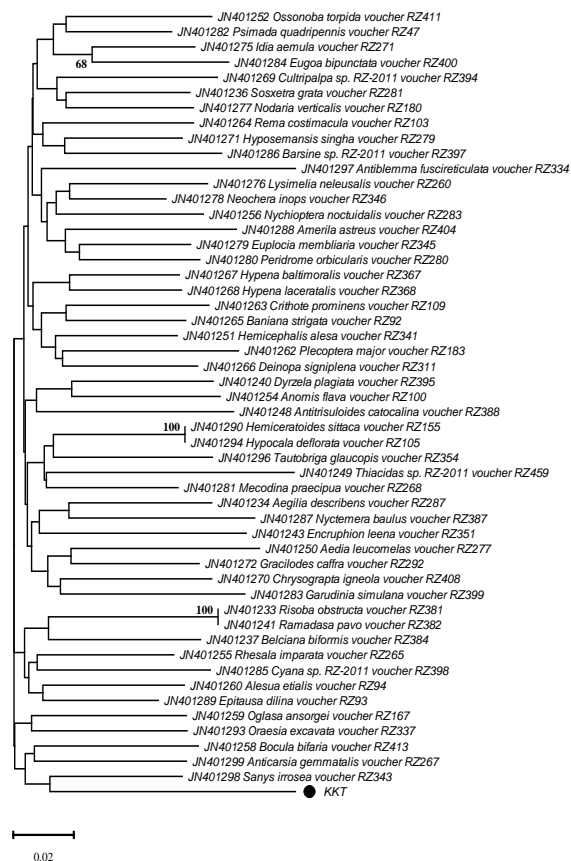


Figure 1. The dendrogram generated using Neighbor Joining (N-J) algorithm with p-distance analysis.

The tree was generated using the partial sequence (598 bp) of *COI* gene. *Sanys irrosea* sample which is marked with solid black dot was compared with the reference insect samples used in the study of Mutanen et al. (2010). The statistical accuracy of the tree was evaluated by bootstrap confidence analysis according to 1.000 repetitions and bootstrap values of 70% or higher were specified in the tree. The scale located under the tree shows the degree of dissimilarity.

Bacteria grown in petri dishes, where bacterial colonies can be evaluated separately, were counted and the number of culturable bacteria per larva was calculated as follows. The numbers of total bacteria in first, second, third, fourth and fifth instar larvae were determined as  $1.2 \times 10^7$  bacteria/larva,  $1.9 \times 10^7$  bacteria/larva,  $2.1 \times 10^8$  bacteria/larva,  $3.6 \times 10^8$  bacteria/larva, and  $0.6 \times 10^9$  bacteria/larva, respectively.

A total of 22 culturable bacterial isolates were obtained from different development stages of *S. irrosea*. Among them, six isolates from first instar, six isolates from second instar, two isolates from third instar, three isolates from fourth instar, and five isolates from fifth instar larvae were isolated. All bacterial isolates were identified at species or genus level using 16S rRNA sequence analysis. Blast results of 16S rRNA genes are given in Table 1.

Table 1.

Percentage identities of *S. irrosea* bacterial isolates with their the most closely associated bacteria in GenBank according to the Blast search of 16S rRNA gene sequences

Instar	Strain	Species	GenBank ID	Query coverage (%)	Percent (%) Similarity
First Instar	KT1.1	<i>Micrococcus yunnanensis</i> SJU9	MN511766	99%	99.57%
		<i>Micrococcus</i> sp. NJS11	MN833053	99%	99.64%
		<i>Micrococcus yunnanensis</i> 190306H2421	MT225720	99%	99.50%
	KT1.2	<i>Staphylococcus haemolyticus</i> B-16	KC139451	99%	99.57%
		<i>Staphylococcus haemolyticus</i> N15	KX507089	99%	99.57%
		<i>Staphylococcus</i> sp. CLC-F26	MH518208	100%	99.50%
	KT1.3	<i>Micrococcus</i> sp. 185	EU714334	98%	99.71%
		<i>Micrococcus luteus</i> 10240	CP041689	99%	99.71%
		<i>Micrococcus luteus</i> NCCP 16831	CP043842	99%	99.71%
	KT1.4	<i>Acinetobacter lwoffii</i> O27	MG594818	99%	99.57%
		<i>Acinetobacter</i> sp. NMS3	MN515076	99%	99.57%
		<i>Acinetobacter lwoffii</i> WST 5	DQ289068	99%	99.57%
	KT1.5	<i>Bacillus anthracis</i> 7-6	JX867748	99%	99.93%
		<i>Bacillus</i> sp. SRG13	MK743992	99%	99.93%
		<i>Bacillus albus</i> XM4	MT023381	99%	99.93%
	KT1.6	<i>Arthrobacter agilis</i> AU D4.2	KY775493	100%	97.94%
		<i>Arthrobacter</i> sp. ITT16	FR667186	100%	97.94%
		<i>Arthrobacter agilis</i> UMCV2	CP024915	100%	97.80%
Second Instar	KT2.1	<i>Staphylococcus capitis</i> IAE36	MK414980	100%	99.19%
		<i>Staphylococcus capitis</i> BQEN3-03	FJ380955	100%	99.19%
		<i>Staphylococcus capitis</i> BBN3T-04d	FJ357614	100%	99.19%
	KT2.2	<i>Staphylococcus</i> sp. PaD1.45b1	GQ406605	99%	99.79%
		<i>Staphylococcus</i> sp. PaH2.43b	GQ391961	99%	99.79%
		<i>Staphylococcus epidermidis</i> BBEN-01d	FJ357583	99%	99.79%
	KT2.3	<i>Staphylococcus capitis</i> BBN3T-04d	FJ357614	99%	99.86%
		<i>Staphylococcus capitis</i> BBN3P-01d	FJ357608	99%	99.79%
		<i>Staphylococcus epidermidis</i> BQNIN-02d	FJ380964	99%	99.79%
	KT2.4	<i>Bacillus simplex</i> EH12	MN750767	99%	100%
		<i>Bacillus thuringiensis</i> EGI94	MN704417	99%	100%
		<i>Bacillus simplex</i> EGI87	MN704413	99%	100%
	KT2.5	<i>Micrococcus</i> sp. N36(2010)	HQ188562	99%	98.12%
		<i>Micrococcus yunnanensis</i> KA-20	KX108873	99%	98.12%
		<i>Micrococcus</i> sp. Actino-13	MH671510	99%	98.05%
KT2.6	<i>Clavibacter</i> sp. PDD-59b-50	KR922173	99%	98.77%	
	<i>Clavibacter michiganensis</i> PDD-57b-26	KR922121	100%	98.70%	
	<i>Clavibacter michiganensis</i> Cmm VT3	HQ144242	100%	98.70%	
Third Instar	KT3.1	<i>Staphylococcus hominis</i> CU1-6	MT373476	99%	98.75%
		<i>Staphylococcus hominis</i> K23	KU922442	99%	98.75%
		<i>Staphylococcus hominis</i> H45	KU922315	99%	98.75%
	KT3.2	Uncultured <i>Staphylococcus</i> sp. clone TJ-3	JQ858218	99%	99.93%
		<i>Staphylococcus haemolyticus</i> SR4-27	MN421506	99%	99.86%

		<i>Staphylococcus haemolyticus</i> M2	KC182061	99%	99.86%
Fourth Instar	KT4.1	<i>Moraxella</i> sp. CRE4	MT380814	100%	99.64%
		<i>Moraxella osloensis</i> NT4	MK571189	100%	99.64%
		<i>Moraxella osloensis</i> NT4	MK571171	100%	99.64%
	KT4.2	<i>Micrococcus yunnanensis</i> SJU9	MN511766	99%	99.86%
		<i>Micrococcus yunnanensis</i> L7-617	JQ659453	99%	99.86%
		<i>Micrococcus</i> sp. T7	MN049740	99%	99.86%
	KT4.3	<i>Kocuria rosea</i> RR75	MK532258	100%	98.22%
		<i>Kocuria rosea</i> PGRS5	MH489032	100%	98.22%
		<i>Kocuria</i> sp. H200-662	MG754440	100%	98.22%
Fifth Instar	KT5.1	<i>Micrococcus</i> sp. DMO-7	MT294696	100%	99.49%
		<i>Micrococcus luteus</i> 1910ICU142	MT225650	100%	99.49%
		<i>Micrococcus yunnanensis</i> QT410	MT033093	100%	99.49%
	KT5.2	Uncultured <i>Staphylococcus</i> sp. TJ-3	JQ858218	100%	99.72%
		<i>Staphylococcus haemolyticus</i> SR4-27	MN421506	100%	99.65%
		<i>Staphylococcus haemolyticus</i> BQNIL-01d	FJ380961	100%	99.65%
	KT5.3	<i>Bacillus aerius</i> CJLT	JN852814	99%	99.29%
		<i>Bacillus licheniformis</i> YC1-A	HQ634208	99%	99.29%
		<i>Bacillus licheniformis</i> SIITMB5	MG892780	99%	99.22%
	KT5.4	<i>Staphylococcus</i> sp. PGT-LC	KY490691	100%	99.79%
		<i>Staphylococcus hominis</i> OsEnb_ALM_C9	MN889343	99%	99.79%
		<i>Staphylococcus</i> sp. CIFRI PTSB-29	JF784037	100%	99.72%
	KT5.5	<i>Staphylococcus</i> sp. ST5-08	KF891400	100%	99.79%
		<i>Staphylococcus hominis</i> OsEnb_ALM_C9	MN889343	99%	99.79%
		<i>Bacterium</i> MTL7-24	MH151280	99%	100%

According to the BLAST search and phylogenetic analysis, the bacterial isolates were identified as *Micrococcus yunnanensis* KT1.1, *Staphylococcus haemolyticus* KT1.2, *Micrococcus luteus* KT1.3, *Acinetobacter lwoffii* KT1.4, *Bacillus* sp. KT1.5, *Arthrobacter agilis* KT1.6, *Staphylococcus capitis* KT2.1, *Staphylococcus* sp. KT2.2, *Staphylococcus capitis* KT2.3, *Bacillus* sp. KT2.4, *Micrococcus* sp. KT2.5, *Clavibacter michiganensis* KT2.6, *Staphylococcus hominis* KT3.1, *Staphylococcus hemolyticus* KT3.2, *Moraxella osloensis* KT4.1, *Micrococcus yunnanensis* KT4.2, *Kocuria rosea* KT4.3, *Micrococcus* sp. KT5.1, *Staphylococcus haemolyticus* KT5.2, *Bacillus* sp. KT5.3, *Staphylococcus* sp. KT5.4 and *Staphylococcus* sp. KT5.5 (Figure 2).

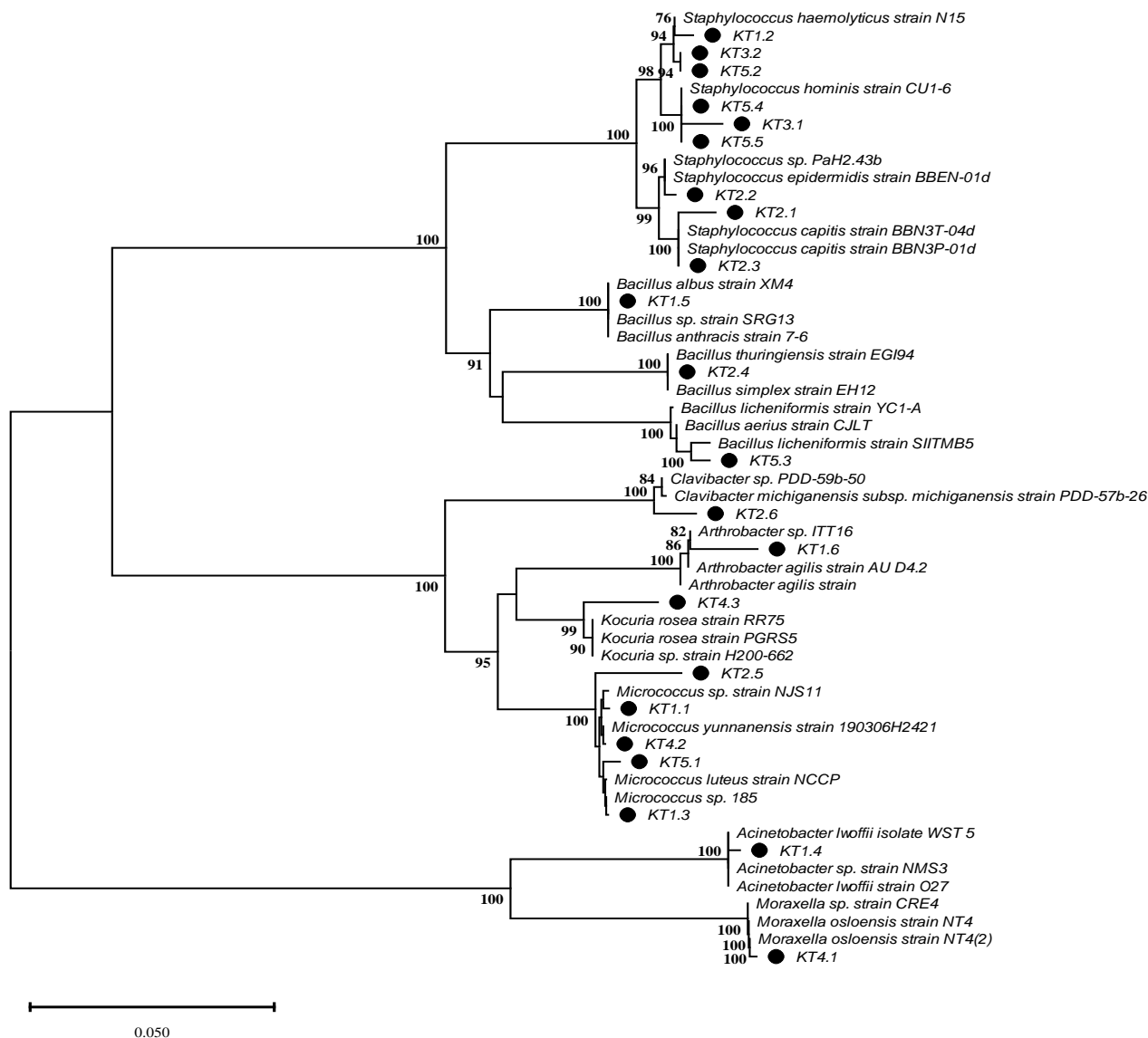


Figure 2. The dendrogram generated using Neighbor Joining (N-J) algorithm with p-distance analysis.

The tree was generated using the partial sequence (approximately 1.500 bp) of 16S rRNA gene. The bacterial isolates used in this study which are marked with solid black dot were compared with the reference species or strains taken from GenBank based on their percent identities with the bacterial isolates. The statistical accuracy of the tree was evaluated by bootstrap confidence analysis according to 1.000 repetitions and bootstrap values of 70% or higher were specified in the tree. The scale located under the tree shows the degree of dissimilarity.

Insects are the most crowded animal group in Arthropoda phylum in terms of class, taxon and species number and they have the biggest number of species in the world. Their evolutionary success partly depends on their interaction with many prokaryotic and eukaryotic microorganisms (Scudder, 2009). These microorganisms which live inside insects are responsible for many important features in insect's life cycle such as enzymatic degradation of nutrients, synthesis of essential metabolites like vitamins, protection of the hosts against biotic and abiotic factors and regulation of development and reproduction of insects (Douglas, 2014). For Lepidopteran insects, there are some evidence that instar-specific bacterial communities should be available for some insects (Chen et al., 2016). Moreover, insect symbiotic bacteria are good candidate for manipulating them using genetic engineering techniques to protect beneficial insects against their enemies and to combat with harmful insects (pests). Based on all this, it is important to study and identify bacterial species that live in insects.

In this study, we found that the gut bacteria (or microbiome) of *S. irrosea* showed great variability consisting of different members of Bacillaceae, Staphylococcaceae, Micrococcaceae, Moraxellaceae and Microbacteriaceae families. Many of the isolated bacteria in this study such as *Staphylococcus*, *Micrococcus*, *Bacillus*, *Acinetobacter* and *Arthrobacter* have been isolated from many insects including Lepidopteran pests (Sevim et al., 2012; Minard et al., 2013). Within these bacteria, *Bacillus* species (*Bacillus* sp. KT1.5, KT2.4 and KT5.3) draw an attention since bacterium *B. thuringiensis* (Bt) is located in this genus and widely used as biological insecticides against many pest's species worldwide (de Maagd, Bravo & Crickmore, 2001). However, it is very hard to distinguish this species from other *Bacillus* members based on 16S rRNA sequence analysis. Therefore, it should be interesting to identify these isolates at species level, to search crystal proteins (if there is) and to test them against a numbers of insect pests to determine their biocontrol potential.

We isolated two interesting bacteria (*Moraxella osloensis* KT4.1 and *Kocuria rosea* KT4.3) regarding insect-bacterium relation. Both species were isolated from fourth instar larvae. *M. osloensis* is known as a bacterial symbiont of *Phasmarhabditis hermaphrodita* which is a slug-parasitic nematode, and this bacterium is transported to the shell cavity of the slug via the nematode and kills the host (Crawford, Hutton & Chapman, 1975). The members of *Kocuria* genus includes gram-positive bacteria that normally inhabit skin and mucous membrane of human and many animals. But there are some evidences that these bacteria might be related to human infections with weakened immune systems (Kandi et al., 2016). In terms of insect-bacteria associations, these two bacteria seem to be novel for further investigations. Especially, due to pathogenic properties of these bacteria, it should be interesting to study a potential transmission of these bacteria to other animals or humans.

In this study, we also isolated a *Clavibacter michiganensis* subsp. *michiganensis* KT2.6 which is a plant pathogenic bacterium causing a bacterial wilt and canker in tomatoes (Gartemann et al., 2003). It has been known that some bacterial pathogens colonizing and living in the vascular systems of plants (phloem or xylem) can be transmitted by several insects such as whiteflies, aphids, and leafhoppers (Perilla-Henao & Casteel, 2016). That means some insects can serve a vector of important plant pathogenic bacteria. Therefore, studying vector-pathogen-host (etc. insects) is a crucial issue to understand the epidemiology of plant diseases. There are some evidences that some plant pathogenic subspecies of *Clavibacter michiganensis* can be transmitted from plant to plant via insect vectors such as Colorado potato beetles and the green peach aphid (Christie, Sumalde, Schulz & Gudmestad, 1991). In addition, nematodes *Dylenchus dipsaci* can serve a vector of *C. michiganensis* causing bacterial wilt in alfalfa (Hawn, 1971). Therefore, it should be interesting to study a vector potential of *S. irrosea* with respect to *C. michiganensis*, at least for non-agricultural plants.

We isolated different bacterial species from different development stages (instars) of *S. irrosea*. Based on our results, we did not determine a clear pattern regarding changes in gut microbiota diversity for different instars. In the literature, it has been demonstrated that although development stages do not affect the bacterial community in some insect species, bacterial diversity or communities can change in other insects such as *Spodoptera littoralis* (Boisduval, 1833) according to the developmental stages (Chen et al., 2016; Mereghetti, Chouaia & Mantagna, 2017). Based on these, it can be said that there is no general rule regarding bacterial diversity or composition could be changed according to the developmental stages of insects.

#### 4. Conclusion

We determined a bacterial diversity in different developmental stages (instars) of *S. irrosea* using the culture-dependent technique and showed that there is no specific pattern with respect to the bacterial diversity in different instars.

#### Author Contributions

Ali Sevim: Conception/design of study, data acquisition, data analysis and interpretation, drafting manuscript, critical revision of manuscript.

Elif Sevim: Data acquisition, data analysis and interpretation.

#### Conflicts of Interest

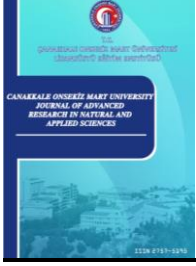
The authors declare no conflict of interest.



## References

- Altschul, S. F., Gish, W., Miller, W., Myers, E. W., & Lipman, D. J. (1990). Basic local alignment search tool. *J Mol Biol*, 215(3), 403-10. doi: [https://doi.org/10.1016/S0022-2836\(05\)80360-2](https://doi.org/10.1016/S0022-2836(05)80360-2)
- Anand, A. A., Vennison, S. J., Sankar, S. G., Prabhu, D. I., Vasani, P. T., Raghuraman, T., Geoffrey, C. J., & Vendan, S. E. (2010). Isolation and characterization of bacteria from the gut of *Bombyx mori* that degrade cellulose, xylan, pectin and starch and their impact on digestion. *Journal of Insect Sci*, 10, 107. doi: <https://doi.org/10.1673/031.010.10701>
- Basset, Y., Cizek, L., Cuenoud, P., Didham, R. K., Guilhaumon, F., Missa, O., Novotny, V., Odegaard, F., Roslin, T., & Leponce, M. (2012). Arthropod diversity in a tropical forest. *Science*, 338(6113), 1481-1484. doi: [10.1126/science.1226727](https://doi.org/10.1126/science.1226727)
- Ben-Dov, E. (2014). *Bacillus thuringiensis* subsp. *israelensis* and its dipteran-specific toxins. *Toxins (Basel)*, 6(4), 1222-1243. doi: <https://doi.org/10.3390/toxins6041222>
- Benson, D. A., Karsch-Mizrachi, I., Clark, K., Lipman, D. J., Ostell, J., & Sayers, E. W. (2012). GenBank. *Nucleic Acids Res*, 40(Database issue), D48-53. DOI: <https://doi.org/10.1093/nar/28.1.15>
- Campbell, A. M., Lawrence, A. J., Hudspath, C. B., & Gruwell, M. E. (2014). Molecular Identification of Diaspididae and Elucidation of Non-Native Species Using the Genes 28s and 16s. *Insects*, 5(3), 528-538. doi: <https://doi.org/10.3390/insects5030528>
- Chen, B., The, B. S., Sun, C., Hu, S., Lu, X., Boland, W., & Shao, Y. (2016). Biodiversity and Activity of the Gut Microbiota across the Life History of the Insect Herbivore *Spodoptera littoralis*. *Sci Rep*, 6, 29505. doi: <https://doi.org/10.1038/srep29505>
- Christie, R. D., Sumalde, A. C., Schulz, J. T., & Gudmestad, N. C. (1991). Insect transmission of the bacterial ring rot pathogen. *Am Potato J*, 68(6), 363-372. doi: <https://doi.org/10.1007/BF02853617>
- Crawford, R. L., Hutton, S. W., & Chapman, P. J. (1975). Purification and properties of gentisate 1,2-dioxygenase from *Moraxella osloensis*. *J Bacteriol*, 121(3), 794-9. doi: <https://doi.org/10.1128/jb.121.3.794-799.1975>
- de Maagd, R. A., Bravo, A., & Crickmore, N. (2001). How *Bacillus thuringiensis* has evolved specific toxins to colonize the insect world. *Trends Gen*, 17(4), 193-199. doi: [https://doi.org/10.1016/S0168-9525\(01\)02237-5](https://doi.org/10.1016/S0168-9525(01)02237-5)
- Douglas, A. E. (2014). The molecular basis of bacterial-insect symbiosis. *J Mol Biol*, 426(23), 3830-3837. doi: <https://doi.org/10.1016/j.jmb.2014.04.005>
- Douglas, A. E. (2015). Multiorganismal insects: diversity and function of resident microorganisms. *Ann Rev Entomol*, 60, 17-34. doi: <https://doi.org/10.1146/annurev-ento-010814-020822>
- Engel, P., & Moran, N. A. (2013). The gut microbiota of insects - diversity in structure and function. *FEMS Microbiol Rev*, 37(5), 699-735. doi: <https://doi.org/10.1111/1574-6976.12025>
- Folmer, O., Black, M., Hoeh, W., Lutz, R., & Vrijenhoek, R. (1994). DNA primers for amplification of mitochondrial cytochrome c oxidase subunit I from diverse metazoan invertebrates. *Mol Mar Biol Biotechnol*, 3(5), 294-9.
- Gartemann, K. H., Kirchner, O., Engemann, J., Gräfen, I., Eichenlaub, R., & Burger, A. (2003). *Clavibacter michiganensis* subsp. *michiganensis*: First steps in the understanding of virulence of a Gram-positive phytopathogenic bacterium. *J Biotechnol*, 106(2), 179-191. doi: <https://doi.org/10.1016/j.jbiotec.2003.07.011>
- Hall, T. A. (1999). BioEdit: A user-friendly biological sequence alignment editor and analysis program for Windows 95/98/NT. *Nucleic Acids Symp Ser*, 41, 95-98.
- Hawn, E. J. (1971). Mode of Transmission of *Corynebacterium insidiosum* by *Ditylenchus dipsaci*. *J Nematol*, 3(4), 420-1.
- Janda, J. M., & Abbott, S. L. (2007). 16S rRNA gene sequencing for bacterial identification in the diagnostic laboratory: pluses, perils, and pitfalls. *J Clin Microbiol*, 45(9), 2761-4. doi: <https://doi.org/10.1128/JCM.01228-07>
- Kandi, V., Palange, P., Vaish, R., Bhatti, A. B., Kale, V., Kandi, M. R., & Bhoomagiri, M. R. (2016). Emerging Bacterial Infection: Identification and Clinical Significance of *Kocuria* Species. *Cureus*, 8(8), e731. doi: <https://doi.org/10.7759/cureus.731>
- Kumar, S., Stecher, G., Li, M., Niyaz, C., & Tamura, K. (2018). MEGA X: Molecular Evolutionary Genetics Analysis across Computing Platforms. *Mol Biol Evol*, 35(6), 1547-1549. doi: [10.1093/molbev/msy096](https://doi.org/10.1093/molbev/msy096)

- Lacey, L. A., Grzywacz, D., Shapiro-Ilan, D. I., Frutos, R., Brownbridge, M., & Goettel, M. S. (2015). Insect pathogens as biological control agents: Back to the future. *J Invertebr Pathol*, *132*, 1-41. doi: <https://doi.org/10.1016/j.jip.2015.07.009>
- Liu, W., Li, Y., Guo, S., Yin, H., Lei, C. L., & Wang, X. P. (2016). Association between gut microbiota and diapause preparation in the cabbage beetle: a new perspective for studying insect diapause. *Sci Rep*, *6*, 38900-38900. doi: <https://doi.org/10.1038/srep38900>
- Madigan, M. T., Martinko, J. M., Parker, J., & Brock, T. D. B. (2003). *Brock Biology of Microorganisms*. New York, NY: Prentice Hall.
- Mereghetti, V., Chouaia, B., & Montagna, M. (2017). New Insights into the Microbiota of Moth Pests. *Int J Mol Sci*, *18(11)*, 2450. Doi: <https://doi.org/10.3390/ijms18112450>
- Minard, G., Tran, F. H., Raharimalala, F. N., Hellard, E., Ravelonandro, P., Mavingui, P., & Moro, C. V. (2013). Prevalence, genomic and metabolic profiles of *Acinetobacter* and *Asaia* associated with field-caught *Aedes albopictus* from Madagascar. *FEMS Microbiol Ecol*, *83(1)*, 63-73. doi: <https://doi.org/10.1111/j.1574-6941.2012.01455.x>
- Moore, S. J., & Warren, M. J. (2012). The anaerobic biosynthesis of vitamin B12. *Biochem Soc Trans*, *40(3)*, 581-6. doi: <https://doi.org/10.1042/BST20120066>
- Mutanen, M., Wahlberg, N., & Kaila, L. (2010). Comprehensive gene and taxon coverage elucidates radiation patterns in moths and butterflies. *Proc Roy Soc B*, *277(1695)*, 2839-2848. doi: <https://doi.org/10.1098/rspb.2010.0392>
- Novotny, V., Basset, Y., Miller, S. E., Weiblen, G. D., Bremer, B., Cizek, L., & Drozd, P. (2002). Low host specificity of herbivorous insects in a tropical forest. *Nature*, *416(6883)*, 841-844. doi: <https://doi.org/10.1038/416841a>
- Perilla-Henao, L. M., & Casteel, C. L. (2016). Vector-Borne Bacterial Plant Pathogens: Interactions with Hemipteran Insects and Plants. *Front Plant Sci*, *7*, 1163-1163. doi: <https://doi.org/10.3389/fpls.2016.01163>
- Peterkova-Koci, K., Robles-Murguía, M., Ramalho-Ortigao, M., & Zurek, L. (2012). Significance of bacteria in oviposition and larval development of the sand fly *Lutzomyia longipalpis*. *Parasites Vectors*, *5*, 145. Doi: <https://doi.org/10.1186/1756-3305-5-145>
- Ruiu, L. (2015). Insect Pathogenic Bacteria in Integrated Pest Management. *Insects*, *6(2)*, 352-67. doi: <https://doi.org/10.3390/insects6020352>
- Scudder, G. G. E. (2009). The importance of insects. Footitt R G, Adler PH, editors. *Insect Biodiversity* (pp. 7-32). Oxford: Blackwell Publishing Ltd.
- Sevim, E., Çelebi, Ö., & Sevim, A. (2012). Determination of the bacterial flora as a microbial control agent of *Toxoptera aurantii* (Homoptera: Aphididae). *Biologia*, *67(2)*, 397-404. doi: <https://doi.org/10.2478/s11756-012-0022-0>
- Souza, R. S., Virginio, F., Riback, T. I. S., Suesdek, L., Barufi, J. B., & Genta, F. A. (2019). Microorganism-Based Larval Diets Affect Mosquito Development, Size and Nutritional Reserves in the Yellow Fever Mosquito *Aedes aegypti* (Diptera: Culicidae). *Front Physiol*, *10*, 152. doi: <https://doi.org/10.3389/fphys.2019.00152>



## Üretim Sektöründe Sürdürülebilirlik için Sosyal Yaşam Döngüsü Değerlendirmesi: Çimento Üretimi Örneği

Büşra Cici<sup>1</sup>, Beyhan Pekey<sup>2</sup>, Simge Çankaya<sup>3\*</sup>

<sup>1</sup>Fen Bilimleri Enstitüsü, İş Sağlığı ve Güvenliği A.B.D, Kocaeli Üniversitesi, Kocaeli, Türkiye

<sup>2,3</sup>Çevre Mühendisliği Bölümü, Mühendislik Fakültesi, Kocaeli Üniversitesi, Kocaeli, Türkiye

### Makale Tarihiçesi

Gönderim: 30.03.2022

Kabul: 04.07.2022

Yayın: 15.12.2022

### Araştırma Makalesi

**Öz** – Günümüzde çimento üretimi, kullanımı ve bertarafı sırasında sosyal konuların değerlendirilmesi, şirketlerin sürdürülebilir kalkınmaya yönelik sosyal sorumlulukları açısından giderek daha önemli hale gelmektedir. Sosyal Yaşam Döngüsü Değerlendirmesi (S-LCA), bir ürünün veya hizmetin yaşam döngüsündeki faaliyetlerin çeşitli paydaşlar üzerindeki olası sosyal etkilerini belirleyerek, şirketlerin sosyal olarak sorumlu bir şekilde çalışmalarını kolaylaştırmayı sağlayan bir tekniktir. Bu çalışmada çimento üretimi gerçekleştirilen bir işletmede sosyal yaşam döngüsü, Birleşmiş Milletler Çevre Programı/Çevresel Toksikoloji ve Kimya Derneği (UNEP/SETAC) tarafından önerilen paydaş kategorileri dikkate alınarak çalışan paydaşı açısından incelenmiştir. Çalışan paydaşının alt kategorileri iş sağlığı ve güvenliği (İSG), fırsat eşitliği/ayrıcılık, adil maaş, çocuk işçi, sosyal yardım/sosyal güvenlik, çalışma saatleri, zorla çalıştırma, sendikalaşma ve toplu pazarlık özgürlüğüdür. Çimento üretim süreçlerinde mavi ve beyaz yaka çalışanların sosyal ve sosyo-ekonomik yönlerinin ve bunların sosyal yaşam döngüsünü kapsayan olumlu ve olumsuz etkileri karşılaştırmalı olarak değerlendirilmiştir. Envanter analizi aşamasında, çalışanlarla gerçekleştirilen anketler aracılığı ile sahaya özgü veriler toplanmıştır. Belirlenen alt kategorilerin etki değerlendirilmesinde, 0 ile 4 arasında puanlama yöntemi kullanılmıştır. Çalışma sonucunda mavi yaka çalışanlar açısından en olumsuz sosyal etkiye sahip alt kategoriler 2 puan ile sosyal yardım/sosyal güvenlik ve sendikalaşma ile toplu pazarlık özgürlüğü olmuştur. Beyaz yaka çalışanlar açısından sosyal etkiler ise olumlu sonuçlanmış ve tüm alt kategoriler 4'er puan olarak hesaplanmıştır.

**Anahtar Kelimeler** – Beyaz Yaka, çalışan paydaşı, çimento, mavi yaka, sosyal yaşam döngüsü değerlendirilmesi.

## Social Life Cycle Assessment for Sustainability in Production Sector: A Cement Production Case Study

<sup>1</sup>Institute of Natural and Applied Science, Kocaeli University, Kocaeli, Türkiye

<sup>2,3</sup>Department of Environmental Engineering, Faculty of Engineering, Kocaeli University, Kocaeli, Türkiye

### Article History

Received: 30.03.2022

Accepted: 04.07.2022

Published: 15.12.2022

### Research Article

**Abstract** – Nowadays, the analysis of social issues during the production, use and disposal of cement becomes important for companies in terms of their social responsibilities for sustainable development. Social life cycle assessment (S-LCA) is a method that facilitates companies to work in a socially responsible manner, by providing information about the social impact of products or services, activities in the life cycle, worker, society, consumers, local community, value chain actors on their stakeholders. In this study, the S-LCA of an enterprise whose main activity is cement production has been examined in terms of worker stakeholder among the stakeholder categories proposed by UNEP/SETAC. Social and socio-economic aspects of blue- and white-collar employees working in cement production stages and their positive and negative impacts covering the S-LCA were evaluated comparatively. In inventory analysis, site-specific data were collected through questionnaires conducted with employees, and a scoring method between 0- 4 was used in the impact assessment of the determined subcategories. As a result of the study, the subcategories which have the most negative social impact were social assistance/social security and freedom of association and collective bargaining (2 score) for blue-collar employees. Considering white collar employees, social impacts were positive, and all subcategories were calculated as 4 score.

**Keywords** – White collar, worker stakeholder, cement, blue collar, social life cycle assessment.

<sup>1</sup> busracici94@gmail.com

<sup>2</sup> bpekey@kocaeli.edu.tr

<sup>3</sup> simge.taner@kocaeli.edu.tr

\*Sorumlu Yazar

## 1. Giriş

Sürdürülebilir kalkınma tartışması çevresel, sosyal ve ekonomik etkileri değerlendirme yöntemleri konusunda girişimleri teşvik etmiştir. Bu gelişme ile son yıllarda ürün ve sistemlerin çevresel yaşam döngüsü değerlendirmesine, sosyal yönlerin dâhil edilmesine yönelik artan bir ilgi olmuştur (Hunkeler, 2006). Ürünlerin üretimi, kullanımı ve bertarafı sırasında sosyal konuların değerlendirilmesi, şirketlerin sürdürülebilir kalkınmaya yönelik sosyal sorumlulukları açısından giderek daha önemli hale gelmektedir (Karlewski ve diğ. 2019).

Sağladığı iş gücü ve yarattığı katma değerle ülke ekonomimize doğrudan katkı sağlayan ve sanayinin önemli yapı taşları arasında yer alan çimento üreticisi firmalar, sürdürülebilirlik stratejileri ve politikaları belirlemiş ve çeşitli sürdürülebilirlik projeleri geliştirmeye başlamıştır (Uysal, 2019). Ülkemizdeki entegre çimento tesislerinin birçoğunda her yıl yayınlanan entegre faaliyet raporlarında sürdürülebilirlik performans alt başlığında kuruluşun sosyal performansları değerlendirilmektedir.

Sosyal yaşam döngüsü değerlendirmesi (S-LCA), bir ürünün veya hizmetin tüm yaşam döngüsü boyunca sosyal ve sosyo-ekonomik etkilerinin değerlendirildiği bir tekniktir (UNEP/SETAC, 2009). Bu sosyal etki değerlendirme tekniği ile hammaddenin temininden, ürün/hizmetin üretimi, kullanım ömrü sonunda işlenmesi, geri dönüşümü ve nihai bertarafına (beşikten mezara) kadar ürünün/hizmetin tüm yaşam döngüsünü kapsayan olası olumlu ve olumsuz sosyal etkilerinin değerlendirilmesi amaçlanmaktadır. Literatürde çimento üretim sektörü ile benzer özellikler gösteren beton üretimi sektöründe uygulanmış S-LCA ile ilgili çalışmalar bulunmakla birlikte (Hosseiniyou ve diğ. 2014; Navarro ve diğ. 2018; Roh ve diğ. 2018); bilginiz dahilinde, çimento üretim sektöründe olası sosyal etkilerin değerlendirildiği bir S-LCA çalışması bulunmamaktadır.

Bu çalışmada, ülkemizde ana faaliyeti çimento üretimi olan bir işletmede UNEP/SETAC (2009) tarafından yayınlanan kılavuz temel alınarak sosyal yaşam döngüsü değerlendirmesi gerçekleştirilmiştir. Çalışma kapsamında UNEP/SETAC (2009) tarafından önerilen paydaş kategorileri içinden çalışan paydaşı seçilmiş; beyaz ve mavi yaka çalışanların sosyal yaşam döngüsü değerlendirmesi karşılaştırmalı olarak incelenmiştir. Söz konusu çalışmada, çimentonun yaşam döngüsündeki çalışanlarını etkileyen faaliyetlerine odaklanılmıştır. Gerçekleştirilen bu S-LCA çalışmasının sonuçları, seçilen çimento tesisinin entegre faaliyet raporunda yayınlanmıştır.

## 2. Materyal ve Yöntem

Bu çalışmada, çimento sektörüne uygulanan sosyal yaşam döngüsü değerlendirmesi dört aşamadan oluşmaktadır: (1) Amaç ve kapsam tanımlanması, (2) envanter analizi, (3) etki değerlendirme, (4) yorumlama aşamalarıdır (UNEP/SETAC, 2009).

### 2.1. Amaç ve Kapsam Tanımlanması

Sosyal yaşam döngüsü değerlendirmesinin ilk aşamasında, çalışmanın amaç ve kapsamı açıkça tanımlanmaktadır. Bu S-LCA çalışmasının amacı, çimento üretim sektöründeki mavi yaka ve beyaz yaka çalışanların sosyal ve sosyo-ekonomik yönlerinin ve bunların yaşam döngüsünü kapsayan olası olumlu ve olumsuz etkilerinin değerlendirilmesidir. Mevcut çalışma ile seçilen entegre çimento üretim tesisinde çalışan mavi ve beyaz yakanın sosyal ve sosyo-ekonomik açıdan olumlu ve olumsuz etkilerinin ortaya konması ve olumsuz etkilerinin iyileştirilmesinin sağlanması hedeflenmektedir. Bu sayede işletmenin sosyal performansı da olumlu yönde artacaktır.

Çalışmanın kapsamı, hammadde temini ve hazırlanması, farin üretimi, klinker üretimi, çimento üretimi, çimento öğütülmesi ve üretilen çimentonun nakliyesi süreçlerinde çalışanların olası sosyal koşullarının değerlendirilmesini kapsayan “beşikten kapıya” olarak belirlenmiştir. Şekil 1’de çalışmanın sistem sınırları sunulmaktadır.

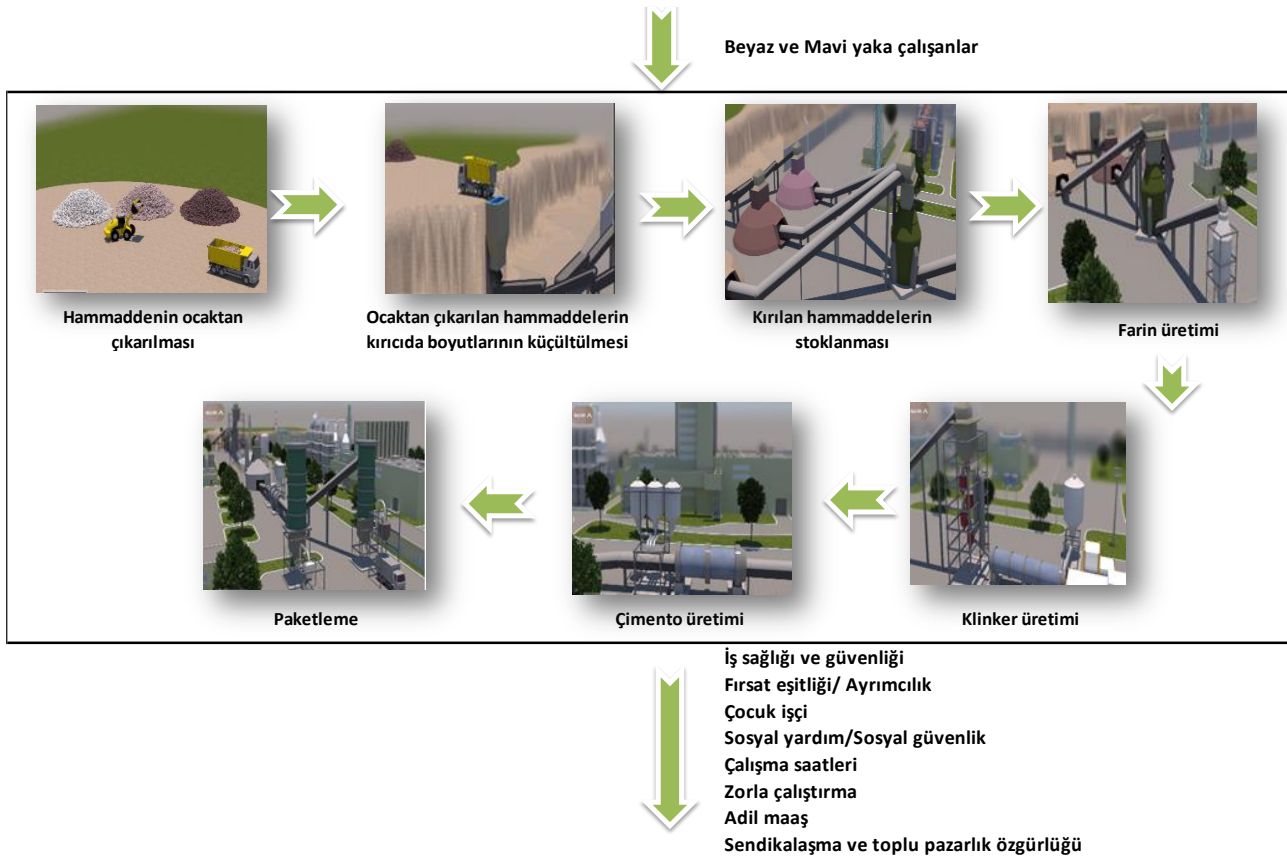
Çalışma kapsamında UNEP/SETAC tarafından yayınlanan kılavuzdaki paydaş kategorilerinden iş sağlığı ve güvenliği konularını da içeren alt kategorilerden oluşan (çocuk işçilik, adil maaş, çalışma saatleri, zorla çalıştırma, fırsat eşitliği/ayrımcılık, iş sağlığı ve güvenliği, sosyal güvenlik/sosyal yardım, sendikalaşma ve toplu

pazarlık özgürlüğü) çalışan paydaş kategorisi seçilmiştir. Çalışan paydaş kategorisinin etki kategorisi olan insan hakları ve çalışma koşulları değerlendirilmiştir.

Sosyal yaşam döngüsü değerlendirmesi çalışmalarında nitel ve yarı nitel göstergeler kullanılması halinde etki sonuçlarının fonksiyonel birim ile ilişkilendirilmesi zor olduğundan, S-LCA çalışmalarında fonksiyonel birim kullanımı ilk geliştirildiği yıllardan itibaren tartışılan bir konudur (Jørgensen ve diğ. 2008, Yıldız-Geyhan ve diğ. 2017; Hossain ve diğ. 2018, Haryati ve diğ. 2022). Bu çalışmada yarı nitel yaklaşım kullanıldığından, çalışma kapsamında incelenen beyaz ve mavi yaka çalışanların sosyal yaşam döngüsü değerlendirmesi fonksiyonel birim ile ilişkilendirilmeden gerçekleştirilmiştir.

## 2.2. Yaşam Döngüsü Envanter Analizi

Bu aşamada, çimento kuruluşunda çalışanlar ile ilgili sosyal konuları içeren daha önceden belirlenen sekiz alt kategorinin sahaya özgü verileri, kurumdaki mavi ve beyaz yaka çalışanlara özel olarak geliştirilen anketler aracılığı ile toplanmıştır. Anket soruları UNEP/SETAC tarafından yayınlanan “S-LCA’nın Alt Kategorileri için Metodolojik Tablolar” rehberi ve literatürde gerçekleştirilen çalışmalardan yararlanılarak oluşturulmuştur.



Şekil 1. Çalışmanın sistem sınırları

Literatürde yapılan çalışmalarda anket soruları açık uçlu veya evet/hayır tipi soruları içermektedir (Petti ve diğ. 2018; Sining ve diğ. 2022). Çalışanların evet/hayır tipi sorulara verdikleri yanıtların açık uçlu sorulara verdikleri yanıtlara göre daha kolay değerlendirilmesi nedeniyle, bu çalışmada anket sorularında evet/hayır tipi sorular tercih edilmiştir. Çalışanların sorulan soru hakkında fikrinin olmaması da göz önünde bulundurularak ankette yanıt kısmına fikrim yok seçeneği eklenmiştir. Ayrıca anket soruları oluşturulurken yoruma dayalı sorular yerine uluslararası sözleşmeler ve anlaşmalar ile karşılaştırma yapılabilecek sorular tercih edilmiştir. Çalışmada kullanılan anketler için Kocaeli Üniversitesi Fen ve Mühendislik Bilimleri Etik Kurulundan onay alınmıştır.

Anketler, çalışanlarla yüz yüze görüşmeler yapılarak uygulanmıştır. Beyaz yaka ve mavi yaka çalışanlar için özel anket soruları oluşturulmuştur. Tablo 1’de çalışmada uygulanan anket sorularının alt kategori dağılımı yer almaktadır.

Gerçekleştirilen anket çalışmasında mavi yaka çalışanlara toplam otuz yedi, beyaz yaka çalışanlara ise yirmi yedi soru sorulmuştur. Çalışma kapsamında uygulanan anket soruları beyaz yaka çalışanlar için yedi alt kategoriye, mavi yaka çalışanlar için ise sekiz alt kategoriye içermektedir. Beyaz yaka çalışanlar sendikaya üye olmadıkları için sendikalaşma ve toplu pazarlık özgürlüğü alt kategorisi anket sorularına dâhil edilmemiştir. Seçilen çimento üretim tesisinde toplam 674 çalışan bulunmaktadır; bunların 193'ü beyaz yaka, 481'i ise mavi yakadan oluşmaktadır. Çalışma kapsamında 120 beyaz yaka, 180 mavi yaka olmak üzere toplam 300 çalışana anket uygulanmıştır.

Tablo 1

Çalışmada seçilen anket soru sayıları dağılımı

Alt kategoriler	Beyaz Yaka	Mavi Yaka
İş sağlığı ve güvenliği	5	5
Fırsat eşitliği/ayrımcılık	5	5
Çocuk işçilik	1	1
Sosyal yardım/Sosyal güvenlik	5	4
Çalışma saatleri	4	5
Zorla çalıştırma	3	3
Adil maaş	4	5
Sendikalaşma ve toplu pazarlık özgürlüğü	-	9
Toplam	27	37

### 2.3. Yaşam Döngüsü Etki Değerlendirme

Literatürde S-LCA çalışmalarında uluslararası kabul gören herhangi bir etki değerlendirme yöntemine rastlanmamıştır. Dolayısıyla bu çalışmada, envanter sonuçlarını değerlendirmek için Foolmaun ve Ramjeeawon (2013) tarafından önerilen yöntem kullanılmıştır. UNEP/SETAC S-LCA kılavuzuna uygun olarak önerilen bu yöntem üç adımdan oluşmaktadır. İlk adımda, tüm gösterge sonuçları yüzdelere dönüştürülmüştür. Bu dönüşüm için Denklem (2.1) ve (2.2) kullanılmıştır:

$$\text{Evet yüzdesel dağılım (\%)} = \frac{\text{Ankete katılan çalışanların evet yanıtı veren sayısı}}{\text{Ankete katılan sayısı-Fikrim yok yanıtı veren sayısı}} \times 100 \quad (2.1)$$

$$\text{Hayır yüzdesel dağılım (\%)} = \frac{\text{Ankete katılan çalışanların hayır yanıtı veren sayısı}}{\text{Ankete katılan sayısı-Fikrim yok yanıtı veren sayısı}} \times 100 \quad (2.2)$$

İkinci adımda, sekiz alt kategorinin anket sonuçlarının kendi içinde yüzdesel ortalaması alınmış ve her bir alt kategoriye buldukları yüzde aralığına göre (%0-20, %21-40, %41-60, %61-80 ve %81-100) 0 ile 4 arasında puan verilmiştir (Tablo 2). En düşük puan (0) en olumsuz sosyal etkileri, en yüksek puan (4) ise en olumlu sosyal etkileri temsil etmektedir. Son adımda ise daha önce sıralanan puanlar herhangi bir ağırlık faktörü ile çarpılmadan toplanmıştır ve UNEP/SETAC'da sunulan sosyal konular için verilen kriterlere göre değerlendirilmiştir.

### 2.4. Yorumlama

Sosyal yaşam döngüsü değerlendirme çalışmasının son aşaması olan yorumlama aşamasında, envanter analizi ve etki değerlendirmesi aşamalarındaki bulgular göz önünde bulundurularak, çalışmanın amacı ve kapsamı doğrultusunda sonuçlar ortaya konmuş, kısıtlar açıklanmış ve tavsiyelerde bulunularak şeffaf bir şekilde sunulmuştur.

## 3. Bulgular ve Tartışma

### 3.1. Çimento Üretim Tesisinde Çalışanlara Ait Demografik Bilgiler

Seçilen çimento üretim tesisinde, gerçekleştirilen S-LCA çalışması sistem sınırları kapsamında bulunan 180 mavi yaka ve 120 beyaz yaka çalışan ile yapılan anket çalışmasında ilk bölümde kişisel bilgiler kısmında cinsiyet, yaş, öğrenim durumu ve hizmet süresi olmak üzere demografik sorular yöneltilmiştir.

Anket sonuçlarına göre, çimento üretim tesisindeki mavi yaka çalışanların %98'i erkek, %2'si ise kadındır. Mavi yaka çalışanların %67'si kırk yaş üstü, %33'ü kırk yaş altı aralığındadır. Öğrenim durumu %24 ilkokul, %59 lise, %15 ön lisans, %1 lisans ve %1 yüksek lisans mezunu mavi yaka çalışan olarak verilmiştir. Hizmet süresi ile ilgili soruyu ise çalışanların %44'ü 0-5 yıl, %20'si 5-10 yıl, %19'u 10-15 yıl, %5'i 15-20 yıl ve %12'si 20 ve üstü yıl şeklinde cevaplamıştır.

Ankete katılım sağlayan beyaz yaka çalışanların %21'i kadın, %79'u ise erkektir. Beyaz yaka çalışanların %59'u kırk yaş altı ve %41'i kırk yaş üstüdür. Öğrenim durumu %16 lise, %7 ön lisans, %54 lisans ve %23 yüksek lisans mezunu olan beyaz yaka çalışan ankete katılmıştır. Beyaz yaka çalışanlar arasında ilkokul mezunu yoktur. Hizmet süresi ile ilgili soru ise %32'si 0-5 yıl, %25'i 5-10 yıl, %11'i 10-15 yıl, %13 15-20 yıl ve %19'u 20 ve üstü yıl şeklinde cevaplanmıştır.

Tablo 2

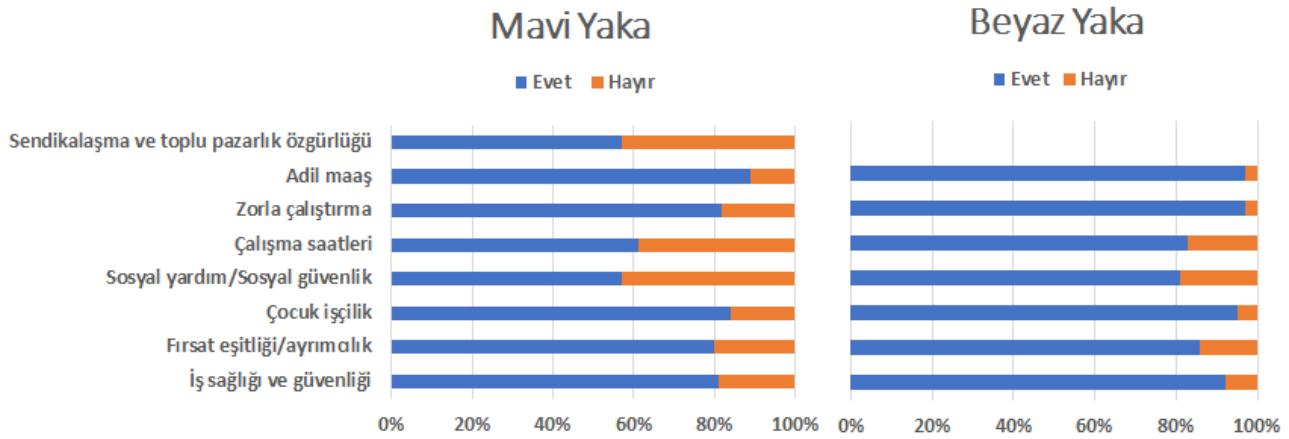
Çalışmada kullanılan puanlama sistemi (Foolmaun ve Ramjeeawon, 2013'den uyarlandı.)

Alt kategori göstergeleri	Yüzdeler	Puan
Çocuk işçilik	0-20	0
	21-40	1
	41-60	2
	61-80	3
	81-100	4
Adil maaş	0-20	0
	21-40	1
	41-60	2
	61-80	3
	81-100	4
Zorla çalıştırma	0-20	0
	21-40	1
	41-60	2
	61-80	3
	81-100	4
Sosyal yardım/Sosyal güvenlik	0-20	0
	21-40	1
	41-60	2
	61-80	3
	81-100	4
Fırsat eşitliği/ayrımcılık	0-20	0
	21-40	1
	41-60	2
	61-80	3
	81-100	4
İş sağlığı ve güvenliği	0-20	0
	21-40	1
	41-60	2
	61-80	3
	81-100	4
Sendikalaşma ve toplu pazarlık özgürlüğü	0-20	0
	21-40	1
	41-60	2
	61-80	3
	81-100	4

### 3.2. Sosyal Yaşam Döngüsü Değerlendirme Sonuçları

Mavi ve beyaz yaka çalışanlara uygulanan tüm anket sorularının sonuçları Şekil 2'de sunulmuştur. Mavi yaka anket sonuçlarının evet oranlarının yüzdesi; iş sağlığı ve güvenliği %81, sosyal yardım/sosyal güvenlik

%57, çalışma saatleri %61, adil maaş %89, sendikalaşma ve toplu pazarlık özgürlüğü %57 olarak hesaplanmıştır. Beyaz yaka anket sonuçlarının evet oranlarının yüzdesi ise; iş sağlığı ve güvenliği %92, sosyal yardım/sosyal güvenlik %81, çalışma saatleri %83, adil maaş %97 olarak hesaplanmıştır. Fırsat eşitliği/ayrımıcılık alt kategorisinin değerlendirilmesi için, kuruluştaki çalışanlara eşit fırsatların verildiği ve ayrımcılık yapılmadığına dair dört soru yöneltilmiştir (Ek 1 ve Ek 2). Mavi yaka çalışanların %80'i, beyaz yaka çalışanların ise %86'sı çalışanlara eşit fırsatların verildiği ve ayrımcılık yapılmadığı şeklinde cevap vermiştir. Kuruluştaki çocuk işçi çalıştırılmadığına yönelik, çalışanlara ankette tek bir soru yöneltilmiştir (Ek 1 ve Ek 2). Anket sonuçlarına göre mavi yaka çalışanların %84'ü; beyaz yaka çalışanların ise %95'i kuruluştaki çocuk işçi çalıştırılmadığını belirtmiştir. Zorla çalıştırma alt kategorisine yönelik ise anketlerde üç soru sorulmuş (Ek 1 ve Ek 2); mavi yaka çalışanların %82'si, beyaz yaka çalışanların ise %97'si zorla çalıştırma yapılmadığı şeklinde cevaplandırmıştır.



Şekil 2. Mavi ve beyaz yaka anket yüzdelilerinin dağılımı

Tablo 3' de ise çimento sektöründeki mavi yaka ve beyaz yaka çalışanların sosyal yaşam döngüsü değerlendirmesi sonuçları yer almaktadır. Anketlere evet/hayır olarak verilen yanıtlar puanlama sistemi kullanılarak nitel envanter verilerinden nicel envanter verilerine dönüştürülmüştür. Bu puanlama sisteminde beyaz yaka çalışanların verdikleri evet yanıtlarının tümü %80'nin üzerinde bulunduğu için en yüksek olumlu sosyal etkiyi gösteren 4 puan verilmiştir. Mavi yaka çalışanlarda ise aynı durum söz konusu değildir. Değerlendirilen alt kategorilerin puanlarında farklılıklar görülmektedir. İş sağlığı ve güvenliği, çocuk işçilik, zorla çalıştırma ve adil maaş alt kategorilerine 4'er puan verilmiştir. Fırsat eşitliği/ayrımıcılık ve çalışma saatleri alt kategorileri ise 3'er puan almıştır. Sosyal yardım/sosyal güvenlik ve sendikalaşma ve toplu pazarlık özgürlüğü alt kategorisi ise alt kategoriler arasında en düşük puana (2) sahiptir. Mavi yaka çalışanlar için değerlendirme kapsamındaki tüm alt kategoriler toplamda 26 puan olarak hesaplanırken, beyaz yaka çalışanların tüm alt kategoriler toplamı 28 puan olarak hesaplanmıştır. Mavi yaka çalışanlarla gerçekleştirilen ankette 8, beyaz yaka çalışanlarla gerçekleştirilen ankette 7 sosyal alt kategori olmasına rağmen mavi yaka ve beyaz yaka çalışanlar arasında 2 puanlık bir fark görülmektedir. Bu durumun nedeni, mavi yaka çalışanların çalışma kapsamındaki sosyal alt kategorilerinde beyaz yaka çalışanlara göre daha olumsuz etkilere sahip olmasıdır.

Çalışma sonucunda İş Sağlığı ve Güvenliği alt kategorisinde ankete katılan mavi yaka çalışanların %81'i kuruluşun sosyal performansını olumlu görürken %19'unun olumsuz gördüğü sonucuna varılmıştır. Mavi yaka çalışanların %29'u bu alt kategorideki en olumsuz yanıtı çalışan sağlığını ve iş güvenliğini sağlama konusundaki verilen eğitimler ve programlar ile ilgili soruya vermişlerdir. Çalışanların İş Sağlığı ve Güvenliği Eğitimlerinin Usul ve Esasları Hakkındaki Yönetmelikte "çok tehlikeli işyerlerinde her çalışan için en az on altı saat İSG eğitiminin verilmesinin gerektiği" yer almaktadır (28.06.2018 tarih ve 30430 sayılı Resmî Gazete). Kuruluşun 2019 yılında kişi başına düşen İSG eğitimi süresinin yaklaşık otuz saat olmasına rağmen mavi yaka çalışanların %29'nun verilen İSG eğitimini yetersiz bulduğu anlaşılmaktadır. Mavi yaka çalışanlar söz konusu eğitimi yetersiz bulma nedenlerini eğitim sürelerinin kısalığı, eğitim içeriğinde kaza kök neden, 5S, Kaizen gibi konuların eksikliği olarak açıklamışlardır. Ayrıca kuruluştaki genel İş Sağlığı ve Güvenliği



önlemlerini artırmak için yapılan İSG Koçları Uygulaması, İş İzin Sistemi, İSG Mühendisleri Projesi, saha denetimleri gibi uygulamaların mavi yaka çalışanların %29'u için yetersiz olduğu söylenilebilir. Ankete katılan beyaz yaka çalışanların %92'si kuruluşun bu alt kategorideki sosyal performansını yeterli, %8'i yetersiz bulmaktadır. Anket sonuçlarına bakıldığında beyaz yaka çalışanların %22'sinin çalışma koşullarının ergonomik olmadığını belirtmeleri dikkat çekmiştir. İSG eğitimleri ve çalışma koşulları konularında yapılacak iyileştirmeler ile çalışanlar gözünde kuruluşun İSG alt kategorisindeki sosyal performansının olumlu yönde daha da artacağı düşünülmektedir.

Tablo 3

Mavi ve beyaz yaka çalışanların alt kategori puanlarının özeti

Alt kategoriler	Puan	
	Mavi Yaka	Beyaz Yaka
İş sağlığı ve güvenliği	4	4
Fırsat eşitliği/ayrımcılık	3	4
Çocuk işçilik	4	4
Sosyal yardım/Sosyal güvenlik	2	4
Çalışma saatleri	3	4
Zorla çalıştırma	4	4
Adil maaş	4	4
Sendikalaşma ve toplu pazarlık özgürlüğü	2	-
Toplam	26	28

Fırsat eşitliği ve ayrımcılık alt kategorisinde ankete katılan mavi yaka çalışanların %80'i kuruluşun sosyal performansını olumlu gördüğü için bu alt kategori değerlendirme sonucunda 3 puan; beyaz yaka çalışanların ise %86'sı kuruluşun bu kategorideki sosyal performansını olumlu gördüğü için 4 puan almıştır. Anket sonuçları incelendiğinde mavi yaka (%35) ve beyaz yaka (%27) çalışanların bu alt kategorideki en olumsuz yanıtı işe alım ve uygun işe yerleştirme süreçleriyle ilgili soruya verdikleri dikkat çekmiştir. Beyaz yaka çalışanlar anketlerin açıklama bölümlerine çalışan bireyler arasında performans değerlendirmesinin yapılarak pozisyon ve maaş artışlarının yapılmasının gerektiğini belirtmişlerdir. Kuruluşta liderlik pozisyonunda çalışan kadın sayısı 6, erkek sayısı ise 62'dir. Liderlik pozisyonunda çalışan kadın sayısında artış sağlanırsa çalışanlar için bu alt kategorinin sonuçlarının olumlu yönde artacağı düşünülmektedir.

Çocuk işçilik alt kategorisinde mavi yaka (%84) ve beyaz yaka çalışanlar (%95) kuruluşta çocuk işçinin çalıştırılmadığını belirtmiştir. Çalışmanın gerçekleştirildiği süreçte kuruluşta çocuk işçiye rastlanmamıştır ve kuruluş yetkilileri ile yapılan görüşmelerden alınan bilgiye göre çocuk işçi çalıştırılmamaktadır. Ayrıca 4857 sayılı İş Kanunu'nun 71. Maddesine göre ağır ve tehlikeli işlerde çocuk işçi çalıştırılması yasaktır.

Sosyal yardım/sosyal güvenlik alt kategorisinde ankete katılan mavi yaka çalışanların %57'si, kuruluşun sosyal performansını yeterli bulduğu için bu alt kategori değerlendirme sonucunda 2 puan almıştır. Bu alt kategori diğer alt kategorilerle kıyaslandığında, mavi yaka çalışanlar için daha düşük olumlu sosyal performans gösterdiği göze çarpmıştır. Mavi yaka çalışanlarla yüz yüze gerçekleştirilen anketler esnasında beyaz yaka çalışanlara sağlanan sosyal yardımlar arasında özel sağlık sigortasının da olduğu ancak bu sosyal yardımın mavi yaka çalışanlara sağlanmadığını belirtilmiştir. Ayrıca, anketlerin açıklama bölümlerinde de özel sağlık sigortasının sadece beyaz yaka çalışanlara yapıldığını belirtmişlerdir. Bu bilgilere dayanarak, ankete katılan mavi yaka çalışanların kuruluşun sosyal performansını olumsuz görme nedeninin özel sağlık sigortasından faydalanmamalarından kaynaklı olabileceği düşünülmektedir. Beyaz yaka çalışanların ise %81'i kuruluşun sosyal yardım/sosyal güvenlik alt kategorisindeki performansının olumlu olduğunu belirtmiştir. Bu alt kategorideki en olumsuz yanıtlar incelendiğinde ise beyaz yaka çalışanların %28'i kişisel gelişim imkânlarının yeterli olmadığını belirtmiştir.

Çalışma saatleri alt kategorisinde ankete katılan mavi yaka çalışanların %61'inin kuruluşun sosyal performansını olumlu görmesi nedeniyle bu alt kategori 3 olarak puanlandırılmıştır. Bu kategorinin olumsuz

etkiye sahip olmasının nedeninin bakım bölümlerindeki mavi yaka çalışanların mesaiye kalma durumunda günlük çalışma saatlerinin 11 saatten fazla olmasından kaynaklandığı düşünülmektedir. Beyaz yaka çalışanların %83'ü çalışma saatleri alt kategorisinde kuruluşun sosyal performansının olumlu olduğunu düşünürken, %17'si olumsuz görmektedir. Bu alt kategorideki en olumsuz yanıt incelendiğinde, ankete katılan beyaz yaka çalışanların %31'i resmî tatil ve bayramlarda çalıştıkları gün için ayrıca izin kullanamadıklarını belirtmiştir.

Zorla çalıştırma alt kategorisinde ankete katılan mavi yaka çalışanların %82'si, beyaz yaka çalışanların ise %97'si kuruluşun sosyal performansını olumlu görmektedir. Bu alt kategorideki en olumsuz yanıtlar incelendiğinde mavi yaka çalışanların %21'i ve beyaz yaka çalışanların %5'i yüksekte çalışma, siklon açma, silo temizliği gibi zorunlu çalışma durumunda alınan önemlerin yeterli olmadığını belirtmiştir.

Adil maaş alt kategorisinde ankete katılan mavi yaka çalışanların %89'u; beyaz yaka çalışanların ise %97'si kuruluşun sosyal performansını olumlu görmektedir. Bu alt kategorideki en olumsuz yanıtlara bakıldığında mavi yaka çalışanların %16'sı ve beyaz yaka çalışanların %5'i kadın çalışanlar ile erkek çalışanlar arasında eşit maaş politikası uygulanmadığını belirtmiştir.

Sendikalaşma ve toplu pazarlık özgürlüğü alt kategorisinde sadece mavi yaka çalışanlara anket uygulanmıştır. Anket sonuçları değerlendirildiğinde mavi yaka çalışanların anket sorularının geneline olumsuz yanıtlar verdiği göze çarpmış ve bu alt kategori 2 olarak puanlandırılmıştır. Mavi yaka çalışanların %56'sı sendika temsilcisinin şirketteki büyük değişikliklerin planlanmasında katkısının olmadığını belirtmiştir. Sendikalı çalışanların %52'si fikir ve önerilerini üst yönetimle paylaşabilecekleri iletişim kanallarının yeterli olmadığını belirtmiştir. Ankete katılan mavi yaka çalışanların %50'si toplu sendika toplantılarına katılmadıklarını belirtmiştir. Sendikalaşma ve toplu pazarlık özgürlüğü alt kategorisinde sendikanın kuruluştaki etkin bir rol oynamadığı düşünülmektedir.

Literatürde çimento üretiminin sosyal yaşam döngüsünün değerlendirilmesi konusunda yapılan bir çalışmaya rastlanmamış olmakla birlikte, diğer sektörler için yapılan S-LCA çalışmalarının çalışan paydaş kategorisi açısından sonuçları incelendiğinde; ülke, sektör, işletme şartları ve sosyal yapı farklılıkları nedeniyle beklenebilecek farklı etkilerin öne çıkmasının yanında bu çalışmanın sonuçları ile benzer etkiler de tespit edilmiştir. Hosseinijou ve diğ. (2014) tarafından iki farklı yapı malzemesinin (çelik ve beton) karşılaştırmalı sosyal yaşam döngüsü değerlendirmesi gerçekleştirilmiştir. Söz konusu çalışmanın "çalışan" paydaş kategorisine ait sonuçları incelendiğinde çalışan paydaşının alt kategorileri olan adil maaş ve iş sağlığı kategorilerinde beton yapı malzemesinin çeliğe göre daha olumlu sosyal etkiye sahip olduğu belirlenmiştir. Bizim çalışmamızda da bu alt kategorilerdeki sosyal etkiler olumlu olarak değerlendirilmiştir. Buna karşılık, beton ve çimento endüstrisinin sosyal profilinin çimento üretiminin yerel topluluk paydaş kategorisinin bir alt kategorisi olan "güvenli ve sağlıklı yaşam koşulları" üzerindeki olumsuz etkisi nedeniyle zarar gördüğü ortaya konmuştur. Aynı çalışmada, çimento üretim alanlarına yakın yaşayan insanlar tarafından çeşitli şikayetlerde (yüksek seviyede hava ve gürültü kirliliği, kaynak tükenmesi vb. nedenlerden dolayı) bulunduğu belirtilmiştir. Bununla birlikte, bizim çalışmamızda sadece "çalışan" paydaş kategorisi ve buna bağlı alt kategorilere göre değerlendirme gerçekleştirilmiş; yerel topluluk paydaş kategorisi ile ilgili bir çalışma ve değerlendirme gerçekleştirilmemiştir. Roh ve diğ (2018), Güney Kore'de farklı işletim sistemlerine sahip (doğrudan işletilen, özel beton üreticileri tarafından işletilen, çimento tedarikçileri tarafından işletilen) üç tip beton santralının sosyal etkilerini değerlendirmek için S-LCA tekniğini kullanmışlardır. Bu çalışmada; çalışan paydaş kategorisi açısından çocuk işçilik, adil maaş, çalışma saatleri, zorla çalıştırma, fırsat eşitliği/ayrımcılık, iş sağlığı ve güvenliği, sosyal güvenlik/sosyal yardım, sendikalaşma ve toplu pazarlık özgürlüğü, eğitim ve öğretim, istihdam ilişkileri ve iş memnuniyeti olmak üzere 11 sosyal konu üzerine odaklanmışlardır. Değerlendirme sonucunda en yüksek pozitif sosyal etkinin çimento tedarikçileri tarafından işletilen beton santralinde, daha sonra sırasıyla özel beton üreticileri tarafından işletilen ve doğrudan işletilen beton santralinde olduğu ortaya konmuştur. Bu pozitif sosyal etkinin en önemli bileşeninin adil maaş alt kategorisi olduğu ve beton santralleri arasında bu farklılığı yaratan durumun doğrudan işletilen beton santrali çalışanlarına sadece yasal asgari ücret ödenirken diğer santrallerde asgari ücrete ek olarak fabrika ödenekleri, yeterlilik ödenekleri, iletişim maliyeti ve öğrenim ücretleri gibi çeşitli ek ödeneklerin sağlanması olduğu tespit edilmiştir.

Petti ve diğ. (2011) yapmış oldukları S-LCA çalışmasında “Cuore di Bu” adı verilen bir İtalyan domates çeşidinde alt kategori değerlendirme yöntemi kullanarak bitkilerin yetiştirilmesinden piyasaya sürülüp tüketicilere ulaşana kadar olan süreçlerin sosyal performanslarını değerlendirmeyi amaçlamışlardır. S-LCA çalışması sonucunda çalışan paydaş kategorisinin tüm alt kategorilerine (çocuk işçi, adil maaş, çalışma saatleri, zorla çalıştırma, fırsat eşitliği ve ayrımcılık, iş sağlığı ve güvenliği, sosyal yardım ve sosyal güvenlik, sendikalaşma ve toplu pazarlık özgürlüğü) 3'er puan verilmiştir. En düşük puan 1 ve en yüksek puan 4'tür. Değerlendirme yapılırken çalışanlarla gerçekleştirilen anketin sonuçları ve ILO (Uluslararası Çalışma Örgütü) Sözleşmeleri göz önünde bulundurulmuştur. Çalışanlar herhangi bir sendikaya üye değildir ama sendikalaşma özgürlüğü haklarına saygı gösterilerek bir kooperatif halinde gruplandırılmıştır. 15 yaşından küçükler çalıştırılmamaktadır ve çocuk işçi çalıştırılmaması için politika oluşturulmuştur. En düşük maaş İtalyan tarım sektörünün asgari ücretine eşit veya daha yüksektir. Haftalık çalışma süreleri sektör kanunlarına uygundur. Zorla çalıştırmanın önüne geçmek için politika oluşturulmuştur. Kuruluş, çalışanları için eşit fırsatları desteklemektedir. Kazaları önlemek için programlar hazırlanmış ve çalışanlara eğitimler verilmiştir. Çalışanlara temel gereksinimler listesindeki ikiden fazla sosyal yardım sağlanmıştır. Çalışma sonucunda, seçilen domates üretim sektörünün, çalışan paydaş kategorisindeki çoğu alt kategorinin ilgili ILO sözleşmeleri tarafından tanımlanan asgari standartları karşıladığı anlaşılmaktadır.

Foolmaun ve Ramjeeawon (2013) tarafından gerçekleştirilen bir çalışmada, kullanılmış polietilen tereftalat (PET) şişelerin seçilen alternatif dört bertaraf yöntemi senaryoları ile (%100 düzenli depolama, %40 flake üretimi ve %60 düzenli depolama, %75 yakma ve %25 düzenli depolama, %75 flake üretimi ve %25 düzenli depolama) çevresel ve sosyal etkileri araştırılmış ve karşılaştırılmıştır. Envanter sonuçlarına göre, flake üretim endüstrisinde ve yakma tesisinde çocuk işçinin çalıştırılmadığı, zorla çalıştırma vakalarının olmadığı ve tüm çalışanların sosyal yardımlardan faydalandığı çalışanlar tarafından onaylanmıştır. Düzenli depolama tesisinde zorla çalıştırmanın %21,45 olduğu hesaplanmıştır; düzenli depolama tesisinde işçilerin %63,75'i, yakma tesisindeki işçilerin ise %30'u mevcut maaşlarından memnun değilken, flake üretim endüstrisinde çalışan işçilerin %80'i mevcut maaşlarından memnun olduğunu belirtmişlerdir. Ayrıca, düzenli depolama tesisinde çalışan işçilerin %51,25'i hiçbir zaman iş sağlığı ve güvenliği konularında bilgilendirilmezken, flake üretim endüstrisinde çalışan işçilerin sadece %8'i ve yakma tesisinde çalışanların %10'u bu konuda bilgilerinin olmadığını söylemişlerdir. Yaralanma oranı düzenli depolama tesisinde %7,5 ile %10 arasında değişirken, yakma tesisinde çalışan işçiler için herhangi bir yaralanma vakası bildirilmemiştir. Sonuçlar ayrıca tüm çalışanlara çalıştıkları kuruluşlar tarafından koruyucu ekipman sağlandığını göstermiştir. Flake üretim endüstrisinde ve yakma tesisinde çalışan işçiler, acil durum/kaza durumunda izlenecek prosedürlerin tam olarak farkındayken, düzenli depolama tesisindeki işçilerin sadece %25'i bu prosedürlerin farkındadır. Her bir alt kategoriye, bir önceki adımda hesaplanan yüzdelerin bulunduğu beş aralığa (%0-20, %21-40, %41-60, %61-80 ve %81-100) göre 0 ile 4 arasında puan verilmiştir. Önerilen puanlama sistemi ve envanter sonuçlarına göre, flake üretim endüstrisinde ve yakma tesisinde çocuk işçilik, sosyal yardım/sosyal güvenlik, ayrımcılık alt kategorilerine 4 puan verilmiştir. Adil maaş alt kategorisi flake üretim endüstrisinde 3, düzenli depolama tesisinde 1 ve yakma tesisinde ise 3 puan almıştır. Zorla çalıştırma ve iş sağlığı ve güvenliği alt kategorisi flake üretim endüstrisinde ve yakma tesisinde 4 puan olarak hesaplanmıştır. Zorla çalıştırma alt kategorisi düzenli depolama tesisinde 3 puan ve iş sağlığı ve güvenliği alt kategorisi ise 3,5 puan almıştır. Üç tesis için puanlar toplandığında, en az puan düzenli depolama tesisi ve en yüksek puan flake üretim endüstrisi tarafından elde edilmiştir.

Prasara-A ve Gheewala (2018) tarafından gerçekleştirilen bir çalışmada, S-LCA tekniğinin Tayland şeker endüstrisi sektörüne uygulanabilirliği test edilmiştir. Seçilen paydaşlar; çalışanlar, tüketiciler, yerel toplum ve değer zinciri aktörleridir. Kullanılan göstergeler, her bir sosyal alt kategori için tasarlanan sorulara evet / hayır cevabı veren paydaşların yüzdesi olarak hesaplanmıştır. Çalışanlar tarafından en önemli görülen sosyal alt kategorilerin yüzdeleri: %53 adil maaş, %27 iş sağlığı ve güvenliği, %10 ayrımcılık, %7 ile zorla çalıştırma olmuştur. Paydaşlar tarafından belirlenen sosyal alt kategoriler dikkate alındığında, en önemli alt kategorilerin adil ücretler ile iş sağlığı ve güvenliği (çalışanlar, yerel tüketici ve yerel topluluk için) olduğu görülmektedir. İşçilerin %30'u şeker kamışı çiftliklerinin koruyucu ekipman sağlamadığı yanıtını vermiştir. Buna ek olarak, çalışanların %20'si işverenlerin kişisel koruyucu ekipmanı tedarik ettiğini ancak çalışanlar tarafından kullanılmadığını belirtmiştir. Adil ücret alt kategorisinde, hükümet tarafından belirlenen asgari ücretten daha düşük ücretlere çalıştığını belirten %93 işçi olmasına rağmen, işçilerin %90 adil ücret aldıklarını bildirmesi

ilginçtir. Bu çalışmada adil ücret alt kategorisi için elde edilen sonuçlara göre, şeker endüstrisinin bu alt kategoride olumsuz performanslara neden olup olmadığı konusunda net bir cevap bulunmamaktadır. Ayrımcılık alt kategorisi için kullanılan iki gösterge vardır, farklı cinsiyetlere göre ücret ayrımcılığı ve erkek ve kadın çalışanların yüzdesi. İlk göstergenin sonucu hiçbir etki göstermezken ikinci gösterge negatif performans (-%80) göstermiştir. Bunun nedeni, bu alanda çalışan kadın işçilerin yüzdesinin erkek işçilerinkinden daha yüksek olmasıdır. Bununla birlikte, işçilerle yapılan görüşmelerde elde edilen bilgilere göre, işçileri işe alma konusunda cinsiyet ayrımcılığının olmadığı belirtilmiştir. Erkek işçilerin daha yüksek ücret ödeyen diğer sektörleri tercih ettiklerini sözlerine eklemiştir. Sosyal yardımlar alt kategorisi de negatif performans göstermektedir. Bu alt kategori için kullanılan gösterge, çalışanların işverenlerden sosyal yardım alıp almadığıdır. Tüm çalışanlar, işverenlerden hiçbir sosyal yardım almadığını bildirmiştir (-%100). Çocuk işçilik, çalışma saatleri, zorla çalıştırma, sendikalaşma ve toplu pazarlık özgürlüğü alt kategorileri olumlu ya da olumsuz bir etki göstermemiştir.

Literatürde S-LCA ile ilgili yapılan çalışmalar genel olarak değerlendirildiğinde, farklı paydaş gruplarının dahil edildiği çalışmalarda, kuruluşların sosyal performansını olumlu/olumsuz olarak değiştiren faktörlerin öncelikle çalışan paydaş grubunu doğrudan etkileyen adil maaş ve iş sağlığı ve güvenliği gibi faktörler olduğu tespit edilmiştir. Bu durum dikkate alındığında, kuruluşların sosyal performanslarını artırmak için öncelikle çalışan paydaş grubunun alt kategorilerindeki sorunları tespit edip, bu sorunları azaltmaya ve/veya tamamen gidermeye odaklanmalarının önemli olduğu söylenebilir.

#### 4. Sonuçlar

Bu çalışmada, çimento üretim süreci kapsamında mavi ve beyaz yaka çalışanların sosyal koşulları ve genel sosyo-ekonomik performansı yaşam döngüsü yaklaşımıyla karşılaştırmalı olarak değerlendirilmiştir. Çalışan paydaşının alt kategorileri olan sendikalaşma ve toplu pazarlık özgürlüğü, iş sağlığı güvenliği, fırsat eşitliği/ayrımcılık, çocuk işçilik, sosyal yardım/sosyal güvenlik, çalışma saatleri, zorla çalıştırma ve adil maaş 0 ile 4 arasında puanlandırılarak etki değerlendirilmesi gerçekleştirilmiştir. Çalışmanın sonucunda mavi yaka çalışanlarının sosyal yardım/sosyal güvenlik (2), sendikalaşma ve toplu pazarlık özgürlüğü (2), çalışma saatleri (3) ve fırsat eşitliği/ayrımcılık (3) sosyal konularının iyileştirilmesi halinde kuruluşun sosyal performansının artacağı sonucuna varılmıştır. Beyaz yaka çalışanların verdikleri yanıtlar doğrultusunda tüm alt kategorilere 4 puan verilmiştir. Bu yüzden alt kategori yerine en olumsuz sosyal etkiye sahip anket sorularının değindiği konulara yönelik iyileştirmeler yapılması gerektiği sonucuna varılmıştır. Ülkemizde sosyal yaşam döngüsü değerlendirilmesi çalışmaları oldukça sınırlı sayıdadır. Bu çalışma ile ortaya konan sonuçların, çimento üretimi gerçekleştirilen kuruluşta çalışanların sosyal ve sosyo-ekonomik yönlerinin olumlu ve olumsuz etkileri konusunda fikir sahibi olunması ve buna göre karar vericilere kuruluşun sosyal performansının geliştirilmesi için farklı bir bakış açısı sağlayacağı, ayrıca ileride yapılacak çalışmalar için referans noktası oluşturacağı düşünülmektedir. S-LCA çalışmalarının en önemli kısıtlarından biri, hâlen uluslararası anlamda kabul edilmiş bir standart bir yöntemin bulunmamasıdır. Çeşitli özel yazılımlar aracılığıyla S-LCA çalışmaları uygulamalarında kullanılabilecek Social Hot-Spot Database, Product Social Impact Life Cycle Assessment Database gibi veri tabanları mevcut olmakla birlikte; hem mevcut veri tabanlarına erişimde kolaylığın sağlanması hem de S-LCA için uluslararası düzeyde kabul gören standart yöntemlerin geliştirilmesi; ürün, hizmet ve servislerin yaşam döngüsü sürdürülebilirlik değerlendirmelerinin tam ve güvenilir olarak gerçekleştirilebilmesi açısından önem taşımaktadır.

#### Yazar Katkıları

Büşra Cici: Literatür taramasını yapmış, veri toplamış, analizini yapmış ve sonuçları yorumlamıştır.

Beyhan Pekey: Çalışma konusunu belirlemiş, çalışmayı planlamış, yönetmiş, sonuçları yorumlamış ve değerlendirmiştir.

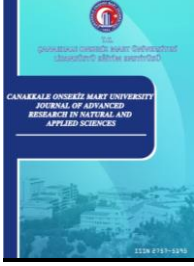
Simge Çankaya: Literatür taramasını yapmış, sonuçları yorumlamış ve makaleyi yazmıştır.

#### Çıkar Çatışması

Yazarlar çıkar çatışması bildirmemişlerdir.

**Kaynaklar**

- Foolmaun R.K., Ramjeeawon T. (2013). Comparative Life Cycle Assessment and Social Life Cycle Assessment of Used Polyethylene Terephthalate (PET) Bottles in Mauritius, *The International Journal of Life Cycle Assessment*, 18(1), 155-171. doi:<https://doi.org/10.1007/s11367-012-0447-2>.
- Haryati, Z., Subramaniam, V., Noor, Z. Z., Hashim, Z., Loh, S. K., & Aziz, A. A. (2022). Social life cycle assessment of crude palm oil production in Malaysia. *Sustainable Production and Consumption*, 29, 90-99. doi: <https://doi.org/10.1016/j.spc.2021.10.002>.
- Hossain, M., Poon, C. S., Dong, Y. H., Lo, I., & Cheng, J. C. (2018). Development of social sustainability assessment method and a comparative case study on assessing recycled construction materials. *The International Journal of Life Cycle Assessment*, 23(8), 1654-1674. doi: <https://doi.org/10.1007/s11367-017-1373-0>.
- Hosseinijou S.A., Mansour S., Shirazi M.A. (2014). Social Life Cycle Assessment for Material Selection: a Case Study of Building Materials, *The International Journal of Life Cycle Assessment*, 19(3), 620-645. doi: <https://doi.org/10.1007/s11367-013-0658-1>.
- Hunkeler D. (2006). Societal LCA Methodology and Case Study ,*The International Journal of Life Cycle Assessment*, 11(6), 371-382. doi:<https://doi.org/10.1065/lca2006.08.261>.
- Jørgensen, A., Le Bocq, A., Nazarkina, L., & Hauschild, M. (2008). Methodologies for social life cycle assessment. *The International Journal of Life Cycle Assessment*, 13(2), 96-103. doi: <https://doi.org/10.1065/lca2007.11.367>.
- Karlewski H., Lehmann A., Ruhland K., Finkbeiner M., A (2019). Practical Approach for Social Life Cycle Assessment in the Automotive Industry, *Resources*, 8(3), 146. <https://doi.org/10.3390/resources8030146>.
- Navarro I.J., Yepes V., Martí J.V. (2018). Social Life Cycle Assessment of Concrete Bridge Decks Exposed to Aggressive Environments, *Environmental Impact Assessment Review*, 72, 50-63. doi: <https://doi.org/10.1016/j.eiar.2018.05.003>.
- Petti, L., Sanchez Ramirez, P. K., Traverso, M., & Ugaya, C. M. L. (2018). An Italian tomato “Cuore di Bue” case study: challenges and benefits using subcategory assessment method for social life cycle assessment. *The International Journal of Life Cycle Assessment*, 23(3), 569-580. doi: <https://doi.org/10.1007/s11367-016-1175-9>.
- Prasara-A, J., & Gheewala, S. H. (2018). Applying social life cycle assessment in the Thai sugar industry: challenges from the field. *Journal of Cleaner Production*, 172, 335-346. doi:<https://www.sciencedirect.com/science/article/abs/pii/S0959652617324198>
- Roh S., Tae S., Kim R., Martínez D.M., Analysis of Worker Category Social Impacts in Different Types of Concrete Plant Operations: A Case Study in South Korea, (2018). *Sustainability*, 10(10), 3661. doi: <https://doi.org/10.3390/su10103661>.
- Sining, M., Sharaai, A. H., & Wafa, W. (2022). A study of social well-being among university students. *The International Journal of Life Cycle Assessment*, 1-13. doi:<https://doi.org/10.1007/s11367-022-02029-w>.
- UNEP/SETAC, Guidelines for Social Life Cycle Assessment of Products, *United Nations Environment Programme-Society of Environmental Toxicology and Chemistry Life Cycle Initiative*, 2009, ISBN: 978-92-807-3021-0.
- Uysal R., *Çalışanların İş Sağlığı ve Güvenliği Algısı: As Çimento A.Ş. Örneği* (Yüksek Lisans Tezi), 2019. Erişim adresi: <https://tez.yok.gov.tr/UlusalTezMerkezi>.
- Yıldız-Geyhan, E., Altun-Çiftçiöğlü, G. A., & Kadirgan, M. A. N. (2017). Social life cycle assessment of different packaging waste collection system. *Resources, Conservation and Recycling*, 124, 1-12. doi:<https://doi.org/10.1016/j.resconrec.2017.04.003>.



# Makine Öğrenmesi Yöntemleri ile Türkiye’de Covid-19’a İlişkin Günlük Vaka, Ağır Hasta, Vefat ve İyileşen Sayısı Tahmini

Figen Özen<sup>1,\*</sup>

<sup>1</sup>Elektrik-Elektronik Mühendisliği Bölümü, Mühendislik Fakültesi, Haliç Üniversitesi, İstanbul, Türkiye

## Makale Tarihçesi

Gönderim: 10.01.2022  
Kabul: 18.07.2022  
Yayın: 15.12.2022

## Araştırma Makalesi

**Öz** – Covid-19 içinde bulunduğumuz yüzyılın ilk pandemidir ve bundan önceki pandemilere kıyasla süresi, neden olduğu can kaybı, yarattığı psikolojik, sosyolojik ve ekonomik etkileri dolayısıyla farklılık göstermektedir. Bu süreçte virüs pek çok varyant üretmiştir ve üretmeye de devam etmektedir. Dünya üzerindeki hareketliliğin sıklığı ve miktarı düşünüldüğünde, bu durumun yakın gelecekte değişmesi mümkün gözükmemektedir. Pandeminin gidişatını anlamak, bundan sonraki olası pandemiler için hazırlıklı olmak konusunda faydalı olacaktır. Bu amaçla, T.C. Sağlık Bakanlığı tarafından yayınlanan günlük veri incelenmiş, farklı veri grupları üzerinde gerek özelliklerini anlama gerekse geleceğe yönelik tahmin gerçekleştirme amacıyla, güncel bir yaklaşım olan makine öğrenmesi yöntemleri kullanılmıştır. Kullanılan veri grupları oldukça karmaşık birer zaman serisi yapısındadır ve günlük vaka sayısı, ağır hasta sayısı, günlük vefat sayısı ve günlük iyileşen sayısı olarak seçilmiştir. Polinom regresyon, en küçük kareler polinom uyumu ve kübik eğri uyumu sonuçları ile tahminler bu makalede incelenmiştir. Sonuçlar gerek grafikler yoluyla gerekse zaman serisi tahmininde kabul görmüş bir performans kriteri olan Canberra uzaklığının ortalama, medyan, standart sapma ve toplam değerleriyle, sayısal olarak belirtilmiştir. Yukarıda belirtilen dört zaman serisi için en iyi sonuçların, kübik eğri uyumu yöntemiyle alındığı görülmektedir. Tahminlerde kullanılan eğrilerin dereceleri, zaman serisine göre değişiklik göstermektedir. Elde edilen tahmin sonuçları, zaman serisine bağlı olarak değişen yüksek doğruluk oranı sağlamıştır.

**Anahtar Kelimeler** – Covid-19, en küçük kareler polinom uyumu, kübik eğri uyumu, makine öğrenmesi, polinom regresyon

## Estimation of Daily Cases, Deaths, Serious Patients and Recovering Patients of Covid-19 in Turkey with Machine Learning Methods

Department of Electrical and Electronics Engineering, Faculty of Engineering, Haliç University, İstanbul, Turkey

## Article History

Received: 10.01.2022  
Accepted: 18.07.2022  
Published: 15.12.2022

## Research Article

**Abstract** – Covid-19 is the first pandemic of the century and differs from previous pandemics due to its duration, loss of life, and psychological, sociological and economic effects. In this process, the virus has produced and continues to produce many variants. Considering the frequency and amount of mobility on Earth, this situation does not seem likely to change soon. Understanding the course of the pandemic will be helpful in being prepared for the next possible pandemics. To this end, the daily data published by the Turkish Ministry of Health was examined, and machine learning methods, which is an up-to-date approach, were used to understand the features and make predictions for the future on different data groups. The data groups used are in a very complex time series structure and were chosen as the number of daily cases, severe patients, deaths, and recoveries per day. The results of polynomial regression, least squares polynomial fit, and cubic spline fit, and estimations are shown in this article. The results are presented graphically, and by means of an accepted performance criterion in time series estimation, namely by the mean, median, standard deviation, and total values of the Canberra distance. It is seen that the best results for the time series mentioned above are obtained by the cubic spline fit method. The degrees of the curves used in the estimations vary according to the time series. The estimation results obtained provided a high accuracy rate that varies depending on the time series.

**Keywords** – Covid-19, cubic spline fit, least squares polynomial fit, machine learning, polynomial regression

<sup>1</sup> figenozen@halic.edu.tr

\*Sorumlu Yazar

## 1. Giriş

Dünya Sağlık Örgütü tarafından açıklanan rakamlara göre, 29 Temmuz 2022 itibarıyla 572.239.451 doğrulanmış vaka ve 6.390.401 ölü sayısı ile, yirmi birinci yüzyılın şu ana dek en büyük pandemisi olan Covid-19, 2020 yılının ilk aylarından itibaren ülkemizde de etkili olmuştur. Dünya Sağlık Örgütü'nün istatistiklerinde 29 Temmuz 2022 tarihinde Türkiye için doğrulanmış vaka sayısı 15.524.071, vefat sayısı ise 99.184 olarak verilmiştir. Bu rakamlarla, Türkiye, vaka sayısı bakımından dünyada 10. sırada, vefat sayısı bakımından ise 19. sırada yer almaktadır. Türkiye'de her 100 kişiye düşen aşı dozu 25 Temmuz 2022 itibarıyla 177,3 olmuştur ve bu oranla, Türkiye ortalama aşı dozu bakımından 81. sıradadır. 25 Temmuz 2022 tarihine dek uygulanan toplam aşı dozu sayısı 12.248.795.623'tir. Dünya ortalaması 25 Temmuz 2022 tarihinde 157,15 olarak gerçekleşmiştir (World Health Organization, 2022). Tahminlere göre Covid-19 yayılımını ve ondan kaynaklanan ölümleri yakın bir tarihte durdurmak mümkün görünmemektedir.

Türkiye'de pandemi ile ilgili bilgiyi T.C. Sağlık Bakanlığı'nın web sitesinden takip etmek mümkündür. Bakanlığın verisi incelendiğinde, bütün veri çeşitlerinin aynı tarihte başlamadığı ve eşit sayıda bilgiye ulaşmanın mümkün olmadığı görülmektedir. Ayrıca, süreç boyunca Türkiye'de ve dünyada veri ilan standartlarının değişime uğradığı gözlenmektedir. Başlarda günlük verinin düzenli olarak yayınlandığı görülürken, süre uzadıkça, ayrıntılı olarak ilan edilen tabloların daha az veri çeşidi için düzenlendiği görülmektedir (T.C. Sağlık Bakanlığı, 2022).

Covid-19 salgınının başlamasından bu yana gerek zaman serisi bilgisinden yola çıkarak, gerekse görüntü işleme yöntemleriyle pandeminin geleceği hakkında çeşitli tahminler yürütülmeye çalışılmıştır. Bu çalışmanın konusu zaman serisi analizi ve tahmini olduğundan, aşağıda zaman serisi üzerine yapılan çalışmalara örnekler verilmiştir.

### 1.1. Covid-19 Zaman Serisi Konusunda Yapılan Çalışmalar

Gambhir, Jain, Gupta ve Tomer 154 günlük veriyle Hindistan'da hastalığın seyrini polinom regresyonu ile analiz ederek, 3 haftalık geleceği tahminde %93 başarı elde etmişlerdir (Gambhir vd., 2020). Mandayam, Rakhshith, Siddesha ve Niranjana John Hopkins Üniversitesi tarafından yayınlanan veriyle ve doğrusal regresyon ve destek vektör regresyonu ile tahmin yaptıklarında, doğrusal regresyonun daha iyi sonuç verdiği karar vermişlerdir. Bunun, verinin doğrusal yapısından kaynaklandığını belirtmişlerdir (Mandayam vd., 2020).

Kurniawan vd. Worldometers verisi ile 200 ülkeyi pandemilerinin benzerliği bazında kümelere ayırmışlardır (Kurniawan vd., 2020). Rustam vd. John Hopkins Üniversitesi tarafından yayınlanan veriyle, doğrusal regresyon, LASSO algoritması, destek vektör makineleri ve üstel yumuşatma yöntemlerini kullanarak, 10 gün içinde yeni vaka, vefat ve iyileşen sayılarını tahmin etmişlerdir. En iyi sonucun üstel yumuşatma algoritmasıyla elde edildiğini bildirmişlerdir (Rustam vd., 2020).

Ramchandani, Fan ve Mostafavi derin öğrenme yoluyla yaptıkları tahminde kullanılan özniteliklerin analizini yapmışlardır (Ramchandani vd., 2020). Yang ve Chen, ABD'de sınırlı sayıda eyaletin Twitter verisini kullanarak, ülkenin tamamındaki vaka sayısını regresyon modelleri ile tahmin etmeye çalışmışlardır (Yang ve Chen, 2020).

Singh ve Dalmia Hindistan için doğrusal regresyon ile vaka sayısı verildiğinde vefat sayısını tahmin etmişlerdir (Singh ve Dalmia, 2020). Bhadana, Jalal ve Pathak, Hindistan için sonraki 5 günde vaka, vefat ve iyileşen sayısını doğrusal regresyon, karar ağacı, LASSO, destek vektör makineleri ve rastgele orman algoritmaları ile hesaplamışlardır. Polinom regresyonunun en iyi sonucu verdiğini belirtmişlerdir (Bhadana vd., 2020).

Hazarika ve Gupta Brezilya, Hindistan, Peru, Rusya ve ABD verisini kullanarak, dalgacık bağlantılı rastgele vektör fonksiyonel bağlantı ağı ile Covid 19 yayılımı tahmin edilmiştir (Hazarika ve Gupta, 2020). Seveli ve Başer, John Hopkins Üniversitesi verisiyle ve Facebook Prophet modeliyle vaka, vefat ve iyileşen sayılarını tahmin etmişlerdir (Seveli ve Başer, 2020). Leon, Iqbal, Azim ve Mamun, Bangladeş verisini kullanarak polinom regresyon, destek vektör regresyonu, Holt Winter, ARIMA ve Facebook Prophet modelleriyle vaka ve vefat sayılarını tahmin etmişlerdir, En yakın sonucun Facebook Prophet modeliyle elde edildiğini belirtmişlerdir (Leon vd., 2021).

Kumari vd. Hindistan verisini kullanarak çoklu regresyon ve otoregresyon ile 30 gün sonrası için vaka, vefat ve iyileşen sayısını tahmin etmişlerdir (Kumari vd., 2021).

Gupta, Gupta, Kumar ve Sardana, Hindistan için rastgele orman, destek vektör makineleri, karar ağacı ve yapay sinir ağı modelleriyle vaka, vefat ve iyileşen sayısını tahmin etmişlerdir. En yakın sonuçları rastgele orman modeliyle aldıklarını belirtmişlerdir (Gupta vd., 2021). Yudistra, Sumitro, Nahas ve Riama Covid 19 yayılımına etki eden unsurları evrişimli uzun kısa süre bellekli model ile incelemişlerdir (Yudistira vd., 2021).

ArunKumar vd. pandemiden çokça etkilenen 16 ülkeyi seçerek 60 günlük vaka, vefat ve iyileşen sayısını ARIMA ve SARIMA modelleriyle tahmin etmişlerdir. SARIMA model tahminlerinin daha gerçekçi olduğunu belirtmişlerdir (ArunKumar vd., 2021). Kumar ve Susan, parçacık sürü optimizasyonu ve bulanık zaman serisi tahminini birleştirerek 10 ülke için vaka sayısı tahminini gerçekleştirmişlerdir (Kumar ve Susan, 2021).

Yukarıdaki çalışmalar, yapıldığı ülke için geçerlidir ve başarılıdır. Ancak her ülkenin pandemi yanıtı kendine özgü bir yapı göstermektedir. Bu nedenle, tek bir model oluşturup, her ülke için bir açıklama getirmek mümkün değildir. Türkiye'deki durumu inceleyen çalışmalara ilişkin örnekler arasında (Koçak, 2020), (Ergül, Yavuz, Aşık ve Kalay, 2020), (Taşdelen ve Yıldırım, 2020), (Akay ve Akay, 2021), (Karcioğlu vd., 2021) yer almaktadır. Koçak, çeşitli AR (otoregresif) modelleri kıyaslamış ve sonuçlarını 7 Nisan 2020 tarihinde varolan veri için belirtmiştir (Koçak, 2020). Ergül vd., 10 Nisan 2020 tarihine dek varolan veri ile Türkiye'deki pandemi seyrini 22 ülke ile karşılaştırmışlar ve en iyi zaman serisi modellemesini Box-Cox yöntemiyle elde ettiklerini ifade etmişlerdir (Ergül, Yavuz, Aşık ve Kalay, 2020). Taşdelen ve Yıldırım, ilk iki ayın verisini kullanarak Poisson regresyon yöntemiyle çalışmışlar ve bazı dönemlerde tahminlerin daha başarılı sonuçlar verdiğini belirtmişlerdir (Taşdelen ve Yıldırım, 2020). Akay ve Akay, 11 Mart-24 Ağustos 2020 aralığında ARIMA modeliyle çalışmışlar, iki haftalık tahmin modeli oluşturduklarını belirtmişlerdir (Akay ve Akay, 2021). Karcioğlu, Tanışman ve Bulut, günlük vaka ve vefat sayılarında ARIMA modelinin, günlük iyileşen sayılarında LSTM modelinin daha iyi sonuç verdiğini belirtmişlerdir (Karcioğlu vd., 2021).

Sözü geçen çalışmalarda kullanılan veri, pandemi hala sürmekte olduğundan, kısıtlıdır ve öte yandan pandemiye ilişkin zaman serisi, çeşitli toplumsal gelişmelerin de etkisiyle günden güne değişim göstermektedir. Dolayısıyla, daha güncel veriyle yapılan çalışmalara ihtiyaç bulunmaktadır.

Bu çalışma, Türkiye'deki Covid-19 salgınının seyrini, T.C. Sağlık Bakanlığı tarafından yayınlanan günlük veriyi baz alarak incelemek ve günlük vaka, ağır hasta, vefat ve iyileşen sayıları konusunda gidişatı tahmin etmek ve buna ek olarak veri karakteristiğini incelemek için yapılmıştır. Yukarıda belirtilen ve Türkiye verisi için gerçekleştirilen çalışmalardaki verinin zaman kısıtı nedeniyle, hem Covid-19 pandemisinin nasıl geliştiğine, hem de gelecekteki olası pandemilerin seyrinin nasıl olabileceğine dair bilgi ve fikir vermesi açısından böyle bir çalışmanın fayda sağlayacağı düşünülmektedir.

Yukarıda verilen örneklerde kullanılan yöntemlerin basit regresyon modellerinden başlayıp LSTM gibi daha karmaşık olanlarına dek geniş bir skalada bulunduğu görülmektedir. Bu çalışmada, Türkiye'ye ait pandemi verisini mümkün olduğunca basit ve açıklanabilir modellerle ifade etmek amacı güdülmüştür. Kullanılan yöntemler, makine öğrenmesi yöntemlerinden polinom regresyon, en küçük kareler polinom uyumu ve kübik eğri uyumudur. Bu yöntemler, karmaşık yapıdaki veriyi mümkün olduğunca basit ve bilgisayar yardımıyla hızlı bir şekilde ifade edebilmek ve bu konuda yapılan diğer çalışmalara bir alternatif sunmak için tercih edilmiştir. Daha karmaşık yöntemler kullanılarak elde edilen sonuçlarda açıklanabilirlik problemiyle karşılaşmaktadır. İkinci bölümde, çalışmada kullanılan yöntemler açıklanmaktadır.

## 2. Materyal ve Yöntem

Bu çalışma, Türkiye'de Covid-19 hastalığının seyrini izlemek için, T.C. Sağlık Bakanlığı tarafından yayınlanan veri baz alınarak gerçekleştirilmiştir (T.C. Sağlık Bakanlığı, 2022). Bu veriyi anlamlı bir şekilde ifade ve tahmin edebilmek amacıyla, çeşitli makine öğrenmesi yöntemleri kullanılmıştır. Kullanılan yöntemlerin geçerliliği gerek görsel gerekse sayısal yöntemlerle incelenmiş ve karşılaştırılmıştır.

Bu çalışmada incelenen veri kümelerinin gerçek ve tahmini değerlerini karşılaştırmak amacıyla, makine öğrenmesi yöntemleri simülasyon yoluyla uygulanmıştır ve çeşitli tahmin yöntemleri denenmiştir. Ancak gerek sayısal performans kriterleri gerekse görsel olarak, grafikler yardımıyla ulaşılan sonuçların incelenmesiyle, üç yöntemin daha anlamlı sonuç verdiği görülmüştür. Bunlar polinom regresyon, en küçük kareler polinom uyumu ve kübik eğri uyumudur.

Performansın değerlendirilmesi için bazı çalışmalarda yapıldığı gibi normalizasyona başvurulmamış ve gerçek ölçek üzerinden çalışılmıştır. Literatürde toplam sayıların tahminine yönelik çeşitli çalışmalar bulunmaktadır ancak toplam sayılar yüksek olduğu ve tanım gereği artış trendinde olduğu için buralarda yapılan makul seviyeli hatalar, sonuçta bir problem olarak görülmeyebilir. Öte yandan günlük verideki dalgalı ve değişken



yapı ile ilgili çalışma yapıldığında, daha küçük hatalarda bile performans düşüşü gözle görülür hale gelmektedir. Bu tür bir yaklaşım, daha gerçekçi bir sonuç doğurduğu için bu çalışmanın verisi günlük seçilmiştir.

İzleyen paragraflarda, polinom regresyon, en küçük kareler uyumu ve kübik eğri uyumu yöntemleri hakkında bilgi verilmekte, bir sonraki bölümde ise alınan sonuçlar detaylandırılmaktadır. Zaman serisi verisi için daha farklı yöntemler de kullanmak mümkündür, bu çalışma için doğrusal regresyon, Bayes regresyonu, sinüzoidal uyum fonksiyonları ile de çalışılmıştır, ancak Covid-19 veri seti için anlamlı sonuç üretmedikleri görülmüştür. Bu yaklaşımlardan olumlu sonuç alınmaması, verinin oldukça nonlineer yapıda olmasından ve sözü geçen uyum fonksiyonlarının bu tür nonlineer yapıları ifade etmekte zayıf kalmasından kaynaklanmaktadır.

## 2.1. Polinom Regresyon

Polinom regresyon metodu, veri noktalarını en iyi şekilde modelleyebilecek bir polinom ifadesi bulmayı amaçlar. Ancak, incelenen veri setine benzer durumlarda çözümün bulunması pek kolay değildir. Bunun nedeni, hem çok sayıda veri noktası kullanılması, hem de karakteristiğın zaman içinde, varyantlar, kapanmalar dolayısıyla kişiler arası temasın azalması, kontrollü normalleşme, aşılardan sisteme dahil edilmesi gibi etkenler yüzünden sık sık dramatik değişikliklere uğramasıdır. Bu tür etkilerin yapıyı değiştirmedikleri durumlarda, veri kümesi  $n$  noktadan oluşuyorsa,  $n - 1$  dereceli bir polinomla bütün noktaları içeren bir ifadeye ulaşılabilir (Ertel, 2017). Ancak bu yaklaşım gereksiz karmaşıklıkta bir sonuç doğuracaktır. Bunun yerine, mümkün olduğunca düşük dereceli bir polinom kullanılmalıdır.

Genel olarak, polinom regresyon kullanılarak yapılan bir tahmin, Eşitlik 2.1'deki modelle ifade edilebilir:

$$\hat{y}(n) = w_0 + w_1x(n) + w_2x^2(n) + \dots + w_dx^d(n), \quad n = 1, 2, 3, \dots \quad (2.1)$$

Modelde  $\{w_0, w_1, \dots, w_d\}$  olmak üzere,  $d+1$  ağırlık parametresi kullanılmaktadır. Denklemden  $x(n)$ ,  $n$  anındaki veriyi,  $\hat{y}(n)$ ,  $n$  anındaki tahmin değerini,  $d$  ise kullanılan modelin derecesini simgelemektedir (Aggarwal, 2018). Veri noktası sayısından daha az dereceli bir polinom kullanıldığında, hata olması kaçınılmazdır. Dolayısıyla, gerçek değer  $y(n)$  ile tahmin edilen değer  $\hat{y}(n)$  arasında fark oluşur. Önemli olan, bunun kabul edilebilir sınırlar içinde tutulmasıdır.

Polinom regresyon uygulamalarında verinin üsleri kullanılmakta ve görünürde doğrusal olmayan bir yaklaşım izlenimi uyandırmaktadır. Ancak probleme hesaplanması gereken katsayılar açısından bakıldığında, polinom regresyonun doğrusal bir regresyon olduğu anlaşılmaktadır. Zaman serisi probleminin bu şekilde çözümü, doğrusal tahmin ile gerçek değer arasındaki karesel hatayı minimize eden bir çözümdür ve Eşitlik 2.2'de gösterilen ifadeyi küçültmeyi amaçlar:

$$\sum_{i=1}^N (y_i - \hat{y}_i)^2 \quad (2.2)$$

Burada  $y_i$  gerçek değeri,  $\hat{y}_i$  tahmin edilen değeri,  $N$  ise veri setindeki toplam veri sayısını simgelemektedir. Gerçekleştirilen minimizasyon işlemi, Eşitlik 2.1'deki ağırlıkları güncellemek içindir.

## 2.2. En Küçük Kareler Polinom Uyumu

Bu yöntem, Eşitlik 2.2'yi küçültmeyi amaçlar, ancak kullandığı yaklaşım Eşitlik 2.1'den farklıdır ve Eşitlik 2.3 ile ifade edilmektedir:

$$\hat{y}(n) = w_0x(n-d) + w_1x(n-d+1) + \dots + w_dx(n), \quad n = 1, 2, 3, \dots \quad (2.3)$$

Burada  $x(n)$ ,  $n$  anındaki veriyi,  $\hat{y}(n)$ ,  $n$  anındaki tahmin değerini,  $d$  ise kullanılan modelin derecesini simgelemektedir (Theodoridis ve Koutroumbas, 2009).

### 2.3. Kübik Eğri Uyumu

Bu yöntem, verilen noktaların aralarındaki ilişkileri üçüncü dereceden kübik eğriler kullanarak ifade etmeye yarar. Parçalı süreklilik içerir, veriyi çeşitli parçalara ayırarak inceler. Parçalara ilişkin sınır değerler düğüm noktaları adını alır ve kübik eğriler arasındaki geçişleri yumuşatmak için bu değerlerde ikinci türevler sıfıra eşitlenir. Modelin karmaşıklığı, kullanılan düğüm noktalarının sayısı ile artar. Eşitlik 2.4'te tahmin değerinin hesaplanması gösterilmektedir:

$$\hat{y}(n) = w_0 + w_1x(n) + w_2x^2(n) + w_3x^3(n) + w_4[x(n) - \alpha_1]_+^3 + w_5[x(n) - \alpha_2]_+^3 + \dots, n = 1, 2, \dots \quad (2.4)$$

Burada  $\alpha_i$ , i. düğüm noktasını simgelemektedir (Harrell Jr., 2015). Eşitlik 2.4'te kullanılan notasyonun açıklaması Eşitlik 2.5'tedir:

$$[x(n) - \alpha_i]_+ = \begin{cases} x(n) - \alpha_i, & x(n) - \alpha_i > 0 \\ 0, & x(n) - \alpha_i \leq 0 \end{cases} \quad (2.5)$$

Eğer kullanılan düğüm sayısı  $m$  ise,  $m + 4$  adet regresyon katsayısı hesaplanmalıdır. Ağırlık parametrelerini simgeleyen  $\{w_0, w_1, \dots, w_d\}$  çeşitli optimizasyon yöntemleri kullanılarak hesaplanabilir. Düğüm noktalarının yerleri, incelenen eğrideki değişimlerle uyumlu olacak şekilde, optimizasyon algoritmalarıyla belirlenebilir. Ancak bu tür bir yaklaşım, anlık veriyi tahmine dahil etmek konusunda iyi bir yaklaşım değildir. Bu nedenle, daha sık kullanılan yöntem, belli sayıda düğüm noktası kullanmak şeklindedir.

### 2.4. Canberra Uzaklığı

Zaman serilerinin tahmininde başarıyı ölçmek için kullanılan bir yöntemdir. Öklid uzaklığının tekilliklere olan hassasiyetini yenmek için tercih edilmektedir (Zhao vd., 2021). Burada Covid-19 verisinde bulunan tekillikler dolayısıyla tercih edilmiştir. Canberra uzaklığı, gerçek veriye ne kadar yaklaşıldığını ölçmek için Eşitlik 2.6'daki hata kriterini kullanır:

$$e(n) = \frac{|y(n) - \hat{y}(n)|}{|y(n)| + |\hat{y}(n)|} \quad (2.6)$$

Burada  $y(n)$ ,  $n$  anındaki gerçek değeri,  $\hat{y}(n)$  ise tahmin edilen değeri simgelemektedir. Uzaklık formülü, yapısı gereği bir normalizasyon içermekte ve değerler 0 ve 1 arasında değişmektedir. Bu nedenle yorumlanması kolaydır. Canberra uzaklığının ortalamasını, standart sapmasını hesaplamak, tahminin başarısı hakkında bilgi verir. Canberra uzaklığı, çeşitli çalışmalarda kullanılmıştır (Al-wakeel, Wu ve Jenkins, 2017), (Saxena, Kaur ve Bhatnagar, 2019), (Badre ve Thepade, 2016), (Phiri vd., 2021).

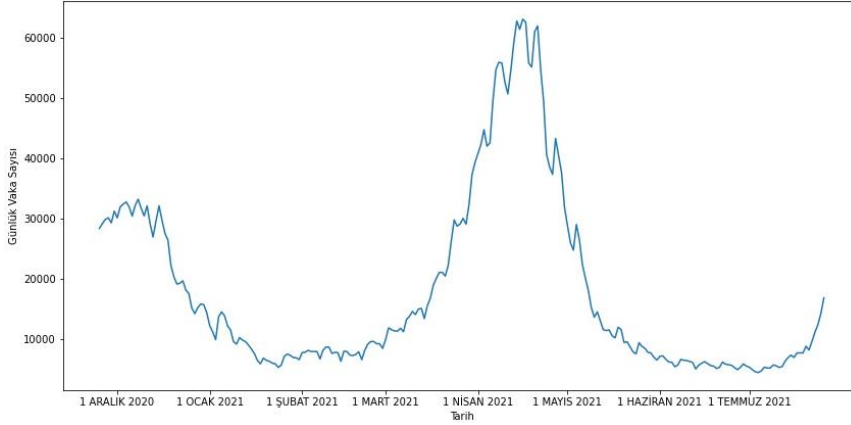
## 3. Bulgular ve Tartışma

Günlük vaka, ağır hasta, vefat ve iyileşen veri kümelerinin karakteristikleri birbirinden farklı olduğundan, ulaşılan sonuçların da spesifik veri kümesi koşullarında değerlendirmesi gerekmektedir. İncelenen zaman zarfında Covid-19 için alfa, beta ve delta varyantlarının etkilerini görmek mümkündür. Kullanılan verinin son zamanlarında en baskın olan varyantın delta olduğu bilinmektedir. Yayınlanan istatistik bilgileri her zaman bütün veriyi içermediğinden, farklı tarih aralıkları kullanmak gerekmiştir.

Bu bölümde yer alan ve tahmin içeren bütün grafiklerde kırmızı noktalar gerçek değerleri, mavi çizgiler ise tahmini değerlerin eğrisini temsil etmektedir.

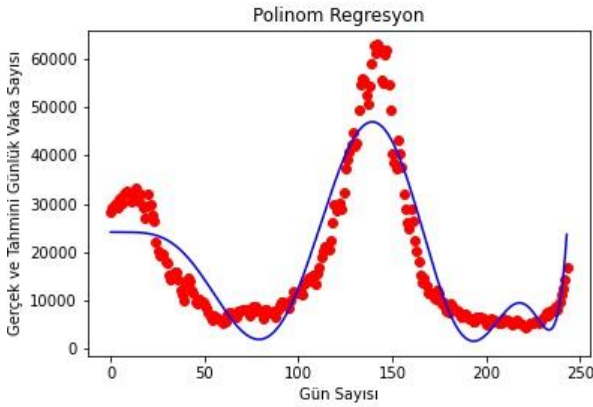
### 3.1. Günlük Vaka Sayısı Bulguları

Gerçekleşen günlük vaka sayısı verisinin grafiği Şekil 1'de gösterilmiştir. Değerlerin geniş bir skalada oluştuğu ve 60.000 sınırının da ötesine geçebildiği gözlemlenmektedir. Günlük vaka verisi toplam 244 gün için değerlendirilmiştir. Burada hem zaman zaman uygulanan sokağa çıkma kısıtlamalarının, hem de verinin son dönemlerine denk gelen aşı uygulamalarının etkilerini gözlemlemek mümkündür.

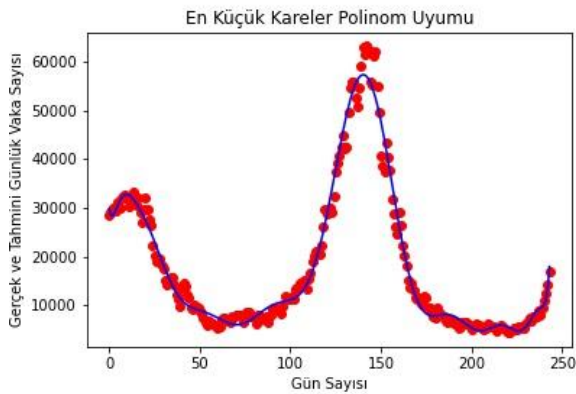


Şekil 1. Günlük vaka sayısı

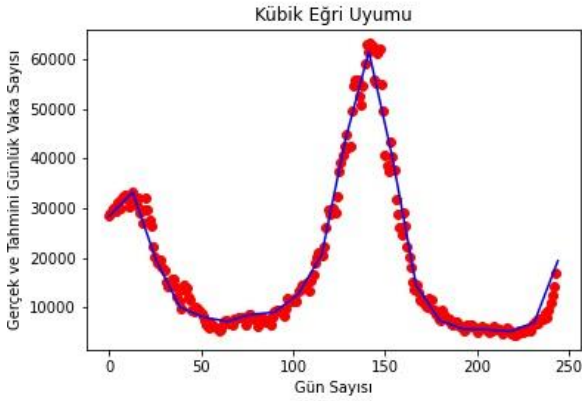
Günlük vaka sayısının tahmini değerlerine ulaşmak için kullanılan ilk yöntem polinom regresyondur. Elde edilen sonuç Şekil 2’de gösterilmiştir. Polinom regresyon için kullanılan derece 10’dur. Küçük değerler kullanıldığında son derece karmaşık bir karakteristiğe sahip olan eğriyi gerçekçi biçimde tahmin edebilmek mümkün değildir, çok yüksek değerler kullanıldığında ise benzer şekilde karakteristikten uzaklaşmaktadır. İkinci tahmin yöntemi olarak en küçük kareler polinom uyumu kullanılmıştır. Sonuçta elde edilen grafik, Şekil 3’te gösterilmiştir. Burada model derecesi 18 seçilmiştir ve polinom regresyon tahmininden daha iyi sonuç elde edilmiştir. En büyük farkın pik noktası civarında olduğu görülmektedir. Bunun yanında ani düşüşlerde de tahmin polinom regresyona göre daha isabetlidir. Tahmin için kullanılan son yöntem, kübik eğri uyumudur. Sonuç Şekil 4’te gösterilmiştir. 244 veriden oluşan küme, Eşitlik 2.4 ve 2.5’te belirtildiği biçimde, 20 eşit parçaya ayrılarak, her parça üzerinde üçüncü dereceden eğri kullanımıyla bir uyum oluşturulmaya çalışılmıştır. Sonucun hem pik hem de dip noktalar dahil, önceki iki tahminden daha iyi olduğu görülmektedir.



Şekil 2. Polinom regresyon ile günlük vaka tahmini



Şekil 3. En küçük kareler polinom uyumu ile tahmin



Şekil 4. Kübik eğri uyumu ile günlük vaka tahmini

Yapılan tahmin çalışmalarını sayısal açıdan karşılaştırmak için Canberra uzaklığı kullanılmıştır. Tablo 1’de her üç yöntem için hesaplanan ortalama, medyan, toplam Canberra uzaklıkları ve standart sapma değerleri verilmiştir. Toplam uzaklık rakamı en düşük olan kübik eğri uyumu yaklaşımıdır ve bu durum, Şekil 4 ile görsel açıdan da desteklenmektedir.

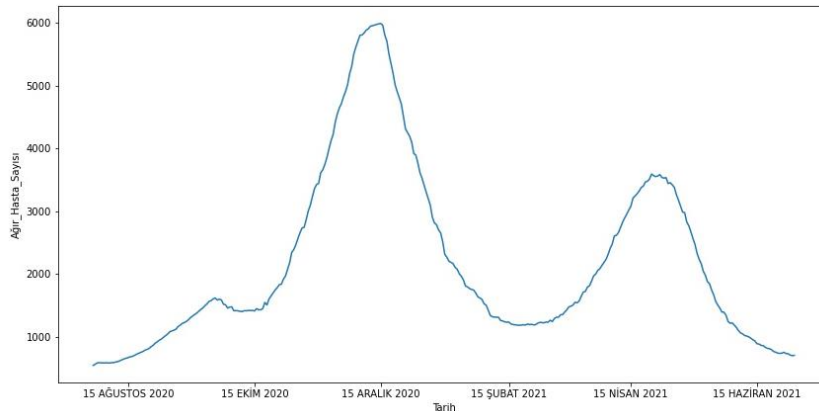
Tablo 1

Günlük vaka tahmini sayısal performans karşılaştırması

Yöntem	Ortalama	Medyan	Standart Sapma	Toplam
Polinom regresyon	0.38	0.42	0.19	92.47
En küçük kareler polinom uyumu	0.05	0.04	0.04	12.69
Kübik eğri uyumu	0.41	0.47	0.23	8.25

### 3.2. Ağır Hasta Sayısı Bulguları

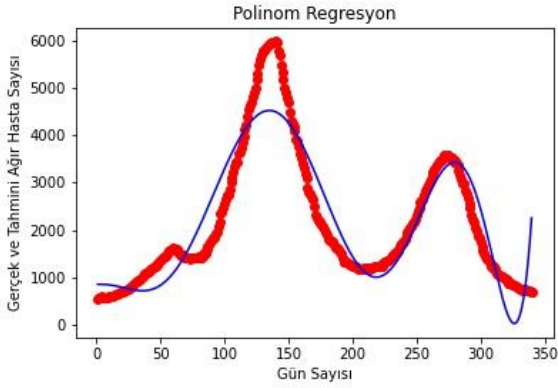
Gerçekleşen günlük ağır hasta sayısı verisinin grafiği Şekil 5’te gösterilmiştir. Değerlerin geniş bir skalada oluştuğu ve 6.000 sınırını zorladığı gözlemlenmektedir. Günlük ağır hasta verisi, toplam 340 gün için değerlendirilmiştir. Buradaki veri setinin vaka sayısına ilişkin veri setinden daha yumuşak bir yapısı olduğu gözlemlenmektedir.



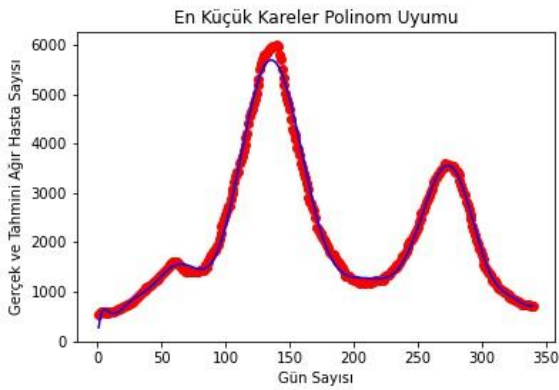
Şekil 5. Günlük ağır hasta sayısı

Polinom regresyon yöntemiyle tahminde ulaşılan sonuç Şekil 6’da gösterilmiştir. Kullanılan derece 8’dir. Şekil 1 ve 5 karşılaştırıldığında, ağır hasta sayısının daha yumuşak bir eğri çizdiği ve daha düşük derecele tahmin yapılabileceği görülmektedir. En küçük kareler polinom uyumu ile elde edilen grafik, Şekil 7’de gösterilmiştir.

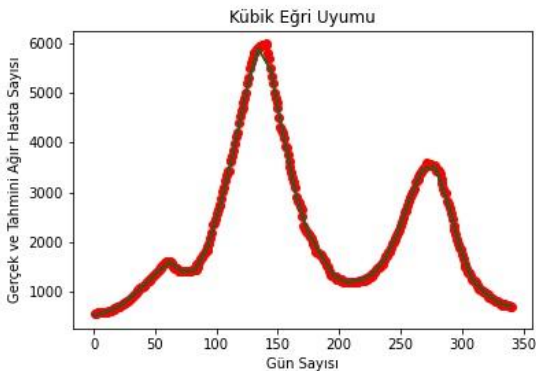
Burada model derecesi, günlük vaka sayısının tahminine benzer şekilde, 18 seçilmiştir ve paralel biçimde, polinom regresyon tahmininden daha iyi sonuç elde edilmiştir. En büyük fark, iki pik noktasından daha yüksek olanı civarındadır, ani düşüşlerde tahmin daha isabetlidir. Kübik eğri uyumunun sonucu Şekil 8’de gösterilmiştir. 340 veriden oluşan küme 34 eşit parçaya ayrılarak, her parça üzerinde bir uyum oluşturmaya çalışılmıştır. Sonucun hem pik hem de dip noktalar dahil, önceki iki tahminden daha iyi olduğu görülmektedir.



Şekil 6. Polinom regresyon ile günlük ağır hasta tahmini



Şekil 7. En küçük kareler polinom uyumu ile tahmin



Şekil 8. Kübik eğri uyumu ile günlük ağır hasta tahmini

Ağır hasta tahmin çalışmalarını karşılaştırmak için, Canberra uzaklığı değerleri Tablo 2’de verilmiştir. Toplam uzaklık rakamı en düşük olan kübik eğri uyumu yaklaşımıdır.

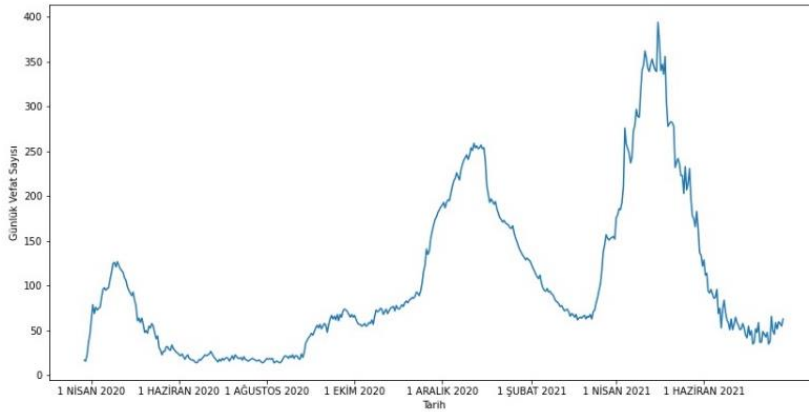
Tablo 2

## Ağır hasta tahmini sayısal performans karşılaştırması

Yöntem	Ortalama	Medyan	Standart Sapma	Toplam
Polinom regresyon	0.38	0.34	0.22	129.96
En küçük kareler polinom uyumu	0.02	0.02	0.02	7.53
Kübik eğri uyumu	0.01	0.01	0.01	0.45

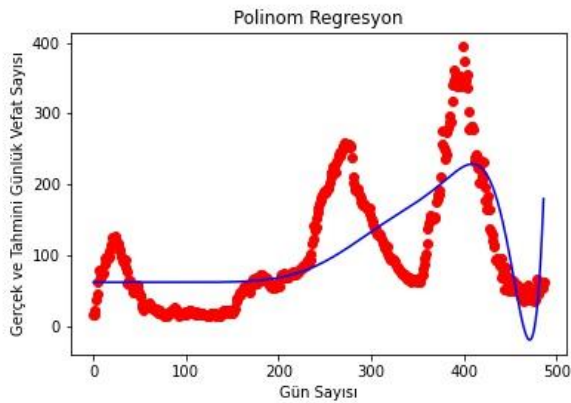
## 3.3. Vefat Sayısı Bulguları

Gerçekleşen günlük vefat sayısı verisinin grafiği Şekil 9’da gösterilmiştir. Değerlerin en yüksek olduğu günlerde 400 sınırını zorladığı ve eğrinin düzensiz bir karakteristiğe sahip olduğu gözlemlenmektedir. Günlük vefat verisi, toplam 487 gün için değerlendirilmiştir.

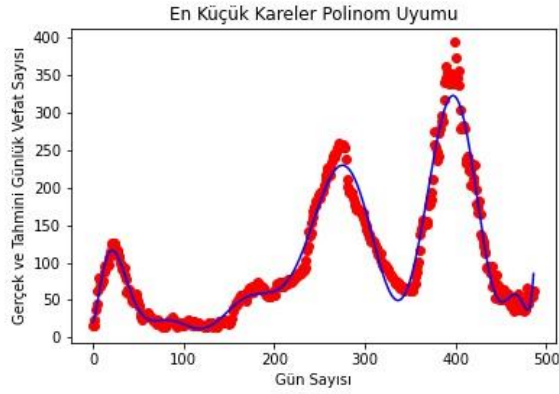


Şekil 9. Günlük vefat sayısı

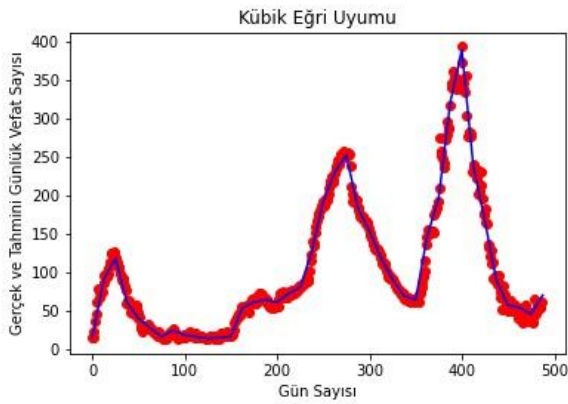
Polinom regresyon yöntemiyle tahminde ulaşılan sonuç Şekil 10’da gösterilmiştir. Kullanılan derece 15’dir. Gerçeğe yakın bir tahmin yapmak mümkün olmamıştır. Bunu karakteristiğinin aşırı değişkenliğine bağlamak mümkündür. En küçük kareler polinom uyumu ile elde edilen grafik, Şekil 11’de gösterilmiştir. Burada model derecesi, 17 seçilmiştir ve diğer çalışmalarla aynı şekilde, polinom regresyon tahmininden daha iyi sonuç elde edilmiştir. En büyük fark, iki en yüksek pik noktası civarındadır, ani düşüşlerde tahminde gecikme gözlenmektedir. Kübik eğri uyumunun sonucu Şekil 12’de gösterilmiştir. 487 veriden oluşan küme, 40 eşit parçaya ayrılarak, her parça üzerinde bir uyum oluşturmaya çalışılmıştır. Sonucun hem pik hem de dip noktalar dahil, önceki iki tahminden daha iyi olduğu görülmektedir, ayrıca gecikme sorunu ortadan kalkmıştır.



Şekil 10. Polinom regresyon ile günlük vefat tahmini



Şekil 11. En küçük kareler polinom uyumu ile tahmin



Şekil 12. Kübik eğri uyumu ile günlük vefat tahmini

Vefat tahmin çalışmalarını karşılaştırmak için, Canberra uzaklığı değerleri Tablo 3'te verilmiştir. Toplam uzaklık rakamı en düşük olan kübik eğri uyumu yaklaşımıdır ve bu durum, Şekil 12 ile uyum içindedir.

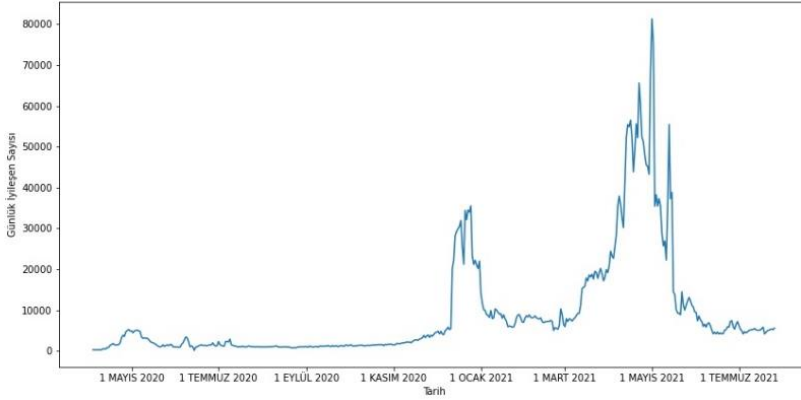
Tablo 3

Vefat tahmini sayısal performans karşılaştırması

Yöntem	Ortalama	Medyan	Standart Sapma	Toplam
Polinom regresyon	0.33	0.35	0.22	160.44
En küçük kareler polinom uyumu	0.07	0.06	0.06	35.55
Kübik eğri uyumu	0.31	0.25	0.22	12.27

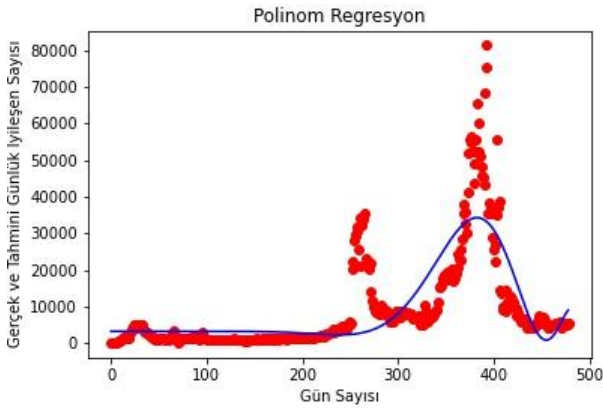
### 3.4. İyileşen Sayısı Bulguları

Gerçekleşen günlük iyileşen sayısı verisinin grafiği Şekil 13'te gösterilmiştir. Değerlerin en yüksek olduğu günlerde 400 sınırını zorladığı ve eğrinin düzensiz bir karakteristiğe sahip olduğu gözlemlenmektedir. Günlük vefat verisi, toplam 479 gün için değerlendirilmiştir.

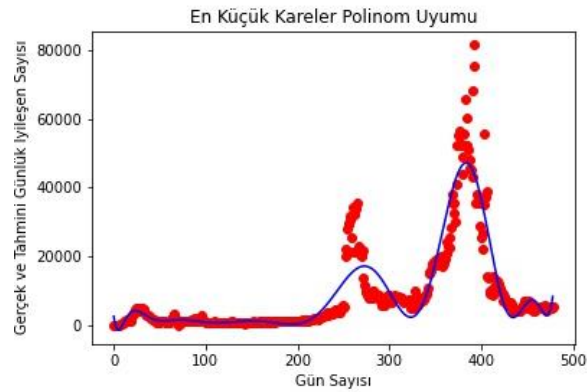


Şekil 13. Günlük iyileşen sayısı

Polinom regresyon yöntemiyle tahminde ulaşılan sonuç Şekil 14'te gösterilmiştir. Kullanılan derece 15'tir, ancak tıpkı vefat sayısında olduğu gibi, gerçeğe yakın bir tahmin yapmak mümkün olmamıştır. Bunu, benzer şekilde, karakteristiğın aşırı değişkenliğine bağlamak mümkündür. En küçük kareler polinom uyumu ile elde edilen grafik, Şekil 15'te gösterilmiştir. Burada model derecesi, ağır hasta tahmininde olduğu gibi, 17 seçilmiştir ve polinom regresyon tahmininden daha iyi sonuç elde edilmekle beraber, tatminkar olmaktan uzaktır. En büyük fark, pik noktaları civarındadır. Kübik eğri uyumunun sonucu Şekil 16'da gösterilmiştir. 479 veriden oluşan küme, 40 eşit parçaya ayrılarak, her parça üzerinde bir uyum oluşturmaya çalışılmıştır. Sonucun hem pik hem de dik noktalar dahil, önceki iki tahminden daha iyi olduğu görülmektedir.

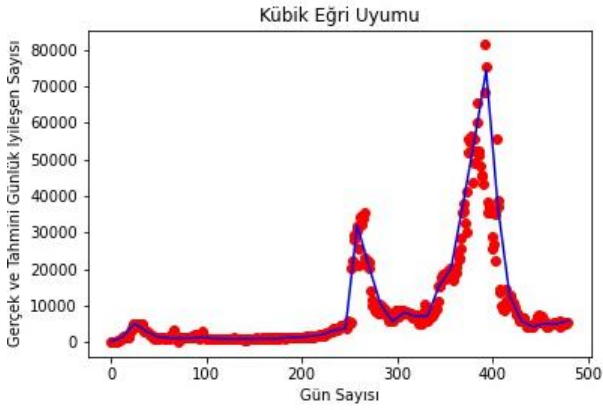


Şekil 14. Polinom regresyon ile günlük iyileşen tahmini



Şekil 15. En küçük kareler polinom uyumu ile günlük iyileşen tahmini





Şekil 16. Kübik eğri uyumu ile günlük iyileşen tahmini

İyileşen tahmin çalışmalarını karşılaştırmak için, Canberra uzaklığı değerleri Tablo 4’te verilmiştir. Toplam uzaklık rakamı en düşük olan, kübik eğri uyumu yaklaşımıdır ve sonuç, Şekil 16 ile uyum içindedir.

Tablo 4

İyileşen tahmini sayısal performans karşılaştırması

Yöntem	Ortalama	Medyan	Standart Sapma	Toplam
Polinom regresyon	0.45	0.44	0.22	215.74
En küçük kareler polinom uyumu	0.20	0.16	0.17	96.27
Kübik eğri uyumu	0.39	0.33	0.28	15.79

İncelenen zaman serilerinin birbirinden farklı yapısı dolayısıyla kullanılan modellerin dereceleri farklılıklar göstermektedir. Parametreler, karşılaştırma için kolaylık sağlaması açısından Tablo 5’te toplu halde gösterilmiştir. Tabloda görülen parametreler, benzetim çalışmaları sırasında optimize edilerek kararlaştırılmıştır.

Tablo 5

Kullanılan modellerin dereceleri

Zaman Serisi	Veri sayısı	Yöntem	Model Derecesi
Vaka sayısı	244	Polinom regresyon	10
		En küçük kareler polinom uyumu	18
		Kübik eğri uyumu	20
Ağır hasta sayısı	340	Polinom regresyon	8
		En küçük kareler polinom uyumu	18
		Kübik eğri uyumu	34
Vefat sayısı	487	Polinom regresyon	15
		En küçük kareler polinom uyumu	17
		Kübik eğri uyumu	40
İyileşen sayısı	479	Polinom regresyon	15
		En küçük kareler polinom uyumu	17
		Kübik eğri uyumu	40

Bu çalışmada, Türkiye’de meydana gelen Covid-19 vakalarının karakteristik yapısı anlaşılmasına çalışılmıştır. Zaman serilerinin incelenmesiyle, zaman içerisinde yayılımın oldukça karmaşık bir yapıyı takip ettiği anlaşılmıştır. Hiç kuşkusuz, gerek varyantların çeşitliliği, gerekse alınan önlemlerin etkisi, karakteristiklerin karmaşık yapısına katkıda bulunmaktadır. Karantina uygulaması, nispeten başlarda gündeme gelmiştir. Maske kullanımı ilk vakanın görülmesinden bir süre sonra başlamıştır. Aşı uygulaması, bundan aylar sonra gündeme gelmiştir. Ayrıca zaman zaman gerçekleşen tam ve kısmen kapanmaların etkisi de söz konusudur. Dolayısıyla, çalışmaya konu olan karakteristikler, sadece basit birer zaman eğrisi olmaktan öte, çok yönlü tıbbi ve sosyal olguları da temsil etmektedir. Değerlendirme bu düşüncelerin ışığında yapılmalıdır. Elbette ki, etki eden unsurlar ayrıştırılmaz ve birbirini doğrusal olmayan biçimlerde etkileyen özelliktedir.

Günlük vaka, ağır hasta, vefat ve iyileşen karakteristikleri birbirine benzememektedir. Bunları, 1, 5, 9 ve 13 numaralı şekillerden görmek mümkündür. Çalışmada kullanılan yöntemlerden kübik eğri uyumunun en iyi sonuçları verdiği görülmüştür. Bu çalışma veri karakteristikleri ile ilgili olarak gerçekleştirilmiştir, ancak karakteristiklere etki eden maske kullanımının zorunlu hale gelmesi, sokağa çıkma kısıtlamaları gibi unsurlar birer parametreye dönüştürülmemiştir. Bu konuların Ergül vd.’nin çalışmasında olduğu gibi (Ergül vd., 2020) ayrıca incelenmesi gerekmektedir.

#### 4. Sonuçlar

Bu çalışmada, Türkiye’de Covid-19 vakalarının karakteristik yapısı anlaşılmasına çalışılmıştır. T.C. Sağlık Bakanlığı tarafından yayınlanan günlük veri ışığında günlük vaka, ağır hasta, vefat ve iyileşen sayılarının veri karakteristiği incelenmiş, polinom regresyon, en küçük kareler polinom uyumu ve kübik eğri uyumu yöntemleri ile tahmin yapılmıştır. En iyi sonuç, uyum esnekliği ve verideki değişimleri takip etmeye yönelik olarak daha fazla sayıda parametre kullanması, dolayısıyla daha fazla serbesti derecesine sahip olması sebebiyle kübik eğri uyumu yaklaşımıyla elde edilmiştir. Canberra uzaklığının bu çalışmada anlamlı olup olmadığını saptayabilmek amacıyla, görsel olarak performansın yakın olduğu izlenimini yaratan günlük ağır hasta sayısına ilişkin ortalama mutlak yüzde hata hesaplanmıştır. Bu değer, en küçük kareler polinom uyumu için %4.37, kübik eğri uyumu için ise %2.20 olmuştur. Dolayısıyla ağır hasta günlük verisi için en iyi sonucun %97.8 başarı oranıyla kübik eğri uyumu tarafından elde edildiği sonucuna varılmıştır. Bu kıyaslama, Canberra uzaklığı hesaplarıyla uyum içindedir. Bundan sonraki çalışmada, bu çalışmaya konu olan dönemde gerçekleşen farklı sosyal olguların zaman serilerine etkileri incelenmeye çalışılacaktır. Bu şekilde daha az hata içeren tahminler yapılabilir. Bu yaklaşımda, hesaplama zamanının artacağı göz önünde bulundurulmalıdır. Sonuçta, benzer uygulamalarda harcanan çaba ve programın çalışması için gereken zamanın da elde edilen doğruluğa ek olarak, birer kritere dönüştüğü bilinmektedir. Ayrıca bir sonraki aşamada, başka ülkelerden örnekler seçilerek karşılaştırmalar yapılması hedeflenmektedir.

#### Yazar Katkıları

Figen Özen: Araştırmayı yapmış, veriyi ayıklamış, gerekli analizi, programların yazılmasını, değerlendirmelerin yapılmasını ve makalenin yazılmasını gerçekleştirmiştir.

#### Çıkar Çatışması

Yazar çıkar çatışması bildirmemiştir.

#### Kaynaklar

- Aggarwal, C. C. (2018). *Neural Networks and Deep Learning*. Springer.
- Akay, S. ve Akay, H. (2021). Time series model for forecasting the number of COVID-19 cases in Turkey. *Turkish Journal of Public Health*, 19(2), 140–145. doi:https://doi.org/10.20518/tjph.809201
- Al-wakeel, A., Wu, J. ve Jenkins, N. (2017). k -means based load estimation of domestic smart meter measurements. *Applied Energy*, 194, 333–342. Doi:https://doi.org/10.1016/j.apenergy.2016.06.046
- ArunKumar, K. E., Kalaga, D. V., Sai Kumar, C. M., Chilkoor, G., Kawaji, M. ve Brenza, T. M. (2021). Forecasting the dynamics of cumulative COVID-19 cases (confirmed, recovered and deaths) for top-16 countries using statistical machine learning models: Auto-Regressive Integrated Moving Average (ARIMA) and Seasonal Auto-Regressive Integrated Moving Averag. *Applied Soft Computing*,

- 103(December 2019), 107161. doi: <https://doi.org/10.1016/j.asoc.2021.107161>
- Badre, S. R. ve Thepade, S. D. (2016). Novel video content summarization using Thepade's sorted n-ary block truncation coding. *Procedia - Procedia Computer Science*, 79, 474–482. doi: <https://doi.org/10.1016/j.procs.2016.03.061>
- Bhadana, V., Jalal, A. S. ve Pathak, P. (2020). A comparative study of machine learning models for Covid-19 prediction in India. *IEEE 4th Conference on Information & Communication Technology (CICT)*. doi: <https://doi.org/10.1109/CICT51604.2020.9312112>
- Ergül, B., Yavuz, A. A., Aşık, E. G. ve Kalay, B. (2020). Dünya'da ve Türkiye'de Nisan ayı itibariyle COVID-19 salgın verilerinin istatistiksel değerlendirilmesi. *Anadolu Kliniği Tıp Bilimleri Dergisi*, 25(1), 130–141. doi: <https://doi.org/10.21673/adoloklin.719629>
- Ertel, W. (2017). *Introduction to artificial intelligence* (2nd ed.). Springer.
- Gambhir, E., Jain, R., Gupta, A. ve Tomer, U. (2020). Regression analysis of COVID-19 using machine learning algorithms. *2020 International Conference on Smart Electronics and Communication, Icosec*, 65–71. doi: <https://doi.org/10.1109/ICOSEC49089.2020.9215356>
- Gupta, V. K., Gupta, A., Kumar, D. ve Sardana, A. (2021). Prediction of COVID-19 confirmed, death, and cured cases in India using random forest model. *Big Data Mining and Analytics*, 4(2), 116–123. doi: <https://doi.org/10.26599/BDMA.2020.9020016>
- Harrell Jr., F. E. (2015). *Regression modeling strategies* (2nd ed.). Springer.
- Hazarika, B. B. ve Gupta, D. (2020). Modelling and forecasting of COVID-19 spread using wavelet-coupled random vector functional link networks. *Applied Soft Computing Journal*, 96, 106626. doi: <https://doi.org/10.1016/j.asoc.2020.106626>
- Karcıoğlu, A. A., Tanışman, S. ve Bulut, H. (2021). Türkiye'de COVID-19 bulaşısının ARIMA modeli ve LSTM Ağı Kullanılarak zaman serisi tahmini. 32, 288–297. doi: <https://doi.org/10.31590/ejosat.1039394>
- Koçak, M. (2020). A comparison of time-series models in predicting COVID-19 cases. *Türkiye Klinikleri Biyoistatistik Dergisi*, 12(1), 89–96. Doi: <https://doi.org/10.5336/biostatic.2020-75402>
- Kumar, N. ve Susan, S. (2021). Particle swarm optimization of partitions and fuzzy order for fuzzy time series forecasting of COVID-19. *Applied Soft Computing*, 110, 107611. doi: <https://doi.org/10.1016/j.asoc.2021.107611>
- Kumar, S., Rup, S. ve Swamy, M. N. S. (2021). An improved scheme for multifeature-based foreground detection using challenging conditions. *Digital Signal Processing*, 113, 103030. doi: <https://doi.org/10.1016/j.dsp.2021.103030>
- Kumari, R., Kumar, S., Poonia, R. C., Singh, V., Raja, L., Bhatnagar, V. ve Agarwal, P. (2021). Analysis and predictions of spread, recovery, and death caused by COVID-19 in India. *Big Data Mining and Analytics*, 4(2), 65–75. doi: <https://doi.org/10.26599/BDMA.2020.9020013>
- Kurniawan, R., Abdullah, S. N. H. S., Lestari, F., Nazri, M. Z. A., Mujahidin, A. ve Adnan, N. (2020). Clustering and correlation methods for predicting coronavirus COVID-19 risk analysis in pandemic countries. *2020 8th International Conference on Cyber and IT Service Management, CITSM 2020*. doi: <https://doi.org/10.1109/CITSM50537.2020.9268920>
- Leon, M. I., Iqbal, M. I., Azim, S. M. ve Al Mamun, K. A. (2021). Predicting COVID-19 infections and deaths in Bangladesh using machine learning algorithms. *2021 International Conference on Information and Communication Technology for Sustainable Development, ICICT4SD 2021 - Proceedings*, 70–75. doi: <https://doi.org/10.1109/ICICT4SD50815.2021.9396820>
- Mandayam, A. U., Rakshith, A. C., Siddesha, S. ve Niranjan, S. K. (2020). Prediction of Covid-19 pandemic based on Regression. *Proceedings - 2020 5th International Conference on Research in Computational Intelligence and Communication Networks, ICRCICN 2020*, 1–5. doi: <https://doi.org/10.1109/ICRCICN50933.2020.9296175>
- Phiri, C. C., Valle, C., Botzheim, J., Ju, Z. ve Liu, H. (2021). Fuzzy rule-based model for outlier detection in a topical negative pressure wound therapy device. *ISA Transactions*, 117, 16–27. doi: <https://doi.org/10.1016/j.isatra.2021.01.046>
- Ramchandani, A., Fan, C. ve Mostafavi, A. (2020). DeepCOVIDNet: An interpretable deep learning model for predictive surveillance of COVID-19 using heterogeneous features and their interactions. *IEEE Access*, 8, 159915–159930. doi: <https://doi.org/10.1109/ACCESS.2020.3019989>
- Rustam, F., Reshi, A. A., Mehmood, A., Ullah, S., On, B. W., Aslam, W. ve Choi, G. S. (2020). COVID-19 future forecasting using supervised machine learning models. *IEEE Access*, 8, 101489–101499.

- doi:<https://doi.org/10.1109/ACCESS.2020.2997311>
- Saxena, R., Kaur, S. ve Bhatnagar, V. (2019). Identifying similar networks using structural hierarchy. *Physica A*, 536, 121029. doi: <https://doi.org/10.1016/j.physa.2019.04.265>
- Sevli, O. ve Başer, V. G. (2020). Covid- 19 salgınına yönelik zaman serisi verileri ile Prophet model kullanarak makine öğrenmesi temelli vaka tahminlemesi. *European Journal of Science and Technology*. 19, 827–835. Erişim Linki:<https://dergipark.org.tr/en/pub/ejosat/issue/54511/766623>
- Singh, M. ve Dalmia, S. (2020). Prediction of number of fatalities due to Covid-19 using Machine Learning. *2020 IEEE 17th India Council International Conference, INDICON 2020*. doi:<https://doi.org/10.1109/INDICON49873.2020.9342390>
- T.C. Sağlık Bakanlığı. (2022). *Covid 19*. Erişim Linki:<https://covid19.saglik.gov.tr/TR-66935/genel-koronavirus-tablosu.html>
- Taşdelen, B. ve Yıldırım, D. D. (2020). Türkiye ' de COVID - 19 Vaka Sayılarının Poisson Regresyon ile Tahmini ve Alınan Önlemlerin İnsidans Hızı Tahminlerine Etkisi. *Türkiye Klinikleri Biyoistatistik Dergisi*, 12(3), 293–302. doi: <https://doi.org/10.5336/biostatic.2020-77595>
- Theodoridis, S. ve Koutroumbas, K. (2009). *Pattern Recognition* (4th Ed). Academic Press, Elsevier.
- Vakula Rani, J. ve Jakka, A. (2020). Forecasting COVID-19 cases in India using machine learning models. *Proceedings of the International Conference on Smart Technologies in Computing, Electrical and Electronics, ICSTCEE 2020*, 466–471. doi: <https://doi.org/10.1109/ICSTCEE49637.2020.9276852>
- World Health Organization. (2022). *Data Table*. <https://covid19.who.int/>
- Yang, Z. ve Chen, K. (2020). Machine Learning Methods on COVID-19 Situation Prediction. *Proceedings - 2020 International Conference on Artificial Intelligence and Computer Engineering, ICAICE 2020*, 78–83. doi: <https://doi.org/10.1109/ICAICE51518.2020.00021>
- Yudistira, N., Sumitro, S. B., Nahas, A. ve Riama, N. F. (2021). Learning where to look for COVID-19 growth: Multivariate analysis of COVID-19 cases over time using explainable convolution–LSTM. *Applied Soft Computing*, 109, 107469. doi: <https://doi.org/10.1016/j.asoc.2021.107469>
- Zhao, F., Gao, Y., Li, X., An, Z., Ge, S. ve Zhang, C. (2021). A similarity measurement for time series and its application to the stock market. *Expert Systems With Applications*, 182(November 2020), 115217. doi: <https://doi.org/10.1016/j.eswa.2021.115217>



## Group-Based Authentication Methods in The OneM2M Ecosystem

İbrahim Uğur Aba<sup>1,\*</sup>, Erhan Taşkın<sup>2</sup>

<sup>1</sup>Department of Computer Engineering, Faculty of Engineering, University of Turkish Aeronautical Association, Ankara, Türkiye

<sup>1</sup>Department of Artificial Intelligence Technology, Graduate School of Natural and Applied Sciences, Ankara University, Ankara Türkiye

<sup>2</sup>Cloud DevOps Architect at Afiniti, İstanbul, Türkiye

### Article History

Received: 09.12.2021

Accepted: 20.07.2022

Published: 15.12.2022

### Research Article


**Abstract** – The essential element of the Internet of Things (IoT) environment, the number of devices has traditionally exceeded the number of devices connected to the Internet. This situation is considered positive for the IoT concept but still has negative consequences. Undoubtedly, the most prominent and most important among these results is the security of the devices and the constructed IoT environment. Group-based authentication and authorization methods are crucial to ensure the safety of many IoT devices and the environment. In this study, the “auth” mechanism that performs group-based authentication and authorization processes, serving from the first moment when the devices in the IoT environment are included in the system until they leave the system, has been developed. In the development process of the “auth” mechanism, the Mobius IoT platform, which is evaluated as a golden sample by the oneM2M global organization and developed as an open-source code, is taken as the basis. The “auth” mechanism tested in three different test environments, including simulation, physical, and cloud environments, were tested using five different test scenarios. By using the group management module provided by the IoT service platform and the “auth” mechanism's together, it has been observed that the computational overhead on the devices and the signal traffic in the environment provide up to 4 times efficiency according to performance measurements. With the development of the “auth” mechanism with a flexible structure, it can be operated independently from the IoT server platform, allowing interoperability between oneM2M-based IoT server platforms.


**Keywords** – Group-based authentication, internet of things, oneM2M, open-source IoT server platform, security

## 1. Introduction

The internet of things (IoT) is a new network structure in which all devices are connected and may communicate with each other via the internet. IoT can be relevant for numerous application fields such as smart transportation, tourism service, medical treatment, energy management, and education (Su, Wong, & Chen, 2016). In addition to these, smart homes, smart cities, and smart production stand out as other important application areas. IEEE defines this notion as “A network of items - each embedded with sensors - which are connected to the Internet” (Define IoT, 2015).

The Gartner research business shows the current and near-future situation of the Internet of Things through several studies. A study done in 2019 anticipated that the number of terminal units utilized in the corporate and automobile industries would reach 5.81 billion in 2020. That number translates to an increase of 21 percent compared to the previous year. Also, it is noted in the report that the sector where the tremendous increase will be in-building automation with 42 percent (Gartner, Inc., 2019). In another study by research company Gartner done in 2018, 20 percent of institutions surveyed stated that 2015 to 2018 be exposed to at least one IoT-based cyberattack. Researchers believe that the expenditure made in 2018 to assure security in the IoT will reach 1.5 billion dollars, and by 2021 this amount will climb to 3.5 billion dollars (Gartner, Inc., 2018). The analysis conducted by the IoT analytics research organization published in November 2020 indicated similar results

<sup>1</sup>  ugur.aba@gmail.com

<sup>2</sup>  erhantaskin@gmail.com

\*Corresponding Author

with Gartner's investigations. The analysis found that despite the COVID-19 global pandemic's detrimental consequences, the IoT market continues to flourish and grow in 2020. The most interesting information revealed by the study was that for the first time in 2020, the number of IoT devices surpassed the number of devices that can typically connect to the Internet (computers, phones, tablets, etc.). At the end of 2020, it was anticipated that 11.7 billion of 21.7 billion active internet-connected devices world-wide, about 54 percent, will be IoT devices. It was also projected that the number of IoT devices would climb to 30 billion in 2025, and 4 IoT devices will be used per person according to the world population (IoT Analytics, 2020). In the study published by IoT Analytics in May 2022 and explaining the status of IoT in 2022, it was stated that terminal devices will increase by 18 percent and reach 14.4 billion end devices globally. While this supports the results of previous studies, it shows that the recovery in the IoT markets, where the chip shortage continues. In 2021, the number of global IoT connections increased by 8% to 12.2 billion active endpoints, a significantly lower rate than in previous years. Despite a surge in demand for IoT solutions and good attitude in the IoT community and most IoT end markets, IoT Analytics anticipates the chip shortage to have a long-term impact on the number of connected IoT devices. The ongoing COVID-19 pandemic and general supply chain interruptions are also challenges for IoT industries. The Internet of Things industry is estimated to expand 18% to 14.4 billion active connections by 2022. It is predicted that there will be around 27 billion linked IoT devices by 2025, as supply restrictions ease and demand increases (IoT Analytics, 2022).

The participation of so many IoT devices in the ecosystem poses numerous issues. In the study conducted by AIOTI, it was revealed that there are more than 100 protocol recommendations in 9 key categories (The Alliance for Internet of Things Innovation, 2019). The large amount of study and development on classical authentication and key agreement (AKA) and group-based AKA. The key objective of these research carried out is to perform mutual authentication and key exchange between end devices; It has been noticed as guaranteeing confidentiality and data integrity, and minimizing bandwidth usage, and defining the most efficient and uncompromising AKA method.

The earliest proposal of the group-based authentication and authorization strategy is the G-AKA technique (Chen, Wang, Chi & Tseng, 2010). In this protocol, a mobility management entity (MME) can authenticate additional end devices in the group using information comprising of authentication of the first end device. Thus, bandwidth usage for authentication for other end devices in the group has greatly lowered. However, it does not give a solution to the signal traffic that arises when several end devices wish to do authentication synchronously, which is vulnerable to the widely used man-in-the-middle (MitM) and denial-of-service (DoS) attacks. SE-AKA (Lai, Li, Lu & Shen, 2013) and EG-AKA (Jiang, Lai, Luo, Wang & Wang, 2013) have been presented, which are based on G-AKA and provide safety standards not found in G-AKA. Thus, the high computational burden due to asymmetric key operations attracts attention as the weak point of both protocols. The NOVEL-AKA protocol employs symmetric keys to lessen the computational cost, however it raises security difficulties (Lai, Li, Li & Cao, 2013). The GBAAM-AKA protocol proposes that to strengthen security in group-based AKA protocols (Cao, Ma & Li, 2015). However, the usage of asymmetric keys produces a high transaction burden and cannot secure privacy. PRIVACY-AKA employs asymmetric cryptography to provide secrecy (Fu, Song, Li, Zhang & Zhang, 2016). Although the protocol is robust to assaults, it creates a significant processing burden and does not offer forward and backward privacy. GLARM-AKA protocol has been designed to decrease the computational and communication overhead; protocol beneficial for resource-constrained end devices; It is not effective in terms of impersonation attack and privacy protection (Lai, Lu, Zheng, Li & (Sherman) Shen, 2016). The GR-AKA protocol has been suggested to assure security and privacy (Li, Wen & Zheng, 2016).). The sophisticated and time-consuming Lagrange Multiplier (LC) is employed in the GR-AKA protocol. GBS-AKA protocol, which is resistant to assaults and lowers the communication burden (Yao, Wang, Chen, Wang & Chen, 2016). However, the technique is subject to preserving secrecy, impersonation, and DoS attacks. The SEGB-AKA method has been suggested to strengthen the security of group-based protocols (Parne, Gupta & Chaudhari, 2018). However, the protocol cannot give protection against DoS assaults. GSL-AKA protocol, which has the same structure as GBS-AKA and SEGB-AKA, has been suggested by developing features (Modiri, Mohajeri & Salmasizadeh, 2018). It is noted that it successfully overcomes recognized security and non-security challenges while protecting the secrecy of end devices and groups.

The study, published in 2019 by Şahinaslan, looked at encryption technologies for protocols used on the internet of things. The article explains the Markov Chain and RSA asymmetric encryption approach for wireless IoT devices. The MAC session key provides cryptographic control over the information while also providing security against potential attacks. The paper also explains how to avoid the KRACK vulnerability

that happens during the key exchange phase by employing the DragonFly key exchange mechanism (Şahinaslan, 2019). Aydın et al. propose a lightweight Group authentication system (GAS) that significantly reduces device energy consumption, saving more than 80% when compared to state-of-the-art alternatives. Their approach is also resistant to replay and man-in-the-middle attacks. In mMTC situations, the proposed approach also tackles key agreement and key distribution concerns. That solution is also useful in both centralized and decentralized group authentication scenarios. The proposed solution can meet the rapid authentication requirements of the envisioned agile 6G networks, which will be supported by aerial networking nodes (Aydın et al, 2020). Padmashree et al. suggested Group Key Exchange and Authentication with Elliptic Curve Cryptography (ECC), or GKEAE for short, on the Internet of Things to establish safe key distribution and improve security. When an IoT device joins or leaves a group, ECC is used for authentication. Integrating access authentication and data transfer improves the serviceability of IoT devices. The GKEAE delivers a faster group key distribution computation time than the quick authentication system (Padmashree et al, 2022).

Suggesting different protocols for each application area and not settling on one protocol produces a highly undesirable standardization situation. To define technical standards for architectural structure, API, and security solutions in M2M and IoT technologies, in 2012, the world's main standardization authorities joined together to form an organization named OneM2M. OneM2M foundation represents nearly 200 enterprises and universities. The OneM2M standard offers a basic horizontal platform design based on a three-tier paradigm of applications, services, and networks (OneM2M, 2012).

Mobius, an open-source IoT service platform, was created by the Korean Electronic Technologies Institute (KETI, 1991), a member of the OneM2M organization, as part of an open alliance for IoT standard (OCEAN) investigations. Mobius IoT service platform gains notice by becoming the first application to acquire a oneM2M compliance certificate. It is also used as a gold sample to evaluate test cases and test systems. Mobius presents common service functions (CSF) as middleware for multiple service areas to IoT applications (IoT OCEAN, 2017).

In this study, based on the Mobius IoT service platform, a “auth” mechanism has been designed that executes group-based authentication and authorization operations from the moment the IoT devices in the IoT environment joined the ecosystem until they exit the system. The “auth” process has been evaluated in three separate test contexts: simulation, physical, and cloud environments. In the test scenarios, the benefit of the “auth” method with the group-based authentication procedure was examined. According to the results obtained by testing the “auth” mechanism using five different test scenarios in three different test environments, the computational overhead on the nodes and the signal traffic in the IoT environment have been significantly reduced by running the mechanism together with the group management module provided by the IoT service platform. It has been established that the proposed “auth” method contributes 1ms computational overhead to the IoT service platform, delivering an optimal benefit between 2 and 25 IoT devices and providing up to 4 times efficiency.

## 2. Materials and Methods

This section outlines the tools and apps utilized in the study. The environment produced by the introduction of open-source software and the enhancements made to it is presented in the architectural design. In addition, information about the methods used in the test scenarios on the generated environment is presented.

### 2.1. Open-Source Applications

#### 2.1.1. Mobius IoT Server Platform

Mobius is an open-source IoT server platform based on the oneM2M standards developed by KETI as part of OCEAN studies. Mobius provides CSFs (enrollment, data management, subscription/notification, security) middleware for IoT applications of different service domains. Mobius can successfully connect oneM2M-compatible and non-oneM2M-compatible devices. Within the global oneM2M organization, Mobius has been awarded the “oneM2M compliance certificate” by Telecommunications Technology Association (TTA). This certification guarantees that Mobius meets the oneM2M specifications and testing requirements that ensure interoperability with oneM2M products. As it is the first application to receive oneM2M certification, it is used as a gold example for validating test scenarios and test systems (IoT OCEAN, 2017).

### Functional Architecture of the Server Platform

The Mobius IoT server platform created by KETI is architecturally based on the OneM2M functional reference architecture stated in the document named “TR-0025 Application Developer Guide” issued with version 2A of the OneM2M global organization (TR-0025 Technical Report, 2018).

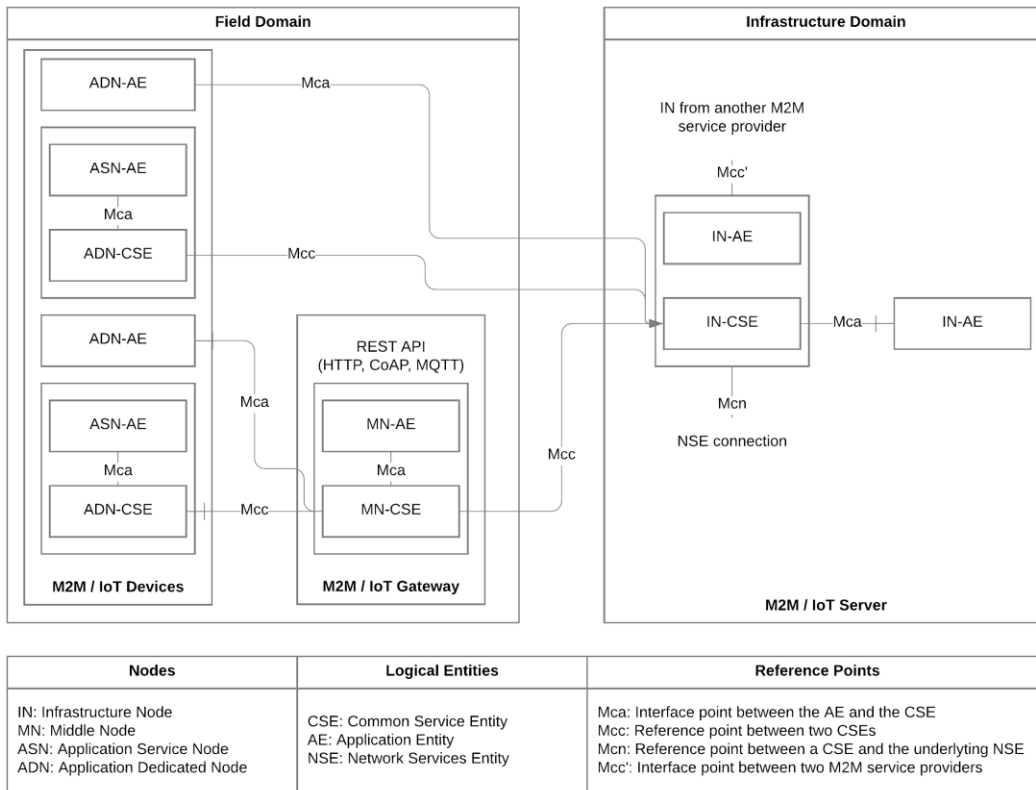


Figure 1. Functional architecture of the IoT server platform (Kim, Choi, Yun & Lee, 2016).

As shown in Figure 1, the oneM2M architecture divides M2M and IoT environments into two different domains (Field Domain and Infrastructure Domain). It defines four different node types for use in these domains. An IN (infrastructure node) can exist in the infrastructure domain of any M2M (machine-to-machine) service provider, while any oneM2M node group, including MN (middle node), ASN (application server node), and ADN (application dedicated node), even non-oneM2M nodes can exist in the field domain.

### Improvements on the IoT server platform

The Mobius IoT server platform created by KETI is architecturally based on the OneM2M functional reference architecture stated in the document named “TR-0025 Application Developer Guide” issued with version 2A of the OneM2M global organization (TR-0025 Technical Report, 2018).

The IoT service platform leverages access control policies (ACP) under oneM2M standards for authorization processes in security operations (TS-0001 Technical Specification, 2016). However, it does not give a solution for authentication processes. In this method, when a common service entity (CSE) seeks to access a resource in a working structure, it is sufficient to conduct merely ACP's. The fact that the element that attempts to get access during the creation of a new resource or accessing an existing resource does not perform the authentication process puts the system open to possible attacks.

Within the scope of the study, the “auth” mechanism, which will conduct the operations of two fundamental categories (Identification and Authentication, Authorization) for the “Security Functions Layer” of the oneM2M security architecture, has been created (TS-0003 Technical Specification, 2018). Passport.js (Passport.js) and jsonwebtoken (RFC7519) libraries are used for authentication and authorization operations as it is suitable with the IoT service platform created in the Node.js working environment using the JavaScript dynamic programming language. In the created “auth” method, MongoDB is used independently from the MySQL database used by the IoT service platform (MongoDB). The usage of a distinct database management



system permitted flexibility in the IoT network structure to be established. It was also feasible to establish a separate server that could execute authentication and authorization operations.

The “auth” method was created with group-based authentication and authorization operations in mind. Accordingly, when a group administrator initially authenticates, the system creates a token value that other members of the group can use for a limited period. By using this token value, which is specified as a Group Common Key (GCK), other members of the group can be added to the system avoiding the authentication stage if the GCK information is valid. After the validity of the produced token value expires, the group administrator must execute an authentication procedure again. The jsonwebtoken (RFC7519) library is used to construct the token structure that executes the GCK job.

Table 1  
Comparison of OneM2M Token Structure and Generated Token Structure

OneM2M Token Structure	Generated Token Structure	Description
version	keyID	Token version
tokenID	jwtID	Token unique id
holder	subject	The ID of the token holder
issuer	issuer	The ID of the token issuer
notBefore	notBefore	The token is valid from this moment
notAfter	expiresIn	The token expires after this moment
tokenName	header	Token name (optional)
audience	audience	CSE’s ID list (optional)
permissions	-	Associated permissions
extension	-	Application-specific information

The generated token value is supplied in the header named “authorization” which is appended to HTTP requests according to the format provided in the document named oneM2M “TS-0009 Protocol Binding” (TS-0009 Technical Specification, 2016).

Table 1 explains the token structure specified in the technical specification of oneM2M TS-0003 and the attributes used in the generated token structure. The generated token value is for sending in HTTPS requests.

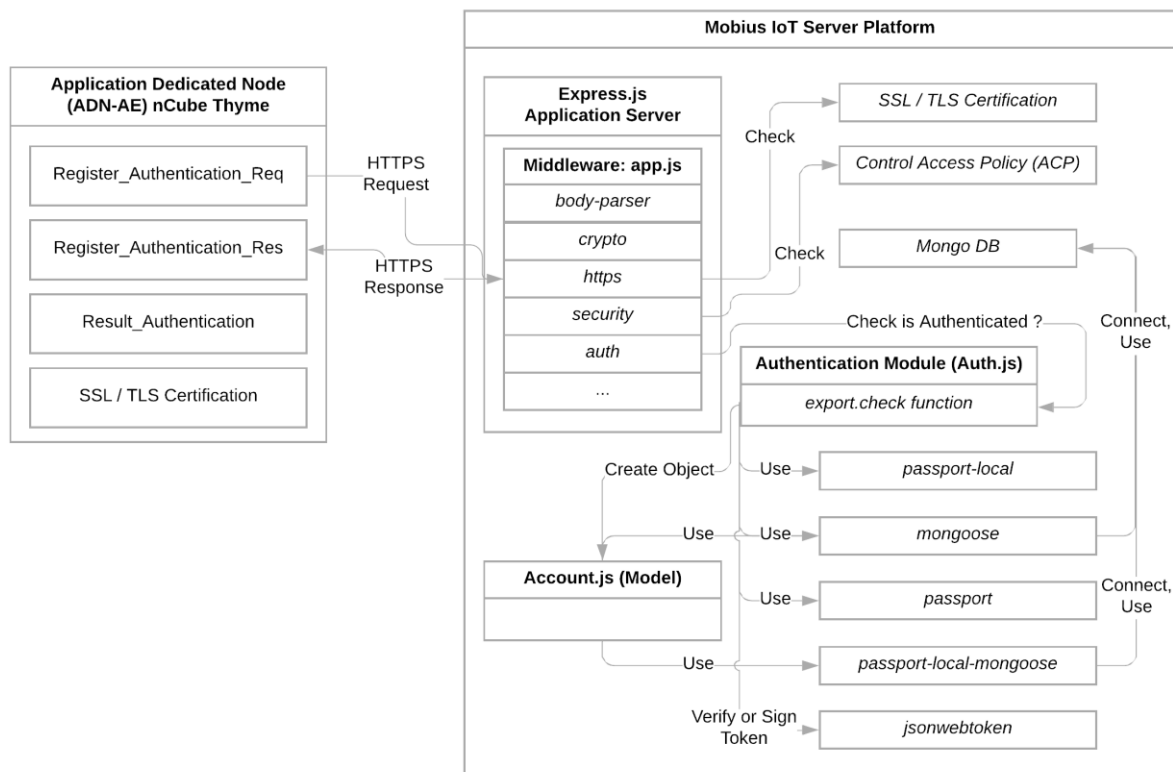


Figure 2. The architectural design of the IoT service platform after the inclusion of the auth mechanism.

To increase security, all sent and received HTTP requests must be transmitted over a secure channel. Therefore, the HTTPS protocol is for communication between the nodes in the field domain and IN. The architectural design formed after the operations performed on Mobius is shown in Figure 2.

The established “auth” method must not compromise the IoT platform's compliance with oneM2M requirements. For this reason, the token structure developed must also conform with the criteria described in the paper published by the worldwide oneM2M organization, named “TS-0003 Security Solutions”. Accordingly, a token is for carrying authorization information, which can be roles given to the owner or ACPs valid for the owner (TS-0003 Technical Specification, 2018).

### 2.1.2. nCube

The nCube is specified as the general name of the nodes in the field domain, based on the oneM2M standards created by KETI within the framework of OCEAN research. Developed as open source, the nCube program contains five different versions (Rosemary, Thyme Node.js, Lavender, Thyme Arduino, Thyme Java) that may operate as three separate oneM2M node structures. Within the scope of this investigation, the first three node types were employed. The nCube Rosemary is an open-source IoT gateway platform based on oneM2M standards.

The nCube Rosemary application, used to deliver proximity based IoT services, gives CSFs to oneM2M apps and other oneM2M devices. Serving as the MN-CSE, nCube Rosemary also supports interoperability services using interworking proxy application entity (IPE), as stated in the oneM2M standards. It links to IN-CSE utilizing CSEs in ASN and ADNs, which are additional nodes in the field domain (nCube-Rosemary, 2018). The nCube Thyme is an open-source IoT device application element based on oneM2M standards. Thyme has three separate versions: node.js, java, and android. Node.js version is employed within the scope of this study. The nCube Thyme application may be linked to MN-CSE or IN-CSE (nCube-Thyme, 2018). The nCube Lavender is also an open-source IoT device platform based on oneM2M standards. The nCube Lavender, one of the oneM2M platforms, delivers CSFs to oneM2M device apps operating on the same device (nCube-Lavender, 2018). In this sense, although it is comparable to the nCube Rosemary application, nCube Rosemary acts as an MN in the oneM2M domain, whereas the nCube Lavender application serves as an ASN.

### Improvements on the nCube application

Several provisions have been made for the nCube application to function in harmony with the “auth” mechanism created on the IoT service platform. These arrangements are based on the nCube Thyme application and the “auth\_usr” and “auth\_pwd” headers have been added to the HTTPS request submitted for registration to the “auth” mechanism. In addition, the IoT service platform is alerted that the “auth” mechanism established by the title “use auth” has the value of “enable”. If the title “auth\_useprotocol” is provided as “local”, the system applies the authentication processes using the information on the MongoDB. If a group header also known as administrator will establish a connection with the “auth” mechanism for the first time, while transmitting the above-mentioned “auth\_usr” and “auth\_pwd” headers, the other members of the group will use to token value created by the “auth” mechanism, which is used as GCK, by the TS-0009 technical specification under the “authorization” heading (TS-0009 Technical Specification, 2016).

## 2.2. Test Environments

In the study, three distinct environments are built by employing the IoT service platform, in which the “auth” method is integrated. Performance measurements were done on equipment with varying technical parameters.

### 2.2.1. Simulation Environment

A simulation environment has been constructed to assess the performance of the “auth” method on hardware with restricted resources. Oracle VM VirtualBox program, a free and open-source hypervisor created by Oracle, was used to construct the virtual environment used. The technical parameters of the virtual machines utilized instead of the nodes in the oneM2M IoT ecosystem in the simulation environment are provided in Table 2.

Table 2

Technical Specifications of Machines in the Simulation Environment

Machine Name	CPU	RAM	Storage	Operating System
IN-Mobius	2 Virtual Cores	2048 MB	20 GB SSD	Ubuntu 20.04 (64-bit)
MN-Rosemary	2 Virtual Cores	2048 MB	20 GB SSD	Ubuntu 20.04 (64-bit)
ASN-Lavender	1 Virtual Core	2048 MB	20 GB SSD	Ubuntu 20.04 (64-bit)
ADN-AE-Thyme	1 Virtual Core	1024 MB	20 GB SSD	Ubuntu 20.04 (64-bit)
JMeter Xubuntu	2 Virtual Cores	2048 MB	20 GB SSD	Ubuntu 20.04 (64-bit)

The technical specifications of the computer, which runs virtual machines throughout the development phase, include Intel Core i7-5600U 2.60 GHz CPU, 8 GB RAM, 64-bit Windows 10 Pro operating system, and 500 GB SSD. While developing the “auth” method, the Postman program was used to transmit HTTPS requests from the host system to virtual machines and to execute unit tests. A NAT network has been setup in the Oracle VM VirtualBox program to correctly conduct HTTPS requests.

### 2.2.2. Physical Environment

In the simulation environment, test scenarios were achieved by allocating restricted resources to virtual computers with nodes and IoT service platforms. In the physical environment experiments, a laptop computer with technical characteristics that can function as an MN in the oneM2M IoT ecosystem and a desktop computer with technical capabilities that can work as an IN was utilized. The technical parameters of the physical devices utilized instead of the nodes in the oneM2M ecosystem in the physical environment are presented in Table 3.

Table 3

Technical Specifications of Machines in the Physical Environment

Machine Name	CPU	RAM	Storage	Operating System
MN-Windows	Intel i7 5600U	8 GB	500 GB SSD	Windows 10 (64-bit)
IN-Mobius	AMD FX-8320	32 GB	256 GB SSD	Ubuntu 20.04 (64-bit)

The machine named MN-Windows is in Lapseki, Çanakkale, whereas the machine called IN-Mobius is located in Kepez, Çanakkale. There is around 40 KM between the two mentioned locations. To perform the test scenarios, a test program named Postman was installed on the MN-Windows machine and the tests were run.

### 2.2.3. Cloud Environment

To test the established “auth” technique in the cloud context, an EC2 is built on Amazon Web Services (AWS). The built EC2 machine is picked in t2.large type, us-east-1e region, and North-ern Virginia location, and the IoT service platform is deployed and served. The technical parameters of the physical and virtual computers utilized instead of the nodes in the oneM2M ecosystem in the cloud environment are provided in Table 4.

Table 4

Technical Specifications of Machines in the Cloud Environment

Machine Name	CPU	RAM	Storage	Operating System
MN-Windows	Intel i7 5600U	8 GB	500 GB SSD	Windows 10 (64-bit)
IN-Mobius-EC2	Intel Xeon 2 vCPU	8 GB	20 GB EBS	Ubuntu 20.04 (64-bit)

HTTPS requests are made to the IoT service platform on the virtual machine name IN-Mobius-EC2 with IP number 54.227.195.58 utilizing the virtual private cloud (VPC) on the physical machined called MN-Windows. The HTTPS requests made from the MN-Windows computer is moved to the VPC when it reaches the internet gateway on AWS. Considering the security information, the HTTPS requests are sent to the EC2 machine with the t2.large type IoT service platform in the private subnet via the NAT gateway.

## 2.3. Testing Tools

### 2.3.1. Postman

During the creation of the “auth” mechanism, the Postman program was utilized to execute unit tests (Postman API Platform). During the testing utilizing Postman version 7.27.0, nCube open-source apps were emulated and operations were carried out on the IoT service platform. A collection of all HTTPS requests performed for unit testing of the “auth” method has been built.

### 2.3.2. Apache JMeter

In the study, Apache JMeter v5.3 application was utilized to assess the efficiency offered by the developed “auth” method (Apache JMeter). The test application was executed on the virtual machine named “JMeter Xubuntu” defined in the simulation environment section. The test application took part in various test scenarios as a group administrator or group member, which formed the foundations of the group-based authentication and authorization framework.

## 3. Results and Discussion

In this part, five distinct test situations in which we tested the “auth” method will be explained. Then, three distinct test methods that we devised utilizing these situations will be discussed. Finally, the outcomes seen in the test situations will be compared and assessed using the defined test methodologies.

### 3.1. Test Scenarios

#### 3.1.1. Test Scenario 1: Determination of Core Values

In the technical standard named TS-0003 issued by oneM2M, the methods to be given for authentication and authorization are outlined. In addition, the IoT service platform, which is described as the golden example by oneM2M and produced by KETI, has been built by TS-0003 and other technical specifications released by oneM2M. In the technical specification designated TS-0003, it is recommended to employ ACPs for security and authorization processes (TS-0003 Technical Specification, 2018).

Since the IoT service platform is established by the given technical standards, no separate authentication and authorization module has been developed on the platform. In circumstances when ACP and the “auth” method are not employed, there is no security mechanism on the IoT service platform. The “auth” mechanism has been designed as a module that is meant to be used together with the ACP mechanism, not as a substitute for the ACP mechanism.

To estimate the contribution of the “auth” mechanism, which provides group-based authentication and authorization, the default results should be calculated as fundamental values. At this point, fundamental values were measured by deactivating the group feature of the “auth” mechanism produced owing to the absence of an authentication and authorization module operating on the IoT service platform.

In the test scenario carried out, the application entity (AE) registration request of the node units was issued, rising in floating slices between 100 up to 1000. The “auth” method, designed with each HTTPS request delivered independently, is offered to execute authentication and authorization. The outcomes when test case 1 is executed in the simulation, physical, and cloud settings are presented in Table 5, accordingly.

Table 5  
Results of Test Scenario 1

# Of nodes	Simulation Environment			Physical Environment			Cloud Environment		
	Avg. (ms)	Min. (ms)	Max. (ms)	Avg. (ms)	Min. (ms)	Max. (ms)	Avg. (ms)	Min. (ms)	Max. (ms)
100	975	844	2104	504	468	2382	1029	982	1649
200	897	822	2157	486	457	2335	1047	980	1605
300	909	832	2049	495	466	2933	1105	982	2797
400	1088	834	2020	483	459	2120	1115	981	2957
500	1021	818	2565	492	467	2756	1048	979	1723
600	1111	826	2530	481	455	2395	1072	978	2612
700	1115	838	2315	478	457	2266	1142	979	6336
800	1120	926	2581	480	458	2555	1078	988	4568
900	1138	929	2338	478	458	2279	1017	978	2154
1000	1111	821	2318	477	455	2248	1036	983	1463

According to the results of test scenario 1, where the core values were determined, the operation of the “auth” mechanism for the first HTTPS request sent when the IoT service platform was started for the first time and the response time of the platform to the request create the maximum value for each test. It is shown that the number of nodes employed in the functional design of the oneM2M ecosystem is directly related to the hardware on which the IoT service platform is operating and will cease to be stable if it is more than a specific quantity.

### 3.1.2. Test Scenario 2: Single Retrieve of CIN Source

A key benefit of group-based authentication and authorization procedures with the group management module is that activities may be conducted on many resources by submitting a single HTTPS request. To notice this benefit, a core data set should be constructed identical to the prior test case. In this test scenario, it is targeted to provide the <ContentInstance> resources described with the abbreviation CIN in the oneM2M ecosystem to the nodes that make the request from the IoT service platform. The CIN resource represents the resources containing application-specific data generated in cooperation with the oneM2M ecosystem.

There are varied numbers of sensors and nodes in apps created to function in the IoT ecosystem. In the research done to examine the performance gain offered by group-based authentication and authorization procedures in the IoT ecosystem, it was established that the most ideal outcome was the construction of 100 groups in an IoT ecosystem with 500 nodes (Su, Wong & Chen, 2016).

Considering the findings of the research indicated in the previous paragraph, the fact that the number of nodes creating a group is between 100 and 1000, rather than between 1 and 100, is in keeping with the applications created for the IoT environment. Considering this information, the number of nodes in the test scenario was determined as 1, 2, 3, 5, 10, 25, 50, 70, 90, and 100. The outcomes when test case 6 is executed in the simulation, physical, and cloud settings are presented in Table 6, correspondingly.

According to the results of test scenario 2, which was carried out in the simulation environment and where the CIN resource was retrieved individually without using group management, an irregular increase was observed in the maximum values obtained after the test using 25 nodes, as indicated by the column representing the maximum value. Although the average and minimum values do not reach the ideal values more than 25 nodes submit single HTTPS requests to result in the IoT service platform delivering irregular results.

Table 6  
Results of Test Scenario 2

# Of nodes	Simulation Environment			Physical Environment			Cloud Environment		
	Avg. (ms)	Min. (ms)	Max. (ms)	Avg. (ms)	Min. (ms)	Max. (ms)	Avg. (ms)	Min. (ms)	Max. (ms)
1	100	100	100	282	282	282	712	712	712
2	84	66	102	147	66	229	459	186	733
3	89	43	170	111	62	210	357	180	711
5	75	34	144	91	58	216	292	184	723
10	50	30	124	75	57	212	248	190	752
25	49	30	103	62	52	200	207	183	730
50	53	15	342	57	49	197	203	190	755
70	45	20	126	54	49	185	196	183	730
90	44	16	248	55	46	204	196	185	738
100	36	15	102	54	50	205	189	182	743

In the test scenario established in the physical environment, it is apparent that there is an increase owing to network latency when the results are analyzed despite the increase in CPU power. When the average values of the results achieved in the simulation environment and the results obtained in the practical environment are compared, an increase in the range of 15–20ms was seen in the test cluster with more than 5 nodes. Considering that these values are caused by network delay, it has been proved that the IoT service platform operates reliably in both scenarios. When the findings are reviewed independently of the network latency, irregular results have been created after the test in which the number of 25 nodes is employed when the values acquired are executed on a virtual machine with restricted processing capacity in the simulation environment. However, it has been noticed that the results produced by operating the IoT service platform on hardware that is used in the actual world and has higher processing power, continue to be stable up to 100 nodes. In the test scenario done in the cloud environment, it was found that the efficiency fell, and the results rose owing to the variables such as

shared EC2 usage and network latency. When the data were evaluated, it was revealed that the efficiency reduced by 4 times compared to the results in the physical environment. The findings acquired in the minimum column coincide with the values in the maximum column obtained in the test scenario in the physical environment. Considering this condition, it should be recognized that the technical characteristics of the EC2 machine used in the cloud environment are raised and the efficiency will rise if it approaches the test machine that hosts the IoT service platform in the test scenario used in the physical environment.

### 3.1.3. Test Scenario 3: Group-Based Authentication and Authorization

The group feature of the “auth” mechanism produced in this test scenario has been enabled to measure the benefit offered by the “auth” mechanism designed for group-based authentication and authorization procedures and to compare it with the findings in test scenario 1. The test scenario 3 carried out is based on the G-AKA research, which is considered as the beginning of group-based authentication and authorization processes. According to the G-AKA research, a group authentication key (GAK) information is created when the administrator knew the header of the group enrolled in the system completes a full authentication and authorization procedure. After the GAK information is established is shared with the other members of the group through the group header. Other members of the group can be located and processed on the system utilizing this information (Chen et al., 2012).

The GAK information produced as a result of a full authentication authorization process of the group header was sent to the IoT service platform by the group members under the "authorization" heading of the HTTPS package transmitted over a secure channel, as specified in the TS-0009 technical specification published by oneM2M, in the test, based on the number of nodes specified in test scenario 1 (TS-0009 Technical Specification, 2016).

Table 7

Results of Test Scenario 3

# Of nodes	Simulation Environment			Physical Environment			Cloud Environment		
	Avg. (ms)	Min. (ms)	Max. (ms)	Avg. (ms)	Min. (ms)	Max. (ms)	Avg. (ms)	Min. (ms)	Max. (ms)
100	30	15	165	69	59	250	204	195	749
200	26	13	139	62	50	332	206	197	749
300	22	11	113	78	61	277	205	195	779
400	21	10	103	64	59	264	209	192	809
500	20	9	98	67	61	263	205	193	856
600	19	9	81	68	59	301	197	189	758
700	19	7	98	66	60	231	204	189	798
800	19	9	101	69	59	363	203	189	832
900	20	8	150	66	59	364	200	191	774
1000	22	8	307	66	58	377	203	189	842

In the executed test scenario, AE registration requests were issued utilizing the group resources produced by the nodes, increasing in floating slices between 100 and 1000. The findings when test case 3 is executed in the simulation, physical, and cloud settings are presented in Table 7, accordingly.

In the executed test scenario, AE registration requests were issued utilizing the group resources produced by the nodes, increasing in floating slices between 100 and 1000. The results reported in Table 7 do not contain the values of the HTTPS request, in which full authentication and authorization are made by the group header. As noted in Table 7, optimal values have been attained in the operations performed over the group resource consisting of 600, 700, and 800 nodes. According to the findings of the test scenario established in the physical environment, which is described in detail in Table 7 and indicates the maximum values, is examined, it is seen that the maximum value occurs in the initial HTTPS request issued for each test owing to network delay. When the results in the physical environment and the results in the simulation environment are compared, it is notable that the average values created in the physical environment and the average values formed in the simulation environment rise by two or three times. Considering that the IoT service platform tries to minimize the difference between the processing power and the processing power of the hardware on which it works in the physical environment, and the distance between the client and server pair in the physical is approximately 40 KM, it is thought that the difference is due to network latency. Likewise, the findings of the test scenario performed in the cloud environment agree with the results of the actual environment. In the test scenario outlined in Table

7, average values were measured in the range of 197-209ms. In addition, the average and lowest values established created a 10 percent gap between themselves, comparable to those in the actual world.

### 3.1.4. Test Scenario 4: Retrieving CIN Resource Using Group Resource

The group management CSF is responsible for group-related operations. HTTP or HTTPS request is issued for batch actions such as reading, writing, subscribing, notification, device management enabled by the group, as well as controlling a group or its member. Group administration is responsible for gathering group answers and alerts when a request or subscription is made through the group (TS-0001 Technical Specification, 2016).

The designed “auth” mechanism provides authentication and authorization processes in all operations done on the IoT service platform, starting from the time the nodes are included in the system and during the full process, they are in system. In the test scenario where the group management module offered by the IoT platform, which was developed by the group management features specified in the technical specification named TS-0001 published by oneM2M, is used, it is aimed to call the previously created daemon resources using a single HTTPS request.

To assess the benefit offered by the group management and the “auth” mechanism, test scenario 4 was carried out based on the identical node counts as the previous test scenario 2. Accordingly, the efficiency offered by the “auth” method and group management was seen in the test scenario employing group resources consisting of 1, 2, 3, 5, 10, 25, 50, 70, 90, and 100 nodes, respectively.

Table 8  
Results of Test Scenario 4

# Of nodes	Simulation Environment, Time Elapsed (ms)	Physical Environment, Time Elapsed (ms)	Cloud Environment, Time Elapsed (ms)
1	122	118	217
2	107	161	242
3	200	204	247
5	280	232	278
10	579	353	341
25	840	681	532
50	2120	1185	1006
70	2662	1450	1142
90	3590	1876	1445
100	3554	2033	1476

The results when test case 4 is run in the simulation, physical, and cloud environments are shown in Table 8, respectively.

According to the findings of test scenario 4, when the CIN resource is obtained collectively utilizing group management, the most efficient results were reached in the test phase carried out on a single group re-source in which 25 nodes were included as indicated in Table 8. The findings obtained in instances where group resources with more than 25 nodes are included offer efficiency compared to the case where the group management module is not employed, but the efficiency supplied by the growth in the number of nodes is seen to be inversely proportional. According to the findings of test scenario 4 performed in the simulation environment, efficiency cannot be attained in the test set if a group resource consisting of one node is employed. The lowest number of nodes that a group resource is efficient is determined to be 2. It has been observed that the optimum conditions in the results obtained with the growth in the processing capacity of the hardware employed in the physical environment compared to the simulation environment have altered. As the processing power of the actual hardware rises, the efficiency given by the established “auth” mechanism increases in direct proportion. When the column, which is presented in Table 8 and represents the time taken for the process, is inspected, it is apparent that the benefit offered by the mechanism starts with the test set consisting of 2 nodes and gives the optimal level of efficiency up to the test cluster in which 50 nodes are employed. However, although the efficiency given by the “auth” mechanism is de-creasing, it remains to be evident in the test set consisting of 100 nodes. In the fulfillment of the test scenario, which was produced utilizing the group management of the previously constructed CIN resources, on the cloud environment, the results were acquired in a way that verifies the values received from the prior two settings.

As observed in the test results performed in the physical environment, it has been observed that the “auth” mechanism and the group management module developed from the group resource using 2 nodes to the group resource with 50 nodes, and the group management module, are similarly efficient at the optimum level in the

test conducted in the cloud environment. However, the benefit given declines when more than 50 nodes are employed, as in the actual environment. According to the data provided in Table 8, the resultant times rise in direct proportion to the number of nodes. In group resources where more than 50 nodes are employed, forming more than one group by splitting the nodes that make up the groups allows the efficiency offered by the group module and the “auth” method to be delivered at the optimal level.

### 3.1.5. Test Scenario 5: Computational Overhead of Auth Mechanism

It is of considerable importance that the established “auth” mechanism maintains its compliance with the technical standards given by oneM2M, as well as maintaining security by successfully completing AKA transactions on the IoT service platform.

Table 9

Creation of group administrator resources in the simulation environment

# Of nodes	Average (ms)	Minimum (ms)	Maximum (ms)
100	816	764	985
200	809	764	954
300	824	764	3276
400	823	764	1035
500	834	764	1120
600	1115	767	6516
700	904	776	3810
800	1098	795	2120
900	1161	999	1704
1000	1198	788	2051

Table 10

AKA transactions performed by the group header and members in the simulation environment

# Of nodes	Average (ms)	Minimum (ms)	Maximum (ms)
100	1,12	0	985
200	1,2	0	967
300	1,18	0	1032
400	1,09	0	1032
500	1,03	0	1071
600	1,08	0	988
700	1,11	0	1028
800	1,08	0	1081
900	1,24	0	1068
1000	1,18	0	1044

Table 11

Creation of group administrator resources in the physical environment

# Of nodes	Average (ms)	Minimum (ms)	Maximum (ms)
100	282	264	387
200	278	264	351
300	277	265	378
400	277	264	359
500	277	264	361
600	279	264	383
700	282	264	440
800	276	261	357
900	277	261	378
1000	277	263	374



Table 12

AKA transactions performed by the group header and members in the physical environment

# Of nodes	Average (ms)	Minimum (ms)	Maximum (ms)
100	3,92	0	356
200	2,19	0	361
300	1,63	0	358
400	1,34	0	355
500	1,1	0	354
600	1,04	0	356
700	0,95	0	348
800	0,87	0	358
900	0,8	0	354
1000	0,76	0	340

Table 13

Creation of group administrator resources in the cloud environment

# Of nodes	Average (ms)	Minimum (ms)	Maximum (ms)
100	273	268	383
200	272	268	357
300	271	268	356
400	272	268	367
500	271	268	413
600	271	267	426
700	271	268	360
800	271	267	360
900	270	267	386
1000	272	267	36

Table 14

AKA transactions performed by the group header and members in the cloud environment

# Of nodes	Average (ms)	Minimum (ms)	Maximum (ms)
100	3,82	0	362
200	2	0	357
300	1,61	0	398
400	1,27	0	392
500	0,98	0	363
600	0,92	0	391
700	0,78	0	356
800	0,73	0	360
900	0,76	0	452
1000	0,59	0	360

However, the small computational overhead of the “auth” process is vital for the system to be accepted and employed in subsequent investigations. In group-based AKA procedures, only the group leader also known as an administrator executes a full AKA process. However, for each HTTPS request sent independently, a complete AKA process must be executed. In addition, the computational cost while completing AKA transactions by other members of the group using the token value described as GCK, which happens after a full AKA transaction of the group header was assessed.

While creating the group header resource of the developed “auth” mechanism, an average set of values in the range of 800-1200ms was produced in the test scenario 5 made in the simulation environment, as shown in Table 9. Table 10 shows the results of AKA transactions made by the group header and its members using the “auth” mechanism in the simulation environment. According to the results shown in Table 10, the computational overload of the “auth” mechanism on the system was measured as 1ms on average. The column showing

the maximum values shows the values resulting from a full AKA operation of the group header. When test scenario 5 is performed in the physical environment, the results obtained decreased with the increase of the processor power, as determined in the results of the previous tests. The average values obtained according to the results indicated in Table 11 were measured in the range of 276-282ms. According to these results, efficiency between two and three times is provided in the test performed in the physical environment compared to the simulation environment. In addition, the computational overhead of the “auth” mechanism on the hardware used in the physical environment and running the IoT service platform was measured as 1.4ms on average. When the column showing the average values in test scenario 5 performed in the physical environment is examined, the average of the values formed is like the simulation environment. In addition, when the maximum values specified in Table 12 are examined, it is observed that the results are 3 times less than in the simulation environment. In the tests carried out in the cloud environment, it has been revealed once again that the computational overhead brought to the system by the “auth” mechanism is the lowest level. It has been observed that the values obtained as a result of AKA operations performed in the AWS environment and performed by the header of the group in Table 13 are 3 times more efficient than in the simulation environment. When columns showing the minimum and average values in Table 13 are examined, EC2 and network structure used in the AWS environment stand out as another result that was found to have the most efficient and stable bandwidth among the three different test environments.

As with other findings, the maximum numbers always indicate the time taken for the delivered value in response to the initial HTTPS request at the start of the tests. As in the previous results, the “auth” mechanism maintains the level of efficiency it provided, as the GCK value of the developed “auth” mechanism is used by other members of the group as a result of the request made by the group header, and the results obtained from the structure forming the second part of the test. Also, the average of the column showing the average values in Table 14, the value is determined as 1.34ms.

According to the numbers obtained with test scenario 5 executed in three separate test settings, the additional computational overload given to the system by the “auth” mechanism, which carries out group-based authentication and authorization operations, is 1.13, 1.46, and 1.34 accordingly.

## 3.2. Test Methods

### 3.2.1. Test Method 1: Group-Based and Non-Group-Based AE Enrollment Process

The results of test scenarios 1 and 3 are compared to measure the efficiency of the created “auth” method, which leverages the authentication and authorization module of more than one AE resource during the registration phase of the IoT service platform. While making this comparison, instead of making the system secure using just ACPs, the mechanism was controlled by performing AKA actions at the position where the group feature was switched off in the “auth” mechanism.

As indicated in the part where test scenarios 1 and 3 are presented, the comparison was done based on the G-AKA study in addition to the relevant measures (Chen et al., 2012). In Table 15, the efficiency given by the “auth” method established in the place where the group feature is active is noticed.

Table 15

Test Method 1: Group-Based and Non-Group-Based AE Enrolment Process

# Of nodes	Average with Group Feature Off (ms)			Average with Group Feature On (ms)		
	Simulation	Physical	Cloud	Simulation	Physical	Cloud
100	975	504	1029	30	69	204
200	897	486	1047	26	62	206
300	909	495	1105	22	78	205
400	1088	483	1115	21	64	209
500	1021	492	1048	20	67	205
600	1111	481	1072	19	68	197
700	1115	478	1142	19	66	204
800	1120	480	1078	19	69	203
900	1138	478	1017	20	66	200
1000	1111	477	1036	22	66	203

According to the findings presented in Table 15, by integrating the built “auth” mechanism with the IoT service platform, the outcomes in the off and on group feature were compared. In tests done in simulation, physical

and cloud settings, 897-1138, 477-504, and 1017-1142ms intervals were measured while the group feature turned off, accordingly. However, when the group feature was active, 19-30, 64,78, and 197-209ms intervals were recorded, respectively.

According to these data, the “auth” method created to execute group-based authentication and authorization operations give 4 times efficiency in the worst-case situation. In the oneM2M IoT environment, signal traffic is decreased by employing the created “auth” method, while AKA transactions between the nodes in the field and IN are carried out in a secure environment.

**3.2.2. Test Method 2: HTTPS Requests Made with Single and Group Resource**

It is of vital importance that the identities of the nodes registered to the system using the “auth” method be validated from the minute they join the system to the moment they exit the system and that they may only do the transactions they are permitted to accomplish. Working with the group management module of the “auth” mechanism built in HTTPS requests utilizing CSFs offered by the IoT service platform, it has become feasible to make transactions on the system in a safe, efficient, and collective method.

In this manner, the test results acquired in test scenarios 2 and 4, in which the group-based AKA transactions of the previously developed CIN sources are active, but the group management module is tested in both active and passive positions, are compared. In test scenario 4, one HTTPS request was issued to get numerous CIN resources utilizing only one group resource. However, in test scenario 2, distinct HTTPS requests are issued for each CIN resource. Therefore, to directly compare test cases 2 and 4, the real average value of test case 2 is computed using equation 3.2.2a.

$$Unique, Real Average = Number\ of\ Nodes * Average\ Value \tag{3.2.2a}$$

$$Efficiency = Unique, Real Average / Average\ with\ Group\ (ms) \tag{3.2.2b}$$

For a group to be efficient, as shown in Table 16, at least two nodes must be included in the group. However, the efficiency value was calculated for each test set as shown in equation 3.2.2b.

Calculated efficiency values were carried out for three separate test scenarios: simulation, physical, and cloud environments. In the simulation scenario, the greatest efficiency is assessed as 1,570ms, which happens when a group resource consists of 2 nodes. However, when the administrative efficiency of the IoT environment is taken into consideration, this number is estimated to be 1,458ms which happens when a group resource with 25 nodes is deployed.

Table 16  
Test Method 2: HTTPS Requests Made with Single and Group Resource

# Of nodes	Single Average (ms)			Average with Group (ms)			Efficiency		
	Simulation	Physical	Cloud	Simulation	Physical	Cloud	Simulation	Physical	Cloud
1	100	282	712	122	118	217	0,819	2,39	3,281
2	168	294	918	107	161	242	1,57	1,826	3,793
3	267	333	1071	200	204	247	1,335	1,632	4,336
5	375	455	1460	280	232	278	1,339	1,961	5,252
10	500	750	2480	579	353	341	0,863	2,125	7,273
25	1225	1550	5175	840	681	532	1,458	2,276	9,727
50	2650	2850	10150	2120	1185	1006	1,25	2,405	10,089
70	3150	3780	13720	2662	1450	1142	1,183	2,607	12,014
90	3960	4950	17640	3590	1876	1445	1,103	2,639	12,208
100	3600	5400	18900	3554	2033	1476	1,012	2,656	12,808

When the results of the values acquired in the physical and cloud environments are analyzed, the first aspect to be noted is that the network latency in the tests done in these two settings affected all HTTPS requests. According to the calculation done in 3.2.2a, it is shown that the most efficient condition in the cloud environment is 2,656 efficiency values created by a group resource consisting of 100 nodes. However, in the cloud environment, this number appeared with an efficiency value of 12,808 in the test set when a resource consisting of 100 nodes was utilized.

According to these results, the effectiveness of the “auth” mechanism created in small, medium, and large-scale application regions for IoT settings that are meant to be constructed as oneM2M-based differs. If the

hardware with the IN utilized in the IoT environment to be constructed has restricted technological characteristics, the outcomes will mirror the simulated environment. As the technological qualities of the hardware with the IN in-crease, the efficiency will grow accordingly.

### 3.2.3. Test Method 3: Computational Overhead of the Designed Auth Mechanism

The computational overhead that the “auth” mechanism established within the scope of the study provides to the system during the AKA activities done on the IoT service platform must be at a low level for the mechanism to be utilized and accepted in further studies. As indicated before, there is no module supplied on the IoT service platform that executes AKA transactions. For this reason, to assess the computational cost of the created “auth” mechanism to the system, the results of the AKA transactions performed by the group header and other members of the group acquired in test scenario 5 are compared.

Table 17

Test Method 3: Computational Overhead of the Designed Auth Mechanism

# Of nodes	Single Average (ms)			Average with Group (ms)		
	Simulation	Physical	Cloud	Simulation	Physical	Cloud
100	816	282	273	1,12	3,92	3,82
200	809	278	272	1,2	2,19	2
300	824	277	271	1,18	1,63	1,61
400	823	277	272	1,09	1,34	1,27
500	834	277	271	1,03	1,1	0,98
600	1115	279	271	1,08	1,04	0,92
700	904	282	271	1,11	0,95	0,78
800	1098	276	271	1,08	0,87	0,73
900	1161	277	270	1,24	0,8	0,76
1000	1198	277	272	1,18	0,76	0,59

When the group management module offered by the IoT service platform is not used, each result will be the same as the result a group header would obtain after a full AKA operation. As noted in Table 17, conducting a full AKA operation by a group header was measured, on average, in simulated, physical, and cloud settings, and it was observed that it took a time in the range of 800-1198, 276-282, and 270-273ms, respectively. As shown in Table 17, when the members of the group using the “auth” mechanism designed to perform AKA operations transmit the GCK value, the computational overhead imposed by the mechanism on the system is measured 1.13, 1.46, and 1.34ms on average in simulated, physical and cloud environments, respectively.

## 4. Conclusion

Within the scope of the study, the “auth” mechanism that executes group-based authentication and authorization procedures were established based on the Mobius IoT service platform, which was issued a oneM2M compliance certificate by the oneM2M worldwide organization and produced as open source by KETI. By combining the “auth” method and the group management module supplied by the IoT service platform together, the computational overload and signal traffic on the nodes in the field domain are greatly decreased. According to the findings of the test scenarios carried out, the computational overhead of the “auth” mechanism on the IoT service platform is in the range of 800-1198, 276-282, and 270-273ms for single transactions in simulation, physical, and cloud environments, respectively. It was assessed as 1.13 – 1.46 and 1.34ms on average for processes using the source. In the testing for accessing CIN resources, it is noticed that HTTPS requests with the group feature enabled give up to 4 times efficiency, starting from 2 nodes to the test cluster employing 50 nodes. For an IoT environment to be developed utilizing restricted resources in the OneM2M ecosystem, it is advised to form groups of 25 nodes, provided that one of them is the group header.

The signal traffic on the internet of things environment has dropped as a result of the deployment of group-based authentication systems. It is anticipated that the nodes energy usage will go down as a result of the nodes' effective communication with one another. In this study, group-based transactions, particularly authentication and authorization procedures, maintain a high level of security on the Internet of Things contexts while maintaining a measurably low overhead in computing and communication. In future studies, the “auth” mechanism built based on this study can execute group-based AKA transactions on a standalone server. Developing a

structure that can interact with more than one IoT service platform in the oneM2M ecosystem would boost the possibilities of interoperability across IoT service platforms.

### Author Contributions

İbrahim Uğur Aba: Graduated MSc student. Collected data and performed the tests. Performed statistical analysis and wrote the paper.

Erhan Taşkın: Thesis supervisor. Conceived and designed the analysis.

### Conflicts of Interest

The authors declare no conflict of interest.

### References

- Aydin, Y., Kurt, G. K., Ozdemir, E., & Yanikomeroglu, H. (2020). A flexible and lightweight group authentication scheme. *IEEE Internet of Things Journal*, 7(10), 10277-10287. Doi: <https://www.doi.org/10.1109/jiot.2020.3004300>
- Apache JMeter. Retrieved from: <http://jmeter.apache.org>
- Cao, J., Ma, M., & Li, H. (2015). GBAAM: Group-based access authentication for MTC in LTE networks. *Security and Communication Networks*, 8(17), 3282-3299. doi: <https://www.doi.org/10.1002/sec.1252>
- Chen, Y., Wang, J., Chi, K., & Tseng, C. (2010). Group-based authentication and key agreement. *Wireless Personal Communications*, 62(4), 965-979. doi: <https://www.doi.org/10.1007/s11277-010-0104-7>
- Define IOT. (2015, May 25). Retrieved October 22, 2019, from <https://iot.ieee.org/definition.html>
- Fu, A., Song, J., Li, S., Zhang, G., & Zhang, Y. (2016). A privacy-preserving group authentication protocol for machine-type communication in LTE/LTE-A networks. *Security and Communication Networks*. doi: <https://www.doi.org/10.1002/sec.1455>
- Gartner says 5.8 billion enterprise and automotive IoT endpoints will be in use in 2020. (2019, August 29). Retrieved from: <https://www.gartner.com/en/newsroom/press-releases/2019-08-29-gartner-says-5-8-billion-enterprise-and-automotive-iot>
- Gartner says worldwide IoT security spending will reach \$1.5 billion in 2018. (2018, March 21). Retrieved from: <https://www.gartner.com/en/newsroom/press-releases/2018-03-21-gartner-says-worldwide-iot-security-spending-will-reach-1-point-5-billion-in-2018>
- IoT Analytics, state of the IoT 2018: Number of IoT devices now at 7B – market accelerating. (2018, August 08). Retrieved from: <https://iot-analytics.com/state-of-the-iot-update-q1-q2-2018-number-of-iot-devices-now-7b>
- IoT Analytics, state of the IoT 2022: Number of connected IoT devices growing 18% to 14.4 billion globally. (2022, May 18). Retrieved from: <https://iot-analytics.com/number-connected-iot-devices>
- IoT OCEAN. (2017, July 9). Retrieved from: <http://developers.iotocean.org/archives/module/mobius>
- Jiang, R., Lai, C., Luo, J., Wang, X., & Wang, H. (2013). EAP-based group authentication and key agreement protocol for machine-type communications. *International Journal of Distributed Sensor Networks*, 9(11), 304601. doi: <https://www.doi.org/10.1155/2013/304601>
- RFC7519. (2015, May). Retrieved from: <https://datatracker.ietf.org/doc/html/rfc7519>
- KETI. (1991, August). Retrieved from: <https://www.keti.re.kr>
- Kim, J., Choi, S., Yun, J., & Lee, J. (2016). Towards the oneM2M standards for building IoT ecosystem: Analysis, implementation, and lessons. *Peer-to-Peer Networking and Applications*, 11(1), 139-151. doi: <https://www.doi.org/10.1007/s12083-016-0505-9>
- Lai, C., Li, H., Li, X., & Cao, J. (2013). A novel group access authentication and key agreement protocol for machine-type communication. *Transactions on Emerging Telecommunications Technologies*, 26(3), 414-431. doi: <https://www.doi.org/10.1002/ett.2635>
- Lai, C., Li, H., Lu, R., & Shen, X. (2013). SE-AKA: A secure and efficient group authentication and key agreement protocol for LTE networks. *Computer Networks*, 57(17), 3492-3510. Doi: <https://www.doi.org/10.1016/j.comnet.2013.08.003>
- Lai, C., Lu, R., Zheng, D., Li, H., & (Sherman) Shen, X. (2016). GLARM: Group-based lightweight authentication scheme for resource-constrained machine-to-machine communications. *Computer Networks*, 99, 66-81. doi: <https://www.doi.org/10.1016/j.comnet.2016.02.007>
- Li, J., Wen, M., & Zhang, T. (2016). Group-based authentication and key agreement with dynamic policy updating for MTC in LTE-A networks. *IEEE Internet of Things Journal*, 3(3), 408-417. doi:

- <https://www.doi.org/10.1109/jiot.2015.2495321>
- Modiri, M. M., Mohajeri, J., & Salmasizadeh, M. (2018). GSL-AKA: Group-based secure lightweight authentication and key agreement protocol for M2M communication. *2018 9th International Symposium on Telecommunications (IST)*. doi: <https://www.doi.org/10.1109/istel.2018.8661145>
- MongoDB: The application data platform. (2007). Retrieved from: <http://www.mongodb.com>
- nCube-Lavender. Retrieved from: <http://developers.iotocean.org/archives/module/ncube-lavender>
- nCube-Rosemary. Retrieved from: <http://developers.iotocean.org/archives/module/ncube-rosemary>
- nCube-Thyme Nodejs. Retrieved from: <http://developers.iotocean.org/archives/module/ncube-thyme-nodejs>
- OneM2M, the global community that develops standards for IoT. (2012). Retrieved from: <http://www.onem2m.org>
- Parne, B. L., Gupta, S., & Chaudhari, N. S. (2018). SEGB: Security enhanced group-based AKA protocol for M2M communication in an IoT enabled LTE/LTE-A network. *IEEE Access*, 6, 3668-3684. Doi: <https://www.doi.org/10.1109/access.2017.2788919>
- Padmashree, M. G., Mallikarjun, Arunalatha, J. S., & Venugopal, K. R. (2022). GKEAE: Group key exchange and authentication with ECC in internet of things. *Intelligent Systems*, 1-10. Doi: [https://www.doi.org/10.1007/978-981-19-0901-6\\_1](https://www.doi.org/10.1007/978-981-19-0901-6_1)
- Passport.js. Retrieved from: <http://www.passportjs.org>
- Postman API platform. Retrieved from: <https://www.postman.com>
- Su, W., Wong, W., & Chen, W. (2016). A survey of performance improvement by group-based authentication in IoT. *2016 International Conference on Applied System Innovation (ICASI)*. doi:<https://www.doi.org/10.1109/icasi.2016.7539800>
- Şahinaslan, O. (2019). Encryption protocols on wireless IOT tools. *AIP Conference Proceedings*. doi: <https://www.doi.org/10.1063/1.5095121>
- The alliance for internet of things innovation. (2019, October). IoT LSP Standard Framework Concepts, Release 2.9 AIOTI WG03 - IoT Standardization
- TR-0025 Technical Report. (2018, March 12). TR-0025 V2.0.2 Application Developer Guide.
- TS-0001 Technical Specification. (2016, August 30). TS-0001 V2.10.0 Functional Architecture.
- TS-0003 Technical Specification. (2018, March 12). TS-0003 V2.12.1 Security Solutions.
- TS-0009 Technical Specification. (2016, August 30). TS-0009 V2.6.1 HTTP Protocol Binding.
- Yao, J., Wang, T., Chen, M., Wang, L., & Chen, G. (2016). GBS-AKA: Group-based secure authentication and key agreement for M2M in 4G network. *2016 International Conference on Cloud Computing Research and Innovations (ICCCRI)*. Doi: <https://www.doi.org/10.1109/icccri.2016.15>



# Validation of Colchicine Assay Method for Therapeutic Drug Monitoring in Human Plasma

Fadime Canbolat<sup>1,\*</sup>

<sup>1</sup>Department of Pharmacy Services, Vocational School of Health Services, Çanakkale Onsekiz Mart University, Çanakkale, Türkiye

## Article History

Received: 13.06.2022

Accepted: 29.07.2022

Published: 15.12.2022

## Research Article

**Abstract** - Colchicine (COL) reduces the frequency of attacks in Familial Mediterranean Fever (FMF) patients and is effective in preventing and arresting renal amyloidosis in most patients. COL has a narrow therapeutic window. The blood concentration to achieve therapeutic effects can be determined by Therapeutic Drug Monitoring (TDM). However, the use of selective and sensitive analytical methods is necessary for achieving success with TDM. The purpose of this study is to develop and validate a new method for quantitative assay of COL in human plasma samples by liquid chromatograph- tandem mass spectrometry (LC-MS/MS). In our study, to 1ml plasma sample, 0.25 ml internal standard solution was added. The solution was extracted by liquid-liquid extraction (LLE). The method was validated according to the European Medicines Agency (EMA). The total run time was 8 min in LC-MS/MS. The method has been validated over the 0.25 - 8.0 ng/mL calibration range for COL. It was seen that the method has been validated since the results of the analysis meet the EMA criteria. In our study, COL plasma levels were found to be approximately 1.097±0.42 ng/ml in 40 FMF patients using an oral dose of 1.5-2 mg/day. A validated, rapid, simple, cost-effective, and sensitive LC-MS/MS method was developed and optimized for quantitation of COL in plasma. It has been thought that pharmacokinetic studies of COL in plasma can be performed easily using this validated method

**Keywords** – Colchicine, plasma, therapeutic drug monitoring, validation, LC-MS/MS

## 1. Introduction

The pyrin protein is responsible for producing fever symptoms in people with Familial Mediterranean Fever (FMF). Mutations in the MEFV gene can lead to this disease (Cerquaglia et al., 2005). Colchicine (COL; C<sub>22</sub>H<sub>25</sub>NO<sub>6</sub>) reduces the frequency of attacks in FMF patients and is effective in preventing and arresting renal amyloidosis in most patients (Niel & Scherrmann, 2006; Cocco, Chu & Pandolfi, 2010). COL is a neutral, lipophilic alkaloid derived from the plant *Colchicum Autumnale*. In oral administration, it is rapidly and easily absorbed from the gastrointestinal tract. The maximum peak plasma concentration of COL, after oral administration, is reached within 0.5-2 hours (Tateishi et al., 1997). It is mainly absorbed in the ileum. Liver Cytochrome P450 (CYP) enzymes are effective in COL biotransformation (Angelidis et al., 2018). COL is metabolized to inactive metabolites which are 2-demethyl colchicine and 3-demethyl colchicine by CYP3A4 within 48 hours (Lidar et al., 2004; Wason, Di Giacinto & Davis, 2012). COL is eliminated by biliary excretion, 20 % of an oral dose is recovered unchanged in the urine. Elimination half time of COL (T<sub>1/2</sub>) is about 23-41 hours. COL has a narrow therapeutic window because the therapeutic level of COL is 0.5-3 ng/ml and the toxic level of COL is 5 ng/ml (Niel & Scherrmann, 2006). It can lead to acute, subacute, and chronic toxicity. To achieve therapeutic effects and avoid toxic effects, drug blood concentration analysis is widely used in Therapeutic Drug Monitoring (TDM). Knowing the monitoring of the drug's blood level by physicians increases the benefits of rational drug therapy. The use of TDM has become the norm to optimize the prescribed

<sup>1</sup> fadime.canbolat@comu.edu.tr

\*Corresponding Author

dose for a large number of drugs. However, the use of selective and sensitive analytical methods is necessary for achieving success with TDM. The purpose of this study is to develop and validate a new method for quantitative assay of COL in human plasma samples. In this way, a successful TDM follow-up for COL can be performed using the validated method.

## 2. Materials and Methods

### 2.1. Standards and Reagents

Colchicine (COL), and the deuterated compounds used as an internal standard colchicine-d3 (COL-d3) were purchased from Sigma (Sigma-Aldrich, St. Louis, Missouri, USA). Also, all HPLC solvents and organic solvents were purchased from Merck (Merck, Kenilworth, New Jersey, USA).

### 2.2. Preparation of Calibration Standards and Quality Control Samples (QCs)

The stock standard solution was prepared by dissolving COL in methanol (c: 0.1 mg/ml). The diluted standard solution (100 ng/ml) was obtained by diluting the stock standard solution of COL with methanol: water [30:70, v/v]. Calibration standards and quality control samples (QCs) were prepared using this diluted standard solution. The COL-d3 internal stock standard solution was prepared by dissolving COL-d3 (as internal standard) in methanol (c: 0.01 mg/mL). The diluted internal standard solution (c: 10 ng/mL) was obtained by diluting the internal stock standard solution of COL-d3 with methanol: water [30:70, v/v]. All solutions were stored at 4°C until required. Diluted standard solution of COL was added to different volumes of blank plasma to prepare seven calibration standards and five QCs. The calibration standards included concentrations of 0.25, 0.5, 1.0, 2.0, 4.0, 6.0, 8.0 ng/mL for COL. QCs included concentrations of 0.25, 0.75, 4.0, 6.0, 8.0 ng/mL for COL.

### 2.3. LC-MS/MS Conditions

HPLC was performed on an Agilent 1200 HPLC system. COL was performed using an X Terra RP18 analytical column (3mm\*150mm; 3.5mm). Chromatographic separation was performed using the gradient mobile phase system. Mobile phase A was deionized water with formic acid [250:1, v/v], and mobile phase B methanol. The flow rate was 0.5 mL/min under the following conditions: 10% B held 1 min, then increased to 80 % B up to 6 min, and re-equilibrated for 2 min at initial conditions. The column was held at 38°C. MS/MS was performed on an Agilent 6410 B triple-quadrupole LC-MS/MS. Quantitative analysis was performed using multiple reaction modes with electrospray positive ionization (ES+) for COL and COL-d3. Quantification was based on monitoring the parent and product ions of COL m/z 400.2 > 310.3 and COL-d3 m/z 403.3 > 359.2, as shown in Table 1.

Table 1

Quantitation parameters for COL and COL-d3

Compound name	Retention time (RT, min)	Parent (m/z)	Quantifier product mass (m/z)	Fragment voltage (V)	Quant collision energy (eV)	Cell Accelerator voltage (V)	Polarity
COL	3.05	403.3	359.2	80	20	7	+
COL-d3	3.05	400.2	310.3	85	25		

COL; Colchicine, COL-d3; Colchicine-d3 (as internal standard)

### 2.4. Extraction Method of COL from Plasma Sample

To 1ml plasma sample, 0.25 ml internal standard solution (COL-d3; (10 ng/ml)) was added. The solution was extracted with 8 ml ether: dichloromethane [70:30; v/v] and mixed by vortex for 15 min. The phases were centrifuged for 1 min, 4000 rpm. The organic phase was then evaporated to dryness under a stream of nitrogen at 40°C. The residue dissolved in 250 µl methanol was injected 30 µl into the system.



## 2.5. Validation of COL Method

The method was validated for selectivity, calibration curve range, accuracy and precision, matrix effect, stability, and lower limit of quantification (LLOQ) according to the European Medicines Agency (EMA) guidelines for bioanalytical methods validation and other literature that has done bioanalytical method validation studies (Jones, Singer & Bannach, 2002; Chèze, Deveaux & Pèpin, 2006; EMA, 2011; Gowda, 2014). In the selectivity study, the blank plasma sample and the lowest level of calibration standard sample were compared at COL and internal standard retention time. In the calibration curve study, seven calibration standards were analyzed by using the extraction method of COL from the plasma sample. In the accuracy and precision study, five QCs were analyzed by using the extraction method of COL from a plasma sample. The QC1 level (0.25 ng/mL) was the same as the level of the lowest calibration standard (0.25 ng/mL). The QC2 level (0.75 ng/mL) was three times the lowest calibration standard (0.25 ng/mL). The QC3 level (4 ng/mL) was the middle level of the calibration curve range. The QC4 level (6 ng/mL) was about 80% of the highest calibration standard (8 ng/mL). The QC5 level (8 ng/mL) was the same as the level of the highest calibration standard (8 ng/mL). Six samples were prepared from each QC sample for intraday (within) batch analysis. 18 samples were prepared for between-batch (batch to batch) analysis. In the matrix effect study, QC2 and QC4 prepared in plasma were compared with QC2 and QC4 prepared in methanol. In the stability analysis, QC2 and QC4 samples kept at room temperature for 72 hours were compared with fresh prepared QC2 and QC4 samples. For the LLOQ analysis, it was noted that the signal-to-noise ratio was about 10 and was higher than the interference area in the blank sample.

## 2.6. Using The Validated Method for TDM Analysis

In our previous studies (2015a, 2015b), the plasma samples of 40 FMF patients treated at the Marmara University Training and Research Hospital Rheumatology Unit have been analyzed by this developed method (Canbolat et al., 2015a; Canbolat et al., 2015b). We have applied to the Ethics Committee of Marmara University and this study has been approved by the Ethics Committee of Marmara University. We have applied to Marmara University Ethics Committee to analyze patient blood samples. Our ethics committee application was approved by protocol no MAR-YC-2013.0179. To determine TDM, 2 mL blood samples were drawn from each patient 30 minutes before the next COL dose. All plasma samples were stored at -20° C until required.

## 3. Results and Discussion

### 3.1. Validation of COL Assay Method

#### *Selectivity*

A good analytical method should be able to separate the analytes from the endogenous components in the matrix. Selectivity should be proven by using at least six different plasma sources to find the appropriate sample of blank plasma to be used in the analysis. The criteria of the selectivity study are that the interference area in the blank sample is less than 20% of the LLOQ area and 5% of the internal standard area (EMA, 2011). In our study, blank plasma and LLOQ samples were analyzed by using the extraction method of COL from a plasma sample. As a result of the analysis, it was determined that there was no peak in the blank sample and methanol at the retention time (RT) of approximately 3.05 minutes for both COL and internal standard as seen in Figure 1. It was seen that the method with good selectivity has been developed since the results of the analysis meet the EMA selectivity criteria (Jones, Singer & Bannach, 2002; Chèze, Deveaux & Pèpin, 2006; EMA, 2011; Gowda, 2014).

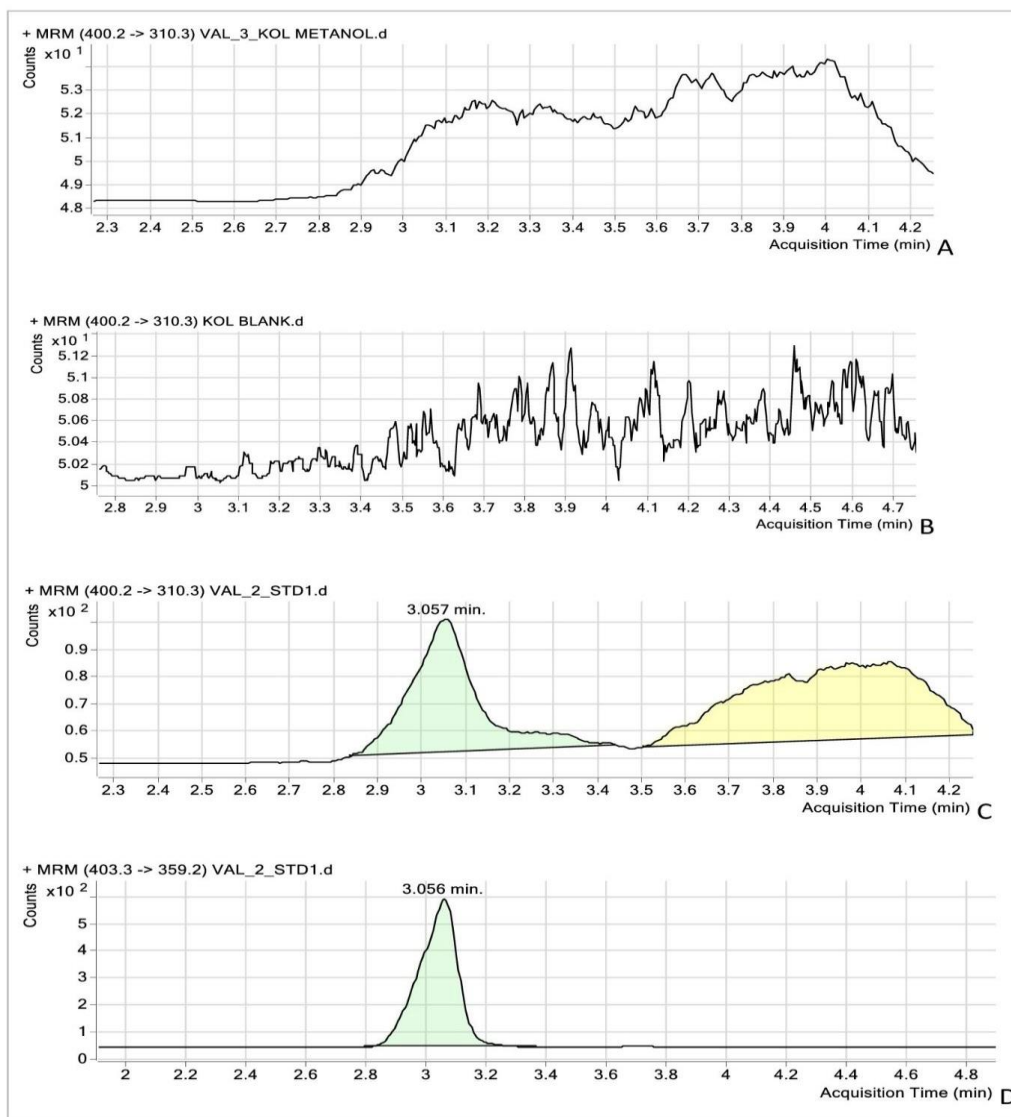


Figure 1. Chromatograms of the analysis samples. Chromatogram of methanol (as a solvent) (A); Chromatogram of blank sample (B); Chromatogram of COL (LLOQ) m/z: 400.2 > 310.3, RT: 3.05 min. (C); Chromatogram of COL-d3 m/z: 403.3 > 359.2, RT: 3.05 min. (as an internal standard) (D).

### Calibration curve range

Before performing the validation of the analytical method, it should be known in which concentration range it will be studied. This calibration curve should be covered by the lowest calibration standard and the highest calibration standard. Calibration standards with at least six different concentrations should be used. Along with the standard samples, blank and zero samples should also be analyzed. According to EMEA criteria, the calculated LLOQ level must be within  $\pm 20\%$  of the nominal value of LLOQ. The calculation of the other calibration standard level must be within  $\pm 15\%$  of the nominal value of standards. At least 75% of the calibration standards must meet this criterion.

In our study, the method has been validated over the 0.25 - 8.0 ng/mL calibration range for COL. The calibration range was established with seven calibration standards and five QCs. The calibration curve was calculated by a least-squares linear regression model. Out of seven standards, only one standard was out of the nominal value. Since the calculated standards and QC values were close to the nominal values, the calibration curve was accepted. The calibration curve are given in Figure 2. It was seen that the method with a good calibration curve has been developed since the results of the analysis meet the EMEA criteria (Jones, Singer & Bannach, 2002; Chèze, Deveaux & Pèpin, 2006; EMEA, 2011; Gowda, 2014).

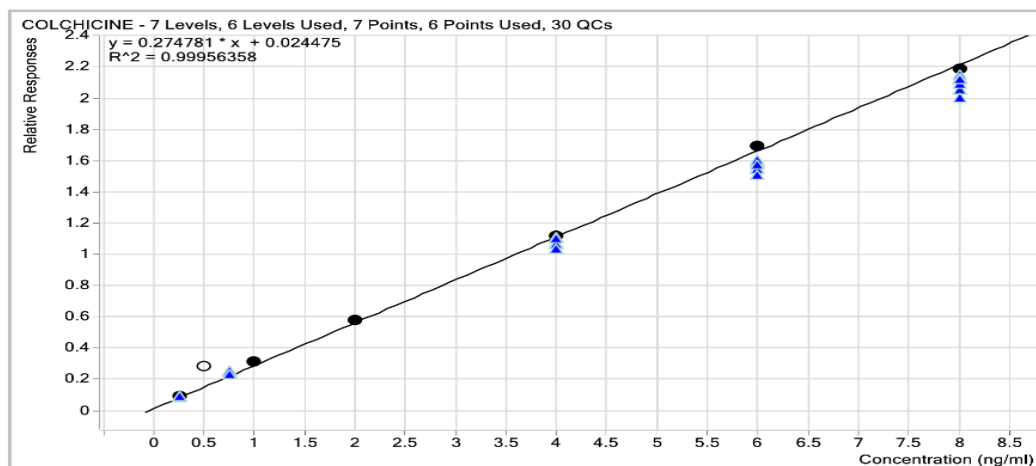


Figure 2. Calibration curve. Small circles represent the calibration standard, and small arrows represent QCs. Calibration standards and QC values were accepted when they were close to nominal values:  $\pm 15\%$  for the high and middle levels and  $\pm 20\%$  for both the LLOQ and lowest QC level.

### Accuracy and Precision

The accuracy of an analytical method is that the calculated analyte value is close to the nominal concentration of the analyte. It should be assessed on QCs. The QCs are analyzed according to the calibration curve and the calculated QC levels are compared with the nominal value. Accuracy is assessed among QCs obtained within the batch and between batches. According to EMEA criteria, the calculated QC1 level must be within  $\pm 20\%$  of the nominal value of QC1. The calculation of the other QC levels must be within  $\pm 15\%$  of the nominal value of QCs.

In our study, within-batch accuracy was determined by analyzing in a single run six samples per level at five QC levels. Also, between-batch accuracy was determined by analyzing in different three runs. The mean concentration was within  $\pm 15\%$  of the nominal values for the QCs in the intra-day (within batch) and inter-day (between batch or batch to batch). The results are given in Table 2.

The precision of the analytical method is determined by the close of the repeated analyte measurements to each other. It is the random error of accuracy (coefficient of variation; % CV). Precision is assessed among QCs obtained within the batch and between batches. We have found that the CV value was lesser than 15% for the QCs in intra-day (within batch) and inter-day (between batch or batch to batch) (Table 2). It was seen that the method with good accuracy and precision has been developed since the results of the analysis meet the EMEA criteria (Jones, Singer & Bannach, 2002; Chèze, Deveaux & Pèpin, 2006; EMEA, 2011; Gowda, 2014).

Table 2.

#### Intra-day and Inter-day statistics of precision and accuracy for QCs of COL

Intra-day	Correlation Coefficient ( $r^2$ )	Mean % Accuracy Range (QCs)					Precision (% CV) Range (QCs)				
		0.25 ng/mL	0.75 ng/mL	4 ng/mL	6 ng/mL	8 ng/mL	0.25 ng/mL	0.75 ng/mL	4 ng/mL	6 ng/mL	8 ng/mL
Batch 1	0.99597	95.85	100.09	104.71	104.18	104.51	5.88	6.82	1.28	3.57	2.65
Batch 2	0.99792	94.85	102.64	96.74	93.68	96.17	5.16	4.17	1.12	3.65	3.81
Batch 3	0.99956	99.49	108.14	95.82	93.35	94.05	4.49	3.98	2.56	2.16	2.54
Inter-day analysis results											
Batch to batch	Mean % Accuracy Range (QCs)					Precision (% CV) Range (QCs)					
	0.25 ng/mL	0.75 ng/mL	4 ng/mL	6 ng/mL	8 ng/mL	0.25 ng/mL	0.75 ng/mL	4 ng/mL	6 ng/mL	8 ng/mL	
	96.78	103.62	99.09	97.07	98.25	5.26	5.95	4.55	5.99	5.46	

### Matrix Effect

Matrix effects should be determined when using mass spectrometric methods. The internal standard normalized matrix factor (IS normalized MF) is used to determine the matrix effect. The CV of IS normalized MF

calculated for the QCs should not be greater than 15%. The matrix factor was calculated according to the calculation specified in the EMEA guideline (EMEA, 2011). Firstly, the matrix factor (MF) is calculated for the analyte as seen in Equation 3.1 and IS as seen in Equation 3.2. Then, The IS normalized MF is calculated by dividing the MF of the analyte by the MF of the IS (EMEA, 2011).

$$MF_{\text{analyte}} = \frac{\text{peak area of analyte in blank}}{\text{peak area of analyte in methanol}} \quad (3.1)$$

$$MF_{\text{IS}} = \frac{\text{peak area of IS in blank}}{\text{peak area of IS in methanol}} \quad (3.2)$$

In our study, this calculation was done at a low and at a high level of QC. The CV of the IS-normalised MF was calculated lesser than 15 %. It was seen that the method with a good matrix effect has been developed since the results of the analysis meet the EMEA criteria (Jones, Singer & Bannach, 2002; Chèze, Deveaux & Pèpin, 2006; EMEA, 2011; Gowda, 2014).

### Stability

The QCs prepared stability study was analyzed against a calibration curve. Room temperature stability was performed at low QC and high QC levels, and the CV values were within  $\pm 15\%$ . The stability results in our study were compared with the EMEA criteria. It has been shown that the samples prepared are stable at room temperature for over 72 hours.

### LLOQ

LLOQ of the method is the lowest concentration level with suitable precision and accuracy. LLOQ for COL in human plasma was set at 0.25 ng/mL. The chromatograms are given in Figure 1.

When we look at the studies conducted in the last 30 years, there are studies on the plasma level of COL. In the Tracqui et al. (1996) study, the LLOQ of COL in plasma was 0.6 ng/ml (Tracqui et al., 1996). In the Bourgogne et al. (2013) study, the run time of COL analysis was 9.5 minutes and the LLOQ level was 0.3 ng/ml (Bourgogne et al., 2013). In the Fabresse et al. (2017) study, the LLOQ of COL level was determined as 0.5 ng/ml (Fabresse et al., 2017). In our study, the LLOQ of COL level was 0.25 ng/ml, and run time was 8 minutes. Considering the short run time of COL analysis and LLOQ of COL level of the validated method, a fast and sensitive analysis method has been developed compared to other studies. Even though COL has a narrow therapeutic window, analytical research on this drug is limited. The research mostly includes toxic case reports. In the Goldbart et al. study, a case report of poisoning with the use of 2 mg of COL was included. It has been shown that the cause of intoxication was the interaction of the drug with nutrients, as a result of which the level of COL was higher than expected (Goldbart, Press, Sofer & Kapelushnik, 2000). In our previous studies, COL plasma levels were found to be approximately  $1.097 \pm 0.42$  ng/ml in 40 FMF patients using an oral dose of 1.5-2 mg/day (Canbolat et al., 2015a; Canbolat et al., 2015b). Since the therapeutic plasma concentration of COL is relatively low (0.5-3 ng/ml), many analytical studies (non-specific radioimmunoassay, chromatography methods) for the determination of COL to date have lagged behind expectations for measurements at the therapeutic level. Physicians need to determine the levels of COL in the patient's plasma to ensure an appropriate and safe therapeutic dose. The fact that the plasma level of COL can be analyzed with a rapid and sensitive method becomes important to achieving the therapeutic effect of COL. Considering the superiority of the validated method over other COL analysis methods in the literature, it is thought that the validated method can be easily used in TDM analysis.

### 4. Conclusion

Current studies show the importance of plasma drug monitoring both to evaluate the clinical response and to prevent drug toxicity. We, therefore, decided to develop a highly specific and sensitive LC-MS/MS method for the determination and quantitation of COL in plasma. A validated, rapid, simple, cost-effective, and accurate LC-MS/MS method was developed and optimized for the quantitation of COL in plasma. It is also a practical and easy method for pharmacokinetic studies involving the evaluation of TDM of COL.

## Acknowledgment

I would like to thank Gulsen Ozen, Ali Ugur Unal, Guzide Nevsun Inanc, Pamir Atagunduz, and Haner Direskeneli for supporting the collection of patient blood samples in our previous study. Thank you Selma Ozilhan, Kasif Nevzat Tarhan, and deceased Salih Tuncel Ozden for providing laboratory facilities.

## Author Contributions

Fadime Canbolat: The author takes part in the development and validation of the colchicine assay method, analysis of samples, and writing of the manuscript.

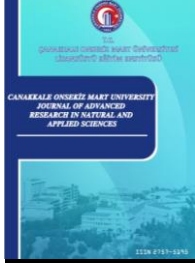
## Conflicts of Interest

The author declares no conflict of interest.

## References

- Angelidis, C., Kotsialou, Z., Kossyvakis, C., Vrettou, A. R., Zacharoulis, A., Kolokathis, F., Vasilios, K., & Giannopoulos, G. (2018). Colchicine pharmacokinetics and mechanism of action. *Current pharmaceutical design*, 24(6), 659-663. doi: <https://doi.org/10.2174/1381612824666180123110042>
- Bourgogne, E., Soichot, M., Latour, C., & Laprèvote, O. (2013). Rugged and accurate quantitation of colchicine in human plasma to support colchicine poisoning monitoring by using turbulent-flow LC-MS/MS analysis. *Bioanalysis*, 5(23), 2889-2896. doi: <https://doi.org/10.4155/bio.13.258>
- Canbolat, F., Ozen, G., Ozilhan, S., Gulturk, S., Ozcetin, A., Unal A.U., Inanc, N., Atagunduz, P., Direskeneli, H., & Ozden, T. (2015a). Relationship Between Colchine Plasma Level and Frequency of Familial Mediterranean Fever Attacks. *ACR/ARHP Annual Meeting*, Abstract 941, USA. Retrieved from: <https://acrabstracts.org/abstract/relationship-between-colchine-plasma-level-and-frequency-of-familial-mediterranean-fever-attacks/>
- Canbolat, F., Ozen, G., Ozilhan, S., Gulturk, S., Ozcetin, A., Unal, A. U., Inanc, N., Atagunduz, P., Direskeneli, H., & Ozden, T. (2015b). THU0549 Relationship Between Colchine Plasma Level and Frequency of Familial Mediterranean Fever Attacks. *BMJ Journals Annals of The Rheumatic Diseases*, 74 (2). Retrieved from: [https://ard.bmj.com/content/74/Suppl\\_2/399.2](https://ard.bmj.com/content/74/Suppl_2/399.2)
- Cerquaglia, C., Diaco, M., Nucera, G., Regina, M. L., Montalto, M., & Manna, R. (2005). Pharmacological and clinical basis of treatment of Familial Mediterranean Fever (FMF) with colchicine or analogues: an update. *Current Drug Targets-Inflammation & Allergy*, 4(1), 117-124. doi: <https://doi.org/10.2174/1568010053622984>
- Cocco, G., Chu, D. C., & Pandolfi, S. (2010). Colchicine in clinical medicine. A guide for internists. *European journal of internal medicine*, 21(6), 503-508. doi: <https://doi.org/10.1016/j.ejim.2010.09.010>
- Chèze, M., Deveaux, M., & Pèpin, G. (2006). Liquid chromatography-tandem mass spectrometry for the determination of colchicine in postmortem body fluids. Case report of two fatalities and review of the literature. *Journal of analytical toxicology*, 30(8), 593-598. doi: <https://doi.org/10.1093/jat/30.8.593>
- EMA Committee for Medicinal Products for Human Use (2011). *Guideline on bioanalytical method validation*. European Medicines Agency EMA. CHMP/EWP/192217/2009: 1-22 (cited 2011 August 01). Retrieved from: [www.ema.europa.eu/ema/pages/includes/document/open\\_document.jsp](http://www.ema.europa.eu/ema/pages/includes/document/open_document.jsp)
- Fabresse, N., Allard, J., Sardaby, M., Thompson, A., Clutton, R. E., Eddleston, M., & Alvarez, J. C. (2017). LC-MS/MS quantification of free and Fab-bound colchicine in plasma, urine and organs following colchicine administration and colchicine-specific Fab fragments treatment in Göttingen minipigs. *Journal of Chromatography B*, 1060, 400-406. doi: <https://doi.org/10.1016/j.jchromb.2017.06.034>
- Goldbart, A., Press, J., Sofer, S., & Kapelushnik, J. (2000). Near fatal acute colchicine intoxication in a child. A case report. *European journal of pediatrics*, 159(12), 895-897. doi: <https://doi.org/10.1007/PL00008364>
- Gowda, B. G. (2014). High-Performance liquid chromatographic determination of colchicine in pharmaceutical formulations and biological fluids. *Int. J Pharm Pharm Sci*, 6, 335-337. Retrieved from: [https://web.archive.org/web/20180413121507id\\_/http://ijppsjournal.com/Vol6Issue6/9624.pdf](https://web.archive.org/web/20180413121507id_/http://ijppsjournal.com/Vol6Issue6/9624.pdf)
- Jones, G. R., Singer, P. P., & Bannach, B. (2002). Application of LC-MS analysis to a colchicine

- fatality. *Journal of analytical toxicology*, 26(6), 365-369. doi: <https://doi.org/10.1093/jat/26.6.365>
- Lidar, M., Scherrmann, J. M., Shinar, Y., Chetrit, A., Niel, E., Gershoni-Baruch, R., Langevitz, P., & Livneh, A. (2004). Colchicine nonresponsiveness in familial Mediterranean fever: clinical, genetic, pharmacokinetic, and socioeconomic characterization. In *Seminars in arthritis and rheumatism* (Vol. 33, No. 4, pp. 273-282). WB Saunders. doi: [https://doi.org/10.1053/S0049-0172\(03\)00137-9](https://doi.org/10.1053/S0049-0172(03)00137-9)
- Niel, E., & Scherrmann, J. M. (2006). Colchicine today. *Joint Bone Spine*, 73(6), 672-678. doi: <https://doi.org/10.1016/j.jbspin.2006.03.006>
- Tateishi, T., Soucek, P., Caraco, Y., Guengerich, F. P., & Wood, A. J. (1997). Colchicine biotransformation by human liver microsomes: identification of CYP3A4 as the major isoform responsible for colchicine demethylation. *Biochemical pharmacology*, 53(1), 111-116. doi: [https://doi.org/10.1016/S0006-2952\(96\)00693-4](https://doi.org/10.1016/S0006-2952(96)00693-4)
- Tracqui, A., Kintz, P., Ludes, B., Rouge, C., Douibi, H., & Mangin, P. (1996). High-performance liquid chromatography coupled to ion spray mass spectrometry for the determination of colchicine at ppb levels in human biofluids. *Journal of Chromatography B: Biomedical Sciences and Applications*, 675(2), 235-242. doi: [https://doi.org/10.1016/0378-4347\(95\)00386-X](https://doi.org/10.1016/0378-4347(95)00386-X)
- Wason, S., DiGiacinto, J. L., & Davis, M. W. (2012). Effects of grapefruit and Seville orange juices on the pharmacokinetic properties of colchicine in healthy subjects. *Clinical therapeutics*, 34(10), 2161-2173. doi: <https://doi.org/10.1016/j.clinthera.2012.08.007>



## Evaluation of Consumers' Aspects on Organic Farming Products by Regions

Başak Aydın<sup>1,\*</sup>, Murat Doğu<sup>2</sup>, Ayten Aşkın Kılınç<sup>3</sup>, Sunay Demir<sup>4</sup>, Bülent Tarım<sup>5</sup>, Duygu Aktürk<sup>6</sup>, Filiz Pezikoğlu<sup>7</sup>, Volkan Burucu<sup>8</sup>, Mustafa Aslan<sup>9</sup>

<sup>1</sup>Atatürk Soil Water and Agricultural Meteorology Research Institute, Kırklareli, Türkiye  
<sup>2,3,4,5</sup>Poultry Research Institute, Ankara, Türkiye

<sup>6</sup>Department of Agricultural Economics, Faculty of Agriculture, Çanakkale Onsekiz Mart University, Çanakkale, Türkiye

<sup>7</sup>Atatürk Horticultural Central Research Institute, Yalova, Türkiye (retired)

<sup>8</sup>Agricultural Economic and Policy Development Institute, Ankara, Türkiye

<sup>9</sup>General Directorate of Plant Production, Republic of Turkey Ministry of Agriculture and Forestry, Ankara, Türkiye

### Article History

Received: 17.04.2022

Accepted: 04.08.2022

Published: 15.12.2022

### Research Article

**Abstract** – The main purposes of this study were to analyze the attitude and behavior of the consumers regarding to purchase of the organic food, the socio-economic comparison of the consumers consuming and non-consuming organic food and to determine the organic food consumption in consideration of different regions. This research was carried out by a questionnaire study with 1494 consumers, consuming organic and non-organic products in six regions in accordance with their socio-economic development index values. By making use of average, percentage and cross tables during the analysis of the data obtained, some of the socio-economical characteristics of the consumers were determined. Factor analysis was used to evaluate the attitudes of the producers consuming organic products regarding the organic products. 25.60% of the consumers in the first region, 47.59% of the consumers in second region, 31.33% of the consumers in third region, 20.48% of the consumers in fourth region, 27.11% of the consumers in the fifth region, 13.86% of the consumers in sixth region declared that they were consuming organic food. Associated with showing and alteration according to the regions, the most consumed organic products were, in respectively, egg, fruit, milk, vegetable. While the 91.30% of the consumers that did not consume organic products in the first region, so did the 94.74% of the third region, 92.42% of the fourth region, 94.21% of the fifth region, 95.80% of the sixth region expressed a positive opinion about consuming organic products, this ratio was determined as 78.16% in the second region.

**Keywords** – Consumer behaviours, consumption, organic farming, organic product, Turkey

## 1. Introduction

Increasing environmental pollution and problems in human health have created many problems for producers and consumers. Over time, producers and consumers have started to produce organic agricultural products, which is a production method that does not harm people and the natural environment. The products

<sup>1</sup> [basakaydin\\_1974@yahoo.com](mailto:basakaydin_1974@yahoo.com)

<sup>2</sup> [mrtdogu@hotmail.com](mailto:mrtdogu@hotmail.com)

<sup>3</sup> [aytenaskinkilinc@gmail.com](mailto:aytenaskinkilinc@gmail.com)

<sup>4</sup> [sunay.demir@tarimorman.gov.tr](mailto:sunay.demir@tarimorman.gov.tr)

<sup>5</sup> [bulent.tarim@tarimorman.gov.tr](mailto:bulent.tarim@tarimorman.gov.tr)

<sup>6</sup> [akturk@comu.edu.tr](mailto:akturk@comu.edu.tr)

<sup>7</sup> [filiz.pezikoglu@gmail.com](mailto:filiz.pezikoglu@gmail.com)

<sup>8</sup> [volkanburucu@gmail.com](mailto:volkanburucu@gmail.com)

<sup>9</sup> [mustafa.aslan@tarimorman.gov.tr](mailto:mustafa.aslan@tarimorman.gov.tr)

\*Corresponding Author

produced with the organic farming method have become products that are preferred by conscious and high-income consumers in the world and have a wide market potential (Aktürk, 2012). While organic agriculture had an agricultural production philosophy in which ecology was completely addressed at the beginning, it has transformed into a marketing structure that has been reduced to the level of "brand" in order to take part in the globalizing world trade and has been registered with the name "organic".

Since 1980, organic agriculture has gained a commercial dimension by being removed from family business with the increasing demand of consumers and has started to be applied in the USA and EU countries (Turhan, 2005). Organic agricultural production is carried out without harming people and the environment. It aims to improve the natural balance in the natural environment, which has been damaged by the wrong application of chemical substances and these chemical substances. In other words, it is expressed as an agricultural method that is guaranteed by a certain control and certification process and is carried out without the use of synthetic chemical inputs and pesticides (Eti, 2014).

An organic product is all kinds of products produced, processed, packaged, labelled and put on the market as certified by the entrepreneur with the organic farming method. Organic products are defined as foodstuffs containing plant and animal foods in which genetic engineering, artificial and similar fertilizers, protectors, colorants, additives, chemicals, brightening agents and chemical packaging materials are not used in their cultivation and processing (Akın, Çiçek, İnal & Toksarı, 2010).

The consumption of organic products is increasing in Turkey as well as in the world, depending on the awareness of the consumers and the increase in the income level. Due to the increasing consumer awareness in recent years, consumers are faced with the risk of encountering health problems and safety of foodstuffs and as their concerns increase, they tend to organic products instead of products grown with pesticides, hormones and various chemicals (Özer, 2008). Organic agriculture activities in Turkey started not due to the increase in domestic demand, but to the demands of consumers in developed countries, and the main purpose was to increase exports of Turkey's basic agricultural products and enter new markets (Ataseven & Güneş, 2008).

Consumers in Turkey as well as all over the world; show more and more sensitivity about the environment, health and safe nutrition. This sensitivity increases the interest and demand of consumers for organic foods, and enables the domestic market in organic food products. In Turkey, it is necessary to increase the knowledge level of consumers about organic foods and their benefits, and in the marketing process of organic foods, the consumer trends and the demographic information of the consumers should be investigated, and this is also important for the growth of the domestic market. It is not possible to keep organic food products in stocks, and the production amounts of organic food products are determined in line with the demands in the domestic and foreign markets (Sarıkaya, 2007). In this direction, it is important for both implementers and researchers to learn organic food purchasing motivations in order to increase the purchasing potential of consumers. Considering the importance of organic food consumption in terms of human health, this state will have positive effects on consumers (Cengiz & Şenel, 2017).

While 150 kinds of organic products were produced by 12,428 producers on 89,827 hectares of land in 2002, 278 kinds of organic products were produced by 52,600 producers in 346,767.40 hectares of land in 2020. In terms of organic animal production, the number of farmers, which was 10 in 2004, increased to 114 in 2020; and the number of animals increased from 26,500 to 1,130,165. The number of farmers engaged in organic beekeeping, which was 256 in 2004, increased to 494 in 2020 and the number of hives, which was 38,792, increased to 89,128 (Anonymous, 2022).

In order for the enterprises to continue their existence in the organic food market, it is necessary to determine the purchasing behaviors of consumers, to develop products and marketing strategies suitable for the needs of the target market. Encountering the needs of consumers and consumer satisfaction is extremely important in the development of marketing strategies. In this study attitudes and behaviors of the consumers about purchasing organic food in Turkey were determined. The research was conducted in six regions determined according to the socio-economic development index and the regions were compared. When the studies on the subject are examined, it is striking that the studies are generally carried out on a provincial basis. This study is a first in terms of being carried out throughout Turkey and making regional comparisons.



## 2. Materials and Methods

The research was conducted in 2018 in six regions in Turkey classified in terms of development levels according to socio-economic development index values, and 32 provinces were selected by taking into account the index values. The target group of the study consisted of consumers selected by sampling. The primary data of the research consisted of data collected from these consumers by face-to-face interview technique. Survey forms prepared in accordance with the purpose of the research were filled by the researchers through face-to-face surveys. Thus, the primary data were obtained directly from the consumers. Secondary data, on the other hand, were obtained by using the relevant literature and statistics.

Provinces in Turkey are classified in six levels in terms of their development levels according to their socio-economic development index values. The index values of the provinces in the first level are greater than 1, the index values of the provinces in the 2nd, 3rd, 4th and 5th levels are between 1 and -1, and the index values of the provinces in the 6th level are less than -1. There are 8 provinces in the first level, 13 provinces in the second level, 12 provinces in the third level, 17 provinces in the fourth level, 16 provinces in the fifth level and 15 provinces in the sixth level. Approximately 25% of the number of provinces at each level was selected purposefully, taking into account the index values, and the population numbers of the provinces were obtained. The population of the selected provinces corresponds to 68% of the total population of Turkey (79,814,871). The total population of the provinces of İstanbul, Ankara and İzmir, which are in the first level, corresponds 30.53% of the total population of Turkey. Considering the total population of the provinces at each level, the number of consumers to be surveyed was determined by the proportional sampling formula (2.1.) given below (Newbold, 1995). The number of surveys was distributed proportionally to the provinces. Sampling was done separately for the provinces of İstanbul, Ankara and İzmir. Since the characteristics of the consumers constituting the main population were not known at the beginning,  $p=0.5$  was taken to maximize the sample size.

$$n = \frac{N \cdot p(1-p)}{(N-1)\sigma^2 p + p(1-p)} \quad (2.1)$$

In the formula;

$n$  = sample size

$N$  = Population size (total population size)

$p$  = Estimation ratio (consumption rate of organic products) (based on 50% assumption)

$\sigma_p^2$  = Variance of the ratio (calculated according to a certain confidence interval and margin of error)

According to 99% confidence interval and 0.10 margin of error;

$Z_{\alpha/2\sigma_p} = r$

$2.58 \sigma_p = 0.10$

$\sigma_p = 0.03876$ .

As a result of the sampling, the number of consumers surveyed was determined as 1494. The provinces where the survey was conducted and the number of consumers are given in Table 1.

Table 1

The provinces where the survey was conducted and the number of surveys

Region	Provinces	Number of surveys	Region	Provinces	Number of surveys
1	İstanbul	166	4	Kırıkkale	12
1	Ankara	166	4	Malatya	35
1	İzmir	166	4	Hatay	69
1	Kocaeli	38	4	Kastamonu	17
1	Antalya	49	4	Bartın	9
1	Bursa	61	4	Çorum	24
1	Eskişehir	18	5	Çankırı	9
2	Bolu	8	5	Erzurum	39
2	Adana	61	5	Kahramanmaraş	57
2	Kayseri	37	5	Ordu	39
2	Konya	60	5	Yozgat	22
3	Burdur	10	6	Diyarbakır	59
3	Karabük	9	6	Iğdır	7
3	Zonguldak	23	6	Batman	21
3	Gaziantep	75	6	Bingöl	10
3	Samsun	49	6	Şanlıurfa	69

In the analysis of the obtained data, by using descriptive statistics such as mean, percentage and cross tables; some socio-economic characteristics of the surveyed consumers were determined. The chi-square test was used in discrete data whether there was a difference between the groups that consumed organic products and those that did not. In continuous data, firstly, the variables with and without normal distribution were determined by using Kolmogorov-Smirnov test. As the number of groups was 2, t-test was used for normally distributed variables, and the Mann-Whitney U test for non-normally distributed variables.

Factor analysis was used to evaluate the judgments of producers consuming organic products about organic products. Factor analysis is a multivariate analysis technique used by the researcher to understand the relationships between the concepts in the data set more easily by revealing the main factors belonging to a data set consisting of many variables that are related to each other. In other words, it is a technique that makes many variables related to each other less meaningful and completely independent from each other (Kleinbaum, Lawrence & Keith, 1998).

Factor analysis is carried out in four basic stages. First, the evaluation of the suitability of the data for factor analysis, obtaining the factors, rotation of the factors and naming the factors. Three methods are used to evaluate whether the data set is appropriate. These are the creation of the correlation matrix, Kaiser-Meyer-Olkin (KMO) and Bartlett tests (Akgül & Çevik, 2003). In the calculation of the correlation matrix, a high correlation relationship between the variables is searched. Variables with very strong correlations will generally be in the same factor.

Another indicator of the relationship between variables is the partial correlation coefficient. The Kaiser-Meyer-Olkin (KMO) test is an index that compares the size of the observed correlation coefficients. KMO value is considered as excellent if it is above 0.90, very good between 0.80-0.90, good between 0.70-0.80, moderate between 0.60-0.70, weak between 0.50-0.60 and unacceptable below 0.50 is considered (Sharma, 1996).

The Bartlett Test of Sphericity is used to test whether the correlation matrix is a unit matrix with all diagonal terms 1 and non-diagonal terms 0. This test requires that the data originate from multiple normal distributions (Hair, Anderson, Tahtam & Black, 1998). In determining the number of factors, the eigenvalue and scree test chart are mostly used. In determining according to eigenvalues, factors with eigenvalues greater than 1 are derived. In the scatter diagram (Scree test) method, the graph of the eigenvalues is examined and the factors up to the point where the vertical line becomes horizontal are included in the solution (Lewis, 1994). Vertical rotation techniques such as Varimax, Quartimax, Orthomax, Biquartimax, Equamax, and oblique rotation techniques such as Oblimax, Quartimin, Oblimin are used for better interpretation of the factors. In the most widely used Varimax method, some factor loadings in each column are approached to 1, while many of the remaining values are approached to 0. In this method proposed by Kaiser, rotation is performed to ensure that the factor variances are maximized (Çokluk, Şekercioğlu & Büyüköztürk, 2010).

Factors related to considerations on organic food products were subjected to cluster analysis based on the factor scores obtained. Cluster analysis has taken its place among the multivariate statistical methods that are frequently used in classifying grouped data according to their similarities. Cluster analysis focuses on the clusters or groups that will emerge by calculating the values of individuals or objects observed in the research on all measured variables. In order to determine the similarities between individuals or objects, distance measures, correlation measures or similarity measures of qualification data are used (Kalaycı, 2009).

### 3. Results and Discussion

Organic product consumption status by regions is given in Table 2. 25.60% of the consumers in the first region, 47.59% of the consumers in the second region, 31.33% of the consumers in the third region, 20.48% of the consumers in the fourth region, 27.11% of the consumers in the fifth region, 13.86% of the consumers in the sixth region stated that they consume organic products. It was determined that the region where organic products were consumed the most was the second region. The fact that the production of vegetables and fruits is quite common in most of the provinces in the second region, the majority of the provinces are located in the Marmara and Aegean regions, and the awareness level of the consumers in these regions is higher, can be shown among the reasons for the higher consumption of organic products in this region.

As a result of the chi-square test performed to determine whether or not the difference in organic product consumption status was statistically significant between the regions, it was determined that there was a difference at 1% ( $p=0.000$ ) significance level.

Table 2

Consumption of organic products by regions

Organic product consumption	Region 1		Region 2		Region 3		Region 4		Region 5		Region 6		Total		
	No.	%	No.	%	No.	%	No.	%	No.	%	No.	%	No.	%	
Yes	170	25.60	79	47.59	52	31.33	34	20.48	45	27.11	23	13.86	403	26.97	
No	494	74.40	87	52.41	114	68.67	132	79.52	121	72.89	143	86.14	1,091	73.03	
Total	664	100.00	166	100.00	166	100.00	166	100.00	166	100.00	166	100.00	1,494	100.00	
Chi-square: 56.104		p: 0.000													

While the average age of consumers consuming organic products was 34.67, the average age of consumers who did not consume organic products was 37.79. The monthly average food expenditure of consumers consuming organic products was determined as 1,323.33 TL whereas the monthly average food expenditure of consumers who did not consume organic products was determined as 1,149.87 TL. The education period of the consumers consuming and not consuming organic products were found as 12.89 and 11.60 years. As a result of the Mann-Whitney U test carried out to determine whether or not the difference in age, monthly food expenditure and education period of consumers was statistically significant between the groups, it was determined that there was a difference at 1% ( $p=0.000$ ) significance level (Table 3).

Table 3

Some socio-cultural indicators of consumers

Socio-cultural indicators	Age		Monthly food expenditure		Education period	
	Average	P	Average	P	Average	P
Consuming organic products	34.67	0.002	1,323.33	0.000	12.89	0.000
Non-consuming organic products	37.79		1,149.87		11.60	

#### 3.1. Consumers' Level of Knowledge about Organic Products

The opinions of consumers about organic products are given in Table 4. 68.61% of the consumers in both groups stated that organic products were products or foods that were not produced by using chemicals, 60.78% were products or foods from natural production, 60.51% were products or foods that were not produced by using hormones. 27.51% of the consumers stated that organic products were products or foods coming from

production that did not harm nature and the environment. In addition, 11.38% of the consumers stated that organic products were certified products or foods, while very few of the consumers declared that organic products were traceable and highly efficient products or foods. Organic foods are considered reliable because they do not use artificial chemical inputs in their production, the use of genetically modified organisms is prohibited, they are produced with methods that do not harm the environment, and they are controlled and certified at every stage of production. As a result of the study, it was seen that the most important judgment of the consumer about organic foods was being healthy.

In the study conducted by Doğan & Gürel (2016), it was determined that 64.86% of the consumers described organic products as products for which the use of drugs, hormones and chemicals was prohibited or limited.

Table 4

Consumers' considerations on organic products

What is an organic product?	Consuming organic products		Non-consuming organic products		Total*	
	Number	%	Number	%	Number	%
Chemical-free products/food	294	72.95	731	67.00	1025	68.61
Products/foods from natural production	275	68.24	633	58.02	908	60.78
Hormone-free products/foods	278	68.98	626	57.38	904	60.51
Products/foods from production that does not harm nature and the environment	157	38.96	254	23.28	411	27.51
Certified products/foods	81	20.10	89	8.16	170	11.38
Traceable products/food	43	10.67	42	3.85	85	5.69
High yield products/ foods	18	4.47	32	2.93	50	3.35

\*Multiple options marked

Consumers were asked about their considerations on products produced with traditional methods (Table 5). The ratio of consumers who stated that there were drugs, hormones and antibiotics in products produced by traditional methods was almost the same in both groups, and it was determined as 76%. Chi-square test results showed that consumers' considerations on products produced by traditional methods did not change according to consumer groups.

Table 5

Consumers' considerations on products produced with traditional methods

Are there drugs, hormones, antibiotics in products produced by traditional methods?	Consuming organic products		Non-consuming organic products		Total	
	Number	%	Number	%	Number	%
Yes	309	76.67	832	76.26	1141	76.37
No	65	16.13	149	13.66	214	14.32
No idea	29	7.20	110	10.08	139	9.30
Total	403	100.00	1,091	100.00	1,494	100.00

Chi-square: 3.897      p: 0.142

Consumers were asked whether organic products had a certified and controlled production process (Table 6). While 63.28% of consumers consuming organic products stated that organic products had a certified and controlled production process, this ratio was determined as 41.70% in the consumer group who did not consume organic products. It was observed that consumers who consumed organic products had a higher level of knowledge about organic agricultural products. As a result of the chi-square test carried out to determine whether the difference in the opinions of consumers about the certified and controlled production process of organic products was statistically significant between the groups, it was determined that there was a difference at 1% (p=0.000) significance level.

Table 6

## Consumers' considerations on the certified and controlled production process of organic products

Do organic products have a certified and controlled production process?	Consuming organic products		Non-consuming or- ganic products		Total	
	Number	%	Number	%	Number	%
Yes	255	63.28	455	41.70	710	47.52
No	64	15.88	423	38.77	487	32.60
No idea	84	20.84	213	19.52	297	19.88
Total	403	100.00	1,091	100.00	1,494	100.00

Chi-square: 76.379      p: 0.000

Consumers were asked about their considerations on the effect of certified organic products on consumption (Table 7). 63.52% of the consumers consuming organic products and 59.12% of the non-consumers stated that certified organic products had an impact on consumption. While 10.67% of consumers consuming organic products stated that they were undecided on this issue, this ratio was determined as 24.01% in the consumer group that did not consume organic products. As a result of the chi-square test conducted to determine whether the difference in the opinions of consumers regarding the effect of certified organic products on consumption was statistically significant between the groups, it was determined that there was a difference at 1% ( $p=0.000$ ) significance level.

Table 7

## Consumers' considerations on the effect of certified organic products on consumption

The effect of certified organic products on consumption	Consuming organic products		Non-consuming or- ganic products		Total	
	Number	%	Number	%	Number	%
Not effective	5	1.24	22	2.02	27	1.81
Not very effective	26	6.45	89	8.16	115	7.70
I'm undecided	43	10.67	262	24.01	305	20.41
Effective	256	63.52	645	59.12	901	60.31
Very effective	73	18.11	73	6.69	146	9.77
Total	403	100.00	1,091	100.00	1,494	100.00

Chi-square: 68.006      p: 0.000

	Average	Standard deviation	Average	Standard deviation	Average	Standard deviation
	3.91	0.807	3.60	0.811	3.69	0.821

1: not effective, 2: not very effective, 3: Undecided, 4: effective, 5: very effective

Information sources of the consumers about organic products were investigated within the scope of the research (Table 8). 51.67% of the consumers in both groups stated that they obtained information about organic products from the internet and social media, 46.92% from television, and 46.12% from the friends. In addition, 11.85% of consumers stated that they obtained information from printed publications, 11.18% from doctors, 9.77% from the Ministry of Agriculture and Forestry, and 9.44% from fairs. It was observed that the sources of information that consumers obtained the most information about organic products were the internet, social media and television. Published publications and institutions, which were thought to be among other sources of information, had little impact. It is thought that the studies on creating the education process and awareness from the producer to the consumer will be effective on organic product consumption. The trainings provided by the Ministry of Agriculture and Forestry, the Ministry of Health, the Ministry of National Education for producers, consumers and students should be increased.

In the study conducted by Gülgör (2017), it was determined that the primary sources of information about organic products of the consumers were friend advice and the internet whereas the most important information sources of the consumers about organic products were visual media and the internet in Doğan & Gürel (2016) literature.

**Table 8**  
**Information resources of consumers about organic products**

Information sources of consumers about organic product	Consuming organic products		Non-consuming organic products		Total*	
	Number	%	Number	%	Number	%
Internet, social media	257	63.77	515	47.20	772	51.67
TV	191	47.39	510	46.75	701	46.92
Friends	187	46.40	502	46.01	689	46.12
Magazine-newspaper (printed publications)	59	14.64	118	10.82	177	11.85
Doctors	82	20.35	85	7.79	167	11.18
Ministry of Agriculture and Forestry	35	8.68	111	10.17	146	9.77
Fairs	49	12.16	92	8.43	141	9.44

\*Multiple options marked

The required criteria to be applied for more consumption of organic products were asked to the consumers and their answers are given in Table 9. Consumers were asked to rank the answers according to their status of finding it important, and the answers were scored from the most important to the least important. Organic product consumers stated that access to organic food should be easy in order to consume more organic products, while consumers who did not consume organic products stated that organic products should primarily be reliable. Consumers in both consumer groups stated that more promotion of organic products would have less impact on organic product consumption. It is possible to say that the easy access to organic products and the high prices of organic products were highly effective on consumption. The fact that organic product prices are at a more reasonable level will be very effective in the tendency of all individuals to consume organic products.

In the study carried out by Shepherd, Magnusson & Sjöden (2005), it was determined that health benefits were demonstrated to be more strongly related to attitudes and behavior toward organic foods than were perceived environmental benefits. Unal, Görgün Deveci & Yıldız (2019) determined in their study that consumption motives of healthiness, easiness, mood, and convenience-price of organic foods motivated consumers to buy organic foods. Eynade, Mushunje & Gbolahan Yusuf (2021) determined that the health and safety of organic products was important for consumers' consumption of organic products. In the study carried out by Cavite, Mankeb, Kerdsriserm, Joedsak, Direksri & Suwanmaneepong (2022), it was revealed that subjective norms, perceived behavioral control, health, consciousness, and knowledge of product traceability significantly affected consumers' intention to purchase traceable organic rice. In the study carried out by Ben Khadda, Ezrari, Radouane, Boutagayout, El Housni, Lahmamsi, Zahri, Houssaini, El Ghadraoui, Elamine & Guiné, Raquel (2022), it was revealed that the price was very important for the majority of consumers in terms of organic product consumption.

**Table 9**  
**Criteria to be applied for more consumption of organic products**

What should be/should be done to consume more organic products?	Consuming organic products		Non-consuming organic products	
	Total score	Order	Total score	Order
Organic food should be easy to access	1,486	1	3,214	4
Must be reliable	1,470	2	4,447	1
Prices should be lower	1,288	3	3,670	2
Income should be more	1,119	4	3,370	3
More promotion should be done	721	5	1,675	5

Consumers were asked about their considerations on purchasing organic products for children (Table 10). 98.51% of consumers consuming organic products and 91.02% of non-consumers stated that organic products should be purchased for children. As a result of the chi-square test, which was conducted to determine whether the difference in consumers' considerations about purchasing organic products for children was statistically significant between groups, it was determined that there was a difference at 1% (p=0.000) significance level.

Table 10  
Consumers' considerations on buying organic products for children

Should organic products be purchased for children?	Consuming organic products		Non-consuming organic products		Total	
	Number	%	Number	%	Number	%
Yes	397	98.51	993	91.02	1390	93.04
No	6	1.49	98	8.98	104	6.96
Total	403	100.00	1,091	100.00	1,494	100.00

Chi-square: 25.517      p: 0.000

Consumers were also asked about their considerations on whether organic product preference was important in baby care and growth or not (Table 11). 36.97% of the consumers consuming organic products and 31.81% of non-consumers stated that they fully agreed with the importance of choosing organic products in baby care and growth. While 2.98% of the consumers consuming organic products stated that they were undecided on this issue, this ratio was determined as 8.07% in the non-consumer group. As a result of the chi-square test, it was determined that there was a difference at 1% (p=0.000) significance level on the considerations of the consumers about whether or not organic product preference was important in baby care and growth.

Table 11  
Consumers' thoughts on organic product preference in baby care and growth

Is organic product preference important in baby care and growth?	Consuming organic products		Non-consuming organic products		Total	
	Number	%	Number	%	Number	%
I never agree	2	0.50	2	0.18	4	0.27
I do not agree	5	1.24	39	3.57	44	2.95
No idea	12	2.98	88	8.07	100	6.67
I agree	235	58.31	615	56.37	850	56.89
I totally agree	149	36.97	347	31.81	496	33.20
Total	403	100.00	1,091	100.00	1,494	100.00

Chi-square: 22.515      p: 0.000

	Average	Standard deviation	Average	Standard deviation	Average	Standard deviation
	4.30	0.636	4.16	0.730	4.20	0.708

### 3.2. Findings Concerning Consumers Consuming Organic Products

The time for consumers to start consuming organic products was determined within the scope of the study (Table 12). It was determined that consumers in all regions mostly started to consume organic products for more than 5 years. This result was similar to the findings of Gülgör (2017).

It was observed that the consumer group, whose time to start consuming organic products was between 3-5 years, had the highest rate in the sixth region and the lowest rate in the fourth region. The consumer group, whose time to start consuming organic products was between 1-3 years, resided in the third region with the highest ratio. The ratios of the consumers who stated that they started to consume organic products in the last year and in the last six months were quite low in all regions, and 13.04% of the consumers residing only in the sixth region stated that they started consuming organic products a year ago. When Table 12 was examined, it was possible to say that consumers were mostly experienced in organic product consumption.

Table 12  
Start time of consuming organic products

Organic product consumption time	Region 1		Region 2		Region 3		Region 4		Region 5		Region 6		Total	
	No.	%	No.	%	No.	%	No.	%	No.	%	No.	%	No.	%
More than 5 years	106	62.35	49	62.03	28	53.85	27	79.41	30	66.67	10	43.48	250	62.03
3-5 years	37	21.76	17	21.52	14	26.92	2	5.88	7	15.56	8	34.78	85	21.09
1-3 years	21	12.35	8	10.13	9	17.31	1	2.94	6	13.33	2	8.70	47	11.66
Last year	5	2.94	2	2.53	0	0.00	1	5.88	1	2.22	3	13.04	13	3.23
In the last 6 months	1	0.59	3	3.80	1	1.92	2	5.88	1	2.22	0	0.00	8	1.99
Total	170	100.00	79	100.00	52	100.00	34	100.00	45	100.00	23	100.00	403	100.00

Organic agricultural products consumed by regions are given in Table 13. Although it varied according to the regions, it was determined that the most consumed organic products were eggs, fruits, milk and vegetables, respectively. These were followed by chicken meat, honey, red meat, dairy products, legumes and meat products, respectively.

The three most consumed organic products in the first region were eggs, milk, fruit, respectively; vegetables, fruits, eggs in the second region; fruit, vegetables, eggs in the third region; milk, eggs, vegetables in the fourth region; fruit, egg, milk in the fifth region and milk, egg and fruit in the sixth region.

It was determined that organic egg consumption was highest in the first and sixth regions, fruit consumption was highest in the fifth region, milk consumption was the highest in the fourth and sixth regions, and vegetable consumption was the highest in the second and fourth regions.

It was determined that the consumption of organic chicken meat, honey, red meat, dairy products and meat products of consumers residing in the fourth region, and organic legumes consumption of consumers residing in the second region were higher than the consumers in other regions.

According to the average of the regions, consumption of legumes, meat products, organic jam, fruit and vegetable juices, canned food, flour/macaroni, tea/coffee, dried fruit/vegetables was determined to be below 5%.

When the Table was examined, it was seen that organic vegetable consumption was higher in the second region. It was considered that the higher production of vegetables and fruits in most of the provinces in this region can be a factor in this situation. In the study conducted by İlter & Yılmaz (2016), it was determined that the most consumed organic products by consumers were eggs, fruits, vegetables and milk, which was similar to the research result.

Table 13

## Consumed organic agricultural products

Consumed organic products	Region 1		Region 2		Region 3		Region 4		Region 5		Region 6		Total	
	No.	%	No.	%	No.	%	No.	%	No.	%	No.	%	No.	%
Egg	114	67.06	44	55.70	25	48.08	21	61.76	27	60.00	16	69.57	247	61.29
Fruit	99	58.24	49	62.03	29	55.77	20	58.82	33	73.33	12	52.17	242	60.05
Milk	109	64.12	36	45.57	24	46.15	24	70.59	25	55.56	17	73.91	235	58.31
Vegetable	83	48.82	50	63.29	26	50.00	21	61.76	22	48.89	11	47.83	213	52.85
Chicken meat	42	24.71	17	21.52	7	13.46	11	32.35	10	22.22	4	17.39	91	22.58
Honey	26	15.29	11	13.92	14	26.92	12	35.29	6	13.33	4	17.39	73	18.11
Meat	12	7.06	13	16.46	12	23.08	10	29.41	7	15.56	3	13.04	57	14.14
Dairy products	7	4.12	15	18.99	5	9.62	7	20.59	7	15.56	4	17.39	45	11.17
Legumes	10	5.88	13	16.46	2	3.85	3	8.82	3	6.67	3	13.04	34	8.44
Meat products	7	4.12	7	8.86	2	3.85	6	17.65	5	11.11	1	4.35	28	6.95
Jam	9	5.29	5	6.33	1	1.92	4	11.76	0	0.00	0	0.00	19	4.71
Fruit/vegetable juice	7	4.12	2	2.53	1	1.92	1	2.94	0	0.00	0	0.00	11	2.73
Canned foods	3	1.76	3	3.80	2	3.85	2	5.88	0	0.00	0	0.00	10	2.48
Flour/macaroni	5	2.94	1	1.27	1	1.92	2	5.88	0	0.00	0	0.00	9	2.23
Tea, coffee	4	2.35	2	2.53	1	1.92	2	5.88	0	0.00	0	0.00	9	2.23
Dried fruit/vegetable	3	1.76	3	3.80	1	1.92	2	5.88	0	0.00	0	0.00	9	2.23

\*Multiple options marked

Consumers were asked about the criteria they paid attention to when purchasing organic products (Table 14). Consumers were asked to rank the answers according to their status of finding it important, and the answers were scored from the most important to the least important. While the consumers in the first region stated that they primarily paid attention to the appearance, taste and smell while purchasing organic products, the consumers in the other regions stated that they primarily paid attention to the expiration date when purchasing organic products. It was determined that the second important issue for the consumers in the first region was the expiration date, the second important issue for the consumers in the fifth region was the price, and the second important issue for the consumers in the other regions was the appearance, taste and smell of the product.



Table 14  
Criteria to consider when purchasing organic products

Criteria	Region 1		Region 2		Region 3		Region 4		Region 5		Region 6	
	Total score	Order	Total score	Order	Total score	Order	Total score	Order	Total score	Order	Total score	Order
Appearance-taste-smell	743	1	349	2	212	2	147	2	182	3	97	2
Expiration date	729	2	368	1	248	1	164	1	204	1	102	1
Price	590	3	225	5	165	4	110	3	183	2	90	3
Packaging	543	4	208	6	130	6	88	6	104	6	60	6
Certification institution	494	5	261	4	165	5	100	5	115	5	67	5
Label	478	6	269	3	175	3	107	4	161	4	69	4

Consumers were also asked whether they paid attention to the logo of the organic product they purchased (Table 15). While 77.65% of consumers in the first region, 67.31% of the consumers in the third region, 70.59% of the consumers in the fourth region, 66.67% of the consumers in the fifth region, 69.57% of the consumers in the sixth region stated that they paid attention to the logo of the organic product they purchased, this ratio was below 50% (46.84%) among the consumers in the second region. Considering the high consumption of organic products in the second region, it is possible to say that consumers living in this region were more conscious about organic product consumption.

Table 15  
Consumers' attention to the logo of the organic products

Attention to the logo	Region 1		Region 2		Region 3		Region 4		Region 5		Region 6		Total	
	No.	%	No.	%	No.	%	No.	%	No.	%	No.	%	No.	%
Yes	132	77.65	37	46.84	35	67.31	24	70.59	30	66.67	16	69.57	274	67.99
No	28	16.47	31	39.24	15	28.85	7	20.59	11	24.44	7	30.43	99	24.57
No idea	10	5.88	11	13.92	2	3.85	3	8.82	4	8.89	0	0.00	30	7.44
Total	170	100.00	79	100.00	52	100.00	34	100.00	45	100.00	23	100.00	403	100.00

Consumers were also asked whether they made certification inquiries for organic products (Table 16). While 24.05% of consumers in the second region, 30.77% of the consumers in the third region, 35.29% of the consumers in the fourth region, 31.11% of the consumers in the fifth region, 30.43% of the consumers in the sixth region stated that they made certification inquiries for products, this ratio was very low for the consumers in the first region (12.94%).

Table 16  
Status of consumers making certification inquiries of organic products

Making certification inquiry	Region 1		Region 2		Region 3		Region 4		Region 5		Region 6		Total	
	No.	%	No.	%	No.	%	No.	%	No.	%	No.	%	No.	%
Yes	22	12.94	19	24.05	16	30.77	12	35.29	14	31.11	7	30.43	90	22.33
No	139	81.76	56	70.89	34	65.38	21	61.76	26	57.78	16	69.57	292	72.46
No idea	9	5.29	4	5.06	2	3.85	1	2.94	5	11.11	0	0.00	21	5.21
Total	170	100.00	79	100.00	52	100.00	34	100.00	45	100.00	23	100.00	403	100.00

Consumers were asked to list their reasons for choosing organic products, and their answers are given in Table 17. Consumers were asked to rank the answers according to their status of finding it important, and the answers were scored from the most important to the least important. While consumers in the sixth region stated that they preferred organic products primarily as they were healthy, the primary reason for consumers in other regions was the absence of drugs and harmful substances in organic products. The last time consumers in all regions prefer organic products. It was determined that the last criterion of the consumers for preferring organic products was the environmental friendliness of organic products in all regions.

In the research conducted by Armağan & Özdoğan (2005), the fact that 75.8% of consumers stated their preference for being healthy and safe supported the findings of this study. In the study conducted by Karabaş & Gürler (2012), health and trust factors were found to be important by consumers. Ben Khadda, Ezrari, Radouane, Boutagayout, El Housni, Lahmamsi, Zahri, Houssaini, El Ghadraoui, Elamine & Guiné, Raquel (2022), determined in their study that the majority of consumers consumed organic products because they were healthy.

Table 17

## Reasons for choosing organic products

Reasons for choosing organic products	Region 1		Region 2		Region 3		Region 4		Region 5		Region 6	
	Total score	Order	Total score	Order	Total score	Order	Total score	Order	Total score	Order	Total score	Order
No drug-harmful substance	715	1	323	1	233	1	141	1	180	1	90	2
Healthy	670	2	317	2	201	2	129	2	173	2	100	1
Rich in nutrients	385	4	230	3	135	3	93	3	127	3	64	3
Taste-smell-image	444	3	211	4	131	4	93	4	127	4	57	4
Environmentally friendly	335	5	131	5	89	5	54	5	80	5	34	5

It was also determined how consumers distinguished organic products from non-organic products (Table 18). While 52.94% of the consumers in the first region and 55.88% of the consumers in the fourth region distinguished the organic products by the certificate and logo, 49.37% of the consumers in the second region, 65.38% of the consumers in the third region, 57.78% of the consumers in the fifth region and 47.83% of the consumers in the sixth region stated that they distinguished the organic products with their appearance.

When all regions were evaluated together, it was concluded that consumers distinguished organic products from non-organic products with their images, certificate-logo, label, taste and smell, respectively. Gülgör (2017), on the other hand, emphasized that the most important factors in distinguishing organic products from non-organic products were certificate-logo, taste, image and label information, respectively.

Table 18

## Criteria for consumers to distinguish organic products from non-organic products

Criteria	Region 1		Region 2		Region 3		Region 4		Region 5		Region 6		Total*	
	No.	%	No.	%	No.	%	No.	%	No.	%	No.	%	No.	%
Image	90	52.94	39	49.37	34	65.38	19	55.88	26	57.78	11	47.83	219	54.34
Certificate-logo	100	58.82	32	40.51	29	55.77	19	55.88	14	31.11	10	43.48	204	50.62
Label information	83	48.82	31	39.24	27	51.92	9	26.47	19	42.22	10	43.48	179	44.42
Taste	51	30.00	32	40.51	17	32.69	20	58.82	16	35.56	8	34.78	144	35.73
Smell	34	20.00	25	31.65	22	42.31	19	55.88	16	35.56	4	17.39	120	29.78

\*Multiple options marked

### 3.3. Evaluation of the Considerations of Organic Food Consuming Consumers about Organic Food Product by Factor Analysis

Consumers consuming organic products were also asked about their considerations on the organic food product (Table 19).

Table 19

## Considerations of the consumers about organic food product

Statements on organic food product	Significance					Avg.	Std. deviation
	1	2	3	4	5		
Organic food products are beneficial for my health.	5	5	7	243	143	4.28	0.68
Consuming organic food products protects me against diseases.	7	20	15	240	121	4.11	0.83
Organic food products are reliable because they are strictly inspected.	13	30	48	230	82	3.84	0.94
Organic food products are beneficial for the development of children.	3	5	17	242	136	4.25	0.66
Organic products are of higher quality because they are grown naturally.	2	14	19	265	103	4.12	0.69
Organic products are hormone-free.	2	32	14	251	104	4.05	0.81
Those who consume organic food products have stronger immune systems.	2	19	29	250	103	4.07	0.75
Consuming organic food products protects against cancer.	2	24	37	243	97	4.01	0.79
Organic food products do not contain GMOs.	6	29	32	247	89	3.95	0.85
Organic food products are tastier.	2	15	28	253	105	4.10	0.72
While growing organic products, nature is not harmed.	4	18	37	241	103	4.04	0.78
Organic food products do not contain chemicals.	6	28	17	258	94	4.01	0.83
Organic food products are easy to cook.	27	104	58	161	53	3.27	1.18
The products I buy from the village are organic.	62	118	32	147	44	2.98	1.31
Considering the cost of producing organic food, it is not expensive.	20	90	23	210	60	3.50	1.14
Organic food products must be certified.	4	15	19	256	109	4.12	0.74
Organic food products are expensive.	10	35	16	262	80	3.91	0.90
The price I pay for organic food products is not too much for my health.	8	62	33	227	73	3.73	0.99
Organic food products smell good.	2	17	39	259	86	4.02	0.72
Organic food products are beneficial to sick people.	4	13	42	268	76	3.99	0.72
If the fruit is wormy, it is organic.	30	105	61	165	42	3.21	1.16
All organic products on the market are organic.	86	212	39	49	17	2.25	1.06

1. Strongly disagree 2. Disagree 3. Undecided 4. Agree 5. Strongly agree

Consumers agreed with the statements that organic food products were beneficial to health, protected against diseases, were beneficial for the development of children, were of high quality as they were grown naturally, were hormone-free, immune systems of those who consumed organic food products were stronger, consuming organic food protected against cancer and organic food products were more delicious. In addition, it was seen that they agreed with the statements that nature was not harmed while growing organic products, organic products did not contain chemicals, organic products must be certified, organic food products smelled good and organic products were beneficial for sick people. It was determined that they tended to agree with the judgments that organic food products were reliable as they were strictly inspected, there are no GMOs in organic food products, organic products were expensive, but the price paid for organic food products was not high for health. It was determined that they were undecided about the judgments that the products obtained from the village were organic, organic food products were easily cooked, organic food was not expensive considering the production cost, and the fruit was organic if it was wormy. In addition, it was determined that consumers did not agree with the statement that all organic products in the market were organic (Table 19).

Factor analysis was performed using 22 variables. The 22 variables in Table 19 were reduced to 4 factors according to their degree of relationship. The communality was taken into account in testing the applicability of the factor analysis method. The communalities of the variables were found to be high and the average was 0.610. This indicated that the variables used were applicable for factor analysis.

First, the correlation matrix was created. Then, the KMO criterion expressed in Table 20, which compares the magnitudes of the correlation coefficients with the magnitudes of the partial correlation coefficients, was examined, and since the significance of the test was found to be significant according to this criterion, factor

analysis was considered appropriate. In other words, the KMO coefficient was found as 0.932, so the result was very good. For this reason, the sample size was sufficient for the study. According to Table 20, it was seen that the Bartlett test significance level value was 0.000. Since this value was less than 5% margin of error, the H0 hypothesis was rejected. In other words, the Bartlett test of Sphericity was found significant (chi-square = 4,741.934,  $p = 0.000$ ).

Table 20  
Suitability test for factor analysis (KMO and Bartlett test)

KMO and Bartlett test		
Kaiser-Meyer-Olkin fitness measure		0.932
Bartlett sphericity test	Approximate chi-square	4,741.934
	Degree of freedom (df)	231
	Significance	0.000

As seen in Table 21, 61.043% of the total variance was explained with 4 factors instead of 22 variables at the beginning. Whether the factors were significant or not was determined by examining the correlation matrix's eigenvalues greater than 1. The variance explanation percentages of these factors gave the total variance explained, the eigenvalues before and after the transformation and showed that there were 4 factors. The first factor explained 32.942% of the total variance, the second factor explained 10.989% of the total variance, the third factor explained 9.063% of the total variance, and the fourth factor explained 8.049% of the total variance. The cumulative amount of variance explained by the eigenvalues was 61.043% of the total variance.

Table 21  
Total variance and variance explanation percentages of factors

Factors	Initial eigenvalues			Sum of translated squared weights		
	Total	Variance (%)	Cumulative (%)	Total	Variance (%)	Cumulative (%)
1	9.091	41.324	41.324	7.247	32.942	32.942
2	1.981	9.003	50.327	2.418	10.989	43.931
3	1.297	5.896	56.223	1.994	9.063	52.994
4	1.060	4.820	61.043	1.771	8.049	61.043
5	0.965	4.385	65.428			
6	0.845	3.842	69.270			
7	0.763	3.469	72.739			
8	0.711	3.230	75.970			
9	0.611	2.778	78.747			
10	0.552	2.510	81.257			
11	0.487	2.212	83.469			
12	0.474	2.156	85.625			
13	0.444	2.019	87.644			
14	0.420	1.908	89.552			
15	0.376	1.711	91.263			
16	0.368	1.672	92.936			
17	0.321	1.458	94.394			
18	0.307	1.397	95.791			
19	0.295	1.343	97.134			
20	0.234	1.066	98.199			
21	0.202	0.917	99.117			
22	0.194	0.883	100.000			

In order to interpret the factors, factor rotation was performed. Varimax method was preferred while performing factor rotation. As a result, the transformative factor loading matrix obtained from 22 variables and 4 factors is shown in Table 22.

When the criteria that constituted the F1 factor were examined, it was seen that these criteria were related to the benefits of organic food products to the health and environment. When the criteria constituting this factor were examined, it was seen that the criteria of "The immune systems of those who consume organic food products are stronger" was the variable with the highest factor loading with a factor load of 0.840, the average factor load of all criteria was 0.695, and the percentage of variance that can be explained was 32.942%. This factor was named as "Health and Environmental Benefits" because it included consumers' statements about the health and environmental benefits of organic products.

When the criteria that constituted the F2 factor were examined, it was seen that these criteria were related to the prices of organic products. While the criteria constituting this factor were examined, it was seen that "Organic food is not expensive considering the cost of production" had the loading of 0.816, "The price I pay for organic food products is not too much for my health" had factor loadings of 0.551, the average factor loading of these criteria was 0.684, and the variance percentage that can be explained was 10.989%. This factor was named as "Price" because it consisted of criteria that included the considerations of the consumers about the prices of organic products.

The average factor loadings of the criteria which were effective on F3 factor such as "All organic products in the market are organic", "The products I buy from the village are organic" and "Organic food products are easy to cook" was found as 0.640 and the explained variance percentage was 9.063%. This factor was defined as "Trust" because it consisted of criteria that included the trust of the consumers to the organic products.

It was seen that the criteria of "Organic food products are expensive (0.818)" and "Organic food products must be certified (0.654)" represented the awareness level of consumers about organic products. For this reason, it was considered appropriate to call this factor "Level of Consciousness". The mean factor loadings of these criteria was found as 0.736 and the percentage of variance explained was 8.049%.

Table 22  
Rotating factor loads matrix

Variables	Factors			
	1	2	3	4
Those who consume organic food products have stronger immune systems.	<b>0.840</b>	0.076	0.111	-0.003
Organic food products are beneficial for the development of children.	<b>0.776</b>	-0.009	-0.049	0.263
Organic products are hormone-free.	<b>0.767</b>	0.204	0.073	0.058
Consuming organic food products protects me against diseases.	<b>0.764</b>	0.021	-0.021	0.103
Consuming organic food products protects against cancer.	<b>0.754</b>	0.245	0.206	-0.032
Organic products are of higher quality because they are grown naturally.	<b>0.745</b>	0.269	-0.038	0.251
While growing organic products, nature is not harmed.	<b>0.697</b>	0.390	0.092	0.169
Organic food products do not contain GMOs.	<b>0.691</b>	0.194	0.211	-0.125
Organic food products do not contain chemicals.	<b>0.664</b>	0.452	0.073	0.073
Organic food products are beneficial for my health.	<b>0.656</b>	0.037	-0.063	0.461
Organic food products smell good.	<b>0.610</b>	0.483	0.161	0.130
Organic food products are tastier.	<b>0.608</b>	0.357	0.047	0.230
Organic food products are beneficial to sick people.	<b>0.595</b>	0.361	0.104	0.301
Organic food products are reliable because they are strictly inspected.	<b>0.566</b>	0.361	0.104	0.301
Considering the cost of producing organic food, it is not expensive.	0.153	<b>0.816</b>	0.095	0.028
The price I pay for organic food products is not too much for my health.	0.412	<b>0.551</b>	0.096	0.246
All organic products on the market are organic.	-0.073	-0.033	<b>0.797</b>	0.002
If the fruit is wormy, it is organic.	0.190	-0.006	<b>0.729</b>	0.090
The products I buy from the village are organic.	-0.047	0.290	<b>0.673</b>	0.129
Organic food products are easy to cook.	0.225	0.345	<b>0.360</b>	-0.089
Organic food products are expensive.	0.037	-0.029	0.198	<b>0.818</b>
Organic food products must be certified.	0.324	0.334	-0.042	<b>0.654</b>

Factors related to the considerations on organic food products were subjected to cluster analysis based on the factor scores obtained (Table 23). Producers at different scales were gathered in different numbers of clusters,

and it was determined that producers at a scale of 10 units gathered in seven clusters. The obtained factors were analysed as seven clusters with the K-means cluster method. The first cluster comprised 0.25% of the main population, the second cluster 23.82%, the third cluster 4.47%, the fourth cluster 41.44%, the fifth cluster 2.48%, the sixth cluster %4.71 and the seventh cluster constituted 22.83% of the population. "Trust" in the first and fourth clusters, "Health and Environmental Benefits" in the second and seventh clusters, "Level of Consciousness" in the third cluster, and "Price" in the sixth cluster were determined as the most prominent factors.

Table 23

Cluster analysis results on judgments about organic food product

Main Factors	Clusters						
	1	2	3	4	5	6	7
Health and Environmental Benefits (F1)	-1.30435	0.60774	-1.79852	-0.16621	-2.62353	-1.29139	0.58547
Price (F2)	-3.02319	0.69681	-1.27002	0.37420	-0.54921	0.87286	-1.24559
Trust (F3)	3.51773	-0.92572	-1.11556	0.75092	-0.93211	-0.48062	-0.01652
Consciousness Level (F4)	-5.03680	-0.18086	1.78902	0.04722	-2.17442	0.76856	-0.11465
Number of observations	1	96	18	167	10	19	92
Ratio in the population (%)	0.25	23.82	4.47	41.44	2.48	4.71	22.83

### 3.4. Findings Concerning Consumers Not Consuming Organic Products

Consumers who did not consume organic products were also asked whether they wanted to consume organic products (Table 24). It was determined that 91.30% of consumers in the first region, 94.74% of the consumers in the third region, 92.42% of the consumers in the fourth region, 94.21% of the consumers in the fifth region, 95.80% of the consumers in the sixth region expressed a positive opinion about consuming organic products while this ratio was slightly lower in the second region (78.16%). In the study conducted by Sandallıoğlu (2014) in Adana province, 56.3% of the consumers who did not consume organic products stated that they were considering purchasing organic products in the future.

Table 24

Consumers' considerations on organic product consumption

Would you like to consume organic products?	Region 1		Region 2		Region 3		Region 4		Region 5		Region 6		Total*	
	No.	%	No.	%	No.	%	No.	%	No.	%	No.	%	No.	%
Yes	451	91.30	68	78.16	108	94.74	122	92.42	114	94.21	137	95.80	1,000	91.66
No	43	8.70	19	21.84	6	5.26	10	7.58	7	5.79	6	4.20	91	8.34
Total	494	100.00	87	100.00	114	100.00	132	100.00	121	100.00	143	100.00	1,091	100.00

Consumers who stated that they wanted to consume organic products were also asked in which situations they would buy organic products (Table 25). 66.52% of consumers in the first region, 86.76% of the consumers in the second region, 76.85% of the consumers in the third region, 72.95% of the consumers in the fourth region, 82.46% of the consumers in the fifth region, 70.80% of consumers in the sixth region stated that they would consume organic products if they truly believed that they were organic. 66.30% of consumers in the first region, 60.29% of the consumers in the second region, 71.30% of the consumers in the third region, 72.95% of the consumers in the fourth region, 62.28% of the consumers in the fifth region, 81.75% of consumers stated

that they would consume organic products if they were cheaper. According to the average of the regions, 26.70% of consumers stated that they would consume organic products if their income was higher, and 24.10% of them stated that they would consume more organic products if they could find more in the market. In the study conducted by Gülgör (2017), it was concluded that consumers would consume organic products if they were cheaper, more available in the market, and if they truly believed that they were produced organically.

It was striking that most of the consumers in all regions would buy organic products if they relied on organic products and the products were sold at more affordable prices. Organic products should be included more in the written and visual media.

Table 25

Organic product purchasing criteria of consumers

Criteria	Region 1		Region 2		Region 3		Region 4		Region 5		Region 6		Total*	
	No.	%	No.	%	No.	%	No.	%	No.	%	No.	%	No.	%
If I really believe it's organic	300	66.52	59	86.76	83	76.85	89	72.95	94	82.46	97	70.80	722	72.20
If it's cheaper	299	66.30	41	60.29	77	71.30	89	72.95	71	62.28	112	81.75	689	68.90
If I have a higher income	120	26.61	6	8.82	36	33.33	33	27.05	21	18.42	51	37.23	267	26.70
If I can find more in the market	114	25.28	23	33.82	19	17.59	28	22.95	26	22.81	31	22.63	241	24.10
If there are more products from my area	23	5.10	10	14.71	11	10.19	18	14.75	9	7.89	16	11.68	87	8.70
If there are more seasonal products	32	7.10	8	11.76	8	7.41	6	4.92	8	7.02	16	11.68	78	7.80
If I have a small child	51	11.31	2	2.94	6	5.56	2	1.64	4	3.51	4	2.92	69	6.90
If I know organic product/logo better	15	3.33	9	13.24	5	4.63	8	6.56	11	9.65	15	10.95	63	6.30
If there is more product variety	17	3.77	4	5.88	3	2.78	5	4.10	4	3.51	5	3.65	38	3.80
If only there is more information in the media.	14	3.10	3	4.41	2	1.85	3	2.46	4	3.51	10	7.30	36	3.60
If it has better/shorter cooking time	6	1.33	3	4.41	4	3.70	1	0.82	1	0.88	6	4.38	21	2.10
If they last longer	8	1.77	4	5.88	1	0.93	0	0.00	5	4.39	2	1.46	20	2.00
If they are better looking and tasty	9	2.00	1	1.47	2	1.85	3	2.46	4	3.51	1	0.73	20	2.00
If I have more time to look for organic products.	7	1.55	2	2.94	0	0.00	1	0.82	1	0.88	3	2.19	14	1.40
If it contains less packaging	3	0.67	1	1.47	3	2.78	1	0.82	0	0.00	5	3.65	13	1.30

\*Multiple options marked

#### 4. Conclusion

With this study, the attitudes and behaviours of consumers in Turkey about purchasing organic food were analysed. The research was conducted in six regions determined according to the socio-economic development index and the regions were compared. Increasing the awareness of consumers about organic foods and their benefits and determining consumer trends in the marketing process of organic foods is also very important for the growth of the domestic market. Since there will be no consumption without production, steps should be taken to enable producers to pass to organic agriculture within the scope of projects. In particular, local governments should identify regions that are suitable for organic farming, with very low or no chemical use, and work for the producers to pass to organic farming. The increase in the number of public markets may contribute to the spread of organic foods and make the organic products easily available to consumers. Besides, the public markets make possible for the producer to sell their goods directly to the consumer and contributes the more reasonable prices of organic products over time by increasing the awareness of organic products. Studies such as creating a healthy database, working to improve consumer awareness, giving priority to advertising activities, teaching the concept of organic products in schools, increasing the specialty stores and making sales by raising the awareness of the consumers in these stores, contributing to the market by increasing and developing the producer unions, can be suggested for the development of the organic market.

#### Acknowledgement

This study was carried out within the scope of the project "Determination of the Factors Affecting the Organic Farming Products of the Consumers" supported by the Ministry of Agriculture and Forestry, General Directorate of Agricultural Research and Policies.

## Author Contributions

Başak Aydın: Data input, performed the statistical analysis and wrote the paper.

Murat Doğu: Collected data.

Ayten Aşkın Kılınç: Collected data.

Sunay Demir: Collected data.

Bülent Tarım: Collected data.

Duygu Aktürk: Interpretation of the results.

Filiz Pezikoğlu: Interpretation of the results.

Volkan Burucu: Collected data.

Mustafa Aslan: Interpretation of the results.

## Conflicts of Interest

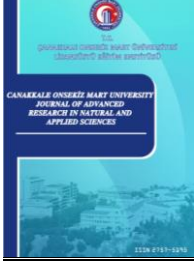
The authors declare that they do not have any conflict of interest.

## References

- Akgül, A., & Çevik, O. (2003). *İstatistiksel analiz teknikleri*, Emek Ofset, Ankara.
- Akın, M., Çiçek, R., İnal, M. E., & Toksarı, M. (2010). Niğde ilindeki tüketicilerin sosyo-demografik özellikleri ile organik gıdalara ilişkin tutum ve bireysel değerleri arasındaki farklılığın incelenmesine yönelik bir araştırma. *Dokuz Eylül Üniversitesi SBE Dergisi*, 12(1), 29-56. Retrieved from: <https://arastirmax.com/en/system/files/dergiler/591/makaleler/12/1/arastirmax-nigde-ilindeki-tuketicilerin-sosyo-demografik-ozellikleri-ile-organik-gidalara-iliskin-tutum-bireysel-degerleri-arasindaki-farklilikin-incelenmesine-yonelik-bir.pdf>
- Aktürk, D. (2012). Organik ürünlerin pazarlama kanalları: Türkiye için uygun bir model önerisi. *International Food, Agricultural and Gastronomy Congress*, (pp. 1-2), Antalya, Türkiye.
- Anonymous (2022). Retrieved from: <https://www.tarimorman.gov.tr/Konular/Bitkisel-Uretim/Organik-Tarim/Istatistikler>
- Armağan, G., & Özdoğan, M. (2005). Ekolojik yumurta ve tavuk etinin tüketim eğilimleri ve tüketici özelliklerinin belirlenmesi. *Hayvansal Üretim*, 46(2), 14-21. Retrieved from: <https://dergipark.org.tr/tr/download/article-file/85119>
- Ataseven, Y., & Güneş, E. (2008). Türkiye’de işlenmiş organik tarım ürünleri üretimi ve ticaretindeki gelişmeler. *Uludağ Üniversitesi Ziraat Fakültesi Dergisi*, 22(2), 25-33. Retrieved from: <https://dergipark.org.tr/tr/download/article-file/154075>
- Ben Khadda, Z., Ezrari, S., Radouane, N., Boutagayout, A., El Housni, Z., Lahmamsi, H., Zahri, A., Houssaini, T.S., El Ghadraoui, L., Elamine, Y., & Guiné, Raquel, P.F. (2022). Organic food consumption and eating habit in Morocco, Algeria, and Tunisia during the COVID-19 pandemic lockdown. *Open Agriculture*, 7(1), 21-29. doi: <https://doi.org/10.1515/opag-2022-0064>
- Cavite, H.J., Mankeb, P., Kerdsriserm, C., Joedsak, A., Direksri, N., & Suwanmaneepong, S. (2022). Do behavioral and socio-demographic factors determine consumers' purchase intention towards traceable organic rice? Evidence from Thailand. *Organic Agriculture*. doi: <https://doi.org/10.1007/s13165-022-00387-1>
- Cengiz, H., & Şenel, M. (2017). Tüketicilerin organik gıda satın alma motivasyonlarının zaltman metafor çıkarım tekniği aracılığıyla incelenmesi. *Karabük Üniversitesi Sosyal Bilimler Enstitüsü Dergisi*, 7(1), 56-69. Retrieved from: <https://dergipark.org.tr/tr/pub/joiss/issue/30785/323318>
- Çokluk, Ö., Şekercioğlu, G., & Büyüköztürk, Ş. (2010). *Sosyal bilimler için çok değişkenli istatistik*. Pagem Akademi, Ankara.
- Doğan, H.G., & Gürel, E. (2016). Kırşehir ili merkez ilçede yaşayan tüketicilerin organik ürün tüketimindeki tutum ve davranışlarının belirlenmesi. *Gaziosmanpaşa Üniversitesi Ziraat Fakültesi Dergisi*, 33(3), 147-156. doi: <https://doi.org/10.13002/jafag1033>
- Eti, H.S. (2014). *Marketing of organic food and analysis of consumer attitude and behavior towards organic food* (Unpublished doctoral dissertation). Namık Kemal University, Tekirdağ, Turkey.
- Eyinade, G.A., Mushunhe, A.M., & Gbolahan, S.F. (2021). The willingness to consume organic food: A review. *Food and Agricultural Immunology*, 32(1), 78-104, doi: <https://doi.org/10.1080/09540105.2021.1874885>
- Gülgör, E. (2017). *Economy of organic farming and consumer trends* (Unpublished master’s thesis). Namık Kemal University, Tekirdağ, Turkey.



- Hair, J.F., Anderson, R.E., Tahtam, R.L., & Black, W.C. (1998). *Multivariate data analysis* (5th ed.). Upper Saddle River, N.J. : Prentice Hall.
- İlter, B., & Yılmaz, B.S. (2016). Understanding determinants of organic food consumption: Turkey example. *Acta Universitatis Danubius. OEconomica*, 12(4), 372-389. Retrieved from: [https://econpapers.repec.org/article/dugacta/y\\_3a2016\\_3ai\\_3a4\\_3ap\\_3a372-389.htm](https://econpapers.repec.org/article/dugacta/y_3a2016_3ai_3a4_3ap_3a372-389.htm)
- Karabaş, S., & Gürler, A.Z. (2012). Organik ürün tercihinde tüketici davranışları üzerine etkili faktörlerin logit regresyon analizi ile tahminlemesi. *Adıyaman Üniversitesi Sosyal Bilimler Enstitüsü Dergisi*, 5(10), 129-156. doi: <https://doi.org/10.14520/adyusbd.272>
- Kalaycı, Ş. (2009), *SPSS uygulamalı çok değişkenli istatistik teknikleri* (4. Baskı). Asil Yayın Dağıtım, Ankara.
- Kleinbaum, D.G., Lawrence, L.K., & Keith, E.M., (1998). *Applied regression analysis and other multivariable methods* (3rd ed.). Duxbury Press, London.
- Lewis, B.M.S. (1994). *Factor analysis and related techniques*. Sage Publications, London.
- Newbold, P. (1995). *Statistics for business and economics*. Prentice Hall International Editions.
- Özer, O. G. (2008). *Analysis of organic agricultural products in terms of demand: Çanakkale case* (Unpublished master's thesis), Çanakkale Onsekiz Mart University, Çanakkale, Turkey.
- Sandallıoğlu, A. (2014). *Consumption of organic agricultural products and consumer tendencies in Adana* (Unpublished doctoral dissertation), Çukurova University, Adana, Turkey.
- Sarıkaya, N. (2007). Organik ürün tüketimini etkileyen faktörler ve tutumlar üzerine bir saha çalışması. *Kocaeli Üniversitesi Sosyal Bilimler Enstitüsü Dergisi*, 14(2), 110-125. Retrieved from: <https://dergipark.org.tr/tr/pub/kosbed/issue/25706/271251>
- Sharma, S. (1996). *Applied multivariate techniques*. John Wiley & Sons Inc., New York.
- Shepherd, R., Magnusson, M., & Sjöden, P.O. (2005). Determinants of consumer behavior related to organic foods. *Ambio*, 34(4-5), 352-359. doi: <https://doi.org/10.1579/0044-7447-34.4.352>
- Turhan, Ş. (2005). Tarımda sürdürülebilirlik ve organik tarım. *Tarım Ekonomisi Dergisi*, 11(1), 13-24. Retrieved from: <https://dergipark.org.tr/tr/download/article-file/253316>
- Unal, S., Görgün Deveci, F., & Yıldız, T. (2019). Do we know organic food consumers? The personal and social determinants of organic food consumption. *Istanbul Business Research*, 48(1), 1-35 doi: <https://doi.org/10.26650/ibr.2019.48.0019>



## Metalik-Benek Dokulu Sanatsal Seramik Sırların Geliştirilmesi: Yüzey Aşınma Özelliklerinin İncelenmesi

Nihan Ercioğlu Akdoğan<sup>1,\*</sup>, Elif Ubay<sup>2</sup>

<sup>1</sup>Kimya Mühendisliği Bölümü, Mühendislik Fakültesi, Eskişehir Teknik Üniversitesi, Eskişehir, Türkiye

<sup>2</sup>Seranit Seramik Fabrikası, ARGE Merkezi, Eskişehir, Türkiye

### Makale Tarihi

Gönderim: 23.06.2022

Kabul: 13.08.2022

Yayın: 15.12.2022

### Araştırma Makalesi

**Öz** – Dekoratif amaçlı olarak kullanılan, seramik sırların ömrünü belirleyen faktörlerin başında sırn aşınma ve kimyasallara karşı direnci yer almaktadır. Sırn aşınma direnci, sır sertliğinin artırılmasıyla iyileştirilebilmektedir. Sırn sertliğini arttırmanın yollarından biri; camsı matristen daha sert kristal faz ya da fazların geliştirildiği uygun cam seramik sistemlerin oluşturulmasıdır. Geliştirilen metalik sırlı ürünlerin düşük konsantrasyonlu kimyasallara maruz bırakılmasından sonra yüzeylerinde leke tutma ve aşınma gibi yüzey hatalarının meydana geldiği tespit edilmiştir. Bu çalışmada, üretilen metalik yüzeyli ürünlerin yüzey hatalarına karşı dayanımlarını arttırmak için reçeteler geliştirilmesi amaçlanmıştır. Kullanılacak olan hammaddelerin kimyasal analizleri X-Ray flüoresans spektroskopisi ile analiz edilerek bileşenleri tespit edilmiş olup reçeteler bu bilgiler ışığında oluşturulmuştur. Oluşturulan sır reçetesinin karakteristik ergime davranışları, ısı mikroskobu analizi yapılarak tespit edilmiştir. Ticari firmalardan alınan metal oksit tozlarının (demir oksit, bakır oksit, mangan oksit) farklı oranlarda kullanılmasıyla oluşturulan reçetelerin aşınmaya ve metalik/artistik yüzey elde etmek üzerine davranışları araştırılmıştır. Elde edilen metalik sır reçetelerin asit/alkali dayanımlarını geliştirdiği ve buna ek olarak sitrik asit, ev kimyasalları ve yüzme havuzu tuzlarına dayanım sonuçlarının ise iyileştirildiği tespit edilmiştir. Aynı zamanda endüstriyel hızlı pişirim koşullarına uyumlu metalik görünümlü, benek efektli ve aşınmaya dirençli, duvar karosu mat sırlar da geliştirilmiştir.

**Anahtar Kelimeler** – Aşınma, benek efekt, metal oksit, seramik karo, seramik sır

## Development of Metallic-Speck Textured Artistic Ceramic Glazes: Investigation of Surface Abrasion Properties

<sup>1</sup>Department of Chemical Engineering, Engineering Faculty, Eskişehir Technical University, Eskişehir, Türkiye

<sup>2</sup>Seranit Granite Ceramic Factory, Research and Development Center, Eskişehir, Türkiye

### Article History

Received: 23.06.2022

Accepted: 13.08.2022

Published: 15.12.2022

### Research Article

**Abstract** – One of the factors determining the life of ceramic glazes used for decorative purposes is the glaze's resistance to abrasion and chemicals. The abrasion resistance of the glaze can be improved by increasing the hardness of the glaze. One of the ways to increase the hardness of the glaze is the creation of suitable glass-ceramic systems in which a harder crystalline phase or phases are developed from the glassy matrix. It has been determined that surface defects such as staining, and abrasion occur on the surfaces of the metallic glazed products produced after exposure to low-concentration chemicals. In the present study, it was aimed to develop recipe in an attempt to improve the resistance of the produced metallic surface products against surface defects. Chemical analysis of the used raw materials was done by X-Ray fluorescence spectroscopy and their components were determined, and recipes were created in the light of chemical components. The characteristic melting behaviours of the created glaze recipe were determined by performing heat microscopy analysis. The behaviour of the recipes containing different amount of metal oxide powders (iron oxide, copper oxide, manganese oxide) from commercial companies on abrasion and metallic/artistic surface obtainment were investigated. It was determined that the acid/alkali resistance of the obtained metallic glaze recipes, as well as the results of resistance to citric acid, household chemicals, and swimming pool salts were improved. Also, matte glazes for wall tiles with metallic appearance, speck effect, and abrasion-resistant, and compatible with industrial fast-firing conditions have been developed.

**Keywords** – Abrasion, speck effect, ceramic tile, metal oxide, ceramic glaze

<sup>1</sup> nihanercioglu@gmail.com

<sup>2</sup> elif.ubay@seranit.com.tr

\*Sorumlu Yazar

## 1. Giriş

Öğütülmüş uygun bileşimli seramik hammaddelerden elde edilen ve seramik bünye üzerinde pişirme neticesinde cam yapıya benzer bir tabaka oluşturabilen harmanlara sır denilmektedir. Sır, terim anlamı olarak da malzemenin yüzeyini dış etkenlerden korumak veya dayanıklı bir boya ile kaplamak amacıyla yüzeye sürülen saydam veya mat camsı tabaka olarak da tanımlanabilmektedir (Trinitat Pradell, 2020; Kurt Strecker, 2014). Endüstriyel uygulamalarda kullanılmak üzere seramik sektöründe daha büyük boyutlar kazanmaktadır (Karmakar, 2017).

Günümüz seramiklerinde kullanılan modern sırlar birtakım niteliklere sahip olmak zorundadırlar (Karmakar, 2017; Hongjun Huang, 2020). Bu nitelikler; i) kullanım boyunca asit ve sularla temasında aşınmamak, ii) su geçirgenliğinin bulunmaması, iii) kılcal sır çatlamalarının olmaması, iv) pullanmalar ve diğer sır hatalarına karşı dayanıklı olmak, v) dekoratif uygulamalarda kristal sırlar gibi artistik sırların elde edilmesine yatkın olmak ve vi) işletme şartlarında belirlenen ısılarda ergimek, endüstriyel olarak sırların sahip olması gereken özelliklerdendir (Richard A. Eppler, 2000; Encarna Bou, 2006; Gizem Ustunel, 2021).

Artistik sırlar, endüstriyel üretimlerde kullanılması daha kısıtlı olması ile dekoratif uygulamalarda sanatsal seramik çalışmalarında renk ve doku elde etmek amacıyla kullanılarak geliştirilen sırlardır (Casasola, 2011; Leidy Johana Jaramillo Nievesa, 2020). Kullanıldıkları seramik formlara sanatsal değer kazandıran bu sırlar detaylı araştırmalar sonucu oluşturulurlar. Bazen rastlantı eseri meydana gelen sır hataları seramik yüzeylere sanatsal etki vermektedir (Leidy Johana Jaramillo Nievesa, 2020). Bu etkiyi bir kez daha elde etmek kimi zaman mümkün olmamaktadır. Kullanıldığı seramiklere sanatsal değer katan artistik sırlara örnek olarak krakle, toplanmalı, seladon sır, metalik, aventürin, kristal, bitkisel kökenli kül, temmoku, lüster ve raku sayılabilir (Brummel, 2020; Hamdzun Haron, 2014; --Pradell, 2006). Metalik sırlar seramik yüzeylerde metal etkisi gösteren mat/parlak yüzeyli sırlar olarak tanımlanmaktadır. Metalik sırlar genelde normal parlak bir sırnın içerisine renklendirici oksitlerin katılması sonucunda elde edilirler (Trinitat Pradell, 2020; Nergis Kiliç Mirdali, 2019) Renk verici oksitler sırlar içerisinde çözünerek sıra renk verirler. Çözünme, renk verici oksidin sırnı oluşturan çözücü maddelerle birleşmesi sonucunda gerçekleşir ve oksidin cinsine ya da kullanım oranına göre değişmektedir. Sırdaki kullanım miktarı arttıkça çözünme hızı azalır ve sırnın özelliği etkilenir. Buna örnek olarak, bakır oksit, demir oksit verilebilir. Bu oksitler, sır içerisinde çözünmezse metalik siyah renkleri oluştururlar (Pradell, 2006; Olga Opuchovic, 2015; Hongjun Huang, 2020).

Literatürde oksitlerin kullanımı ile çeşitli artistik sır çalışmaları yapılmıştır (Kamuran Özlem Sarıncı, 2007; Ozgu Gundeslioglu, 2016; Serap Ünal, 2020). Divitcioğlu ve ark (Gülşah Divitcioğlu, 2021), zeytinden elde ettikleri külü kullanarak sır elde etmişlerdir. Geliştirdikleri sır reçeteleri içerisine renklendirici oksitleri (demir oksit, mangan oksit, krom oksit ve bakır oksit) ilave ederek renkli sırlar geliştirmişlerdir. Bu oksit türlerinden demir oksit, sırlarında en yaygın kullanılan oksit türüdür. Yüksek sıcaklıklarda pişen ve demir oksit ile renklendirilen sırlarda oldukça yumuşak renk geçişlerinin olduğu gözlenmiştir (Gülşah Divitcioğlu, 2021). Bu renk geçişleri, sırlarda yükseltgen ortamda açık sarıdan koyu kahverengiye kadar değişen renk tonlarını meydana getirmiştir (Zaide Bayer Ozturk, 2010; Gultekin, 2017). Kubat (Kubat, 2020), kestane kabuğu külünü kullanarak geliştirilen sır içerisine bakır oksit ve kobalt oksit ilavesi ile renklendirme yapmışlardır. Sonuçları değerlendirildiğinde, külün cam oluşturucu etkisini kullanarak ve oksit ilavesi ile doku oluşumlarını tespit etmişlerdir. Güneş (Güneş, 2015), renk veren oksit katkılarının çeşitli renk ve yüzey etkilerini araştırmak amacıyla stoneware bünyeler üzerine farklı oranlarda uygulama yaparak stoneware sır geliştirmişlerdir. Kobalt oksit, sırlara çok küçük miktarlarda ilave edilse bile oldukça güçlü bir renklendirici olması sebebiyle renklendirme için yeterli olmuştur. Reçetede farklı oranlarda kullanımı farklı mavi tonlarını elde etmek mümkündür. Reçetelere %0,2 kobalt oksit katkısı ile lacivert renk elde edilirken, reçetede eritici miktarı azaltıldığında gök mavisine kadar değişen renk tonları elde edilebilmiştir (Güneş, 2015). Kobalt oksidin verdiği güçlü renk tonlarını diğer oksitleri de beraber kullanarak şiddetini azaltmak mümkündür. Trinitat ve ark (Pradell, 2006), sırların teknik özelliklerini, tarih boyunca süregelen keşifleri ve kullanımları ve dekoratif tekniklerin bir özetini sunmuşlardır. Bakır oksit, sırlarda özellikle yeşil tonlarını elde etmek en fazla kullanılan oksittir. Reçetelerde, %2- 5 oranlarında bakır oksit katkısı ile yeşil renk oluşurken, %0,2-0,5 bakır oksit katkısı ile su yeşilleri elde edilmektedir. Yüksek oranlarda kullanıldığında ise, (kullanım oranı %8'in üzerine çıktığında) renk siyaha doğru değişmektedir. Mangan dioksit katkılı sırlar ile krem/kahverengi tonları elde edilebilmektedir. Düşük sıcaklıklarda pişirilen sırlara %2 oranında mangan oksit ilavesi ile kahverengi tonları elde edilirken, yüksek sıcaklıklarda pişirilen sırlara %5 ve üzerindeki mangan oksit katkısı ile bu renkler elde edilebilmektedir. Aynı zamanda, düşük oranlarda %0,5-0,8 mangan oksit katkısı ile krem rengi elde

edilebilmektedir. Nikel oksit, yüksek sıcaklıklarda pişirilen sırlarda kullanıldığında (%1 ile %4 oranında) pembe rengini meydana getirmektedir (Trinitat Pradell, 2020; Olivier Bobin, 2003). Harmanlanarak kullanımı (nikel oksit, kobalt oksit ve bakır oksit) sonrasında, gri rengi elde edilebilmektedir. Bunun yanı sıra, nikel oksit katkılı sırların uygulanma miktarına (kalın ve ince uygulamalarla) göre farklı tonlar elde etmek mümkündür. Kalın uygulama yapılması halinde pembe renk meydana gelirken ince uygulanan yerlerde gri rengin oluştuğu görülmüştür (Güneş, 2015; Bakanlık, 2007).

Bu çalışmada, literatürde indirgen atmosfer veya elektrikli fırınlarda geliştirilebilen artistik sırların oluşturulması amaçlanmıştır. Böylece ürünlere katma değer sağlayacak endüstriyel hızlı pişirim koşullarına uyumlu metalik sırlar geliştirilmiştir. Bunun yanı sıra, metalik sırlı yüzeylerin aşınma davranışı incelenecek olup aynı zamanda sırlı yüzeylerin aşınmasını etkileyen parametreler açıklanmıştır. Bu kapsamda çeşitli metal oksitler kullanılarak; aşınma dayanımı yüksek duvar karosu sırlarının geliştirilmesi amaçlanmıştır.

## 2. Materyal ve Yöntem

### 2.1. Sır Formülasyonunun Geliştirilmesi

Endüstriyel olarak kullanımı yapı ve teknik özellikler bakımından uygun olan, metalik özellikte, sır geliştirilmesi için reçetelerde kullanılacak malzemelerin seçimi gerçekleştirilmiştir. Üretimi planlanan metalik sır reçetesinde kullanılacak hammaddelerden, kaolin (Smalticeram Unicer S.P.A.), alümina (Industrie Bitossi Mineral San.A.Ş.), Nefelin (Industrie Bitossi Mineral San.A.Ş.) ve dolomit (Kızıldağ Madencilik Hafriyat Nak.İşt.San.Ve Tic.Ltd Şti.) farklı mevki/ocaklardan temin edilmiştir. Esan Eczacıbaşı Endüstriyel Hammaddeler San. ve Tic. A.Ş firmasından kuvars, zirkon ve potasyum feldspat hammaddeleri tedarik edilmiştir. Hammaddeler kullanılarak, farklı oranlarda olmak üzere 64 adet deneme yapılmıştır. Geliştirilen ve uygun bulunan reçete oranları Tablo 1’de verilmiştir. Reçetenin büyük bir bölümünü oluşturan frit, Torrecid S.A firmasından temin edilmiştir. Geliştirilen sır reçetelerinin reolojik özelliklerinin kontrol altında tutulmasını sağlayan reolojik ajanlardan STTP (Sodyum Tripolifosfat) Esan Eczacıbaşı Endüstriyel Hammaddeler San. ve Tic. A.Ş. firmasından, karboksimetil selüloz (CMC) Lamberti Kimya San. ve Tic. firmasından tedarik edilmiştir. Metalik özellikte sır elde etmek için gerekli oksit numuneleri (Demir oksit, mangan oksit, bakır oksit) Akcoat firmasından tedarik edilmiştir.

Tablo 1

Metalik sır elde etmek için geliştirilen sır kompozisyonu

	Frit	Nefelin	Kaolin	Feldspat	Zirkon	Kuvars	Alümina	Dolomit	Bentonit
R2609 (%)	58	9	9	7-10	3-5	4-6	4-5	4-6	0,5-1

### 2.2. Kimyasal Analiz

Hammaddelerin kimyasal analizleri Rigaku ZSX Primus marka ve model XRF cihazı ile eritiş yöntemi kullanılarak gerçekleştirilmiştir. Platin kroze içerisinde çıkarılan camlaştırılmış numuneler XRF cihazına yerleştirilerek analizleri gerçekleştirilmiştir. Bor’dan Uranyum’a kadar olan elementler için tarama yapılmıştır.

### 2.3. Isı Mikroskobu

Atık numunenin ergime davranışları Misura ODHT HSM 1600-80 marka ısı mikroskobuyla belirlenmiştir. Atık numune toz halde olduğu için doğrudan şekillendirme işlemine geçilmiştir. Numune hazırlama aparatıyla yaklaşık 2x3 mm<sup>2</sup> (çap x yükseklik) ebatlarında preslenen silindirik numuneler alümina altlık üzerinde cihaza yerleştirilip analizleri yapılmıştır. Numunenin karakteristik sıcaklık noktaları tespit edilmiştir. Sinterleme sıcaklığı, numunenin belirgin bir akışkan camsı faza sahip olana kadar boyutunun değişmediği sıcaklık aralığıdır. Bu sinterleme sıcaklığının değeri, cihaz tarafından numunenin belirli oranda (genelde %6) boyut değiştiği nokta olarak belirlenmektedir. İlk görüntü %100 düşünülüğünde, buna göre %6 boyut değişimi bu ilk karakteristik sıcaklığı vermektedir. Yumuşama noktası sıvı fazın numune yüzeyinde görüldüğü noktadır. Küre sıcaklığında numune tamamen sıvı fazdan oluşur ve numunenin şekli yüzey gerilimi tarafından kontrol edilmektedir. Yarı küre sıcaklığı, numunenin yüksekliğinin, genişliğin yarısı olduğu duruma denilmektedir. Ergime sıcaklığı ise, numune ilk yüksekliğinin üçte birinin altına düştüğündeki noktadır (Paganelli & Sighinolfi, 2008; Z.Bayer Ozturk, 2020).

## 2.4. Otoklav Test

Bu test TS EN ISO 10545/11 numaralı standarda uygun olarak yapılmıştır. Testi yapılacak pişmiş numunelerin yüzeylerine malahit yeşili sürülerek yüzeylerinde çatlak, kopuk olup olmadığı kontrol edilmiştir. Numuneler otoklav içerisine yerleştirilerek çalıştırılmıştır. Cihaz otomatik olarak 5 atm basınçta 2 saat bekledikten sonra durarak kendini soğutmak için su sirkülasyonu yapmaktadır. 15 dakika soğutulmasından sonra cihazın buhar boşaltma vanası açılarak içerideki buhar boşaltılmıştır. Cihaz Kapağı açılarak numuneler alınmış ve sırlı yüzeylerine malahit yeşili sürülerek çatlak olup olmadığı kontrol edilmiştir. Yüzeylerinde çatlak olanlar ‘-’ çatlak olmayanlar ‘+’ işareti ile kontrol raporuna kaydedilmiştir.

## 2.5. Spektrofotometrik Analiz

Konica Minolta (CM-26dG) markalı spektrofotometre kullanılarak geliştirilen metalik sırların renk ve parlaklık ölçümleri yapılmıştır. Spektrofotometre vasıtası ile örneğe ışın gönderilerek yüzeyden yansıyan ışık spektral mod ile ölçülmüştür. Ölçüm değerleri L, a, b değerleri olarak kaydedilmiştir. ‘L’; açıklık ( $L^*=100$ ) ve koyuluk ( $L^*=0$ ) arasındaki farkı, ‘a’; yeşillik ( $-a^*$ ) ve kırmızılık ( $+a^*$ ) arasındaki farkı ve ‘b’; mavilik ( $-b^*$ ) ve sarılık ( $+b^*$ ) arasındaki farkı tanımlamaktadır.

## 2.6. Aşınma Direnci ve Yüzey Sertliği Kontrolü

Aşındırma testlerinde Ceramic Instruments Abrasimeter PEI 300/C markalı aşındırma cihazı kullanılarak TS EN ISO 10545/7 numaralı standart referans alınarak yapılmıştır. Aşınma testi kapsamında, numuneler 10x10 cm ebadında kesilmiştir. Kesilen numuneler cihaza yerleştirilerek kapak üzerindeki deliklerden her göze 20 ml saf su konulmuştur. Kapak üzerindeki deliklerden her göze 3'er gram korund ve aşınmada kullanılan bilyeler konularak kapak delikleri kapatılmıştır. Yüzey aşındırma cihazı sırası ile 600-1500-2100 devir sayılarına ayarlanarak çalıştırılmıştır. Her kademede devir sayısı tamamlandıktan sonra numune yüzeyleri kontrol edilmiştir. Aynı devir sayısında birden fazla numunede aşınma görülür ise ondan bir önceki devir sayısı ürünün aşınma direncini ve sınıfını belirlemektedir.

Yüzey sertliğinin ölçümü için; Şekil 1’de verilen Mohs sertlik setinde verilen mineraller numunenin sırlı yüzeyine hafifçe bastırılarak sürülmüştür. Uygulamaya küçük numaralı mineralden başlanarak, yüksek numaraya doğru devam etmiştir. Burada gösterilen 1 numaralı mineral ‘Talk’, 2 numaralı mineral ‘jips’, 3 numaralı mineral ‘kalsit’, 4 numaralı mineral ise ‘florit’ mineralleridir. Bu mineraller ile çizilen yüzeyler çakı ya da iğne ile çizilebilecek çizilme derecesine sahip numuneler olarak adlandırılır. Bunların yanı sıra, ‘Apatit’ minerali 5, feldspat minerali ise ‘6’ sertlik derecesine sahip olup bu değere sahip numuneler, sert çelikle çizilebilir yüzeyler olarak tanımlanırlar. Sertlik derecesi 7, 8 ve 9 olan mineraller ise sırasıyla; kuvars, beril ve korundum minerallerini göstermektedir. Bu sertlik derecesine sahip numuneler cam yüzeyini kuvvet ile çizilebilir tanımlamasına uyan numuneler olarak adlandırılmıştır.



Şekil 1. Sertlik testinde kullanılan mineraller (The minerals using in the hardness test)

## 2.7. Lekelenmeye Dayanıklılık Kontrolü

Bu test TS EN ISO 10545/14 numaralı standarda uygun olarak yapılmıştır. Bu kontrolde 4 çeşit lekendirici kullanılmaktadır. Kullanılan bu lekendiriciler; ince yağ içinde yeşil renklendirici madde (%40 m/m Cr<sub>2</sub>O<sub>3</sub>, %60 m/m Myritol 318), ince yağ içinde kırmızı renklendirici madde (%40 m/m Fe<sub>2</sub>O<sub>3</sub>, %60 m/m Myritol 318), iyot (alkol içerisinde 13 g/lt' lik çözelti), zeytinyağıdır. Bu lekendirici malzemelerden numune yüzeyine 3-4 damla damlatılarak yayılması sağlanmıştır. Lekendirici malzeme numune yüzeyinde 24 saat bekletilmiştir. 24 saat bekleyen lekendiricilere temizleyici maddeler işlem sırasıyla uygulanmıştır. İşlem sırası; sıcak su (55±5) °C sıcaklıkta uygulanmasından sonra zayıf temizleme maddesi (aşındırıcı içermeyen PH 6,5-7,5 aralığında ticari temizlik maddesi) sonrasında güçlü temizleme maddesi (aşındırıcı içeren PH 9-10 aralığında) ve uygun çözücüler (hidroklorik asit çözeltisi (%3'lük), potasyum hidroksit çözeltisi (200g/lt), aseton) uygulanmıştır. Her işlem uygulandığında yüzey kurularak kontrolü yapılmıştır.

## 2.8. Kimyasal Maddelere Direnç Kontrolü

Bu test TS EN ISO 10545/13 numaralı standarda uygun olarak yapılmıştır. Nihai sır reçetelerinden elde edilen numuneler alınarak yüzeyleri temizlenmiştir. 8 cm çapında lastik contanın bir yüzü gres yağı ile hafifçe yağlanarak test edilecek numunenin temizlenen kısmına yapıştırılmıştır. Contanın iç kısmına 5 ml çözelti konularak yabancı maddeler giremeyecek şekilde contanın üstü kapatılmıştır. Kimyasal maddelerde direnç kontrolünde kullanılan çözelti cinsi ve kullanım konsantrasyonları Tablo 2'de verilmiştir. Numuneler, ev kimyasalları, yüzme havuzu tuzları ve düşük konsantrasyonlu çözeltiler içinde 24 saat bekletilmiştir. Süresi dolan test numunelerinin yüzeyleri temizlenerek, incelenmiştir.

Tablo 2

Kullanılan çözelti cinsi ve konsantrasyonları

Ev kimyasalları/ Yüzme havuzu tuzları	Amonyum klorür	100 g/lt
	Sodyum hipoklorit	20 mg/lt
	Asit ve alkaliler	%3 (v/v)
Düşük Konsantrasyonlu Çözeltiler	Hidroklorik asit	%3 (v/v)
	Sitrik asit	100 g/lt
	Potasyum hidroksit	30 g/lt

## 2.9. Optik Mikroskop

Yüzeyin makro görünümünün tespiti için Novel NSZ-606 Binocular Zoom stereo mikroskop kullanılmıştır. Mikroskop incelemeleri 50x büyütmede gerçekleştirilmiştir. Yüzeyde oluşan beneklerin boyutunun tespiti için Image-j programı kullanılmıştır. Beneklerin eninden ve boyundan olmak üzere ölçümler yapılmıştır. Bu ölçüm değerlerinin ortalaması hesaplanmıştır.

## 3. Bulgular ve Tartışma

### 3.1. Hammaddelerin Kimyasal Analizi

Kimyasal dayanıma sahip sır reçete oluşturulurken oksitlerin kimyasal analizi büyük önem taşımaktadır. Hammaddelerin yapısında bulunan bileşenler sır bazının fiziksel ve mekaniksel özelliklerine etki etmiştir. Reçetede %58 oranında kullanılan frit, reçete içerisinde bulunması planlanan fakat suda çözünmeleri sebebiyle kullanılamayan veya zararlı malzemelerin, camlaştırılıp yapıda çözünmez hale getirilerek homojen bir yapının oluşturulması için kullanılmıştır. Diğer hammaddelerden farklı olarak BaO, CaO, ZnO içeren frit, metalik renklerin ortaya çıkmasına avantaj sağlamak için kullanılmıştır. Sır bazı oluştururken kullanılan en önemli bileşen kimyasal dayanıma katkısıyla silisyum oksittir. Tablo 3'te görüldüğü gibi, silisyum oksit, frit ve kuvars içerisinde yüksek oranda bulunmasıyla SiO<sub>2</sub> bileşeninin kaynağını oluşturmuştur. Silisyum oksit, bazik oksitler ile uygun oranda karıştığında yapıda cam oluşumunu sağlamaktadır. Bu sayede sırnın mekanik dayanımı arttırmıştır. Kimyasal analiz sonucunda belirlenen, diğer bir önemli oksit bileşeni ise Al<sub>2</sub>O<sub>3</sub> (alüminyum oksit)'tür. Alüminyumun yanı sıra, kaolin hammaddesi de alüminyum oksit kaynağı olarak kullanılmıştır. Isıl genleşmeyi azaltması sayesinde sırnın sıcaklık karşısında dayanımını artırır ve sırnın mekanik direncinin artmasını sağlar. Bunun yanı sıra, sır bazının içerisinde kullanılan diğer bir ergitici hammadde ise feldspattır. Feldspat

hammaddesi, yüksek silisyum oksit, alüminyum oksit ve sodyum oksit içeriğiyle dikkat çekmektedir. Sırın ergimesini sağlamıştır. Genleşme katsayısını yükseltmesi sebebiyle alüminyum oksidin termal genleşmeyi azaltma özelliğini dengelemek için kullanılmıştır. Alkali oranına katkı sağlayan diğer bir hammadde nefelindir. Reçetede, nefelin hammaddesi sodyum oksit ( $\text{Na}_2\text{O}$ ) ve potasyum oksit ( $\text{K}_2\text{O}$ ) içeriğiyle diğer hammaddelerden ayrılmıştır. Dolomit hammaddesi reçetede magnezyum oksit ( $\text{MgO}$ ) ve kalsiyum oksit ( $\text{CaO}$ ) kaynağı olarak kullanılmıştır. Dolomit kullanımı ile sırın termal şok çatlaklarının önlenmesini sağlamıştır. Zirkon hammaddesinin reçetede en önemli görevi yapıya zirkonyum dioksit ( $\text{ZrO}_2$ ) bileşenini kazandırmasıdır. Yüksek aşınma dayanımına ve korozyon direncine sahip olması reçetede kullanımını kaçınılmaz kılmıştır. Kırılma tokluğunu arttırmasının yanı sıra, sırın fiziko-mekanik özelliklerinin gelişmesine katkı sağlamıştır. Diğer hammaddelerden farklı olarak, kimyasal analizinde, %1,37 oranında Hafniyum (IV) oksit tespit edilmiştir. Oksit özelliği açısından hafniyumun rolü elektriksel olarak yalıtkan olduğundan, yapıya da bu özelliği kazandırabilir. Bentonit hammaddesi sırın plastisitesini sağlayarak, sırın yüzeye yayılmasına yardım etmiştir. Böylece, sırda meydana gelebilecek yüzey hatalarının önüne geçilmiştir. Sırın reolojisini yüksek oranda etkilemesi sebebiyle reçetede düşük miktarda kullanılmıştır.

Tablo 3  
Reçeteyi oluşturan hammaddelerin kimyasal analiz sonuçları

Kimyasal Bileşen (%)	$\text{Na}_2\text{O}$	$\text{MgO}$	$\text{Al}_2\text{O}_3$	$\text{SiO}_2$	$\text{P}_2\text{O}_5$	$\text{SO}_3$	$\text{K}_2\text{O}$	$\text{CaO}$	$\text{TiO}_2$	$\text{Fe}_2\text{O}_3$	$\text{BaO}$	$\text{ZnO}$	$\text{ZrO}_2$	$\text{HfO}_2$	A. Z
Frit	1,97	1,86	18,20	46,04	0,70	-	2,32	7,82	-	0,34	4,86	7,95	4,06	0,10	3,78
Nefelin	10,02	0,01	23,10	60,60	0,02	-	5,20	0,38	0,07	0,12	-	-	-	-	0,48
Kaolin	-	0,19	37,14	47,66	0,08	0,02	1,37	0,06	0,18	1,05	-	-	-	-	12,25
Feldspat	10,69	0,03	17,92	70,68	0,01	-	0,09	0,42	0,08	0,07	-	-	-	-	0,01
Zirkon	-	-	1,43	37,40	-	-	0,03	0,09	-	0,28	-	-	59,03	1,37	0,36
Kuvars	0,40	-	1,73	96,56	0,02	-	0,15	0,26	-	0,66	-	-	-	-	0,16
Alümina	-	-	99,39	0,31	-	-	-	0,03	-	0,14	-	-	-	-	0,13
Dolomit	0,10	16,87	-	0,51	0,01	-	-	37,68	-	0,10	-	-	-	-	44,72
Bentonit	0,97	4,16	14,43	69,85	0,03	0,03	0,83	1,91	-	1,28	-	-	-	-	6,51

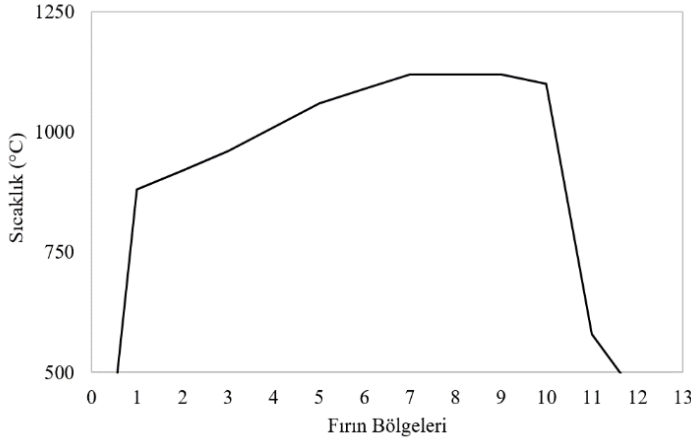
### 3.2. Sır Reçetesinin Hazırlanması

Farklı mevki ve ocaklardan alınan hammaddeler ve fritler ile denemeler yapılmıştır. Elde edilen kompoze sırlarda kurşun, bor ve alkalilik oranına göre oksitlerin meydana getirdiği renkler farklılık göstermiştir. Aynı zamanda geliştirilen birçok sırda, sırın ergimesinin düşük sıcaklıkta gerçekleşmesi nedeniyle sırın yüzeyinde köpürme gibi yüzey hatalarının meydana geldiği görülmüştür. Bu sebeple R2609 kodlu reçete seçilmiştir. Hammaddeler, 500 gram olacak şekilde tartılarak jet değirmenler içerisine %45 oranında su ile ilave edilmişlerdir. Sır reolojisini dengede tutmak için CMC ve STPP; sırasıyla %0,18 ve %0,25 oranlarında ilave edilmiştir. Alümina bilyeli değirmenler 45 dakika boyunca 300 rpm' de karışması sağlanmıştır. Öğütülen kompoze sırın elek bakiyesi 0-0,5 değer aralığında hesaplanmıştır. Sır bazı hazırlandıktan sonra demir oksit, bakır oksit ve mangan oksit farklı oranlarda (%0,5-1-2-5-10) ilave edilerek 5 dakika boyunca tekrar aynı şartlarda karıştırılmıştır. Hazırlanan metalik sır 15x30 cm<sup>2</sup> engoplu duvar karosu üzerine 20-25 gram olacak şekilde uygulanmıştır.

### 3.3. Sinterleme Prosesi

Geliştirilen sır reçetesi 15x30 cm<sup>2</sup> boyutlarında karo üzerine uygulandıktan sonra duvar karosu fırın rejiminde (1120°C-45dk) pişirilmiştir. Duvar karosu, sinterleme eğrisi Şekil 2'de verilmiştir. Şekilde verilen fırının içerisinde bulunan bölümler; kurutma (0-1), ön ısıtma (1-6), ateş bölgesi (6-9), kritik soğutma (9-10), dolaylı soğutma (10-11) ve son soğutma (11-12) olarak adlandırılmıştır. Kurutma bölgesinde, bünyede bulunan fiziksel olarak bağlı su uzaklaştırılmış ve malzemelerin suyun buharlaşma sıcaklığının üzerindeki bir sıcaklığa ısıtılması sağlanmıştır. Kurutma bölgesinden çıkan karo ön ısıtmaya girmiştir. Ön ısıtmada, karodaki kimyasal sular ve bünyedeki  $\text{CO}_3$  ve  $\text{SO}_4$ 'ler atılmıştır. Bu bölümde gerçekleşen en önemli olaylardan biri de  $\alpha$ - $\beta$  kuvars dönüşümüdür. Ateş bölgesi, fırının ortasında bulunmaktadır. Fırının altında ve üstünde brülörler vardır. Brülörlerden her tarafa dengeli sıcaklık dağılımı olmalıdır. Sır bu aşamada en yüksek sıcaklığa erişerek pişmiştir.

Ateş bölgesinden çıkan ürün kritik soğutma bölgesine gelerek, delikli borular ile soğutulmuştur. Dolaylı soğutma aşamasında ise bünye içerisinde  $\beta$ - $\alpha$  kuvars dönüşümü gerçekleşmiştir. Bu kısımda hacimce genişleme meydana geldiğinden dolayı dönüşümün yavaş olması gerekmektedir. Eğer hızlı bir soğutma sağlanırsa sır ve bünyenin genişleme farkından kaynaklı olarak şok çatlakları oluşacaktır. Son soğutma aşamasında karolar, soğutma fanları yardımı ile soğutularak fırından çıkarılmıştır.



Şekil 2. Duvar karosu fırın rejiminin sıcaklık eğrisi

### 3.4. Isı Mikroskobu

Sır bazı numunesinin ergime davranışı ölçüm sonrasında grafik üzerinde incelenmiş olup ergime davranışı ve karakteristik sıcaklık noktaları (sinterleme, yumuşama, tam küre, yarı küre ve akma sıcaklığı) belirlenmiştir. Sır bazına ait ısı mikroskobu ile yapılan ergime davranışı analizinin sonucu aşağıdaki Tablo 4'te sunulmuştur.

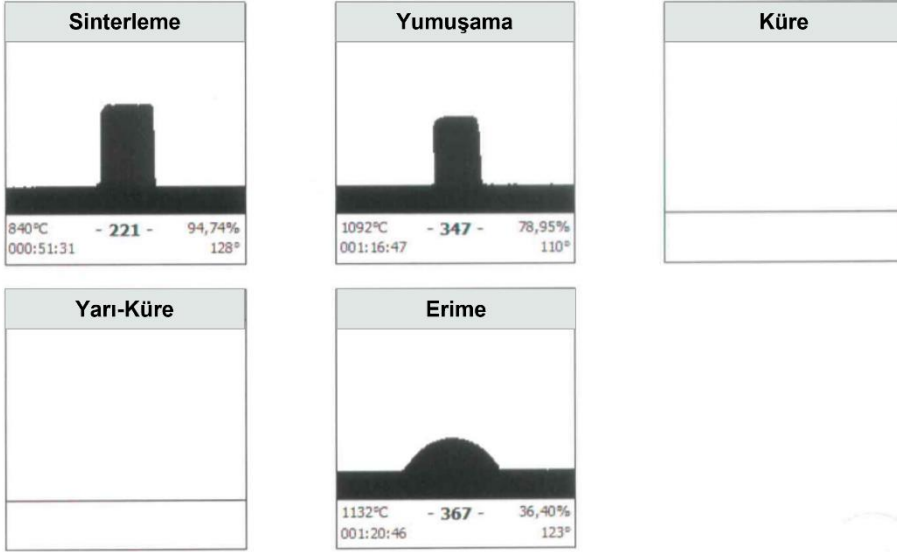
Tablo 4

Sır bazının karakteristik sıcaklıkları

Numune	Sinterleme Sıcaklığı (°C)	Yumuşama Sıcaklığı (°C)	Tam Küre Sıcaklığı (°C)	Yarı Küre Sıcaklığı (°C)	Akma Sıcaklığı (°C)
Sıcaklık	840	1092	-	-	1132

Sinterlenme sıcaklığında sıcaklık artışıyla sıranın, viskoz akış aktivasyon bariyeri aşılmış ve malzeme sinterleme fazına geçmiştir. Tablo 4'te gösterildiği gibi sinterleme sıcaklığı 840°C sıcaklığındadır. Bu süreçte numunenin boyutu azalmış, ancak gerçek şeklinde değişme olmamıştır. Malzemenin sinterlenmesi tamamlanıncaya kadar, yüzey geriliminin etkisiyle cam taneleri birbirine yaklaşmış ve deforme olmuşlardır. Şekil 3'te numunenin sinterlenme sıcaklığına ulaştığındaki deforme hali gösterilmiştir. Numune maksimum yoğunluğa ulaştığı için bu sıcaklıkta sinterleme aşaması sona ermiştir. Yumuşama sıcaklığı olan 1092°C 'den itibaren Şekil 3'ten de görüldüğü gibi, sıvı fazın yüzey geriliminden dolayı numunenin şekli belirgin bir şekilde değişmiştir. Bu noktayı belirlemek için köşelerin yuvarlaklığı ve numune duvarının üst kısımlarının pürüzsüzlüğü göz önünde bulundurulmuştur. Küre ve yarı küre sıcaklığı tespit edilememiştir. Bunun sebebi, yüzey gerilimi yüzeyi küresel hale getirmeye çalışırken, sıvı fazın yoğunluğuna bağlı olarak oluşan hidrostatik basınç şekli düzleştirmeye çalışmıştır. Bu nedenle numunenin yüksek yoğunluklu ve düşük yüzey gerilimine sahip olduğu düşünülmüştür. Sıcaklık değeri 1132 °C'ye ulaştığında ise numune tamamen sıvı faza geçmiş ve erime noktasına ulaşmıştır.





Şekil 3. R2609 kodlu sır bazının ısı mikroskobu ile ergime davranışları

### 3.5. Otoklav Test


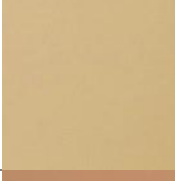
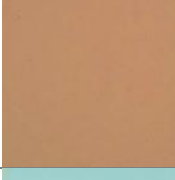
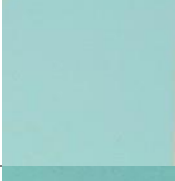


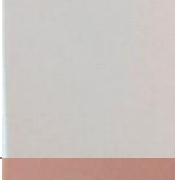


Farklı oranlarda oksit içeren R2609 metalik sır reçetesinin uygulandığı karolar, otoklav içerisinde yüksek basınçtaki buhara maruz bırakıldıktan sonra (5 atm-2 saat) sırlı yüzeylerinde çatlak oluşup oluşmadığını tespit etmek için malahit boyası sürülmüştür. Karoların sırlı yüzeylerinde kılcal çatlaklar oluşup oluşmadığı kontrol edildiğinde oksitlerin kullanım oranının (%0,5-1-2-5-10) ve oksit bileşeninin kılcal çatlak oluşumunu etkilemediği görülmüştür. Tüm denemelerin sonuçları ‘+’ olarak kaydedilmiştir.

### 3.6. Spektrofotometrik Analiz

Temin edilen her bir oksit numunesi %0,5-1-2-5-10 oranlarında R2609 sır bazı içerisine katkılanarak renk değişimleri ve metalik etkileri gözlenmiştir. Denemelerin spektrofotometrik değerleri, parlaklıkları ve görselleri Tablo 5 ve Tablo 6’da verilmiştir. Demir oksit numunesi içeren sır bazının renginde artan oranlarla birlikte krem renginden kahverengiye geçiş olduğu gözlenmiştir. Sır bazı içerisine %0,5-1-2 oranında demir oksit ilavesi ile sır üzerinde metalik etki meydana gelmemiştir. Artan oranlarla numunelerin beyazlığında azalma ve parlaklığında artış meydana gelmiştir. Yüzeyde sır bazındaki oksit miktarının artması ile pinol adı verilen deliklenme meydana gelmiştir. Bu yüzey hatasının meydana gelmesinin sebebi; demir oksidin, sırnın ergime noktasını düşürmesi ve böylece sinterlenmenin daha erken olmasına neden olduğu düşünülmüştür (Güneş, 2015). Bakır oksidin diğer oksit türlerine kıyasla yüzey hatalarına neden olmadığı görülmüştür. Bakır oksit katkılı (%0,5-1-2) sır bazlarının pişirim sonrası renkleri artan oranlarla açık turkuaz renginden maviye dönüşmüştür. %2 oranında bakır oksit ilavesi ile metalik etki artmış ve yüzeyde benek efektinin oluşumları gözlenmiştir. Bakır oksit oranının artması ile ‘L’ değeri olan beyazlıkta azalma parlaklıkta ise artış görülmüştür. Kırmızılık/yeşillik (+a; -a) değerleri arasındaki fark oldukça azken sarılık/mavilik değeri, oksit oranının artması ile sararma (+b) yönünde değişmiştir. Sır bazı içerisine mangan oksit katkısı ile artan oranlarla sır renginde toz-pembeden mor rengine doğru koyulaşma olduğu tespit edilmiştir. Bunu sebebi, mangan oksidin, kurşun oranı yüksek olan sırlarda kahverengi, bor içerikli sırlarda kahve-mor, alkalilik oranı yüksek sırlarda ise mor renklerinin oluşmasına katkı sağlamasıdır. Bunun yanı sıra, mangan oksit oranının artması ile sırnın matlaştığı tespit edilmiştir. Bu sonuç, mangan oksidin diğer oksitlere kıyasla sır bazının ergimesini yükselterek pişirim sıcaklığı arttırdığını göstermiştir. Renginin pembe mor tonlarında olması sebebiyle ‘a’ değerinde diğer oksitlere kıyasla daha fazla artış gözlenmiştir. Metalik etki gözlenmemiştir. Oksit numunelerinin, %0,5-1 ve %2 oranlarında sır bazı içerisine ilavesinin yüzeylerdeki metalik etkinin oluşmasına yeterli katkıyı sağlayamadığı bu sebeple bu oranın artması gerekliliğine karar verilmiştir. Tablo 6’da sır bazı içerisine %5-10 oranlarında oksit ilavesinin yüzey rengine, metalik ve benek efektine etkisi incelenmiştir.

Tablo 5

Oksit katkılı sırların spektrofotometre değerleri ve farklı oksit katkılı sırların yüzey görüntüsü





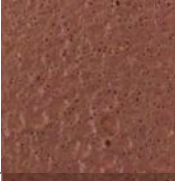

Numune	L	a	b	Parlaklık	Görüntüsü
R2609/0,5Fe	74,72	7,59	17,01	12,44	
R2609/1Fe	69,39	8,79	20,39	14,48	
R2609/2Fe	65,05	8,55	16,82	16,95	
R2609/0,5Cu	84,64	-10,99	-0,78	10,99	
R2609/1Cu	77,39	-12,96	0,37	12,09	
R2609/2Cu	67,41	-12,12	2,36	14,11	
R2609/0,5Mn	82,21	3,97	4,47	23,42	
R2609/1Mn	74,93	5,60	4,92	14,24	
R2609/2Mn	67,36	6,35	5,19	12,43	

Tablo 6’da görüldüğü gibi, %5 ve %10 oranında demir oksit ilavesi ile sırların rengi kahverengi tonunda koyulaşarak ‘43,56’ değerine gerilemiştir. Aynı zamanda, parlaklık değeri de artan oranlarla artmıştır. ‘a’ değerleri karşılaştırıldığında R2069/5Fe ve R2069/10Fe numuneleri arasında fark gözlenmemiştir. Metalik etki bu oran bandında da demir oksit numunesi için tespit edilmemiştir. Bunlara ek olarak, R2609/2Cu numunesinde ortaya

çıkan küçük beneklenme görüntüleri ve metalik efektler, oksit oranının %5 ve %10'a artırılması ile daha belirgin benek oluşumlarının meydana gelmesine neden olmuştur. Tablo 6'da sır görüntülerinde gözleendiği gibi %5 oranında bakır oksit ilavesi ile sır koyu yeşil renginde iken, %10 oranında ilave edildiğinde siyah rengin almıştır. Bunun yanı sıra, bakır oksit ilavesi ile sıran parlaklığı artmıştır. İki oran sonucunda da metalik etki gözlenmiştir. Mangan oksit miktarının artması ile sıran ergime noktası düşmüş bu sebeple pişirim sıcaklığında yüzeyde köpürme meydana gelmiştir. Oranın artması ile yüzey matlaşarak koyulaşmış ve metalik etki gözlenmiştir.

Tablo 6

%5 ve %10 oranında demir, bakır ve mangan oksit katkılı sırların spektrofotometrik sonuçları ve bu sırların yüzey görünüşleri

Numune	L	a	b	Parlaklık	Görüntüsü
R2609/5Fe	53,86	10,78	26,73	17,44	
R2609/10Fe	43,56	10,17	18,51	18,91	
R2609/5Cu	49,91	-5,45	5,42	16,29	
R2609/10Cu	43,46	0,72	3,82	19,11	
R2609/5Mn	53,15	6,36	5,02	15,45	
R2609/10Mn	45,11	5,28	4,29	13,07	

Bu çalışmalara ek olarak, mangan oksit içeren sırlarda meydana gelen köpürme probleminin önüne geçebilmek için kurumanın, sır kalınlığının ve reçete içerisine ergime sıcaklığını arttıracak hammadde ilavesinin etkisi incelenmiştir. Mangan oksit katkılı sırlarda görülen köpürme problemi kurutulan karolarda da devam etmektedir. Bunun yanı sıra sırların uygulama yüzeyindeki kalınlığının etkisini incelemek için 15x30 cm<sup>2</sup> yüzey üzerine 15-20 gram sır uygulanarak pişirilmiştir. Bunun sonucunda; köpürme probleminin azaldığı görülmüştür. Fakat sır kalınlığının azaltılması ile elde edilen denemelerde karo yüzeylerindeki metalik etkinin de azaldığı tespit edilmiştir. Metalik özellik gösteren R2609/10Mn sırası içerisine sıran sinterlenme sıcaklığını arttırmak için %2 oranında alümina ilave edilerek yüzey köpürmesine etkisi incelenmiştir. İlave sonrası yüzeyde köpürme hatasının azaldığı fakat yüzeyin yüksek oranda matlaştığı ve metalik etkisini kaybettiği görülmüştür.

### 3.7. Lekelenme ve Kimyasal Direnç Kontrolü

Yüzeylerinde metalik etki ve beneklenme efekti görülen numuneler lekelenme ve kimyasal dayanım testlerine tabi tutulmuşlardır. Elde edilen sonuçlar Tablo 7’de verilmiştir. Asit alkali ve ev kimyasalları testleri sırbazı ve içerisinde bakır oksit katkısı olan sırlar için ‘LA’ ve ‘A’ olarak tespit edilmiştir. Bu ifadeler, yüzeyin asit alkalilere ve kimyasallara karşı yüksek düzeyde dayanımı olduğunu göstermektedir. Oksit miktarının artması yüzeyin lekelenme ve kimyasal maddelere karşı dayanımını değiştirmemiştir. Bakır oksit katkısı, sırbazının erime noktasını yükselttiği ve sinterleme sıcaklığını arttırdığı için yüzeyler diğer oksit katkılı sırlara göre daha mattır. Bu da katkılı sırların daha yüksek sıcaklıkta sinterlenebildiği anlamına gelmektedir. Yüksek sıcaklıkta sinterlenen sırlar genellikle düşük sıcaklıkta elde edilen sırlara göre daha sert, dayanıklı ve asitlere karşı dayanıklı olma özelliklerine sahiptirler (Encarna Bou, 2006). Elde edilen sonuçlarda bu bilgiyi doğrular niteliktedir.

Tablo 7

Bakır oksit katkılı sırların lekelenme ve kimyasal maddelere dayanım sonuçları

Testler	Asit Alkali		Ev Kimyasalları			Lekelenme		
	HCl	KOH	Sitrik Asit	NH <sub>4</sub> Cl	NaClO	Yeşil Leke	Zeytin Yağı	İyot
R2609	LA	LA	LA	A	A	5	5	5
R2609/2Cu	LA	LA	LA	A	A	5	5	5
R2609/5Cu	LA	LA	LA	A	A	5	5	5
R2609/10Cu	LA	LA	LA	A	A	5	5	5

### 3.8. Aşınma Direnci ve Yüzey Sertliği Kontrolü

Yüzeyinde metalik ve benek efekti görülen sırların (R20609/2Cu, R20609/5Cu, R20609/10Cu) yüzey aşınma dayanımlarının sınıflandırılması, TS EN 10545-17 standardında belirtilen teste göre yapılmış olup sonuçlar Tablo 8’de verilmiştir. Aşınma dayanımları PEI sınıfınca değerlendirilmiştir. Tüm numunelerin PEI değeri ‘5’ olarak tespit edilmiştir. Bu değer, yaya trafiğinin yoğun olduğu ve aşındırıcı maddelerin çok olduğu zeminlerde kullanımının uygun olduğunu göstermektedir. Aşınma değeri sırların yüzeylerinde yeterli camsı faz meydana gelmesi sebebiyle dayanımı yüksek ölçülmüştür. Camsı faz yüzeyde bulunan gözenekleri doldurarak, gözenekli yapıdan kaynaklı meydana gelen mikro çatlak oluşumunu engeller. Böylece, çatlakların çoğalmalarını önler. Yüzey sertlik değerleri sırbazı için ‘6’ olarak tespit edilirken, bakır oksit katkılı numuneler için ‘8’ olarak tespit edilmiştir. Bakır oksit katkısı numunenin yüzeyde mekanik direncin oluşmasını yüzeyi sertleştirmiştir. Bu sayede yüzeyin çizilmesini önlemiştir.

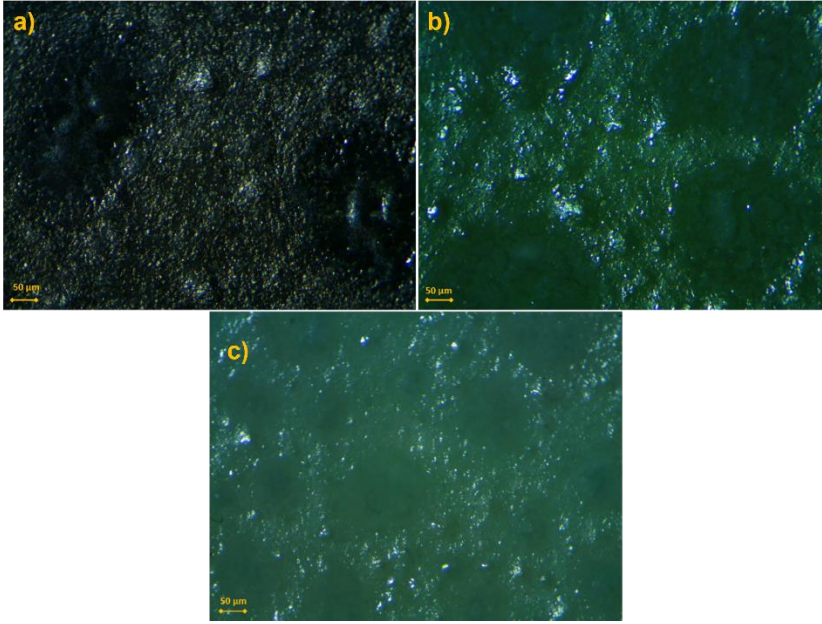
Tablo 8

Bakır oksit katkılı sırların aşınma ve yüzey sertliği değerleri

Test	Aşınma Değeri (PEI)	Yüzey Sertliği (Mohs)
R2609	5	6
R2609/2Cu	5	8
R2609/5Cu	5	8
R2609/10Cu	5	8

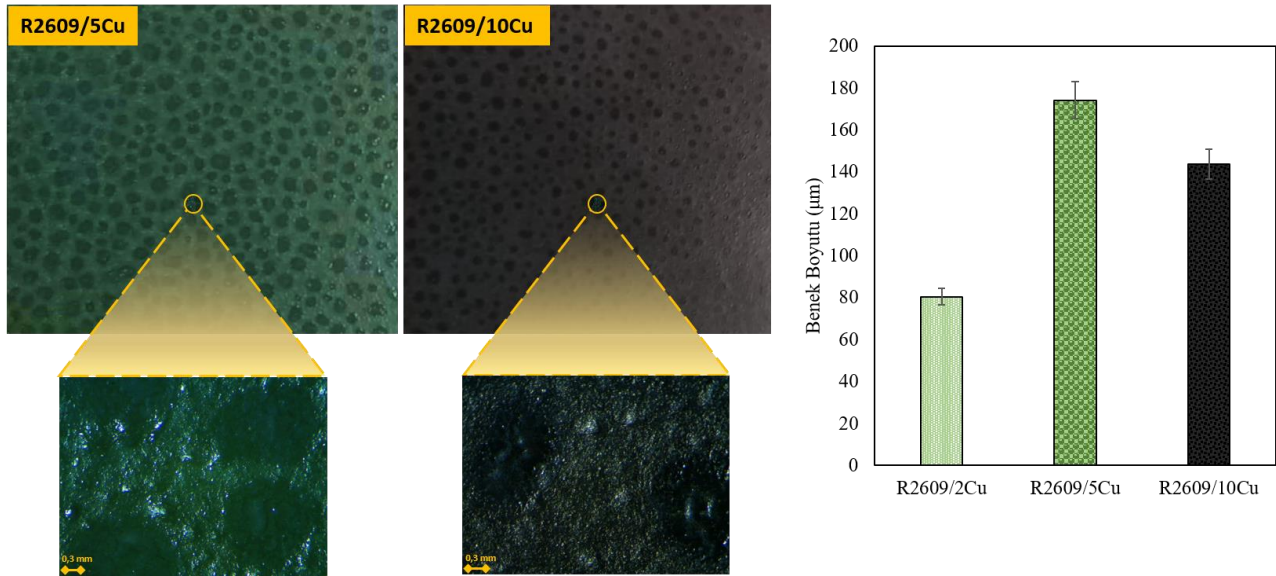
### 3.9. Optik Mikroskop

Yüzey morfolojisinin analiz edilmesi için optik mikroskop görüntüleri incelenmiştir. Şekil 4’de yüzeylerinde beneklenme ortaya çıkmış olan, R2609/2Cu, R2609/5Cu ve R2609/10Cu numunelerinin yüzey görüntüsü verilmiştir. Optik mikroskop görüntüleri incelendiğinde, %10-5 ve 2 oranlarında bakır oksit içeren numunelerin hepsinde beneklenme gözlenmiştir. Benek oluşumu %2 bakır oksit ilavesinden sonra meydana gelmiştir. R2609/2Cu numunesinde diğerlerine oranla daha küçük ve sık miktarlarda benek oluşumu görülmüştür. Bakır oksit miktarının artması ile benekler bir araya gelerek daha büyük boyutlarda beneklerin oluşumuna neden olmuşlardır.



Şekil 4. Bakır oksit katkılı sırlarda oluşan metalik ve benek efektli yüzeylerin optik mikroskop görüntüleri a) %10, b) %5 ve c) %2 bakır oksit ilaveli sır

Optik mikroskop ile tespit edilen benek boyutlarının karşılaştırılması Şekil 5'te verilmiştir. Bakır oksit ilaveli sırlarda %2 oranına kadar benek oluşumu gözlenmezken %2 oranında beneklerin meydana geldiği görülmüştür. %2 oranında bakır oksit ilaveli R2609/2Cu kodlu sırnın benek boyutu  $80,5 \pm 6$   $\mu\text{m}$  olarak hesaplanmıştır. Bunun yanı sıra, bakır oksit ilave edilmesi ile beneklerin boyutunun büyüdüğü gözlenmiştir. %5 oranında bakır oksit katkılanması ile benek boyutunun  $174,2 \pm 4$   $\mu\text{m}$  boyutuna ulaştığı hesaplanmıştır. Bu sonuçlardan yola çıkarak bakır oksitin sır içinde çözünmeye devam ettiği belirlenmiştir. Sır içerisindeki bakır oksit oranının %10'a ulaşması ile benek boyutu  $143,6 \pm 7$   $\mu\text{m}$  olarak ölçülmüş olup benek boyutu küçülmeye başlamıştır. Bunun sebebinin sırnın bakır oksit doygunluğuna ulaşması ve artık çözünemediğinden kaynaklandığı tespit edilmiştir. Bakır oksidin çözünmediğine dair diğer bir gösterge ise sırnın renginin siyaha dönmesidir. Buradan yola çıkarak, sır yüzeyinde meydana gelen beneklerin %2 bakır oksit ilavesi ile önce arttığı daha sonra bakır oksit oranının artması ile önce büyüüp sonra küçülmeye başladığı tespit edilmiştir.



Şekil 5. Bakır oksit ilavesinin benek boyutuna etkisi

#### 4. Sonuçlar

Çalışmanın en önemli sonucu, oksitlerin sır içerisinde kullanımı ile meydana gelen seramik yüzeyler üzerinde oluşan dokusal etkilerdir. Endüstriyel duvar karosu fırın koşullarında meydana gelen benek görüntüsü oldukça ilgi çekicidir. Demir oksit ve mangan oksit kullanımının %5 oranından düşük olduğu denemelerde metalik etki gözlenmemiştir. Bakır oksit katkısının artması ile sır yüzeyinin metalik özelliğinin arttığı ve benek efektinin ortaya çıktığı tespit edilmiştir. Bakır oksit ilavesinin artması ile beneklerin önce büyüdüğü sonra oksidin sır içinde çözünmesinden kaynaklı olarak küçüldüğü gözlenmiştir. Bu nedenle özellikle artistik yüzey görünümleri için bakır oksit kullanımı önerilmektedir. Sır denemelerinin bütününe bakıldığında çatlama, kavlama, toplanma vb. yüzeysel hatalara rastlanmamıştır. Bunun yanı sıra, farklı metalik renklerde olmak üzere elde edilen sırların, yüzey özellikleri incelendiğinde asit alkali ve kimyasallara karşı dayanımının arttığı görülmüştür. Uluslararası TS EN 14411 standartlarının sonuçlarına göre sır yüzeylerinin kimyasal dayanımı geliştirilerek ürünlere katma değer sağlanmıştır. Bir diğer önemli sonuç ise, sır kalınlığının efekt oluşuma etkisidir. Sır uygulama kalınlığının büyük önem taşıdığı tespit edilmiştir. Uygulama kalınlığının artması ile yüzeyde benek oluşumlarının meydana geldiği gözlenmiştir. Bir diğer dikkat çekici özellik ise sır uygulama kalınlığının aynı zamanda benek oluşumunu da etkilemiş olmasıdır. Bakır oksit ile üretilen metalik-benek etkili sırlar seri üretim için uygun olup endüstriyel seramik fırınlarında üretilebilir. Bu sayede hem yeni, ticari ve katma değerli bir yüzey elde edilmiş hem de geliştirilen sır bazı ile aşınma ve kimyasal dayanım artırılmıştır.

#### Teşekkür

Proje çalışmaları süresince finansal destek sağlayarak çalışmanın ortaya çıkmasını sağlayan Sinpaş Holding yönetim kuruluna ve Seranit Seramik Fabrikası yönetim kuruluna teşekkür ve saygılarımı sunarım.

#### Yazar Katkıları

Nihan Ercioğlu Akdoğan: Analizi planlamış ve tasarlamış ve makaleyi yazmıştır.

Elif Ubay: Veri toplamış ve analizini yapmıştır.

#### Çıkar Çatışması

Yazarlar çıkar çatışması bildirmemişlerdir.

#### Kaynaklar

- Bakanlığı, M. E. (2007). *Seramik ve Cam Teknolojisi*. Ankara: Mesleki Eğitim ve Öğretim Sisteminin Güçlendirilmesi Projesi. Retrieved from: <https://docplayer.biz.tr/9178467-T-c-milli-egitim-bakanligi-megep-mesleki-egitim-ve-ogretim-sisteminin-guclendirilmesi-projesi-seramik-ve-cam-teknolojisi.html>
- Brummel, L. (2020). *The Development of an Innovative Glazing Technique for the Raku Kiln*. Avustralya: Central Queensland University (Master's thesis). Retrieved from: [https://acquire.cqu.edu.au/articles/thesis/The\\_development\\_of\\_an\\_innovative\\_glazing\\_technique\\_for\\_the\\_Raku\\_Kiln/17009255](https://acquire.cqu.edu.au/articles/thesis/The_development_of_an_innovative_glazing_technique_for_the_Raku_Kiln/17009255)
- Casasola, R. J. (2011). Glass-ceramic glazes for ceramic tiles: a review. *Journal of Materials Science*, 553-582. doi: <https://doi.org/10.1007/s10853-011-5981-y>
- Encarna Bou, A. M. (2006). Microstructural study of opaque glazes obtained from frits of the system: SiO<sub>2</sub>-Al<sub>2</sub>O<sub>3</sub>-B<sub>2</sub>O<sub>3</sub>-(P<sub>2</sub>O<sub>5</sub>)-CaO-K<sub>2</sub>O-TiO<sub>2</sub>. *Journal of the European Ceramic Society*, 1791-1796. doi: <https://doi.org/10.1016/j.jeurceramsoc.2006.04.148>
- Gizem Ustunel, C. Y. (2021). Prevention of mat glazed acid permeability used in monoporosa wall ceramics. *Environmental Technology & Innovation*, 101628. doi: <https://doi.org/10.1016/j.eti.2021.101628>
- Gultekin, E. E. (2017). Fe<sub>2</sub>O<sub>3</sub> içeren hammaddenin şeffaf sıra renklendirme etkisi. *Dicle Üniversitesi Mühendislik Dergisi*, 8(4), 865-870. Retrieved from: <https://dergipark.org.tr/tr/pub/dumf/issue/33630/408861>
- Gülşah Dıvıçoğlu, M. F. (2021). Usage olive seed ash in artistic ceramic glazes. *Journal of Awareness*, 155-164. doi: <https://doi.org/10.26809/joa.6.3.07>
- Güneş, P. Ç. (2015). Renk Veren Oksitlerle Geliştirilen 'Stoneware' Sır Araştırmaları. *Yedi: Sanat, Tasarım ve Bilim Dergisi*, 135-142. Retrieved from: <https://dergipark.org.tr/tr/download/article-file/203774>
- Hamdzun Haron, S. A. (2014). The Formulation of Ceramic Bodies using the Toba Volcanic Ash of Lenggong.



- Jurnal Teknologi*, 99-104. doi: <https://doi.org/10.11113/jt.v67.2383>
- Hongjun Huang, J. Y. (2020). Preparation of A High-Performance Frit Glaze Using High-Potassium Feldspar. *IOP Conf. Series: Earth and Environmental Science*. Japan: IOP Publishing. Retrieved from: <https://iopscience.iop.org/article/10.1088/1755-1315/943/1/012018/pdf>
- Kamuran Özlem Sarnıç, L. K. (2007). Eskişehir Bölgesi Şeker Pancarı Küspesi Küllerinin Sır Bileşeni ve Renklendirici Olarak Kullanılabilirliğinin Araştırılması. *IV Uluslararası Katılımlı Seramik Cam Emaye Sır ve Boya Semineri*, (s. 204-2014). Eskişehir. Retrieved from: <http://kamuranozlemsarnic.com/uploads/dosyalar/bildiri/serez2008.pdf>
- Karmakar, B. (2017). Functional glass-ceramics. B. Karmakar içinde, *Functional Glasses and Glass-Ceramics Processing, Properties and Applications* (s. 119-208). Birleşik Krallık: Butterworth-Heinemann. Retrieved from: <https://www.elsevier.com/books/functional-glasses-and-glass-ceramics/karmakar/978-0-12-805056-9>
- Kubat, L. (2020). Kestane Kabuğu Külünün Sır Bileşeni Olarak Kullanılabilirliğinin Araştırılması . *Akademik Sanat*, 61-70. Retrieved from: <https://dergipark.org.tr/en/download/article-file/1075843>
- Kurt Strecker, H. B. (2014). Formulation of Ceramic Glazes by Recycling Waste Glass. *Materials Science Forum*, 635-641. doi: <https://doi.org/10.4028/www.scientific.net/MSF.775-776.635>
- Leidy Johana Jaramillo Nievesa, A. V. (2020). Digital decoration for ceramic tiles: The effect of glazes particle size distribution on the inkjet decoration. *Boletín de la Sociedad Española de Cerámica y Vidrio*, 44-48. doi: <https://doi.org/10.1016/j.bsecv.2019.06.005>
- Nergis Kiliç Mirdali, M. D. (2019). Development and characterization of low temperature metallic glazes in Na<sub>2</sub>O-B<sub>2</sub>O<sub>3</sub>-SiO<sub>2</sub> (NBS) system. *Ceramics International*, 45(17), 21661-21667. doi: <https://doi.org/10.1016/j.ceramint.2019.07.164>
- Olga Opuchovic, A. K. (2015). Historical hematite pigment: synthesis by an aqueous sol-gel method, characterization and application for the coloration of ceramic glazes. *Ceramic International*, 4509. doi: <https://doi.org/10.1016/j.ceramint.2014.11.145>
- Olivier Bobin, M. S.-F. (2003). Coloured metallic shine associated to lustre decoration of glazed ceramics: A theoretical analysis of the optical properties. *Journal of Non-Crystalline Solids*, 28-34. doi: <https://doi.org/10.1016/j.jnoncrysol.2003.08.084>
- Ozgu Gundeslioglu, K. T. (2016). Bir Sera Atığı Olarak Patlıcan Dalı Külünün Düşük Dereceli Seramik Sırlarında Kullanımı. *Akdeniz Sanat Dergisi*, 11-20. Retrieved from: <https://dergipark.org.tr/tr/download/article-file/275523>
- Paganelli, M., & Sighinolfi, D. (2008). Understanding the behaviour of glazes with the automatic heating microscope. *Ceramic Forum International*, 85(5), E63-E67. Retrieved from: [https://www.researchgate.net/publication/292709377\\_Understanding\\_the\\_behaviour\\_of\\_glazes\\_with\\_the\\_automatic\\_heating\\_microscope](https://www.researchgate.net/publication/292709377_Understanding_the_behaviour_of_glazes_with_the_automatic_heating_microscope)
- Pradell, T. J. (2006). Luster decoration of ceramics: mechanisms of metallic luster formation. *Applied Physics A*, 203-208. doi: <https://doi.org/10.1007/s00339-006-3508-1>
- Richard A. Eppler, D. R. (2000). Glazes and glass coatings. *Glazes and glass coatings* (s. 29-80). Amer Ceramic Society. Retrieved from: <https://www.amazon.com/Glazes-Glass-Coating-Richard-Eppler/dp/1574980548>
- Serap Ünal, E. A. (2020). Gül posası külünün seramik yüzeylerde kullanımı. *Akademik Sanat*, 90-104. DOI:10.34189/asd.5.10.006
- Trinitat Pradell, J. M. (2020). Ceramic technology. How to characterise ceramic glazes. *Archaeological and Anthropological Sciences*, 12-189. doi: <https://doi.org/10.1007/s12520-020-01136-9>
- Z.Bayer Ozturk, A. K. (2020). Effects of alumina and white fused alumina addition on technological properties of transparent floor tile glazes. *Journal of Thermal Analysis and Calorimetry*, 142, 1215-1221. doi: <https://doi.org/10.1007/s10973-019-09171-y>
- Zaide Bayer Ozturk, N. A. (2010). The effect of ferrochromium fly ash as a pigment on wall tile glaze. *Advances in Science and Technology*, 68, 213-218. doi: <https://doi.org/10.4028/www.scientific.net/AST.68.213>



# Sentiment Analysis from Face Expressions Based on Image Processing Using Deep Learning Methods

Orhan Emre Aksoy<sup>1</sup>, Selda Güney<sup>2\*</sup>

<sup>1,2</sup>Department of Electrical & Electronics Engineering, Faculty of Engineering, Başkent University, Ankara, Turkey

## Article History

Received: 12.01.2022

Accepted: 13.08.2022

Published: 15.12.2022

## Research Article

**Abstract** – In this study, the classification study of human facial expressions in real-time images is discussed. Implementing this work in software have some benefits for us. For example, analysis of mood in group photos is an interesting instance in this regard. The perception of people's facial expressions in photographs taken during an event can provide quantitative data on how much fun these people have in general. Another example is context-aware image access, where only photos of people who are surprised can be accessed from a database. Seven different emotions related to facial expressions were classified in this context; these are listed as happiness, sadness, surprise, disgust, anger, fear and neutral. With the application written in Python programming language, classical machine learning methods such as k-Nearest Neighborhood and Support Vector Machines and deep learning methods such as AlexNet, ResNet, DenseNet, Inception architectures were applied to FER2013, JAFFE and CK+ datasets. In this study, while comparing classical machine learning methods and deep learning architectures, real-time and non-real-time applications were also compared with two different applications. This study conducted to demonstrate that real-time expression recognition systems based on deep learning techniques with the most appropriate architecture can be implemented with high accuracy via computer hardware with only one software. In addition, it is shown that high accuracy rate is achieved in real-time applications when Histograms of Oriented Gradients (HOG) is used as a feature extraction method and ResNet architecture is used for classification.

**Keywords** – Classification, convolutional neural network, deep learning, emotion analysis, image processing

## 1. Introduction

One of the biggest problems encountered within the scope of face based, computer-generated image applications are the variety of expressions in facial images (Yang & Kriegman, 2002). Although many system suggestions have been put forward, regarding the resistance to facial expressions, the problem could not be resolved (Frank, 2019). The face, which is easy to access and has a high distinctiveness, has been the subject of researchers for many years. Facial diagnosis and recognition studies have contributed not only to the development of security surveillance systems, but also to the development of neurology and psychology sciences (Yang & Kriegman, 2002). Negative aspects of the examination of facial images are mainly related to head posture, lighting conditions and facial expressions. Today, accessing and processing three-dimensional (3D) facial information has become extremely easy. This situation contributed significantly to the solution due to the pose and illumination, which does not change due to the nature of the data. Similar developments are also observed in facial expression

<sup>1</sup>  [orhanemreaksoy@gmail.com](mailto:orhanemreaksoy@gmail.com)

<sup>2</sup>  [seldaguney@baskent.edu.tr](mailto:seldaguney@baskent.edu.tr)

\*Corresponding Author



recognition (Göngör & Tutsoy, 2018; Tutsoy et al., 2017; Zhao et al., 2015; Kuo et al., 2018; Jung et al., 2015; Abdullah, et al., 2021). Göngör & Tutsoy proposed a facial emotion recognition system to use in humanoid robot. They used eigenface method to extract the features. Then these features were classified by using Artificial Neural Network (ANN). They achieved promising results as a result of this study (Göngör & Tutsoy, 2018). The results appear to be open to improvement. With the widespread use of deep learning, Zhao et al. analysed a deep learning method for facial emotion recognition in 2015 (Zhao et al., 2015). But they didn't examine the real time applications in facial emotion recognition. Kuo et. al. analysed deep learning methods both real time and non-real time applications. The results showed that the accuracy rate decrease for the real time applications (Kuo et al., 2018).

The recognition of facial expressions is used in wide area such as, the fields of security and visual surveillance and security, medical diagnosis, emotional research, law enforcement, and education (Li et al., 2020).

Facial expressions that provide important clues about people's emotional states, cognitive activities, and interest orientations; is also among the main factors affecting face-to-face communication. This makes machine-human interaction as important as expressions. Classification of facial expressions is also very important in terms of precautions that can be taken against these changes (Li & Liam, 2021). If the subject is handled in terms of security applications, it will be possible for face detection and recognition systems to give higher accuracy results by classifying two-dimensional (2D) face images according to the expressions they contain (Bhattacharya, 2021).

Facial expressions can be considered as concrete indications of individuals' feelings, understanding, characters and psychological states, and they are also an important tool in people's relations with each other. Mehrabian states that listeners are significantly influenced by their facial expressions (Mehrabian, 2016). Darwin argued that humans and animals contain some innate emotions in their nature and that these emotions are reflected as facial expressions. After this first study on facial expression analysis, it was revealed by Ekman and Friesen in 1971 that there are 6 basic emotions and each of them is reflected with different facial expressions; these are listed as anger, disgust, fear, happiness, sadness and surprise (Karaboyacı, 2009).

The use of still images and sequences of images has enabled facial expression analysis to cease to be a research topic that remains only within the boundaries of psychology. Developments in this area such as face detection, face tracking and face recognition in images have led to an increase in the number of studies on facial expression analysis. Facial expressions are formally determined by the deformation of certain regions on the face. By contractions of the facial muscles, especially the eyebrows, eyelids, lips, facial skin, facial features such as nose and temporary undergo changes because of the location of these temporary changes to a few seconds, the intensity and determination of the dynamics, in terms of detection and classification of facial expressions is of major importance. The extent and duration of such changes; it can change in line with the person, age, race, and gender, making the problem very stratified and difficult to solve. Pantic and Rothkrantz identified 3 main problems that emerged in studies on facial expression analysis. These are detection of facial parts in the image, extracting the features of facial expressions and facial expressions classification (Pantic & Rothkrantz, 2001).

It is seen that the studies in the literature also focus on solving the three main problems mentioned above. Kotsia and Pitas used support vector machines (SVM) for facial expression analysis over image sequences (Kotsia & Pitas, 2005). Within the scope of the study, they carried out, expression classification is made according to the displacement with the following images by referring to the points placed in the first image in the image sequence. Classify six different facial expressions, Otsuka used classifiers based on the Hidden Markov Model (HMM) (Pantic & Rothkrantz, 2001). Within the scope of their studies using Gabor features in expression analysis, suggested the AdaSVM method developed by them (Islam & Al-Murad, 2017); Cohn and Kanade achieved extremely high success rates in the facial expression dataset (Lucey et al., 2010). "Feature selection", which is one of the three main problems defined by Pantic and Rothkrantz, is a part of the extraction of features of facial expressions,

and it is a research topic in which studies on classification of expressions are carried out continuously (Pantic & Rothkrantz, 2001).

In Donato's approach, techniques for facial recognition were initially used (Yang & Kriegman, 2002). In the face image, there is also the identity information along with the expression; to perform a detailed expression analysis, it is useful to remove the identity information from the image. By taking sequences of images from the video, a difference image is created, and expressions were classified according to different spatial analyzes with optical flow estimation. Again, in Pantic and Rothkrantz's approach, facial movement units (Action Units) were determined by fitting point-based face models to the image; These movements have been used to classify emotional expressions (Pantic & Rothkrantz, 2001). In Colmenarez's work, feature points are also used for face modeling (Colmenarez et al., 1999). On the other hand, it should be said that the excessive dependence on the accuracy of the feature points is a disadvantage for such approaches. Numerous studies have been conducted on facial expression tracking and expression classification. These studies generally consist of three basic steps: face detection, facial feature extraction and facial expression recognition (Dhavaliker and Kulkarni, 2014). In determining the facial region, features such as skin color and the geometric structure of the face are considered. The fact that the real world is 3D in computer vision and 2D image processing brings with it some difficulties. It is extremely difficult to solve the face detection problem with a computer model. Therefore, face detection must also be accurate for an accurate and reliable facial expression recognition system. In the studies, two feature selection approaches are used to determine the ones that carry the most information about the expression analysis of the selected features (Güneş & Polat, 2009). The common features of the approaches can be listed as transforming the multiple classification problem into a binary classification problem, applying the feature selection, and then combining the selected features and using them for classification. For the real time facial expression recognition system, various studies have been done by using deep learning algorithms (Buhari et al., 2022; Umer et al., 2022; Bisogni et al., 2022). Umer et al. examined the effects of data augmentation methods to classify facial emotions for different database (Umer et al., 2022). Also they obtained successful accuracy results but they didn't examine the results of real time application. Similarly, Bisogni et al analyzed deep learning approaches for the facial emotion recognition problem. As a result of these approaches, successful results were obtained for different data sets (Bisogni et al., 2022). However, they did not calculate accuracy for real-time systems as in the study of Umer et al.. Buhari et al. proposed a new method to recognize real-time facial emotion. In their studies, the accuracy rate was obtained as 87% in SMIC dataset (Buhari et al., 2022). Although good results have been obtained for the real-time application, it seems that there are results that are open to improvement. Saurav et al. improved dual integrated Convolutional Neural Network (CNN) architectures and they obtained the accuracy results for the different database (Saurav et al., 2022). Their study didn't include real time face emotion recognition. All these studies indicate the need to increase accuracy for real-time systems in facial expression recognition. It seems that it is difficult to achieve high classification success in real-time systems due to various environmental (light, camera) factors (Buhari et al., 2022; Devrim et al., 2019, Engin et al., 2017 ). The classification accuracy in this regard needs to be improved. For these reasons, the aim of this study is to increase the success of facial emotion recognition for real-time systems.

In this study, different algorithms were evaluated to find best method for real-time facial recognition system. In this context, detailed analyzes are included in this study. After feature extraction in image processing, successful results can be obtained with traditional machine learning methods (Nagaraj & Banala, 2021). For this reason, in this study traditional machine learning algorithms and convolutional neural networks were compared. Also different databases were used to compare the effects of the databases in the algorithms. In addition to these, two practices were applied to all databases and algorithms to compare real-time and non-real time applications. The rest of this study is organized as follows: the dataset, deep learning models, methods, and techniques are given in Sect. 2. The results of real time applications are reported in Section 3. Also the discussion of the results is given in Section3. Section 4 consist of conclusion.

## **2. Materials and Methods**

Facial recognition system is an integrated system consisting of software and the best deep learning facial system recognition. In this study, we have analyzed the different machine learning algorithms to understand which method is proper for the real time emotion recognition system. While the public datasets were used in the creation of the models, the test phase was carried out with 2 different practices to objectively test the success of these algorithms. In practice 1, all models were tested using images consisting of 70 image data (Mena-Chalco et al., 2009) not used in the training set. In practice 2, images captured from webcam were used to test the models.

The aim of this study is to create a real-time face recognition system with the Python programming language. Since it worked with the three different databases, a laptop computer with powerful hardware was chosen to run the software. To obtain the best results, the application and different parameters and tests were repeated several times on the Spyder and Anaconda development environment using Python language on an 8-core Intel Core i7 processor HP laptop. Python is an object-oriented, interpretative, modular, and interactive high-level programming language. Simple syntax based on indentations makes the language easy to learn and remember. This gives it the feature of being a language where programming can be started without wasting time with the details of syntax (Python Software Foundation, 2012). It is using only CPU cores for all other phases except the face recognition phase. The laptop's GPU is not used because, as mentioned above, the goal is to develop a system that can run with very few computational resources. Also, Logitech C270 720p webcam was used externally from the laptop to capture images and videos to test the system on a standard laptop. In this study, the camera was set to be directly opposite and this program was run in a bright environment to obtain more accurate results.

TensorFlow is an open-sourced end-to-end platform, a library for multiple machine learning tasks, while Keras is a high-level neural network library that runs on top of TensorFlow, whereas OpenCV is a computer vision library (Terra, 2022). OpenCV is library developed specifically for computer vision algorithms. Tensorflow is framework for machine learning problems. Though it is suited for more general problems as well, such as: classification, clustering and regression, you can do image recognition with TensorFlow. Keras is a high-level neural networks API, written in Python and capable of running on top of Tensorflow. It concludes that Tensorflow being a machine learning framework is widely adapted for deep learning tasks in research and industrial community. (Mokhtari, 2021) Most of the open-sourced deep learning models are written in either Tensorflow. With OpenCV, you can test simple face detection techniques like SVM and Histograms of Oriented Gradients (HOG).

In this study, three different public databases were used to train the model. These are FER2013, JAFFE and CK+ databases. These datasets were chosen because they are widely used public datasets. Chen et al. analyze and compare facial expression recognition methods. In this study, they propose some evaluation dimensions and discuss possible directions for future research by using CK+ database (Chen & Wu, 2018). Feature extraction is important issue in real-time application in terms of processing time. To extract the feature, HOG method was used. Different machine learning algorithms were used to classify these extracted features. These are k-Nearest Neighbor (k-NN), SVM and CNN methods. Also transfer learning was used in CNN architecture to improve the performance of the network.

### **2.1 FER2013 Database**

The FER2013 dataset used to create the model in this study includes 35,887 face images. These images are in gray format with 48x48 pixels. Label parts of these photos are included in this data set. The photographs that contain 7 different emotions -happiness, sadness, surprise, disgust, anger, fear and neutral - described in the previous sections are a data set is open source. Some images used in the FER2013 data set are given in Figure 1.



Figure 1. FER2013 dataset (Verma & Verma, 2020)

## 2.2 JAFFE Database

The JAFFE database is a publicly available dataset of 213 facial expression images of 10 Japanese women, called the Japanese Female Facial Expression (JAFFE). Each subject displayed 7 basic emotions, and each expression included 3 - 4 images per subject. This database, which contains 30 angry, 29 disgust, 33 fear, 30 happiness, 31 sad, 30 surprise and 30 neutral expressions and it is a grayscale and has a resolution of 256 x 256 pixels. All facial images were created under similar, highly controlled lighting conditions, without any environmental factors such as hair or glasses. Some images used in the JAFFE data set are given in Figure 2.

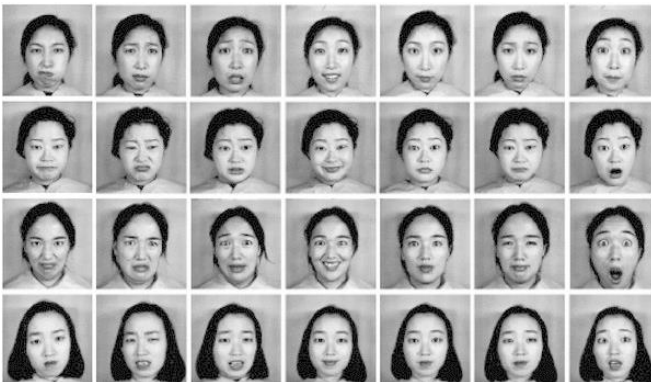


Figure 2. JAFFE dataset (Akinrotimi, 2018)

## 2.3 CK+ Database

The expanded Cohn-Kanade (CK+) dataset includes 593 images from a total of 123 different subjects aged 18 to 50 years, of various genders. Each image is in 640x480 pixel resolution and mostly in gray format. 327 of these images were tagged with one of the seven expressions. The CK+ database is considered the most widely used laboratory-controlled facial expression classification database available and is used in most facial expression classification methods. Some images used in the CK+ data set are given in Figure 3.



Figure 3. CK+ dataset (Lucey et al., 2010)

## 2.4 Feature Selection Method Used in the Application

In this study, a real-time facial expression recognition software was studied. Different models were composed by using different machine learning methods. These models are basically based on recognizing 7 basic emotions. This software is based on the determination of facial expressions and their classification through decision mechanisms. For the classification of facial expressions, the main features expressing emotions should be extracted. In this study, these processes are carried out with the method named HOG. An example image with the HOG method is given in Figure 4. The histogram of directed gradients is a feature selection method used in computer vision and image processing for object detection, a feature descriptor often used for object detection. It relies on the property of objects within an image to have the distribution of density gradients or edge directions. Gradients are calculated within one image per block. A block is considered a pixel grid from which gradients are created from the magnitude and direction of the change in pixel intensities within the block.

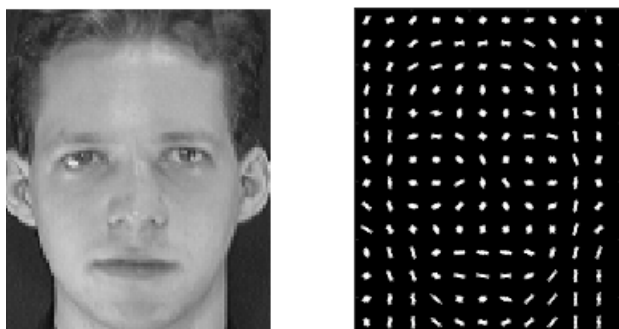


Figure 4. HOG sample face photo (Islam & Al-Murad, 2017)

A window size of 128 x 128 pixel was used for face images because it covers human faces (Yang & Kriegman, 2002). In HOG methods, identifiers are calculated on blocks of 8 x 8 pixels. For each pixel on the 8 x 8 block, these descriptive values are quantized into 9 bins, where each bin represents a directional gradient angle and the value in that bin, which is the sum of the magnitudes of all pixels with the same angle. Also, the histogram is then normalized to a block size of 16 x 16, which means four 8 x 8 blocks are normalized together to minimize light conditions. This mechanism reduces the accuracy drop due to a change in light.

In this study, one of the deep learning libraries of the Python programming language, Keras - TensorFlow was used in this software. The block diagram of the proposed method is shown in Figure 5. When the program is run, it takes face images from the webcam and after a preprocessing called preprocessing, face detection is made. Then, features are extracted with the HOG method. The features are performed automatically with the designed convolutional neural network. By extracting features of face, seven universal emotions can be classified as happiness, sadness, anger, disgust, surprise, neutral and fear.

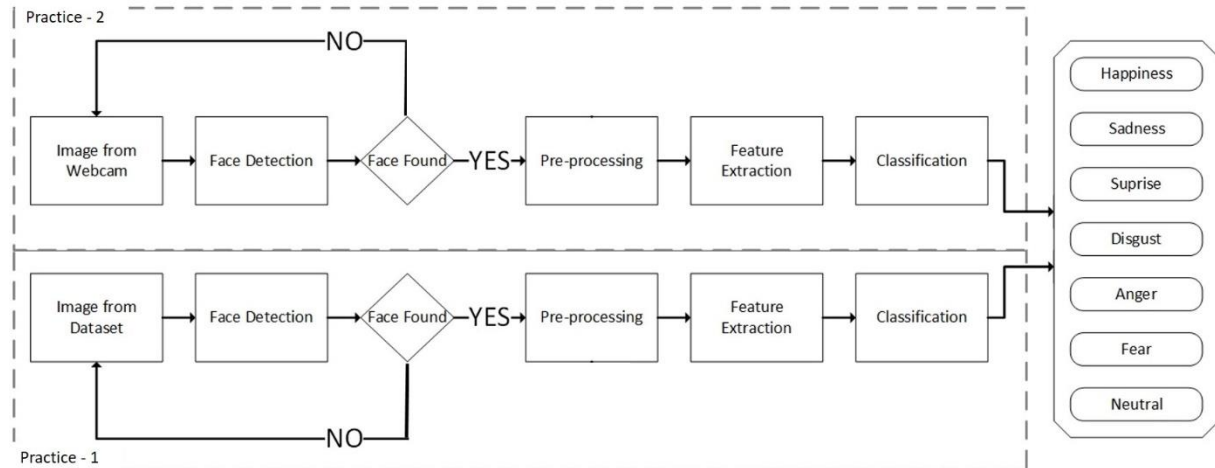


Figure 5. The proposed emotion recognition system from facial expression based on image processing

## 2.5 Methods

In this study, 3 different machine learning methods were used to classified. SVM and k-NN are traditional machine learning algorithms. CNN is one of the deep learning algorithm. Thus, in this study, traditional methods and deep learning can be compared for emotion recognition application.

SVM is a supervised machine learning algorithm used in classification and regression problems. In classification applications, SVM method is a binary classifier. In the SVM algorithm, each data is represented as a point in n-dimensional space, with the value of a particular coordinate. It then finds the hyperplane that best separates the two classes. The algorithm classifies the data according to which side of this hyperplane it is (Khoong, 2021).

k-NN is one of the supervised machine learning algorithms. So the algorithm uses the labeled dataset. The class of the new observation is determined according to the classes of the k nearest observations. The new observation is classified according to the class with the highest votes among its k nearest neighbors (Srivastava,2018).

CNN is a deep learning network that is very successful in image processing. It is developed by analogy from the visual cortex. CNN architecture processes the image by passing it through various layers. The commonly used layers are convolution layer, pooling layer, flattened layer, fully connected layer and softmax layer. Different architectures can be obtained stacking of these layers (Verma & Verma, 2020). Alexnet is the first large-scale CNN architecture to succeed in the Imagenet competition (Çınar, 2018). Alexnet architecture composes of 5 convolution layers and 3 fully connected layers. It was trained with approximately 1.3 million images with 1000 classes. Residual Network (ResNet) is another CNN architecture. The main basic element of the Resnet architecture is residual blocks. To prevent vanish gradient problem, residual links are used in this architecture (Özdemir et al., 2019). There are different ResNet architectures with different number of layers. In this study, Resnet50 consisting of 50 layers was preferred. While training neural networks, losses occur in the feature map due to convolution and pooling operations. Dense net architecture has been proposed to prevent this. It is a CNN architecture consisting of dense blocks. The layers within the blocks are densely interconnected (Özdemir et al., 2019). And lastly, InceptionV3 CNN architecture was used. This architecture proposes an initial model that combines multiple different sized convolutional filters into a new filter (Islam & Al-Murad, 2017). This model reduces the number of parameters to be trained. This also reduces the computational complexity of the model.

## 2.6 Transfer Learning

Reuse of a previously trained model on a new problem is defined as transfer learning in machine learning. Transfer learning is the reuse of information learned by one network in another dataset to improve the performance of another network (Sharma, 2021).

A machine uses knowledge learned from a previous assignment to increase insight into a new task in transfer learning. When training a classifier to predict whether an image contains anything, information acquired during training can be used to distinguish faces. If a simple classifier is trained to predict whether an image contains a smiling human face, the model's training information can be used to identify other facial expressions.

Transfer learning is commonly applied in sentiment analysis (Li & Lima,2021). Neural networks typically aim to detect edges in the first layer, forms in the middle layer, and task-specific features in the later layers(Çinar, 2018). The early and central layers are used in transfer learning, and the later layers are only retrained. As the newly created model is trained to recognize facial expressions at earlier levels, subsequent layers are retrained to understand what distinguishes a smiley from other expressions (Akinrotimi, 2018).

This information learned by a deep network is used by adapting the model to improve the performance of another network and to develop a network that is not suitable for the training set. The situations where the model trained and used for a different data set is called model adaptation. The purpose of this method; the knowledge of the previous model is used by creating a new model on top of the models at a certain level that have learned the subject well (Goodfellow et al., 2017)

### 3. Results and Discussion

JAFFE, FER2013 and CK+ databases as facial expression databases are applied to observe the difference between the management applied in this study and the methods in the literature. OpenCV library for face reading and face recognition processes were used. Studies were carried out with k-NN and SVM classifiers and AlexNet, ResNet, DenseNet and Inception learning algorithms. All the results are given in Table 1.

Table 1

The comparison of accuracy rate and performances of different algorithms for practice 1

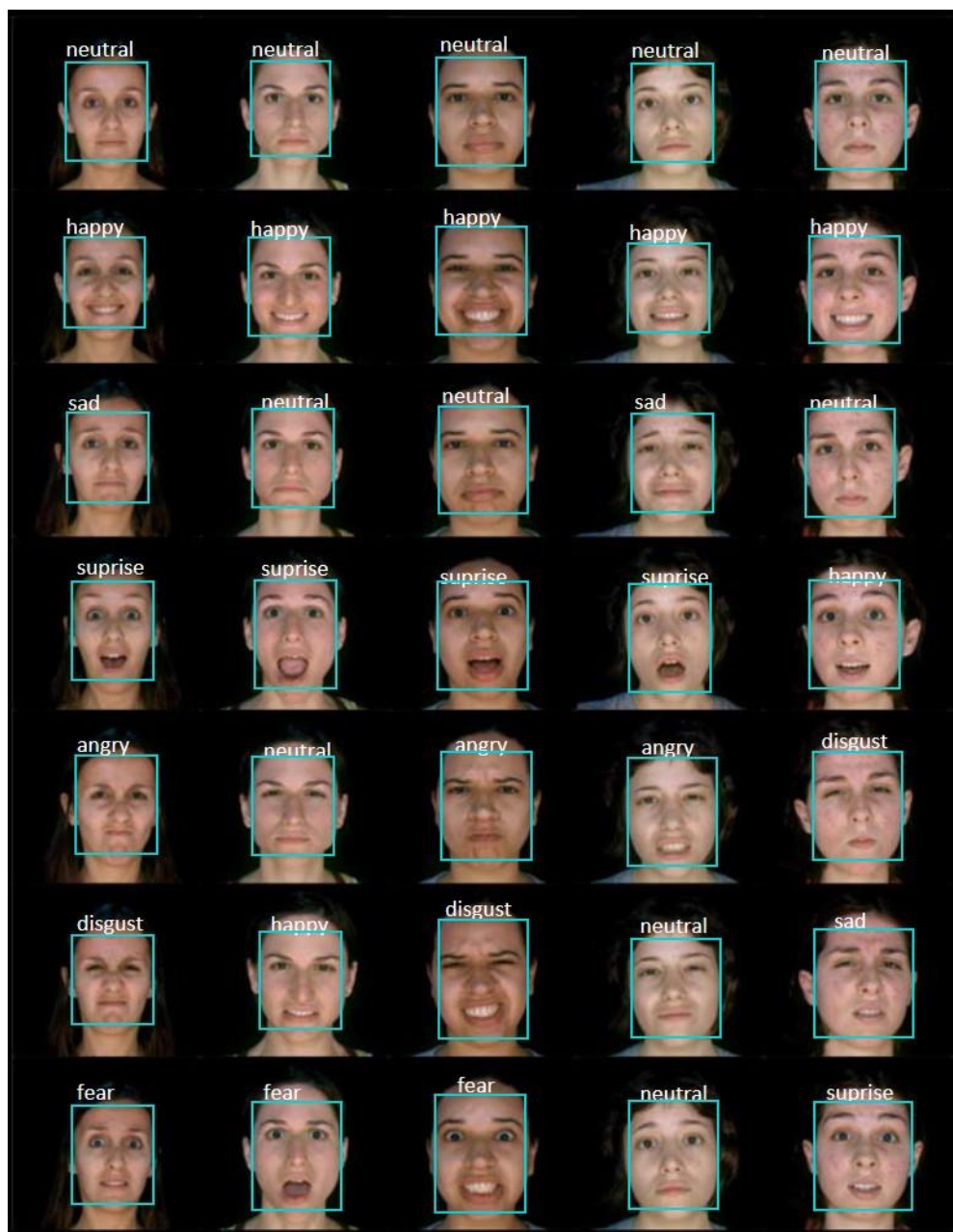
	Database	Practice-1	Practice-2	Training Time
		Accuracy	Accuracy	(sec)
SVM	JAFFE	73,08%	74,80%	11
	FER2013	71,88%	73,22%	12
	CK+	72,74%	74,45%	11
KNN	JAFFE	72,58%	74,98%	12
	FER2013	77,39%	78,92%	14
	CK+	73,94%	76,71%	13
AlexNet	JAFFE	81,67%	83,48%	30
	FER2013	83,42%	84,70%	34
	CK+	82,26%	84,11%	32
ResNet50	JAFFE	90,34%	91,64%	22
	FER2013	93,85%	94,51%	26
	CK+	92,11%	93,12%	25
DenseNet121	JAFFE	89,82%	90,26%	28
	FER2013	92,04%	92,30%	31
	CK+	90,79%	91,54%	30
InceptionV3	JAFFE	84,58%	87,52%	16
	FER2013	86,73%	89,30%	19
	CK+	85,07%	87,85%	17

In this study, accuracy and time analyzes of two different applications were carried out. In practice 1, facial expressions belonging to 10 different people (Mena-Chalco, 2009) were shown the model to test. In practice 2, it was tried to perform the emotion recognition function from facial expression in real time by using web-cam image. The accuracy rates obtained during these applications and the time spent in each training round in machine / deep learning methods are given in seconds. All transfer learnings were performed in 100 rounds to get the best results. The epoch, batch size, momentum and learning



rate are selected as 100, 32, 0.9 and 0.01 respectively in all transfer learning architectures. Adam optimization algorithm was used to update network weights. To obtain overfitting problem dropout was applied and dropout rate was selected as 0,2. In terms of accuracy, it is observed that deep learning networks have a very high accuracy rate.

In the first application, all methods, and their effects on three different databases (JAFPE - FER2013 - CK+) were tested with a total of 70 images of 10 different people. The expressions shown in Figure 6 shows the emotions detected by the application.



(a)





(b)

Figure 6. The faces images used in the practice-1 for test a) first five-person b) last five person (Mena-Chalco, 2009)

In second practice, the webcam images shown in Figure 7 classified for the facial expression in real – time. When the model was trained with the FER2013 database and classified by using SVM method, the confusion matrix shown in Figure 8 is obtained for practice 2. The color bar in Figure 8 indicates that if the color in the confusion matrix is approaching red, the value is approaching 100%. If it is going towards the dark blue color, it indicates that it is approaching 0%. The model achieved the highest success in recognizing the "neutral" expression. The lowest accuracy rate was recorded in the facial expressions of "surprise".

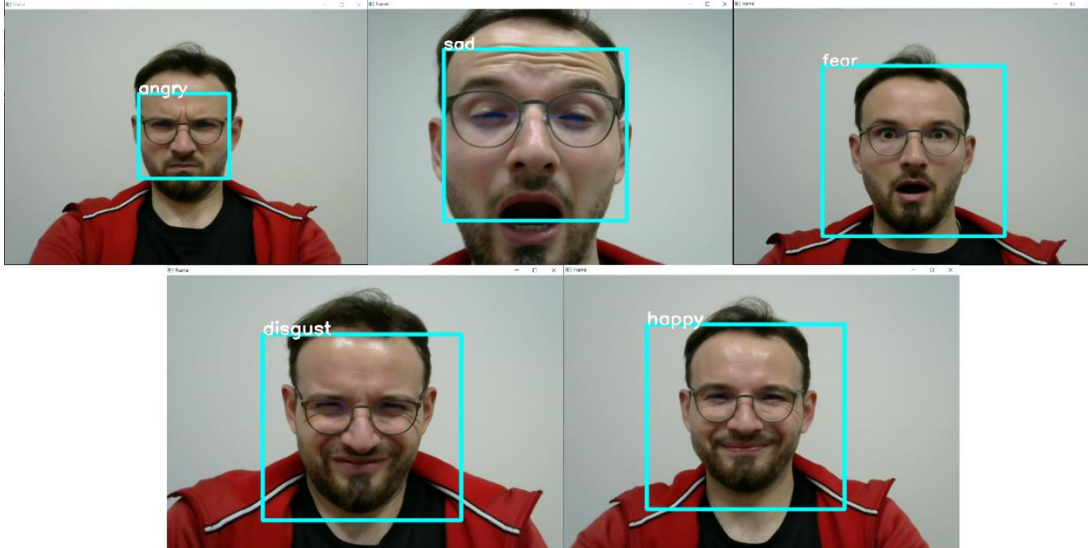


Figure 7. Screenshot images (angry, sad, fear, disgust and happy) from real-time face emotion recognition application

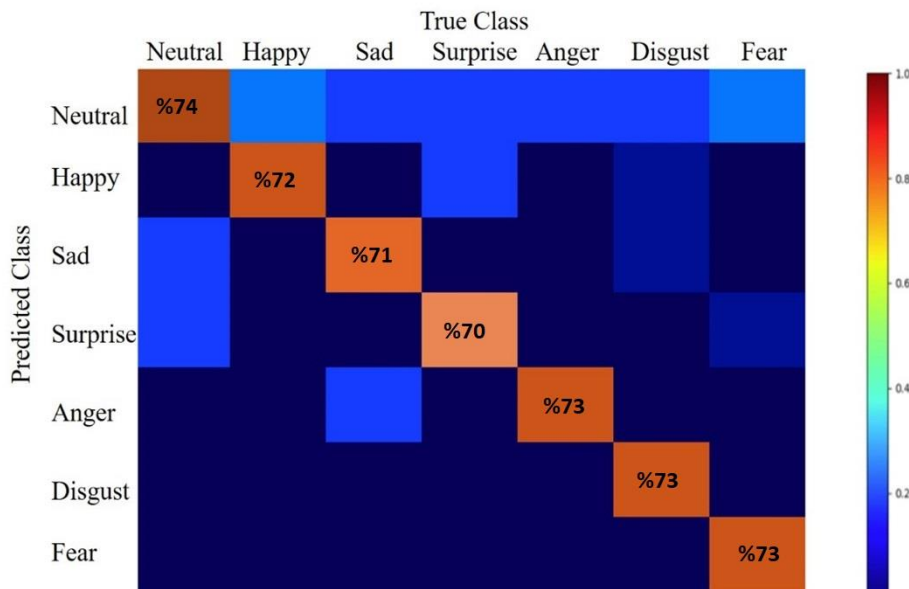


Figure 8. The confusion matrix when the model is trained with FER2013 database and the SVM algorithm is used for classification in practice 2

In another model, the highest accuracy rate was obtained for the practice 2 when the model was trained with FER2013 database in ResNet architecture, which is one of the transfer learning methods. In this model, the lowest accuracy rate was observed in the expressions "disgust" and "surprise", while the highest accuracy rate was observed in the expression "neutral". The confusion matrix of this study is also given in Figure 9.

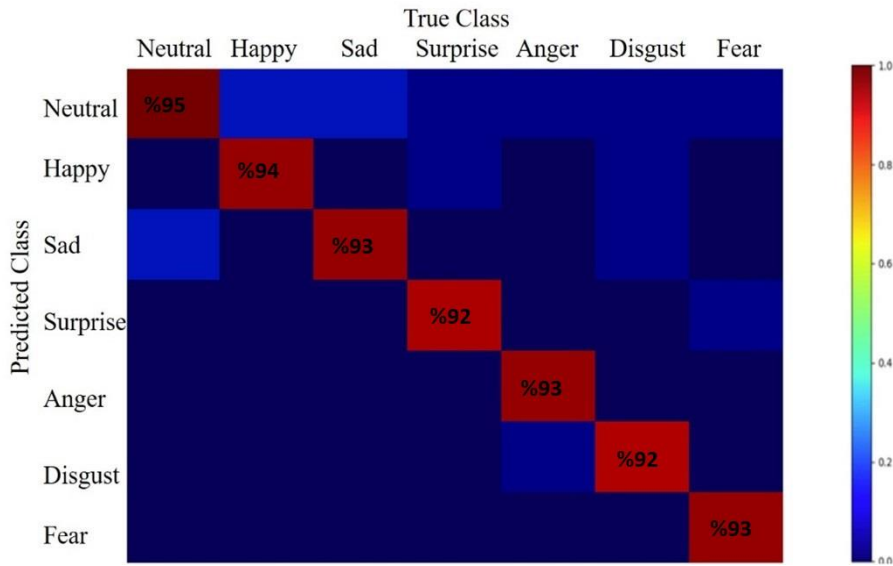


Figure 9. The confusion matrix when the model is trained with FER2013 database and ResNet architecture is used for classification in practice 2.

The confusion matrix, which includes the accuracy rates according to the seven different expressions that are considered as a basis. Neutral expression was mostly observed as the expression with the highest accuracy rate. The main reason for this is that a neutral facial expression can be created on the face without activating any facial muscles. Many different muscles of the face must be activated and contracted at the same time in the other facial expression. These contractions occur differently on each face. These differences detected better as the dataset gets larger and random. Thus, as the data set grows, the expression detection rate also increases. The FER2013 dataset contains the most data from the datasets used in this study. As can be seen from Figure 10, the highest success was achieved in all methods except SVM when FER2013 data was used in training stage. SVM is a method that is successful even when the number of features is high and the number of measurements is low (Güneş & Polat, 2009) For this reason, this study also achieves a certain success in data sets with a small number of data such as JAFFE dataset.

In practice 2, tests were carried out in real time and the expressions taken by the webcam The results of our application show that the tests were more successful in real-time application. The reason for this is that preprocessing, and feature extraction processes are successful in real-time applications when suitable conditions are created.

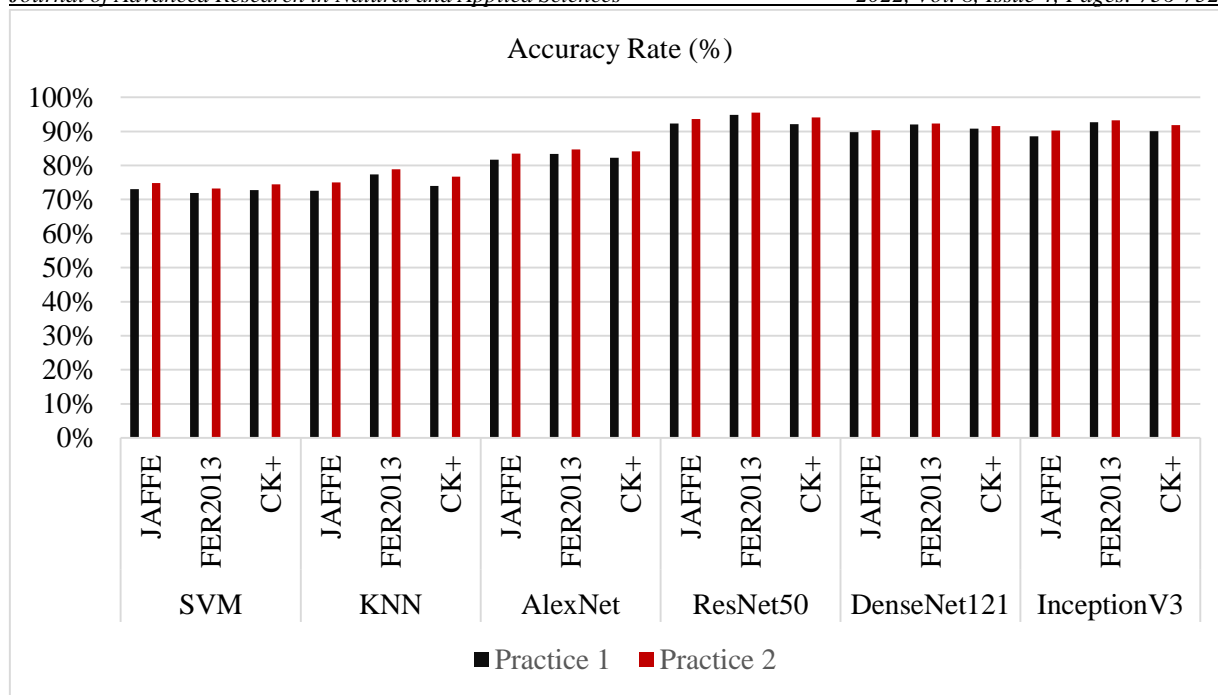


Figure 10. The comparison of accuracy rates of different algorithms for practice 1 and 2.

In the Figure 10, which method gives better results in which application and which method achieves higher accuracy are detailed. ResNet50 was observed in the FER2013 dataset with an accuracy rate of 94.51%. Also classification successes given in Table 2 are analyzed according to each facial expression. Neutral expression is mostly observed as the expression with the highest accuracy rate like the practice 1. For the same reason as in application 1, it is thought that the success obtained in neutral expression is high.

Table 2

Classification accuracies of each facial expression for practice 2.

Method	Dataset	Neutral (%)	Happy (%)	Sad (%)	Surprise (%)	Anger (%)	Disgust (%)	Fear (%)
SVM	JAFFE	73,63	73,87	71,24	71,92	72,94	71,63	73,36
	FER2013	73,45	71,39	70,75	69,83	72,22	72,98	72,46
	CK+	73,15	73,48	71,13	71,26	71,91	71,56	72,54
KNN	JAFFE	73,46	73,43	72,91	71,82	72,67	71,83	71,92
	FER2013	78,64	77,84	76,97	76,58	77,42	76,24	76,43
	CK+	74,65	74,18	74,81	72,26	75,27	72,74	73,36
AlexNet	JAFFE	82,29	82,45	80,91	79,83	80,19	80,13	81,59
	FER2013	83,86	83,89	83,56	81,76	83,47	83,61	83,72
	CK+	82,93	82,79	81,65	81,26	82,73	81,88	82,46
ResNet50	JAFFE	90,83	90,61	90,14	90,50	89,73	89,84	90,89
	FER2013	94,83	93,42	92,84	91,76	92,51	91,79	92,23
	CK+	92,61	92,17	91,68	91,13	92,09	91,49	91,88
DenseNet121	JAFFE	89,42	89,35	89,07	88,59	89,29	89,12	89,20
	FER2013	92,18	91,28	91,07	90,69	91,68	90,83	92,05
	CK+	90,12	90,25	90,92	90,87	91,26	90,45	91,62
InceptionV3	JAFFE	86,17	85,97	85,57	84,74	85,21	85,15	85,23
	FER2013	88,59	88,21	86,65	86,41	86,26	85,42	85,33
	CK+	86,13	85,70	85,42	84,69	84,57	84,12	84,24

When the results obtained in this study are compared with the results of the literature, it seems that successful results have been obtained with the proposed method. The results are given in Table 3. Feature extraction with the HOG method and then classification of the obtained feature extracted image

with the resnet50 architecture has been successful in all datasets. When the literature results are examined, there are higher successful results. However, since these results do not include real-time application, a full comparison cannot be made. The results show that the overall success of the proposed method is high for all data sets.

### 3. 2 Application Restrictions

For software to achieve higher accuracy and to work with better performance, some of the restriction steps we encountered in our system are listed below.

- Real-time recognition becomes very difficult for 720p and higher images. This is because the time it takes to execute the face position step is also significantly extended on the platform. Therefore, our system's real-time recognition is limited to images in sizes from 180p to 720p.
- The system can detect and recognize faces from about 50 to 100 cm from the webcam. Outside of this range, the system will perform poorly.
- Since no extra flash or lighting system is used in the system, the angle of the camera and the amount of light in the environment also affect the performance of the system. For best performance, the camera should be positioned so that it does not reflect overhead lighting or daylight.

Table 3

The comparison of accuracy rates with literature for each dataset

Study	Dataset	Feature Extraction Method	Classification Method	Real Time	Accuracy (%)
Saxena, A., 2020	JAFFE	MLP	ANN	x	73
Saxena, A., 2020	JAFFE	Haar	ADABOOST	x	92
Saxena, A., 2020	GWI	Spectral Embedding	GABOR	x	62,3
Chen, Y., 2018	CK+	-	SVM	x	79
Sebe, N., 2004	-	Optical Flow	K-NN	✓	86
Devrim, M., O., 2019	JAFFE	Viola Jones	DenseNet	✓	90,18
Devrim, M., O., 2019	JAFFE	Viola Jones	InceptionV3	✓	87,50
Devrim, M., O., 2019	JAFFE	Viola Jones	ResNet	✓	91,52
Özdemir, M., A., 2019	FER2013	BPSO	ResNet	x	83,40
Engin, D., 2017	CK+	LBP	ResNet	✓	93,21
Engin, D., 2017	CK+	LBP	InceptionV3	✓	85,77
Zhao, X. 2015	JAFFE	CNN	RELM*	x	96,8
Zhao, X. 2015	CK+	CNN	RELM*	x	86,5
Zhao, X. 2015	FER2013	CNN	RELM*	x	62,5
This Study	JAFFE	HOG	Resnet50	✓	91,64
This Study	FER2013	HOG	Resnet50	✓	94,51
This Study	CK+	HOG	Resnet50	✓	93,12

\*Regularized Extreme Learning Machine

### 4. Conclusion

Computer-based expression recognition models have a wide range of uses in daily life. In this study, a facial expression recognition system was developed to detect seven facial expressions based on facial mimics in real time. Different classification methods, were compared in terms of accuracy rates and training times with training images in databases which have different number images. Spyder software, Keras, Tensorflow and OpenCv libraries have been installed in the computer environment. Among the classification methods, k-NN, SVM, AlexNet, ResNet, DenseNet and Inception were preferred. JAFFE, FER2013 and CK+ were preferred as databases because these are open source. A comprehensive analysis was performed for the different datasets and different methods. According to the results of the applications made in these different methods and databases, the highest accuracy rate was observed in

the model using the FER2013 dataset and the ResNet. With CNN architectures, much more successful results have been obtained in this application compared to traditional methods. It was observed that the accuracy rate increased as the amount of data in the data set increased. When the feature is extracted with HOG and then classified with ResNet, good results have been obtained with this proposed method. The highest accuracy rate was obtained as 95,1% with the proposed method in real time application. By using this application on different datasets, using with different classifiers during training, and increasing the training data, the system can be improved for the future studies. The results of the performance analysis carried out within the scope of this study can be improved by testing more classification methods on different data sets.

### Authors Contribution

Selda Güney: Conceived of the presented idea.

Orhan Emre Aksoy: Verified the analytical methods.

All authors developed the theory, performed the computations, discussed the results and contributed to the final manuscript.

### Conflicts of Interest

The authors declare no conflict of interest.

### References

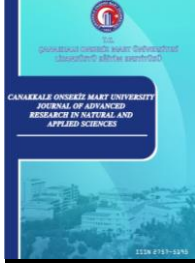
- Abdullah, S. M. S., and Abdulazeez, A. M. (2021). Facial expression recognition based on deep learning convolution neural network: A review. *Journal of Soft Computing and Data Mining*, 2(1), 53-65. Retrieved from: <https://publisher.uthm.edu.my/ojs/index.php/jscdm/article/view/7906>
- Akinrotimi, A. O. (2018). Facial Emotion Recognition Using Principal Component Analysis and Support Vector Machine. *Computing, Information Systems, Development Informatics & Allied Research Journal*, 9(2), 12-20. Retrieved from: [https://www.researchgate.net/publication/336120020\\_Facial\\_Emotion\\_Recognition\\_Using\\_Principal\\_Component\\_Analysis\\_and\\_Support\\_Vector\\_Machine](https://www.researchgate.net/publication/336120020_Facial_Emotion_Recognition_Using_Principal_Component_Analysis_and_Support_Vector_Machine)
- Bhattacharya, S. (2021). A Survey on: Facial Expression Recognition Using Various Deep Learning Techniques. *Advances in Intelligent Systems and Computing, Advanced Computational Paradigms and Hybrid Intelligent Computing*, 619–631. doi:[https://doi.org/10.1007/978-981-16-4369-9\\_59](https://doi.org/10.1007/978-981-16-4369-9_59)
- Bisogni, C., Castiglione, A., Hossain, S., Narducci, F, and Umer S. (2022). Impact of Deep Learning Approaches on Facial Expression Recognition in Healthcare Industries. *IEEE Transactions on Industrial Informatics*, 18(8), 5619-5627. Retrieved from: <https://ieeexplore.ieee.org/document/9674818>
- Buhari A. M., Ooi, C. P., Baskaran, V.M., Phan, R. CW, Wong, K. and Tan, W-H. (2022). Invisible emotion magnification algorithm (IEMA) for real-time micro-expression recognition with graph-based features. *Advances in Soft Computing Techniques for Visual Information-based Systems*, 81, 9151–9176. doi:<https://doi.org/10.1007/s11042-021-11625-1>
- Chen, Y., Wu, H. (2018). A Comparison of Methods of Facial Expression Recognition. *2018 WRC Symposium on Advanced Robotics and Automation (WRC SARA)*, 261-268. Retrieved from: <https://ieeexplore.ieee.org/document/8584202>
- Coşar, S., (2008). *Facial Feature Point Tracking Based On A Graphical Model Framework* (Master Thesis). Retrieved From: [https://vpa.sabanciuniv.edu/vpadb/findfile\\_get\\_anonymous\\_paper.php?f=1954](https://vpa.sabanciuniv.edu/vpadb/findfile_get_anonymous_paper.php?f=1954)
- Çınar, A., C., (2018) .Deep Learning . Retrieved From: <https://www.ahmetcevahircinar.com.tr/2017/08/11/imagenet-classification-with-deep-convolutional-neural-networks/>
- Colmenarez, A., Frey, B. and Huang, T.S. (1999). A probabilistic framework for embedded face and facial expression recognition. *Proceedings 1999 IEEE Computer Society Conference on Computer Vision and Pattern Recognition (Cat. No PR00149)*, 592-597, doi: 10.1109/CVPR.1999.786999.

- Devrim, M., O. (2019). *Farklı Derin Evrimsel Sinir Ağlarının Yüz İfadesi Tanıma İşleminde Karşılaştırılması* (Master Thesis). Retrieved from: <https://tez.yok.gov.tr/UlusalTezMerkezi/tezDetay.jsp?id=vLQ0gfV9vTaOpH16k6kjMA&no=ZgJjiVHnbVeqxh9M0L2OHg>
- Dhavalikar, A., Kulkarni, R., K., (2014). Face detection and facial expression recognition system. *International Conference on Electronics and Communication Systems (ICECS)*, 1-7. Retrieved From: <https://ieeexplore.ieee.org/document/6892834>
- Engin, D., (2017). *Facial Expression Pair Matching* (Master Thesis) Retrieved from: [https://tez.yok.gov.tr/UlusalTezMerkezi/tezDetay.jsp?id=2bQ8F7EJQFFi10i\\_DbMMkQ&no=pooo j2n8rQ268jwzPwoqw](https://tez.yok.gov.tr/UlusalTezMerkezi/tezDetay.jsp?id=2bQ8F7EJQFFi10i_DbMMkQ&no=pooo j2n8rQ268jwzPwoqw)
- Frank, M., G., (2001). *Facial Expressions*. International Encyclopedia of the Social & Behavioral Sciences, Pergamon, 5230-5234. doi:<https://doi.org/10.1016/B0-08-043076-7/01713-7>
- Goodfellow, I., Bengio, Y., Courville, A. (2016). *Deep Learning. Regularization for Deep learning*. 228-270, Cambridge, Massachusetts: MIT Press. Retrieved From: <http://www.deeplearningbook.org>
- Güneş, T., Polat, E. (2009). Feature Selection In Facial Expression Analysis And Its Effect On Multi-Svm Classifiers. *23rd International Symposium on Computer and Information Sciences*, 1-5, doi:10.1109/ISCIS.2008.4717874.
- Göngör, F., and Tutsoy, O. (2018). Eigenface based emotion analysis algorithm and implementation to humanoid robot. *In International Science and Academic Congress*, 1-17. Retrieved from: [https://www.researchgate.net/publication/329557854\\_Eigenface\\_Based\\_Emotion\\_Analysis\\_Algorithm\\_and\\_Implementation\\_to\\_Humanoid\\_Robot](https://www.researchgate.net/publication/329557854_Eigenface_Based_Emotion_Analysis_Algorithm_and_Implementation_to_Humanoid_Robot)
- Islam, K., Al-Murad, A. (2017). Performance of SVM, CNN, and ANN with BoW, HOG, and Image Pixels in Face Recognition. *2nd International Conference on Electrical & Electronic Engineering (ICEEE)*, 1-4. Retrieved from: <https://ieeexplore.ieee.org/document/8412925>
- Jung H. et al., (2015). Development of deep learning-based facial expression recognition system. *21st Korea-Japan Joint Workshop on Frontiers of Computer Vision (FCV)*, 1-4. doi: 10.1109/FCV.2015.7103729.
- Karaboyacı, C., (2009). *Geometrical Feature Based Automated Facial Expression Analysis* (Master Thesis). Retrieved from: <https://polen.itu.edu.tr/bitstream/11527/339/1/9597.pdf>
- Khoong, W., H., (2021). *When Do Support Vector Machines Fail?* Retrieved From: <https://towardsdatascience.com/when-do-support-vector-machines-fail-3f23295ebef2>
- Kotsia, I., Pitas, I., (2008). Facial Expression Recognition in Image Sequences Using Geometric Deformation Features and Support Vector Machines. *IEEE Transactions on Image Processing*, 16(1), 172-187. doi: 10.1109/TIP.2006.884954. Retrieved From: <https://ieeexplore.ieee.org/document/4032815>
- Kuo, C., Lai, S. and Sarkis, M. (2018). A Compact Deep Learning Model for Robust Facial Expression Recognition. *2018 IEEE/CVF Conference on Computer Vision and Pattern Recognition Workshops (CVPRW)*, 2202-2208, Retrieved from: <https://ieeexplore.ieee.org/document/8575457>
- Lucey, P., Cohn, J., Kanade T. (2010) .The Extended Cohn-Kanade Dataset (CK+): A complete dataset for action unit and emotion-specified expression. Retrieved From: <https://ieeexplore.ieee.org/document/5543262>
- Li, B. and Lima, D. (2021). Facial expression recognition via ResNet-50. *International Journal of Cognitive Computing in Engineering*, 2, 57-64. doi: <https://doi.org/10.1016/j.ijcce.2021.02.002>
- Li, S. (2020). Deep Facial Expression Recognition: A Survey. *IEEE Transactions on Affective Computing*, 1-20. Retrieved From: <https://ieeexplore.ieee.org/document/9039580>
- Mehrabian, A. (2016), [https://en.wikipedia.org/wiki/Albert\\_Mehrabian](https://en.wikipedia.org/wiki/Albert_Mehrabian), 01.06.2022.
- Mena-Chalco, J.P., Macedo, I., Velho, L. and Cesar, R.M. (2009). 3D face computational photography using PCA spaces. *Visual Computer*, 25, 899-909. doi:<https://doi.org/10.1007/s00371-009-0373-x>
- Mokhtari, N., I., (2021). Which is Better for Your Machine Learning Task. Retrieved From: <https://towardsdatascience.com/which-is-better-for-your-machine-learning-task-opencv-or-tensorflow-ed16403c5799>
- Nagaraj, P., Banala, R., (2021). Real Time Face Recognition using Effective Supervised Machine Learning Algorithms. *J. Phys.: Conf. Ser.* 012007, 1-6. doi:10.1088/1742-6596/1998/1/012007 Retrieved From: <https://iopscience.iop.org/article/10.1088/1742-6596/1998/1/012007/pdf>



- Özdemir, M., A., Elagöz, B., Alaybeyoğlu, A., Akan, A. (2019). Real Time Emotion Recognition from Facial Expressions Using CNN Architecture. *2019 Medical Technologies Congress (TIPTEKNO)* DOI: 10.1109/TIPTEKNO.2019.8895215. Retrieved from: <https://ieeexplore.ieee.org/document/8895215>
- Özdemir and Hanbay. (2022). Deep feature selection for facial emotion recognition based on BPSO and SVM. *Journal of Polytechnic*, Early Access. Retrieved From: <https://dergipark.org.tr/tr/pub/politeknik/issue/33364/992720>
- Pantic, M., Rothkrantz, J., (2001), Automatic Analysis of Facial Expressions: The State of the Art. *IEEE Transactions on Pattern Analysis and Machine Intelligence*, 22(12), 1424-1445. doi: 10.1109/34.895976. Retrieved from: <https://ieeexplore.ieee.org/document/895976>
- Paleari, M., Velardo, C., Huet, B., Dugelay, J. (2009). Face dynamics for biometric people recognition. *2009 IEEE International Workshop on Multimedia Signal Processing*, 1-5, doi: 10.1109/MMSP.2009.5293300. Retrieved From: <https://ieeexplore.ieee.org/document/5293300>
- Python Software Foundation (2012) Retrieved from: <https://web.archive.org/web/20121024164224/http://docs.python.org/faq/general.html>
- Saurav, S., Gidde, P., Saini, R., and Singh, S. (2022). Dual integrated convolutional neural network for real-time facial expression recognition in the wild. *The Visual Computer*, 38, 1083–1096. Retrieved from: <https://doi.org/10.1007/s00371-021-02069-7>
- Saxena, A., Khanna, A., Gupta, D. (2020). Emotion Recognition and Detection Methods. *Journal of Artificial Intelligence and Systems*, 2, 53-79. Retrieved from: <https://iecsce.org/uploads/jpapers/202003/dnQToaqdF8IRjhE62pflovCkDJ2jXAcZdK6KHRz M.pdf>
- Saraçbaşı, N. Z. (2021). *Face Recognition Using Facial Dynamics of Emotional Expressions* (Master Thesis). Retrieved From: <https://tez.yok.gov.tr/UlusalTezMerkezi/tezSorguSonucYeni.jsp>
- Sebe, N., Cohen, I., Huang, T.S (2004). *Multimodal Emotion Recognition*. Handbook of Pattern Recognition and Computer Vision, 387-409. doi:[https://doi.org/10.1142/9789812775320\\_0021](https://doi.org/10.1142/9789812775320_0021)
- Sharma, P. (2021). Understanding Transfer Learning for Deep Learning. Retrieved from: <https://www.analyticsvidhya.com/blog/2021/10/understanding-transfer-learning-for-deep-learning/>
- Srivastava, T., (2018). Introduction to k-Nearest Neighbors. Retrieved From: <https://www.analyticsvidhya.com/blog/2018/03/introduction-k-neighbours-algorithm-clustering/>
- Terra, J., (2022). Key Differences Among the Deep Learning Framework. Retrieved From: <https://www.simplilearn.com/keras-vs-tensorflow-vs-pytorch-article#:~:text=TensorFlow%20is%20an%20open%2Dsourced,because%20it's%20built%2Din%20Python.>
- Tutsoy, O., Güngör, F., Barkana, D. E., & Köse, H. (2017). An emotion analysis algorithm and implementation to NAO humanoid robot. *The Eurasia Proceedings of Science Technology Engineering and Mathematics*, 1, 316-330. Retrieved From: <http://www.epstem.net/tr/download/article-file/381431>
- Umer, S., Rout, R.K., Pero, C., and Nappi, M. (2022). Facial expression recognition with trade-offs between data augmentation and deep learning features. *Journal of Ambient Intelligence and Humanized Computing*, 13, 721–735. doi:<https://doi.org/10.1007/s12652-020-02845-8>
- Verma, G., Verma, H. (2020). Hybrid-Deep Learning Model for Emotion Recognition Using Facial Expressions. *The Review of Socionetwork Strategies*. doi:<https://doi.org/10.1007/s12626-020-00061-6>
- Yang, M., H., Kriegman, D., (2002). Detecting Faces in Images: A Survey. *IEEE Transactions on Pattern Analysis and Machine Intelligence*, 24(1), 34-58. Retrieved from: <https://ieeexplore.ieee.org/document/982883?arnumber=982883>
- Zhao, X., Shi X. and Zhang, S. (2015). Facial Expression Recognition via Deep Learning. *IETE Technical Review*, 32(5), 347-355, Retrieved From: <https://ieeexplore.ieee.org/document/7043872>





# A Methodology for Clustering Items with Seasonal and Non-seasonal Demand Patterns for Inventory Management

Burak Kandemir<sup>1,\*</sup>

Koç Digital Çözümler A.Ş., İstanbul, Türkiye

## Article History

Received: 10.05.2022

Accepted: 12.07.2022

Published: 15.12.2022

## Research Article

**Abstract** – Item clustering has become one of the most important topics in terms of effective inventory management in supply chains. Classification of items in terms of their features, sales or consumption volume and variation is a prerequisite to determine differentiated inventory policies as well as parameters, most common of which is service levels. Volume classification is easily obtained by well-known Pareto approach while coefficient of variance is usually used for variation dimension. Hence, it is not always applicable to classify items under different product families with different demand patterns in terms of variation. In this paper, we propose two algorithms, one based on statistical analysis and the other an unsupervised machine learning algorithm using K-means clustering, both of which differentiate seasonal and non-seasonal products where an item's variation is evaluated with respect to seasonality of the product group it belongs to. We then calculate the efficiency of two proposed approaches by standard deviation within each cluster and absolute difference of percentage of volume and item numbers. We also compare the outputs of two algorithms with the methodology which is based on coefficient of variance and is currently in use at the company which is a leading major domestic appliance manufacturer. The results show that the statistical method we propose generates superior outputs than the other two for both seasonal and non-seasonal demand patterns.

**Keywords** – Inventory control, item classification, K-means clustering, supply chain management, seasonality

## 1. Introduction

Effective inventory management is one of the major area of studies in supply chain management. Optimization of service levels with respect to inventory carrying and operating costs enables companies to determine their supply chain strategies in terms of customer and product-specific policies. It is almost a necessity to differentiate service levels since obtaining a high service for all product and customer combinations becomes infeasible in terms of cost and working capital management.

A well-known approach to differentiate products for service level differentiation is grouping items based on their volume and one can easily deduce that the well-known ABC classification of items has a great area of use for its validity and simplicity. ABC classification takes Vilfredo Pareto's rule as a basis where the majority of the consequences are determined by a small portion of the items or causes which affect them. Hence, classification of items in order to generate effective inventory policies does not only depend on volume but other features as well. These features may depend on the dynamics of the related industry and production and distribution requirements of the items and thus, some of the various studies and applications will be mentioned afterwards. However, one of the most important features for item classification is taken as the variability of the items' consumption, since variability is also a major feature in terms of inventory management, such as determining the safety stock levels.

<sup>1</sup>  [burak.kandemir@gmail.com](mailto:burak.kandemir@gmail.com)

Corresponding Author

We have conducted this study in one of the leading major domestic appliance manufacturers in the world, which started its industrial life in 1950s and has been producing a wide range of products under various brands at its factories and exports to more than 130 countries since then. The company’s supply chain faces challenges in effective planning, especially in terms of inventory management due to high complexity of channel requirements, products, and different demand patterns. The company has the well-known periodically reviewed order-up-to inventory control policy in use, and in order to establish a robust supply chain planning infrastructure, their major area of focus is differentiating the service levels among the high number of product portfolio.

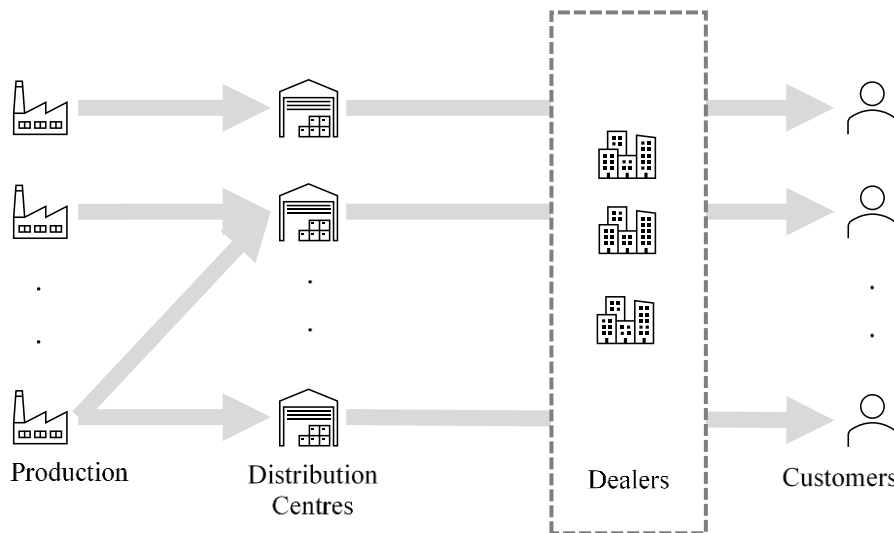


Figure 1. Distribution network of the company's supply chain

As determining the differentiated service levels in such a complex supply chain structure becomes a prerequisite for inventory planning, our study focuses on clustering the products for the abovementioned service level differentiation within a single market, the distribution network of which is shown in Figure 1. Within the order-up-to policy for inventory control, the company uses a classical ABC-XYZ classification of items where ABC classes are determined by volume and XYZ classes by demand variation, and we take the same two dimensions of clustering methodology focusing on variation sub-clusters.

Currently, the company uses the coefficient of variance (CoV) parameter for the XYZ clustering in which the CoV value for SKU  $i$  is calculated by (1.1);

$$CoV_i = \frac{\sigma_i}{\mu_i} \tag{1.1}$$

where;

$\sigma_i$ : standard deviation of sales of SKU  $i$

$\mu_i$ : average of sales of SKU  $i$

and

$$i \in \begin{cases} X & ; \text{if } CoV_i \leq a \\ Y & ; \text{if } a < CoV_i < b \\ Z & ; \text{if } b \leq CoV_i \end{cases}$$

Hence, this classification has two major lacking points. First, the outcome of this methodology is highly dependent on the chosen  $a$  and  $b$  parameters. The company uses 0.7 and 1.1 values respectively for threshold values but there is no scientific methodology nor an optimisation algorithm for determining the mentioned parameters. Selecting the best-fit parameters will require deep industrial knowledge but will also be open to challenges related to dynamic environmental changes in the industry and will demonstrate a weak argument for deployment. The second lacking point lies in the nature of the demand pattern of different products. The

clustering methodology is on SKU level by nature, but the company uses same threshold values as well as classifying the products with the same criteria of standard deviation where the product portfolio includes highly seasonal products together with non-seasonable ones. One can easily guess that the standard deviation of seasonal and non-seasonal products will show difference on the basics, and it would neither be theoretically nor practically correct to evaluate these two groups in the same manner.

## 2. Literature Review

Researchers and practitioners have conducted numerous studies for item classification in inventory control. (Raja et al., 2016) used hierarchical clustering in which they have converted non-metric variables to metric for improving inventory performance in inventory management of spare parts. (Pujiarto et al., 2021) developed a method based on Partitioning Around Medoids algorithm for locating optimal picking points based on cluster classifications. (Razavi Hajiagha et al., 2021) proposes a hybrid fuzzy-stochastic multi-criteria method using possibilistic chance-constrained programming. They have considered demand information as stochastic due to its time-varying nature and cost information as fuzzy due to its cognitive ambiguity and classified items into three groups naming their level of importance. (López-Soto et al., 2017) designed a multi-start constructive algorithm to train a discrete artificial neural network in order to classify new units based on their attributes. Another multi-criteria framework for inventory classification is developed by (Lolli et al., 2017) and applied to intermittent demand. They emphasize the importance of inventory classification with respect to its effect on ordering and replenishment policies. (Rezaei & Dowlatshahi, 2010) also proposed a rule-based multi-criteria approach to inventory classification in which they have taken into account the inherent ambiguities that exist in the reasoning process of the classification system. They have also compared their results with analytic hierarchy process (AHP) method. (Cakir & Canbolat, 2008) proposed multi-criteria decision support system using fuzzy analytic hierarchy process. (Bacchetti et al., 2013) developed a hierarchical multi-criteria classification method and applied it in a spare parts inventory management case study. (Ladhari et al., 2016) developed a hybrid model to overcome the conflicts of various multiple criteria inventory classification model and evaluated the efficiency of consensus outputs.

(Ernst & Cohen, 1990) developed a statistical clustering method using operations related groups (ORGs). The groups they used took into consideration all the related product characteristics that have impact on operations management. They also included an application of the mentioned methodology in spare parts distribution in automotive industry with substantial advantages of outputs. (Ramanathan, 2006) built a weighted linear optimisation model scheme with illustrated application. (Russo, 2019) conducted widespread research and proposed alternative method for ABC-XYZ classification of items in multi-echelon structures, identifying the most important features for classification. (Chu et al., 2008) combined ABC analysis and fuzzy classification to handle variables with both nominal and non-nominal attitudes and implemented their approach on the data of Keelung Port with satisfactory outcomes. (Park et al., 2014) suggested a cross-evaluation-based linear optimisation for multiple criteria inventory clustering which incorporates the cross-efficiency for ranking of inventory items. They also conducted a comparative experiment with the previous related investigations by simulation. (Rossetti & Achlerkar, 2011) evaluated multi-item group policies and grouped multi-item individual policies and compared them to ABC analysis via a set of experiments. (Yang et al., 2017) investigated the dynamic integration and optimisation of inventory classification to maximise the net present value of profit over the planning horizon using mixed-integer linear programming. (Tavassoli et al., 2014) used data envelopment analysis (DEA) to classify inventory items into three groups with weight restrictions in order to allow managerial preferences. Another model simultaneously optimises the number of inventory groups, corresponding service levels and assignment of SKUs within the group (Millstein et al., 2014). (Narkhede & Rajhans, 2022) discusses an integrated approach where they use rank order clustering (ROC) technique to redesign inventory management strategies for small and medium-sized enterprises.

While the use of multi-criteria decision making, linear optimisation, fuzzy systems and analytic hierarchy process is widespread, methodologies for item clustering is not limited to them, especially with the increasing application of machine learning techniques. Many studies take into account k-means algorithm, which is an incremental approach and dynamically adds one cluster centre through a deterministic global search procedure consisting of executions with the number of data points (Likas et al., 2003). (Balugani et al., 2018) used k-

means and Ward’s method algorithms to cluster items into homogenous groups with uniform inventory control policies. (T. Kanungo et al., 2002) proposed an efficient k-means algorithm together with its analysis and implementation. (Mohamad & Usman, 2013) analysed the performances of three standardization methods on conventional k-means algorithm on dataset of infectious diseases. They conclude that the z-score standardization method is more effective and efficient than min-max and decimal scaling methods. (Bellini et al., 2022) proposed a recommendation system based on a multi-clustering approach of items and users in fashion retail, where their proposed solution relies on mining techniques. (Liu et al., 2022) uses dynamic clustering scheduling for optimisation of big data parallel scheduling tasks. Their approach can also be adapted to item scheduling for inventory management where multiple criteria are used. Another strong technique which can be adapted to inventory management is linear programming (LP)-rounding to be used in machine learning and used for facility location clusters (Negahbani, 2022).

### 3. Methodology

Within the light of listed studies with various methods, we have generated a statistical and a k-means based methodologies to overcome the lacking features of current clustering technique which is based on simple sorting of CoV values for each SKU. To do so, we start by determining each SKUs variability relative to the variation of the product group it belongs to, and therefore we first define the coefficient of variance of product group  $p$  by (3.1);

$$CoV_p = \frac{\sigma_p}{\mu_p} \tag{3.1}$$

where;

$\sigma_p$ : standard deviation of sales of product group  $p$

$\mu_p$ : average of sales of product group  $p$

Hence, we would like to obtain the relative variability of a single SKU with respect to variability of the product group it belongs to, and combining (1) and (2), we define the ratio of variability  $\phi$  as in (3.2):

$$\phi_i^p = \frac{CoV_i}{CoV_p} \tag{3.2}$$

Generating the  $\Phi_i$  values for each SKU, we apply two approaches for clustering -a statistical approach where the classes are formed by the distance of  $\Phi_i$  to the median of the  $\Phi_i$  values within that product group, and an unsupervised machine learning algorithm using k-means clustering. For the statistical modelling that is based on median values, we first determine the range of  $\Phi$  values by the difference of maximum and minimum of the parameter within each product group (3.3a) and obtain the quartiles with respect to the median of  $\Phi$  data set (3.3b and 3.3c). The XYZ clusters are formed based on comparing the  $\Phi$  value of the SKU with obtained quartiles:

$$R_{i,p}^\phi = Max\phi_i^p - Min\phi_i^p \tag{3.3a}$$

$$Q_{i,p,1}^\phi = med(\phi_i^p) - (R_{i,p}^\phi/4) \tag{3.3b}$$

$$Q_{i,p,3}^\phi = med(\phi_i^p) + (R_{i,p}^\phi/4) \tag{3.3c}$$

$$i \in \begin{cases} X & ; \text{if } \phi_i^p \leq Q_{i,p,1}^\phi \\ Y & ; \text{if } Q_{i,p,1}^\phi < \phi_i^p < Q_{i,p,3}^\phi \\ Z & ; \text{if } Q_{i,p,3}^\phi \leq \phi_i^p \end{cases}$$

In addition to the statistical method we have developed, we have also used a k-means clustering algorithm. K-means methodology requires the number of clusters to be obtained as the initial step and this parameter is usually generated by additional techniques such as elbow method. Since the number of clusters we need is

already three, we pre-set this parameter. Then each  $\Phi_i$  within the product group  $p$  is iteratively grouped based on the cluster of nearest data point and the XYZ clusters are iteratively finalized.

#### 4. Results and Discussion

As stated above, our methodology fundamentally aims to differentiate seasonal and non-seasonal products and generates a new parameter of SKU variation with respect to product groups' variation. We therefore analyse the outputs of the two algorithms based on this new parameter of relative coefficient of variation and compare the results with the current sorting method as well as with each other both for seasonal and non-seasonal product groups. We start with visualising the distribution of relative coefficient of variation, where the distribution of obtained  $\Phi_i$  points is given in Figure 2.

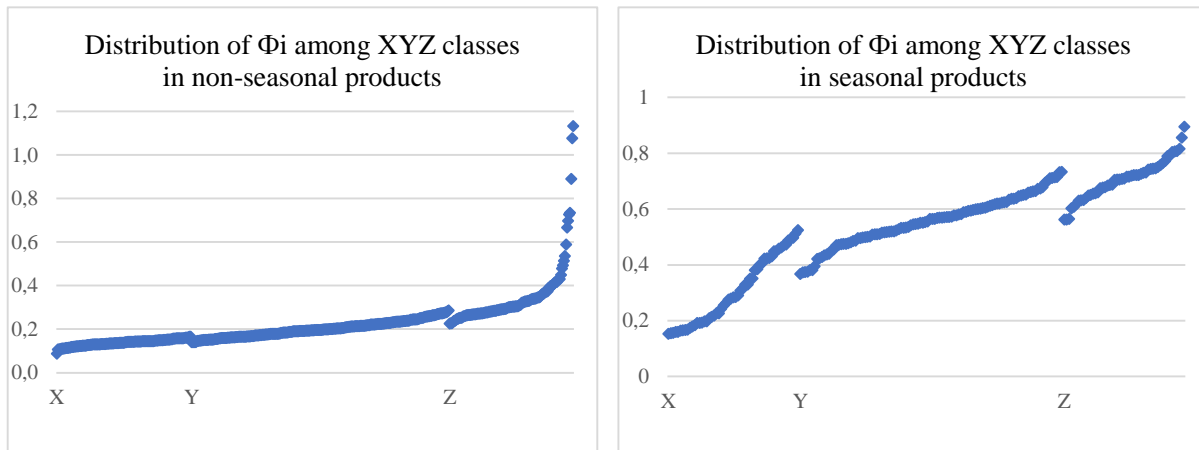


Figure 2. Distribution of  $\Phi_i$  data points in non-seasonal and seasonal product groups

In order to determine the efficiency of the three methods, we first analyse the correspondence of each cluster with respect to volume. We obtain this efficiency by calculating the absolute value of the difference of percentage of volume and percentage of number of items within that cluster as in (4.1).

$$\delta_i^{p,q} = |\chi_v^{p,q} - \chi_i^{p,q}| \tag{4.1}$$

where;

$\chi_v^{p,q}$ : Percentage of volume of cluster  $q$  within product group  $p$

$\chi_i^{p,q}$ : Percentage of number of SKUs in cluster  $q$  within product group  $p$

$\delta_i^{p,q}$ : Absolute value of difference of percentages

The outputs of this calculation are shown in Figure 3. Both for seasonal and non-seasonal products, statistical method gives the biggest sum of absolute values with 41.7% and 55.2% of values respectively. K-means algorithm has 35.8% for seasonal and 3.6% for non-seasonal products while sorting method has 10.1% and 1.0% values with the same order. Considering these values statistical method gives the best output, however for seasonal products, 21 points of 41.7% arises from cluster X in reverse side, which means 25.5% of number of items in cluster X corresponds to only 4.6% turnover. These numbers enable to question the absolute efficiency of the algorithm, leading to carry out further analysis.

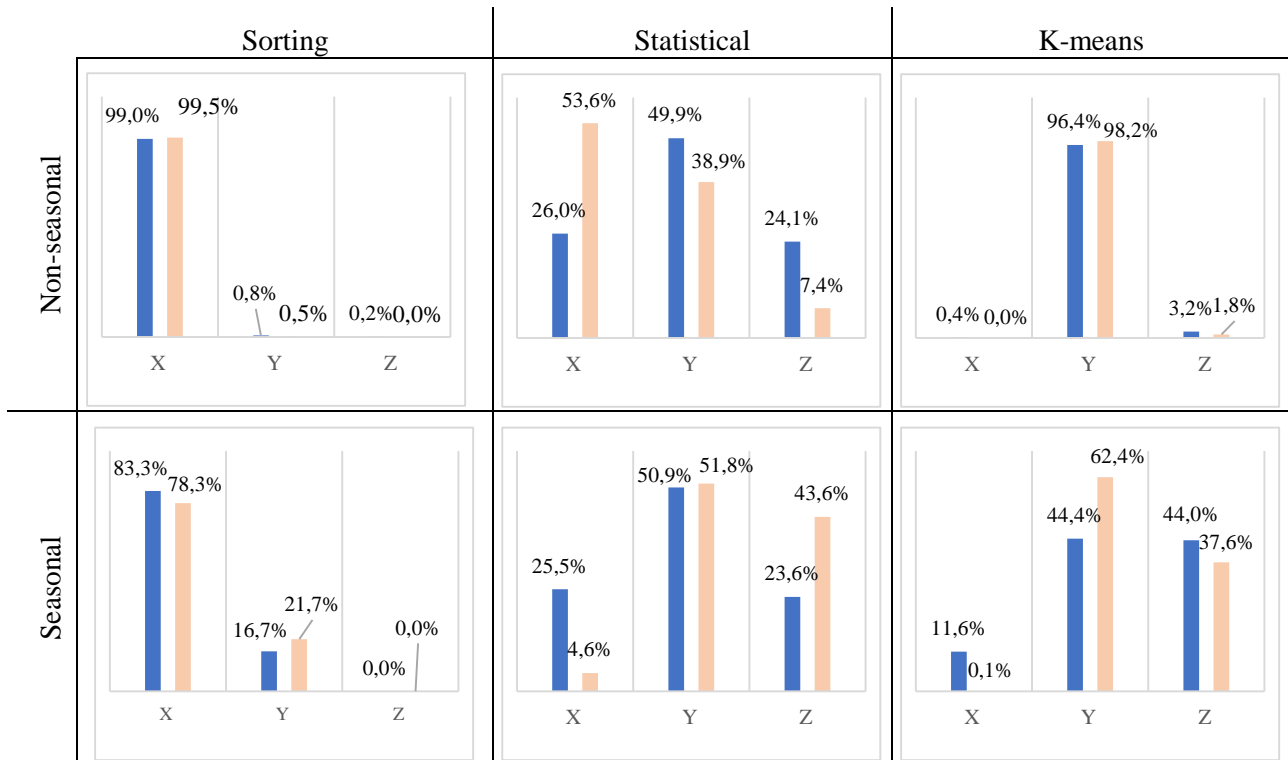


Figure 3. Correspondence of items within clusters to volume (■ number of items, ■ volume)

Our second analysis is based on the standard deviation of  $\Phi_i$  values within each cluster. It can easily be concluded that the smaller the standard deviation within each cluster, the more efficient the clustering algorithm would be. However, since the main parameter for clustering is coefficient of variation for sorting method, we have taken standard deviation of CoV values for it. Standard deviation values of  $CoV_i$  and  $\Phi_i$  within each cluster for both type of product groups is given in Table 1.

Table 1

Analysis of standard deviation of clusters for seasonal and non-seasonal items

	Seasonal			Non-seasonal		
	X	Y	Z	X	Y	Z
Sorting	.3159	.1649	-	.1935	.3879	-
Statistical	.1202	.0877	.0726	.0151	.0359	.1467
K-means	.0321	.0694	.0808	.0186	.0699	.3022

Since sorting method yields to only one data point in cluster Z, we do not have any calculated standard deviation figure for that cluster. Deep-diving into the calculated values, we again observe statistical algorithm outperforming both sorting and k-means algorithms. The exceptional figure is again cluster X of seasonal products where the standard deviation value of k-means algorithm is less than statistical algorithm. These outputs lead us to conclude that the analysis of standard deviation is in line with our first figure namely correspondence of percentages in terms of items and volume. Therefore, the statistical algorithm based on median value and defining quartiles as the threshold values outperforms simple sorting and k-means algorithms, except cluster X of seasonal products.

### 5. Conclusion

This study is conducted in major domestic appliances industry which has a highly complex supply chain structure in terms of demand and distribution characteristics, and therefore requires a sophisticated inventory management policy. The base of effective inventory management lies on setting differentiated service levels for different types of products, which brings item clustering as a prerequisite. The company where this study

is conducted uses a simple sorting method for clustering in which they use coefficient of variation parameter as the indicator for all product range. This paper analyses the clustering methodology of items based on their sales (consumption) variation with the fundamental aim of differentiating seasonal and non-seasonal product groups. In order to execute this idea of differentiation, we have generated a new relative variation indicator in which an item's variation is measured with respect to the product group's variation that the item belongs to. Having generated this indicator, we have developed two algorithms in order to form XYZ clusters. The first algorithm is based on a statistical analysis, where the quartiles are obtained around the median of the relative variation data set and clusters are formed based on these quartile threshold values. The second algorithm uses the classical k-means machine learning techniques where the number of clusters is set to three and data points are assigned to each cluster iteratively.

We have analysed the results of the three algorithms in terms of two main perspectives: correspondence of percentage of items in each cluster to the percentage of volume, and standard deviation of data points within each cluster. The result of the analysis demonstrates that both statistical and k-means algorithms overperform the simple sorting method which is currently used by the company and proves our idea of differentiating seasonal and non-seasonal products would provide better results for effective inventory management. In addition, the statistical method we have developed provides better results rather than k-means algorithm both in seasonal and non-seasonal product groups, except the X cluster of seasonal products. Considering the higher computational effort of k-means algorithm as well, it is more advantageous for the company to apply the statistical method based on quartiles around the median value.

However, deep-dived data analysis might provide additional insights for the performance of the two algorithms, especially for product groups with higher seasonality. Also, our study is limited to one industry only and takes into account only historic sales variation. Especially for highly seasonal products, future demand variation may differ from historic data. Therefore, further studies would be much more enlightening especially in different industries with both seasonal and non-seasonal products, focusing on the features that affect the demand pattern and variation. We have only tried to establish a base for differentiation of products, and various techniques can be added in order to enrich the study.

### Conflicts of Interest

The author declares no conflict of interest.

### References

- Aktepe A., Turker A.K., Ersoz S., Dalgic A., & Barisci N. (2018). An inventory classification approach combining expert systems, clustering, and fuzzy logic with the ABC method, and an application. *South African Journal of Industrial Engineering*, 29(1), 49–62. doi: <https://doi.org/10.7166/29-1-1784>
- Bacchetti, A., Plebani, F., Saccani, N., & Syntetos, A. A. (2013). Empirically-driven hierarchical classification of stock keeping units. *Focusing on Inventories: Research and Applications*, 143(2), 263–274. doi: <https://doi.org/10.1016/j.ijpe.2012.06.010>
- Bala, P. K. (2009). Data Mining for Retail Inventory Management. In *Advances in Electrical Engineering and Computational Science* (Vol. 39, pp. 587–598). Springer, Dordrecht.
- Bala, P. K. (2012). Improving inventory performance with clustering based demand forecasts. *Journal of Modelling in Management*, 7(1), 23–37. doi: <https://doi.org/10.1108/17465661211208794>
- Balugani, E., Lolli, F., Gamberini, R., Rimini, B., & Regattieri, A. (2018). Clustering for inventory control systems. *16th IFAC Symposium on Information Control Problems in Manufacturing INCOM 2018*, 51(11), 1174–1179. doi: <https://doi.org/10.1016/j.ifacol.2018.08.431>
- Bellini, P., Palesi, L. A. I., Nesi, P., & Pantaleo, G. (2022). Multi Clustering Recommendation System for Fashion Retail. *Multimedia Tools and Applications*. doi: <https://doi.org/10.1007/s11042-021-11837-5>
- Cakir, O., & Canbolat, M. S. (2008). A web-based decision support system for multi-criteria inventory classification using fuzzy AHP methodology. *Expert Systems with Applications*, 35(3), 1367–1378. doi: <https://doi.org/10.1016/j.eswa.2007.08.041>
- Chiou, Y.-C., & Lan, L. W. (2005). Ordering and Warehousing Strategies for Multi-item Multi-Branch Firm's Inventory: Clustering Approaches. *Journal of the Eastern Asia Society for Transportation Studies*, 6, 2809–2821. doi: <https://doi.org/10.11175/easts.6.2809>

- Chu, C.-W., Liang, G.-S., & Liao, C.-T. (2008). Controlling inventory by combining ABC analysis and fuzzy classification. *Computers & Industrial Engineering*, 55(4), 841–851. doi: <https://doi.org/10.1016/j.cie.2008.03.006>
- Ernst, R., & Cohen, M. A. (1990). Operations related groups (ORGs): A clustering procedure for production/inventory systems. *Journal of Operations Management*, 9(4), 574–598. doi: [https://doi.org/10.1016/0272-6963\(90\)90010-B](https://doi.org/10.1016/0272-6963(90)90010-B)
- Errasti, A., Chackelson, C., & Poler, R. (2010). An Expert System for Inventory Replenishment Optimization. *An Expert System for Inventory Replenishment Optimization*, 129–136.
- F. Wang, H. Y. Ng, & T. E. Ng. (2018). Novel SKU Classification Approach for Autonomous Inventory Planning. *2018 IEEE International Conference on Industrial Engineering and Engineering Management (IEEM)*, 1441–1445. doi: <https://doi.org/10.1109/IEEM.2018.8607736>
- Flores, B. E., Olson, D. L., & Dorai, V. K. (1992). Management of multicriteria inventory classification. *Mathematical and Computer Modelling*, 16(12), 71–82. doi: [https://doi.org/10.1016/0895-7177\(92\)90021-C](https://doi.org/10.1016/0895-7177(92)90021-C)
- K. P. Sinaga & M. Yang. (2020). Unsupervised K-Means Clustering Algorithm. *IEEE Access*, 8, 80716–80727. doi: <https://doi.org/10.1109/ACCESS.2020.2988796>
- Ladhari, T., Babai, M. Z., & Lajili, I. (2016). Multi-criteria inventory classification: New consensual procedures. *IMA Journal of Management Mathematics*, 27(2), 335–351. doi: <https://doi.org/10.1093/imaman/dpv003>
- Likas, A., Vlassis, N., & J. Verbeek, J. (2003). The global k-means clustering algorithm. *Biometrics*, 36(2), 451–461. doi: [https://doi.org/10.1016/S0031-3203\(02\)00060-2](https://doi.org/10.1016/S0031-3203(02)00060-2)
- Liu, F., He, Y., He, J., Gao, X., & Huang, F. (2022). Optimization of Big Data Parallel Scheduling Based on Dynamic Clustering Scheduling Algorithm. *Journal of Signal Processing Systems*. doi: <https://doi.org/10.1007/s11265-022-01765-4>
- Lolli, F., Ishizaka, A., Gamberini, R., & Rimini, B. (2017). A multicriteria framework for inventory classification and control with application to intermittent demand. *Journal of Multi-Criteria Decision Analysis*, 24(5–6), 275–285. doi: <https://doi.org/10.1002/mcda.1620>
- López-Soto, D., Angel-Bello, F., Yacout, S., & Alvarez, A. (2017). A multi-start algorithm to design a multi-class classifier for a multi-criteria ABC inventory classification problem. *Expert Systems with Applications*, 81, 12–21. doi: <https://doi.org/10.1016/j.eswa.2017.02.048>
- Millstein, M. A., Yang, L., & Li, H. (2014). Optimizing ABC inventory grouping decisions. *International Journal of Production Economics*, 148, 71–80. doi: <https://doi.org/10.1016/j.ijpe.2013.11.007>
- Mohamad, I., & Usman, D. (2013). Standardization and Its Effects on K-Means Clustering Algorithm. *Research Journal of Applied Sciences, Engineering and Technology*, 6(17), 3299–3303.
- Narkhede, G., & Rajhans, N. (2022). An integrated approach to redesign inventory management strategies for achieving sustainable development of small and medium-sized enterprises: Insights from an empirical study in India. *Business Strategy & Development*, 1(14). Doi: <https://doi.org/10.1002/bsd2.200>
- Negahbani, Maryam. (2022). *Approximation Algorithms for Clustering: Fairness and Outlier Detection*. Guarini School of Graduate and Advanced Studies Dartmouth College.
- Park, J., Bae, H., & Bae, J. (2014). Cross-evaluation-based weighted linear optimization for multi-criteria ABC inventory classification. *Computers & Industrial Engineering*, 76, 40–48. doi: <https://doi.org/10.1016/j.cie.2014.07.020>
- Pujiarto, B., Hanafi, M., Setyawan, A., Imani, A. N., & Prasetya, E. R. (2021). A Data Mining Practical Approach to Inventory Management and Logistics Optimization. *International Journal of Informatics and Information Systems; Vol 4, No 2: September 2021 DO - 10.47738/Ijiiis.V4i2.109*. Retrieved from: <http://ijiiis.org/index.php/IJIIIS/article/view/109>
- Raja, A. M. L., Ai, T. J., & Astanti, R. D. (2016). A Clustering Classification of Spare Parts for Improving Inventory Policies. *IOP Conference Series: Materials Science and Engineering*, 114, 012075. doi: <https://doi.org/10.1088/1757-899x/114/1/012075>
- Ramanathan, R. (2006). ABC inventory classification with multiple-criteria using weighted linear optimization. *Computers & Operations Research*, 33(3), 695–700. doi: <https://doi.org/10.1016/j.cor.2004.07.014>
- Razavi Hajiagha, S. H., Daneshvar, M., & Antucheviciene, J. (2021). A hybrid fuzzy-stochastic multi-criteria ABC inventory classification using possibilistic chance-constrained programming. *Soft Computing*, 25(2), 1065–1083. doi: <https://doi.org/10.1007/s00500-020-05204-z>



- Rezaei, J., & Dowlatshahi, S. (2010). A rule-based multi-criteria approach to inventory classification. *International Journal of Production Research*, 48(23), 7107–7126. doi: <https://doi.org/10.1080/00207540903348361>
- Rossetti, M. D., & Achlerkar, A. V. (2011). Evaluation of segmentation techniques for inventory management in large scale multi-item inventory systems. *International Journal of Logistics Systems and Management*, 8(4), 403–424. doi: <https://doi.org/10.1504/IJLSM.2011.039598>
- Russo, F. (2019). *Adaptive product classification for inventory optimization in multi-echelon networks*. Erasmus University.
- S. Na, L. Xumin, & G. Yong. (2010). Research on k-means Clustering Algorithm: An Improved k-means Clustering Algorithm. *2010 Third International Symposium on Intelligent Information Technology and Security Informatics*, 63–67. Doi: <https://doi.org/10.1109/IITSI.2010.74>
- SAP Library ABC-XYZ Analysis. (n.d.). Retrieved from: [https://help.sap.com/doc/saphelp\\_scm700\\_ehp02/7.0.2/en-US/4d/33d92edb9e00d3e10000000a42189b/content.htm?no\\_cache=true](https://help.sap.com/doc/saphelp_scm700_ehp02/7.0.2/en-US/4d/33d92edb9e00d3e10000000a42189b/content.htm?no_cache=true)
- Sheikh-Zadeh, A., Rossetti, M. D., & Scott, M. A. (2021). Performance-based inventory classification methods for large-Scale multi-echelon replenishment systems. *Omega*, 101, 102276. doi: <https://doi.org/10.1016/j.omega.2020.102276>
- T. Kanungo, D. M. Mount, N. S. Netanyahu, C. D. Piatko, R. Silverman, & A. Y. Wu. (2002). An efficient k-means clustering algorithm: Analysis and implementation. *IEEE Transactions on Pattern Analysis and Machine Intelligence*, 24(7), 881–892. doi: <https://doi.org/10.1109/TPAMI.2002.1017616>
- Tavassoli, M., Faramarzi, G. R., & Farzipoor Saen, R. (2014). Multi-criteria ABC inventory classification using DEA-discriminant analysis to predict group membership of new items. *International Journal of Applied Management Science*, 6(2), 171–189. doi: <https://doi.org/10.1504/IJAMS.2014.060904>
- Yang, L., Li, H., Campbell, J. F., & Sweeney, D. C. (2017). Integrated multi-period dynamic inventory classification and control. *International Journal of Production Economics*, 189, 86–96. doi: <https://doi.org/10.1016/j.ijpe.2017.04.010>



# Fretting behavior of piston ring-cylinder liner components of a diesel engine running on TiO<sub>2</sub> nanolubricant

Ali Can Yılmaz<sup>1,\*</sup>

<sup>1</sup>Department of Motor Vehicles and Transportation Technologies, Adana Vocational School, Cukurova University, Adana, Türkiye

## Article History

Received: 30.04.2022

Accepted: 16.08.2022

Published: 15.12.2022

## Research Article

**Abstract** – This experimental research presents the friction and wear characteristics of piston ring-cylinder liner component of a diesel engine running on commercial engine oil (5W-30) and TiO<sub>2</sub> nanoparticle (~20 nm, ≥99.5% trace metals basis) incorporated 5W-30 engine oil (nanolubricant) to observe the performance parameters in terms of mean effective pressures and smoke emissions. Dynamic light scattering was utilized to examine the nanoparticle dispersion in the lubricant. Thermo-gravimetric analysis on nanoparticles was conducted to examine the thermal endurance during abrasion tests. The samples directly cut from the spare piston ring of the test engine underwent severe friction and wear tests via linear friction module. Coefficient of friction was considered as comparison parameter to understand the tribological behavior of friction pairs submerged in two different lubricants. Scanning electron microscopy analysis was conducted to observe morphology of the nanoparticle and to analyze the surface structure of the samples before and after the abrasion tests. Atomic force microscopy analysis was done to obtain the 3D images of the worn surfaces and to make a comprehensive comparison of tribological performance between engine lubricant and nanolubricant. The results depicted that, TiO<sub>2</sub> is effective in reducing coefficient of friction by an average of 10.37% and wear rate by 33.58% as well as improving brake mean effective pressure by an average of 4.95% and reducing friction mean effective pressure by an average of 9.34% when compared to those of the engine oil. In parallel with reduced friction, TiO<sub>2</sub> incorporation in engine oil yielded an average reduction of 9.11% in smoke opacity. The experiments suggest promising results in terms of utilization of low friction, fuel efficient and environmental friendly internal combustion engines fulfilling strict emission regulations.

**Keywords** – Diesel engine, mean effective pressure, smoke emission, tribology, TiO<sub>2</sub> nanoparticle;

## 1. Introduction

Friction between solid surfaces in relative motion is a complex process due to wide variation in the magnitude of forces exerted onto the contact surfaces. Thus, various lubrication regimes occur in the piston ring-cylinder liner (PRCL) of a running engine. Basically, three regimes are observed in PRCL system: (i) Boundary lubrication generally occurs when the piston is at top dead center (TDC) and bottom dead center (BDC). The oil film is only formed by squeeze effect as the piston velocity is zero at these dead points. This causes thinner oil film at TDC and BDC, where fretting effects reach maximum. (ii) Hydrodynamic lubrication is expected to be seen at mid-strokes where higher piston velocity values are observed. As the piston moves, the lubrication ring distributes the lubricant on the cylinder liner. The oil film is thicker and metal-metal contact is minimum within mid-stroke region. (iii) Mixed lubrication represents the transition from boundary regime to hydrodynamic regime (Yin, Li, Fu, & Yun, 2012). Stribeck diagram is used to define lubrication regimes in which the Hersey number (HN) (1.1) is plotted against coefficient of friction. “f” can be expressed in terms of dry and hydrodynamic friction as depicted in 1.2 (Heywood, 2018):

<sup>1</sup>  [acyilmaz@cu.edu.tr](mailto:acyilmaz@cu.edu.tr)

Corresponding Author

$$HN = \eta N / \Gamma \quad (1.1)$$

$$f = \sigma f_d + (1 - \sigma) f_h \quad (1.2)$$

where;

$\eta$ : dynamic viscosity of the lubricant (Pa.s)

$N$ : entrainment speed of the lubricant (m/s)

$\Gamma$ : loading force per length of the tribological contact (N/m)

$\sigma$ : metal-metal contact constant ( $0 < \sigma < 1$ )

$f_d$ : dry friction coefficient

$f_h$ : hydrodynamic friction coefficient

As  $\sigma \rightarrow 1$  and  $f \rightarrow f_d$ , boundary friction occurs, that is, solid surfaces are nearly in contact (very thin oil layer in between). On the other hand, as  $\sigma \rightarrow 0$  and  $f \rightarrow f_h$ , hydrodynamic friction occurs where the thickness of the oil layer is adequate to fully separate the solid surfaces (Heywood, 2018).

In reciprocating engines, fretting pairs become deteriorated in time and piston ring assembly is responsible for 45% of total friction (Taylor, 1998). Thus, tribological characteristic of PRCL system is directly related to the lubrication performance of the engine (Dimkovski, Anderberg, Ohlsson, & Rosén, 2011; Guo, Yuan, Liu, Peng, & Yan, 2013).

Intriguing studies have been carried out by several researchers focusing on reducing frictional using various methods such as coating of contact surfaces (Kovalchenko, Ajayi, Erdemir, Fenske, & Etsion, 2005; Kumar, Sinha, & Agarwal, 2019; K. Y. Li, Zhou, Bello, Lee, & Lee, 2005; Lin, Wei, Bitsis, & Lee, 2016; Tung & Gao, 2003; Wróblewski & Koszalka, 2021), surface texturing (Kovalchenko et al., 2005; Podgornik, Vilhena, Sedlaček, Rek, & Žun, 2012; Ronen, Etsion, & Kligerman, 2001), organic friction modifiers as engine lubricant additives (Fry, Chui, Moody, & Wong, 2020; Guegan, Southby, & Spikes, 2019; Ratoi, Niste, Alghawel, Suen, & Nelson, 2014). Though undisputable advantageous features of these techniques in terms of reducing frictional losses within PRCL system, they may bring a huge cost burden to the researcher or his/her institution as they require expensive experimental set-ups. In this context, incorporation of nanoparticle additives in engine oil steps forward to improve the tribological behavior of PRCL pair, little amount of nanoparticle introduction into the engine oil is generally sufficient and very effective as well as requiring no special and high cost experimental set-ups. Furthermore, one does not need to make modifications on the test engine. Nanoparticles are characterized by their specific features that manipulate the lubrication mechanisms such as polishing (K. Lee et al., 2009), rolling (Liu et al., 2004), mending (Tao, Jiazheng, & Kang, 1996) and third body (Padgurskas, Rukuiza, Prosyčevs, & Kreivaitis, 2013) effects. Therefore, recently, metallic nanoparticles in elemental form such as Ag (Ghaednia, Babaei, Jackson, Bozack, & Khodadadi, 2013; J. Ma, Mo, & Bai, 2009), Cu (Hu, Peng, & Ding, 2013; Pan & Zhang, 2010; Wang, Yin, Zhang, Wang, & Zhao, 2013; Yang, Zhang, Zhang, Yu, & Zhang, 2013; Yu et al., 2008), Fe (Chen et al., 2015; S. Ma, Zheng, Cao, & Guo, 2010; Nabhan, Ghazaly, Mousa, & Rashed, 2020; Song et al., 2012; Yilmaz, 2020b, 2020a), Ni (Chou et al., 2010), Pd (Abad & Sánchez-López, 2013) or in compound form (Chen et al., 2015; Hernandez Battez et al., 2006; S. Ma et al., 2010; Nabhan et al., 2020; Song et al., 2012) have been studied by several researchers. Among nanoparticles as engine oil additives, TiO<sub>2</sub> nanoparticles have been attracting attention due to its higher corrosion endurance, wear resistance and thermal stability as well as entrainment ability onto the metal surface crevices (higher viscosity of nano-oil) to reduce friction (Cao et al., 2018; Ćurković, Ćurković, Salopek, Renjo, & Šegota, 2013; Dhiflaoui, Kaouther, & Larbi, 2018; Langlet et al., 2001; Wan, Chao, Liu, & Zhang, 2011).

Indicated mean effective pressure (IMEP) and brake mean effective pressure (BMEP) are useful parameters for comparison of engine performance. Researchers have been implementing valuable studies related to IMEP improvement such as developing fuel adjustment systems for CI engines (Shi, Sun, & Deng, 2016; Kokjohn, Hanson, Splitter, & Reitz, 2011; Bedoya, Saxena, Cadavid, Dibble, & Wissink, 2012), observation of fuel injection timing (Agarwal et al., 2013; Su, Ji, Wang, Shi, Yang, & Cong, 2017) and establishment of dual-fuel spark ignition engines running on various fuels (Liu, Wang, Long, & Wang, 2015). IMEP directly relates to the work done by engine and can be measured via optical pressure sensors (Nagashima, Kawa, & Tsuchiya,

2003) or it can be estimated as an area in a closed curve under P-V indication diagram using numerical integration. The average pressures in the engine cylinders are referred to as BMEP and it defines the work done by the crankshaft per swept volume as shown in 1.3 (Heywood, 2018; Pahmi et al., 2019):

$$\text{BMEP} = 2 * \pi * n * T / V_d \quad (1.3)$$

BMEP: brake mean effective pressure (Pa)

n: number of revolutions per power stroke (n=2 for 4-stroke engines)

T: brake torque (Nm)

V<sub>d</sub>: displacement volume (m<sup>3</sup>)

Friction mean effective pressure (FMEP) is another parameter defining the pressure loss between IMEP and BMEP due to friction occurring in the PRCL system. It is the mean effective pressure to overcome engine friction (Heywood, 2018). Thus, it is related to the lubrication conditions between contact surfaces and can be approximated by using 1.4:

$$\text{FMEP} = \text{IMEP} - \text{BMEP} \quad (1.4)$$

Smoke emissions (soot formation) are of great concern especially in diesel engines. Diesel engines are prone to emit smoke from the exhaust pipe under high loads due to lack of adequate oxygen to oxidize the most of the fuel (Abdullah, Abdullah, & Bhatia, 2008; Mishra & Prasad, 2014). Furthermore, at high loads, short ignition delay period (short time for mixing of air-fuel) at high fuel injection pressures deteriorate formation of homogeneous mixture, that is, increased smoke emissions (Celikten, 2003). Diesel particulate filter (DPF) has been a compulsory equipment in recent years to fulfill the strict emission regulations. DPFs are effective in reducing particulate matter (Nguyen, Sung, Lee, & Kim, 2011) and may be more effective with a reduction in frictional losses. Reducing frictional losses in PRCL system will make the engine deliver the same power with lesser fuel or more power with the same fuel amount yielding lower smoke emissions.

The goal of this study is to observe the tribological effects of TiO<sub>2</sub> nanolubricant on performance (IMEP, BMEP, FMEP) and smoke emissions of a diesel engine by conducting comprehensive friction and wear analyses on the samples made up of same material with the piston ring-cylinder liner components. Though there are several studies on tribological enhancement effects of TiO<sub>2</sub> nanoparticles as engine oil additive, literature review shows that no study has been conducted to investigate the performance and smoke emissions of a diesel engine running on TiO<sub>2</sub> nanolubricant. Furthermore, to the author's knowledge, no studies have been established related to the combination of tribological improvement of TiO<sub>2</sub> nanoparticles and in-cylinder mean effective pressure parameters as well as smoke emissions.

## 2. Experimental Procedure

In the first step of the study, scanning electron microscopy (SEM) analysis was carried out to observe the morphology of TiO<sub>2</sub> nanoparticles (~20 nm, ≥99.5% trace metals basis). In the next step, thermal stability (TG) analysis was carried out to investigate the thermal endurance of TiO<sub>2</sub> nanoparticles during friction tests under harsh conditions to determine any decomposition and/or deterioration at high temperatures. In the subsequent step, before friction tests, SEM image of sample surface (unworn cast iron sample directly cut from the spare piston ring of the test engine) was taken. Then, the sample was submerged in the engine oil and TiO<sub>2</sub> nano-oil ambients to undergo friction tests under the same experimental conditions (oil temperature, sliding distance, normal friction load exerted on the samples). Nanoparticle dispersion in engine oil has substantial effects on tribological performance as nanoparticle clusters formed in the oil are highly responsible for agglomeration between the contact surfaces. Therefore, it is essential to prepare a nano-oil in which the nanoparticles suspend homogeneously. Firstly, the nanoparticle incorporated lubricant was ultrasonicated for 1 h to make a homogeneous dispersion of the nanoparticles. Dynamic light scattering (DLS) technique was utilized to confirm the homogenous dispersion of the nanoparticles in the oil. DLS is one of the most widely used techniques for detecting size distributions, dispersion, and morphologies of dry and powdered nanoparticles in

liquids. It uses a He–Ne laser operating at a certain wavelength (651 nm for this study) and a detection angle (174° for this study) (Murdock, Braydich-Stolle, Schrand, Schlager, & Hussain, 2008; Pecora, 2000). The beam coming out of the laser source is focused on the nano-oil suspension via a lens and scattered beams from the nanoparticles are detected by a high speed camera. A software computes the zeta potential ( $\zeta$ -p) value from the beam data detected by the camera and processed by a data acquisition system (Figure 1). Zeta potential defines the particle agglomeration, sedimentation, contact and complexation of nanoparticles with other media elements in suspension and this value must be higher than 30 mV for a stable and homogeneous nano-oil (Krishna Sabareesh, Gobinath, Sajith, Das, & Sobhan, 2012; J. H. Lee et al., 2008; Streng, 1995). Average  $\zeta$ -p value of nanolubricant was over 30 mV even 10 days after its preparation. Technical specifications of the DLS device is tabulated in Table 1. Experiments showed that TiO<sub>2</sub> incorporation in engine oil above 0.5 wt.% causes sedimentation on the sample surface and coefficient of friction (CoF) tends to depict a sharp increase. Thus, 0.5 wt.% was considered as the nanoparticle amount in the engine oil during experiments. Subsequent to friction tests, worn sample surfaces were SEM analysed to compare the surface images before and after the fretting trials. Atomic force microscopy (AFM) analyses were also implemented on sample surfaces before and after the abrasion tests to observe wear characteristics. At the beginning of the friction tests, samples were cleaned in diluted HCl bath to get rid of contaminations. Then, the surfaces were washed with pure water and blown by nitrogen gas (drying process). The normal force during abrasion tests was maintained at 40 N due to excessive damage formed on the sample surface. The specifications of the friction test conditions are given in Table 2.

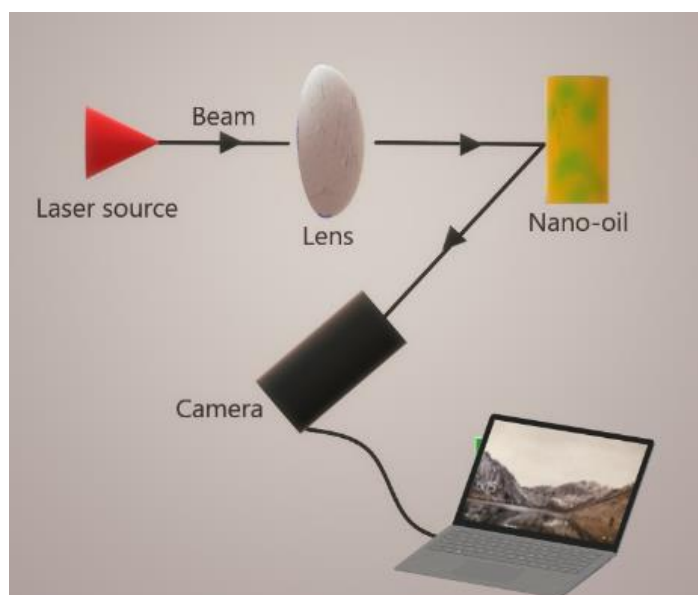


Figure 1. Illustration of DLS technique

Table 1

DLS device technical specifications

Diameter measurement range	3.8–100 $\mu$ m
Mobility range	$\pm$ 20 $\mu$ cm/Vs
Zeta potential range	$>$ $\pm$ 500 mV
Measurement sensitivity	$\pm$ 2 mV
Beam	He-Ne laser
Motion capture	CCD camera
Minimum sample volume	12 $\mu$ L
Maximum conductivity	200 mS/cm
Zeta potential measurement	15 days after its preparation

Table 2

## Friction test specifications

Sample material	Cast iron
Sample size (LxWxH)	20x20x4 mm
Module motion	Reciprocating
Scratcher	Steel ball (Ø5 mm)
Scratcher linear speed	2000 mm/min
Scratcher distance travelled	200 m
TiO <sub>2</sub> mass fraction	0.5 wt.%
Oil bath temperature	25°C
Normal load	40 N
Oil vessel volume	150 mL

The final stage of the study includes the single cylinder 4-stroke diesel engine tests with normal 5W-30 engine oil and TiO<sub>2</sub> incorporated (0.5 wt.%) engine oil (nano-oil). The comparison of these two lubricants in terms of in-cylinder mean effective pressures and smoke emissions was also conducted. The technical specifications of the test engine are shown in Table 3.

Table 3

## Technical data of the single cylinder water cooled diesel test engine

Air induction	Naturally aspirated
Fuel feeding system	Direct injection
Bore	85 mm
Stroke	78 mm
Displacement	481 cc
Compression ratio	18:1
Lubrication	Pump in oil sump
Max. rev.	3200 rpm
Max. power	7.8 kW@2800 rpm
Max. torque	29.5 Nm@1850 rpm
Mass	55 kg

During running of the engine, each instantaneous pressure value was measured via a piezoelectric pressure sensor (Table 4) and transferred to the software by a data acquisition system. The crank angle corresponding to instantaneous volume values was also measured utilizing a crank sensor which is connected to the same data acquisition system. Thus, each instantaneous pressure datum subtending to each instantaneous crank angle was recorded. Then, crank angle values were approximately converted to the corresponding volume data. The area under the closed loop P-V diagram gives the net indicated work which is computed via cyclic integration of the piston work (P.dV). In other words, IMEP can be defined as the net indicated work per swept volume (V<sub>s</sub>) as presented in 2.1:

$$\text{IMEP} = [1/V_s] [\oint P.dV] \quad (2.1)$$

Table 4

## Technical data of the piezoelectric pressure sensor

Measuring range	0-300 bar
Sensitivity	-30 pC/bar
Natural frequency	≥65 kHz
Operating temp. range	-20–1560°C
Capacitance (no cables)	12 pF
Connector	10-32 UNF

The test engine was loaded via electromagnetic forces utilizing an eddy current dynamometer with arm length of 185 mm. Each engine test was carried out at normal engine operating temperature, same ambient

temperature (25°C) and relative humidity (55%) under wide open pumping (max. rpm at 0% load) conditions. The loading process was done gradually until the engine starts to stammer. A digital smokemeter with  $\pm 1\%$  precision was used to measure the smoke opacity. The device was initially calibrated with checks at 0% and 100% smoke opacity. General schematic of the test rig is demonstrated in Figure 2.

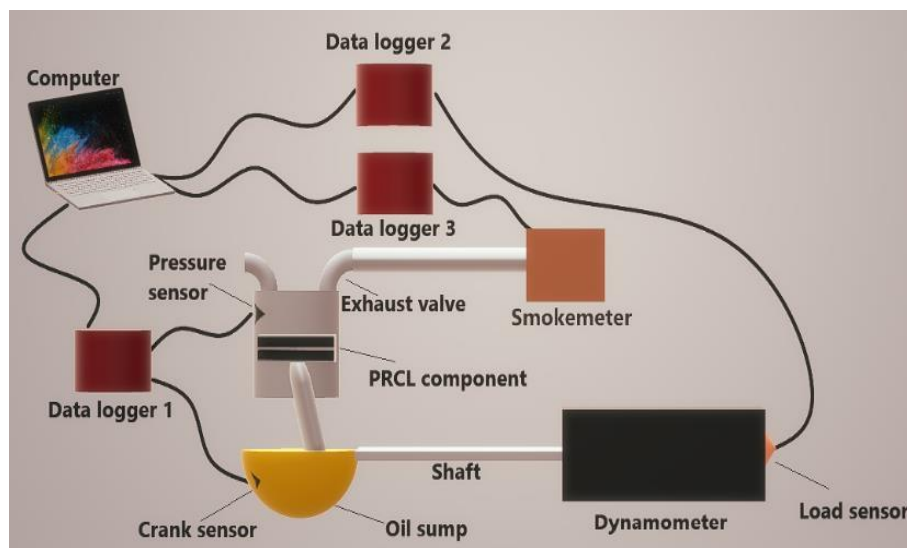


Figure 2. Schematic of the test rig

### 3. Results and Discussion

#### 3.1. Morphology and thermo-gravimetric (TG) analysis

Nanoparticle geometry highly affects the friction and wear characteristics between contact surfaces (Zhang, Hu, Feng, & Wang, 2013). In general, the geometry is spherical throughout the structure (Figure 3) and rolling effect is expected to be dominant in reducing friction between solid pairs at moderate lubricant temperatures.

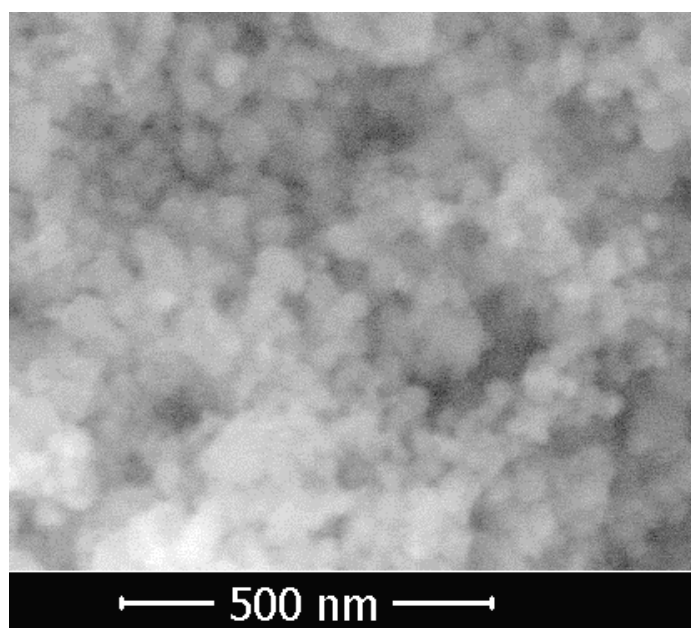


Figure 3. SEM image of  $\text{TiO}_2$  nanoparticles

Thermo-gravimetric methods reveal the changes in the structure of nanoparticles as a result of temperature variations. Chemical reactions, polymerization, and crystallization processes are commonly represented by exothermic peaks, while phase shifts, dehydration, degradation, and reduction reactions are represented by

endothermic peaks. The lack of peaks suggests that the sample's thermal stability is high, implying that no degradation during the work performed at that temperature range (Ali et al., 2016; Peng, Hu, & Wang, 2007; Zin et al., 2014). As can be seen in Figure 4, TiO<sub>2</sub> nanoparticles were able to perform high resistance to harsh thermal conditions even above 600°C (no sharp peaks). Mass increase with the increase in temperature is related to the oxidation of metals on the surface during the heating process in an oxygen-rich environment. Mass loss with increased temperature, on the other hand, may signal a possible breakdown response (S. Li & Bhushan, 2016).

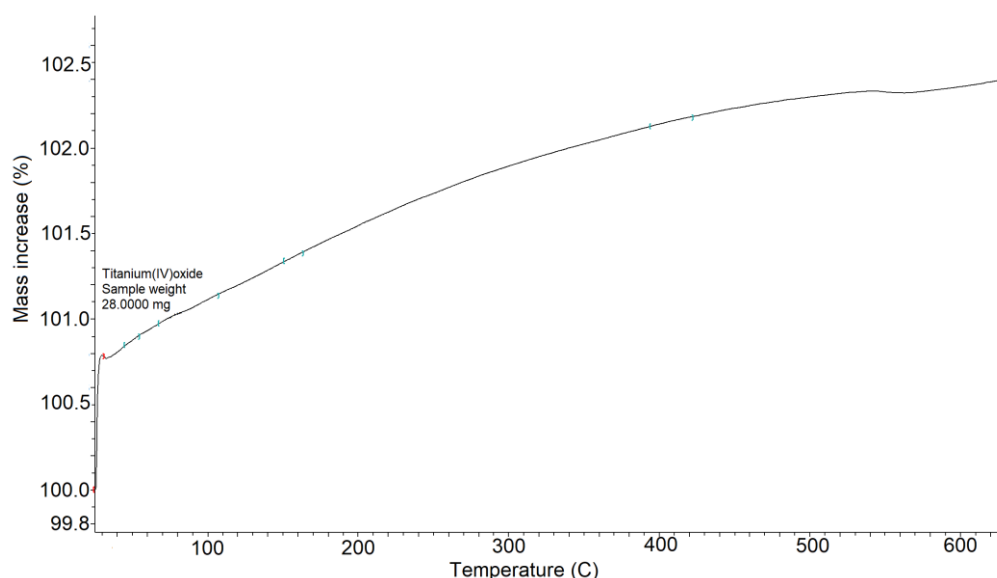


Figure 4. Thermo-gravimetric behavior of the TiO<sub>2</sub> nanoparticles

### 3.2. Friction and wear analysis

Friction between two solid surfaces can be reduced by either lowering the contact surface area (rolling effect) or decreasing the surface roughness (polishing effect). The CoF data procured from the linear friction module are depicted in Figure 5. For both lubricant modes, mixed lubrication (transition from boundary to hydrodynamic) can be observed until approximately sliding distance of 200 m. As of 200 m, hydrodynamic friction occurs due to increase in shear stress in oil film arising from high scratcher velocity at mid-strokes (mid-sliding distance). The average CoF in TiO<sub>2</sub> nano-oil is 10.37% lower than that of neat 5W-30 engine oil. The reduction in CoF is due to: (i) the spherical shape of TiO<sub>2</sub> nanoparticles which reveals the rolling effect and extra separation influence on fretting pairs, (ii) average zeta potential of 85 mV of the nano-oil that confirms the homogeneous dispersion of nanoparticles in the engine oil, ensuring smoother operation, (iii) filling of asperities with nano size TiO<sub>2</sub> particles yielding polishing effect and smoother contact regions, (iv) higher viscosity of nano-oil that provides more stable tribofilm between friction pairs and increase in load bearing capacity.



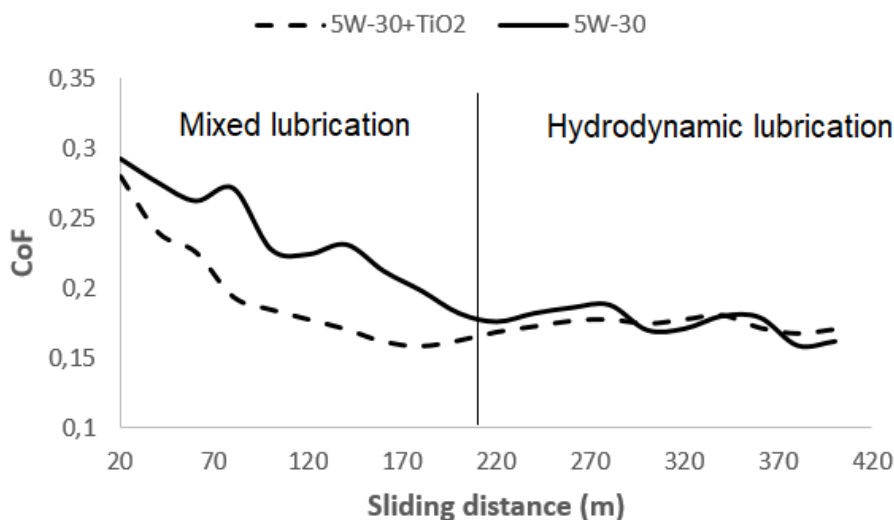


Figure 5. CoF with respect to sliding distance

Wear analysis on friction pairs is based on SEM (Figure 6) and AFM (Figure 7) images of surfaces before and after abrasion tests. The wear rate and surface roughness data (Table 5) were also collected to make a comprehensive wear study. It is clearly seen from both SEM and AFM results that the surface of the specimen submerged in the nano-oil is smoother than the one in the engine oil. The average surface roughness ( $R_a$ ) experiments were conducted in triplicate and average of these values were taken into account. The SEM image of the unworn surface was shown to make a before-after comparison. For nano-oil ambient, average reductions of 33.58% and 15.85% were determined in wear rate and average  $R_a$ , respectively. Higher viscosity of nano-oil yields a slight increase in pressure of oil film and thus, separation of contact surfaces. Lower average CoF values for nano-oil also confirm this phenomenon. Reduced wear tracks on the surface submerged in nano-oil ambient may also be explained based on TG results (no melting at even high temperatures). High thermal endurance of  $TiO_2$  nanoparticles provides maintenance of spherical geometry and rolling effect. Furthermore, polishing effect of nano size particles favors reduced wear tracks.

Table 5  
Wear and average surface roughness test results

Lubricant	Wear rate ( $mm^3/Nm$ )	$R_a$ ( $\mu m$ )			Average $R_a$ ( $\mu m$ )
		Test 1	Test 2	Test 3	
5W-30	$32.28 \times 10^{-9}$	0.92	0.81	0.73	0.82
5W-30+TiO <sub>2</sub>	$21.44 \times 10^{-9}$	0.84	0.72	0.51	0.69
<b>Reduction</b>	<b>33.58%</b>				<b>15.85%</b>

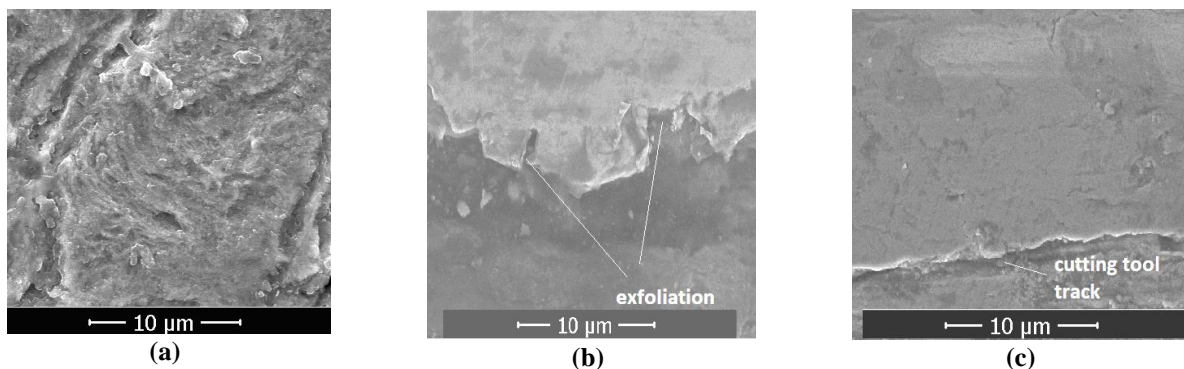


Figure 6. SEM images of (a) unworn raw sample surface, (b) worn sample surface in engine oil, (c) worn sample surface in  $TiO_2$  nano-oil

3D-AFM images of the unworn and worn surfaces also clearly confirm that wear rate (mass loss) is higher in engine oil than that of nano-oil according to the average surface roughness height shown in vertical axis. Smoother surface is clearly observed on the sample underwent friction tests in nano-oil than that of engine oil. The “plains” are dominant compared to “hills” on the surface processed in nano-oil. The small amount of sharp points on the images are due to AFM gain oscillation measurement errors.

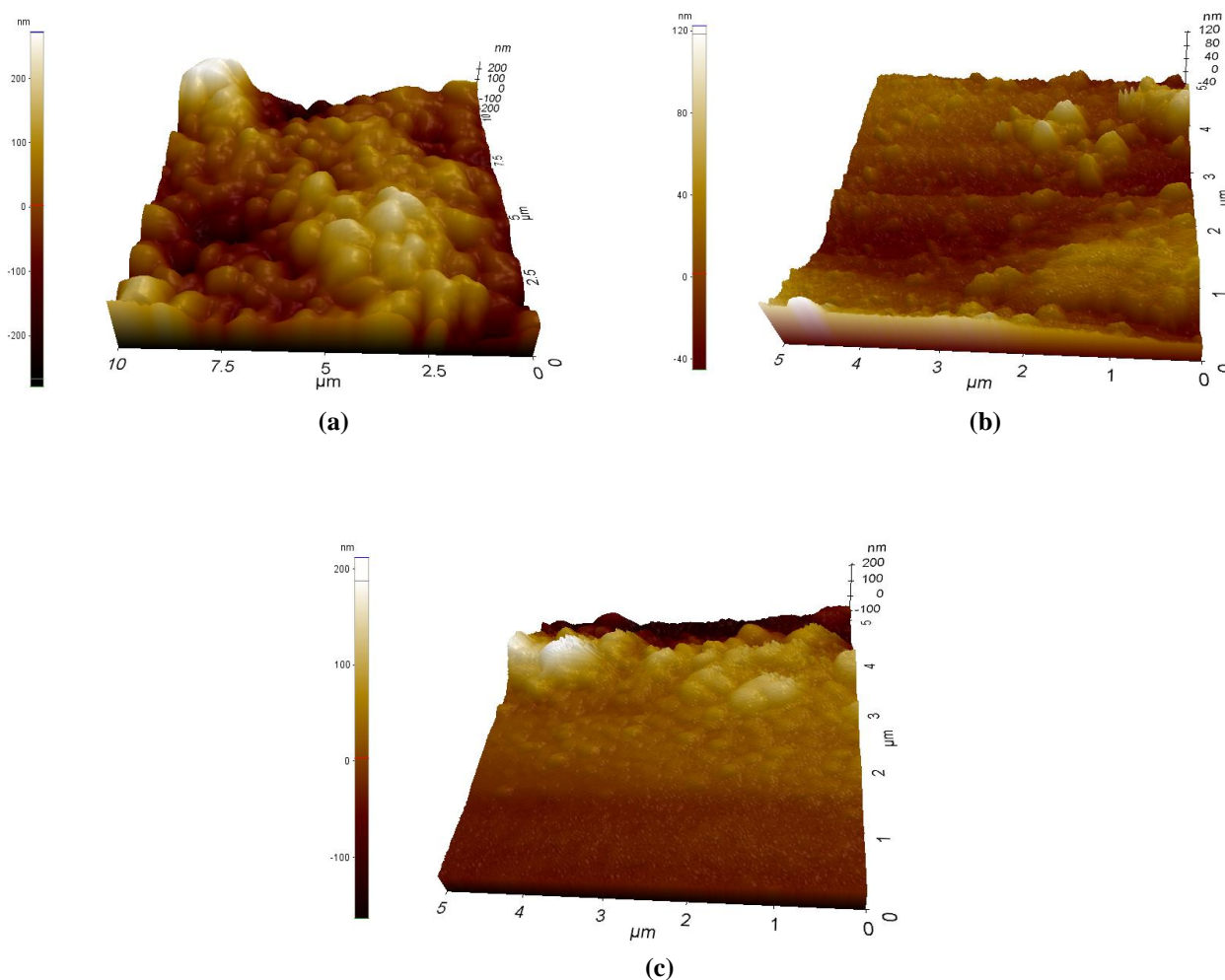


Figure 7. 3D-AFM images of (a) unworn raw sample surface, (b) worn sample surface in engine oil, (c) worn sample surface in TiO<sub>2</sub> nano-oil

### 3.3. Mean effective pressure and smoke emission analyses

In-cylinder IMEP is a good comparison parameter in terms of combustion efficiency and work done by combustion force exerted onto the piston head. This study includes the indirect determination of IMEP using P-V indicator diagram (Figure 8) plotted by means of the data taken from the pressure and crank sensors. Each volume datum subtending to each crank angle was recorded as mentioned in the previous section. The area integration of the closed loop gives the net indicated work delivered by the engine and IMEP is calculated using 2.1 as depicted above.

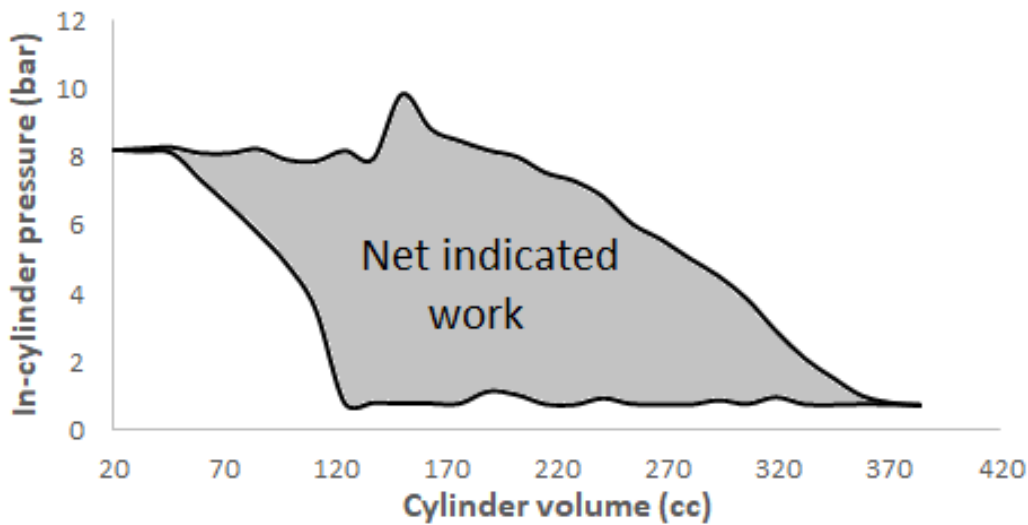


Figure 8. P-V indicator diagram of the engine

BMEP was used as another performance comparison parameter for the test engine running on two lubricant modes. Dynamometer load cell provides the torque values corresponding to each engine speed via data logger and a software. BMEP data were obtained substituting in 1.3. To observe the effects of fretting behavior on mean pressure drops due to frictions, FMEP data were also computed considering the difference between IMEP and BMEP (1.4). Mean effective pressure values were plotted against engine speed as seen in Figure 9. Torque is prone to increase until mid-revs and reaches maximum at about 2000 rpm due to development of mixture (more time for fuel to participate combustion). As approaching mid-revs, developed mixture unites with lower heat loss, thus maximum torque is achieved. Above 2000 rpm, torque tends to decrease as there was very insufficient time for combustion due to short opening time of intake valve. Recalling the direct proportion between torque and BMEP, the same trend is expected for BMEP. FMEP stands for the mean pressure loss and, hence, is inversely proportional to BMEP. Minimum FMEP is expected where the BMEP reaches its maximum and vice versa. Especially at high revs, an escalation in FMEP increase rate was observed which can be ascribed to elevated shear stress in tribofilm between fretting pairs.

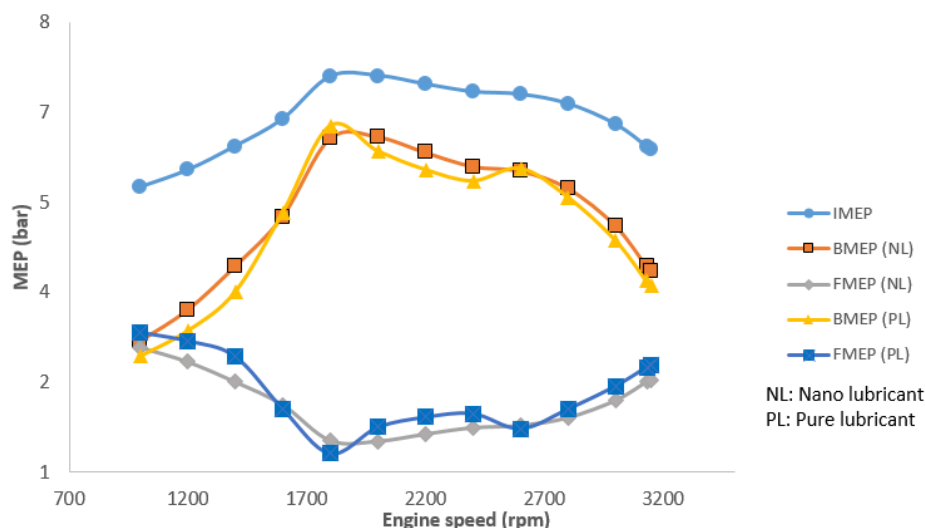


Figure 9. Mean effective pressures vs. engine speed for both lubrication modes

Smoke emission is one of the biggest problem of diesel engines due to its environmental and health hazards. Figure 10 demonstrates the variation of smoke opacity with respect to engine speed. As the load increases (rpm decreases), more fuel is to be injected into the combustion chamber to overcome the inverse forces exerted by the dynamometer. If there is no adequate time for sufficient air to enter the cylinder, some of the fuel will not

find air for oxidation and combustion will remain incomplete causing unburned solid fuel particles in the exhaust system. Reducing fretting forces entails smooth engine operation in which the injectors will spray lesser fuel to overcome the decreased frictional forces and thus, lower smoke emissions. Improved tribological features of the TiO<sub>2</sub> nanolubricant is the main reason in reducing smoke in comparison to that of the neat engine oil.

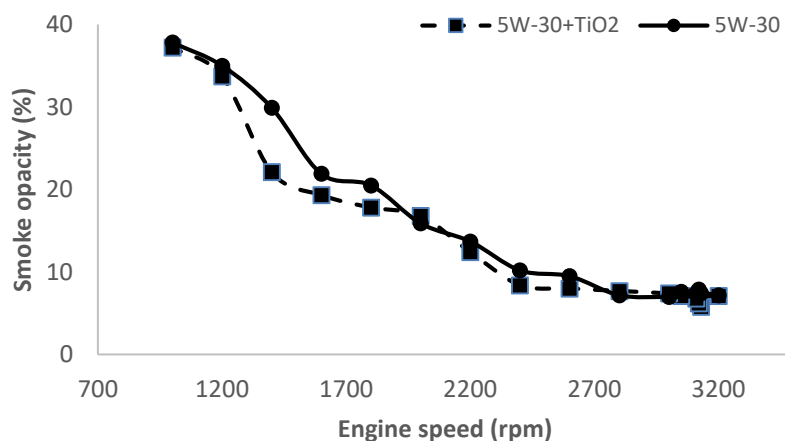


Figure 10. Variation of smoke opacity with respect to engine speed

#### 4. Conclusions

This experimental study reveals the tribological improvement features of TiO<sub>2</sub> nanoparticle incorporation in commercial engine oil in the context of reducing frictional losses between PRCL components of a single cylinder diesel engine via comprehensive analyses. The results prove the effectiveness of TiO<sub>2</sub> nanoparticles in engine oil in terms of reducing frictional losses, enhancing performance and decreasing smoke emissions. The results seem to be promising due to attainment of 10.37% reduction in CoF, 4.95% improvement in BMEP, 9.34% and 9.11% reductions in FMEP and smoke emissions, respectively. Furthermore, TiO<sub>2</sub> nanolubricant provides reductions of 15.85% and 33.58% in surface roughness and wear rate, respectively. High thermal resistance of TiO<sub>2</sub> nanoparticles also facilitates its usage in engine oil, as very severe conditions may exist in the PRCL system of an internal combustion engine especially at the end of compression and at the time of combustion in which pressure and temperature reach very high levels.

#### Acknowledgment

This study was conducted in Cukurova University, Adana Vocational School, Automotive Laboratories and fiscally supported by Cukurova University, Scientific Research Projects, under Grant number FBA-2021-14009.

#### Author Contributions

Ali Can Yılmaz: Participation in the concept, design, analysis, writing, and revision of the manuscript.

#### Conflict of interest

The author declares no conflict of interest.

#### References

Abad, M. D., & Sánchez-López, J. C. (2013). Tribological properties of surface-modified Pd nanoparticles for electrical contacts. *Wear*, 297(1–2), 943–951. doi: <https://doi.org/10.1016/j.wear.2012.11.009>

- Abdullah, A. Z., Abdullah, H., & Bhatia, S. (2008). Improvement of loose contact diesel soot oxidation by synergic effects between metal oxides in  $K_2O-V_2O_5/ZSM-5$  catalysts. *Catalysis Communications*, 9(6), 1196–1200. doi: <https://doi.org/10.1016/j.catcom.2007.11.003>
- Agarwal, A. K., Srivastava, D. K., Dhar, A., Maurya, R. K., Shukla, P. C., & Singh, A. P. (2013). Effect of fuel injection timing and pressure on combustion, emissions and performance characteristics of a single cylinder diesel engine. *Fuel*, 111, 374–383, doi: 10.1016/j.fuel.2013.03.016
- Ali, M. K. A., Xianjun, H., Mai, L., Bicheng, C., Turkson, R. F., & Qingping, C. (2016). Reducing frictional power losses and improving the scuffing resistance in automotive engines using hybrid nanomaterials as nano-lubricant additives. *Wear*, 364–365, 270–281. doi: <https://doi.org/10.1016/j.wear.2016.08.005>
- Bedoya, I. D., Saxena, S., Cadavid, F. J., Dibble, R. W., & Wissink, M. (2011). Experimental study of biogas combustion in an HCCI engine for power generation with high indicated efficiency and ultra-low  $NO_x$  emissions. *Energy Conversion and Management*, 53(1), 154–162. doi: 10.1016/j.enconman.2011.08.016
- Cao, L., Liu, J., Wan, Y., Yang, S., Gao, J., & Pu, J. (2018). Low-friction carbon-based tribofilm from poly-alpha-olefin oil on thermally oxidized  $Ti_6Al_4V$ . *Surface and Coatings Technology*, 337, 471–477. doi: <https://doi.org/10.1016/j.surfcoat.2018.01.057>
- Çelikten, I. (2003). An experimental investigation of the effect of the injection pressure on engine performance and exhaust emission in indirect injection diesel engines. *Applied Thermal Engineering*, 23(16), 2051–2060. doi: [https://doi.org/10.1016/S1359-4311\(03\)00171-6](https://doi.org/10.1016/S1359-4311(03)00171-6)
- Chen, B., Gu, K., Fang, J., Jiang, W., Jiu, W., & Nan, Z. (2015). Tribological characteristics of monodispersed cerium borate nanospheres in biodegradable rapeseed oil lubricant. *Applied Surface Science*, 353, 326–332. doi: <https://doi.org/10.1016/j.apsusc.2015.06.107>
- Chou, R., Battez, A. H., Cabello, J. J., Viesca, J. L., Osorio, A., & Sagastume, A. (2010). Tribological behavior of polyalphaolefin with the addition of nickel nanoparticles. *Tribology International*, 43(12), 2327–2332. doi: <https://doi.org/10.1016/j.triboint.2010.08.006>
- Ćurković, L., Ćurković, H. O., Salopek, S., Renjo, M. M., & Šegota, S. (2013). Enhancement of corrosion protection of AISI 304 stainless steel by nanostructured sol-gel  $TiO_2$  films. *Corrosion Science*, 77, 176–184. doi: <https://doi.org/10.1016/j.corsci.2013.07.045>
- Dhiflaoui, H., Kaouther, K., & Larbi, A. B. C. (2018). Wear behavior and mechanical properties of  $TiO_2$  coating deposited electrophoretically on 316 L stainless steel. *Journal of Tribology*, 140(3). DOI: <https://doi.org/10.1115/1.4038102>
- Dimkovski, Z., Anderberg, C., Ohlsson, R., & Rosén, B. G. (2011). Characterization of worn cylinder liner surfaces by segmentation of honing and wear scratches. *Wear*, 271(3–4), 548–552. doi: <https://doi.org/10.1016/j.wear.2010.04.024>
- Fry, B. M., Chui, M. Y., Moody, G., & Wong, J. S. S. (2020). Interactions between organic friction modifier additives. *Tribology International*, 151. DOI: <https://doi.org/10.1016/j.triboint.2020.106438>
- Ghaednia, H., Babaei, H., Jackson, R. L., Bozack, M. J., & Khodadadi, J. M. (2013). The effect of nanoparticles on thin film elasto-hydrodynamic lubrication. *Applied Physics Letters*, 103(26). doi: <https://doi.org/10.1063/1.4858485>
- Guegan, J., Southby, M., & Spikes, H. (2019). Friction Modifier Additives, Synergies and Antagonisms. *Tribology Letters*, 67(3). doi: <https://doi.org/10.1007/s11249-019-1198-z>
- Guo, Z., Yuan, C., Liu, P., Peng, Z., & Yan, X. (2013). Study on influence of cylinder liner surface texture on lubrication performance for cylinder liner-piston ring components. *Tribology Letters*, 51(1), 9–23. doi: <https://doi.org/10.1007/s11249-013-0141-y>
- Hernandez Battez, A., Fernandez Rico, J. E., Navas Arias, A., Viesca Rodriguez, J. L., Chou Rodriguez, R., & Diaz Fernandez, J. M. (2006). The tribological behaviour of  $ZnO$  nanoparticles as an additive to PAO6. *Wear*, 261(3–4), 256–263. doi: <https://doi.org/10.1016/j.wear.2005.10.001>
- Heywood, J. B. (2018). Internal Combustion Engine Fundamentals, Second Edition. In Internal Combustion Engine Fundamentals Second Edition. Retrieved from <https://www.accessengineeringlibrary.com/content/book/9781260116106%0>
- Hu, H., Peng, H., & Ding, G. (2013). Nucleate pool boiling heat transfer characteristics of refrigerant/nanolubricant mixture with surfactant. *International Journal of Refrigeration*, 36(3), 1045–1055. doi: <https://doi.org/10.1016/j.ijrefrig.2012.12.015>
- Kokjohn, S. L., Hanson, R. M., Splitter, D. A., & Reitz, R. D. (2011). Fuel reactivity controlled compression

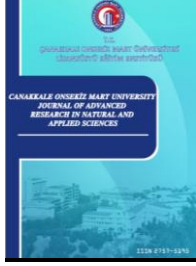
- ignition (RCCI): a pathway to controlled high-efficiency clean combustion. *International Journal of Engine Research*, 12(3), 209–226. doi: 10.1177/1468087411401548
- Kovalchenko, A., Ajayi, O., Erdemir, A., Fenske, G., & Etsion, I. (2005). The effect of laser surface texturing on transitions in lubrication regimes during unidirectional sliding contact. *Tribology International*, 38(3), 219–225. doi: <https://doi.org/10.1016/j.triboint.2004.08.004>
- Krishna Sabareesh, R., Gobinath, N., Sajith, V., Das, S., & Sobhan, C. B. (2012). Application of TiO<sub>2</sub> nanoparticles as a lubricant-additive for vapor compression refrigeration systems - An experimental investigation. *International Journal of Refrigeration*, 35(7), 1989–1996. doi: <https://doi.org/10.1016/j.ijrefrig.2012.07.002>
- Kumar, V., Sinha, S. K., & Agarwal, A. K. (2019). Wear evaluation of engine piston rings coated with dual layer hard and soft coatings. *Journal of Tribology*, 141(3). doi: <https://doi.org/10.1115/1.4041762>
- Langlet, M., Burgos, M., Coutier, C., Jimenez, C., Morant, C., & Manso, M. (2001). Low temperature preparation of high refractive index and mechanically resistant sol-gel TiO<sub>2</sub> films for multilayer antireflective coating applications. *Journal of Sol-Gel Science and Technology*, 22(1–2), 139–150. doi: <https://doi.org/10.1023/A:1011232807842>
- Lee, J. H., Hwang, K. S., Jang, S. P., Lee, B. H., Kim, J. H., Choi, S. U. S., & Choi, C. J. (2008). Effective viscosities and thermal conductivities of aqueous nanofluids containing low volume concentrations of Al<sub>2</sub>O<sub>3</sub> nanoparticles. *International Journal of Heat and Mass Transfer*, 51(11–12), 2651–2656. doi: <https://doi.org/10.1016/j.ijheatmasstransfer.2007.10.026>
- Lee, K., Hwang, Y., Cheong, S., Choi, Y., Kwon, L., Lee, J., & Kim, S. H. (2009). Understanding the role of nanoparticles in nano-oil lubrication. *Tribology Letters*, 35(2), 127–131. doi: <https://doi.org/10.1007/s11249-009-9441-7>
- Li, K. Y., Zhou, Z. F., Bello, I., Lee, C. S., & Lee, S. T. (2005). Study of tribological performance of ECR-CVD diamond-like carbon coatings on steel substrates Part 1. The effect of processing parameters and operating conditions. *Wear*, 258(10), 1577–1588. doi: <https://doi.org/10.1016/j.wear.2004.10.006>
- Li, S., & Bhushan, B. (2016). Lubrication performance and mechanisms of Mg/Al-, Zn/Al-, and Zn/Mg/Al-layered double hydroxide nanoparticles as lubricant additives. *Applied Surface Science*, 378, 308–319. doi: <https://doi.org/10.1016/j.apsusc.2016.03.220>
- Lin, J., Wei, R., Bitsis, D. C., & Lee, P. M. (2016). Development and evaluation of low friction TiSiCN nanocomposite coatings for piston ring applications. *Surface and Coatings Technology*, 298, 121–131. doi: <https://doi.org/10.1016/j.surfcoat.2016.04.061>
- Liu, G., Li, X., Qin, B., Xing, D., Guo, Y., & Fan, R. (2004). Investigation of the mending effect and mechanism of copper nano-particles on a tribologically stressed surface. *Tribology Letters*, 17(4), 961–966. doi: <https://doi.org/10.1007/s11249-004-8109-6>
- Liu, H., Wang, Z., Long, Y., & Wang, J. (2015). Dual-Fuel Spark Ignition (DFSI) combustion fuelled with different alcohols and gasoline for fuel efficiency. *Fuel*, 157, 255–260. doi: 10.1016/j.fuel.2015.04.042
- Ma, J., Mo, Y., & Bai, M. (2009). Effect of Ag nanoparticles additive on the tribological behavior of multialkylated cyclopentanes (MACs). *Wear*, 266(7–8), 627–631. doi: <https://doi.org/10.1016/j.wear.2008.08.006>
- Ma, S., Zheng, S., Cao, D., & Guo, H. (2010). Anti-wear and friction performance of ZrO<sub>2</sub> nanoparticles as lubricant additive. *Particuology*, 8(5), 468–472. doi: <https://doi.org/10.1016/j.partic.2009.06.007>
- Mishra, A., & Prasad, R. (2014). Preparation and application of perovskite catalysts for diesel soot emissions control: An overview. *Catalysis Reviews - Science and Engineering*, 56, 57–81. doi: <https://doi.org/10.1080/01614940.2014.866438>
- Murdock, R. C., Braydich-Stolle, L., Schrand, A. M., Schlager, J. J., & Hussain, S. M. (2008). Characterization of nanomaterial dispersion in solution prior to in vitro exposure using dynamic light scattering technique. *Toxicological Sciences*, 101(2), 239–253. doi: <https://doi.org/10.1093/toxsci/kfm240>
- Nabhan, A., Ghazaly, N. M., Mousa, H. M., & Rashed, A. (2020). Influence of TiO<sub>2</sub> and SiO<sub>2</sub> nanoparticles additives on the engine oil tribological properties: Experimental study at different operating conditions. *International Journal of Advanced Science and Technology*, 29(1), 845–855.
- Nagashima, K., Kawa, T., & Tsuchiya, K. (2003). Indicated mean effective pressure measuring method using optical fiber pressure sensor. *SAE Technical Papers*. doi: <https://doi.org/10.4271/2003-01-2013>
- Nguyen, L. D. K., Sung, N. W., Lee, S. S., & Kim, H. S. (2011). Effects of split injection, oxygen enriched air

- and heavy EGR on soot emissions in a diesel engine. *International Journal of Automotive Technology*, 12(3), 339–350. DOI: <https://doi.org/10.1007/s12239-011-0040-x>
- Padgurskas, J., Rukuiza, R., Prosyčevs, I., & Kreivaitis, R. (2013). Tribological properties of lubricant additives of Fe, Cu and Co nanoparticles. *Tribology International*, 60, 224–232. doi: <https://doi.org/10.1016/j.triboint.2012.10.024>
- Pahmi, A., Hisyam Basri, M., Mustafa, M. E., Yaakob, Y., Sharudin, H., Ismail, N. I., & Talib, R. J. (2019). Intake pressure and brake mean effective pressure analysis on various intake manifold design. *Journal of Physics: Conference Series*, 1349(1). doi: <https://doi.org/10.1088/1742-6596/1349/1/012080>
- Pan, Q., & Zhang, X. (2010). Synthesis and tribological behavior of oil-soluble Cu nanoparticles as additive in SF15W/40 lubricating oil. *Xiyou Jinshu Cailiao Yu Gongcheng/Rare Metal Materials and Engineering*, 39(10), 1711–1714. doi: [https://doi.org/10.1016/s1875-5372\(10\)60129-4](https://doi.org/10.1016/s1875-5372(10)60129-4)
- Pecora, R. (2000). Dynamic light scattering measurement of nanometer particles in liquids. *Journal of Nanoparticle Research*, 2(2), 123–131. DOI: <https://doi.org/10.1023/A:1010067107182>
- Peng, Y., Hu, Y., & Wang, H. (2007). Tribological behaviors of surfactant-functionalized carbon nanotubes as lubricant additive in water. *Tribology Letters*, 25(3), 247–253. doi: <https://doi.org/10.1007/s11249-006-9176-7>
- Podgornik, B., Vilhena, L. M., Sedlaček, M., Rek, Z., & Žun, I. (2012). Effectiveness and design of surface texturing for different lubrication regimes. *Meccanica*, 47(7), 1613–1622. doi: <https://doi.org/10.1007/s11012-012-9540-7>
- Ratoi, M., Niste, V. B., Alghawel, H., Suen, Y. F., & Nelson, K. (2014). The impact of organic friction modifiers on engine oil tribofilms. *RSC Advances*, 4(9), 4278–4285. doi: <https://doi.org/10.1039/c3ra46403b>
- Ronen, A., Etsion, I., & Kligerman, Y. (2001). Friction-reducing surface-texturing in reciprocating automotive components. *Tribology Transactions*, 44(3), 359–366. doi: <https://doi.org/10.1080/10402000108982468>
- Shi, L., Sun, Y., & Deng, K. (2016). Fuel adjustment to achieve a smooth net indicated mean effective pressure during mode switching from homogeneous charge compression ignition to conventional diesel compression ignition in a transient hydrocarbon emissions study. *Proceedings of the Institution of Mechanical Engineers, Part D: Journal of Automobile Engineering*, 230(13), 1758–1766. doi: [10.1177/0954407015623408](https://doi.org/10.1177/0954407015623408)
- Song, X., Zheng, S., Zhang, J., Li, W., Chen, Q., & Cao, B. (2012). Synthesis of monodispersed ZnAl<sub>2</sub>O<sub>4</sub> nanoparticles and their tribology properties as lubricant additives. *Materials Research Bulletin*, 47(12), 4305–4310. doi: <https://doi.org/10.1016/j.materresbull.2012.09.013>
- Streng, K. (1995). Introduction to Modern Colloid Science. *Zeitschrift Für Physikalische Chemie*, 189(2), 277–278. doi: [https://doi.org/10.1524/zpch.1995.189.part\\_2.277a](https://doi.org/10.1524/zpch.1995.189.part_2.277a)
- Su, T., Ji, C., Wang, S., Shi, L., Yang, J., & Cong, X. (2017). Effect of spark timing on performance of a hydrogen-gasoline rotary engine. *Energy Conversion and Management*, 148, 120–127. doi: [10.1016/j.enconman.2017.05.064](https://doi.org/10.1016/j.enconman.2017.05.064)
- Tao, X., Jiazheng, Z., & Kang, X. (1996). The ball-bearing effect of diamond nanoparticles as an oil additive. *Journal of Physics D: Applied Physics*, 29(11), 2932–2937. doi: <https://doi.org/10.1088/0022-3727/29/11/029>
- Taylor, C. M. (1998). Automobile engine tribology-design considerations for efficiency and durability. *Wear*, 221(1), 1–8. doi: [https://doi.org/10.1016/S0043-1648\(98\)00253-1](https://doi.org/10.1016/S0043-1648(98)00253-1)
- Tung, S. C., & Gao, H. (2003). Tribological characteristics and surface interaction between piston ring coatings and a blend of energy-conserving oils and ethanol fuels. *Wear*, 255(7–12), 1276–1285. doi: [https://doi.org/10.1016/S0043-1648\(03\)00240-0](https://doi.org/10.1016/S0043-1648(03)00240-0)
- Wan, Y., Chao, W., Liu, Y., & Zhang, J. (2011). Tribological performance of Fluoroalkylsilane modification of sol-gel TiO<sub>2</sub> coating. *Journal of Sol-Gel Science and Technology*, 57(2), 193–197. doi: <https://doi.org/10.1007/s10971-010-2341-3>
- Wang, X. L., Yin, Y. L., Zhang, G. N., Wang, W. Y., & Zhao, K. K. (2013). Study on antiwear and repairing performances about mass of nano-copper lubricating additives to 45 steel. *Physics Procedia*, 50, 466–472. doi: <https://doi.org/10.1016/j.phpro.2013.11.073>
- Wróblewski, P., & Koszalka, G. (2021). An Experimental Study on Frictional Losses of Coated Piston Rings



- with Symmetric and Asymmetric Geometry. *SAE International Journal of Engines*, 14(6). doi: <https://doi.org/10.4271/03-14-06-0051>
- Yang, G., Zhang, Z., Zhang, S., Yu, L., & Zhang, P. (2013). Synthesis and characterization of highly stable dispersions of copper nanoparticles by a novel one-pot method. *Materials Research Bulletin*, 48(4), 1716–1719. doi: <https://doi.org/10.1016/j.materresbull.2013.01.025>
- Yilmaz, A. C. (2020a). Performance evaluation of a refrigeration system using nanolubricant. *Applied Nanoscience (Switzerland)*, 10(5), 1667–1678. doi: <https://doi.org/10.1007/s13204-020-01258-5>
- Yilmaz, A. C. (2020b). Tribological Enhancement Features of Various Nanoparticles as Engine Lubricant Additives: An Experimental Study. *Arabian Journal for Science and Engineering*, 45(2), 1125–1134. doi: <https://doi.org/10.1007/s13369-019-04243-5>
- Yin, B., Li, X., Fu, Y., & Yun, W. (2012). Effect of laser textured dimples on the lubrication performance of cylinder liner in diesel engine. *Lubrication Science*, 24(7), 293–312. doi: <https://doi.org/10.1002/lis.1185>
- Yu, H., Xu, Y., Shi, P., Xu, B., Wang, X., & Liu, Q. (2008). Tribological properties and lubricating mechanisms of Cu nanoparticles in lubricant. *Transactions of Nonferrous Metals Society of China (English Edition)*, 18(3), 636–641. doi: [https://doi.org/10.1016/S1003-6326\(08\)60111-9](https://doi.org/10.1016/S1003-6326(08)60111-9)
- Zhang, S., Hu, L., Feng, D., & Wang, H. (2013). Anti-wear and friction-reduction mechanism of Sn and Fe nanoparticles as additives of multialkylated cyclopentanes under vacuum condition. *Vacuum*, 87, 75–80. doi: <https://doi.org/10.1016/j.vacuum.2012.07.009>
- Zin, V., Agresti, F., Barison, S., Colla, L., Mercadelli, E., Fabrizio, M., & Pagura, C. (2014). Tribological properties of engine oil with carbon nano-horns as nano-additives. *Tribology Letters*, 55(1), 45–53. doi: <https://doi.org/10.1007/s11249-014-0330-3>





## Kocaavşar Deresi (Balıkesir) Fitoplankton Ekolojisi

Kemal Çelik<sup>1\*</sup>

<sup>1</sup>Biyoloji Bölüm, Fen-Edebiyat Fakültesi, Balıkesir Üniversitesi, Balıkesir, Türkiye

### Makale Tarihçesi

Gönderim: 12.03.2022

Kabul: 01.07.2022

Yayın: 15.12.2022

### Araştırma Makalesi

**Öz** - Kocaavşar Deresinden Mayıs 2020 ve Ekim 2020 tarihlerinde iki istasyondan su örnekleri alınıp suyun bazı fiziksel ve kimyasal parametreleri ile fitoplanktonik alg florası incelenmiştir. Yapılan analizlerde, su sıcaklığı (T) 10-27°C, pH 8.77-14.70, elektriksel iletkenlik (EK) 322-712 µScm<sup>-1</sup>, nitrat azotu (NO<sub>3</sub>-N) 1.8-2.5 mg l<sup>-1</sup>, toplam azot (TN) 2.8-4 mg l<sup>-1</sup>, fosfat (PO<sub>4</sub>-P) 0.2-0.34 mg l<sup>-1</sup> ve toplam fosfor (TP) 0.26-0.4 mg l<sup>-1</sup> aralıklarında ölçülmüştür. Fitoplankton örneklerinin analizi sonucu, Bacillariophytadan 9, Chlorophytadan 17, Cyanobacteriadan 5 ve Euglenozoadan 1 olmak üzere toplam 32 tür tespit edilmiştir. Bacillariophytadan *Fragilaria capucina*, *Cyclotella glabriuscula*, *Cymbella affinis*, *Diatoma vulgare*, *Pinnularia major*, *Ulnaria ulna* var. *Oxyrhynchus*, *Navicula minuta*, *Nitzschia amphibia*, Chlorophytadan *Pandorina morum* ve Euglenozoadan *Phacus pleuronectes* baskın türler olarak belirlenmiştir. Korelasyon analizleri, Bacillariophyta grubundan baskınlık gösteren *F. capucina* 'nın elektriksel iletkenlik (EK) ve toplam azot (TN) ile, *P. major* pH ile, *N. amphibia* TP ile, *C. affinis* NO<sub>3</sub>-N ve TN ile, *D. vulgare* ve *U. ulna* fosfat (PO<sub>4</sub>-P) ve TP ile yüksek korelasyon göstermişlerdir. Chlorophyta grubunda baskın olan *P. morum* pH ve EK ile, Euglenozoa grubundan *P. pleuronectes* sadece EK ile yüksek korelasyon göstermiştir. Su Kirliliği Kontrolü Yönetmeliği, kıta içi su kütleleri kalite kriterleri ışığında değerlendirildiğinde toplam fosfora göre Kocaavşar Deresinin III. sınıf, nitrat azotuna göre ise I. sınıf su kalitesinde olduğunu göstermiştir. Baskın fitoplankton türlerine göre ise ötrofik karakterli bir su kütlesidir.

**Anahtar Kelimeler** – Ekoloji, fitoplankton, Kocaavşar Deresi, ötrofikasyon, su kalitesi

## Phytoplankton Ecology of Kocaavşar Stream (Balıkesir)

<sup>1</sup>Department of Biology, Faculty of Science and Arts, Balıkesir University, Balıkesir, Turkey

### Article History

Received: 12.03.2022

Accepted: 01.07.2022

Published: 15.12.2022

### Research Article

**Abstract**- Some physical and chemical parameters and planktonic algal flora of the water were examined by taking water samples from two stations from Kocaavşar Stream in May 2020 and October 2020. In the analysis, water temperature (T) ranged from 10 to 27°C, pH from 8.77 to 14.70, electrical conductivity (EC) from 322 to 712 µScm<sup>-1</sup>, nitrate nitrogen (NO<sub>3</sub>-N) from 1.8 to 2.5 mg l<sup>-1</sup>, total nitrogen (TN) from 2.8 to 4 mg l<sup>-1</sup>, phosphate (PO<sub>4</sub>-P) from 0.2 to 0.34 mg l<sup>-1</sup> and total phosphorus (TP) from 0.26 to 0.4 mg l<sup>-1</sup>. Analysis of phytoplankton samples showed that a total of 32 species were identified, 9 from Bacillariophyta, 17 from Chlorophyta, 5 from Cyanobacteria and 1 from Euglenozoa. *Fragilaria capucina*, *Cyclotella glabriuscula*, *Cymbella affinis*, *Diatoma vulgare*, *Pinnularia major*, *Ulnaria ulna* var. *Oxyrhynchus*, *Navicula minuta*, *Nitzschia amphibia* from Bacillariophyta, *Pandorina morum* from Chlorophyta and *Phacus pleuronectes* from Euglenozoa were determined as dominant species. Correlation analysis showed that *F. capucina* was correlated with electrical conductivity (EC) and total nitrogen (TN), *P. major* with pH, *N. amphibia* with TP, *C. affinis* with NO<sub>3</sub>-N and TN, *D. vulgare* and *U. ulna* with phosphate (PO<sub>4</sub>-P) and TP, *P. morum* with pH and EC, and *P. pleuronectes* with EC. According to the Water Pollution Control Regulation, inland water resources quality criteria, based on nitrate- nitrogen values, Kocaavşar Stream is classified as first class, but based on total phosphorus values it is classified as 3<sup>rd</sup> class water quality. According to the dominant phytoplankton species, it is a eutrophic water body.

**Keywords** –Ecology, eutrophication, Kocaavşar Stream, phytoplankton, water quality

<sup>1</sup> kcelik@balikesir.edu.tr

\*Sorumlu Yazar

## 1. Giriş

Akuatik sistemlerde besin zincirinin ilk halkasını oluşturan algler, söz konusu sistemlerde ekolojik durumun belirlenmesi amacıyla incelenen önemli canlı topluluklarından biridir. Çünkü algler yayılış gösterdikleri ortamın ekolojik durumunu gösteren göstergeler türler içermektedir (Wang vd., 2021).

Ülkemizde akarsulardaki pelajik alg komunitelerinin tür içeriği ve zamansal dinamikleri üzerine araştırmalara Manavgat Nehri nehirağzı bölgesi fitoplanktonu (Erdoğan vd., 2012), Köprüçay Nehri Nehirağzı Bölgesi Fitoplanktonu (Erdoğan vd., 2016), Karasu (Fırat) Nehri fitoplankton ve epipelik alg florası (Altuner ve Gürbüz, 1990) ve Çoruh nehri diyatmaları (Atıcı ve Obalı, 1999) örnek verilebilir.

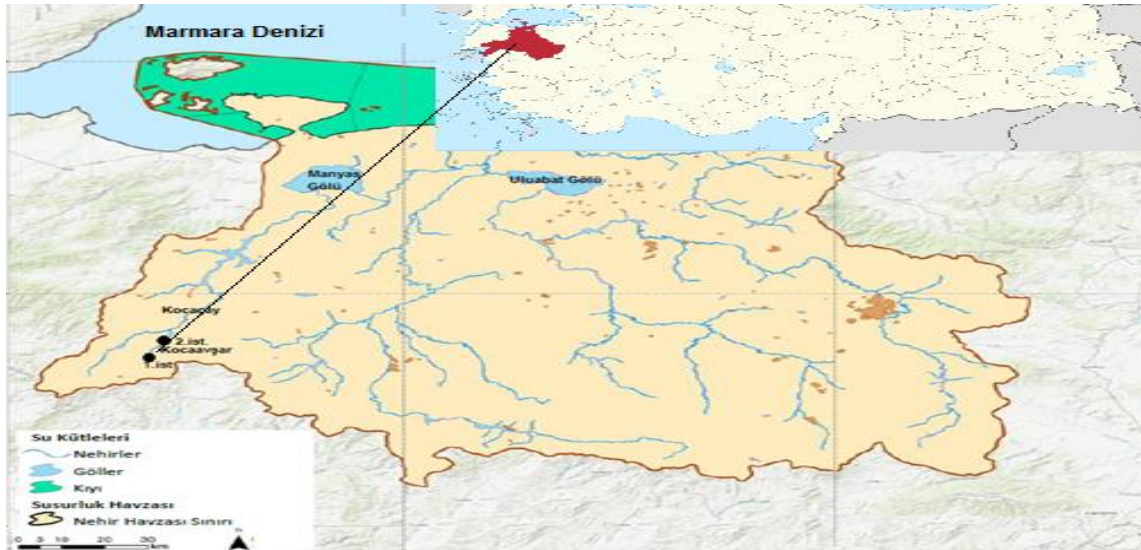
Akarsular çeşitli tür ve sayıda alg türleri barındırırlar. Ülkemizde son zamanlarda alglerin göstergeler olarak kullanıldığı araştırmalar artmaktadır (Atıcı ve Ahıska, 2005; Şen ve Varol, 2014; Tezel Ersanlı ve Öztürk, 2017; Morkoyunlu Yüce, vd., 2018).

Kocaavşar Deresinin fitoplanktonik organizmaları üzerinde şimdiye kadar yapılmış herhangi bir çalışma bulunmamaktadır. Dolayısıyla, bu çalışma Kocaavşar Deresinin fitoplanktonu üzerinde yapılan ilk kapsamlı çalışma niteliğindedir.

Bu çalışmanın amacı, Susurluk havzası içerisinde yer alan Kocaavşar Deresi'nde planktonik alglerin mevsimsel değişimini ve buna bağlı olarak derenin ekolojik durumunun tespit edilip Türkiye akarsu alglerinin envanter oluşturulmasına katkı sağlamaktır.

## 2. Materyal ve Yöntem

Balıkesir merkez Karesi ilçesinde yer alan Kocaavşar Deresi, Madra Dağları'nın kuzeye meyilli yüzü ile Musluk, Uzuncabayır ve Sülyarya Dağlarının sularının toplanmasından oluşup, güneybatıdan Kuzeydoğu'ya doğru akarak Kocaçayla birleşip Manyas Gölü'ne dökülür (**Şekil 1**). Örnekleme için iki istasyon seçilmiştir. 1. İstasyon, Kocaavşar mesire alanının üst tarafından, 2. İstasyon, Kocaavşar mesire alanının alt tarafından seçilmiştir.



Şekil 1. Kocaavşar Deresi ve örnekleme istasyonları

Fitoplankton örnekleri 2020 yılı Mayıs (ilkbahar) ve Ekim (sonbahar) aylarında iki istasyondan alınıp analiz edilip bazı fizikokimyasal değişkenlerle olan bağıntıları tespit edilmiştir.

Fiziksel ve kimyasal parametrelerden su sıcaklığı (S), pH ve elektriksel kondüktivite (EK) örnek alma anında, arazi tipi bir YSI marka 6600 model cihazla ölçülmüştür. Nitrat azotu (NO<sub>3</sub>-N), toplam azot (TN), fosfat (PO<sub>4</sub>-P) ve toplam fosfor (TP) analizleri ise laboratuvarında standart metotlara göre (Baird vd., 2017) spektrofotometrik olarak ölçülmüştür.

Örnekler yüzeyin altından alınıp 0.5 litrelik plastik şişelerle direkt olarak alınıp Lugol solüsyonu ile tespit edilmiştir. Laboratuvarında, 50 ml'lik cam silindirlere konularak 24 saat bekletilmiştir. Daha sonra üstte biriken 45 ml'lik su pipet ile boşaltıldıktan sonra kalan 5 ml incelenme için bir flakona aktarılmıştır. Tür analizleri 0.1

ml'lik alt örnekleme ile bir Palmer-Maloney lamında bir Olympus BX51 mikroskobu (60'luk büyütme) kullanılarak yapılmıştır.

Fitoplankton türlerinin teşhisleri için (Huber-Pestalozzi, 1982; John vd., 2003; Round vd., 1990; Sims, 1996) tayin anahtarlarından yararlanılmıştır. Tespit edilen dominant türlerin bollukları ve fizikokimyasal değişkenler arasındaki Pearson korelasyon (ilişkiler) SAS paket programı kullanılarak tespit edilmiştir (SAS, 2001).

### 3. Bulgular

Kocaavşar Deresinde ölçülen fiziksel ve kimyasal değişkenlerin en yüksek, en düşük, ortalama ve standart sapma değerleri **Tablo 1** de verilmiştir. Tespit edilen değerler Su Kirliliği Yönetmeliğine göre değerlendirildiğinde toplam fosfora göre Kocaavşar Deresinin III. sınıf, nitrat azotuna göre ise I. sınıf su kalitesinde olduğunu göstermiştir.

Tablo 1

Ölçülen fiziksel ve kimyasal parametrelerin en düşük, en yüksek, ortalama ve standart sapma değerleri

	En Düşük	En Yüksek	Standart Sapma	Ortalama	Kıta içi Su Kaynakları Kalite Kriterleri			
					I.Sınıf	II.Sınıf	III.Sınıf	IV.Sınıf
<b>Su Sıcaklığı ( °C)</b>	10.00	27.00	7.36	18.25	25	25	30	>30
<b>pH</b>	8.77	14.70	2.20	11.30	6.5-8.5	6.5-8.5	6.0-9.0	6.0-9.0 dışında
<b>Elektriksel Konduktivite (<math>\mu\text{Scm}^{-1}</math>)</b>	322.00	712.00	132.86	414.25	-	-	-	-
<b>Fosfat (<math>\text{mg l}^{-1}</math>)</b>	0.20	0.34	0.05	0.27	-	-	-	-
<b>Toplam Fosfor (<math>\text{mg l}^{-1}</math>)</b>	0.26	0.40	0.05	0.32	0.02	0.16	0.65	>0.65
<b>Nitrat Azotu (<math>\text{mg l}^{-1}</math>)</b>	1.80	2.50	0.23	2.12	5	10	20	>20
<b>Toplam Azot (<math>\text{mg l}^{-1}</math>)</b>	2.80	4.00	0.38	3.21	-	-	-	-

Kocaavşar Deresinde yapılan bu araştırmada, Bacillariophytadan 9, Chlorophytadan 17, Cyanobacteriadan 5 ve Euglenozoadan 1 olmak üzere 32 fitoplankton türü tespit edilmiştir (Tablo 2). Tespit edilen fitoplankton türlerinin %28'sini Bacillariophyta, %53'ünü Chlorophyta, %16'sını Cyanobacteria ve %3'ünü Euglenozoa grupları oluşturmuştur.

Tablo 2  
Kocaavşar Deresinde tespit edilen fitoplankton türleri

Grup	Mayıs 2020		Ekim 2020	
	İst.1	İst.2	İst.1	İst.2
Bacillariophyta	+	+	+	+
<i>Cyclotella glabriuscula</i> (Grunow) Håkansson	+	-	-	+
<i>Cyclotella stylorum</i> Brightwell	+	+	-	+
<i>Cymbella affinis</i> Kützing	+	+	-	+
<i>Diatoma vulgare</i> Bory	+	+	+	+
<i>Fragilaria capucina</i> Desmazières	+	+	+	+
<i>Fragilaria pinnata</i> Ehrenberg	+	+	+	+
<i>Navicula minuta</i> Skvortsov	-	+	+	-
<i>Nitzschia amphibia</i> Grunow	+	+	+	+
<i>Pinnularia major</i> (Kützing) Rabenhorst	-	+	+	+
<i>Ulnaria ulna</i> var. <i>oxyrhynchus</i> (Kützing) Aboal	+	+	-	+
Chlorophyta	+	+	-	+
<i>Ankistrodesmus falcatus</i> (Corda) Ralfs	+	-	+	-
<i>Closterium acutum</i> Brébisson	-	+	+	+
<i>Crucigenia quadrata</i> Morren	+	+	-	+
<i>Golenkinia radiata</i> Chodat	+	+	-	+
<i>Lagerheimia subsalsa</i> Lemmermann 1	+	+	+	+
<i>Lagerheimia wratislawiensis</i> Schröder	+	+	+	+
<i>Monoraphidium contortum</i> (Thuret) Komárková-Legnerová	+	+	+	+
<i>Pandorina morum</i> (O.F.Müller) Bory	-	+	-	-
<i>Pediastrum tetras</i> (Ehrenberg) Ralfs	+	+	+	+
<i>Scenedesmus arcuatus</i> (Lemmermann) Lemmermann	+	+	+	+
<i>Scenedesmus communis</i> E.Hegewald	+	+	+	+
<i>Scenedesmus longispina</i> Chodat	-	+	-	-
<i>Staurastrum paradoxum</i> Meyen ex Ralfs	+	-	+	+

<i>Tetraëdron caudatum</i> (Corda) Hansgirg	-	+	+	+
<i>Tetraëdron minimum</i> (A.Braun) Hansgirg	-	+	+	+
<i>Tetrabaena socialis</i> (Dujardin) H.Nozaki & M.Itoh	+	-	+	+
<i>Tetrastrum staurogeniiforme</i> var. <i>longispinum</i> G.M.Smith	+	+	+	+
Cyanobacteria				
<i>Anabaena spiroides</i> Klebahn	-	+	-	+
<i>phanocapsa elachista</i> West & G.S.West	-	-	+	-
<i>Gomphosphaeria aponina</i> Kützing	-	+	+	+
<i>Merismopedia glauca</i> (Ehrenberg) Kützing	+	-	-	+
<i>Pseudanabaena catenata</i> Lauterborn	+	+	+	+
Euglenozoa				
<i>Phacus pleuronectes</i> (O.F.Müller) Nitzsch ex Dujardin	-	-	-	+

Korelasyon analizleri sonuçlarına göre, Kocaavşar Deresinde Bacillariophyta grubundan baskınlık gösteren *F.capucina* elektriksel kondüktivite (EK) ve toplam azot (TN) ile, *P. major* pH ile, *N. amphibia* TP ile, *C. affinis* NO<sub>3</sub>-N ve TN ile, *D. vulgaris* ve *U. ulna* fosfat fosforu (PO<sub>4</sub>-P) ve toplam fosfor (TP) ile yüksek korelasyon göstermişlerdir. Chlorophyta grubunda baskın olan *P. morum*, pH ve EK ile, Euglenozoa grubundan *P. pleuronectes* sadece EK ile yüksek korelasyon göstermişlerdir (Tablo 3).

Tablo 3

Kocaavşar Deresinde baskın fitoplankton türleri ile fiziksel ve kimyasal parametreler (Su Sıcaklığı=S, °C; pH; Elektriksel Kondüktivite=EK, µScm<sup>-1</sup>; Fosfat=PO<sub>4</sub>-P, mg l<sup>-1</sup>; Toplam Fosfor=TP, mg l<sup>-1</sup>; Nitrat Azotu=NO<sub>3</sub>-N, mg l<sup>-1</sup>; Toplam azot=TN, mg l<sup>-1</sup>) arasındaki korelasyon değerleri

	<i>F.cap</i>	<i>U.uln</i>	<i>N.amp</i>	<i>C.aff</i>	<i>P.maj</i>	<i>D.vul</i>	<i>P.ple</i>	<i>P.mor</i>
<b>T</b>	-0.223	-0.163	-0.213	0.340	0.368	0.472	0.347	0.305
<b>pH</b>	0.194	0.322	-0.328	-0.124	0.476	0.745*	0.464	0.872**
<b>EK</b>	0.585	0.291	-0.016	0.437	0.413	0.547	0.159	0.703
<b>PO<sub>4</sub>-P</b>	-0.447	0.704	0.093	-0.044	-0.304	0.739*	0.078	0.485
<b>TP</b>	-0.453	0.662	-0.435	0.015	-0.029	0.800*	0.126	0.537
<b>NO<sub>3</sub>-N</b>	0.504	-0.517	0.278	0.826*	0.093	-0.240	-0.072	-0.093
<b>TN</b>	0.591	-0.521	0.291	0.712*	-0.015	-0.314	-0.097	-0.029

\* 0.05 düzeyinde istatistiksel olarak önemli

\*\*0.01 düzeyinde istatistiksel olarak önemli

*Cymbella affinis*: *C.aff*; *Diatome vulgaris*: *D.vul*; *Fragilaria capucina*: *F.cap*; *Nitzschia amphibia*: *N.amp*; *Pinnularia major*: *P.maj*; *Phacus pleuronectes*: *P.ple*; *Pandorina morum*: *P. mor*; *Ulnaria ulna*: *U.uln*,

#### 4.Tartışma ve Sonuç

Kocaavşar Deresi'nin planktonik alglerinin mevsimsel değişimi ve buna bağlı olarak derenin ekolojik durumunu belirlemek amacıyla yapılan bu çalışmada, Bacillariophyta'dan 9, Chlorophyta'dan 17, Cyanobacteria'dan 5 ve Euglenozoa'dan 1 olmak üzere toplamda 32 fitoplankton türü tespit edilmiştir. Chlorophyta toplam türlerin %53'ünü oluşturarak baskın grup olmuştur. Bacillariophyta'dan *P. major*, *N. amphibia*, *C. affinis*, *D. vulgaris*, *U. ulna*, Chlorophyta'dan *P. morum*, Euglenozoa'dan *P. pleuronectes* türleri baskın olup söz konusu türler diğer akarsularda da yaygın olarak bulunmuşlardır (Aysel, 2005; Kalyoncu vd., 2009).

Bere ve Tundisi (2011) Brazilyadaki Monjolinho nehrinde yaptıkları çalışmada *Pinnularia* türlerinin ötrofikasyonla ilişkili odluklarını bilmişlerdir. Lebkuecher vd. (2014) *N. amphibia*'nın Amerika Birleşik Devletlerindeki Sulphur Fork Deresinin ötrofik kısmında yoğun olarak bulunduğunu tespit etmişlerdir.

Fakıoğlu vd. (2013) ötrofik karakterli Tortum Deresinde yaptıkları çalışmada *C. affinis* en sık rastlanan türlerden biri olmuştur. Holmes ve Taylor (2013) Güney Afrikadaki Great Fish Nehrinde yaptıkları çalışmada *D. vulgaris*'in düşük debi ve yüksek fosfor seviyelerini tercih eden ötrofikasyon indikatörü bir tür olduğunu belirtmişlerdir.

Yılmaz (2012) Riva Deresi fitoplanktonu üzerine yaptığı çalışmada derenin yoğun olarak kirletildiği ve *U. ulna* da dereye sıklıkla rastlanan türlerden biri olduğunu belirtmiştir. Piirsoo (2003) *P. morum*'un Estonia akarsularında fitoplanktonu oluşturan türlerden biri olduğunu belirtmiştir. Chen vd. (2016) *P. morum*'un besin tuzlarınca zengin derelerde sıklıkla rastlanan türlerden biri olduğunu belirtmişlerdir.

Trang vd. (2018) Vietnamdaki ötrofik karakterli Nhu Y Nehri fitoplanktonu üzerinde yaptıkları çalışmada *P. pleuronectes*'in ötrof akarsularında bulunabilen kozmopolit bir tür olduklarını belirtmişlerdir.

Bu türlerden bazıları planktonik tür değildir, ancak sediman ve taşlar üzerindeki alglerin dalga hareketleri ile fitoplanktona karıştığı birçok çalışmada belirtilmiştir (Solak vd., 2012; Varol ve Şen, 2014; Çiçek ve Ertan, 2015).

Kocaavşar Deresinde Chlorophyta, Cyanobacteria ve Euglenozoa gruplarına ait türlerin akış nedeni ile diğer grupların türlerine nazaran daha az yoğunlukta geliştiği ancak mevsim sıcaklığının yükseldiği, suyun akış devinim hızının azaldığı sonbahar döneminde geliştikleri tespit edilmiştir. Özellikle, *P. morum*, *P. pleuronectes* ve *G. aponina* diğer akarsularında yapılan çalışmalarda rapor edilmişlerdir (Yıldız, 1987).

Sonuç olarak, Su Kirliliği Kontrolü Yönetmeliğinde, toplam fosfora göre Kocaavşar Deresinin III. sınıf, nitrat azotuna göre ise I. sınıf su kalitesinde olduğunu göstermiştir. Ötrof sularda yayılış gösteren türler (*Bacillariophytadan F. capucina*, *C. glabriuscula*, *C. affinis*, *D. vulgaris*, *P. major*, *U. ulna* var. *oxyrhychnus*, *N. minuta*, *N. amphibia*, Chlorophytadan *P. morum* ve Euglenozoadan *P. pleuronectes*) özellikle sonbahar döneminde yaygın olarak kaydedilmişlerdir (Tezel Ersanlı ve Öztürk, 2017; Memiş, 2019).

## Çıkar Çatışması

Yazar çıkar çatışması bildirmemiştir.

## Kaynaklar

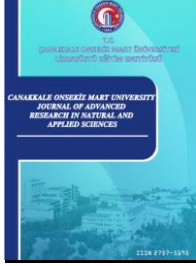
- Altuner, Z. ve Gürbüz, H. (1990). Karasu (Fırat) Nehri'nin epilitik ve epifitik algleri üzerine bir araştırma. *X. Ulusal Biyoloji Kongresi Botanik Bildirileri* (pp. 193- 203). Erzurum, Türkiye.
- Atıcı, T. ve Obalı, O. (1999). A study on diatoms in upperpart of Çoruh River, Turkey. *Gazi Üniversitesi Fen Bilimleri Enstitüsü Dergisi*, 12, 473-496. Erişim Linki: <https://search.trdizin.gov.tr/yayin/detay/24670/>
- Atıcı, T. ve Ahıska, S. (2005). Pollution and algae of Ankara Stream. *Gazi University Journal of Science*, 18, 51-59. Erişim Linki: <https://dergipark.org.tr/tr/pub/gujs/issue/7413/97213>
- Aysel, V. (2005). Check-list of the freshwater algae of Turkey. *Journal of Black Sea/Mediterranean Environment*, 11(1), 1-124. Erişim Linki: <https://dergipark.org.tr/en/download/article-file/103798>
- Baird, R., Eaton, A. D. ve Rice E. W. (2017). *Standard Methods for the Examination of Water and Wastewater* (23<sup>rd</sup> ed.). (Eds.). Standard Methods. American Public Health Association, Washington, D.C., USA. Erişim Linki: [https://www.bookfinder.com/book/9780875532875/?src=google\\_bhdyn8&gclid=EAIaIQobChMIwODH2fnK-QIVD-N3Ch14tAqLEAAyAAEgKYC\\_D\\_BwE](https://www.bookfinder.com/book/9780875532875/?src=google_bhdyn8&gclid=EAIaIQobChMIwODH2fnK-QIVD-N3Ch14tAqLEAAyAAEgKYC_D_BwE)
- Bere, T. ve Tundisi, J. G. (2011). The Effects of Substrate Type on Diatom-Based Multivariate Water Quality Assessment in a Tropical River (Monjolinho), São Carlos, SP, Brazil. *Water Air Soil Pollution*, 216, 391–409. Erişim Linki: <https://link.springer.com/article/10.1007/s11270-010-0540-8>
- Chen, N., Liu, L., Qiao, D., Li, Y., ve Lv, Y. (2016). Seasonal succession patterns of plankton in eutrophic rivers on plains. *International Journal of Limnology*, 52, 217-233 doi: <https://doi.org/10.1051/limn/2016007>
- Dere, Ş., Karacaoğlu, D. ve Dalkıran, N. (2002). A study on the epiphytic algae of the Nilufer Stream (Bursa). *Turkish Journal of Botany*, 26, 219–234. Erişim Linki:

- <https://journals.tubitak.gov.tr/botany/vol26/iss4/4/>
- Erdoğan, Ö., Nezire Lerzan Çiçek, N. L., ve Ertan, Ö. O. 2012. Manavgat Nehri Nehirağzı Bölgesi Fitoplanktonunun Mevsimsel Dağılımı. *Eğirdir Su Ürünleri Fakültesi Dergisi*, 8, 9-21. Erişim Linki: <https://dergipark.org.tr/tr/download/article-file/214246>
- Erdoğan, Ö., Nezire Lerzan Çiçek, N. L., ve Ertan, Ö. O. 2016. Köprüçay Nehri Nehirağzı Bölgesi Fitoplanktonunun Mevsimsel Dağılımı. *Akademia Disiplinlerarası Bilimsel Araştırmalar Dergisi*, 2 (1), 31-41. Erişim Linki: <https://dergipark.org.tr/tr/download/article-file/286487>
- Fakıoğlu, Ö, Köktürk M ve Atamanalp M. (2013). The application of some biodiversity indices in the Tortum Stream, Erzurum, Turkey. *International Journal of Physical Sciences*, 8(46), 2069-2076. Erişim Linki: <https://academicjournals.org/journal/IJPS/article-full-text-pdf/F69572742411>
- Holmes, M. ve Taylor, J. C. (2015). Diatoms as water quality indicators in the upper reaches of the Great Fish River, Eastern Cape, South Africa. *African Journal of Aquatic Science*, 40(4), 321-337. Erişim Linki: <https://www.tandfonline.com/doi/abs/10.2989/16085914.2015.1086722>
- Huber-Pestalozzi, G. (1982). *Das phytoplankton des süßwassers systematik und biologie*, 8.Teil, 1. Halffe Conjugatophyceae Zygnematalesund Desmidiiales (excl. Zygnemataceae). E. Schweizerbarth'sche Verlagsbuchhandlung (Nägele u. Obermiller), Stuttgart, Germany. Erişim Linki: <https://www.schweizerbart.de>
- John, D. M., Whitton, B. A. ve Brook, A. J. (2003). *The freshwater algal flora of the British isles: An identification guide to freshwater and terrestrial algae*. The Natural History Museum and The British Phycological Society. Cambridge University Press, Cambridge, UK. Erişim Linki: [https://books.google.com.tr/books/about/The\\_Freshwater\\_Algal\\_Flora\\_of\\_the\\_Britis.html?id=Sc4897dfM\\_MC&redir\\_esc=y](https://books.google.com.tr/books/about/The_Freshwater_Algal_Flora_of_the_Britis.html?id=Sc4897dfM_MC&redir_esc=y)
- Kalyoncu, H., Barlas, M. ve Ertan, Ö. O. (2009). Aksu Çayı'nın su kalitesinin biotik indekslere (diatomlara ve omurgasızlara göre) ve fizikokimyasal parametrelere göre incelenmesi, organizmaların su kalitesi ile ilişkileri. *TÜBAV Bilim Dergisi*, 2(1), 46-57. Erişim Linki: <https://dergipark.org.tr/tr/download/article-file/200839>
- Lebkuecher, J. G., Tuttle, E. N., Johnson, J. L. ve Willis, N. K. S. (2015). Use of Algae to Assess the Trophic State of a Stream in Middle Tennessee. *Journal Freshwater Ecology*, 30(3), 346-379. Erişim Linki: <https://www.tandfonline.com/doi/full/10.1080/02705060.2014.951883>
- Memiş, Y. (2019). Boğacık Deresi (Giresun) algleri üzerine floristik bir çalışma (Yayımlanmamış yüksek lisans tezi). Giresun Üniversitesi, Giresun. Türkiye.
- Morkoyunlu Yüce, A. , Gönüloğlu, A. , Ertan, Ö. O. & Erkebay, Ş. (2018). Hereke Deresi Alg Florası (Kocaeli-Türkiye). *Journal of Limnology and Freshwater Fisheries Research*, 4(1)25-29. Erişim Linki: <http://www.limnofish.org/tr/pub/issue/36766/366830>
- Piirsoo, K. (2003). Species diversity of phytoplankton in Estonian streams. *Cryptogamie Algologie*, 24 (2), 145-165. Erişim Linki: <https://sciencepress.mnhn.fr/en/periodiques/algologie/24/2/species-diversity-phytoplankton-estonian-streams>
- Round, F. E., Crawford, R. M. ve Mann, D. G. (1990). *The diatoms: Morphology and biology of the genera*. Cambridge University Press, Cambridge, UK. doi: <https://doi.org/10.1017/S0025315400059245>
- Sims, P. A. (1996). *An Atlas of British Diatoms*. Biopress Ltd., Bristol, UK. Erişim Linki: <https://www.worldcat.org/title/atlas-of-british-diatoms/oclc/35906099>
- SAS Institute. (1990). *SAS/STAT Users Guide*, (4<sup>th</sup> ed.). Cary, NC, USA. Erişim Linki: [https://books.google.com.tr/books/about/SAS\\_STAT\\_User\\_s\\_Guide\\_Version\\_6\\_Fourth\\_E.html?id=Dp0EzQEACAAJ&redir\\_esc=y](https://books.google.com.tr/books/about/SAS_STAT_User_s_Guide_Version_6_Fourth_E.html?id=Dp0EzQEACAAJ&redir_esc=y)
- Solak, C. N., Barinova, S., Acs, E. ve Dayıoğlu, H. (2012). Diversity and ecology of diatoms from Felent creek (Sakarya River Basin) Turkey. *Turkish Journal of Botany*, 36(2), 191-203. doi: 10.3906/bot-1102-16
- Sungur, D. (2005). Melen Çayı (Düzce- Adapazarı) bentik algleri ve yoğunluğundaki mevsimsel değişimi (Doktor Tezi). Gazi Üniversitesi, Ankara, Türkiye.
- Tezel Ersanlı, E. ve Öztürk, R. (2017). Karasu Çayı Fitoplankton Topluluğu ve Su Kalitesi Üzerine Ekolojik ve İstatistik Bir Değerlendirme. *Kahramanmaraş Sütçü İmam Üniversitesi Doğa Bilimleri Dergisi*, 20(3), 193-200. doi: <https://doi.org/10.18016/ksudobil.264177>
- Trang, L. T., Luong, Q. D., Vo, T. T. H., ve Nguyen, V. T. (2018). A case study of phytoplankton used as a biological index for water quality assessment of Nhu Y river, Thua Thien - Hue. *Vietnam Journal of Science, Technology and Engineering*, 60, 45-51. doi: [https://doi.org/10.31276/VJSTE.60\(4\).45-51](https://doi.org/10.31276/VJSTE.60(4).45-51)
- Şen, B. ve Varol, M. (2014). Dicle Nehri'nin planktonik alg florası. *Journal of Fisheries Sciences.com*, 8(4),

252-264. Erişim Linki: <https://search.trdizin.gov.tr/yayin/detay/261969/>

- Wang, J. H., Li, C., Xu, Y. P., Li, S. Y., Du, J. S., Han, Y. P. ve Hu, H. Y. (2021). Identifying major contributors to algal blooms in Lake Dianchi by analyzing river-lake water quality correlations in the watershed. *Journal of Cleaner Production*, 315, 128144. doi: <https://doi.org/10.1016/j.jclepro.2021.128144>
- Yıldız, K. (1987). Diatoms of the Porsuk River, Turkey. *Turkish Journal of Biology*, 11, 162-182. Yılmaz, N. (2012). The Relationship Between Phytoplankton Density and Chlorophyll-a in Riva Stream (Istanbul, Turkey). *Balkan Water Observation and Information System (BALWOIS)*. Ohrid, Republic of Macedonia. Erişim Linki: [https://balwois.com/wp-content/uploads/old\\_proc/889.pdf](https://balwois.com/wp-content/uploads/old_proc/889.pdf)





## Effect of Growth Medium on L-Dopa and Dopamine Production Using *Citrobacter freundii* (NRRL B-2643)

Meltem Çakmak<sup>1</sup>, Veyis Selen<sup>2</sup>, Dursun Özer<sup>3</sup>, Fikret Karataş<sup>4\*</sup>, Sinan Saydam<sup>5</sup>

<sup>1,3</sup> Department of Chemical Engineering, Faculty of Engineering, Firat University, Elazığ, Türkiye

<sup>2</sup> Department of Bioengineering, Faculty of Engineering, Firat University, Elazığ, Türkiye

<sup>4,5</sup> Department of Chemistry, Faculty of Science, Firat University, Elazığ, Türkiye

### Article History

Received: 29.04.2022

Accepted: 22.08.2022

Published: 15.12.2022

### Research Article

**Abstract** – In this study, microbial production of L-Dopa and Dopamine which is an important substance for the treatment of Parkinson's disease were investigated by using *Citrobacter freundii* (NRRL B-2643). The effects of carbon source (sucrose) and, salt concentrations (NaCl, CaCl<sub>2</sub>), initial pH, temperature, inoculum level and shaking speed on L-Dopa and dopamine production were investigated. The amounts of extracellular L-dopa and dopamine were determined by using HPLC. Maximum L-dopa and dopamine production, under optimized conditions (sucrose: 2.5 g/L, NaCl and CaCl<sub>2</sub>: 1.0 g/L, inoculum level: 1.0% (v/v), initial pH: 6.5, temperature: 33°C, shaking speed: 200 rpm) were found to be 458 and 592 mg/L, respectively. Although the experiments were carried out for 60 hours, but the maximum production of L-Dopa and Dopamine was realized at around the 30<sup>th</sup> hour of the experiments.

**Keywords** – *Citrobacter*, dopamine, fermentation, *freundii* (NRRL B-2643), L-Dopa, HPLC

## 1. Introduction

Although there are millions of living species in nature, there are common structures and characters among living things is divers. Microorganisms have many genes that humans have, as well as some genes that are not to be found in humans.

Bacteria use cheap carbon sources to reproduce, have the ability to reproduce quickly, and can be modified due to their relatively simple structure. Bacteria are used in the natural synthesis of many drugs used in the health industry, as they provide cheap cost due to these properties (Demain & Vaishnav, 2009). Bacteria is a microscopic single-cell species that prosper in a number of medium, such as soil, water, and can be grouped on the basis of cell structure, cell metabolism or cell component variations such as DNA, fatty acids, pigments, antigens and quinones. *C. freundii* is a member of the Enterobacteriaceae family of anaerobic gram-negative bacteria (O'Hara et al. 1997; Fang et al. 2017).

L-Dopa (3,4-dihydroxy-L-phenylalanine or 2-amino-3-(3,4 dihydroxyphenyl)-propanoic acid) is an amino acid naturally synthesized in the human body from L-tyrosine. L-Dopa is formed as a result of hydroxylation of tyrosine by the tyrosine hydroxylase (TOH) and leads to the biosynthesis of catecholamines such as dopamine, norepinephrine and epinephrine, which have an important biological functions (Nagatsu & Sawada, 2009; Kurt et al. 2009).

<sup>1</sup> [cakmak\\_meltem@hotmail.com](mailto:cakmak_meltem@hotmail.com)

<sup>2</sup> [vselen@firat.edu.tr](mailto:vselen@firat.edu.tr)

<sup>3</sup> [dozer@firat.edu.tr](mailto:dozer@firat.edu.tr)

<sup>4</sup> [fkartas@firat.edu.tr](mailto:fkartas@firat.edu.tr)

<sup>5</sup> [ssaydam@firat.edu.tr](mailto:ssaydam@firat.edu.tr)

\*Corresponding Author

L-Dopa is used as a primary drug in the treatment of Parkinson's disease and neurogenic injury following the myocardium (heart muscle) (Raju & Ayyanna, 1993). Unlike dopamine, the chirality of L-Dopa enables it to selectively cross the blood-brain barrier to the brain. Therefore, L-Dopa is used as the most effective drug in the treatment of Parkinson's patients (Montgomer, 1992). In recent years, in addition to being a dopamine precursor, L-Dopa has been reported to act as a neuromodulator or neurotransmitter in the central nervous system (Misu et al. 2002). Dopamine is the precursor of the mammalian central nervous system neurotransmitters norepinephrine and epinephrine (Kruk & Pycock, 1991). Dopamine is synthesized from L-Dopa by the enzyme dopa decarboxylase (DDC; aromatic L-amino acid decarboxylase, EC 4.1.1.28). Dopamine is a neurotransmitter that is the starting material for the formation of important catecholamines (such as norepinephrine and epinephrine) and also activates dopamine receptors in the brain (Hoffman & Lefkowitz, 1996; Lisbon, 2003). Dopamine synthesis takes place in two stages. In the first stage, L-Dopa is synthesized from substrates such as tyrosine and catechol, while Dopamine is synthesized from L-Dopa in the second stage. While a bacterium (*Symbiobacterium sp*) was needed for the synthesis of L-Dopa, another bacteria was needed for the synthesis of Dopamine (*Streptococcus faecalis*) from L-Dopa (Lee et al. 1999).

Bacteria can reach large masses in suitable nutrient media due to the the highest reproduction rate, the lowest generation time, and they show a logarithmic growth. Many products with high potential for use in various industries are obtained from microorganisms using recombinant techniques. Especially the use of bacteria for the production of drugs used in the treatment of many diseases is of great importance for the pharmaceutical industry.

In this study, simultaneous production of Dopa and dopamine was carried out by using the *Citrobacter freundii* (NRRL B-2643) bacteria. Aimed was to optimize the fermentation conditions (such as sucrose concentration, pH, temperature) for the production of L-Dopa and dopamine.

## 2. Materials and Methods

### 2.1. Material

*C. freundii* (NRRL B-2643) microorganism was obtained from the Biotechnology Laboratory of the Chemical Engineering Department of Firat University. Double distilled (dd H<sub>2</sub>O) water was used throughout the work. All the chemical used are reagent or analytical grade and obtained from Merck or Sigma-Aldrich.

### 2.2. Method

Luria-Bertani (LB) medium was used for the storage and development of *C. freundii* microorganism used in experiments (Bertani, 1951). The prepared stock cultures were cultivated in solid nutrient medium (10.0 g peptone, 5.0 g yeast extract, 10.0 g NaCl and 15 g agar, per liter) and incubated at 37 °C for 18 hours. The culture obtained after incubation was kept at +4 °C as it was used in a short time. Before the bacteria required for the production of L-Dopa and Dopamine are inoculated into the prepared fermentation medium, they are inoculated from the culture storage medium to the development medium and then inoculated into the main fermentation medium. Thus, the fermentation medium is inoculated with fresh culture.

50 ml of the nutrient media (LB) prepared for the experiments were taken and production was carried out in 250 mL erlen mayer after sterilization. The erlen mayers, in which the cultures were inoculated, were placed in an orbital shaker (Selecta Rotabit) with the shaking speed of 150 rpm at 37 °C and incubated for 18 hours to ensure bacterial growth. At the end of the incubation, the microorganisms whose growth was completed were transferred to the L-Dopa and Dopamine production medium at a different amount. L-Dopa and dopamine analysis were performed by taking a sample one erlen mayer from orbital shaker for every 6 hours, and centrifuged at 6000 rpm for 5 minutes then supernatant is separated. Experiments were carried out in three parallels.

### 2.3. L-Dopa and Dopamine Analysis

The amounts of extracellular L-Dopa and Dopamine in the supernatant were determined by HPLC (Shimadzu LC20). L-Dopa and Dopamine were determined at 290 nm by using a mixture of 97/3 (v/v) 25 mM Phosphate Buffer (pH:3.0) and Methanol as the mobile phase in an Inertsil ODS-4 column at a flow rate of 1.0 mL/min. (Aytan E. 2009)

### 3. Results and Discussion

The effects of sucrose concentration, initial pH, temperature, shake speed and salt concentration (NaCl vs. CaCl<sub>2</sub>) on L-Dopa and Dopamine production by *C. freundii* (NRRL B-2643) were investigated. The composition of the medium is the most important parameter affecting the growth of microorganisms and the production of various metabolites. The carbon source is very important as it participates in the synthesis of basic substances that form the building blocks of the microorganism cell, such as polysaccharides, lipids and proteins, and is also used as an energy source (Rehm et al. 1987). Different concentrations of sucrose (1-10 g/L) were used to investigate the effect of carbon source on L-Dopa and Dopamine production. The results obtained are given in Figures 1 and 2.

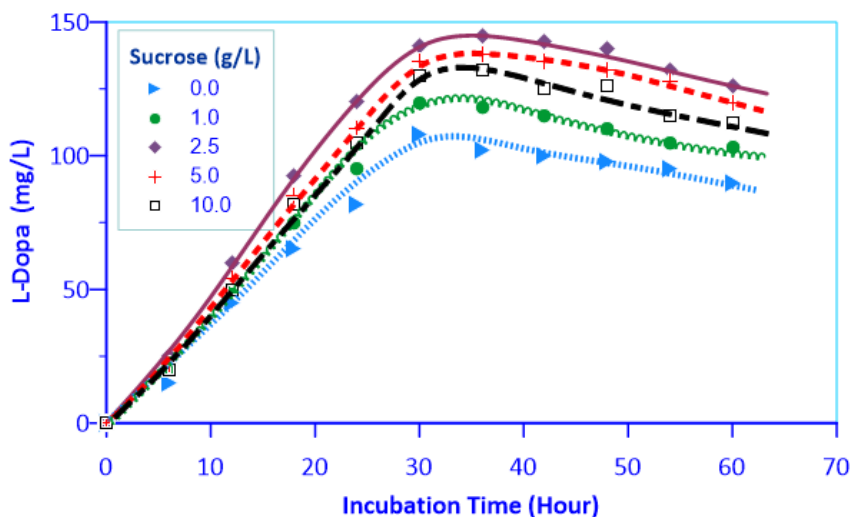


Figure 1. The effect of sucrose concentration on the L-Dopa production

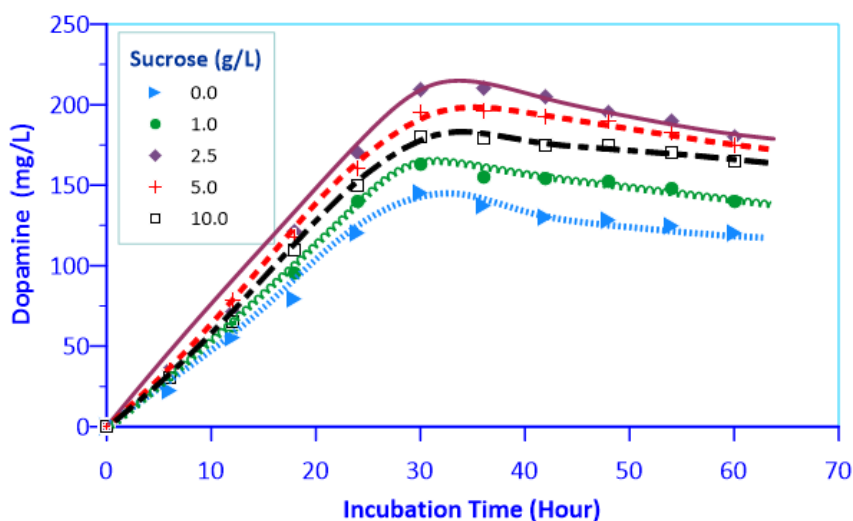


Figure 2. The effect of sucrose concentration on the Dopamine production

As seen in Figures 1 and 2, the highest L-Dopa and Dopamine concentrations were reached at 2.5 g/L sucrose concentration, 141 and 209 mg/L respectively.

It is seen that high sucrose concentration has a negative effect on L-Dopa and Dopamine production and decreases the production level of these metabolites. The reason for this is that the presence of some carbon sources in high concentrations in the nutrient medium reduces the amount of substances produced by making a repression effect on the metabolites secreted by microorganisms (Prudende et al. 1989; Yun & Ryu, 2001; Geckil et al. 2004).

Towards the end of the logarithmic phase, it is seen that the production amount L-dopa and dopamine's are almost fixed, indicating that the production is accompanied by growth. In other words, growth associated products are produced simultaneously with microbial growth.

The decrease in the amount of products towards the end of the incubation period indicates that the products started to deteriorate due to the environmental conditions. Production of L-dopa and dopamine is stopped at the 30 th hour to prevent product loss. Since L-Dopa is the precursor of Dopamine, the variation of product concentrations over time is expected to be parallel (Figures 1 and 2).

Optimum nitrogen source for the production of L-Dopa and Dopamine with the *C. freundii* microorganism were used according to Çakmak, (2016), 10.0 g/L peptone, 5.0 g/L yeast extract, 10.0 g/L NaCl, initial pH: medium pH, inoculum level: 1.0 % v/v, shaking speed: 150 rpm, T: 37 °C. In addition to carbon and nitrogen sources, microorganism needs elements such as Na, Ca, Mg, Fe, Mn, Cu, Zn in order to grow and produce products. Trace elements are sometimes especially added to the growth medium, but it is generally obtained through impurities in water and other media components. These cations are usually obtained from inorganic salts. In addition to their nutritional role, these salts also have a stimulating role on development of microorganism and activate enzymes, in some cases it is a component of some enzymes (Shuler & Kargi, 2002). In order to investigate the effect of Sodium and Calcium, chloride salts were added to the fermentation medium. It was observed that concentrations of NaCl had no effect on the amount of product, but CaCl<sub>2</sub> concentrations had a slightly positive effect on the production of L-dopa and dopamine concentration. It is known that NaCl creates an isotonic balance in fermentation environments (Halkman, 2005). In the continuation of the study, NaCl was added to the fermentation medium at a concentration of 1.0 g/L. In order to investigate the effect of calcium, CaCl<sub>2</sub> was added to the fermentation medium at five different concentrations, 1, 2.5, 5, 7.5 and 10 g/L. The effect of CaCl<sub>2</sub> on L-Dopa and dopamine production is given in Figures 3 and 4.

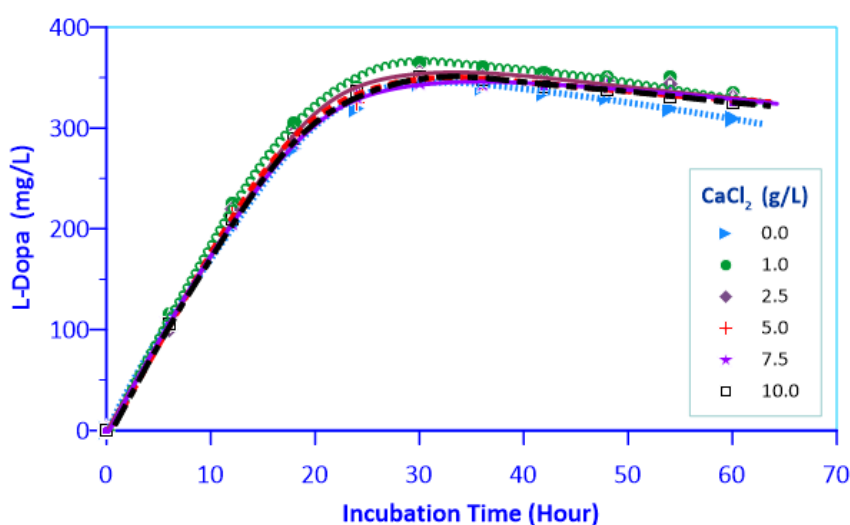


Figure 3. The effect of CaCl<sub>2</sub> concentration on the L-Dopa production

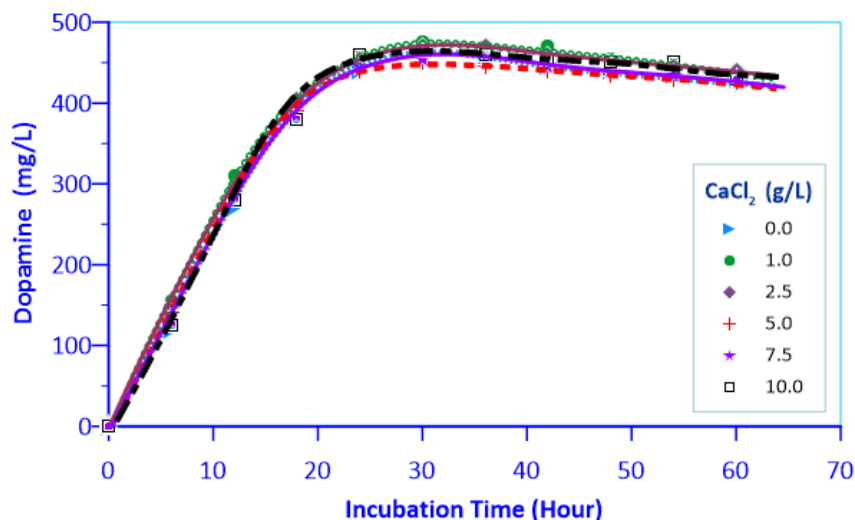


Figure 4. The effect of CaCl<sub>2</sub> concentration on the Dopamine production

As seen in Figures 3 and 4, the highest L-Dopa and Dopamine amounts were obtained at 1.0 g/L CaCl<sub>2</sub> concentration. At this concentration, the amounts of L-Dopa and dopamine were found to be 363 and 471 mg/L, respectively. Since the isotonic balance in the medium is largely achieved with NaCl, the amount of CaCl<sub>2</sub> should be well adjusted. Calcium, helps to regulate the ionic balance, and it also acts to activate some enzymes in the medium (Halkman, 2005).

In the microbial production processes, the pH of the medium changes over time due to the conversion of the carbon sources used into different products, the formation of some intermediate organic acids and their reuse to produce other compounds. pH is very important for microorganism growth and production product (Shuler & Kargi, 2002). The results obtained from the experiments carried out to investigate the effect of initial pH on L-dopa and dopamine production are given in Figures 5 and 6.

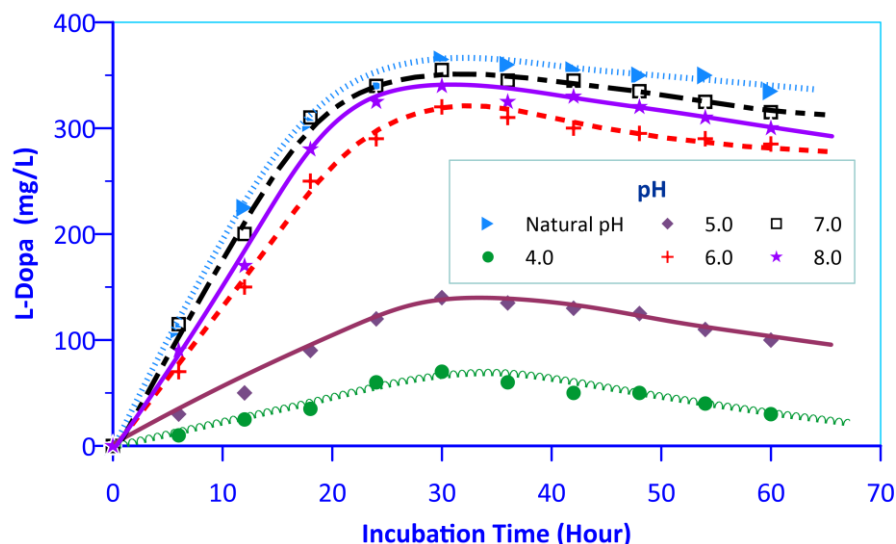


Figure 5. Effect of initial pH on L-Dopa production

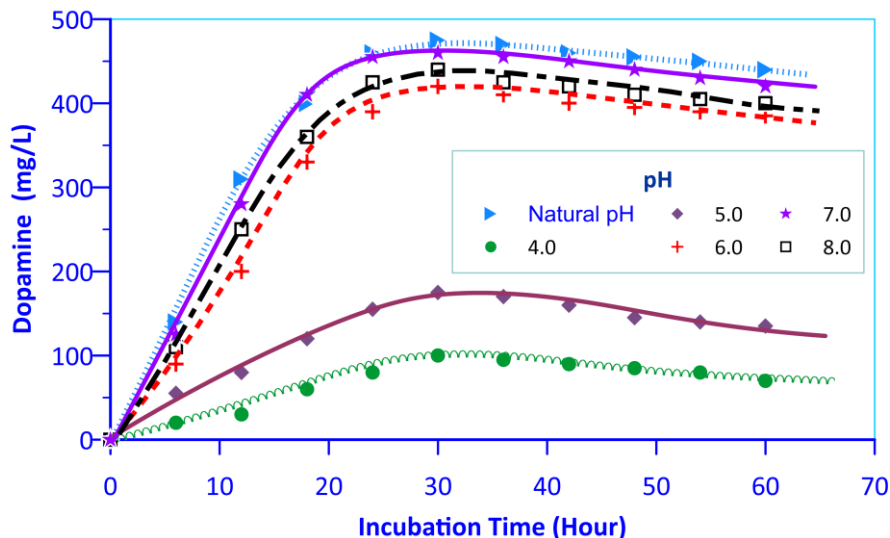


Figure 6. Effect of initial pH on Dopamine production

Maximum production of L-Dopa and Dopamine occurred at the natural pH of the medium (approximately 6.5). The amounts of L-Dopa and dopamine formed at this pH were found to be 363 and 471 mg/L, respectively (Figures 5 and 6). At low pH values, production of L-dopa and dopamine might be reduced, because of low microorganism production at this pH. Apart from natural and near-nature pH values, L-Dopa and dopamine production are adversely affected. Elibol and Ozer (2000) reported in their study that the amount of lipase produced varies depending on the initial pH. Our findings are compatible with the literature.

It is reported that the amount of inoculum affects microbial processes (Elibol et al. 1995). The results obtained in the study conducted to investigate the effect of different inoculum level on L-Dopa and Dopamine production are given in Figures 7 and 8.

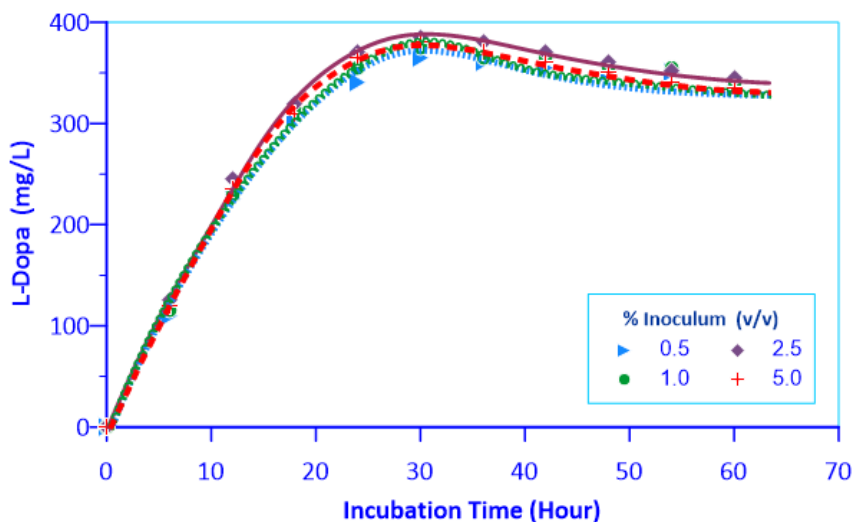


Figure 7. Effect of inoculum level on L-Dopa production

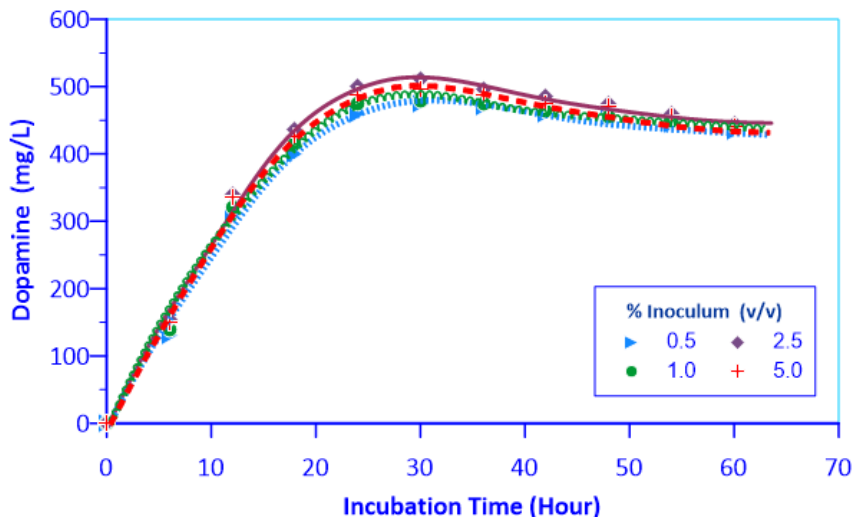


Figure 8. Effect of inoculum level on Dopamine production

As seen in Figures 7 and 8, although the increase in inoculum concentration did not affect L-Dopa and Dopamine production much, the highest production level was reached in the medium where microorganisms were cultivated at a ratio of 2.5% by volume. These values are 382 and 511 mg/L, respectively. Elibol and Özer (2000) reported in their study that the amount of inoculum had no effect on the amount of lipase produced.

Mixing is a very important parameter for microbial growth and production, as it facilitates the microorganism's access to oxygen and nutrients (McDaniel & Bailey, 1969).

The effect of shaking speed on L-dopa and dopamine production is given in Figures 9 and 10.

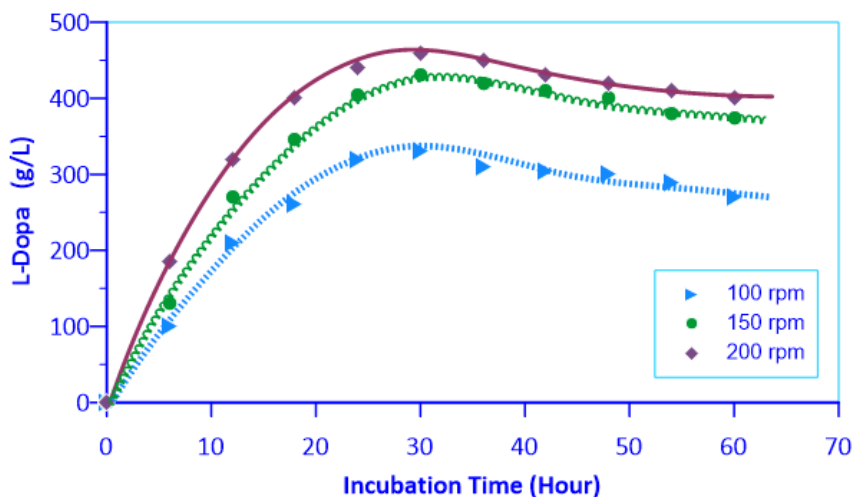


Figure 9. Effect of shaking speed on L-Dopa production

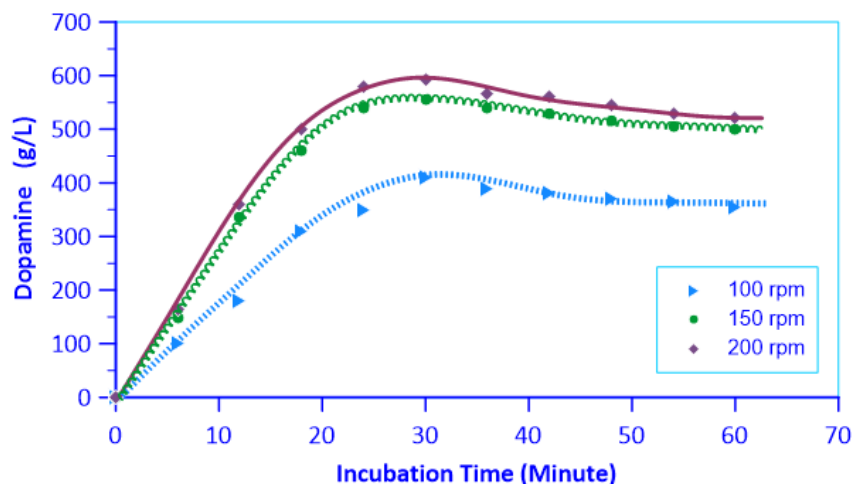


Figure 10. Effect of shaking speed on Dopamine production

It is seen that the amount of product increases depending on the shaking speed. As the film layer around the microorganism cells will be thinned with mixing, the oxygen and nutrient transfer to the cells will increase. If the shaking speed is too high, this create a disadvantage for microorganisms, the speed must be adjusted well. Charm and Wong (1970) reported that high mixing speeds negatively affect the activity of enzymes. Temperature is an important parameter in fermentation processes and needs to be adjusted well. Higher temperature increases cell denaturation and has a negative effect on cell formation. In addition, at high temperature values, the structure of the formed products may deteriorate with the deterioration of microorganism proteins. Since the diffusion of nutrients to the microorganism is reduced at low temperature values, the microorganism cannot develop sufficiently and the production amount decreases (Sodhi et al. 2005; Prakasham et al. 2005).

In order to investigate the effect of temperature on L-Dopa and Dopamine production, the results of experiments performed at different temperatures are given in Figures 11 and 12.

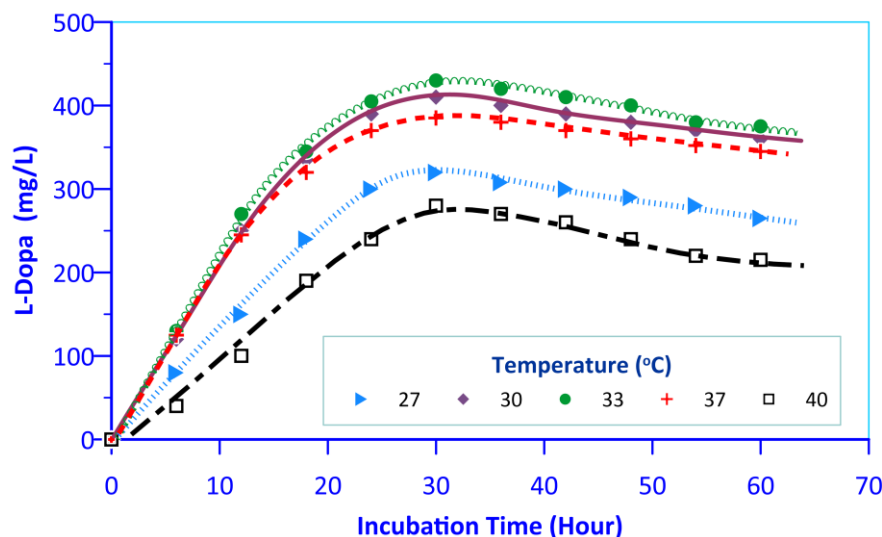


Figure 11. Effect of temperature on L- Dopa production



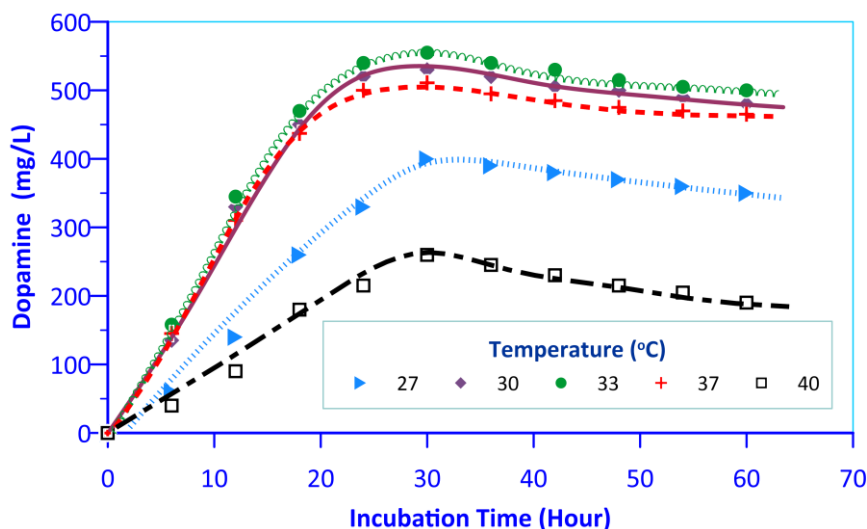


Figure 12. Effect of temperature on Dopamine production

The highest production of L-Dopa and Dopamine occurred at 33 °C. The amounts of L-Dopa and dopamine formed at this temperature are 428 and 553 mg/L, respectively. It is observed that at higher temperatures the amount of L-dopa and dopamine concentration are decreased (Figures 11 and 12). Tanyildizi et al. (2007) reported that amylase production decreased at high temperatures.

#### 4. Conclusion

It has been determined that especially sucrose concentration, temperature, initial pH and mixing speed are very effective on the production of L-Dopa and Dopamine by fermentation. It has been observed that the production of L-Dopa and dopamine reaches its maximum in approximately 30 hours. Extending the fermentation time caused a slight decrease in the amount of both products. Maximum production conditions for L-Dopa and Dopamine were determined to be 2.5 g/L sucrose, 1.0 g/L CaCl<sub>2</sub>, 2.5% (v/v) inoculum, 33 °C temperature and initial natural pH. To increase the production of dopa and dopamine at these conditions, different genetically modified microorganism could be used for further studies. In addition, L-dopa and dopamine production could be investigated by batch and continuous reactors.

#### Conflicts of Interest

The authors declare no conflict of interest.

#### Author Contributions

Meltem Çakmak: Performing the experiments.

Veyis Selen: Performing the experiments.

Dursun Özer: Designing the experiments, evaluating the results and writing.

Fikret Karatas: Designing the experiments, evaluating the results and writing.

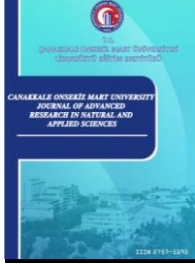
Sinan Saydam: Designing and writing the manuscript.

#### References

- Aytan E., (2009). *Vitreoscilla Hemoglobin Geninin Erwinia herbicola'ya Klonlanması ve L-DOPA Üretimi Üzerine Etkisi*, Yüksek Lisans Tezi, İnönü Üniversitesi, Fen Bilimleri Enstitüsü, Retrieved from: <https://tez.yok.gov.tr/UlusalTezMerkezi>
- Bertani, G. (1951). Studies on lysogenesis. I. The mode of phage liberation by lysogenic *Escherichia coli*,

- Journal of Bacteriology*, 62, 293-300. doi: <https://doi.org/10.1128/jb.62.3.293-300.1951>
- Charm, S.E., & Wong, B.L. (1970). Enzyme inactivation with shearing. *Biotechnology and Bioengineering*, 12, 1103 – 1109. doi: <https://doi.org/10.1002/bit.260120615>
- Çakmak, M., (2016). *Citrobacter freundii* (NRRL B-2643) Mikroorganizması Kullanılarak Farklı Fermantatif Şartlarda L-Dopa Ve Dopamin Üretiminin İncelenmesi, Yüksek Lisans Tezi, Fırat Üniversitesi Fen Bilimleri Enstitüsü. Retrieved from: <https://tez.yok.gov.tr/UlusalTezMerkezi>
- Demain, A.L., & Vaishnav, P. (2009). Production of recombinant proteins by microbes and higher organisms. *Biotechnology Advances*, 27, 297-306. doi: <https://doi.org/10.1016/j.biotechadv.2009.01.008>
- Elibol, M. & Ozer, D., (2000). Lipase production by immobilised *Rhizopus arrhizus*. *Process Biochemistry*, 36, 219 – 223. doi: [https://doi.org/10.1016/S0032-9592\(00\)00191-6](https://doi.org/10.1016/S0032-9592(00)00191-6)
- Elibol, M., Ulgen, K., Kamarulzaman, K., & Mavituna, F. (1995). Effect of inoculum type on actinorhodin production by *Streptomyces coelicolor*. *Biotechnology Letters*, 17, 579–582 doi: <https://doi.org/10.1007/BF00129381>
- Fang, H., Kang, J., & Zhang, D. (2017). Microbial production of vitamin B 12: a review and future perspectives. *Microbial Cell Factories*, 16(15), 1-14 doi: <https://doi.org/10.1186/s12934-017-0631-y>.
- Geckil, H., Gencer, S., & Uckun, M. (2004). *Vitreoscilla* hemoglobin expressing *Enterobacter aerogenes* and *Pseudomonas aeruginosa* respond differently to carbon catabolite and oxygen repression for production of L-asparaginase, an enzyme used in cancer therapy, *Enzyme and Microbial Technology*, 35, 182-189. doi: <https://doi.org/10.1016/j.enzmictec.2004.04.005>
- Halkman, A.K. (2005). *Anonymous, Merck Gıda Mikrobiyolojisi Uygulamaları*. Ed: A. K. Halkman. Başak Matbaacılık Ltd. Şti., Ankara.
- Hoffman, B.B., & Lefkowitz, R.J. (1996). *Catecholamines, sympathomimetic drugs, and adrenergic receptor antagonists*. In: Hardman J.G., Limbird L.E., Molinoff P.B., Ruddon R.W., Goodman L.S., Gilman A., editors. *Goodman & Gilman's the Pharmacological Basis of Therapeutics*. 9th. McGraw-Hill; New York, NY, USA: 1996. pp. 199–248.
- Kruk, Z.L., & Pycocock, C.J. (1991). *Dopamine*. In: *Neurotransmitters and drugs*, Suffolk, UK: St. Edmundsbury Press, 3rd ed., 87–115.
- Kurt, A.G., Aytan, E., Ozer, U., Ates, B., & Geckil, H. (2009). Production of L-DOPA and dopamine in bacteria bearing *Vitreoscilla* hemoglobin gene. *Biotechnolgy Journal*, 4(7), 1077-1088. doi: <https://doi.org/10.1002/biot.200900130>
- Lee, S.G., Hong, S.P., & Sung, M.H. (1999). Development of an enzymatic system for the production of dopamine from catechol, pyruvate, and ammonia, *Enzyme and Microbial Technology*, 25, 298-302. doi: [http://dx.doi.org/10.1016/S0141-0229\(99\)00071-X](http://dx.doi.org/10.1016/S0141-0229(99)00071-X)
- Lisbon, A. (2003). Dopexamine, dobutamine and dopamine increase splanchnic blood flow: What is the evidence? *CHEST*, 123, 460–463. doi: [https://doi.org/10.1378/chest.123.5\\_suppl.460s](https://doi.org/10.1378/chest.123.5_suppl.460s)
- McDaniel, L.E., & Bailey, E.G. (1969). Effect of Shaking Speed and Type of Closure on Shake Flask Cultures, *Applied Microbiology*, 17, 286-290. doi: <https://doi.org/10.1128/am.17.2.286-290.1969>
- Misu, Y., Goshima, Y., & Miyamae, T. (2002). Is DOPA a neurotransmitter? *Trends in Pharmacological Science*, 23(6), 262–268. doi: [https://doi.org/10.1016/s0165-6147\(02\)02013-8](https://doi.org/10.1016/s0165-6147(02)02013-8)
- Montgomer, E.B. (1992). Pharmacokinetics and pharmacodynamics of levodopa. *Neurology*, 42(1 Suppl 1), 17-22. PMID: 1549197
- Nagatsu, T., & Sawada, M. (2009). L-dopa therapy for Parkinson's disease: Past, present, and future, *Parkinsonism & Related Disorders*, 15, S3-S8. doi: [https://doi.org/10.1016/S1353-8020\(09\)70004-5](https://doi.org/10.1016/S1353-8020(09)70004-5)
- O'Hara, C.M., Westbrook, G.L., & Miller, J.M. (1997). Evaluation of Vitek GNI+ and Becton Dickinson Microbiology Systems Crystal E/NF identification systems for identification of members of the family Enterobacteriaceae and other gram-negative, glucose-fermenting and non-glucose-fermenting bacilli. *Journal of Clinical Microbiology*, 35, 3269-3273. doi: <https://doi.org/10.1128/jcm.35.12.3269-3273.1997>
- Prakasham, R.S., Rao, C.S., Rao, R.S., & Sarma, P.N. (2005). Alkaline protease production by an isolated *Bacillus circulans* under solid-state fermentation using agroindustrial waste: Process parameters optimization, *Biotechnology Progress*, 21, 1380-1388. doi: <https://doi.org/10.1021/bp050095e>
- Prudende, K.W., Katz, A., Sugrue, J.A., & Thomson, A. (1989). The effect of glucose on the expression of a cloned *Bacillus amyloliquefaciens*  $\alpha$ -amylase gene in strains *Bacillus subtilis*, *Current Microbiology*, 18(1), 27-31. DOI: <https://doi.org/10.1007/BF01568826>

- Raju, B.G.H., & Ayyanna, C. (1993). Bioconversion of L-tyrosine to L-DOPA Nusing *Aspergillus oryzae*. *CBS Publishers*, 106–110. doi: <https://10.1007/s00726-010-0768-z>
- Rehm, J., Reed, G., & Kennedy, J.F. (1987). *Biotechnology*, Vch. New York, 7a, 5-100.
- Shuler, M.L., & Kargi, F. (2002). *Bioprocess engineering Basic Concepts*, Second edition, Prentice Hall New York. Pp. 46-54. ISBN 0-13-081908-5
- Sodhi, H.K., Sharma, K., Gupta, J.K., & Soni, S.K. (2005). Production of a thermostable alpha-amylase from *Bacillus sp* PS-7 by solid state fermentation and its synergistic use in the hydrolysis of malt starch for alcohol production. *Process Biochemistry*, 40, 525-534. doi: <https://doi.org/10.1016/j.procbio.2003.10.008>
- Tanyildizi, M.S., Ozer, D., & Elibol, M. (2007). Production of bacterial  $\alpha$ -amylase by *B. amyloliquefaciens* under solid substrate fermentation. *Biochemical Engineering Journal*, 37, 294–297. doi: <https://doi.org/10.1016/j.bej.2007.05.009>
- Yun, J.S., & Ryu, H.W. (2001). Lactic acid production and carbon catabolite repression from single and mixed sugars using *Enterococcus faecalis* RKY1. *Process Biochemistry*, 37, 235-240. doi: [https://doi.org/10.1016/S0032-9592\(01\)00205-9](https://doi.org/10.1016/S0032-9592(01)00205-9)



# The Changes in Biochemical Compositions of Five Different Macroalgae and Seagrass (*Halophila stipulacea* (Forsskal) Ascherson 1867) Collected from Iskenderun Bay

Mehmet Naz<sup>1,\*</sup>, Selin Sayin<sup>2</sup>, Zafer Cetin<sup>3</sup>, Eyüp Ilker Saygılı<sup>4</sup>, Ergun Taskin<sup>5</sup>, Oktay Soyler<sup>6</sup>

<sup>1,2</sup>Marine Sciences and Technology Faculty, Iskenderun Technical University, Hatay 31200, Türkiye

<sup>3</sup>Department of Medical Biology, School of Medicine, Sanko University, Gaziantep 27090, Türkiye

<sup>4</sup>Department of Medical Biochemistry, School of Medicine, Sanko University, Gaziantep 27090, Türkiye

<sup>5</sup>Department of Biology, Faculty of Arts and Sciences, Manisa Celal Bayar University, Manisa 45140, Türkiye

<sup>6</sup>Iskenderun Vocational College, Iskenderun Technical University, Hatay 31200, Türkiye

## Article History

Received: 14.03.2022

Accepted: 31.08.2022

Published: 15.12.2022

## Research Article

**Abstract** –In present study, biochemical compositions (ash, lipid and protein) of five different macroalgae ((Green Macroalgae-GMA (*Chaetomorpha linum* and *Caulerpa prolifera*), Red Macroalgae-RMA (*Pterocladia capillacea*), Brown Macroalgae-BMA (*Sargassum vulgare* and *Ericaria amentacea*)) and Angiosperm/Seagrass (*Halophila stipulacea*) collected from Iskenderun Bay were investigated. The differences observed between biochemical compositions such as ash, lipid and protein of five macroalgae species and Angiosperm/Seagrass (*Halophila stipulacea*) were statistically significant ( $p < 0.05$ ). The lowest and highest ash, lipid and protein values of five macroalgae were  $12.19 \pm 1.15\%$  (*Caulerpa prolifera*)-  $21.38 \pm 1.53\%$  (*Ericaria amentacea*),  $1.74 \pm 0.19\%$  (*Caulerpa prolifera*)-  $5.83 \pm 0.68\%$  (*Ericaria amentacea*),  $5.56 \pm 0.06\%$  (*Chaetomorpha linum*)-  $11.45 \pm 0.53\%$  (*Sargassum vulgare*), respectively. Ash, lipid and protein values of Angiosperms/Seagrass (*Halophila stipulacea*) were determined as  $14.56 \pm 2.08\%$ ,  $3.16 \pm 0.48\%$  and  $8.11 \pm 0.07\%$ , respectively. Protein value of Angiosperms/Seagrass (*Halophila stipulacea*) was higher than those of (GMA (*Chaetomorpha linum* and *Caulerpa prolifera*) but not RMA (*Pterocladia capillacea*) and BMA (*Sargassum vulgare* and *Ericaria amentacea*)). Lipid value of Angiosperms/Seagrass (*Halophila stipulacea*) was similar to RMA (*Pterocladia capillacea*). In conclusion, the information of the biochemical compositions of five different macroalgae and Angiosperms/Seagrass (*Halophila stipulacea*) are important for the evaluation of potential sources for commercial and human consumption. In addition, biochemical compositions of tested macroalgae and seagrass could make important contributions to feed formulations and functional foods in future.

**Keywords**-Green algae, brown algae, red algae, seagrass, biochemical compositions

## 1. Introduction

Macroalgae known as primary producers are important for the ocean ecosystem. They include nutritional compounds used different industries such as food, agriculture, feed, cosmetic, medicine, pharmacy. Ak (2015)

<sup>1</sup> mehmet.naz@iste.edu.tr

<sup>2</sup> selin.sayin@iste.edu.tr

<sup>3</sup> zcetin@sanko.edu.tr

<sup>4</sup> isaygili@sanko.edu.tr

<sup>5</sup> ergun.taskin@cbu.edu.tr

<sup>6</sup> oktay.soyler@iste.edu.tr

\*Corresponding Author

showed that macroalgae have contain different photosynthetic pigments such as Chlorophyta (Green Macroalgae-GMA), Rhodophyta (Red Macroalgae-RMA), Ochrophyta (Brown Macroalgae-BMA). Researchers revealed that biological activity potentials, fatty acids, protein and mineral substances of macroalgae were high levels (Dawczynski, Schubert & Jahreis 2007; Wells et al., 2017). Burtin (2003) and Benjama & Masniyom (2011) reported that GMA and RMA have higher protein levels (10–30%) than BMA species (5–15%). Dawczynski et al. (2007) showed that proximate compositions of the mentioned GMA, RMA and BMA change according to the geographical distribution, species, season, water temperature, salinity, light and nutrients and mineral availability.

*Caulerpa* is GMA genera belonging to Caulerpaceae family. Invasive algae have important effects on the ecosystems. *Caulerpa taxifolia* is an invasive alga found in the Mediterranean Sea.

Seagrasses provide an important habitat for fish and crustaceans as well as ecological contribution (Fourqurean et al., 2012). It is known that, seagrasses represent to two families, Potamogetonaceae and Hydrocharitaceae, (Hemminga & Duarte, 2000). *Halophila stipulacea* is seagrass species belonging to the family Hydrocharitaceae. There are 10 species of the genus *Halophila*. *Halophila stipulacea* was first observed in the Mediterranean in 1894 (Lipkin, 1975). Due to its invasive nature, there is increasing interest in understanding the ability to tolerate various environmental conditions. (Malm, 2006).

Biochemical compositions (ash, lipid, protein) of macroalgae and seagrasses are important to determine for industrial potentials. There is need to knowledge about analysis of proximate compositions of macroalgae and seagrasses belonging to different regions. Studies about nutritional composition macroalgae and seagrass tested in this study is not adequate in Iskenderun Bay. Therefore, we aimed to investigate the biochemical compositions (ash, lipid and protein) of five different macroalgae ((GMA (*Chaetomorpha linum* and *Caulerpa prolifera*), RMA(*Pterocladia capillacea*), BMA (*Sargassum vulgare* and *Ericaria amentacea*) and Angiosperms/Seagrass (*Halophila stipulacea*) gathered from Iskenderun Bay.

## 2. Materials and Methods

Macroalgae and Seagrass were gathered from the coasts of Iskenderun Bay (Kale and Arsuz regions in July 2019). Five macroalgae species ((GMA (*Chaetomorpha linum* (O.F.Müller) Kützing 1845 and *Caulerpa prolifera* (Forsskal) J.V.Lamouroux 1809), RMA(*Pterocladia capillacea* (S.G.Gmelin) Santelices & Hommersand 1997), BMA (*Sargassum vulgare* C.Agardh, 1820 and *Ericaria amentacea* (C.Agardh) Molinari & Guiry 2020)) and Angiosperms/Seagrass (*Halophila stipulacea* (Forsskal) Ascherson 1867) were identified. The identification studies of macroalgae and seagrass were carried out with Olympus brand SZX16 model stereo zoom and BX51 model binocular light microscopes (Taşkın & Öztürk, 2013; Rodríguez-Prieto, Ballesteros, Boisset & Afonso-Carrillo, 2013; Cormaci, Furnari & Alongi, 2014)

### 2.1. Preparation of the samples

Five macroalgae and Angiosperms/Seagrass (*Halophila stipulacea*) collected from the coasts of Iskenderun Bay were rinsed in distilled water and then drained. Thus, sand and other unwanted objects were removed. The next step was to dry the samples at 60°C for 3 hours using a laboratory oven (Pradana, Prabowo, Hastuti, Djaeni & Prasetyaningrum, 2019). Thoroughly dried samples were ground with a laboratory type mixer and then, stored at –20°C until analyses.

### 2.2. Biochemical compositions

Biochemical analyses of five macroalgae species ((GMA (*Chaetomorpha linum* and *Caulerpa prolifera*), RMA(*Pterocladia capillacea*), BMA (*Sargassum vulgare* and *Ericaria amentacea*) and

Angiosperms/Seagrass (*Halophila stipulacea*) gathered from the coasts of Iskenderun Bay were made according to the AOAC (2005) and Bligh & Dyer (1959) procedures.

### 2.3. Statistical analysis

Ash, lipid and protein results of five macroalgae species ((GMA (*Chaetomorpha linum* and *Caulerpa prolifera*), RMA(*Pterocladia capillacea*), BMA (*Sargassum vulgare* and *Ericaria amentacea*)) and Angiosperms/Seagrass (*Halophila stipulacea*) were submitted as mean  $\pm$  standard error (SE). Statistical comparisons were made by OneWay Analysis (ANOVA) using SPSS 12. Differences were considered statistically significant when  $p < 0.05$ .

### 3. Results and Discussion

The purpose of study was to reveal biochemical compositions (ash, lipid and protein) of five different macroalgae ((GMA (*Chaetomorpha linum* and *Caulerpa prolifera*), RMA(*Pterocladia capillacea*), BMA (*Sargassum vulgare* and *Ericaria amentacea*)) and Angiosperms/Seagrass (*Halophila stipulacea*). The biochemical compositions of five macroalgae and Angiosperms/Seagrass (*Halophila stipulacea*) are summarized in Table 1.

**Table 1**

Biochemical compositions of macroalgae and seagrass (mean $\pm$ SE)

GMA*	Proximate Compositions		
	Ash (%)	Lipid (%)	Protein (%)
<i>Chaetomorpha linum</i>	17,68 $\pm$ 0,33 <sup>bc</sup>	4,84 $\pm$ 1,68 <sup>b</sup>	5,56 $\pm$ 0,06 <sup>a</sup>
<i>Caulerpa prolifera</i>	12,19 $\pm$ 1,15 <sup>a</sup>	1,74 $\pm$ 0,19 <sup>a</sup>	6,70 $\pm$ 0,07 <sup>b</sup>
RMA**			
<i>Pterocladia capillacea</i>	20,31 $\pm$ 0,63 <sup>c</sup>	3,11 $\pm$ 0,53 <sup>ab</sup>	9,62 $\pm$ 0,35 <sup>d</sup>
BMA***			
<i>Sargassum vulgare</i>	13,19 $\pm$ 0,15 <sup>a</sup>	4,31 $\pm$ 0,42 <sup>ab</sup>	11,45 $\pm$ 0,53 <sup>e</sup>
<i>Ericaria amentacea</i>	21,38 $\pm$ 1,53 <sup>c</sup>	5,83 $\pm$ 0,68 <sup>b</sup>	9,75 $\pm$ 0,07 <sup>d</sup>
Angiosperms/Seagrass	Ash (%)	Lipid (%)	Protein (%)
<i>Halophila stipulacea</i>	14,56 $\pm$ 2,08 <sup>ab</sup>	3,16 $\pm$ 0,48 <sup>ab</sup>	8,11 $\pm$ 0,07 <sup>c</sup>

Different letters between the columns indicate significant difference at 5% by Duncan multiple range test.

\* Green Macroalgae; \*\* Red Macroalgae; \*\*\* Brown Macroalgae

The values found between biochemical compositions such as ash, lipid and protein of five macroalgae species and Angiosperms/Seagrass (*Halophila stipulacea*) were statistically significant ( $p < 0.05$ ). The lowest and highest ash, lipid and protein values of five macroalgae were 12.19 $\pm$ 1.15% (*Caulerpa prolifera*)- 21.38 $\pm$ 1.53% (*Ericaria amentacea*), 1.74 $\pm$ 0.19% (*Caulerpa prolifera*)- 5.83 $\pm$ 0.68% (*Ericaria amentacea*), 5.56 $\pm$ 0.06% (*Chaetomorpha linum*)- 11.45 $\pm$ 0.53% (*Sargassum vulgare*), respectively. Ash, lipid and protein values of Angiosperms/Seagrass (*Halophila stipulacea*) were determined as 14.56  $\pm$ 2.08%, 3.16 $\pm$ 0.48% and 8.11 $\pm$ 0.07%, respectively. Ash, lipid and protein values of *Ericaria amentacea* were the highest except for protein value of BMA *Sargassum vulgare*. Protein values of BMA were higher than those of GMA (*Chaetomorpha linum* and *Caulerpa prolifera*), RMA(*Pterocladia capillacea*) and Angiosperms/Seagrass (*Halophila stipulacea*). Protein value of Angiosperms/Seagrass (*Halophila stipulacea*) was higher than those of GMA (*Chaetomorpha linum* and *Caulerpa prolifera*) but not RMA (*Pterocladia capillacea*) and BMA (*Sargassum vulgare* and *Ericaria amentacea*). Lipid value of Angiosperms/Seagrass (*Halophila stipulacea*) was similar to RMA (*Pterocladia capillacea*). Ash and lipid values of *Caulerpa prolifera* except for protein value were lower than that of *Chaetomorpha linum*. Ash and lipid values of *Ericaria amentacea* except for protein value were lower than that of *Sargassum vulgare*. Ash and protein values of RMA (*Pterocladia capillacea*) except for lipid value were higher than those of GMA (*Chaetomorpha linum* and *Caulerpa prolifera*) and Angiosperms/Seagrass (*Halophila stipulacea*).

According to the results of our study, protein levels of RMA (*Pterocladia capillacea*), BMA (*Sargassum vulgare* and *Ericaria amentacea*) were higher than those of GMA (*Chaetomorpha linum* and *Caulerpa prolifera*). Protein value of RMA (*Pterocladia capillacea*) were similar to *Ericaria amentacea* but lower than that of BA (*Sargassum vulgare*).

It is known that, GMA and RMA contain higher protein contents (10–30%) than BMA (5–15%) (Burtin, 2003; Benjama & Masniyom, 2011). Dawczynski et al. (2007) revealed that protein levels of RMA was higher than those of BMA. However, Aras & Sayın (2020) showed that the protein ratio of *Ellisolandia elongata*, which is the only RMA species is similar to *Sargassum vulgare* and lower than *Dictyota dichotoma* from BMA.

Wahbeh (1997) showed that the protein content of the macroalgae *Padina pavonica* collected at the beach in Aqaba, Jordan was 17.4%. Tabarsa et al. (2012) found a protein content of 11.83% in *Padina pavonica*, which they collected in April in southern Iran (Persian Gulf). Ozgun & Turan (2015) showed that the protein levels of eight brown macroalgae collected from Iskenderun Bay was varied from  $2.897 \pm 0.373\%$  to  $6.519 \pm 0.432\%$ . Gür (2015) determined that protein value of *Dictyota dichotoma* was between 4.42-6.15%. Pakawan, Suriyan, Kriengkrai, & Jintana, (2015) biochemical compositions of 9 macroalgae species belonging to the GMA and RMA *Chaetomorpha crassa*, *Chaetomorpha linum*, *Ulva rigida*, *Caulerpa racemosa*, *Caulerpa brachypus*, *Caulerpa lentillifera*, *Caulerpa taxifolia*, *Gracilaria tenuistipitata* and *Gracilaria fisheri* showed as 12.68–33.83% protein. Uslu et al. (2021) determined that the protein amounts of the macroalgae *Sargassum vulgare* and *Cystoseira compressa* were  $6.29 \pm 0.12\%$  and  $9.50 \pm 0.3\%$ , respectively. Protein levels of *Sargassum vulgare* and *Cystoseira compressa* revealed by Uslu et al. (2021) were lower and similar to report from current study, respectively.

Protein levels of BMA (*Sargassum vulgare* and *Ericaria amentacea*) tested in current study was lower than those of protein levels revealed by Wahbeh (1997) and similar to Tabarsa et al. (2012). However, protein levels of BMA tested were higher than those of Ozgun & Turan (2015), Gür (2015) and Aras & Sayın (2020).

Khairy & El-Shafay (2013) revealed that the highest protein of *Pterocladia capillacea* in the different seasons was  $23.72 \pm 0.03\%$  Mazlum, Yazıcı, Sayın, Habiboğlu & Ugur, (2021) and Aras & Sayın (2020) revealed that protein level of *Jania rubens* and *Ellisolandia elongata* from red macroalgae was  $5.99 \pm 0.773\%$  and  $6.05 \pm 0.03\%$ , respectively. Protein level of RMA (*Pterocladia capillacea*) tested were higher than those of the levels determined by Mazlum et al. (2021) and Aras & Sayın (2020) but not Khairy & El-Shafay (2013) and Pakawan et al. (2015).

Burtin (2003) revealed that protein levels of GMA were generally between 10-30%. Firat, Öztürk, Taşkın & Kurt (2007) showed that protein value of *Caulerpa racemosa* were 12.94-20.18%. Manivannan, Thirumaran, Devi, Hemalatha & Anantharaman (2008) found that protein value of *Ulva intestinalis* was 16-17%. Manas et al. (2017) showed that protein value of *Caulerpa species* were 9.21-17.19%. Magdugo et al. (2020) showed that protein of *Caulerpa racemosa* was 19.9%. Protein level of *Ulva intestinalis* by Aras & Sayın (2020) determined as  $15.77 \pm 0.16\%$ . Protein value of *Ulva lactuca* belonging to GMA was determined as  $16.89 \pm 0.12\%$  by Mazlum et al. (2021). The protein values observed for GMA (*Chaetomorpha linum* and *Caulerpa prolifera*) in present study were lower than the values mentioned by Burtin, (2003); Firat, et al. (2007); Manivannan et al. (2008); Pakawan et al. (2015); Manas et al. (2017); Magdugo et al. (2020); Aras & Sayın (2020) and Mazlum et al. (2021).

McDermid & Stuercke (2003) reported that lipid content of macroalgae was less than 4%. Polat & Ozogul (2008) showed that lipid levels of RMA and BMA were between 1.10-11.53%. Lipid level is generally low in macroalgae, between 1-5% (Peng et al., 2015).

Wahbeh (1997) revealed that the lipid content of the macroalgae *Padina pavonica* collected at the beach in Aqaba, Jordan was 4.4%. Gür (2015) and Sultana, Ambreen, & Tariq (2012) showed that lipid levels of *Dictyota dichotoma* from BMA was 0.9-5.13% and 6.8%. Aras & Sayın (2020) revealed that lipid values of

*Dictyota dichotoma* and *Sargassum vulgare* were  $5.43 \pm 0.23\%$  and  $12.21 \pm 0.52\%$ , respectively. Ahmad, Sulaiman, Saimon, Yee, & Matanjun, (2012) stated that BMA species have higher lipid content than RMA and GMA species. Lipid levels in our study were between  $1.74 \pm 0.19\%$  (*Caulerpa prolifera*)- $5.83 \pm 0.68\%$  (*Ericaria amentacea*) levels stated by Peng et al. (2015). Uslu et al. (2021) determined that the lipid amounts of the macroalgae *Sargassum vulgare* and *Cystoseira compressa* were  $2.58 \pm 0.4\%$  and  $2.00 \pm 0.5\%$ , respectively. Lipid levels of *Sargassum vulgare* and *Cystoseira compressa* revealed by Uslu et al. (2021) were lower than present study. The results of our study were supported by Ahmad et al. (2012), Polat & Ozogul (2008), Peng et al. (2015), Gür (2015) but not Aras & Sayın (2020).

Mazlum et al. (2021) and Aras & Sayın (2020) revealed that lipid level of *Jania rubens* and *Ellisolandia elongata* from RMA were  $0.39 \pm 0.103\%$  and  $0.43 \pm 0.09\%$ , respectively. Lipid level of RMA (*Pterocladia capillacea*) tested was higher than those of Mazlum et al. (2021) and Aras & Sayın (2020).

Khairy & El-Shafay (2013) showed that *Ulva lactuca* ( $4.09 \pm 0.2\%$ ) contained more lipids than *Jania rubens* and *Pterocladia capillacea*. Manas et al. (2017) showed that lipid value of *Caulerpa* species were 1.29-2.44%. Magdugo et al. (2020) determined that lipid value of *Caulerpa racemosa* was 4.5%. Mazlum et al. (2021) and Aras & Sayın (2020) revealed that lipid levels of *Ulva lactuca* and *Ulva intestinalis* were  $1.08 \pm 0.33\%$  and  $1.04 \pm 0.37\%$ , respectively. Lipid levels of GMA (*Chaetomorpha linum* and *Caulerpa prolifera*) tested were higher than those of Mazlum et al. (2021) and Aras & Sayın (2020). Results were supported by Polat & Ozogul (2008) and Peng et al (2015) and similar to Khairy & El-Shafay (2013) except for *Caulerpa prolifera*.

According to the literatures, macroalgae have low lipid potential (Ratana- arporn & Chirapart, 2006). Chakraborty & Bhattacharya (2012) mentioned that lipid contents of macroalgae may vary depending on the type and amount of nutritive elements in the environment. Also, Peng et al. (2015) indicated that low lipid contents of macroalgae depends on light intensity, salinity and temperature conditions. Studies have shown that seasonal changes have caused changes in the biochemical compositions of macroalgae.

Tabarsa et al. (2012) revealed that the ash content of macroalgae varies between 8-40% of their dry weight. Polat & Ozogul (2013) determined that the ash levels varies between 2.28-51.63%. On the other hand, Liu (2017) showed that algae can contain as high as 70% dry matter ash in different locations.

Wahbeh (1997) indicated that the ash content of the macroalgae *Padina pavonica* collected at the beach in Aqaba, Jordan was 23.1%. Ozgun & Turan (2015) showed that the ash levels of 8 BMA gathered from Iskenderun Bay was varied from  $1.66 \pm 0.29\%$  to  $18.19 \pm 2.66\%$ . Uslu et al. (2021) determined that the ash amounts of the macroalgae *Sargassum vulgare* and *Cystoseira compressa* were  $27.05 \pm 0.5\%$  and  $21 \pm 0.1\%$ , respectively. Aras & Sayın (2020) found that the ash levels of BMA (*Dictyota dichotoma* and *Sargassum vulgare*) were  $27.34 \pm 0.72\%$  and  $14.79 \pm 0.19\%$ , respectively. BMA (*Sargassum vulgare* and *Ericaria amentacea*) results were similar to the values determined by Wahbeh (1997), Ozgun & Turan (2015), and Aras & Sayın (2020) and Uslu et al. (2021) except for *Sargassum vulgare*.

Firat et al. (2007) revealed that ash value of *Caulerpa racemosa* were 8.02-19.50%. Manas et al. (2017) showed that ash value of *Caulerpa species* were 23.90-40.27%. Magdugo et al. (2020) revealed that ash value of *Caulerpa racemosa* was 29,4%. Aras & Sayın (2020) and Mazlum et al. (2021) revealed that the ash levels of GMA (*Ulva intestinalis*) and *Ulva lactuca*) were  $27.49 \pm 0.43\%$  and  $26.47 \pm 0.20\%$ . Aras & Sayın (2020) and Mazlum et al. (2021) determined that the ash levels of RMA (*Ellisolandia elongata* and *Janie rubens*) were  $76.75 \pm 0.20\%$  and  $78.740 \pm 0.066\%$ , respectively. Khairy & El-Shafay (2013) indicated that ash content of *Jania Rubens* species were quite high (50.54%). Liu (2017) reveal that algae can contain as high as 70% dry matter ash in different locations. Results belonging to GMA (*Chaetomorpha linum* and *Caulerpa prolifera*) and RMA (*Pterocladia capillacea*) were lower than those of Khairy & El-Shafay (2013), Liu (2017), Manas et al. (2017), Magdugo et al. (2020), Aras & Sayın (2020) and Mazlum et al. (2021). Factors such as geographical location and season might be important factors in change the ash content of macroalgae (Renaud and Luong-Van, 2006; Mohamed, Hashim & Rahman, 2012; Cabrita et al., 2016)



Aketa & Kawamura (2001) found that protein values of *Halophila ovalis* was 6,2%. Coria-Monter & Durán-Campos (2015) showed that the protein, lipid and ash values of three seagrass species (*Thalassia testudinum*, *Halodule wrightii*, and *Syringodium filiforme*) were 8.47%-8.10%-10.43%; 0.83%,-2.33%-2.13%; 38.77%-27.23%-23.43%, respectively. Protein level of Angiosperms/Seagrass (*Halophila stipulacea*) was similar to Aketa & Kawamura, (2001), Kannan, Arumugam & Anantharaman, (2010) and Coria-Monter & Durán-Campos (2015). However, lipid and ash values of *Halophila stipulacea* were higher and lower than those of seagrasses species reported by Kannan et al. (2010) and Kannan, Arumugam, Iyapparaj, Thangaradjou & Anantharaman (2013), respectively. Renaud & Luong-Van (2006) indicated that geographic location, environmental conditions, seasons, and sampling conditions changed the biochemical composition of seagrass.

#### 4. Conclusion

In conclusion, the information of the biochemical compositions of five different macroalgae ((**GMA** (*Chaetomorpha linum* and *Caulerpa prolifera*), **RMA** (*Pterocladia capillacea*), **BMA** (*Sargassum vulgare*. and *Ericaria amentacea*)) and Angiosperms/Seagrass (*Halophila stipulacea*) are important for the evaluation of potential sources for commercial and human consumption. Biochemical compositions of tested macroalgae and seagrass could make important contributions to feed formulations and functional foods in future.

#### Author Contributions

Mehmet Naz: planned the study and statistical analyzes and evaluating the results and writing

Selin Sayın: planned the study and the writing of the manuscript

Zafer Çetin: biochemical analyses of m

acroalgae and he writing of the manuscript

Eyüp İlker Saygılı: biochemical analyses of macroalgae and the writing of the manuscript

Ergun Taşkın: collection of macroalgae and the writing of the manuscript

Oktay Söyler: collection of macroalgae and the writing of the manuscript

#### Conflicts of Interest

The authors declare no conflict of interest.

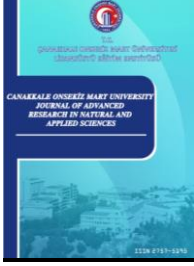
#### References

- Ahmad, F., Sulaiman, M. R., Saimon. W., Yee, C. F., & Matanjun, P. (2012). Proximate compositions and total phenolic content of selected edible seaweed from Semporna, Sabah, Malaysia. *Borneo Science*, 31, 85-96. Retrieved from: <https://jurcon.ums.edu.my/ojums/index.php/borneo-science/article/view/171>
- Ak, İ. (2015). Sucul Ortamın Ekonomik Bitkileri Makro Algler. *Dünya Gıda Dergisi*, 12, 88-97. Retrieved from: [https://www.academia.edu/20226751/Sucul\\_Ortam%C4%B1n\\_Ekonomik\\_Bitkileri\\_Makro\\_Algler](https://www.academia.edu/20226751/Sucul_Ortam%C4%B1n_Ekonomik_Bitkileri_Makro_Algler)
- Aketa, K., & Kawamura, A. (2001). Digestive functions in Sirenians and others (Review). *The Bulletin of Faculty of Biosources*, 27, 85-103. Retrieved from: <https://agris.fao.org/agris-search/search.do?recordID=JP2002004975>
- AOAC (2005). Association of Official Analytical Chemist, Official Methods of Analysis. 18th Edition, AOAC International, Suite 500, 481 North Frederick Avenue, Gaithersburg, Maryland 20877-2417, USA. ISBN 0-935584-77-3
- Aras, A., & Sayın, S. (2020). Geleceğin Fonksiyonel Ürünleri için Bazı Denizel Makroalglerin Potansiyel Belirlenmesi. *MedFAR*, 3(1), 22-35. Retrieved from: <https://dergipark.org.tr/pub/medfar/issue/52185/640946>

- Benjama, O., & Masniyom, P. (2011). Nutritional composition and physicochemical properties of two green seaweeds (*Ulva pertusa* and *Ulva intestinalis*) from the Pattani Bay in Southern Thailand. *Songklanakarin. J. Sci. Technol.*, 33, 575–583. Retrieved from: <https://agris.fao.org/agris-search/search.do?recordID=AV2012081280>
- Bligh, E.G., & Dyer, W.J. (1959). A rapid method of total lipid extraction and purification. *Can. J. Biochem. Physiol.*, 37, 911–917. Retrieved from: <https://cdnsiencepub.com/doi/10.1139/o59-099>
- Burtin, P. (2003). Nutritional value of seaweeds. *Electronic Journal of Environmental, Agricultural and Food Chemistry*, 2: 498-503. Retrieved from: <https://www.semanticscholar.org/paper/Nutritional-value-of-seaweeds-Burtin/32f330e9136c9a9ffc794217f50d4814c7b59326>
- Cabrita, A.R.J., Maia, M.R.G., Oliveira, H.M., Sousa-Pinto, I., Almeida, A.A., Pinto, E., & Fonseca, A.J.M. (2016). Tracing seaweeds as mineral sources for farm-animals. *The Journal of Applied Phycology*, 28, 3135–3150. doi: <https://doi.org/10.1007/s10811-016-0839-y>
- Chakraborty, S., & Bhattacharya, T. (2012). Nutrient composition of marine benthic algae found in the gulf of Kutch Coastline, Gujarat, India. *Journal of Algal Biomass Utilization*, 3 (1), 32 – 38. Retrieved from: <https://www.semanticscholar.org/paper/Nutrient-composition-of-marine-benthic-algae-found-Chakraborty-Bhattacharya/868e550a4149a1456822b56c48096a53ae14e437>
- Coria-Monter, E., & Durán-Campos E. (2015). Proximal analysis of seagrass species from Laguna de Términos, Mexico. *Hidrobiológica*, 25 (2), 249-255. Retrieved from: <https://www.semanticscholar.org/paper/Proximal-analysis-of-seagrass-species-from-Laguna-Coria-Monter-Dur%C3%A1n-Campos/18fa4c4d863e1c5bce006b79334a06daf70a4eb2>
- Cormaci, M., Furnari, G., & Alongi, G. (2014). Flora marina bentonica del Mediterraneo: Chlorophyta. *Boll. Accad. Gioenia Sci. Nat. Catania* 47, 11–436. Retrieved from: [https://www.researchgate.net/publication/311886135\\_Flora\\_marina\\_bentonica\\_del\\_Mediterraneo\\_Chlorophyta](https://www.researchgate.net/publication/311886135_Flora_marina_bentonica_del_Mediterraneo_Chlorophyta)
- Dawczynski, C., Schubert, R., & Jahreis, G. (2007). Amino acids, fatty acids, and dietary fibre in edible seaweed products. *Food Chemistry*, 103(3), 891–899. doi: <https://doi.org/10.1016/j.foodchem.2006.09.041>
- Firat, C., Öztürk, M., Taşkın, E. & Kurt, O. (2007). *Caulerpa racemosa* (Forsskal) J. Agardh'nın (Chlorophyceae=Yeşil Algler) Biyokimyasal İçeriği. *Ege Journal of Fisheries and Aquatic Sciences*, 24 (1), 89-91. Retrieved from: <https://app.trdizin.gov.tr/makale/TnpjME5EQXc/caulerpa-racemosa-forsskal-j-agardh-nin-chlorophyceae-yesil-algler-biyokimyasal-icerigi>
- Fourqurean, J.W., Duarte, C.M., Kennedy, H., Marba, N., Holmer, M., Mateo, M.A., Apostolaki, E.T., Kendrick, G.A., Krause-Jensen, D., McGlathery, K.J., & Serrano, O. (2012). Seagrass ecosystems as a globally significant carbon stock. *Nat. Geosci.*, 5, 505–509. doi: <https://doi.org/10.1038/ngeo1477>
- Gür, İ. (2015). Investigation on the seasonal variations of pigments, antioxidants and nutritional composition in some macroalgae species distributed in the Iskenderun Bay. *Cukurova University Institute of Natural and Applied Sciences*, MSc Thesis, 71 p. Retrieved from: <https://tez.yok.gov.tr/UlusalTezMerkezi/tez-SorguSonucYeni.jsp>
- Hemminga, M.A., & Duarte, C.M. (2000). *Seagrass Ecology*. Cambridge University Press, Cambridge, UK, 298 doi: <https://doi.org/10.1017/CBO9780511525551>
- Kannan R., Arumugam, R., & Anantharaman, P. (2010). Antibacterial potential of three seagrasses against human pathogens. *Asian Pac. J. Trop. Med.*, 3, 890-893. doi: [https://doi.org/10.1016/S1995-7645\(10\)60214-3](https://doi.org/10.1016/S1995-7645(10)60214-3)
- Kannan, R., Arumugam, R., Iyapparaj, P., Thangaradjou, T., & Anantharaman, P. (2013). In vitro antibacterial, cytotoxicity and haemolytic activities and phytochemical analysis of seagrasses from the Gulf of Mannar, South India. *Food Chem.*, 136, 1484-1489. doi: 10.1016/j.foodchem.2012.09.006
- Khairy H. M., and El-Shafay S. M. (2013). Seasonal variations in the biochemical composition of some common seaweed species from the coast of Abu Qir Bay, Alexandria, Egypt. *Oceamologia*, 55(2): 435–452. doi: <https://doi.org/10.5697/oc.55-2.435>

- Lipkin, Y., (1975). *Halophila stipulacea*, a review of a successful immigration. *Aquat. Bot.*, 1, 203–215. doi: [https://doi.org/10.1016/0304-3770\(75\)90023-6](https://doi.org/10.1016/0304-3770(75)90023-6)
- Liu, K. (2017). Characterization of ash in algae and other materials by determination of wetacid indigestible ash and microscopic examination. *Algal Research*, 25, 307-321. doi: <https://doi.org/10.1016/j.algal.2017.04.014>
- Magdugo, R. P., Terme, N., Lang, M., Pliego-Cortés, H., Marty, C., Hurtado, A.Q., Bedoux, G., & Bourgougnon, N. (2020). An Analysis of the Nutritional and Health Values of *Caulerpa racemosa* (Forsskål) and *Ulva fasciata* (Delile)—Two Chlorophyta Collected from the Philippines. *Molecules*, 25 (12), 2901. doi: 10.3390/molecules25122901
- Malm, T. (2006). Reproduction and recruitment of the seagrass *Halophila stipulacea*. *Aquat. Bot.*, 85, 345–349. doi: <https://doi.org/10.1016/j.aquabot.2006.05.008>
- Manas, H. M., Deshmukhe, G., Venkateswarlu, G., Jaiswar, A. K., Divipala, I., Siddaiah G. M. (2017). Nutritional profile of some important *Caulerpa J.V. Lamouroux* species along Maharashtra and Gujarat coast, India. *Journal of Fisheries and Life Sciences*, 2(1), 30-34. Retrieved from: <https://www.semanticscholar.org/paper/Nutritional-profile-of-some-important-Caulerpa-J.V.-Manas-Deshmukhe/9e7320989c69560cff4e83b700ba6de686b14aa5>
- Manivannan, K., Thirumaran, G., Devi, G.K., Hemalatha, A., & Anantharaman, P. (2008). Biochemical composition of seaweeds from mandapam coastal regions along southeast coast of India. *American-Eurasian Journal of Botany.*, 1 (2), 32-37. Retrieved from: <https://www.semanticscholar.org/paper/Biochemical-Composition-of-Seaweeds-from-Mandapam-Manivannan-Thirumaran/69cce43a111aab691880d7ed710aa3cd48c9c4bd>
- Mazlum, Y., Yazıcı, M., Sayın, S., Habiboğlu, O., & Ugur, S. (2021). Effects of two different macroalgae (*Ulva lactuca* and *Jania rubens*) species on growth and survival of juvenile red swamp crayfish (*Procambarus clarkii*) as feed additive. *Mar. Sci. Tech. Bull.*, 10(2), 154-162. Retrieved from: <https://dergipark.org.tr/tr/download/article-file/1378380>
- Mcdermid, K. J., & Stuercke, B., (2003). Nutritional composition of edible Hawaiian seaweeds. *Journal of Applied Phycology.*, 15, 513–524. [10.1023/B:JAPH.0000004345.31686.7f](https://doi.org/10.1023/B:JAPH.0000004345.31686.7f)
- Mohamed, S., Hashim, S.N., & Rahman, H.A. (2012). Seaweeds: a sustainable functional food for complementary and alternative therapy. *Trends Food Sci. Tech.*, 23, 83-96. doi: <https://doi.org/10.1016/j.tifs.2011.09.001>
- Özgün, S. & Turan, F. (2015). Biochemical composition of some brown algae from Iskenderun Bay, The Northeastern Mediterranean coast of Turkey. *Journal of the Black Sea / Mediterranean Environment*, 2, 125-134. [https://blackmedjournal.org/wp-content/uploads/Funda\\_Turan.pdf](https://blackmedjournal.org/wp-content/uploads/Funda_Turan.pdf)
- Pakawan, S., Suriyan, T., Kriengkrai, S., & Jintana, S. (2015). Growth and Nutrients Analysis in Marine Macroalgae. *Kasetsart J. (Nat. Sci.)*, 49, 211-218. Retrieved from: <https://li01.tci-thaijo.org/index.php/annes/article/view/243563>
- Peng, Y., Hu, J., Yang, B., Lin, X. P., Zhou, X. F., Yang, X.W., & Liu, Y. (2015). Chemical composition of seaweeds. In: *Seaweed Sustainability. Academic Press*, 79-124. doi: <https://doi.org/10.1016/B978-0-12-418697-2.00005-2>
- Polat, S., & Ozogul, Y. (2008). Biochemical composition of some red and brown macro algae from the Northeastern Mediterranean Sea. *International Journal of Food Sciences and Nutrition*, 59(7-8), 566-572. doi: <https://doi.org/10.1080/09637480701446524>
- Polat, S., & Özoğul, Y. (2013). Seasonal proximate and fatty acid variations of some seaweeds from the Northeastern Mediterranean coast. *Oceanologia*, 55 (2), 375–391. doi:10.5697/OC.55-2.375
- Pradana G B., Prabowo K B, Hastuti R P., Djaeni M., Prasetyaningrum A., 2019. Seaweed Drying Process Using Tray Dryer with Dehumidified Air System to Increase Efficiency of Energy and Quality Product IOP Conf. Series: Earth and Environmental Science 292, 012070. Retrieved from: <https://iopscience.iop.org/article/10.1088/1755-1315/292/1/012070>
- Renaud, S.M., & Luong-Van, J.T. (2006). Seasonal variation in the chemical composition of tropical Australian marine macroalgae. *J. Appl. Phycol.*, 18,381- 387. doi: <https://doi.org/10.1007/s10811-006-9034-x>

- Ratana-arporn, P., & Chirapart, A. (2006). Nutritional evaluation of tropical green seaweeds *Caulerpa lentilifera* and *Ulva reticulata*. *Kasetsart J. (Nat. Sci.)*, 40,75–83. Retrieved from: <https://www.cabi.org/ISC/abstract/20073167377>
- Rodríguez-Prieto, C., Ballesteros, E., Boisset, F. & Afonso-Carrillo, J. (2013). Guía de las macroalgas y fanerógamas marinas del Mediterráneo occidental. pp. 656. Barcelona: Ediciones Omega, Retrieved from: <https://www.amazon.es/Macroalgas-Faner%C3%B3gamas-Mediterr%C3%A1neo-Occidental-NATU-RALISTA-PECES/dp/8428215928>
- Sultana, V., Ambreen, H.K., & Tariq, A. (2012). Evaluation of biochemical component and antimicrobial activity of some seaweeds occurring at Karachi coast. *Pakistan Journal of Botany*, 44(5), 1799-1803. Retrieved from: <https://agris.fao.org/agris-search/search.do?recordID=PK2017000363>
- Tabarsa, M., Rezaei, M., Ramezanpour, Z., Robert Waaland, J., & Rabiei, R. (2012). Fatty acids, Amino acids, Mineral contents and Proximate composition of Some Brown Seaweeds. *Journal of Phycology*, 48(2), 285-292. doi: 10.1111/j.1529-8817.2012.01122.x
- Taşkın, E., & Öztürk, M. (2013). Türkiye Deniz Algleri. I. Phaeophyceae., p. 1-229, Manisa,Türkiye. Retrieved from: [https://www.researchgate.net/publication/274196118\\_Turkiye\\_Deniz\\_Algleri\\_I\\_Phaeophyceae](https://www.researchgate.net/publication/274196118_Turkiye_Deniz_Algleri_I_Phaeophyceae)
- Uslu, L., Sayın, S., Naz, M., Taskın, E., Soyler, O., Saygılı İ., Çetin, Z., Dinler, ZM., & Işık O. (2021). Proximate Analysis and Fatty Acid Profile of Some Brown Macroalgae Collected from the Northeastern Mediterranean Coast. *Fresenius Environmental Bulletin*, 30(7), 9433-9437. Retrieved from: [https://www.prt-parlar.de/download\\_feb\\_2021/](https://www.prt-parlar.de/download_feb_2021/)
- Wahbeh, M.I. (1997). Amino acid and fatty acid profiles of four species of macroalgae from Aqaba and their suitability for use in fish diets. *Aquaculture*, 159(1-2), 101-109. Retrieved from: [https://doi.org/10.1016/S0044-8486\(97\)00183-X](https://doi.org/10.1016/S0044-8486(97)00183-X)
- Wells, M.L., Potin, P., Craigie, J.S., Raven, J.A., Merchant, S. S., Helliwell, K. E., & Brawley, S. H. (2017). Algae as nutritional and functional food sources: revisiting our understanding. *Journal of Applied Phycology*, 29, 949–982. doi: 10.1007/s10811-016-0974-5



## Yer Radarı (GPR) Uygulaması ile Kısmi Yıkılmış Bir Köprünün Sağlık Durumunun Belirlenmesi

Gökhan Kılıç<sup>1,\*</sup>

<sup>1</sup>İzmir Ekonomi Üniversitesi, İnşaat Mühendisliği Bölümü, İzmir, Türkiye

### Makale Tarihi

Gönderim: 18.03.2022

Kabul: 05.07.2022

Yayın: 15.12.2022

### Araştırma Makalesi

**Öz** – Köprü yapılarının sağlık durumlarının ve yapıların yaşam döngüsü bağlamında durumun değerlendirilmesi mühendisler için hayati öneme sahiptir. Kuşkusuz, yıkılmış köprülerdeki yapısal kusurların önceden tespit edilmesi, özellikle yapı elamanlarındaki çatlaklar, donatıların açığa çıkması ve korozyonun tespiti, mühendislerin gerekli önlemleri alması ve yapının daha uzun süre kullanılabilirliğini sağlamaktadır. GPR uygulamalarının doğru kullanıldığı takdirde, bu gibi kusurların tespitinde etkili olduğu kanıtlanmıştır. GPR yöntemi başka yapılar içerisinde de kullanılmaktadır. GPR verileri işlendikten sonra iki boyutlu görüntüler ayrı ayrı incelenerek ve görüntülere ait radargramlar üzerinde yansımış/saçılmış elektromanyetik (EM) dalga alanları da irdelenmiştir. Sonuç olarak, işlenmiş veriler üzerindeki köprüye ait yansımış/saçılmış dalga alanı konumları, yapısal elamanların konumlarını ve derinliklerini tanımlamaktadır. Elde edilen GPR hiperbollerin tepe genişliği yapısal elamanları belirlemektedir. Bu çalışma, Nisan 2012'de bir nehir üzerindeki köprüde meydana gelen kısmi çöküşü incelemektedir. Bu çöküşün yeterli bir yapısal sağlık izleme programı ile önenebileceği tespit edilmiştir. İncelenen köprünün kısmi yıkılmasını doğrudan etkileyen faktörler arasında yapısal elamanların demir korozyonu, temellerin aşınması ve zayıflamış bir köprü döşemesi bulunmaktadır. Bu çalışmada uygulanan yöntem, korozyondan etkilenen köprülerin GPR uygulaması ile ilgili yapı mühendislerinin ve / veya sorumluların karar vermelerini geliştirmek için kullanılabilir.

**Anahtar Kelimeler** – Köprü, kazısız teknolojiler, sinir ağları, yapı sağlığı, yer radarı

## Health Assessment of a Partially Collapsed Bridge Using Ground Radar (GPR) Application

<sup>1</sup>Department of Civil Engineering, Faculty of Engineering, İzmir University of Economics, İzmir, Türkiye

### Article History

Received: 18.03.2022

Accepted: 05.07.2022

Published: 15.12.2022

### Research Article

**Abstract** – Condition assessment of bridge structures within the context of health monitoring of structures, as well as the life cycle of structures, is of vital significance for engineers. Undoubtedly, the detection of bridge structural defects in the collapsed bridge in particular internal structural elements such as bridge deck delamination, the formation of cracks and corrosion of rebar will enable engineers to take necessary action, and prolong the serviceability of the structure. Applications of GPR have proved to be effective in detecting such imperfections if utilised correctly. GPR is also used in other structures. Since the GPR data was obtained in the form of two dimensional images after processing, the sections were examined in two dimensions and the reflected/scattered electromagnetic (EM) wave fields on the radargrams of the three dimensional images were examined. According to the results, the reflected/scattered wave field locations of the bridge on the processed data define the locations and depths of the structural elements. The apex width of the resulting GPR hyperbolas determines the structural elements. This paper reviews the collapse in April 2012 of a case study bridge over a creek, examining the possibility that this collapse could have been anticipated, and therefore, prevented with an adequate structural health monitoring programme. This paper also presents the results of the application of GPR. Factors which have been identified as having directly contributed to the failure of the case study bridge include the corrosion of rebar, scour of the foundations and a weakened bridge deck. The methodology implemented in this paper can be used to enhance the decision making of structural engineers and/or asset managers relating to the Ground Penetrating Radar application of corrosion affected bridges.

**Keywords** – Bridge, ground penetrating radar, non-destructive technologies, structure health, neural networks

<sup>1</sup> gokhan.kilic@ieu.edu.tr

\*Sorumlu Yazar / Corresponding Author

## 1. Giriş

Tetkik edilen köprü 1951 yılında trafiğe açılmış, dokuz köprü ayağı tarafından desteklenen on açıklıklı betonarme bir yapıdır. 252 metre uzunluğundaki köprünün yaklaşık 48 metresi 6 Nisan 2012 tarihinde saat 04.00'te aniden çökmüştür ve 15 ölümlü sonuçlanmıştır.

Bu çalışmada; köprü çöküşüne neden olan sebepler, bu sebepleri inceleyen raporlar aracılığıyla belirlenmiştir. İncelememiz sonucu, köprü demirlerinin hava koşulları ve dalgalar sonucu sürüklenen taşlar dolayısıyla aşındığı ancak kapsamlı bakım ve onarım çalışması yapılmadığı tespit edilmiştir. (KGM, 2012) tarafından derlenen bir rapora göre, köprünün genel yapı sağlığı incelemesi yapılmamıştır. Bazı onarım çalışmaları Karayolları Genel Müdürlüğü (KGM) tarafından yapılmıştır ancak çok ihtiyaç duyulan köprü yapısına yönelik onarımlar yapılmamıştır (DeNoto, 2022; Cao ve diğ., 2021, Li ve diğ., 2021). Ek olarak; köprü statikğine uygun, taşıyıcı sistemine destek proje çalışmaları yapılmadan, köprüye ekstra yük olan asfalt tabakaları eklenmiştir. Köprüde alt, üst ve etriye donatılarının yerleri bilinmediğinden bu bilgileri elde etmek için GPR kullanılmıştır. Bu çalışma, inşaat mühendisliği kusurlarının yapı aracılığıyla incelenmesi yoluyla tahribata dayanıklı farklı yöntemleri tespit ederek köprü çökmesini önleyebilecek tedbirler konusunda öneriler sunmaktadır. Bu kapsamda, GPR yöntemi, köprü yapısının alt ve üst donatısının konumunu, donatının korozyona uğraması veya nem mevcudiyetini belirlemede, donatı dışındaki betonda çatlak, çökme ve boşlukları belirlemede kullanılır (Parrillo ve Roberts, 2006; Kilic ve Caner, 2021; Benmokrane ve diğ., 2004; Kilic, 2016; Rhazi ve diğ., 2003).

Söz konusu yöntemle tetkik edilen köprü betonunun ciddi şekilde hasar aldığı ve birçok noktada donatıların korozyona uğradığı tespit edilmiştir. Ayrıca, dere yatağının taşıdığı malzeme zaman içinde su debisini değiştirmiş ve bu nedenle köprü ayaklarının altında bulunan ahşap kazıklar ortaya çıkmış, betonarme yapı ve taşıyıcı sistem bozulmuştur. Bu sebeplerin köprünün çökmesinde önemli bir faktör olduğu belirlenmiştir. Bu çalışmanın ilk bölümünde köprünün yapısal bilgileri, yıkılan alanının detaylı bir incelemesi, bulgular, tarihsel veriler ve tavsiyeler bulunmaktadır. İkinci bölümünde ise köprünün döşemesinde kullanılan donatıların alt ve üst konumlarını belirlemek ve GPR uygulamasına odaklanılmaktadır.

Bu araştırma, mevcut köprülerin yıkılma riski altına girmeden, sadece mühendislik gözlem yolu ile değil, diğer tahribatsız ve kazısız teknolojiler yardımı ile köprünün sağlık durumunu belirlemeyi, yıkılma risklerini ortadan kaldırmayı, düzenli kontrol sağlandığı zaman mevcut üst yapıların kullanım ömürlerini uzatmayı hedeflemektedir.

### 1.1.İncelenen Köprü

Köprü, Türkiye'de 1951 yılında Çaycuma deresi üzerinde uzanan 225 m'lik bir açıklıktan oluşan, betonarme / ön gerdirmeli beton bir yapıdan oluşmaktadır (Şekil 1-a). 6 Nisan 2012 tarihinde, yapımından 61 yıl sonra, köprünün belli bir bölümü çökmüş, bu yıkım 15 kişinin hayatını kaybetmesi ile sonuçlanmıştır (Şekil 1-b).



Şekil 1.a Çaycuma Köprüsü'nün Türkiye'deki konumu (KGM, 2012)

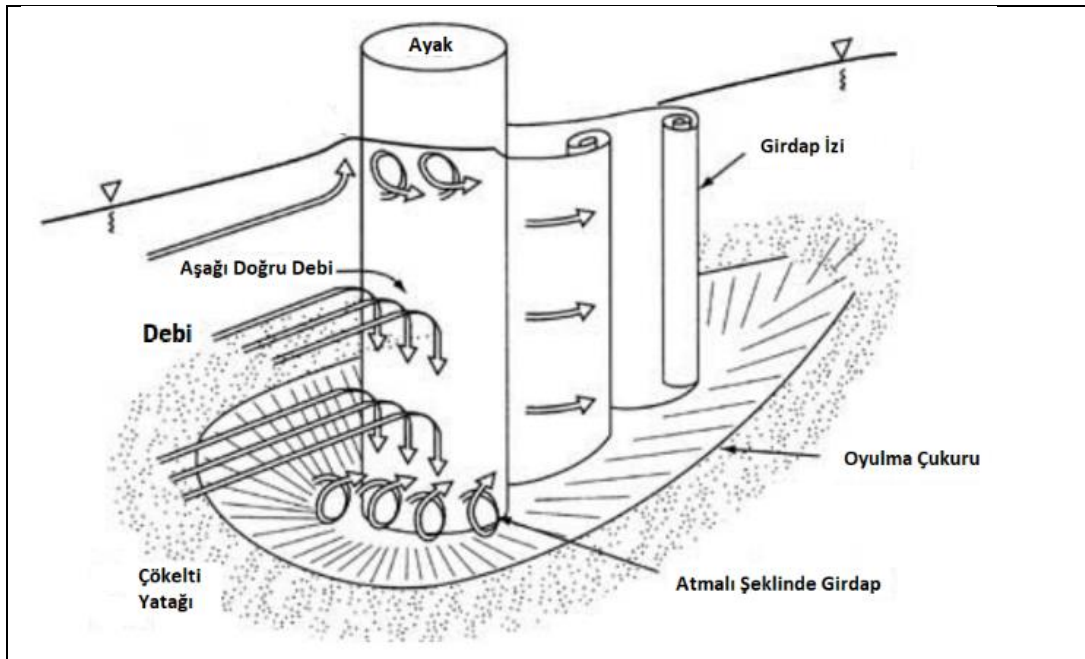


Şekil 1.b İncelenen köprünün kısmi çöken görüntüsü (KGM, 2012)

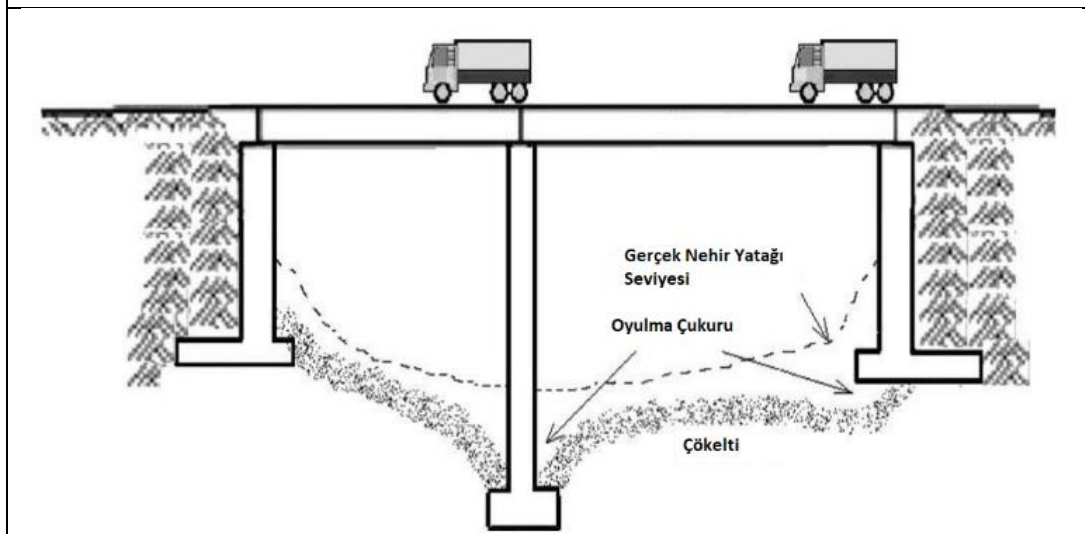


Köprü yapıları, suyun akım şartlarına göre hem doğrusal akarsularda hem de kıvrımlı akarsularda dayanıklı olmalıdır. Bunun yanında köprü yapılarının mukavemeti, hem statik kuvvetlere karşı hem de suyun dinamik etkisine karşı dayanıklı olmalıdır. Yapıların temeli, su kuvveti tarafından oyulma riskine ve taban oyulmalarına dirençli olacak şekilde tasarlanmalıdır.

İncelenen köprünün temeli, akarsuyun debisine ve zemin parametrelerine bakılmaksızın, oyulma riskine karşı herhangi bir önlem alınmadan tasarlanmıştır. Köprünün yıkılımdan sonraki incelemelerde ön değerlendirme olarak, dere boyunca dere yatağından toprak dolgunun alınmasından dolayı, köprü ayakları ve ahşap temel kazıkları olması gereken seviyenin altına düşmektedir. Bu yüzden dere yatağı erozyonuna karşı temel taşıma kapasitesi düşmüş, bu da statik gerginlikten ötürü köprü döşemesinin çökmesine neden olmuştur (Şekil 2-a ve 2-b).



Şekil 2.a Oyma deliğinde girdap oluşumu (Brandimarte ve diğ., 2012)



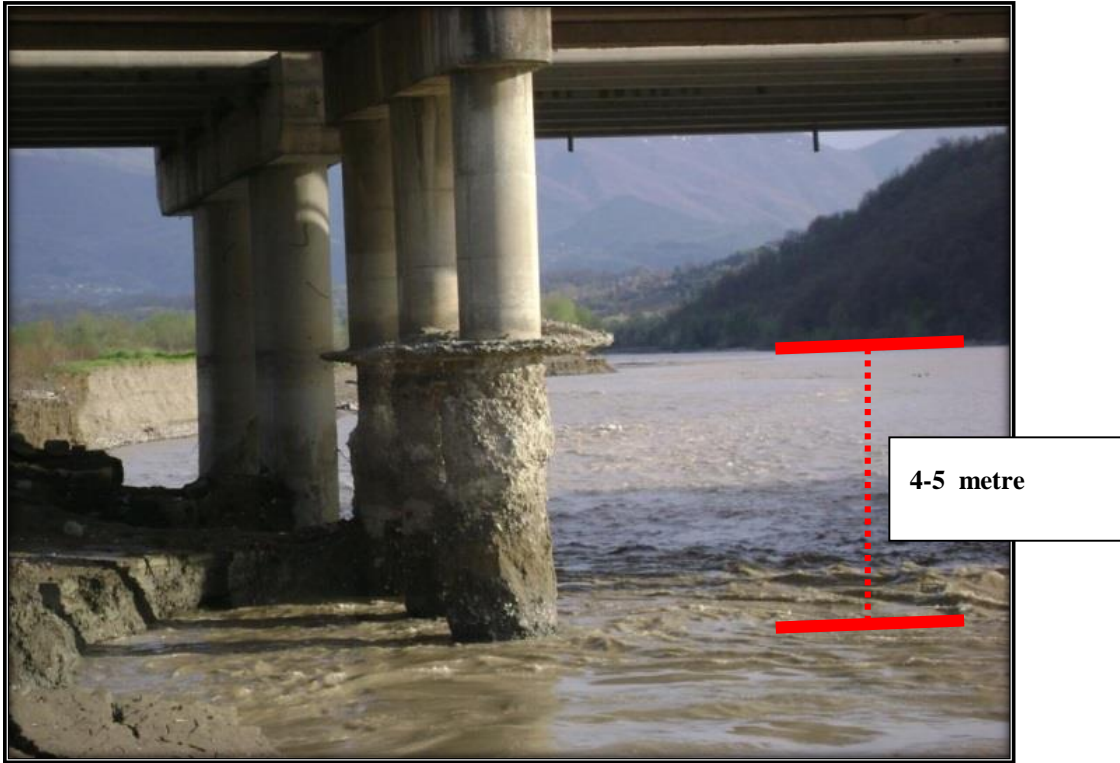
Şekil 2.b Köprünün ayaklarındaki oyulma çukuru (Deng ve Cai, 2010).

Bu gibi çökmelerin önlenmesi için kendi ağırlıkları, trafik yükleri ve ayrıca nehirler ve diğer su kütlelerinin empoze ettiği hidrolik kuvvetlerin birleşimine dayanacak su yollarını kapsayan köprüler tasarlamak

gerekmektedir. Bu arařtırmadaki köprünün yıkılması, sadece yetersiz bakım ve onarımdan ötürü deęil, aynı zamanda erozyonu önleyen setlerin kontrol ve bakımının önemini de ortaya koymaktadır.

## 1.2. İncelenen Köprünün Yıkılması Sebebi Üzerine Arařtırmalar

Tetkik edilen köprünün yıkılmasının öncesi bir kanıt bulunmadığından, bu arařtırma makalesi, inřaat ve tasarım hatalarının ana nedenlerini vurgulamayı amaçlamaktadır. Gelişmekte olan ülkelerdeki köprülerin hasar görmelerinin ana nedenlerinden biri hidrolik faktörlerin yanlış kalibrasyonudur. Amerika Birleşik Devletleri'nde 1989-2000 yılları arasında, 503 köprünün yıkılıř nedenlerini belirlemek için yapılan arařtırmalar, vakaların % 53' ünden fazlasından sellerin sorumlu olduğunu ortaya koymaktadır. Köprülerin yıkılmasının dięer ortak nedenleri arasında araç kazaları, depremler ve aşırı yüklemeler vardır (Yanmaz ve Caner., 2012; Melville ve Coleman., 2000). (Wolforst ve Annandale., 1998; Yanmaz 2002)'e göre nehir akarsuları, köprü ayaklarının etrafındaki fazla çöktelleri temizleyerek yapının sağlamlığını ve güvenilirliğini önemli ölçüde artırır. Şekil 3'te görüldüğü gibi 10 km uzaklıktaki başka bir köprünün taşıyıcı ayaklarının dere yatağından kum alınması sonucu, temellerinin seviyesinin 4-5 metre altında olduğunu tespit edilmiştir.



Şekil 3. Köprünün 10 km yukarısında bulunan başka bir köprü (resim Gokhan Kilic tarafından çekildi, 2012)

Köprü ayaklarının etrafındaki kırılmış beton parçaları yüzünden su akış hızı artmakta ve taşıyıcı ayaklarda oyulmalar daha fazla oranda görülmektedir (Şekil 4 ve 5). Ayrıca taşıyıcı ayaklarda onarım gerektiren bölgeler açıkça Şekil 4'de görülmektedir.





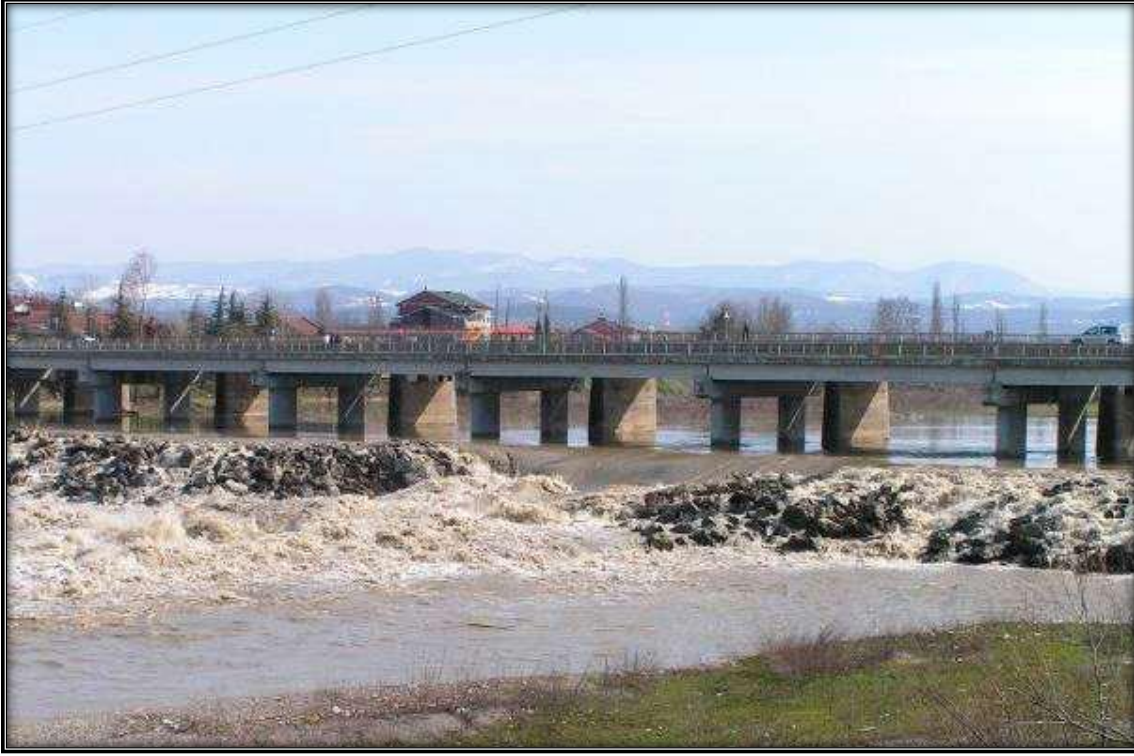
Şekil 4. Köprünün taşıyıcı ayakları ve temelleri (KGM, 2012)

Köprü taşıyıcı ayakları ve ahşap temellerinin üzerinde görünen derin çatlaklar ve açığa çıkmış donatılar Şekil 5'te görünmektedir.



Şekil 5. Köprünün taşıyıcı ayakları ve ahşap temelleri (resim Gokhan Kilic tarafından çekildi, 2012)

Dere yatağı üzerinden izinsiz ve kontrolsüz kum alınması dere akışının seviyesinin değişmesine ve bunun neticesinde köprünün hemen sonrasında bulunan kaya dolgu bariyerinin hasar görmesine sebep olmuştur (Şekil 6).



Şekil 6. Köprünün kaya dolgulu bariyerinin yıkılması (KGM, 2012)

Araştırılan köprünün yıkılmasının ardından, İstanbul Teknik Üniversitesi tarafından yapılan görsel bir inceleme sonucunda; kalan köprü tabliyesi üzerinde derin çatlaklar, beton kalitesinin bozulması, donatı korozyonu, taşıyıcı ayaklar üzerindeki önemli çatlaklar gibi birtakım kusurlar tespit edilmiştir (Şekil 7). Bu ayrıntılı raporda ayrıca, inşaat demiri korozyonunun, taşıma kapasitesi zayıflamış köprü ayaklarının ve döşemesinin de köprünün yıkılmasında etkili olduğu belirtilmiştir.



Şekil 7. Köprünün yıkılmasının ardından köprü tabliyesi (KGM, 2012)

Bu köprünün yıkılmasının birçok nedeni raporda belirtilmektedir. İlk olarak, köprü temelindeki oyulmadan dolayı temel kazıkların ortaya çıkması, Karabük Hidroelektrik Santrali Barajı taşkınlarından (yaklaşık 50 kilometre uzakta) meydana gelen hidrodinamik yüklemdeki artıştan olabileceği de belirtilmektedir. Artan su akışı, temellerin önlerindeki kaya dolgu bariyerinin ortadan kaldırması (Şekil 6), köprünün yapısal bütünlüğünün, özellikle de taşıyıcı ayaklarının taşıma kapasitesinin zayıflamasına neden olmuştur. Bu su akış gücü aynı zamanda köprünün temellerinin aşınmasına neden olmuştur. Ayrıca diğer faktörlerden birisi de eriyen karın neden olduğu su akışındaki yıllık artışlar suyun debisini artırarak taşıdığı ilave molozlar aynı zamanda beton ayaklarına verilen hasarı artırarak köprüdeki donatının açığa çıkmasına ve bu sebeple korozyonun artışına sebep olmuştur.

Köprünün yapısı ile ilgili olarak, uzun yıllar süren yoğun trafik yükleri ve malzemelerdeki doğal şartlar altındaki yıpranmalara ek olarak, köprünün proje dışındaki döşemesi üzerine yapılan ekstra asfalt çalışmasıdır.



Eklenen asfalt kalınlığı yaklaşık 70 cm kalınlığındadır, bu da köprüye 70 cm' ye (Şekil 8), yaklaşık olarak  $0.25 \times 0.70 \times 2,5 = 0.44$  t/m bir ölü yük ile ekstra eklenmektedir.



Şekil 8. Vaka çalışması köprüsünün ve genişletilmiş kaldırımın çöküşü (KGM, 2012)

Köprü yapısı üzerinde bir bütün olarak düzenli standart değerlendirmeler yapılmamıştır. Köprü'nün bazı bölümlerinde çeşitli iyileştirme ve yenileme çalışmaları yapılmış olmasına rağmen, gerekli ciddi onarım ve bakımların hiçbiri yapılmamıştır. Köprüde meydana gelen ciddi hasar belirtilerine rağmen hasarlı köprüye bitişik yeni bir köprü açılmış, tetkik edilen köprü'nün hizmette kalmasına izin verilmiştir. Ek trafik yükünün stresi ve ilave eklenen asfalt ağırlığı, köprü'nün taşıma kapasitesinin zayıflamasına sebep olmuştur.

Kilic, 2013 tarafından ayrıntılı olarak açıklanan böyle bir yaklaşım, tahribatsız tekniklerin bir kombinasyonunu açıklamaktadır: görsel inceleme, GPR, IBIS-S (interferometrik özelliklere sahip gelişmiş temassız bir radar tabanlı sensör sistemidir) ve Sonlu Elemanlar Modellemesi. Tam ve kapsamlı bir görsel inceleme de görünür donatı, köprü ayakları ve döşemesindeki önemli çatlaklar ve anormallikler gibi önemli dış yapısal bozulmayı tanımlamış ve yapısal kusurların yeri hakkında ön bilgi sağlamıştır. IBIS-S incelemesinde köprü sağlığını belirlemede, yük altında oluşan titreşimleri en doğru şekilde aktarmaktadır. Bu incelemede aşırı titreşimler ve yer değiştirmeler, köprü'nün sağlık durumunun çok önemli bir göstergesidir ve ayrıca bir yapının sağlığının bir risk oluşturup oluşturmadığını tahmin edebilecek bir ölçüdür. Başka bir çalışmada, incelenen köprü'nün kapsamlı bir sağlık değerlendirmesinde herhangi bir tam incelemede olduğu gibi, özellikle yoğun olarak kullanılan bir köprü'nün, her zaman gözle inceleme sonucunda bilgilerine ulaşılmamıştır (Hao, 2010). Bu nedenle, yapının sağlık durumunu belirlemek için, köprü gövdesinin iç yapısını, yani nem/su girişinin ve iç çatlakların ve özelliklerin doğru ayrıntılarını belirlemek için bir GPR araştırması yapılmıştır. Hao, 2010 aynı zamanda donatı korozyonunun doğru bir açıklamasını sağlayan bir veri analizi sunar.

Sonuç olarak, tetkik edilen köprü'nün tüm temel bileşenlerinin bozulması sonucunda yıkılmasına yol açmıştır. Sistematik olarak bir köprü sağlığı izleme yaklaşımı uygulandığında, yıkılmasının önlenilebileceği de açıktır. Böyle bir yaklaşım, yapının bir bölümü ile sınırlı olmadığı için, birçok tahribatsız teknik kombinasyonu yardımıyla olmalıdır.

## 2. Yöntem

Betonda donatı korozyonunun, araştırma köprüsünde olduğu gibi, nihayetinde yapısal bozulma ile sonuçlanabilecek betonarme yapıların erken bozulmasındaki ana faktör olduğu yaygın olarak bilinmektedir (Peng Han ve diğ., 2022; Li ve diğ.,2011). Bu korozyon, klorür iyonlarının girmesiyle çöktürülür. Böylece hızlı akan nehirler gibi zorlu çevre koşullarında bulunan yapılar için risk artar. Çatlak veya hasar görmüş yapılarda, klorür iyonları yapısal korumadan geçerek iyon konsantrasyonunun eşik değere ulaşmasına neden olarak, takviye donatıları çevreleyen alanda klorür kaynaklı korozyona neden olabilir. Korozyonun betonarme yapıları üzerindeki etkilerinin analizi esastır çünkü beton genellikle iç korozyona rağmen çatlama gibi herhangi bir dış hasar belirtisi göstermez. Betonarme donatı demirlerinin korozyon oranı da artan streslerle daha da artmaktadır (Enright ve Frangopol,1998).

Pek çok arařtırmada, sırasıyla, betonarme köprü kiriřlerinin dayanımının bozulmasını ve bir betonarme döřemesinin güvenilirliğini inceleyen (Stewart ve Rosowsky, 1998; Darmawan ve Stewart, 2007;Dođan 2008) tarafından geliřtirilenler gibi korozyon modelleri üzerinde detaylı çalıřmalar yapmıřtır. Öngermeli donatıların hacimsel ve zamansal maksimum derinlik verilerini belirlemek için hızlandırılmıř boşluk korozyonu (Haasl ve diđ.,1981) tarafından da incelenmiřtir. (LeBeau ve diđ.,2007) bükülme ve kayma donatılarının boşluk korozyonunun mekanik davranıřının ve yapısal güvenilirlik üzerindeki etkisinin daha ileri analizlerini yapmıřtır. Korozyon iřlemleriyle ilgili daha fazla bilgi için bu ayrıntılı incelemelere başvurulmalıdır. İncelenen köprünün korozyonunu etkileyen ana faktörlerin daha iyi anlaşılmasını kolaylařtırmak için burada sunulan model bilinçli olarak basitleřtirilmiřtir.

## 2.1. Yer Radarı İncelemesi ve Donanımı

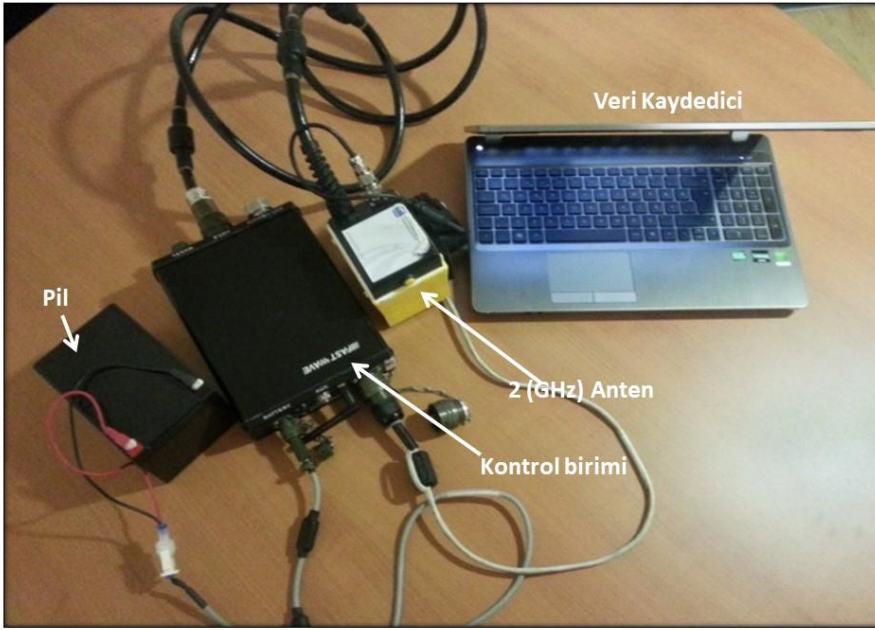
GPR yöntemi öncelikle yapıların sađlık durumlarını belirlemede, zemin yapısının çıkarılmasında, yüzeye yakın zemin birimlerin belirlenmesinde, deprem fay haritasını belirlemede, karstik boşluklarının bulunmasında, yeraltı su seviyesinin belirlenmesinde kullanılır (Li ve diđ., 2022; Asadi ve diđ., 2022).

Köprünün arařtırması, GPR'ın köprünün belirli bölgelerinde bir kılavuz kâğıdı üzerine uygulanmasına dayanmaktadır. GPR ekipmanının kılavuz kâğıdında yatay ve dikey çizgileri boyunca aşamalı olarak hareket ettirerek, incelenen alan hem uzunlamasına hem de enlemesine olarak incelenmiřtir. . Ekipman büyük GPR sistemlerinden oluřmadığı için, arařtırmanın tüm yönlerini tek bir bölgeyi inceleyerek ele almak mümkün deđildir. Bu nedenle, köprünün daha sađlıklı bir analizini gerçekteřtirmek için birkaç küçük alanda arařtırma yapılmıřtır (Şekil 9).



Şekil 9. TR HF (2 GHz) Anteni kullanılarak köprü üzerinde GPR arařtırması

Elde edilen verileri almak, izlemek ve kontrol etmek için K2 Fast-Wave yazılımı kullanılmıřtır. Yazılım normal bir dizüstü bilgisayarla da uyumludur veyüksek kaliteli görüntüler ve tomografi haritaları elde etmek için 2 GHz frekanslı bir Tomography Resistivity High Frequency (TR HF) anteni kullanılmıřtır. (Şekil 10). Bu GPR ekipmanı, köprü hasarlarından sorumlu tüm faktörleri belirleme fırsatlar sunmaktadır.

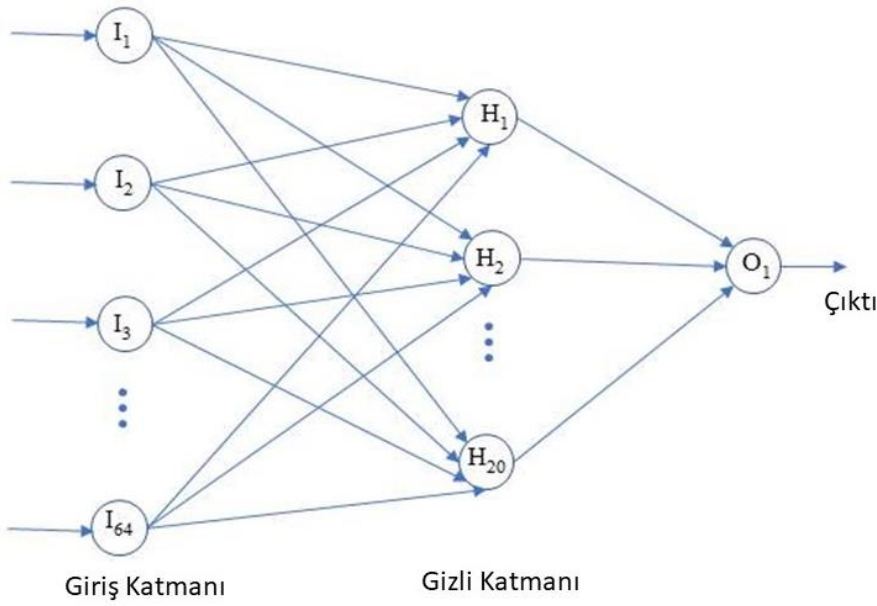


Şekil 10. TR HF (2 GHz) Anteni

Köprünün analizi, veri analizi yazılımı olan IDS GRED kullanılarak yapılmıştır. Analiz incelemesinin tamamı, veri toplama, sıralama ve seçilen verilerin analizini içeren birkaç adımdan oluşur. IDS GRED, donatının derin ve sığ konumlarını otomatik olarak toplayan ve kaydedilen verileri işlemeyen ve bir b-taraması gerçekleştirmeden önce geriye saçılan dalgaları analiz eden akıllı bir sistemdir. Fakat yeterli değildir, bu sebeple incelenen alanın dikey bir bölümünü örneklemek için sinir ağı tasarımı yardımıyla b-taraması azaltılmıştır. Sistem ayrıca kaydedilen verileri yatay ve dikey eksenlerden bir yüksek kaliteli tomografi haritasına toplayabilmektedir.

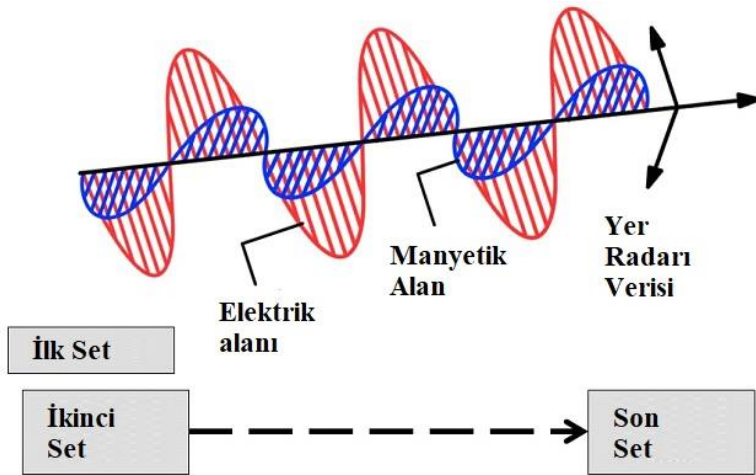
## 2.2.Sinir Ağı Tasarımı

Bu araştırmada ayrıca, Sinir Ağların saçılma elektro manyetik dalga gürültüsü içindeki tespitini yapmak için geri yayılma öğrenme algoritmasını uygulayarak nemi tespit edebilen Sinir Ağlar için tasarım teknikleri yer almaktadır. Giriş, gizli ve çıkış katmanlarından oluşan üç katmanlı Sinir Ağlar, Şekil 11'de görülebilir. Tartışılan teknikler, elektro manyetik dalgalarındaki gürültü içerisindeki belirli alanı belirlemeden önce nemi tespit etme potansiyeline sahiptir. Ek avantajlar gerçek zamanlı işleme, uyarlanabilirlik ve Sinir Ağı eğitimi içerir.



Şekil 11. Giriş, gizli ve çıkış katmanlarından oluşan basit bir Sinir Ağı

Bu ağ tamamen bağlantılı, ileri beslemeli bir Sinir Ağıdır. Uygulamadan önce, en uygun boyuttaki Sinir Ağının, gizli katman sayısı ve her gizli katmandaki gizli nöronların sayısı konusunda kararlar alınmalıdır. Bu tartışmada (Chen ve diğ.,2010; Frein ve Richard, 2011), tek bir gizli katmanın ve 20 gizli nöronun gerekli olan maksimum değer olduğunu düşünmektedir. Doğrulama amacıyla, Sinir Ağı eğitilmiştir ve ortaya çıkan ağ test edilmektedir. Tatminkâr olmayan sonuçların yetersiz bir eğitim seti veya oyundaki aşırı sayıda nöron olması nedeniyle olduğu düşünülmektedir. Daha sonra gerekli ayarlamalar yapılır ve test tekrarlanır. Bu düzen tatmin edici bir doğrulama seti elde edilinceye kadar devam eder.



Şekil 12. Sinir Ağı'nın blok şeması

Köprü'nün incelenen çeşitli bölgelerinde bölümlere ayrılan GPR taramasından elde edilen veriler Sinir Ağına dahil edilmiştir (Şekil 12). Sinir Ağına giriş sinyali oluşturmak için ham bir veri kullanılmıştır; veriler 64 örnek ve iki ardışık set arasında bir örnektir. İlk set, GPR verilerinin başlangıcından elde edilmiştir ve bir sonraki adım, ilk setin sağındaki bir örnektir. Bu kalıp, setteki 1.700 GPR verisinin tüm örneklerini kaplayana kadar kopyalanmıştır.

GPR verileri Sinir Ağına girdi ve çıktı olarak tespit edilmiştir (hatalı) veya tespit edilememiştir (sağlıklı) olarak ikili bir karardır. Her 10 metrede bir veri toplayarak köprüye GPR anketi uygulanmıştır. Görsel inceleme tarafından hatalı olarak etiketlenmiş dört konum vardır ve bunların üçü Sinir Ağı'nı eğitmek için kullanılmıştır. Kalan on altıdan yedisi eğitim için sağlıklı veriler olarak seçilmiştir. Dördüncü hatalı durum ve kalan dokuz

örnek test için kullanılmıştır. Sinir Ağı, dördüncü hatalı durumda ve bir başka numunede (görsel olarak kontrol edilemeyen başka bir yerde) boşluk / nem tespit edilmiştir.

GPRGPR verileri Sinir Ağına dahil edildiğinde, gizli nöronların her çıktısı giriş düğümlerinin ağırlıklı bir toplamıdır ve yanlılık düğümü bir hiperbolik teğet fonksiyonundan geçer (Şekil 11). Gizli nöron'un  $y_j, j=1 \dots L$ , Sinir Ağı'nın sonucu,

$$y_j = \phi\left(\sum_{i=1}^M x(i)w_{ji}^h + \theta^j\right) \quad (2.1)$$

$\phi$  (yanlılık), L 20, M 64'tür ve gizli ve çıkış katmanı için aktivasyon fonksiyonu,  $\phi$  (yanlılık), olarak tanımlanmış,  $\phi()$ , bir teğet hiperbolik fonksiyondur.

$$\phi(y) = \frac{e^y - e^{-y}}{e^y + e^{-y}} \quad (2.2)$$

$x(i)$  terim, GPR verisini içeren girişi  $w_{ji}^h$  temsil ederken,  $j^{\text{th}}$  gizli nöronun  $i^{\text{th}}$  giriş nöronuna olan ağırlığıdır. Sinir Ağı'nın gerçek çıktısı, tüm gizli nöronların ve önyükleme düğümünün ağırlıklı toplamıdır; bu, daha sonra her bir girdi değeri seti için istenen çıktı ile zıtlık oluşturur. Bu çıkışlar arasındaki herhangi bir tutarsızlık bir Sinir Ağı hatası olarak tanımlanır, bu durumda Sinir Ağı'nın ağırlıkları bu çıkış hatasının gradyanı kullanılarak güncellenir (Shi ve diğ.,2011; Li ve diğ.,2010).

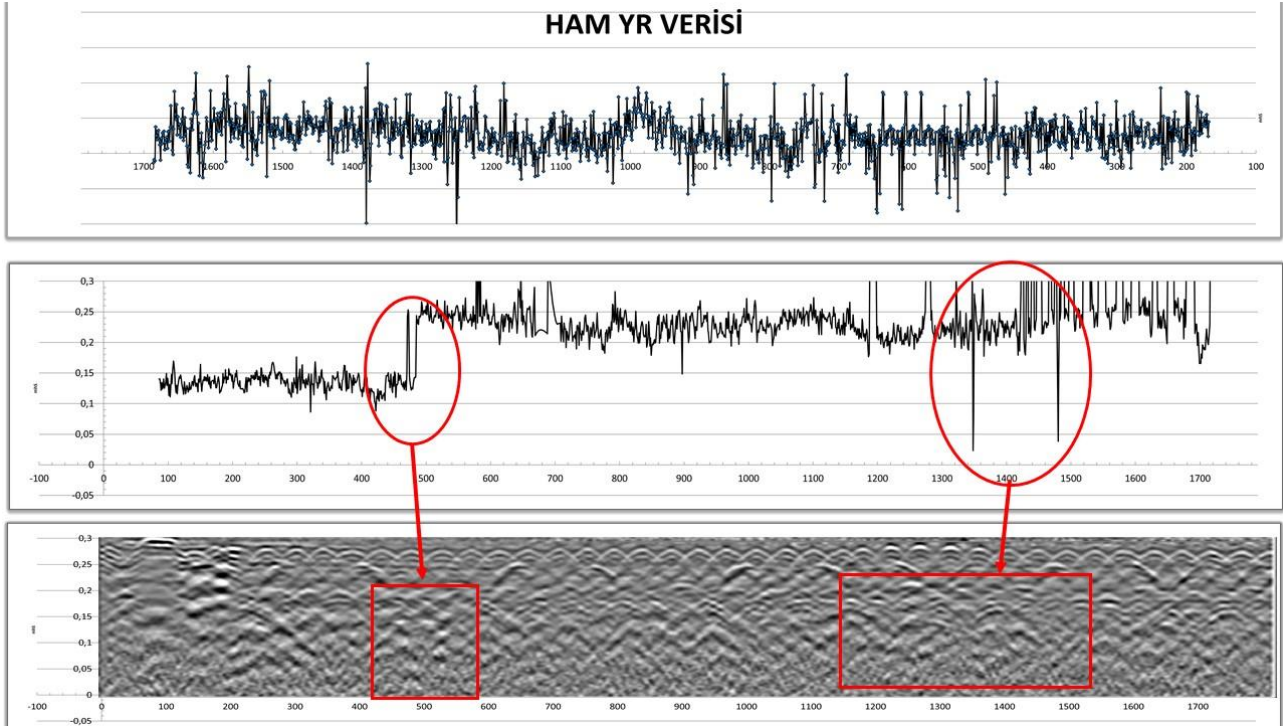
### 3. Bulgular ve Tartışma

#### 3.1. Yer Radarı Sonuçları

Köprünün incelemesi yalnızca GPR incelemesine dayanmakla kalmıyor, aynı zamanda görsel analizleri de yapılmıştır. GPR sonuçları, somut bozulma, su sızıntısı, taşıyıcı sistemlerde büyük çatlaklar ve donatı korozyonu dahil olmak üzere birtakım nedenlerini ortaya koymuştur. Görsel inceleme ayrıca köprü gövdesi yüzeyinde bozulma olduğunu da gösterilmektedir.

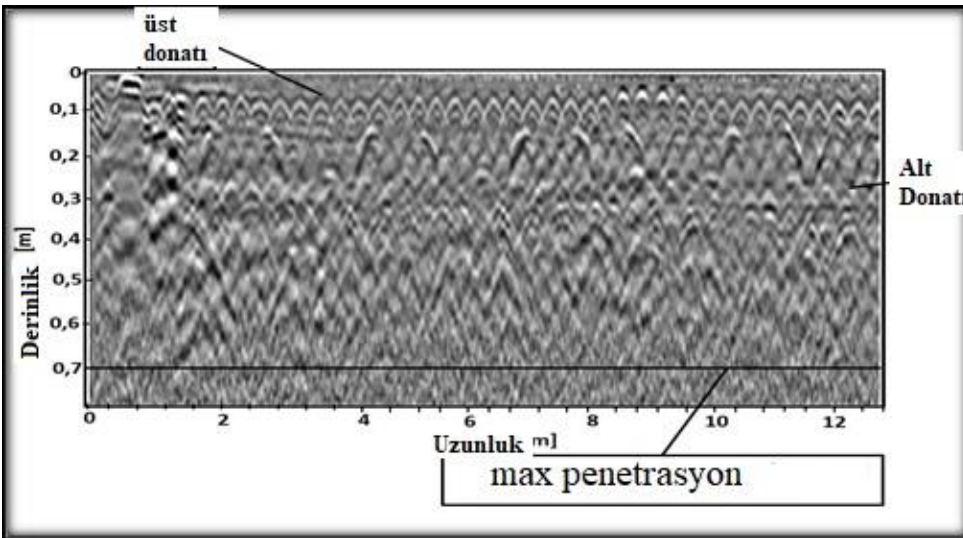
Ham GPR profil verisinden işlenmiş radar profiline geçiş yapılırken Sinir Ağı, düşük frekanslı veya yüksek frekanslı GPR verilerini alacak şekilde tasarlanmıştır. Burada, düşük frekanslı veriler yüzeyde düşük çözünürlük sağlar, ancak daha fazla derinlik bilgisi sağlarken yüksek frekanslı veriler yüzeyde daha yüksek çözünürlük sağlar ancak daha düşük derinlik bilgisi verir. Farklı frekanslar için, boşlukların / nemin saçılma özellikleri oldukça farklı olsa da, test durumlarında ayırım belirgin olarak gözlenmiştir (Şekil 13).





Şekil 13. Ham radar profil verisinden işlenmiş radar profiline geçiş yapılırken uygulanan işlem

İncelemede ayrıca köprünün 70 cm ölçümünün altındaki 5-10 cm arasındaki üst donatı, 30 cm altında alt donatı konumlarının da aşırı nem penetrasyonundan etkilendiğini ortaya çıkarılmıştır. Bu sonuçlar veri toplama ve köprü ve kompozisyonun tüm yönlerinin analizinden elde edildiklerinden (son derece) güvenilir olarak kabul edilir (Şekil 14).

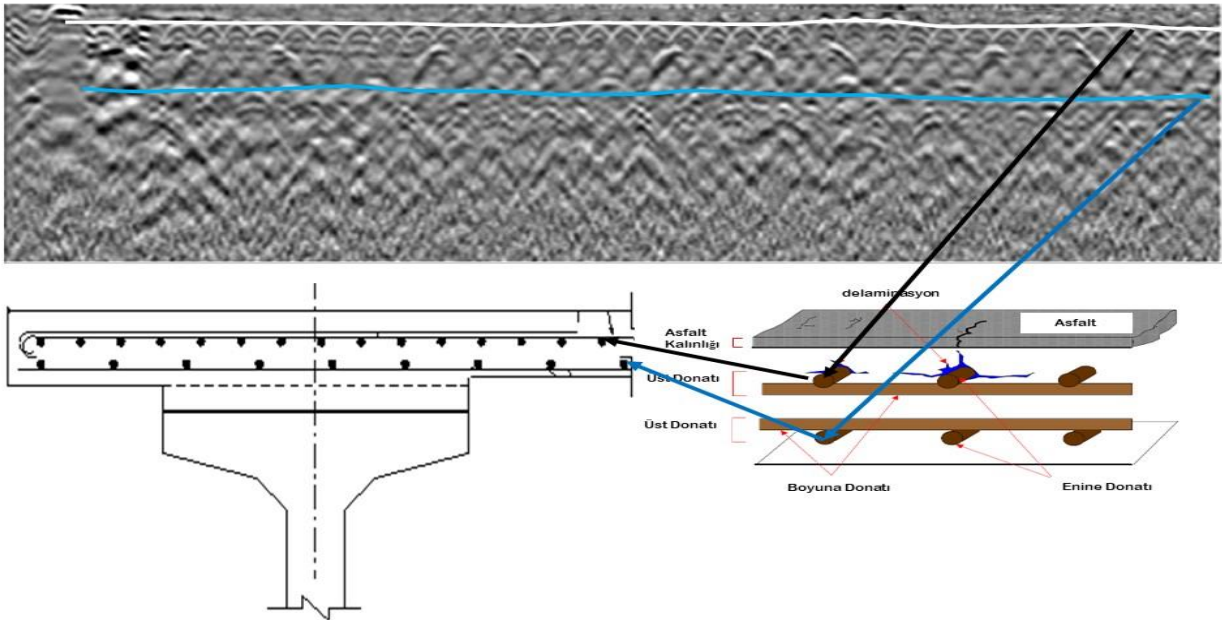


Şekil 14. İşlenmiş 2GHz veri ve daha derin penetrasyonlu köprünün araştırılmasından elde edilen muhtemel açıklamalar (yorumlama)

Yukarıda bahsedildiği gibi, köprünün çeşitli yapısal özelliklerini incelemek için bir TR HF anteni kullanılmıştır. Migrasyon yöntemine dayalı olarak, beton içindeki tahmini yayılma hızı (V), yaklaşık olarak 0.12 m/ns olmuştur ve buna karşılık gelen nispi dielektrik sabiti 6,3'tür. Anten ayrıca 70 cm altındaki alt yüzey katmanlarının kompozisyonunun araştırılmasına da izin vermiştir (Şek. 13). GPR görüntüleri analiz ederek, donatı çubuğunun tam boyut ve konumunu belirlemek mümkün olmuştur. GPR taramasından elde edilen



veriler, alt ve üst donatı konumlandırmalarını analiz etmek için de kullanılmıştır (Şekil 15) (Koşaroğlu vd. 2016 ve Taştan vd. 2017).



Şekil 15. GPR radargramından inşaat demiri konumu (Kilic 2013)

Her ne kadar beton kaplama kalınlığının inşaat demiri korozyonu üzerinde minimum etkiye sahip olduğu düşünülse de, artan kalınlık nehir sedimentinin aşınmasına karşı etkili olduğu ve bu nedenle dalgalanmaya maruz kalan korozyon akımı yoğunluğunu azaltmıştır. Beton kaplama kalınlığı zamanla aşınırken, korozyon akımı yoğunluk değeri artmıştır ve bu da etkili izleme ve bakımın aşırı önemini gösterir. Bu çalışma, köprü döşemesi üzerine eklenen asfalt kalınlığını belirlemede (ölü yükün artması), alt ve üst donatıların konumlarını belirlemede, ve donatılarda korozyon olup olmadığını saptama da araştırma yapılmadığının altını çizen betonarme köprü çöküşü hakkında çok az sayıda rapordan biridir.

#### 4. Sonuçlar

İnceleme neticesinde, köprünün yıkılmasının iki ana nedeninin kontrolsüz asfalt kalınlığının artması ve dere yatağı seviyesindeki doğal değişiklikler olduğu sonucuna varılmıştır. Bunun yanında, köprü yatağı silt ve kumdan oluşan yüksek yoğunluktaki su akımının yatak katmanının içinden yayılmasına maruz kalmıştır.

GPR'ye dayalı incelemede, donatının konumları tam olarak belirlenmiştir. GPR araştırmasının bulguları ve görsel analiz, kapsayıcı sonuçları çıkarmak için birleştirilmiştir. İnceleme sadece köprünün yıkılmasının sebeplerini değil, aynı zamanda yapı kusurlarını göstermek için mühendislerin hibrid analiz tekniklerini benimseme ihtiyacını da vurgulamaktadır. Sadece GPR verileri köprünün mevcut sağlık durumunu ortaya koymaya yeterli değildir. Yıkılan köprünün incelenmesi neticesinde, mega yapı tasarımı için mühendislerin GPR gibi ileri teknikler kullanmalarının yıkılma faktörlerini büyük ölçüde azaltacağı sonucuna varılabilir.

Çalışmamız, köprünün yıkılmasında rol oynayan iki önemli noktayı ortaya çıkarmaktadır: Bunlardan biri uygun muayene tekniklerinin önemidir. Ötekisi ise yapıların yaşlanmadan önce derin incelemelerinin yapılması gereğidir. Bu çalışmada her iki yön de incelenmiştir. Saha incelemesi sırasında, önemli yapısal bozuklukların çökmeye neden olduğu tespit edilmiştir. Yapıdaki temelleri aşındıran su kaymaları, yapıya eklenen fazla yüklenmeden dolayı köprü taşıyıcılığının zayıflaması ve donatıların köprü ayaklarının temelindeki aşınmasıdır. Yazar, bu yapısal başarısızlıkları belirlemede potansiyeli olan basit bir metodoloji önererek, gözle inceleme (yüzeysel ve gözlemlenebilir hataları tanımlamak için) ve GPR taraması (gözle inceleme ile erişilemeyen köprünün iç yapısında bulunan yapısal elamanları veya kusurları ortaya çıkarmak için) kapsamlı bir sağlık değerlendirmesi sistemi önermektedir. Bu nedenle, bu çalışma, tetkik edilen köprünün değerlendirmesini ve hizmet ömrü tahmini için basit, karmaşık olmayan bir güvenilirlik analiz sistemi sunmaktadır. Bu yöntem, büyük olasılıkla saha araştırması tarafından belirlenen yapısal bozulma nedeniyle, çöken köprü için düşük

güvenilirlik indeksini tanımlamıştır. Ayrıca, köprülerin yıkılma olasılığını etkileyen iki önemli faktörün önemli betonarmede kaplama kalınlığı ve hareketli yükün yoğunluğu olduğu tespit edilmiştir. Bu özel durumlarda, mevcut trafik yoğunluk oranı, ek takviye, iyileştirici etki ile azaltılabilir. Bu makalede, incelenen köprünün yıkılmasının sadece bir ön değerlendirmesi yapılmıştır fakat yine de bazı temel nedenleri tanımlayamamaktadır. Dünyada binlerce betonarme köprü vardır, Türkiye'de 6765 köprü (KGM, 2012; Hao, 2010'a göre) ve birçoğunun bu yazıda tartışılan yıkılmaya maruz kalma ihtimalleri vardır. Bu nedenle bu çalışma, köprü yapılarının daha fazla araştırılmasını ve analiz edilmesini teşvik etmeyi amaçlamaktadır.

#### Teşekkür:

Yazar, önemli öneri, kapsamlı inceleme, destek, rehberlik, büyük ilham ve bu yazı için önemli katkılar için Karayolları Genel Müdürlüğünden emekli, rahmetli babası Cemil Kılıç'a minnettedir.

#### Çıkar Çatışması:

Yazar çıkar çatışması bildirmemiştir.

#### Kaynaklar

- Asadi P., Gindy M., Alvarez M., Asadi A., (2020), *A computer vision based rebar detection chain for automatic processing of concrete bridge deck GPR data*, Automation in Construction, Volume 112, 103106, ISSN 0926-5805, doi: <https://doi.org/10.1016/j.autcon.2020.103106>.
- Benmokrane, B., El Salakawy, E. F., El Ragaby, A., Desgagné, G. ve Lackey, T. (2004). *Design, construction and monitoring of four innovative concrete bridge decks using non corrosive FRP composite bars*. Annual Conference & Exhibition of the Transportation Association of Canada. Québec, Canada.
- Brandimarte, L., Paron, P., Di Baldassarre, G. (2012). *Bridge pier scour: A review of processes, measurements and estimates*. Environmental engineering and management journal. 11. 10.30638/eemj.2012.121.Cao R., Agrawal A.K., El-Tawil S., 2021, Overheight impact on bridges: A computational case study of the Skagit River bridge collapse, Engineering Structures, Volume 237, 2021, 112215, ISSN 0141-0296, doi: <https://doi.org/10.1016/j.engstruct.2021.112215>.
- Peng Han, Guofu Qiao, Bingbing Guo, Dongsheng Li, Jinping Ou, 2022, *Investigation of the low-frequency stray current induced corrosion on reinforced concrete infrastructure in high-speed rail transit power supply system*, International Journal of Electrical Power & Energy Systems, Volume 134, 2022, 107436, ISSN 0142-0615, doi: <https://doi.org/10.1016/j.ijepes.2021.107436>.
- Chen, X.-j., Gao, Z.-f., Ma, Y.-e., and Guo, Q., *Application of Wavelet Analysis in Vibration Signal Processing of Bridge Structure*, 2010 International Conference on Measuring Technology and Mechatronics Automation (ICMTMA), Vol. 1, March 13–14, 2010, pp. 671–674, doi: 10.1109/ICMTMA.2010.95.
- Darmawan M. S., Stewart M. G., 2007, *Spatial time-dependent reliability analysis of corroding pretensioned prestressed concrete bridge girders*, Structural Safety, Volume 29, Issue 1, 2007, Pages 16-31, ISSN 0167-4730, doi: <https://doi.org/10.1016/j.strusafe.2005.11.002>.
- Deng L., Cai C.S., (2010), *Bridge Scour: Prediction, Modeling, Monitoring, and Countermeasures*, Review, Practice Periodical on Structural Design and Construction, 15, 125–134., doi/abs/10.1061/%28ASCE%29SC.1943-5576.0000041
- DeNoto G. *Bridged repair of large ventral hernia defects using an ovine reinforced biologic: A case series*, Annals of Medicine and Surgery, Volume 75, 2022, 103446, ISSN 2049-0801, doi: <https://doi.org/10.1016/j.amsu.2022.103446>.
- Doğan A. E., (2008). *Effects Of Collars on Scour Reduction at Bridge Abutments*”. (Mas. Sc. Thesis), Metu, Ankara, <https://etd.lib.metu.edu.tr/upload/3/12610203/index.pdf>
- Enright, M. P., and Frangopol, D. M. (1998). *Probabilistic analysis of resistance degradation of reinforced concrete bridge beams under corrosion*. Eng. Struct., 2011, 960–971., ISSN 0141-0296, doi: [https://doi.org/10.1016/S0141-0296\(97\)00190-9](https://doi.org/10.1016/S0141-0296(97)00190-9).
- Frein de, R. and Rickard, S. T., 2011, *The Synchronized Short-Time-Fourier-Transform: Properties and Definitions for Multichannel Source Separation*, in IEEE Transactions on Signal Processing, vol. 59, no. 1, pp. 91-103, Jan. 2011, doi: 10.1109/TSP.2010.2088392.
- Haasl, D., Roberts, N., Vesely, W., and Goldberg, F., (1981). *Fault Tree Handbook*, U.S. Nuclear Regulatory

- Commission, Washington D.C.
- Hao S., (2010), I-35W *Bridge Collapse*, Journal of Bridge Engineering, 608-614-15-5, doi: [https://doi.org/10.1061/\(ASCE\)BE.1943-5592.0000090](https://doi.org/10.1061/(ASCE)BE.1943-5592.0000090)
- KGM, General Directorate of Highways, 2012, *Republic of Turkiye, General Directorate of Highways, Site Collection Documents, KGM documents*, Istatistikler, Kopru ve Tunel Bilgileri, 2012.
- Kilic G., 2016, *Applications of Ground Penetrating Radar (GPR) to Detect Hidden Beam Positions*, Journal of Testing and Evaluation, 0090-3973 (IF = 1.162) (Category: Q3)
- Kilic G. , Caner A. (2021) *Augmented reality for bridge condition assessment using advanced non-destructive techniques*, Structure and Infrastructure Engineering, 17:7, 977-989, doi: 10.1080/15732479.2020.1782947
- Kilic Gokhan, 2013, (Doktora Tezi) *Application of Advance Non-destructive techniques for Bridge Health Assessment*, PhD Dissertation, 2013, University of Greenwich
- Kosaroglu, Sinan; Bilim, Funda; Tastan, Erkan. (2016). *Cumhuriyet Üniversitesi, Mühendislik Fakültesi Binasının Yer Radarı (GPR) Yöntemi ile Hasarsız İncelenmesi*. Bitlis Eren Üniversitesi Fen Bilimleri Dergisi. 5. 10.17798/beufen.90389.
- LeBeau, K.H. and Wadia-Fascetti, S.J., (2007). *Fault Tree Analysis of Schoharie Creek Bridge Collapse*, Journal of Performance of Constructed Facilities, Vol. 21, No. 4, pg. 320-326. (2007)., doi: [doi/abs/10.1061/%28ASCE%290887-3828%282007%2921%3A4%28320%29](https://doi.org/10.1061/%28ASCE%290887-3828%282007%2921%3A4%28320%29)
- Li R.W., Cao D.S., Wu H., Wang D.F., (2021). *Collapse analysis and damage evaluation of typical simply supported double-pier RC bridge under truck collision*, Structures, Volume 33, 2021, Pages 3222-3238, ISSN 2352-0124, doi: <https://doi.org/10.1016/j.istruc.2021.06.041>.
- Li, F., Yuan, Y., Li, C. Q., (2011). *Corrosion propagation of prestressing steel strands in concrete subject to chloride attack*, Construction and Building Materials, Volume 25, Issue 10, 2011, Pages 3878-3885, ISSN 0950-0618, doi: <https://doi.org/10.1016/j.conbuildmat.2011.04.011>.
- Li, J., Jiang, T., Grzybowski, S., and Cheng, C., (2010). *Scale dependent wavelet selection for de-noising of partial discharge detection*, in IEEE Transactions on Dielectrics and Electrical Insulation, vol. 17, no. 6, pp. 1705-1714, Dec. 2010, doi: 10.1109/TDEI.2010.5658220.
- Liu Z., Gu X., Wu W., Zou X., Dong Q., Wang L., (2022) *GPR-based detection of internal cracks in asphalt pavement: A combination method of DeepAugment data and object detection*, Measurement, Volume 197, 111281, ISSN 0263-2241, doi: <https://doi.org/10.1016/j.measurement.2022.111281>.
- Melville, B.W., and Coleman, S.E. (2000). *Bridge Scour*, Water Resources Publications, LLC, Colorado, ABD. ISBN 13: 978-1-887201-18-6
- Parrillo, R. ve Roberts, R. (2006). *Bridge Deck Condition Assessment using Ground Penetrating Radar*. ECNDT Geophysical Survey Systems. North Salem, NH, USA. ECNDT - Tu.4.2.5
- Rhazi, J., Dous, O., Ballivy, G., Laurens, S. & Balayssac, J. P. (2003). *Non-destructive health evaluation of concrete bridge decks by GPR and half cell potential techniques*. 6th International Conference on Nondestructive Testing in Civil Engineering. Berlin
- Shi, G., Chen, X., Song, X., Qi, F., and Ding, A., (2011) *Signal Matching Wavelet for Ultrasonic Flaw Detection in High Background Noise*, IEEE Trans. Ultrason. Ferr., Vol. 58, No. 4, pp. 776–787. DOI:10.1109/TUFFC.2011.1870
- Stewart, M. G., and Rosowsky, D. V. (1998). *Time-dependent reliability of deteriorating reinforced concrete bridge decks*, Structural Safety, Volume 20, Issue 1, 1998, Pages 91-109, ISSN 0167-4730, doi: [https://doi.org/10.1016/S0167-4730\(97\)00021-0](https://doi.org/10.1016/S0167-4730(97)00021-0).
- Taştan, E. , Koşaroglu, S. & Bilim, F. (2017). *Identifying of structural elements of building using Ground penetrating radar (GPR): A case study of the Cumhuriyet University, Turkey* . Bitlis Eren University Journal of Science and Technology , 7 (1) , 22-26 . doi: 10.17678/beuscitech.295134
- Wolforst J. and Annandale G. (1998) *Channel Degradation due to Gravel Mining: Application of Geomorphic Analysis and Sediment Transport Modeling Approaches*, Proceedings: Unique Functional Consideration for Wetland Restoration, ASCE., doi: [abs/10.1061/40382%281998%29167](https://doi.org/10.1061/40382%281998%29167)
- Web. *Çaycuma Köprüsünün Çökmesi Üzerine Görüşler* [http://www.tkic.org.tr/ documents/caycuma.pdf](http://www.tkic.org.tr/documents/caycuma.pdf). Erişim Tarihi: 29.10.2016.
- Yanmaz, A. M., Caner A. (2012). *Çaycuma Köprüsünün Çökmesi Üzerine Görüşler*. Türkiye Köprü ve İnşaat Cemiyeti", (2012)